



INSTITUTO DE
INVESTIGACIONES QUÍMICAS
CONSEJO SUPERIOR DE
INVESTIGACIONES CIENTÍFICAS

DPTO. QUÍMICA ORGÁNICA
FACULTAD DE QUÍMICA
UNIVERSIDAD DE SEVILLA

Atroposelective Synthesis of (Hetero)biaryls: Dynamic Kinetic and Thermodynamic Control of the Axial Chirality

Memoria presentada por la Graduada
Patricia Rodríguez Salamanca
para optar al grado de Doctora en Química.

Sevilla, enero 2023



INSTITUTO DE
INVESTIGACIONES QUÍMICAS
CONSEJO SUPERIOR DE
INVESTIGACIONES CIENTÍFICAS

DPTO. QUÍMICA ORGÁNICA
FACULTAD DE QUÍMICA
UNIVERSIDAD DE SEVILLA

VºBº El Director de la Tesis

VºBº El Director de la Tesis

Fdo. Dr. José María Lassaletta Simón
Profesor de Investigación del CSIC
Instituto de Investigaciones Químicas

Fdo. Valentín Hornillos Gómez-Recuero
Investigador Ramón y Cajal
Departamento de Química Orgánica
Universidad de Sevilla

El presente trabajo ha sido realizado por la Graduada Patricia Rodríguez Salamanca con un contrato predoctoral (BES-2017-081561) financiado por el Proyecto del Ministerio de Economía, Industria y Competitividad “Desarrollo y Diversificación de Sistemas Catalíticos Innovadores. Aplicaciones en Catálisis Asimétrica” con referencia CTQ2016-76908-C2-1-P, llevándose a cabo en el Grupo de Catálisis Asimétrica del Instituto de Investigaciones Químicas (IIQ) del Consejo Superior de Investigaciones Científicas (CSIC-US). Durante su desarrollo, ha contado con la supervisión del Dr. D. José María Lassaletta Simon, Profesor de Investigación del Instituto de Investigaciones Químicas (CSIC-US) y del Dr. D. Valentín Hornillos Gómez-Recuero, Investigador Ramón y Cajal de la Universidad de Sevilla (US).

Table of Contents

Summary/Resumen	1
Summary.....	1
Resumen.....	2
I. Introduction.	7
I.1. Asymmetric catalysis.....	7
I.2. Axial chirality: atropisomerism.....	11
I.3 Atroposelective synthesis of (hetero)biaryls by kinetic control.....	14
I.3.1. Stereoselective formation of the stereogenic axis.....	15
A. Stereoselective formation of the stereogenic axis <i>via</i> metal-catalyzed cross-coupling reactions.....	15
B. Asymmetric oxidative coupling of two arenes.....	18
C. Asymmetric biaryl synthesis by <i>de novo</i> construction of an aromatic ring.....	22
D. Asymmetric construction of atropisomers by central-to-axial chirality transfer.....	24
I.3.2. Atroposelective transformations of preformed biaryl compounds.....	25
A. Desymmetrizations.....	26
B. Kinetic Resolution (KR).....	37
C. Dynamic Kinetic Resolution (DKR).....	41
D. Dynamic Kinetic Asymmetric Transformation (DYKAT).....	51
I.4. Central and axial chirality: thermodynamic control.....	53
A. Seven-membered bridged biaryls.....	54
B. Eight-membered bridged biaryls.....	57
II. Atroposelective iridium catalyzed transfer hydrogenative allylation of quinolinealdehydes by Dynamic Kinetic Resolution	64
II.1. Introduction.....	64
II.1.1. Isoquinolines.....	64
II.1.1.1. Dynamic Kinetic Asymmetric Transformations.....	66
II.1.1.2. Desymmetrizations.....	72
II.1.1.3. Dynamic Kinetic Resolution.....	75

II.1.2. Quinolines.....	76
II.1.3. C-Carbonyl allylation via transfer hydrogenative coupling	80
II.2. Objectives.....	85
II.3. Results and discussion.....	87
II.3.1. Substrate design and synthesis.	87
II.3.2. Reaction conditions optimization.....	88
II.3.3. Reaction scope.....	93
II.3.4. Control experiments.....	101
II.3.5. Representative transformations.	103
II.4. Conclusions.....	105
II.5. Experimental section.....	106
II.5.1. General procedure for the synthesis of aldehydes 3a-x.	106
II.5.2. General procedure for the Ir-catalyzed asymmetric allylation of aldehydes 4a-x.....	115
II.5.3. Derivatization reactions.	140
III. Biocatalytic atroposelective synthesis of axially chiral N-arylindoles via Dynamic Kinetic Resolution.....	147
III.1. Introduction.....	147
III.1.1. C-N axial chirality.....	147
III.1.2. ADHs as catalyst.	162
III.1.3. Alternative systems.....	171
III.2. Objectives and substrate design.....	172
III.3. Results and discussion.	175
III.3.1. Synthesis of starting materials.	175
III.3.2. DKR of heterobiaryl aldehydes catalyzed by ketoreductases.	176
III.3.2.1. Screening of ketoreductases	176
III.3.3. Reaction scope.	179
III.3.4. Representative transformations.....	186
III.4. Racemization studies.	187
III.5. Conclusions.....	189
III.6. Experimental Section.....	190

III.6.1. General procedure for the synthesis of <i>N,N</i> -Dimethyl-2-(6-methyl-1 <i>H</i> -indol-1-yl)aniline. (16i).....	190
III.6.2. General procedure for the synthesis of 1-(2-(dimethylamino)phenyl)-1 <i>H</i> -indole-2-carbaldehydes. (17a-l).....	191
III.6.3. General procedure for the racemic reduction of 1-(2-(dimethylamino)phenyl)-1 <i>H</i> -indole-2-carbaldehydes. ((±)-18a-l).....	195
III.6.4. General procedure for the enantioselective bioreduction of heterobiaryl aldehydes 17a-l catalyzed by commercially available KREDs.	199
III.6.5. General procedure for the multimilligram bioreduction of heterobiaryl aldehydes 17a-l catalyzed by KREDs.....	200
III.6.6. Derivatization reactions of 18a.....	204
IV. Asymmetric synthesis of dibenzo[<i>b,d</i>]azepines by Cu-catalyzed reductive or borilative cyclization.	210
IV.1. Introduction.....	210
IV.1.1. Synthesis of dibenzoazepine derivatives. State-of-the-art.....	210
IV.1.2. Reductive hydroamination.	218
IV.2. Objectives.	223
IV.3. Results and discussion.	224
IV.3.1. Synthesis of starting materials.....	224
IV.3.2. Asymmetric intramolecular reductive cyclization.....	225
IV.3.2.1. Screening of ligands.	225
IV.3.2.1. Reaction scope.....	227
IV.3.2.3. Kinetic resolution.....	234
IV.3.3. Intramolecular borilative cyclization.	236
IV.3.3.1. Screening of ligands.	236
IV.3.3.2. Reaction scope.....	238
IV.3.4. Representative transformations.	239
IV.3.5. Mechanistic studies.....	241
IV.4. Conclusions.....	250
IV.5. Experimental Section.....	251
IV.5.1. Synthesis of starting materials.....	251
IV.5.1.1. General procedure for the synthesis of amine precursors.	251

IV.5.1.2. General procedure for the synthesis of aldimines substrates.	255
IV.5.2. General procedure for the synthesis of dibenzazepines by CuH-catalyzed intramolecular cyclization.....	266
IV.5.3. General procedure for the kinetic resolution of 25 followed by reduction of the remaining enantioenriched imine.....	280
IV.5.4. General procedure for the synthesis of borylated dibenzazepines 28 by Cu-catalyzed intramolecular borylative cyclization.....	282
IV.5.5. Representative transformations.....	286
APPENDIX I: Abbreviations.....	291
APPENDIX II: General Methods	295

Summary/Resumen

Summary

The main goal of this PhD thesis has been the development of catalytic asymmetric methodologies for the synthesis of axially chiral (hetero)biaryls through dynamization strategies. These methodologies comprise the use of both metal catalysis and biocatalysis *via* kinetic (Dynamic Kinetic Resolution, DKR, Chapter II and III) or thermodynamic control (Chapter IV). The obtained products present interesting structures with potential use as ligands for metal catalysis, precursors for bifunctional organocatalysis, and in biological applications.

In **Chapter I**, a summary of general considerations and contextualization of the research work developed are first reviewed. Moreover, the state-of-the-art of the main methodologies for the catalytic enantioselective synthesis of axially chiral (hetero)biaryls are also discussed. These approaches have been divided in two main sections: kinetic control (construction of the biaryl moiety, using prochiral or racemic heterobiaryls) and thermodynamic control (synthesis of seven to nine-membered bridged biaryls).

In **Chapter II**, a method for the synthesis of axially chiral heterobiaryls presenting central and axial chirality is described. A Lewis acid-base interaction between the carbonyl group from an aldehyde and the N from the quinoline moiety, allowed for the racemization (labilization) of the stereogenic axis in the substrates. In this case, the Lewis acid character is destroyed by an iridium-catalysed asymmetric transfer hydrogenative allylation, enabling the simultaneous generation of central and axial chiral elements, with good control of the diastereoselectivity and excellent enantioselectivities.

Along **Chapter III**, an enantioselective biocatalytic dynamic kinetic resolution (DKR) of configurationally labile *N*-arylidole aldehydes is reported. In this strategy, the racemization of the C-N stereogenic axis takes place through a Lewis pair

interaction between the NMe_2 and the aldehyde groups. The DKR proceed by an atroposelective bioreduction of the carbonyl group using commercial ketoreductases (KREDs). The corresponding axially chiral *N*-arylidole aminoalcohols are thus obtained with high conversions and optical purity, under very mild reaction conditions.

Finally, in **Chapter IV**, a copper-catalyzed asymmetric intramolecular reductive and borylative cyclization for the synthesis of dibenzo[*b,d*]azepine derivatives is described. In this strategy, 7-membered bridged biarylamine containing both central and axial stereogenic elements were synthesized, with excellent control of diastereo-, and enantioselectivities.

Resumen

El objetivo principal de esta Tesis Doctoral ha sido el desarrollo de metodologías de catálisis asimétrica para la síntesis de (hetero)biarilos con quiralidad axial, a través de estrategias de dinamización. Estas metodologías incluyen el uso de catálisis metálica y biocatálisis a través de control cinético (DKR, por sus siglas en inglés Dynamic Kinetic Resolution) o control termodinámico (biarilos- puente). Los productos obtenidos presentan estructuras interesantes con usos potenciales como ligandos para catálisis metálica, precursores de organocatalizadores bifuncionales y moléculas con actividad biológica.

En el **Capítulo I**, se incluyen unas consideraciones generales y se contextualiza el trabajo. Además, se ha llevado a cabo una revisión de las metodologías principales para la obtención de (hetero)biarilos con quiralidad axial a través de catálisis enantioselectiva. Estas metodologías se han dividido en dos apartados principales: control cinético (construcción del fragmento de biarilo, o uso de biarilos racémicos o proquirales como sustratos) o control termodinámico (síntesis de biarilos tipo puente, con ciclos de siete, ocho y nueve miembros).

En el **Capítulo II**, se describe un método para la síntesis de heterobiarilos con quiralidad axial y central basado en DKR. La interacción ácido-base de Lewis entre el

carbonilo del grupo aldehído y el N de la quinolina, es la responsable de la labilización del eje. En este caso, una reacción asimétrica de alilación hydrogenativa por transferencia de hidrógeno catalizada por iridio permite la generación simultánea de elementos de quiralidad central y axial, con buen control de la diastereoselectividad y excelente control de la enantioselectividad, bajo condiciones de reacción suaves.

A lo largo del **Capítulo III**, se describe una resolución cinética dinámica (DKR) enantioselectiva mediante reducción biocatalítica de *N*-arilindol-2-carbaldehídos configuracionalmente lábiles. En esta estrategia, la racemización del eje estereogénico C-N tiene lugar a través de una interacción de pares de Lewis entre el NMe₂ y el grupo aldehído. La DKR se lleva a cabo a través de una bio-reducción atroposelectiva del grupo carbonilo, utilizando ketoreductasas comerciales (KREDs), dando lugar a los correspondientes *N*-arilindoles aminoalcoholes con quiralidad axial, con elevados rendimientos y purezas ópticas.

Por último, en el **Capítulo IV**, se describe una ciclación asimétrica intramolecular reductora o borilativa catalizada por cobre, para la síntesis de dibenzo[*b,d*]acepinas. En esta estrategia, se sintetizaron biarilaminas cíclicas de 7 miembros con quiralidad central y axial, con un control excelente de la diastereo- y la enantioselectividad.

CHAPTER I

Introduction.

I. Introduction.

I.1. Asymmetric catalysis.

The properties of organic molecules are closely related to their shape, which is influenced by the three-dimensional orientation of the substituents in stereocenters, planes or axis.¹ For the former, chirality refers to molecules containing sp^3 -hybridized stereocenters that cannot be superimposed on its mirror image. Therefore, the pair of those mirror images are two different molecules, called enantiomers, that can be isolated.²

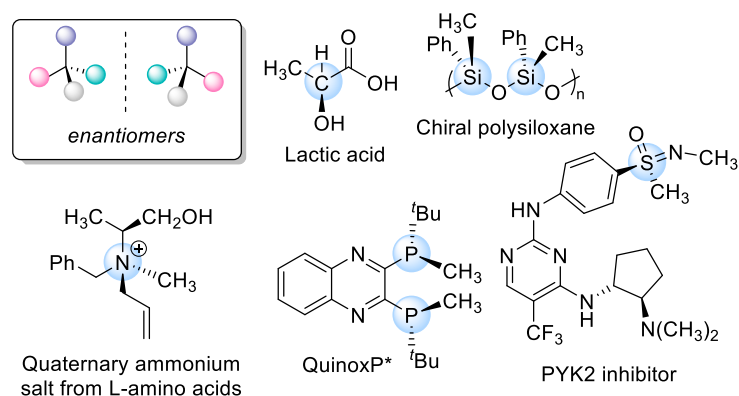


Figure 1: examples of stereogenic centers.

¹ K. W. Quasdorf, L. E. Overman, *Nature* **2014**, 516, 181–191.

² C. Wolf, (2007) *Principles of Chirality and Dynamic Stereochemistry*. In *Dynamic Stereochemistry of Chiral Compounds*, C. Wolf (Ed.); The Royal Society of Chemistry: Cambridge, pp. 6-29.

The most common and well-known stereocenter is a tetrahedral carbon bearing four different substituents, but other heteroatoms such as nitrogen,³ sulphur,⁴ silicon⁵ or phosphorous⁶ can also be a stereogenic center (**figure 1**).

Although central chirality is the most reported, other forms such as axial chirality (allenes⁷ and *ortho*-substituted biaryls,⁸ **figure 2A**), spiro chirality⁹ (**figure 2B**), helical chirality¹⁰ (**figure 2C**) and planar chirality¹¹ (**figure 2D**) have attracted increased interest over the years.

³ H.-F. Wua, W.-B. Lin, L.-Z. Xia, Y.-G. Luo, X.-Z. Chen, G.-Y. Li, G.-L. Zhang, X.-F. Pan, *Helv. Chim. Acta* **2009**, *92*, 677–688.

⁴ a) B. M. Trost, M. Rao, *Angew. Chem. Int. Ed.* **2015**, *54*, 5026–5043. b) S. Otocka, M. Kwiatkowska, L. Madalinska, P. Kiełbasinski, *Chem. Rev.* **2017**, *117*, 4147–4181.

⁵ a) J. Chen, Y. Cao, Y. *Macromol. Rapid Commun.* **2007**, *28*, 1714–1742. b) M. Oishi, Y. Kawakami, *Macromolecules* **2000**, *33*, 1960–1963.

⁶ D. A. Dirocco, Y. Ji, E. C. Sherer, A. Klapars, M. Reibarkh, J. Dropinski, R. Mathew, P. Maligres, A. M. Hyde, J. Limanto, A. Brunskill, R. T. Ruck, L.-C. Campeau, I. W. Davies, *Science* **2017**, *356*, 426–430.

⁷ For reviews on axially chiral allenes, see: a) X. Wang, X. Chen, W. Lin, P. Li, W. Li, *Adv. Synth. Catal.* **2022**, *364*, 1212–12. b) W. Xiao, J. Wu, *Org. Chem. Front.* **2022**, *9*, 5053–5073.

⁸ For reviews on axially chiral biaryls, see: a) G. Bringmann, A. J. P. Mortimer, P. A. Keller, M. J. Gresser, J. Garner, M. Breuning, *Angew. Chem. Int. Ed.* **2005**, *44*, 5384–5427. b) J. A. Carmona, C. Rodríguez-Franco, R. Fernández, V. Hornillos, J. M. Lassaletta, *Chem. Soc. Rev.* **2021**, *50*, 2968–2983. c) J. M. Lassaletta, *Atropisomerism and axial chirality*. **2019**, Ed. World Scientific Publishing Europe Limited. For a review on atropisomeric compounds with an N-C chiral axis, see: d) P. Rodríguez-Salamanca, R. Fernández, V. Hornillos, J. M. Lassaletta, *Chem. Eur. J.* **2022**, *28*, e2021044.

⁹ For reviews on chiral spirocycles see: a) A. K. Franz, N. V. Hanhan, N. R. Ball-Jones, *ACS Catal.* **2013**, *3*, 4, 540–553. b) L. K. Smith, I. R. Baxendale, *Org. Biomol. Chem.* **2015**, *13*, 9907–9933. c) P.-W. Xu, J.-S. Yu, C. Chen, Z.-Y. Cao, F. Zhou, J. Zhou, *ACS Catal.* **2019**, *9*, 3, 1820–1882.

¹⁰ For reviews on helical chiral compounds, see: a) M. Gingras, *Chem. Soc. Rev.* **2013**, *42*, 968–1006. b) M. Gingras, G. Félix, R. Peresutti, *Chem. Soc. Rev.* **2013**, *42*, 1007–1050. c) M. Gingras, *Chem. Soc. Rev.* **2013**, *42*, 1051–1095. d) M. J. Narcis, N. Takenaka, *Eur. J. Org. Chem.* **2014**, *1*, 21–34.

¹¹ For reviews on planar chiral compounds, see: a) S. E. Gibson, J. D. Knight, *Org. Biomol. Chem.* **2003**, *1*, 1256–1269. b) G. C. Fu, *Acc. Chem. Res.* **2006**, *39*, 853–860. c) D. Schaarschmidt, H. Lang, *Organometallics* **2013**, *32*, 5668–5704. d) N. A. Butt, D. Liu, W. Zhang, *Synlett* **2014**, *25*, 615–630. e) S. Arae, M. Ogasawara, *Tetrahedron Lett.* **2015**, *56*, 1751–1761.

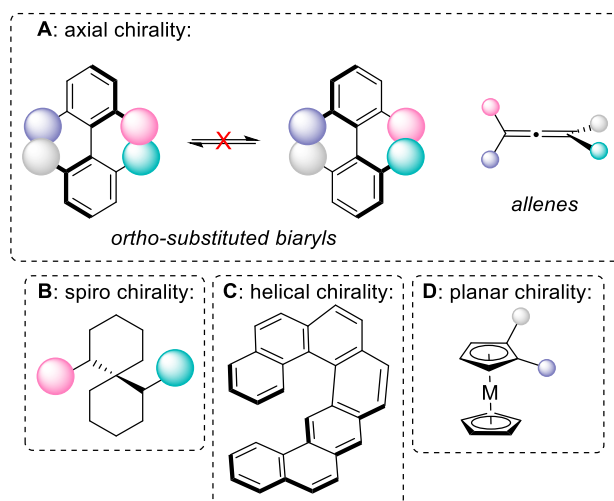


Figure 2: types of chirality.

Chiral molecules are especially relevant for drug discovery, as enantiomers often have different biological activity in the target of interest.¹² It is well-known the case of thalidomide,¹³ whose enantiomers presented different effects in humans, being one of them responsible of teratogenic deformities.

Therefore, efficient synthetic methods to afford enantioenriched complex molecules from available substrates are necessary.

For many years, chiral pool strategies have been the only source for the synthesis of enantiomerically pure compounds, based on the use of optically pure starting materials (*e.g.*, amino acids or sugars); however, the need of stoichiometric amounts of these enantiopure reagents and the lack of the desired configuration in the natural source makes this strategy less desirable.

¹² a) M. Eichelbaum, A. S. Gross, *Adv. Drug Res.* **1996**, *28*, 1–64. b) R. R. Shah, J. M. Midgley, S. K. Branch, *Adverse Drug React. Toxicol. Rev.* **1998**, *17*, 145–90.

¹³ T. Eriksson, S. Bjorkman, B. Roth, A. Fyge, P. Hoglund, *Chirality* **1995**, *7*, 44–52.

On the other hand, resolution of racemic mixtures, which emerged as an interesting alternative approach, only afforded a maximum of 50% yield after separation of the diastereomers.¹⁴

The third approach for the construction of chiral elements from achiral or racemic substrates is asymmetric catalysis, which is very potent and applicable because it only requires sub-stoichiometric amounts of the catalyst to induce chirality in the final products, resulting in atom-efficient processes.¹⁵ Depending on the nature of the catalyst, different strategies could be performed:

A) Organometallic catalysis:¹⁶ most of these reactions involve a transition metal bearing coordinated chiral organic ligands, responsible of the asymmetric induction.

B) Organocatalysis:¹⁷ based on the use of chiral small organic molecules as a catalyst, where an inorganic element is not part of the active principle. There are essentially four types of organocatalysts: Lewis bases, Lewis acids, Brønsted bases, and Brønsted acids.

C) Biocatalysis:¹⁸ based on the ability of enzymes (proteins that can catalyse an organic transformation) to differentiate between pro-*R* and pro-*S* faces in prochiral compounds. These systems present less environmental impact in terms of energy, raw materials, and waste production.

The aim of this PhD thesis is to develop novel catalytic and stereoselective synthetic procedures for the generation of axially chiral compounds. As a result, the

¹⁴ a) K. C. Nicolau, J. S. Chen, (2011). *Classics in Total Synthesis III*; K. C. Nicolau, S. A. Snyder, Eds.; Wiley-VCH: Weinheim. b) N. G. Anderson, *Org. Process Res. Dev.* **2006**, *10*, 3, 683–684. c) C. Kaya, K. Birgül, B. Bülbül, *Chirality* **2022**, 1–25, doi 10.1002/chir.23512.

¹⁵ a) R. A. Sheldon, *Pure Appl. Chem.* **2000**, *72*, 1233–1246. b) B. M. Trost, *Science*, **1999**, *254*, 1471, 1471–1477.

¹⁶ K. W. Quasorf, L. E. Overman, *Nature* **2014**, *516*, 181–191.

¹⁷ B. List, *Chem. Rev.* **2007**, *107*, 12, 5413–5415.

¹⁸ G. de Gonzalo, I. Lavandera, (2021). *Biocatalysis for Practitioners: Techniques, Reactions and Applications* (1st Ed.), Weinheim. Alemania. Wiley-Vch.

characteristics and generation of this type of chirality will be thoroughly discussed in the following sections.

I.2. Axial chirality: atropisomerism.

Axially chiral biaryls, also known as atropisomers, are the most recognized class of compounds featuring axial chirality.⁸ They comprise conformers with restricted rotation around a single bond that allow their isolation in a stable form at room temperature. The configurational stability of these compounds depends on their rotational energy barrier and is generally determined by the number and size of substituents at the *ortho*, *ortho'* positions relative to the stereogenic axis (2,2' and 6,6' in typical 6-membered biaryls). The presence of larger substituents led to higher energy barriers and thus more configurationally stable products.

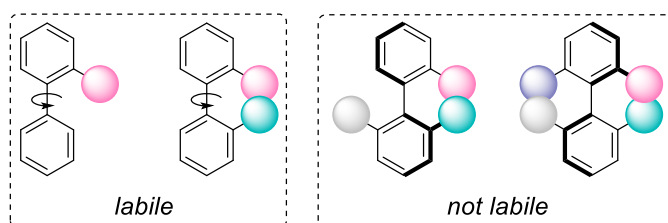


Figure 3: stability of axially chiral biaryls regarding the number of substituents.

The first example of isolation of molecules with restricted axial rotation was described by Christie and Kenner in 1922, using brucine as resolution agent for the separation of both atropisomers of 6,6'-dinitro-2,2'-diphenic acid after fractional recrystallization (**figure 4**).¹⁹ This first example established the groundwork for an emerging research area.

¹⁹ G. H. Christie and J. Kenner, *J. Chem. Soc., Trans.* **1922**, 121, 614–620.

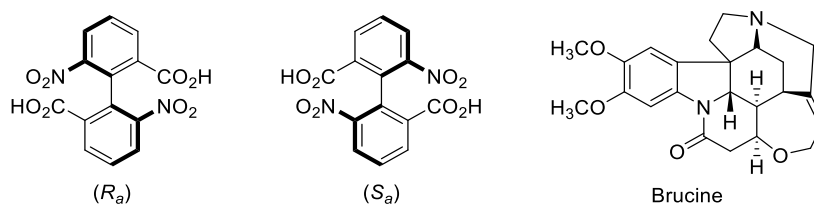


Figure 4: first resolution of atropisomers by Christie and Kenner.

The interconversion of atropisomers is related to time and temperature factors (kinetics) and is an important feature for its characterization. In this regard, Oki proposed that atropisomers should have a half-life time of racemization ($t_{1/2}$) of at least 1000 s^{-1} at room temperature ($22.3 \text{ kJ}\cdot\text{mol}^{-1}$ at 300 K) to allow its isolation.²⁰ On the other hand, LaPlane and Edwards²¹ divided the atropisomeric compounds into three groups based on their rotational energy barriers (class 1, $\Delta E_{\text{rot}} < 20 \text{ kcal}\cdot\text{mol}^{-1}$; class 2 $\Delta E_{\text{rot}} < 20\text{-}30 \text{ kcal}\cdot\text{mol}^{-1}$ and class 3 $\Delta E_{\text{rot}} > 30 \text{ kcal}\cdot\text{mol}^{-1}$); only class 3 atropisomers were found to be kinetically isolable.

On the other hand, in systems with only two substituents at the *ortho*-positions, rotation is not hindered at room temperature, unless the *ortho*-substituents are tethered by bridging atoms (**figure 5**).²² The configurational stability, in this case, is associated with temperature variation, ring size and the presence of substituents. Moreover, the presence of a stereogenic centre in the bridging cycle increases the rigidity and imposes a particular conformation/configuration of the biaryl axis, due to a central-to-axial chirality relay effect.²³

²⁰ M. Oki, *Recent advances in atropisomerism. Topics in stereochemistry* **1983**, *14*, 1-81.

²¹ a) S. R. LaPlane, P. J. Edwards, L. D. Fader, A. Jakalian, O. Hucke, *ChemMedChem* **2011**, *6*, 505–513. b) S. R. LaPlane, L. D. Fader, K. R. Fandrik, D. R. Fandrik, O. Hucke, R. Kemper, S. P. F. Miller, P. J. Edwards, *J. Med. Chem.* **2011**, *54*, 20, 7005–7022.

²² G. Bringmann, A. J. P. Mortimer, P. A. Keller, M. J. Gresser, J. Garner, M. Breuning, *Angew. Chem. Int. Ed.* **2005**, *44*, 5384–5427.

²³ N. Kotwal, Tamanna, P. Chauhan, *Chem. Commun.* **2022**, *58*, 11031–11044.

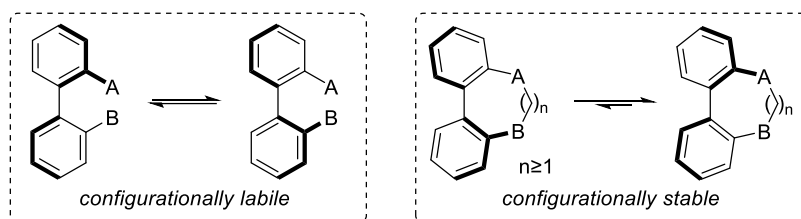


Figure 5: configurational stability of bridged biaryls.

Natural products and bioactive compounds bearing axial chirality are common and diverse. There are many examples of this class of compounds, such as the antibiotic heptapeptide Vancomycin containing three types of stereoelements;²⁴ Knipholone, that presents antimalaria and antitumor activities;²⁵ and Mastigophorene A that has been found to stimulate nerve growth.²⁶ Moreover, asymmetric organometallic catalysis and organocatalysis have been completely transformed by the use of atropisomeric molecules such as ligands and as organocatalyst. Numerous synthetic processes have been reported because of the use of these chiral biaryl scaffolds. Moreover, a family of non-biaryl atropisomers that have attracted considerable attention in recent years comprises those with restricted rotation around a C(sp²)-N(sp²) axis (**figure 6**).^{8d}

²⁴ B. K. Hubbard, C. T. Walsh, *Angew. Chem.* **2003**, *115*, 752–789; *Angew. Chem. Int. Ed.* **2003**, *42*, 730–765.

²⁵ E. Dagne, W. Steglich, *Phytochemistry* **1984**, *23*, 1729–1731.

²⁶ Y. Fukuyama, Y. Asakawa, *J. Chem. Soc. Perkin Trans. 1* **1991**, 2737–2741.

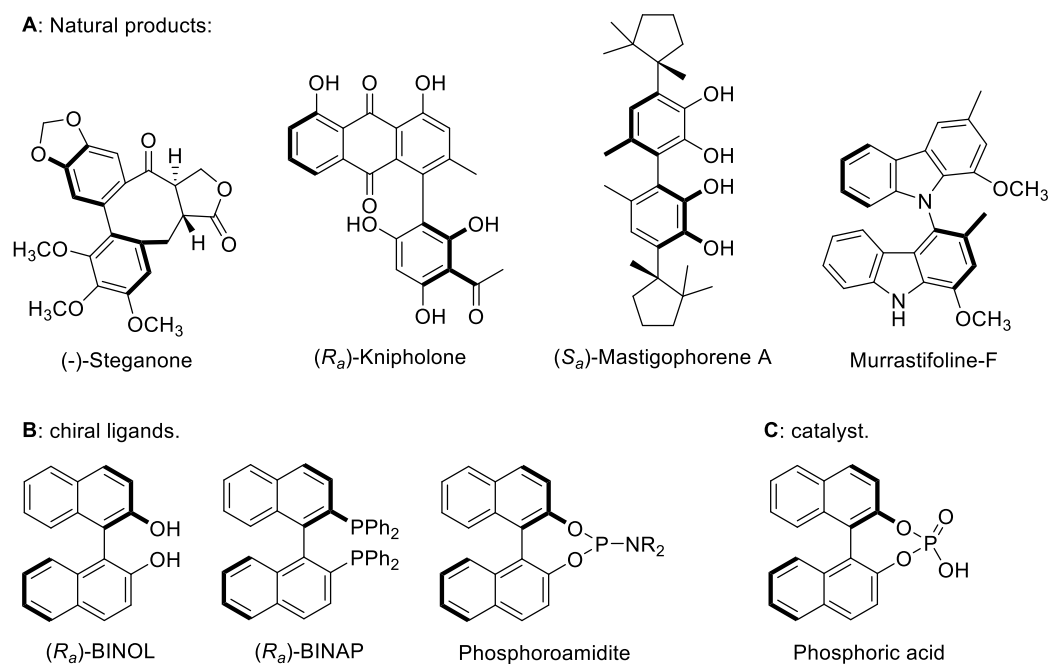


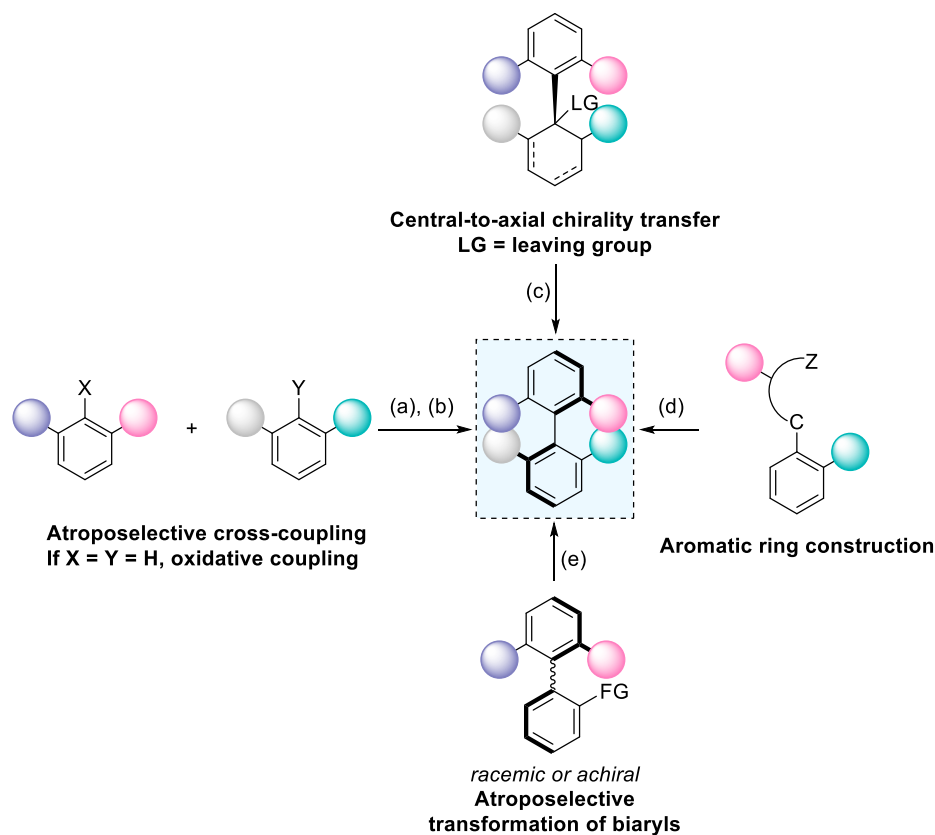
Figure 6: representative examples of natural products, ligands and organocatalyst axially chiral.

I.3 Atroposelective synthesis of (hetero)biaryls by kinetic control.

Synthetic methodologies for the construction of axially chiral (hetero)biaryls has experienced an impressive growth over the last three decades.^{8d} However, new approaches providing access to novel structures are still desirable, due to the unique characteristics of this kind of chiral compounds that present applications for nearly every discipline in which chirality plays an important role.

The atroposelective synthesis of axially chiral (hetero)biaryl derivatives can be divided in five main approaches (**scheme 1**). The most straightforward strategy consists of an asymmetric cross coupling to build the stereogenic axis (a). A related approach is based on oxidative cross-couplings, a challenging methodology that does not require prefunctionalization of the coupling partners (b). The third method involve central-to-axial chirality transfer process, where the axial chirality is formed through the loss of a stereocenter, whose stereochemical information is transmitted to the axis (c). The fourth method is the aromatic ring-construction *via* cycloaddition

or cyclization reactions (d). Finally, the last strategy comprises methods that employ pre-existing (hetero)biaryl atropisomers as substrates (e).



Scheme 1: main methodologies for the catalytic enantioselective synthesis of axially chiral (hetero)biaryls.

I.3.1. Stereoselective formation of the stereogenic axis.

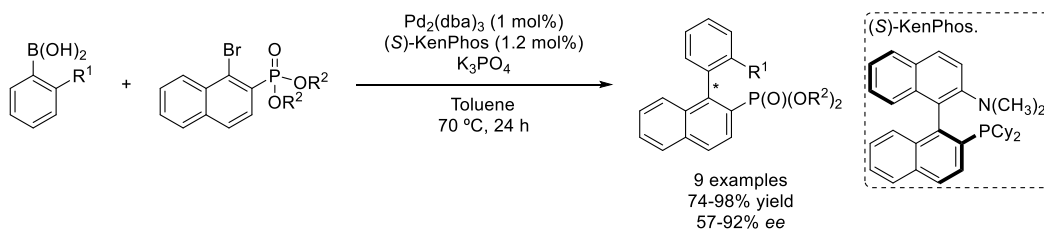
A. Stereoselective formation of the stereogenic axis *via* metal-catalyzed cross-coupling reactions.

The stereoselective formation of aryl-aryl bonds *via* metal-catalyzed cross-coupling reactions is one of the most useful methods to construct biaryl compounds. Moreover, the use of bench stable coupling partners made this reaction very appealing.

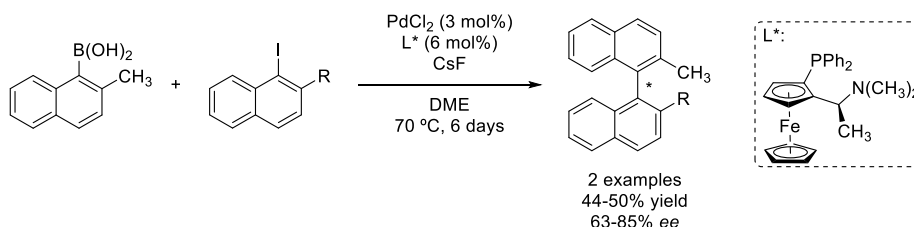
The first enantioselective example of this class was reported by Kumada²⁷ in 1975, using *ortho*-substituted aryl Grignard reagents with aryl halides, in presence of a nickel-phosphine complex. The reaction was later improved by Hayashi and Ito²⁸ using a monodentate ferrocenyl phosphine ligand, obtaining enantioselectivities up to 95% ee. Due to the sensitivity of hard organometallic reagents to air and moisture, as well as their limited functional group tolerance, the atroposelective Suzuki-Miyaura reaction represents a more appealing alternative.

The groups of Buchwald²⁹ (**scheme 2A**) and Cammidge³⁰ (**scheme 2B**) described simultaneously the asymmetric synthesis of biaryl phosphonates and binaphthalenes using (*S*)-KenPhos and a ferrocene-derived phosphine as a chiral ligand, respectively, affording moderate to good enantioselectivities, although with limited substrate scope.

A: Buchwald, 2000:



B: Cammidge, 2000:



Scheme 2: first examples of asymmetric Suzuki-Miyaura coupling.

²⁷ K. Tamao, A. Minato, N. Miyake, T. Matsuda, Y. Kiso, M. Kumada, *Chem. Lett.* **1975**, 4, 133–136.

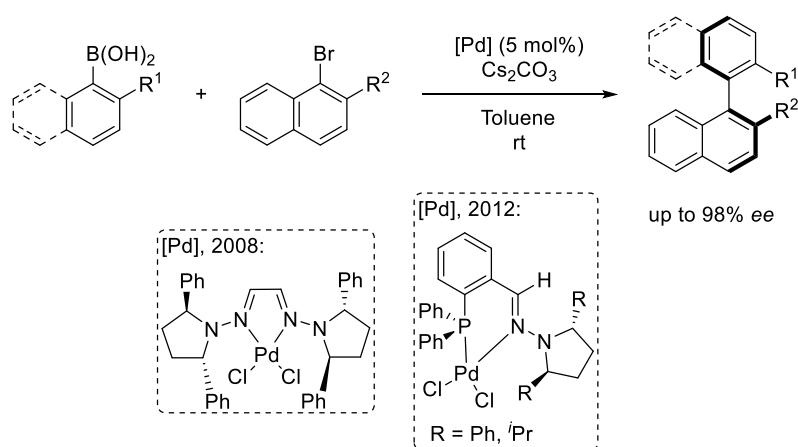
²⁸ T. Hayashi, K. Hayashizaki, T. Kiyoi, Y. Ito, *J. Am. Chem. Soc.* **1988**, 110, 8153–8156.

²⁹ J. Yin, S. L. Buchwald, *J. Am. Chem. Soc.* **2000**, 122, 12051–12052.

³⁰ A. N. Cammidge, K. V. L. Crépy, *Chem. Commun.* **2000**, 1723–1724.

Since these seminal examples, different atroposelective methods have been reported based on Suzuki-Miyaura cross coupling, employing several directing groups.³¹

In 2008, our research group reported an atroposelective Suzuki-Miyaura cross coupling using chiral bis-hydrazones as phosphine-free ligands (**scheme 3**).³² Excellent enantioselectivities (>98% *ee*) under very mild conditions (room temperature) were obtained for a variety of functionalized and nonfunctionalized systems. However, one week reaction time was required. The reaction time could be further decrease to 6-72 h using a phosphino hydrazone as a chiral ligand,³³ although at expenses of enantioselectivities (38-83% *ee*).



Scheme 3: asymmetric Suzuki-Miyaura cross-coupling using C₂-symmetric bis-hydrazones (2008) or phosphino hydrazones (2012) as ligands.

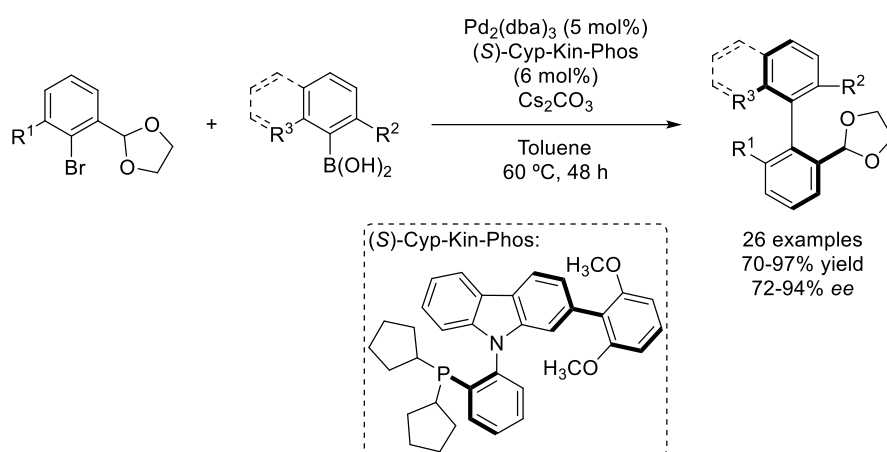
Only few literature procedures have demonstrated their efficiency in enantioselective Suzuki-Miyaura couplings for the synthesis of axially chiral tetra-

³¹ For recent revision, see: a) O. Baudoin, *Eur. J. Org. Chem.* **2005**, *2005*, 4223–4229. b) D. Zhang, Q. Wang, *Coord. Chem. Rev.* **2015**, *286*, 1–16. c) C. Li, D. Chen, W. Tang, *Synlett* **2016**, *27*, 2183–2200. d) F. W. Goetzke, L. V. Dijk, S. P. Fletcher, *PATAI'S Chemistry of Functional Groups*; American Cancer Society, **2019**; 1–54. e) G. Hedouin, S. Hazra, F. Gallou, S. Handa, *ACS Catal.* **2022**, *12*, 4918–4937.

³² A. Bermejo, A. Ros, R. Fernández, J. M. Lassaletta, *J. Am. Chem. Soc.* **2008**, *130*, 47, 15798–15799.

³³ A. Ros, B. Estepa, A. Bermejo, E. Álvarez, R. Fernández, J. M. Lassaletta, *J. Org. Chem.* **2012**, *77*, 4740–4750.

ortho-substituted biaryls.³⁴ Very recently, Gan *et al.* developed a novel class of atropisomeric phosphine ligands bearing C-N axial chirality that resulted very useful for the assembly of steric hindered tetra-*ortho*-substituted biaryls *via* this method (**scheme 4**).³⁵ The approach was based on the two distinctive modes of coordination of the ligand to the metal center (Pd-N and Pd- π), which offered relief for accepting highly steric bulky substrates. Excellent functional group tolerance was observed under the optimized reaction condition. Moreover, a one-pot Miyaura borylation followed by the enantioselective Suzuki coupling could be performed, while maintaining similar yields and enantioselectivities.



Scheme 4: enantioselective Suzuki-Miyaura cross-coupling using a novel atropisomeric C-N ligand.

B. Asymmetric oxidative coupling of two arenes.

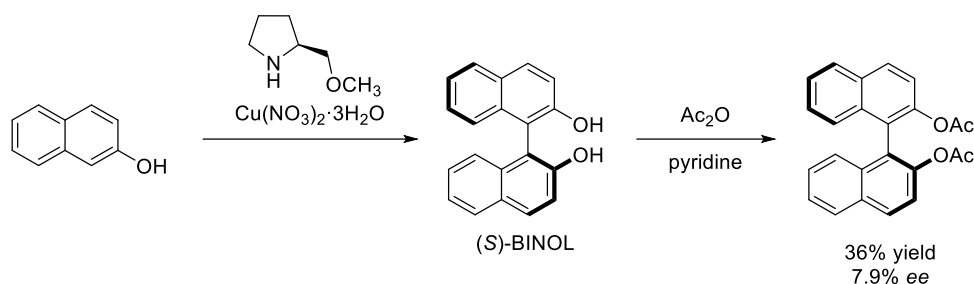
Among the different methodologies for the asymmetric synthesis of axially chiral biaryls, the asymmetric oxidative coupling of two arene moieties without prior functionalization represents the most straightforward and atom-economical method through the net transformation of two C-H bonds into a C-C bond. It has been

³⁴ For selected examples, see: a) M. Genov, A. Almorín, P. Espinet, *Chem. Eur. J.* **2006**, *12*, 9346–9352. b) Y. Uozumi, T. Matsuura, T. Arakawa, Y. M. Yamada, *Angew. Chem., Int. Ed.* **2009**, *48*, 2708–2710. c) D. Shen, Y. Xu, S.-L. Shi, *J. Am. Chem. Soc.* **2019**, *141*, 37, 14938–14945. d) H. Yang, J. Sun, W. Gu, W. Tang, *J. Am. Chem. Soc.* **2020**, *142*, 17, 8036–8043.

³⁵ K. B. Gan, R.-L. Zhong, Z.-W. Zhang, F. Y. Kwong, *J. Am. Chem. Soc.* **2022**, *144*, 14864–14873.

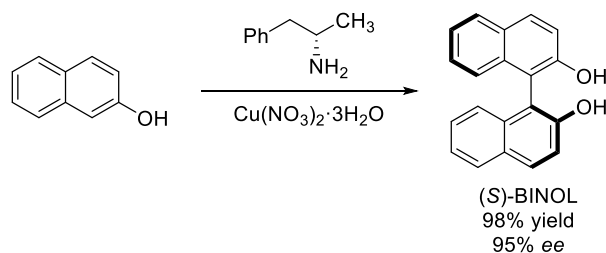
demonstrated that a range of catalytic systems, including transition metal complexes and organocatalysts, can facilitate this type of reaction.³⁶

The first example of asymmetric oxidative coupling was reported in 1978 by Feringa and Wynberg.³⁷ They obtained BINOL, although in very modest enantiomeric excess (up to 7.9% *ee*), through the dimerization of 2-naphthol in presence of stoichiometric amounts of a chiral cupric-amine complex (**scheme 5**).



Scheme 5: syntheses of axially chiral BINOL using a chiral cupric-amine complex.

A few years later, Brussee and co-workers reported the highly enantioselective synthesis of axially chiral BINOL (95% *ee*) using stoichiometric amounts of an (*S*)-amphetamine-copper (II) complex (**scheme 6**).³⁸



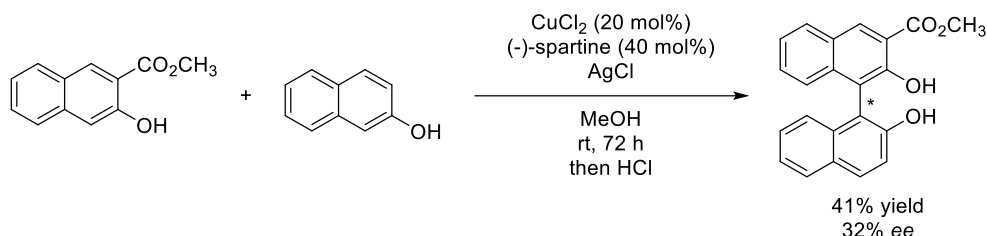
Scheme 6: syntheses of axially chiral binaphthol compounds with chiral copper-amine complexes.

³⁶ C. Zheng, S.-L. You, (2015). *Asymmetric Oxidative Biaryl Coupling Reactions*, RSC Catalysis Ser., ch. 3, vol. 25, pp. 92–125.

³⁷ B. Feringa, H. Wynberg, *Bioorg. Chem.* **1978**, *7*, 397–408.

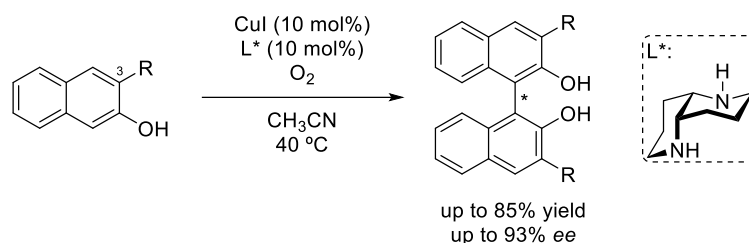
³⁸ a) J. Brussee, A. C. A. Jansen, *Tetrahedron Lett.* **1983**, *24*, 3261–3262; b) J. Brussee, J. L. G. Groenendijk, J. M. te Koppele, A. C. A. Jansen, *Tetrahedron* **1985**, *41*, 3313–3319.

The first catalytic oxidative coupling was described by Kocovsky and co-workers,³⁹ using a mixture of copper(II) chloride and (-)-spartine as ligand, although only a disappointingly 41% yield and 32% *ee* was obtained for a BINOL derivative (**scheme 7**).



Scheme 7: copper-catalyzed oxidative coupling described by Kocovsky.

In 2001, a highly successful catalytic oxidative cross-coupling was reported by Kozlowski and co-workers,⁴⁰ using a C_2 -symmetric (*S,S*)-1,5-diazadecalin as ligand and O_2 as the stoichiometric oxidant, in the presence of CuI (**scheme 8**). The homocoupling of different 2-naphthol derivatives proceeded in good yields with up to 93% *ee*. Importantly, it was found that a coordinating substituent at C3 was crucial to obtain good enantioselectivities.



Scheme 8: first catalytic oxidative coupling described by Kozlowski.

Over the years, numerous examples of asymmetric oxidative couplings for the synthesis of axially chiral biaryl derivatives has been described, using catalytic

³⁹ M. Smrcina, J. Polakova, S. Vyskocil, P. Kocovsky, *J. Org. Chem.* **1993**, *58*, 17, 4534–4538.

⁴⁰ X. Li, J. Yang, M. C. Kozlowski, *Org. Lett.* **2001**, *3*, 8, 1137–1140.

amounts of transition metal complexes, such as copper,⁴¹ vanadium,⁴² ruthenium⁴³ and iron,⁴⁴ as well as organocatalysts.⁴⁵ However, these methodologies still struggle with substrate scope limitations, since most of the reported examples required of 2-naphthol derivatives for the success of the reaction.

Recently, Tan and co-workers reported a novel redox neutral cross-coupling strategy for the synthesis of axially chiral NOBIN and BINAM derivatives,⁴⁶ *via* cross-coupling of 2-naphthols or 2-naphthylamines with azonaphthalene derivatives. Two complementary systems were described, employing either a chiral phosphoric acid-Ca salt combined with $\text{Zn}(\text{BAR}^{\text{F}})_2(\text{CH}_3\text{CN})_6$ complex or a $\text{Ni}(\text{OTf})_2$ /chiral bis(oxazoline) complex (**scheme 9**). Good yields and enantioselectivities were obtained for a wide variety of non- C_2 -symmetrical biaryls. Moreover, the use of the Ni/BOX complex system improved the synthesis of several NOBIN derivatives, and also allowed to explore new substrate classes.

⁴¹ For selected examples, see: a) X. Li, B. Hewgley, C. A. Mulrooney, J. Yang, M. C. Kozlowski, *J. Org. Chem.* **2003**, *68*, 14, 5500–5511. b) K. H. Kim, D.-W. Lee, Y.-S. Lee, D.-H. Ko, D.-C. Ha, *Tetrahedron* **2004**, *60*, 9037–9042. c) S. K. Alamsetti, E. Poonguzhali, D. Ganapathy, G. Sekar, *Adv. Synth. Catal.* **2013**, *355*, 2803–2808.

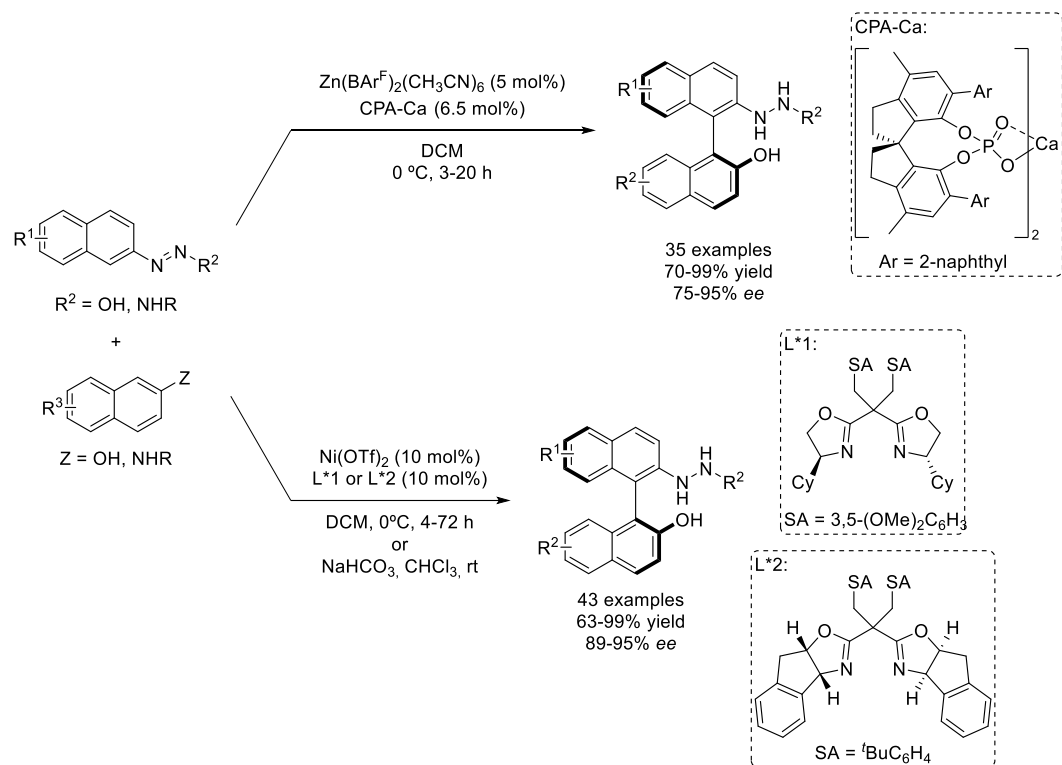
⁴² For selected examples, see: a) D.-R. Hwang, C.-P. Chen, B.-J. Uang, *Chem. Commun.* **1999**, 1207–1208. b) S.-W. Hon, C.-H. Li, J.-H. Kuo, N. B. Barhate, Y.-H. Liu, Y. Wang, C.-T. Chen, *Org. Lett.* **2001**, *3*, 6, 869–872. c) S. Takizawa, J. Koderu, Y. Yoshida, M. Sako, S. Breukers, D. Enders, H. Sasai, *Tetrahedron* **2014**, *70*, 1786–1793.

⁴³ For selected examples, see: a) T. Hamada, H. Ishida, S. Usui, Y. Watanabe, K. Tsumura, K. Ohkubo, *J. Chem. Soc., Chem. Commun.*, **1993**, 909–911. b) R. Irie, K. Masutani and T. Katsuki, *Synlett* **2000**, 1433–1436.

⁴⁴ For selected examples, see: a) H. Egami, T. Katsuki, *J. Am. Chem. Soc.* **2009**, *131*, 17, 6082–6083. b) K. Matsumoto, H. Egami, T. Oguma, T. Katsuki, *Chem. Commun.* **2012**, 48, 5823–5825.

⁴⁵ For selected examples, see: a) G.-Q. Li, H. Gao, C. Keene, M. Devonas, D. H. Ess, L. Kürti, *J. Am. Chem. Soc.* **2013**, *135*, 20, 7414–7417. b) C. K. De, F. Pescioli, B. List, *Angew. Chem., Int. Ed.* **2013**, *52*, 9293–9295.

⁴⁶ L.-W. Qi, S. Li, S.-H. Xiang, J. Wang, B. Tan, *Nature Catalysis* **2019**, *2*, 314–323.



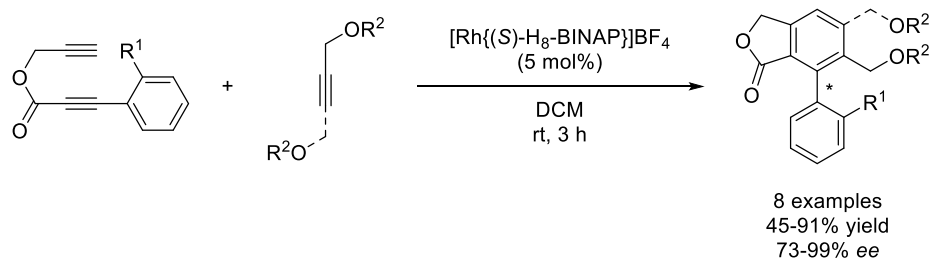
Scheme 9: redox neutral cross-coupling of hydroxyarenes and azonaphthalenes.

C. Asymmetric biaryl synthesis by *de novo* construction of an aromatic ring.

An alternative approach for the atroposelective synthesis of biaryls consist of *de novo* construction of an aromatic ring.

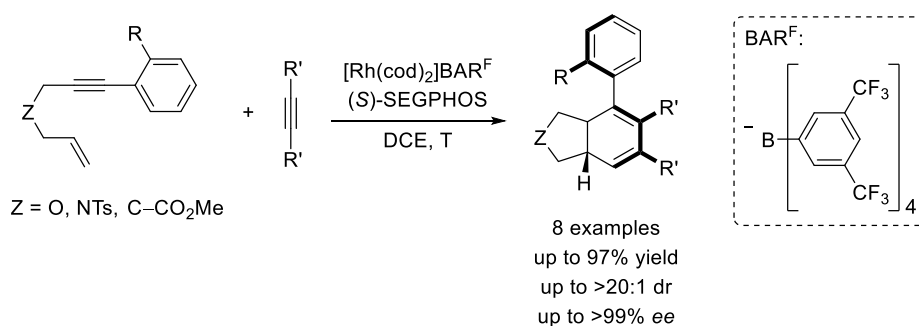
One of the first examples was reported by Tanaka and co-workers. Authors described the enantioselective synthesis of axially chiral phthalides by a cationic $[\text{Rh(I)}(\text{H}_8\text{-BINAP})]$ complex (**scheme 10**).⁴⁷ Good yields and good to excellent enantioselectivities were obtained under mild reaction conditions, using unsymmetrical 1,6-diynes and both terminal and internal alkynes.

⁴⁷ K. Tanaka, G. Nishida, A. Wada, K. Noguchi, *Angew. Chem. Int. Ed.* **2004**, *43*, 6510–6512.



Scheme 10: atroposelective synthesis of phthalides *via* Rh-catalyzed cross alkyne cyclotrimerization.

Moreover, the group of Shibata described the first examples of transition metal-catalyzed cycloaddition reactions for the generation of both central and axial chirality (**scheme 11**).⁴⁸ Through an efficient Rh-catalysed intermolecular [2+2+2] cycloaddition, bicyclic cyclohexa-1,3-dienes were obtained with excellent enantio- and diastereoselectivities.



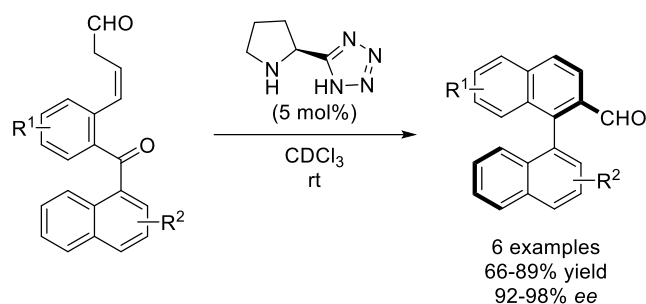
Scheme 11: [2+2+2] cycloaddition for the construction of central and axial chirality catalyzed by Rh.

On the other hand, Link and Sparr developed an organocatalytic arene-forming aldol reaction for the atroposelective synthesis of tri-*ortho*-substituted biaryls.⁴⁹ This methodology involves the formation of an aromatic ring during the dehydration step of the aldol condensation cascade, leading to enantioenriched binaphthyl substrates, in high enantioselectivity and very good functional group tolerance (**scheme 12**). Recently, this research group applied the same catalytic system for the synthesis of atropisomers with up to four stereogenic axes.⁵⁰

⁴⁸ T. Shibata, M. Otomo, Y. Tahara, K. Endo, *Org. Biomol. Chem.* **2008**, *6*, 4296–4298.

⁴⁹ A. Link, C. Sparr, *Angew. Chem. Int. Ed.* **2014**, *53*, 5458–5461.

⁵⁰ D. Lotter, A. Castrogiovanni, M. Neuburger, C. Sparr, *ACS Cent. Sci.* **2018**, *4*, 5, 656–660.



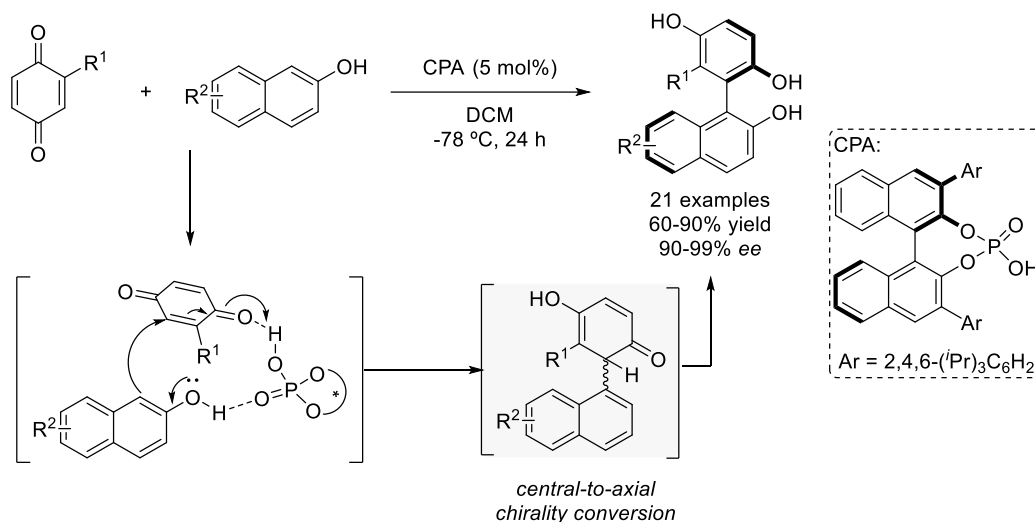
Scheme 12: Sparr's organocatalytic atroposelective aldol condensation.

D. Asymmetric construction of atropisomers by central-to-axial chirality transfer.

Central-to-axial chirality transfer is an interesting transformation in which a stereogenic center of the precursor or an intermediate is destroyed while a new stereogenic axis is generated simultaneously, with transmission of the stereochemical information. In the central-to-axial chirality transfer process, the stereogenic center can exist either as isolated form (substrate), or as *in situ* generated intermediates.

Liu and Tan developed an atroposelective synthesis of axially chiral biaryldiols⁵¹ *via* direct arylation of 2-naphthol and quinone derivatives, using a chiral phosphoric acid as catalyst (**scheme 13**). Mechanistically, the chiral phosphoric acid simultaneously activated the 2-naphthols and the 1,4-benzoquinone derivatives acting as a Brønsted acid/Lewis base bifunctional organocatalyst. The intermediate presenting a chiral center experience *in situ* aromatization, forming the final axially chiral biaryl compound. The resulting biaryldiols were obtained in excellent yields and enantioselectivities.

⁵¹ Y.-H. Chen, D.-J. Cheng, J. Zhang, Y. Wang, X.-Y. Liu, B. Tan, *J. Am. Chem. Soc.* **2015**, *137*, 15062–15065.



Scheme 13: synthesis of axially chiral biaryldiols *via* organocatalytic arylation of 2-naphthols.

A central-to-axial chirality transfer through a CPA-catalyzed arylation of 2-naphthols and 2-naphthylamines⁵² and iminoquinones⁵³ was also described, providing a powerful strategy for the catalytic asymmetric construction of axially chiral frameworks. Moreover, different central-to-axial chirality transfer strategies have also been used by many other groups to obtain axially chiral heterobiaryls.⁵⁴

I.3.2. Atroposelective transformations of preformed biaryl compounds.

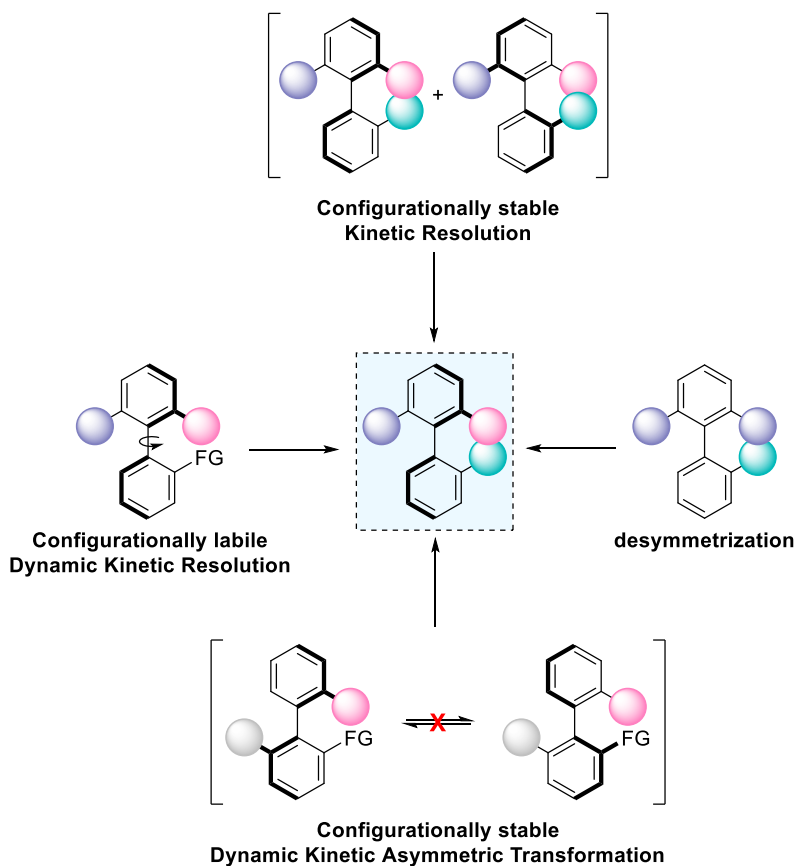
Besides the previously reported approaches, highly efficient alternative methods have been described in which configurationally labile or racemic biaryls are resolved into a stereochemically pure form.

⁵² Y.-H. Chen, L.-W. Qi, F. Fang, B. Tan, *Angew. Chem.* **2017**, *129*, 16526–16530; *Angew. Chem. Int. Ed.* **2017**, *56*, 16308–16312.

⁵³ J.-Z. Wang, J. Zhou, C. Xu, H. Sun, L. Kürti, Q.-L. Xu, *J. Am. Chem. Soc.* **2016**, *138*, 5202–5205.

⁵⁴ For selected examples, see: a) A. Straub, A. Goehrt, *Angew. Chem.* **1996**, *108*, 2832–2834; *Angew. Chem. Int. Ed.* **1996**, *35*, 2662–2664. b) O. Quinonero, M. Jean, N. Vanthuyne, C. Roussel, D. Bonne, T. Constantieux, C. Bressy, X. Bugaut, J. Rodriguez, *Angew. Chem.* **2016**, *128*, 1423–1427; *Angew. Chem. Int. Ed.* **2016**, *55*, 1401–1405. c) D. Bonne, J. Rodriguez, *Chem. Commun.* **2017**, *53*, 12385–12393. d) S.-C. Zheng, Q. Wang, J. Zhu, *Angew. Chem.* **2019**, *131*, 9313–9317; *Angew. Chem. Int. Ed.* **2019**, *58*, 9215–9219.

Therefore, atroposelective functionalization of preformed (prochiral or racemic) biaryls constitutes a key methodology in catalytic asymmetric synthesis of atropisomers, which could take place through desymmetrization, kinetic resolution (KR), dynamic kinetic resolution (DKR) and dynamic kinetic asymmetric transformation (DYKAT) approaches.



Scheme 14: possible routes to obtain axially chiral (hetero)biaryls using preformed (prochiral or racemic) biaryls.

A. Desymmetrizations.

This strategy is based on the modification of an achiral substrate that results in the loss of symmetry. Although the compound presents an axis, it also contains a mirror plane and therefore is not chiral and can be superimposed with its mirror image.

There are three possible desymmetrization strategies to obtain a stereogenic axis, depending on whether the starting biaryl presents restricted rotation around the axis, or there is a fast interconversion between the two enantiomers (being, therefore, conformers).

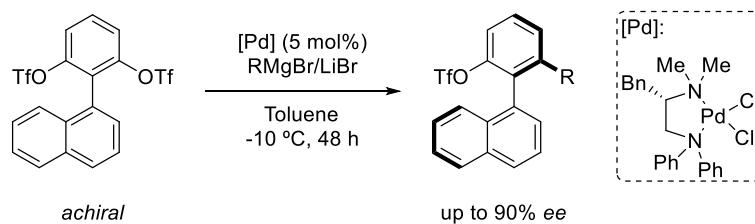
A.1. Desymmetrization of substrates with restricted rotation of the prochiral axis.

A restricted rotation around the aryl-aryl bond is one of the characteristics of biaryl substrates with three or more *ortho*-substituents. However, a perpendicular plane of symmetry emerges when one of the two aryl groups is symmetrically substituted; therefore, this plane of symmetry must be removed to produce axial chirality.

There are two main strategies to break the symmetry of this type of compounds. The first strategy is based on functional group transformation of *ortho* enantiotopic substituents. This transformation would break the symmetry of the biaryl and would generate a stereogenic axis.

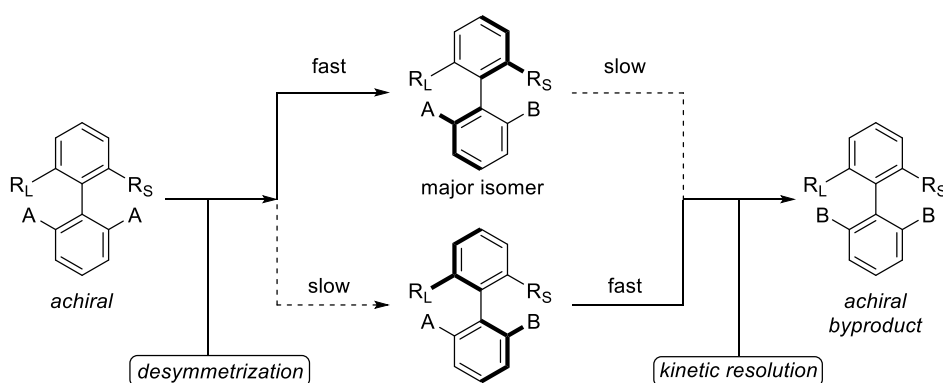
Hayashi and co-workers developed a Kumada coupling⁵⁵ using PdCl₂[(*S*)-Phephos] complex as catalyst for the desymmetrization of achiral biaryl bistriflates, where one of the enantiotopic triflate groups was substituted by an aryl or alkyl group (**scheme 15**), affording up to 90% *ee*, with very little conversion towards the disubstituted product (12% yield).

⁵⁵ a) T. Kamikawa, Y. Uozumi, T. Hayashi, *Tetrahedron* **1999**, 37 (18), 3161–3164. b) T. Kamikawa, T. Hayashi, *Tetrahedron* **1999**, 55 (11), 3455–3466.



Scheme 15: enantioselective arylation of biaryl triflates by Pd-catalyzed Grignard cross-coupling.

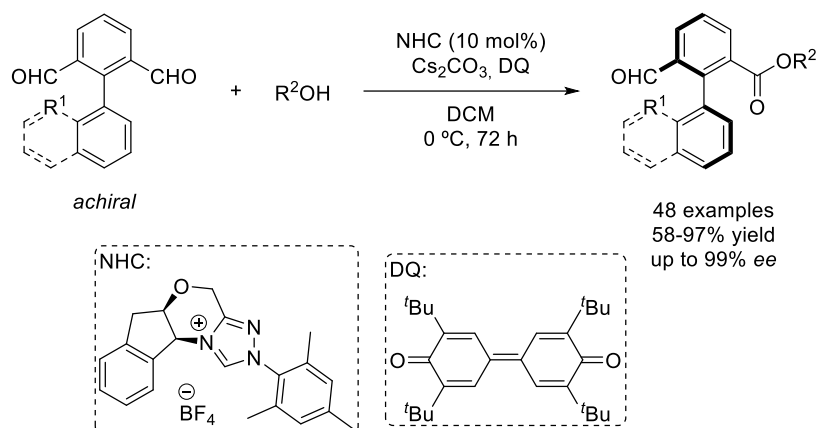
Very recently, Zheng and Zhang reported a NHCs-catalyzed desymmetrization protocol for the synthesis of axially chiral aldehydes. Their approach was based on a desymmetrization reaction with a subsequent kinetic resolution of the minor atropisomer (**scheme 16**), where the high selectivity in the desymmetrization is further enhanced by the following kinetic resolution that led to an achiral byproduct.⁵⁶



Scheme 16: Sequential asymmetric desymmetrization/kinetic resolution reaction.

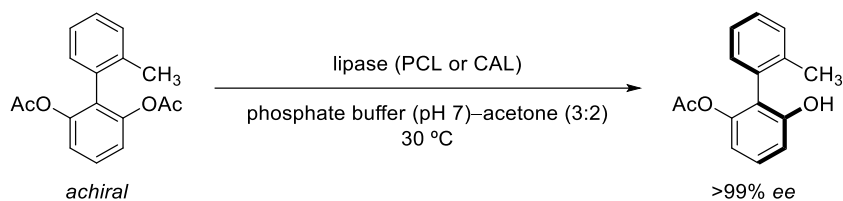
Excellent enantioselectivities (up to 99% *ee*) were obtained in the esterification reaction (**scheme 17**), affording 48 products that includes natural products and bioactive derivatives such as 7-hydroxycoumarin and vitamin E (87-99% *ee*).

⁵⁶ Y. Wu, M. Li, J. Sun, G. Zheng, Q. Zhang, *Angew. Chem. Int. Ed.* **2022**, *61*, e202117340.



Scheme 17: synthesis of axially chiral aldehydes by NHC-catalyzed desymmetrization followed by KR.

Matsumoto and co-workers also used this strategy for the enantioselective enzymatic hydrolysis of symmetric biaryl diacetates, in excellent enantiomeric excess (**scheme 18**).⁵⁷



Scheme 18: biocatalytic desymmetrization strategy developed by the group of Matsumoto.

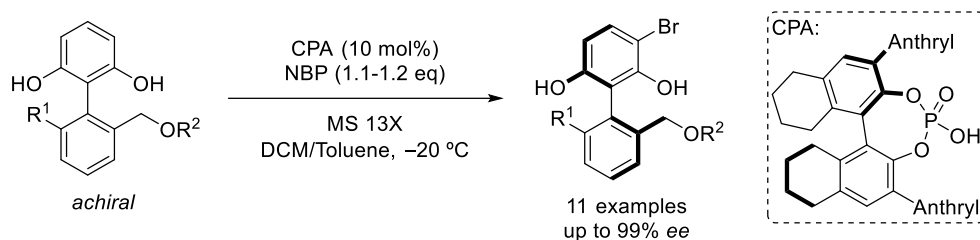
The second strategy to break the symmetry of biaryl compounds with restricted rotation around the axis consist of the introduction of additional substituents in the symmetrical substituted (hetero)aromatic ring.

In 2013, Akiyama described an enantioselective synthesis of biaryls through an electrophilic bromination of achiral dihydroxybiphenyl substrates,⁵⁸ taking advantage of the consecutive desymmetrization/kinetic resolution approach (**scheme 19**). When *N*-bromophthalimide (NBP) was used as brominating agent combined with a chiral phosphoric acid as catalyst, excellent enantioselectivities were

⁵⁷ T. Matsumoto, T. Konegawa, T. Nakamura, K. Suzuki, *Synlett* **2002**, 122–124.

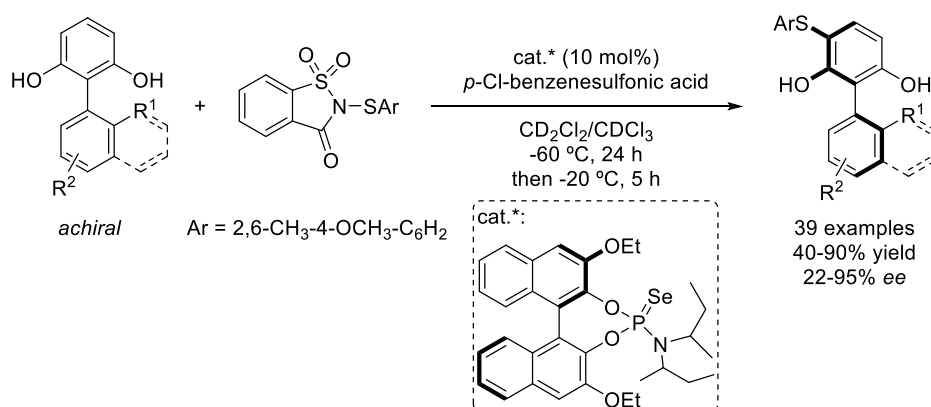
⁵⁸ K. Mori, Y. Ichikawa, M. Kobayashi, Y. Shibata, M. Yamanaka, T. Akiyama, *J. Am. Chem. Soc.* **2013**, *135*, 3964–3970.

obtained for the monobrominated product. DFT analysis determined that the excellent selectivity obtained was achieved *via* a highly organized hydrogen bond system between the substrate, the catalyst, and the brominating reagent.



Scheme 19: chiral phosphoric acid catalyzed electrophilic bromination.

Recently, Luo *et al.* reported an atroposelective sulfenylation reaction for the synthesis of axially chiral sulfur-containing biaryl derivatives,⁵⁹ catalyzed by a combination of a novel 3,3'-disubstituted BINOL-derived selenide catalyst and an achiral sulfonic acid (**scheme 20**). A wide range of biaryls with different electronic substituents were obtained with moderate to excellent yields and enantioselectivities.



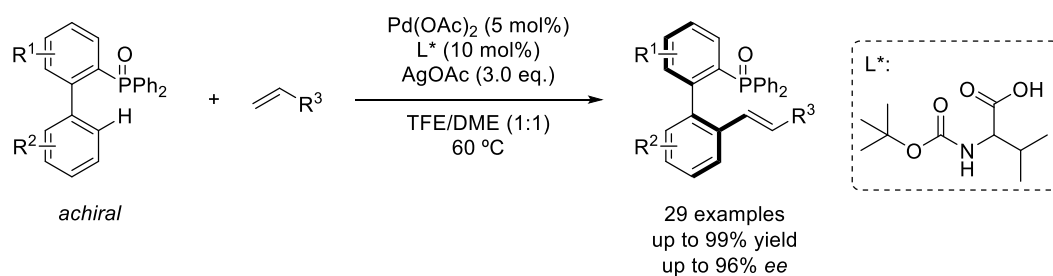
Scheme 20: atroposelective sulfenylation of biaryl phenols *via* a desymmetrization/KR Sequence.

⁵⁹ H.-Y. Luo, Z.-H. Li, D. Zhu, Q. Yang, R.-F. Cao, T.-M. Ding, Z.-M. Chen, *J. Am. Chem. Soc.* **2022**, *144*, 2943–2952.

A.2. Desymmetrization of configurationally labile biaryls via C-H activation/functionalization.

Biaryl atropisomers with low rotational barriers present free rotation around the prostereogenic axis and therefore consist of a rapidly interconverting mixture of conformational enantiomers, thus being achiral. The introduction of an additional substituent at the *ortho*-position is expected to increase their configurational stability, avoiding the interconversion between the enantiomers at room temperature, which results in the generation of axial chirality. In this regard, direct metal-catalyzed C-H activation has been established as an effective method, providing diverse possibilities.

Yang and co-workers developed a method for the synthesis of chiral atropisomeric biaryl phosphine-olefin compounds *via* enantioselective C-H olefination, affording excellent enantioselectivities for a wide variety of compounds (**scheme 21**).⁶⁰



Scheme 21: direct enantioselective C-H olefination towards chiral atropisomeric phosphine biaryls.

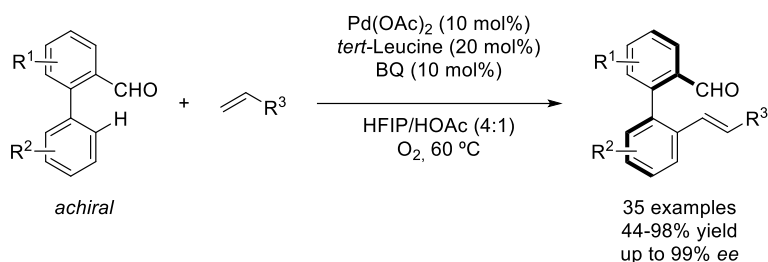
In 2017, Shi and co-workers described an atroposelective oxidative alkenylation of biaryl aldehydes using Pd(OAc)_2 and *tert*-leucine as chiral cocatalyst,⁶¹ affording excellent yields (up to 98%) and enantioselectivities (up to 98% *ee*) for a broad range of substrates (**scheme 22A**). More recently, the same research group

⁶⁰ S.-X. Li, Y.-N. Ma, S.-D. Yang, *Org. Lett.* **2017**, *19*, 1842–1845.

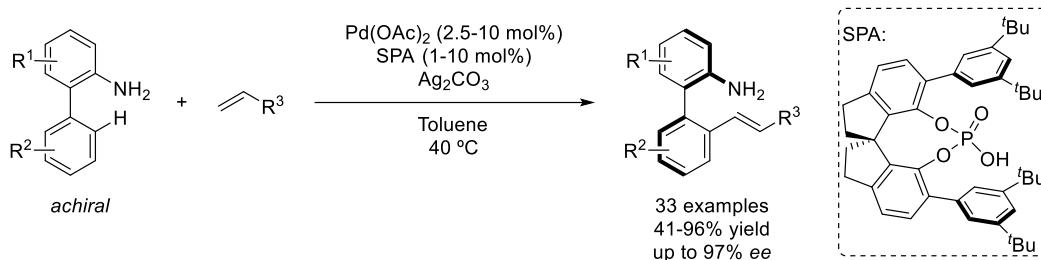
⁶¹ Q.-J. Yao, S. Zhang, B.-B. Zhan, B.-F. Shi, *Angew. Chem. Int. Ed.* **2017**, *56*, 6617–6621.

also reported the use of free amine as directing group⁶² using a spirocyclic phosphoric acid (SPA) combined with Ag₂CO₃ (**scheme 22B**).

A: Shi, 2017:



B: Shi, 2020:

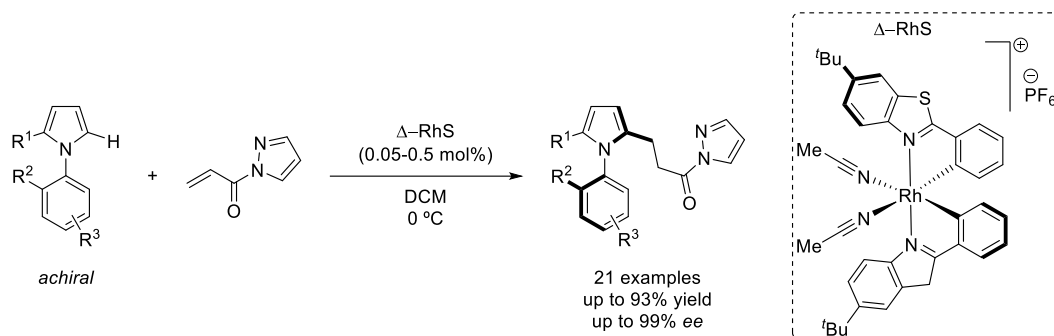


Scheme 22: directed palladium-catalyzed oxidative alkenylation.

The presence of directing groups is not always essential for a successful C-H activation in the synthesis of biaryl atropisomers. Thus, Ye *et al.* recently reported a highly atroposelective alkylation for the synthesis of axially chiral *N*-arylpyrroles by means of a chiral-at-the-metal, cationic Rh complex.⁶³ Moderate to excellent yields and excellent enantioselectivities were reported for a wide range of substrates.

⁶² B.-B. Zhan, L. Wang, J. Luo, X.-F. Lin, B.-F. Shi, *Angew. Chem. Int. Ed.* **2020**, *59*, 3568–3572.

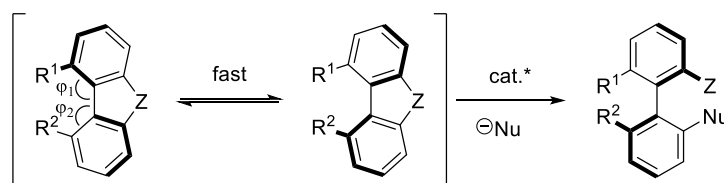
⁶³ C.-X. Ye, S. Chen, F. Han, X. Xie, S. Ivlev, K. N. Houk, E. Meggers, *Angew. Chem. Int. Ed.* **2020**, *59*, 13552 –13556.



Scheme 23: atropselective synthesis of axially chiral N-arylpyrroles by chiral rhodium catalysis.

A.3. Desymmetrization of biaryls *via* ring-opening reactions.

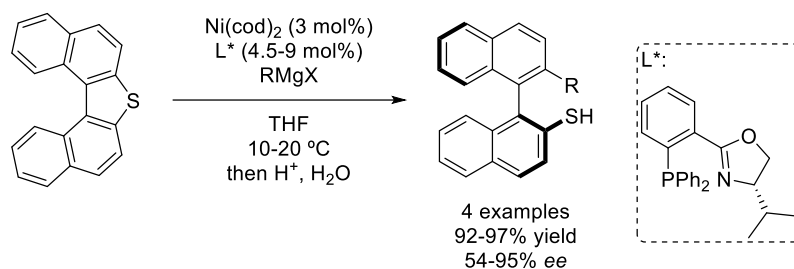
The last type of desymmetrization consist of the catalytic enantioselective five-membered ring opening of strained biaryl compounds. The widening of the φ_1 and φ_2 angles facilitates the labilization of the axis, resulting in a fast interconversion between both enantiomers (**scheme 24**). In these tetra-*ortho* substituted biaryls, the ring opening is facilitated by a decrease of torsional strain, leading to the corresponding configurationally stable products under mild reaction conditions.



Scheme 24: desymmetrization of biaryls featuring five-membered bridges.

The first example of this strategy was described by the group of Hayashi, where the cleavage at the C(sp²)-S bond in dinaphthothiophenes was performed *via* a Ni-catalyzed cross-coupling reaction with different Grignard reagents.⁶⁴ High enantioselectivities were obtained although the scope was very limited (**scheme 25**).

⁶⁴ T. Shimada, Y.-H. Cho, T. Hayashi, *J. Am. Chem. Soc.* **2002**, *124*, 45, 13396–13397.



Scheme 25: desymmetrization of thiophene derivatives *via* Ni-catalyzed coupling with Grignard reagents.

More recently, the asymmetric ring-opening of cyclic diaryliodonium salts for the synthesis of axially chiral biaryl derivatives was reported. This strategy presents two major advantages: (i) the aryl iodide product can be further functionalized to more complex structures, and (ii) various heteroatom-based nucleophiles can be used during the ring-opening processes which increases the structural variability.⁶⁵ Interestingly, bisoxazoline ligands were found to be key for the reactivity and selectivity of the process.

In 2018, the group of Gu reported the Cu-catalyzed enantioselective ring-opening of cyclic diaryliodonium salts with aryl amines,⁶⁶ affording excellent yields and enantioselectivities for a wide range of substrates (**scheme 26A**). It was found that the presence of two substituents at the *ortho* positions was essential for success. Also, non-symmetrical biaryls were suitable substrates, leading to excellent regioselectivities. The same research group further described the ring-opening reactions of cyclic diaryliodoniums with potassium thioates (**scheme 26B**).⁶⁷ Moreover, Zhang and co-workers reported the Cu-catalyzed acyloxylation of iodonium bridged biaryls,⁶⁸ affording excellent yields and enantioselectivities with broad substrate scope (**scheme 26C**). Finally, Gu and co-workers reported a Cu-catalyzed ring-opening phosphorylation reaction of cyclic diaryliodonium salts with

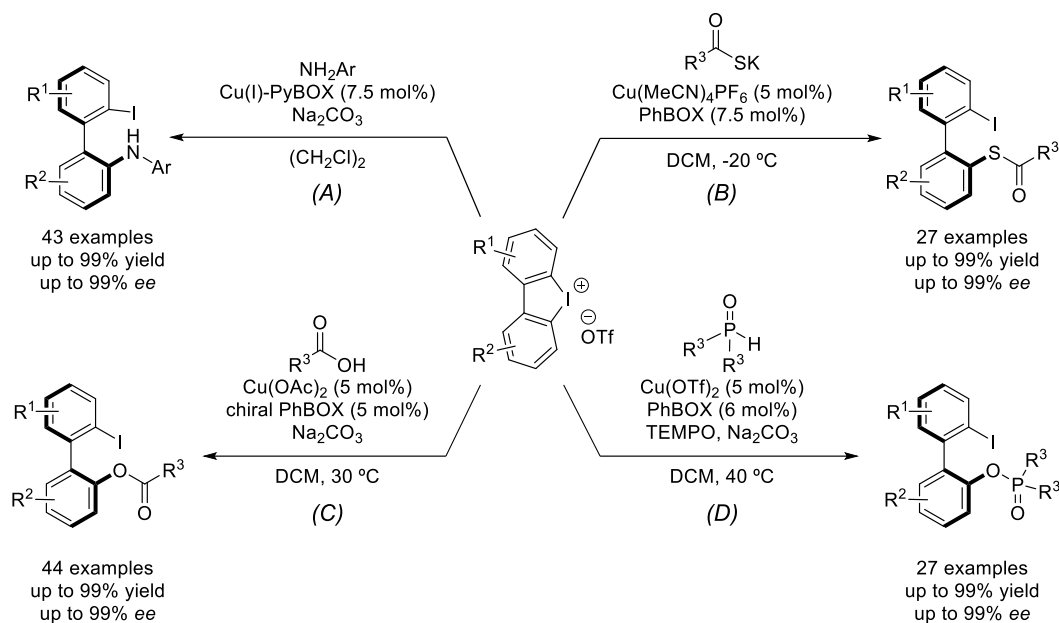
⁶⁵ X. Zhang, K. Zhao, Z. Gu, *Acc. Chem. Res.* **2022**, *55*, 1620–1633.

⁶⁶ K. Zhao, L. Duan, S. Xu, J. Jiang, Y. Fu, Z. Gu, *Chem.* **2018**, *4* (3), 599-612.

⁶⁷ M. Hou, R. Deng, Z. Gu, *Org. Lett.* **2018**, *20*, 5779–5783.

⁶⁸ K. Zhu, K. Xu, Q. Fang, Y. Wang, B. Tang, F. Zhang, *ACS Catal.* **2019**, *9*, 4951–4957.

diarylphosphine oxides,⁶⁹ as a method to add phosphine functionalities to the biaryl atropisomeric skeletons (**scheme 26D**).

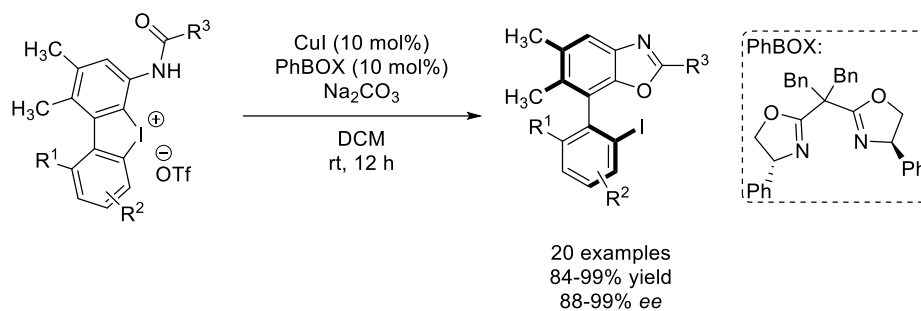


Scheme 26: catalytic enantioselective ring-opening of cyclic diaryliodonium salts.

In 2022, Zhu and co-workers reported an enantioselective ring-opening reaction *via* copper-catalyzed intramolecular oxidation of cyclic diaryliodonium salts, under very mild conditions (**scheme 27**).⁷⁰ The method used a PhBOX derivative as ligand and afforded excellent yields and optical purities for a variety of aryl and alkyl amides.

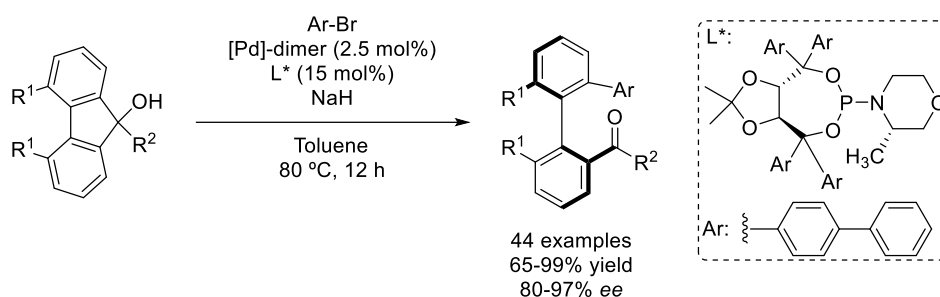
⁶⁹ L. Duan, K. Zhao, Z. Wang, F.-L. Zhang, Z. Gu, *ACS Catal.* **2019**, 9, 9852–9858.

⁷⁰ D. Zhu, Y. Sun, H. Peng, H. Li, Y. Yan, H. Kuang, *Eur. J. Org. Chem.* **2022**, e202101449.



Scheme 27: enantioselective synthesis of axially chiral biaryls by Cu-catalyzed oxidation of cyclic diaryliodoniums.

Notably, all the examples previously described involves the cleavage of carbon-heteroatom bonds. In 2019, the group of Gu reported a carbon-carbon ring opening reaction of different alkyl-substituted bromobenzenes, for the synthesis of biaryl ketones, using a Pd(II)-dimer (**scheme 28**).⁷¹



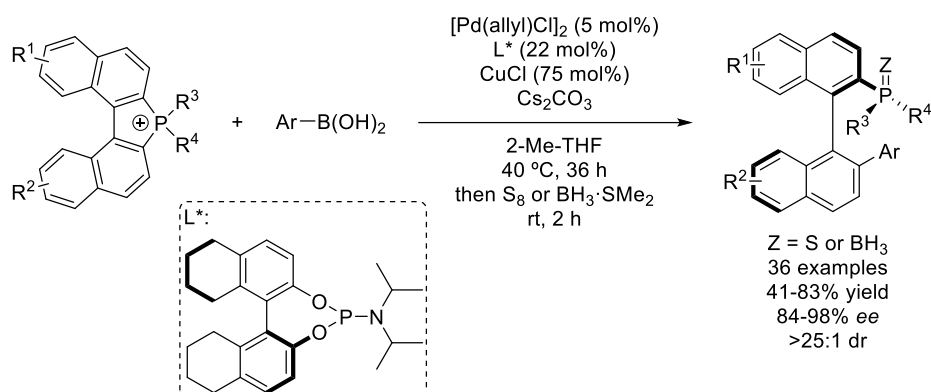
Scheme 28: Pd-catalyzed carbon-carbon ring opening developed by Gu.

Very recently, Pang, Sun *et al.* described an interesting C-P ring opening reaction furnishing atropisomers containing both axial chirality and a P-stereogenic center.⁷² The challenges of this transformation (*e.g.*, control the regioselectivity of the four C-P bonds, the high enantio- and diastereoselection needed for the construction of two chiral elements and the possible P-Pd coordination) were overcome using a palladium-phosphoramidite complex, combined with CuCl (**scheme 29**). It was found that the addition of a Cu(I) salt had an important role to promote the coordination

⁷¹ R. Deng, J. Xi, Q. Li, Z. Gu, *Chem*, **2019**, *5*, 1834–1846.

⁷² L. Pang, Q. Sun, Z. Huang, G. Li, J. Liu, J. Guo, C. Yao, J. Yu, Q. Li, *Angew. Chem. Int. Ed.* **2022**, *61*, e202211710.

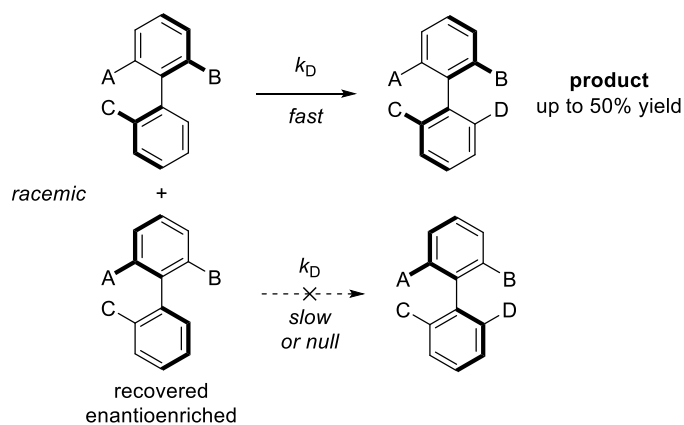
between Pd and the ligand, increasing the efficiency of the process. The reaction presented a good functional group tolerance, affording excellent yields, enantioselectivities and >25:1 dr in all cases.



Scheme 29: enantioselective construction of atropisomers containing a P-stereogenic center.

B. Kinetic Resolution (KR).

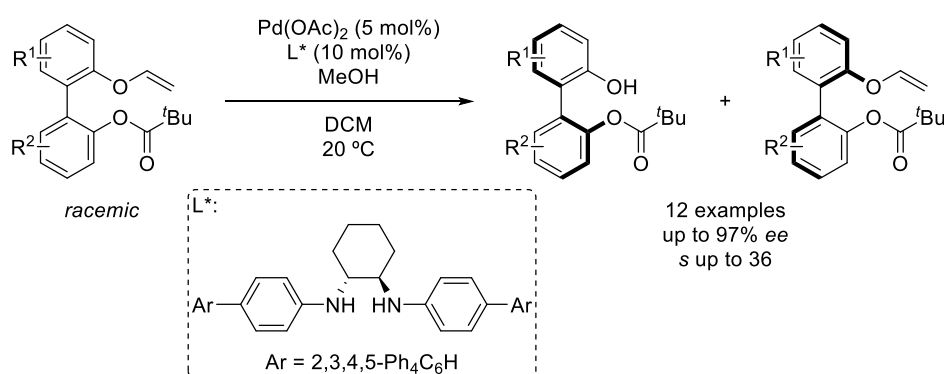
When the biaryl substrate presents a lack of symmetry and there are no dynamic processes involved, the only available strategy is a kinetic resolution. In a catalytic kinetic resolution, the two enantiomers react at different rates, resulting in the transformation of one enantiomer into the desired product with a maximum yield of 50%, and the recovery of the remaining enantioenriched starting substrate.



Scheme 30: classical kinetic resolution of biaryls.

Typically, the efficiency of a KR is determined by a selectivity factor (s), which reflects the energy difference between the two diastereomeric transition states in the enantio-determining step of the catalytic reaction. This methodology has been extensively applied for the synthesis of, among other, BINOL, BINAM and NOBIN derivatives.⁷³

The synthesis of optically active 2,2'-dihydroxy-1,1'-biaryls had traditionally relied on conventional optical resolution or chiral pool methodologies using stoichiometric chiral sources.⁷⁴ In 2005, Tokunaga and Tsuji described the first efficient synthesis of optically active 1,1'-bi-2-phenols⁷⁵ through a Pd-catalyzed methanolysis of vinyl ethers, under mild conditions (**scheme 31**).



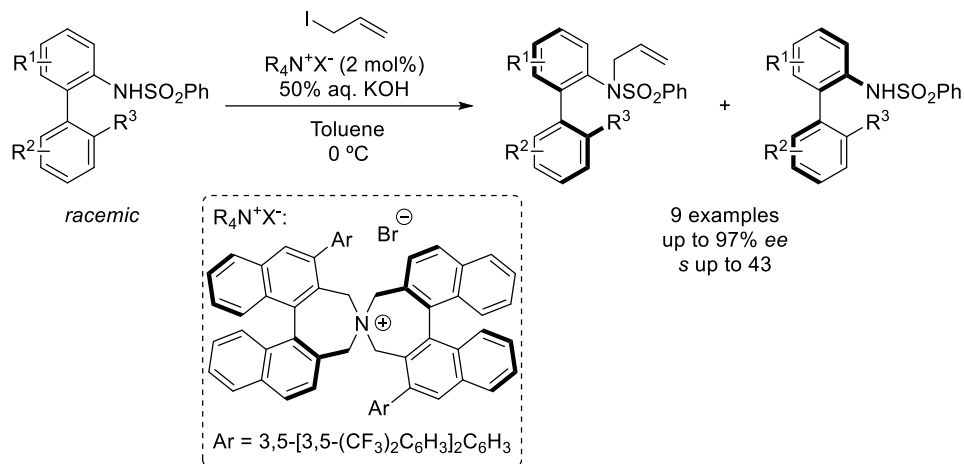
Scheme 31: Pd-catalyzed methanolysis of vinyl ethers *via* kinetic resolution.

⁷³ For selected examples for the synthesis of BINOL and derivatives *via* KR, see: a) B. A. Jones, T. Balan, J. D. Jolliffe, C. D. Campbell, M. D. Smith, *Angew. Chem. Int. Ed.* **2019**, *58*, 4596–4600. b) S. Lu, B. S. Poh, Y. Zhao, *Angew. Chem. Int. Ed.* **2014**, *53*, 11041–11045. c) G. Ma, Y. Deng, M. P. Sibi, *Angew. Chem. Int. Ed.* **2014**, *53*, 11818–11821. d) H. Aoyama, M. Tokunaga, J. Kiyosu, T. Iwasawa, Y. Obora, Y. Tsuji, *J. Am. Chem. Soc.* **2005**, *127*, 10474–10475.

⁷⁴ For selected examples, see: a) G.-Q. Lin, M. Zhong, *Tetrahedron Lett.* **1997**, *38*, 1087-1090. b) F. Toda, K. Tanaka, H. Miyamoto, H. Koshima, I. Miyahara, K. Hirotsu, *J. Chem. Soc., Perkin Trans. 2* **1997**, 1877-1885. c) G. Delogu, D. Fabbri, M. A. Dettori, A. Forni, G. Casalone, *Tetrahedron: Asymmetry* **2000**, *11*, 4417-4427. d) A. I. Meyers, T. D. Nelson, H. Moorlag, D. J. Rawson, A. Meier, *Tetrahedron* **2004**, *60*, 4459- 4473. e) J. M. Brunel, *Chem. Rev.* **2005**, *105*, 857-897.

⁷⁵ H. Aoyama, M. Tokunaga, J. Kiyosu, T. Iwasawa, Y. Obora, Y. Tsuji, *J. Am. Chem. Soc.* **2005**, *127*, 30, 10474–10475.

In 2013, Maruoka and co-workers used a chiral quaternary ammonium phase-transfer catalyst for the *N*-allylation by kinetic resolution of axially chiral 2-amino-1,1'-biaryls (**scheme 32**),⁷⁶ affording high levels of enantiocontrol and selectivity factors (*s*).

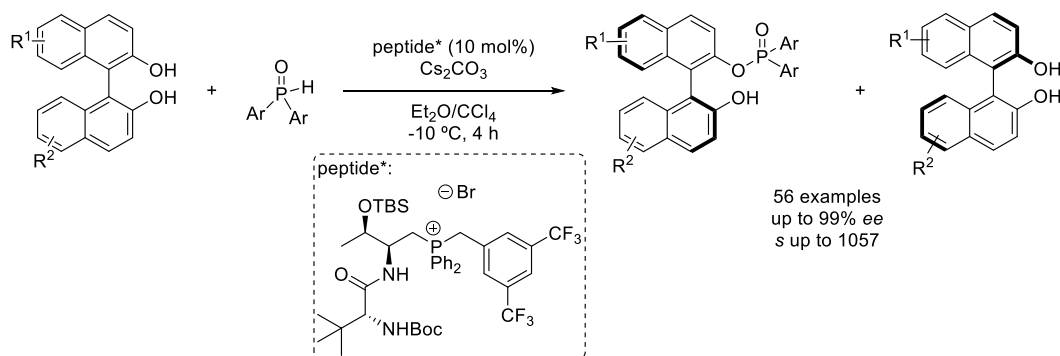


Scheme 32: phase-transfer-catalyzed *N*-allylation of axially chiral 2-amino-1,1'-biaryls.

Recently, the group of Wang described an enantiodivergent organocatalytic kinetic resolution of racemic BINOL by an Atherton–Todd type reaction, using a dipeptide-phosphonium salt as catalyst (**scheme 33**).⁷⁷ The corresponding *O*-phosphorylated biaryls were obtained with excellent selectivity factors and broad substrate scope.

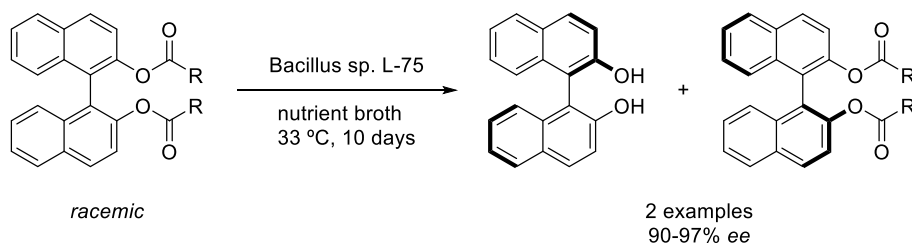
⁷⁶ S. Shirakawa, X. Wu, K. Maruoka, *Angew. Chem., Int. Ed.* **2013**, *52*, 14200–14203.

⁷⁷ S. Fang, J.-P. Tan, J. Pan, H. Zhang, Y. Chen, X. Ren, T. Wang, *Angew. Chem. Int. Ed.* **2021**, *60*, 14921–14930.



Scheme 33: enantiodivergent KR of 1,1''-biaryl-2,2''-diols by dipeptide-phosphonium salt catalysis.

On the other hand, biocatalysis has been widely applied in kinetic resolutions,⁷⁸ with remarkable success. In 1985 Ikekawa and co-workers described the first synthesis of optically pure BINOL, *via* deacylation of the corresponding racemic diester,⁷⁹ using *hydrolase Bacillus sp. L-75* (**scheme 34**). The desired (*R*)-BINOL was obtained with excellent conversion and enantioselectivity, while the remaining unreacted (*S*)-diester was recovered with 94% *ee*. However, only two examples were reported.



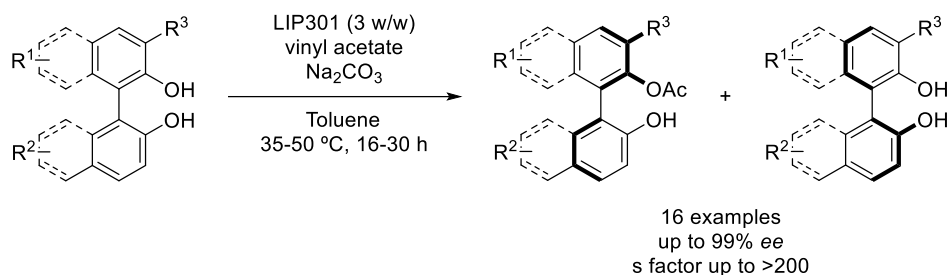
Scheme 34: biocatalytic kinetic resolution for the synthesis of BINOL.

A more recent example of kinetic resolution was described by Akai and co-workers for the synthesis of C₁-symmetric and C₂-symmetric atropoisomeric

⁷⁸ For selected examples, see: a) R. Kazlauskas, *Org. Synth.* **1992**, *70*, 60. b) P.R. Blakemore, S.D. Milicevic, L.N. Zakharov, *J. Org. Chem.* **2007**, *72*, 9368–9371. c) S. Miyano, K. Kawahara, Y. Inoue, H. Hashimoto, *Chem. Lett.* **1987**, *16*, 355–356. d) C. Sanfilippo, G. Nicolosi, G. Delugo, D. Fabbri, M. A. Dettori, *Tetrahedron: Asymmetry* **2003**, *14*, 3267–3270. e) G. Bringman, A.J. Price Mortimer, P.A. Keller, M.J. Gresser, J. Garner, M. Breuning, *Angew. Chem. Int. Ed.* **2005**, *44*, 5384–5427.

⁷⁹ Y. Fujimoto, H. Iwadate, N. Ikekawa, *J. Chem. Soc., Chem. Commun.* **1985**, *19*, 1333–1334.

biaryldiols,⁸⁰ with excellent enantiocontrol, by a lipase-mediated acylation (**scheme 35**).



Scheme 35: base-promoted lipase-catalyzed kinetic resolution described by Akai and co-workers.

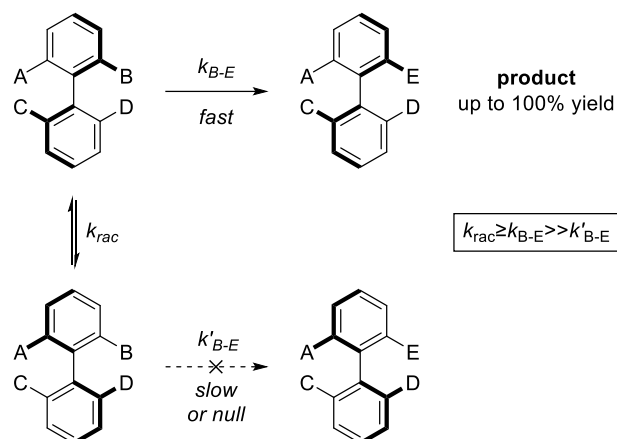
The limitations of kinetic resolutions can be overcome if there is a dynamic process involved in the stereochemical outcome of the reaction, allowing for the interconversion of atropisomeric substrates or intermediates.

There are two possible approaches concerning the nature of the dynamic process: dynamic kinetic resolution (DKR) and dynamic kinetic asymmetric transformation (DYKAT).

C. Dynamic Kinetic Resolution (DKR).

When the racemic biaryl substrate can racemize under the reaction conditions, allowing the constant transformation of the less reactive atropisomer into the more reactive one, and finally to the desired enantioenriched product, a DKR scenario arises. This process allows the obtention of a single enantioenriched product in quantitative theoretical yield (**scheme 36**).

⁸⁰G. A. I. Moustafa, K. Kasama, K. Higashio, S. Akai, *RSC. Adv.* **2019**, 9, 1165–1175.



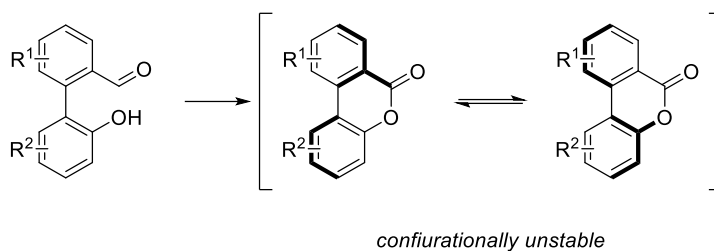
Scheme 36: classical dynamic kinetic resolution of biaryls.

The reaction rates of the two atropisomers are different, but the interconversion into each other is possible. For an efficient DKR, the racemization rate (k_{rac}) must be equal or higher than the reaction rate of the more reactive atropisomer. The constant racemization of the substrate will minimize the formation of the opposite enantiomer, affording higher enantiomeric excesses than in classical KR. On the other hand, a chiral catalyst is not necessarily required for the racemization of the substrate. Although several DKR processes have been reported in literature,⁸¹ there are more limited examples for the synthesis of axially chiral heterobiaryls.

C.1. Bringmann's "lactone concept" and related ring-opening reactions.

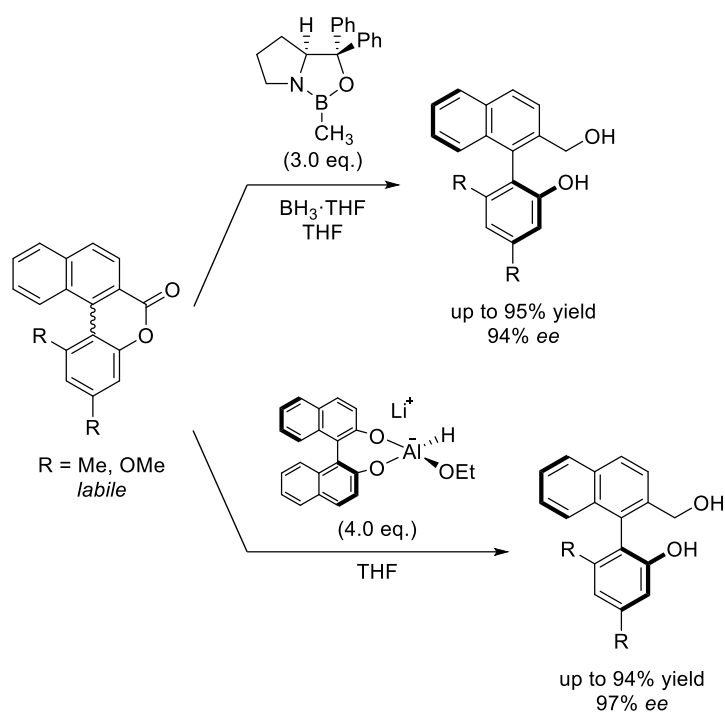
The atroposelective ring opening of six-membered-bridged biaryls are among the most well-known DKR strategies for the synthesis of biaryls. The presence of the lactone bridge allows to decrease the racemization barrier of the system, resulting in a labile biaryl compound. Then, the cleavage of the lactone bond increased the rotational barrier, leading to the corresponding configurationally stable axially chiral biaryl compound (**scheme 37**).

⁸¹ For selected reviews of DKR, see: a) V. Bhat, E. R. Welin, X. Guo, B. M. Stoltz, *Chem. Rev.* **2017**, *117*, 4528–4561. b) H. Pellissier, *Adv. Synth. Catal.* **2011**, *353*, 659–676. c) J. Steinreiber, K. Faber, H. Griengl, *Chem. Eur. J.* **2008**, *14*, 8060–8072. d) F. F. Huerta, A. B. E. Minidis, J.-E. Bäckwall, *Chem. Soc. Rev.* **2001**, *30*, 321–331.



Scheme 37: concept of the “lactone strategy”.

Bringmann pioneered this methodology in 1992 with the first atroposelective ring-opening reduction reaction of biaryl lactones using a stoichiometric chiral hydride transfer reagent, derived from borane,⁸² or (*R*)-BINAL-H⁸³ as nucleophiles (**scheme 38**).



Scheme 38: atroposelective cleavage of bridged biaryl lactones using hydride as nucleophile.

⁸² G. Bringmann, T. Hartung, *Angew. Chem., Int. Ed. Engl.* **1992**, *31*, 761–762.

⁸³ G. Bringmann, T. Hartung, *Tetrahedron* **1993**, *49*, 7891–7902.

The lactone ring-opening reaction was further extended to *N*-⁸⁴ and *O*-nucleophiles⁸⁵ resulting in a powerful methodology, that has been extensively used in the total synthesis of natural products and bioactive compounds. However, the needed of stoichiometric amounts of the nucleophile responsible of the lactone cleavage was an important limitation.

In 2002, Bringmann reported the first example of an atroposelective reduction of biaryl lactones using catalytic amounts of Corey-Bakshi-Shibata (CBS) reagent,⁸⁶ affording the biaryl atropisomers in excellent yield and 88% *ee*. The loading of CBS could be reduced to 10 mol%, although at expensed of a decrease in optical purity (88% *ee*). This protocol represented an important progress to the synthesis of biaryl atropisomers *via* DKR (**scheme 39A**).

A few years later, Yamada and co-workers reported conditions for the reduction of the carbonyl functionality using a β -ketoiminatocobalt(II) complex, affording the products in moderate to excellent enantioselectivities (**scheme 39B**).⁸⁷

In 2016, the group of Wang used a bifunctional quinine-based thiourea catalyst for the atroposelective esterification of labile biaryl-lactones,⁸⁸ with excellent yields and enantioselectivities for a wide range of substrates (**scheme 39C**). A synergistic acid-base mechanism was found to operate, by which the carbonyl was activated by the thiourea, while the tertiary amine in the catalyst directs the nucleophilic attack of the hydroxyl group.

More recently, Hu *et al.* reported the first metal-catalyzed asymmetric transformation of bridged biaryl lactones, using Cu-H as catalyst and PMHS as

⁸⁴ G. Bringmann, M. Breuning, S. Tasler, H. Endress, C. L. J. Ewers, L. Göbel, K. Peters, E.-M. Peters, *Chem. Eur. J.* **1999**, *5*, 3029–3038.

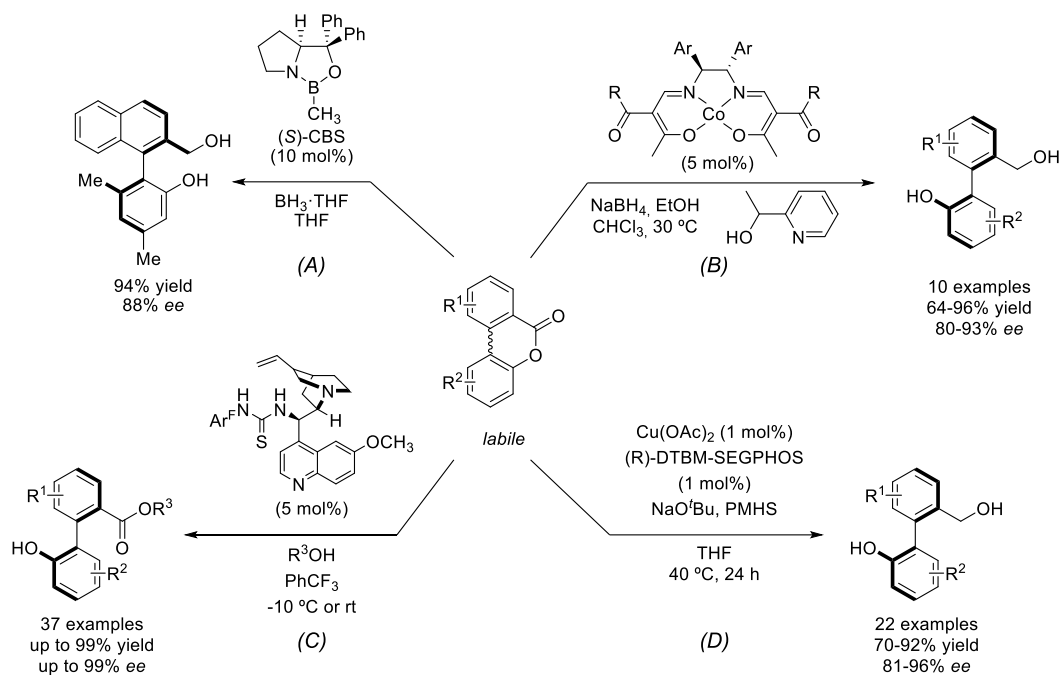
⁸⁵ a) D. Seebach, G. Jaeschke, K. Gottwald, K. Matsuda, R. Formisano, D. A. Chaplin, M. Breuning, G. Bringmann, *Tetrahedron* **1997**, *53*, 7539–7556. b) G. Bringmann, M. Breuning, R. Walter, A. Wuzik, K. Peters, E.-M. Peters, *Eur. J. Org. Chem.* **1999**, 3047–3055.

⁸⁶ G. Bringmann, M. Breuning, P. Henschel and J. Hinrichs, *Org. Synth.* **2002**, *79*, 72.

⁸⁷ T. Ashizawa, S. Tanaka, T. Yamada, *Org. Lett.* **2008**, *10*, 12, 2521–2524.

⁸⁸ C. Yu, H. Huang, X. Li, Y. Zhang, W. Wang, *J. Am. Chem. Soc.* **2016**, *138*, 22, 6956–6959.

reductant.⁸⁹ The reaction present broad scope and good functional group tolerance, while affording moderate to excellent optical purities (**scheme 39D**).



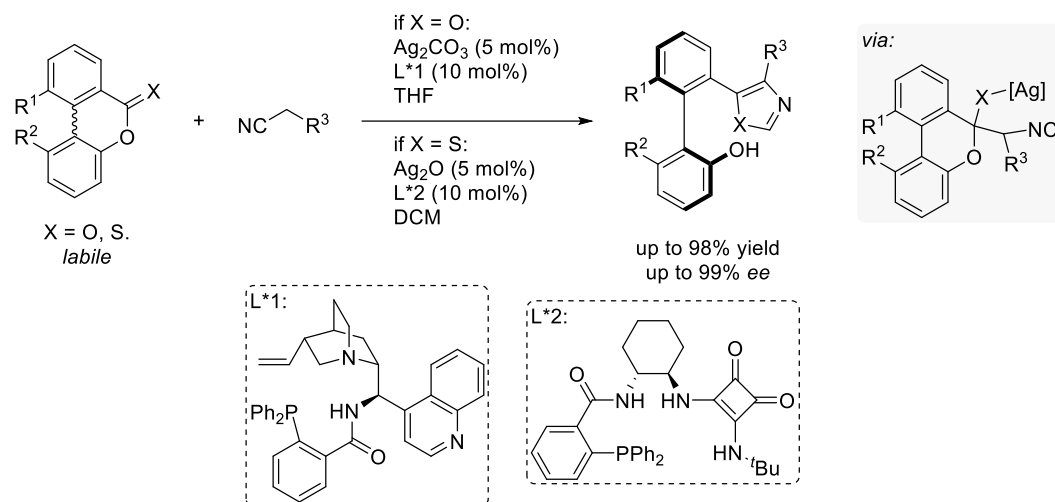
Scheme 39: catalytic asymmetric ring-opening of biaryl lactones.

Recently, Liao and co-workers developed an atroposelective ring-opening of Bringmann's lactones, using *C*-nucleophiles (**scheme 40**).⁹⁰ The reaction proceeds through the formation of very reactive α -isocyanide moiety that undergo rapid cyclization to form the oxazole ring, driven by aromatization. The reactivity could be enhanced by increasing the torsional strain through variations of the two *ortho*-substituents. The reaction required of low temperatures to afford high enantioselectivities, while the conversions remained excellent. Recently, the same

⁸⁹ L. Hu, G.-Q. Chen, B.-J. Lin, Q.-W. Zhang, Q. Yin, X. Zhang, *Org. Lett.* **2019**, *21*, 5575–5580.

⁹⁰ L. Quian, L.-F. Tao, W.-T. Wang, E. Jameel, Z.-H. Luo, T. Zhang, Y. Zhao, J.-Y. Liao, *Org. Lett.* **2021**, *23*, 5086–5091.

research group expanded the scope of this process, using *tri-* and *tetra-ortho*-biaryl thionolactones.⁹¹

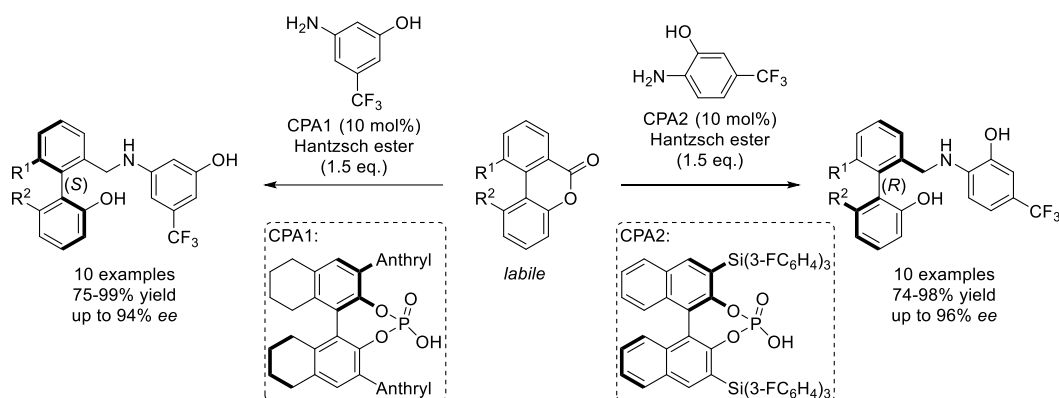


Scheme 40: catalytic atroposelective DKR of biaryl (thiano)lactones with activated isocyanides.

In 2016, Akiyama and co-workers reported a chiral phosphoric acid-catalyzed asymmetric transfer hydrogenation of biaryl lactols, using a Hantzsch ester as hydrogen source (**scheme 41**).⁹² It was possible the control of the axial chirality configuration by changing the substitution pattern of the hydroxylaniline derivative: *ortho*-hydroxylanilines favoured the formation of the *R* isomer, while *meta*-hydroxylanilines favoured the *S* isomer.

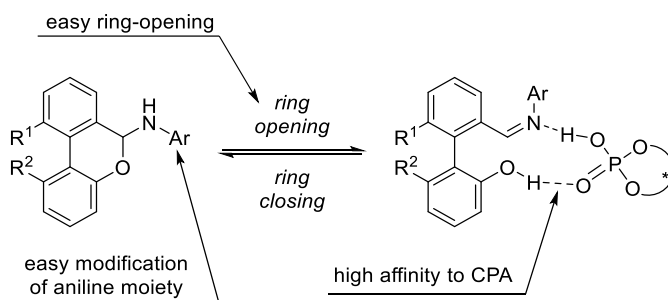
⁹¹ Z.-H. Luo, W.-T. Wang, T.-Y. Tang, S. Zhang, F. Huang, D. Hu, L.-F. Tao, L. Qian, J.-Y. Liao, *Angew. Chem. Int. Ed.* **2022**, *61*, e202211303.

⁹² K. Mori, T. Itakura, T. Akiyama, *Angew. Chem., Int. Ed.* **2016**, *55*, 11642–11646.



Scheme 41: atroposelective synthesis of chiral biaryls by asymmetric transfer hydrogenation.

In this case, the labilization of the axis takes place through the formation of an *N,O*-acetal, obtained from the condensation of a cyclic biaryl acetal and a hydroxylamine, in equilibrium with the imine open form (**scheme 42**). Moreover, the high affinity of the imine for the chiral phosphoric acid and the easy modification of the aromatic ring of the aniline, were key features for the substrate choice.



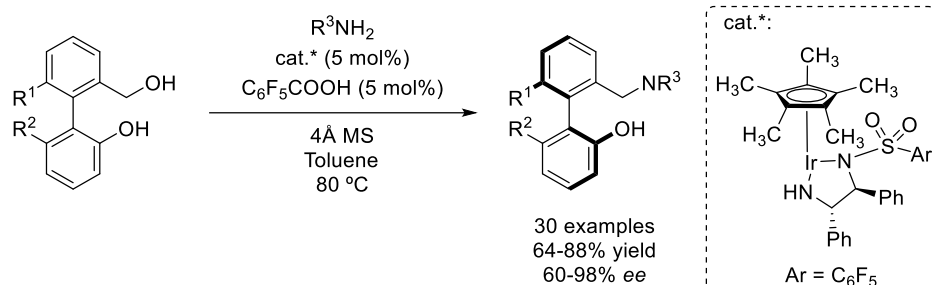
Scheme 42: reasons for the asymmetric transfer hydrogenation substrate selection.

Inspired by this result, other examples of DKR, using biaryl hemiaminal-based substrates, were reported by different authors.

Wang and co-workers reported a redox-neutral amination of biaryl diols, under the cooperative catalysis of a chiral iridium complex and an achiral Brønsted acid (**scheme 43**).⁹³ This method was based on a hydrogen borrowing strategy, starting by the dehydrogenation of a biaryl diol that react with an aniline affording a

⁹³ J. Zhang, J.Wang, *Angew. Chem., Int. Ed.* **2018**, *130*, 474–478.

labile biaryl hemiaminal. The protocol features good functional group tolerance and allows for several structural variations, affording excellent optical purities. The same research group reported a ruthenium-catalyzed atroposelective reductive amination, *via* DKR,⁹⁴ which allowed for the use of previously elusive primary and secondary alkyl amines, with excellent results.

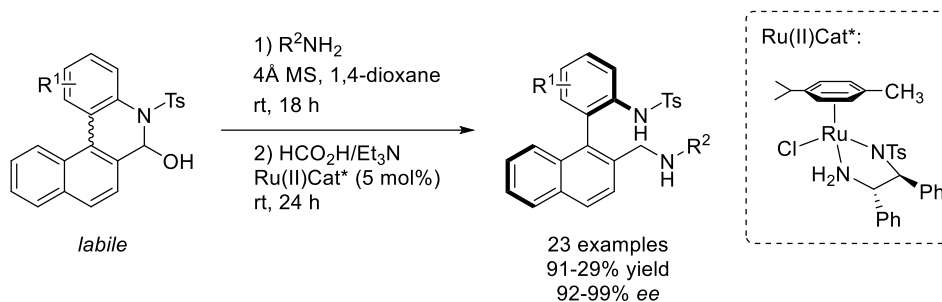


Scheme 43: redox-neutral amination of biaryl compounds through hydrogen borrowing and DKR.

In 2021, our research group developed an efficient asymmetric Ru-catalyzed transfer hydrogenation for the synthesis of BINAM homologues,⁹⁵ *via* dynamic kinetic resolution of cyclic biaryl hemiaminal structures (**scheme 44**). The high levels of enantioselectivities observed for this reaction are due to the rapid interconversion between the two atropisomers of the substrate, by a ring-opening-ring-closing equilibrium between amino-imine structures, followed by a fast transfer hydrogenation.

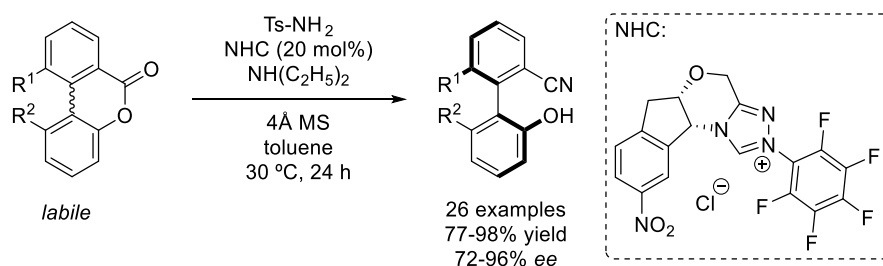
⁹⁴ D. Guo, J. Zhang, B. Zhang, J. Wang, *Org. Lett.* **2018**, *20*, 6284–6288.

⁹⁵ J. A. Carmona, C. Rodríguez-Franco, J. López-Serrano, A. Ros, J. Iglesias-Sigüenza, R. Fernández, J. M. Lassaletta, V. Hornillos, *ACS Catal.* **2021**, *11*, 4117–4124.



Scheme 44: atroposelective transfer hydrogenation of biaryl aminsals *via* dynamic kinetic resolution.

Early this year, the group of Chi reported the synthesis of axially chiral benzonitriles using inexpensive sulfonamides and *N*-heterocyclic carbenes as organocatalyst.⁹⁶ Atropisomeric benzonitriles bearing different substitution patterns were obtained in good to excellent yields and enantioselectivities (**scheme 45**). Computational studies revealed that the loss of the *para*-toluenesulfinate group is the enantiodetermining step and the axial chirality is controlled during the bond dissociation and formation of the new CN group.



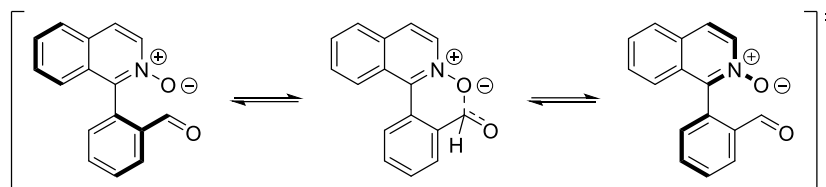
Scheme 45 atroposelective synthesis of axially chiral benzonitriles *via* DKR.

C.2. DKR enabled by non-covalent interactions in cyclic transition states or intermediates.

In the previous section, racemization of the biaryl is facilitated by the formation of a covalent bond between groups at the *ortho* position of the axis. In the next alternative strategy, the formation of a six-membered ring transition states will be responsible for the atropisomerization event.

⁹⁶ Y. Lv, G. Luo, Q. Liu, Z. Jin, X. Zhang, Y. R. Chi, *Nat Commun.* **2022**, *13*, 36.

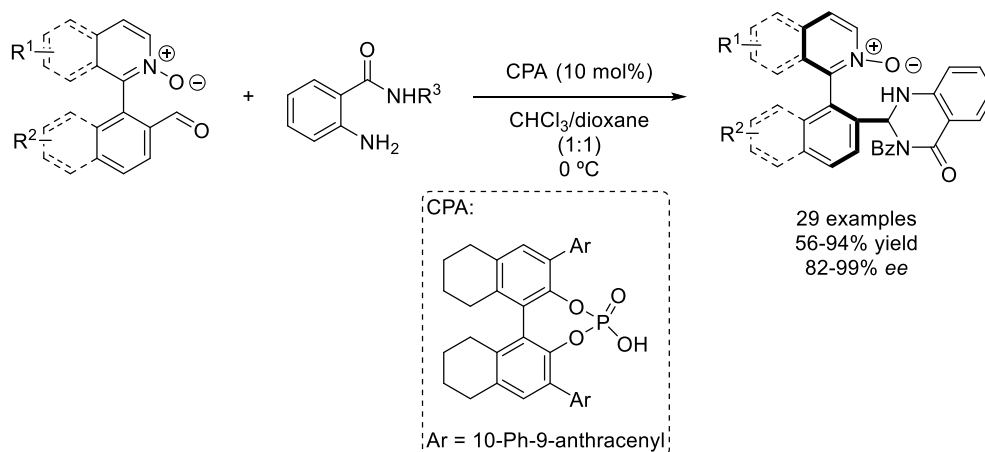
In the first example of this strategy, described by Turner and Clayden, an intramolecular interaction between an *N*-oxide and a carbonyl from an aldehyde facilitate the labilization of the biaryl through the formation of a six-membered transition state (**scheme 46**).⁹⁷



Scheme 46: Dynamic Kinetic Resolution developed by Turner and Clayden.

Based on this approach, authors performed a biocatalytic DKR, that will be further revised in **Chapter III**.

Very recently, Yuan and Wang employed the same system than Turner and Clayden to perform an organocatalytic DKR using a chiral phosphoric acid as organocatalyst (**scheme 47**).⁹⁸



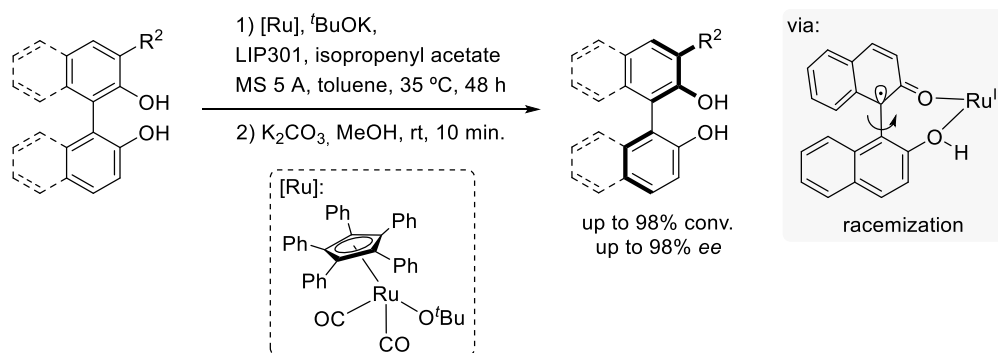
Scheme 47: atropenantioselective synthesis of heterobiaryl *N*-oxides using a chiral phosphoric acid.

⁹⁷ S. Staniland, R. W. Adams, J. J. W. McDouall, I. Maffucci, A. Contini, D. M. Grainger, N. J. Turner, J. Clayden, *Angew. Chem. Int. Ed.* **2016**, *55*, 10755–10759.

⁹⁸ X. Yuan, J. Wang, *Sci. China Chem.* **2022**, 10.1007/s11426-022-1402-9.

C.3. Racemization by hybridization changes.

Recently, Akai and co-workers reported a biocatalytic dynamic kinetic resolution of symmetric BINOL derivatives compatible with lipases, as required for a biocatalytic acylation (**scheme 48**).⁹⁹ The racemization takes place by oxidation of the deprotonated substrate-Ru(II) complex by molecular oxygen, followed by a single electron transfer (SET) process in the resulting Ru(III) binaphtholate complex. Thus, a radical intermediate bearing a sp³ carbon at C1 is formed, thereby enabling the free rotation around the C-C bond before regenerating the stereogenic axis in the racemate. Then, a lipase-catalyzed reaction using isopropenyl acetate as acyl donor takes place, affording atroposelective C₁- and C₂-symmetric diols with excellent enantioselectivities.



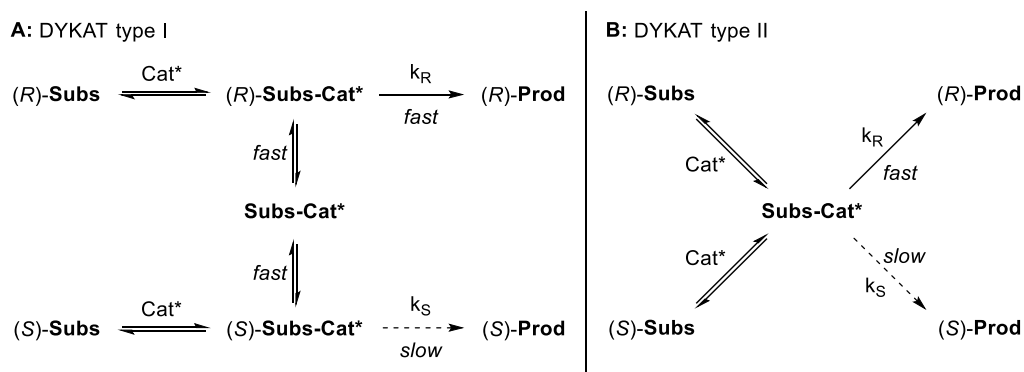
Scheme 48: DKR of BINOL derivatives *via* biocatalytic acylation.

D. Dynamic Kinetic Asymmetric Transformation (DYKAT).

A dynamic kinetic asymmetric transformation takes place for configurationally stable systems (with high rotational barrier that prevents the interconversion between atropisomers), while the reaction conditions do not alter this situation. In this case, a chiral catalysis could promote the racemization event by the formation of a diastereomeric pair that can be interconverted through an achiral

⁹⁹ G.A.I. Moustafa, Y. Oki, S. Akai, *Angew. Chem. Int. Ed.* **2018**, *57*, 10278–10282.

intermediate (**scheme 49A**, DYKAT type I) or a common labile intermediate in which the chiral information is lost (**scheme 49B**, DYKAT type II).⁸



Scheme 49: dynamic kinetic asymmetric transformation.

Regarding the application of the DYKAT strategy, to the best of our knowledge all the reported examples are based on the resolution of heterobiaryl structures.

In 2013, our research group reported the first Pd-catalyzed DYKAT strategy for the atroposelective synthesis of heterobiaryl compounds.¹⁰⁰ At the same time, Virgil, Stoltz and co-workers reported a similar strategy for the synthesis of axially chiral QUINAP.¹⁰¹ This strategy was later extended in our group to the synthesis of different functionalized heterobiaryls, among the most relevant examples included a Pd-catalyzed C-P coupling,¹⁰² a Buchwald-Hartwig amination,¹⁰³ a Cu-free

¹⁰⁰ A. Ros, B. Estepa, P. Ramírez-López, E. Álvarez, R. Fernández, J. M. Lassaletta, *J. Am. Chem. Soc.* **2013**, *135*, 15730–15733.

¹⁰¹ V. Bhat, S. Wang, B. M. Stoltz, S. C. Virgil, *J. Am. Chem. Soc.* **2013**, *135*, 16829–16832.

¹⁰² P. Ramírez-López, A. Ros, B. Estepa, R. Fernández, B. Fiser, E. Gómez-Bengoa, J. M. Lassaletta, *ACS Catal.* **2016**, *6*, 3955–3964.

¹⁰³ P. Ramírez-López, A. Ros, A. Romero-Arenas, J. Iglesias-Sigüenza, R. Fernández, J. M. Lassaletta, *J. Am. Chem. Soc.* **2016**, *138*, 12053–12056.

atroposelective Sonogashira alkynylation,¹⁰⁴ a Pd-catalyzed Heck reaction¹⁰⁵ and finally an asymmetric cross-coupling using *N*-tosylhydrazones.¹⁰⁶

These examples will be reviewed in more detail in **Chapter II**.

I.4. Central and axial chirality: thermodynamic control.

Bridged biaryls are a particular class of atropoisomers in which the biaryl unit is connected by a cyclic system, with the *ortho*, *ortho'* substituents being replaced by a bridge. The size of the bridging ring has a significant impact on the rotation, as well as the nature of substituents placed at the *ortho*-positions to the biphenyl moiety.^{22,23} Bridged biaryls bearing seven-, eight- or nine-membered (hetero)cyclic rings may be resolved as atropisomers.

In systems where the bridge is formed for only one carbon atom (five-membered bridged biaryls), rotation is not hindered at room temperature. A six-membered bridge biaryl still facilitates the rotation; however, Bringmann and co-workers¹⁰⁷ determined that the barrier of racemization increased with the steric hindrance of an extra *ortho*-substituent, and therefore, the enantiomers can be resolved by physical and chemical methods. Among all the structures, eight-membered bridged biaryl present the higher configurational stability due to their rigid-cage-like framework (**figure 7**).¹⁰⁸

Moreover, the presence of a stereogenic center in the bridge can strongly increase the rigidity and influence the thermodynamic equilibrium, adopting the most

¹⁰⁴ V. Hornillos, A. Ros, P. Ramírez-López, J. Iglesias-Sigüenza, R. Fernández, J. M. Lassaletta, *Chem. Commun.* **2016**, 52, 14121–14124.

¹⁰⁵ J. A. Carmona, V. Hornillos, P. Ramírez-López, A. Ros, J. Iglesias-Sigüenza, E. Gómez-Bengoia, R. Fernández, J. M. Lassaletta, *J. Am. Chem. Soc.* **2018**, 140, 11067–11075.

¹⁰⁶ S. Kattela, C. R. D. Correia, A. Ros, V. Hornillos, J. Iglesias-Sigüenza, R. Fernández, J. M. Lassaletta, *Org. Lett.* **2022**, 24, 3812–3816.

¹⁰⁷ a) K. Peters, E.-M. Peters, H. G. von Schnering, G. Bringmann, T. Hartung, O. Schupp, *Z. Kristallogr.* **1992**, 202, 271–274 b) G. Bringmann, M. Heubes, M. Breuning, L. Göbel, M. Ochse, B. Schöner, O. Schupp, *J. Org. Chem.* **2000**, 65, 722–728.

¹⁰⁸ H. Tabata, H. Suzuki, K. Akiba, H. Takahashi and H. Natsuga, *J. Org. Chem.*, **2010**, 75, 5984–5993.

thermodynamically favourable conformation by a central-to-axial chirality relay process.

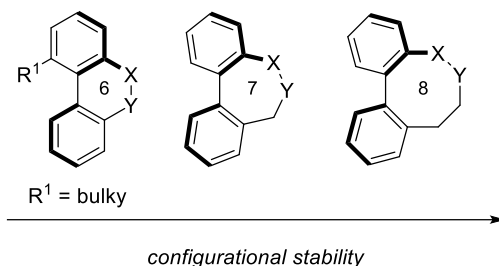


Figure 7: stability of the bridged biaryls.

Medium-size bridged biaryls are present in valuable bioactive molecules, natural products, chiral catalyst and molecular motors.¹⁰⁹ Despite the interesting properties of this class of compounds, their asymmetric synthesis has received less attention compared to other classes of biaryl atropisomers.

A. Seven-membered bridged biaryls.

Most of the catalytic asymmetric synthesis of bridged-biaryls has been described for the construction of seven-membered structures, in particular, *N*-heterocycles and to a lesser extent, carbocycles and silacycles.

The asymmetric synthesis of seven-membered aza-heterocyclic bridged biaryls will be discussed in more detail in **Chapter IV**.

In 2019, Zhou and co-workers described a palladium-catalyzed asymmetric addition of aryl boronic acids to seven-membered cyclic *N*-sulfonyl imides,¹¹⁰ affording chiral ϵ -sultams (**scheme 50A**). Excellent enantioselectivities were obtained for a series of electron-rich and -deficient boronic acids; moreover, the introduction of steric hindrance in the aryl substituents had a minor effect on

¹⁰⁹ For selected examples, see: a) B. Zhang, M. Bao, C. Zeng, X. Zhong, L. Ni, Y. Zeng and X. Cai, *Org. Lett.*, **2014**, *16*, 6400–6403. b) L. Keller, S. Beaumont, J. M. Liu, S. Thoret, J. S. Bignon, J. W. Bakala, P. Dauban and R. H. Dodd, *J. Med. Chem.*, **2008**, *51*, 3414–3421. c) H. J. Lee and K. Maruoka, *Chem. Rec.*, **2022**, e202200004. d) Y. Zhang, Z. Chang, H. Zhao, S. Crespi, B. L. Feringa and D. Zhao, *Chem*, **2020**, *6*, 2420–2429.

¹¹⁰ Z.-B. Zhao, L. Shi, F.-J. Meng, Y. Li, Y.-G. Zhou, *Org. Chem. Front.* **2019**, *6*, 1572–1576.

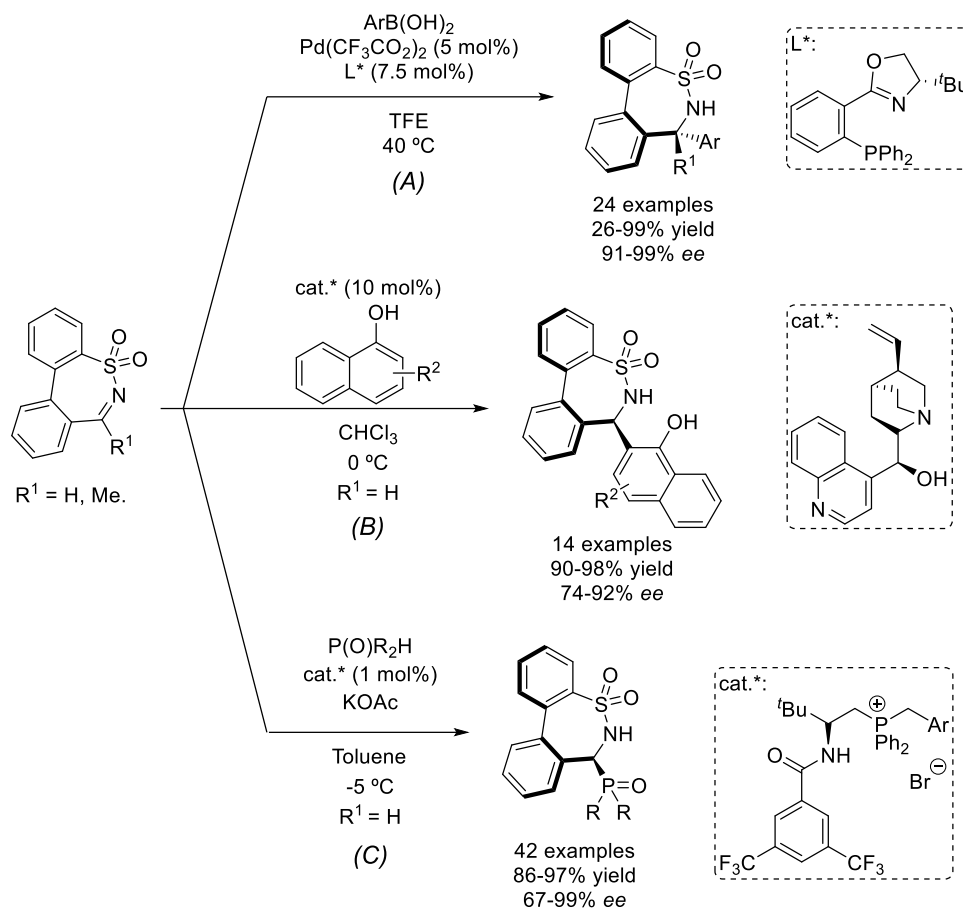
enantioselectivity and reactivity. The origin of the enantioinduction was explained through the coordination of the *N*-sulfonyl imine to the Pd center, minimizing the steric repulsion between the *tert*-butyl and SO₂ groups.

The same research group further reported an aza-Friedel-Crafts reaction using *N*-sulfonyl imines as acceptors.¹¹¹ The reaction was catalyzed by a cinchona alkaloid and afforded excellent yields and optical purities with a variety of 1-naphthols (**scheme 50B**). However, the electronic properties of the cyclic biaryl substrates had an impact on the selectivity of the reaction, as moderate enantioselectivities were obtained for substrates bearing halogen atoms at the *para*-position.

Lastly, the group of Wang reported the synthesis of chiral P-modified ϵ -benzosultams by a hydrophosphonylation reaction, using only 1 mol% of a phase transfer catalyst.¹¹² The phosphorylated products were obtained with moderate to high yields and enantioselectivities (**scheme 50C**), using a series of either aryl or heteroaryl phosphine oxide derivatives. Substitution in the biaryl backbone of the *N*-sulfonyl aldimines also provided the desired ϵ -sutams without compromising the yield or the enantioselectivity.

¹¹¹ Z.-B. Zhao, L. Shi, Y. Li, F.-J. Meng, Y.-G. Zhou, *Org. Biomol. Chem.* **2019**, *17*, 6364–6368.

¹¹² S. Zhang, Z. Feng, C. Jiang, X. Yu, J. Pan, J. Du, Z. Jiang, Y. Chen, T. Wang, *Chem. Eur. J.* **2021**, *27*, 11285–11290.

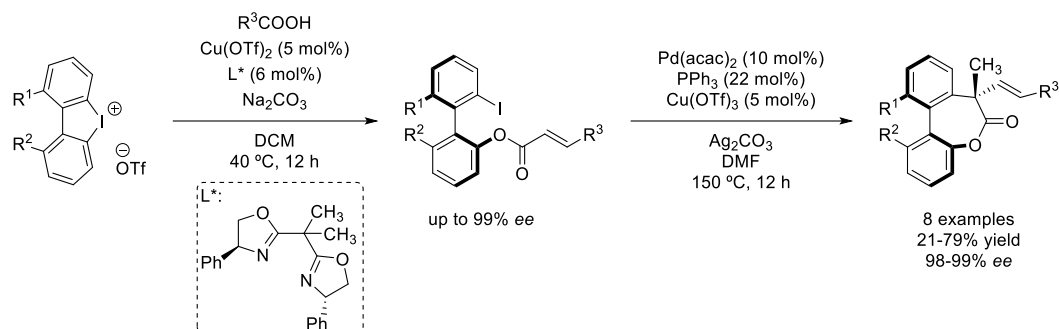


Scheme 50: entantioselective synthesis of seven-membered cyclic sulfonamides.

There is still a lack of synthetic methods for the preparation of seven-membered oxacyclic bridged biaryls. Nonetheless, in 2019, Xue *et al.* reported the enantioselective synthesis of lactone-bridged biaryls using cyclic diaryliodonium salts, that act as double electrophiles in the reaction with α,β -unsaturated carboxylic acids (**scheme 51**).¹¹³ First, axially chiral *tetra*-substituted biaryls are obtained through a ring-opening reaction catalyzed by the chiral copper complex. Next, an intramolecular Heck reaction using $\text{Pd}(\text{acac})_2/\text{PPh}_3/\text{Cu}(\text{OTf})_2$ as catalyst was

¹¹³ X. Xue, Z. Gu, *Org. Lett.* **2019**, *21*, 3942–3945.

performed, obtaining moderate yields but excellent enantioselectivities, with only one diastereomer observed in all cases.



Scheme 51: asymmetric synthesis of lactone-bridged biaryls *via* Pd-catalyzed Heck cyclization.

There are not many straightforward approaches for the synthesis of dibenzocycloheptanes described in the bibliography. The most direct strategies are based on arylation reactions¹¹⁴ or oxidative cross-couplings.¹¹⁵ However, these methods needed several synthetic steps, high temperatures and long reaction times. In 2021, Ramasastry and co-workers described a Morita-Baylis-Hillman reaction of biaryl enone-aldehydes.¹¹⁶

B. Eight-membered bridged biaryls.

Until recently, the catalytic asymmetric synthesis of eight- and -nine-membered bridged biaryls has remained elusive. This could be explained due to the presence of unfavourable transannular interactions arising from the lack of space inside the ring, along with unfavourable enthalpy and entropy factors.¹¹⁷

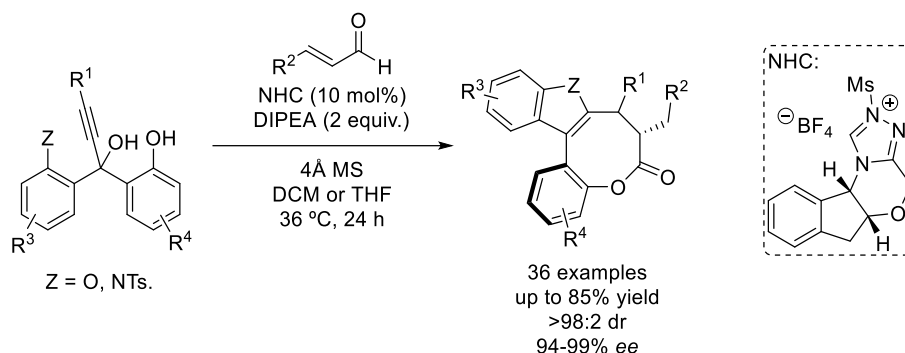
¹¹⁴ a) M. Leblanc, K. Fagnou, *Org. Lett.*, **2005**, *7*, 2849–2852. b) P.-S. Wang, X.-L. Zhou, L.-Z. Gong, *Org. Lett.*, **2014**, *16*, 976–979.

¹¹⁵ K. Hackeloer, G. Schnakenburg, S. R. Waldvogel, *Org. Lett.*, **2011**, *13*, 916–919.

¹¹⁶ A. Mondal, Shivangi, P. Tung, S. V. Wagulde, S. S. V. Ramasastry, *Chem. Commun.*, **2021**, *57*, 9260–9263.

¹¹⁷ R. L. Reyes, T. Iwai and M. Sawamura, *Chem. Rev.*, **2021**, *121*, 8926–8947.

Wong and Zhao described the synthesis of eight-membered bridged heterobiaryls bearing central and axial chirality,¹¹⁸ using an *N*-heterocyclic carbene (NHC) to promote the cyclization between racemic propargylic alcohols and α,β -unsaturated aldehydes (**scheme 52**). Benzofuran- or indole-containing biaryl moieties with an eight-membered lactone bridge were obtained in good yields. It was found that the use of internal alkynes led to lower yields and diastereoselectivities, but without compromising the enantioselectivity.

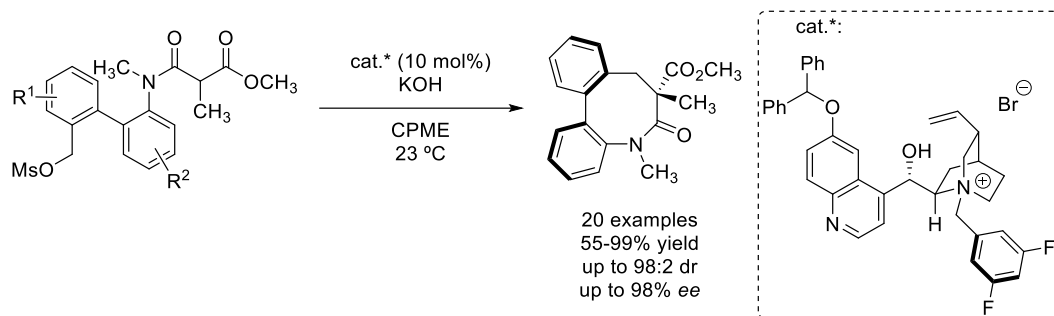


Scheme 52: stereoselective synthesis of eight-membered bridged biaryl lactones *via* NHC-cascade reaction.

Recently, Smith and co-workers reported an enantioconvergent counterion mediated cyclization for the synthesis of highly constrained eight-membered lactams (**scheme 53**).¹¹⁹ A variety of bridged-biaryls bearing different substituents were obtained from racemic substrates, with moderate to excellent yields and excellent enantioselectivities. Mechanistically, the nitrogen pyramidalization help to reduce the rotational barrier in the anilide substrate, thus facilitating the formation of the enolate, and the conformational equilibration of the substrate before the cyclisation.

¹¹⁸ S. Lu, J. Y. Ong, H. Yang, S. B. Poh, X. Liew, C. S. D. Seow, M. W. Wong, Y. Zhao, *J. Am. Chem. Soc.*, **2019**, *141*, 17062–17067.

¹¹⁹ J. Y. Du, T. Balan, T. D. W. Claridge and M. D. Smith, *J. Am. Chem. Soc.*, **2022**, *144*, 14790–14797.



Scheme 53: chiral counterion-mediated synthesis of eight-membered bridged lactams.

CHAPTER II

*Atroposelective Iridium Catalyzed Transfer
Hydrogenative Allylation of
Quinolinealdehydes by Dynamic Kinetic
Resolution.*

Unpublished results.

II. Atroposelective iridium catalyzed transfer hydrogenative allylation of quinolinealdehydes by Dynamic Kinetic Resolution

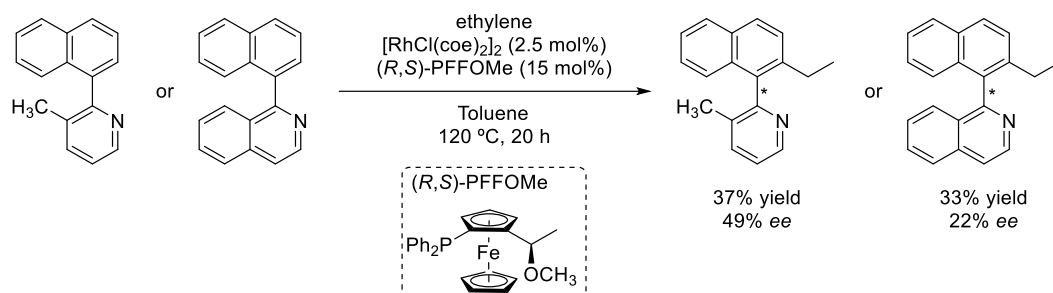
II.1. Introduction.

II.1.1. Isoquinolines.

Over the last 15 years, an important number of methodologies have been developed for the enantioselective synthesis of biaryl compounds bearing a C-C stereogenic axis.^{8b,c} In contrast, methodologies for the synthesis of heterobiaryls atropisomers (*e.g.*, aryl-(iso)quinoline and analogues) are more limited. This is consequence of the coordination of the heteroatoms of the substrate to the metal catalyst, which interfere in the catalytic cycles; and to the relatively lower configurational stability of these compounds.

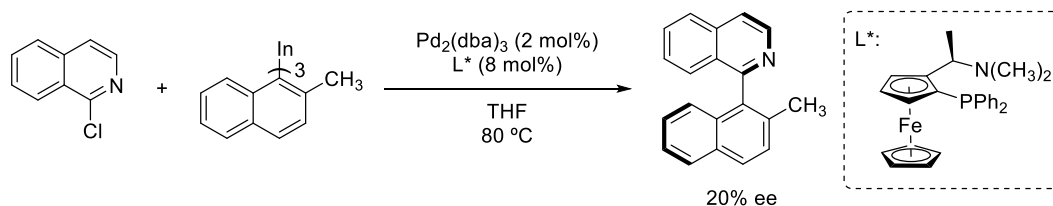
In the earlies 2000, Murai and co-workers reported the first atroposelective desymmetrization of naphtyl isoquinoline or naphtyl 3-methylpyridine derivatives via C-H bond functionalization (**scheme 54**).¹²⁰ The hydroarylation of ethylene was achieved using a rhodium complex catalyst bearing a chiral ferrocenyl phosphine ligand. Nonetheless, the conversion and enantioselectivities achieved for both naphtyl derivatives were low (37% yield and 49% *ee* for naphtyl 3-methylpyridine; 33% yield and 22% *ee* for naphtyl isoquinoline) and attempts to decrease of temperature to 60 °C resulted in an important reduction of the reaction rate. Although yield and enantioselectivities were very modest, this protocol set the bases for the atroposelective synthesis of heterobiaryls compounds.

¹²⁰ F. Kakiuchi, P. Le Gendre, A. Yamada, H. Ohtaki, S. Murai, *Tetrahedron*, **2000**, *11*, 13, 2647–2651.



Scheme 54: first atroposelective alkylation of naphthyl derivatives.

In 2013, Sarandeses y Pérez-Sestelo reported a palladium-catalyzed direct cross-coupling of halonaphthalenes with triaryliindium reagents (**scheme 55**), using a chiral ferrocenyl ligand. Triorganoindium compounds were chosen as reagents due to their excellent performance in the cross-coupling reactions of highly hindered systems.¹²¹ Although good to moderate yields and moderate enantioselectivities were obtained in the reaction, only a single aryl-heterobiaryl coupling product was obtained in moderate yield (78%) but, disappointingly, low 20% enantiomeric excess.



Scheme 55: cross-coupling reaction for the atroposelective synthesis of heterobiaryls developed by Sarandeses.

Highly enantioselective catalytic synthesis of heterobiaryls have also been reported *via* [2+2+2] cycloadditions. Thus, Gutnov and Heller described in 2004 an enantioselective synthesis of 2-arylpyridines through a cobalt(I)-catalyzed cycloaddition of alkynes and nitriles,^{122a} affording excellent enantioselectivities (up

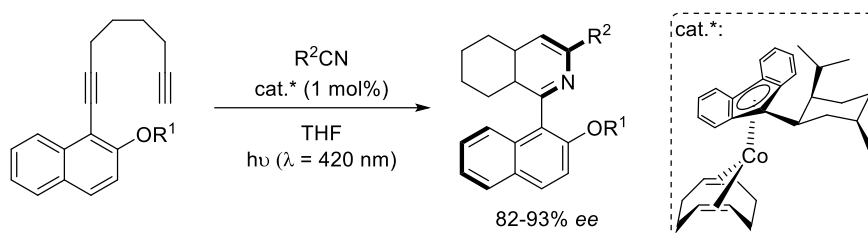
¹²¹ A. Mosquera, M. A. Pena, J. Pérez-Sestelo, L. A. Sarandeses, *Eur. J. Org. Chem.* **2013**, 2555–2562.

¹²² a) A. Gutnov, B. Heller, C. Fischer, H.-J. Drexler, A. Spannenberg, B. Sundermann, C. Sundermann, *Angew. Chem. Int. Ed.* **2004**, 43, 3795–3797. b) M. Hapke, K. Kral, C. Fischer, A. Spannenberg, A. Gutnov, D. Redkin, B. Heller, *J. Org. Chem.* **2010**, 75, 3993–4003.

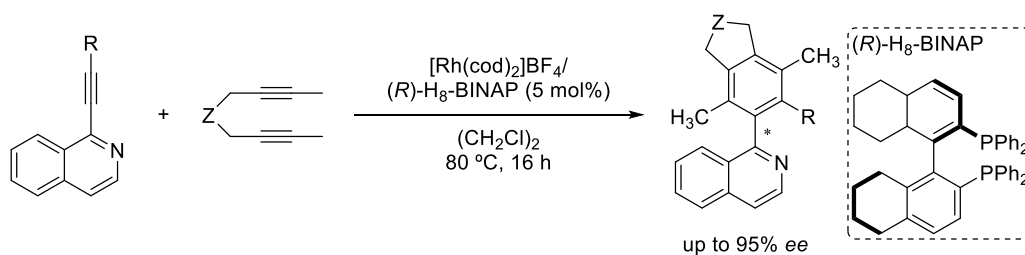
to 98% *ee* after recrystallization), for the use of bulky substrates (**scheme 56A**). The enantioselectivity did not depend on the solvent or the radiation wavelength used, but a reduced conversion was observed by lowering the temperature. In 2010, the scope of the reaction was further extended, using the same catalytic system.^{122b}

One year later, the group of Tanaka described the highly enantioselective synthesis of 1-arylisquinolines featuring axial chirality, via rhodium-catalyzed [2+2+2] intermolecular cycloaddition (**scheme 56B**).¹²³

A: Gutnov, Heller. 2004, 2010.



B: Tanaka, 2011.



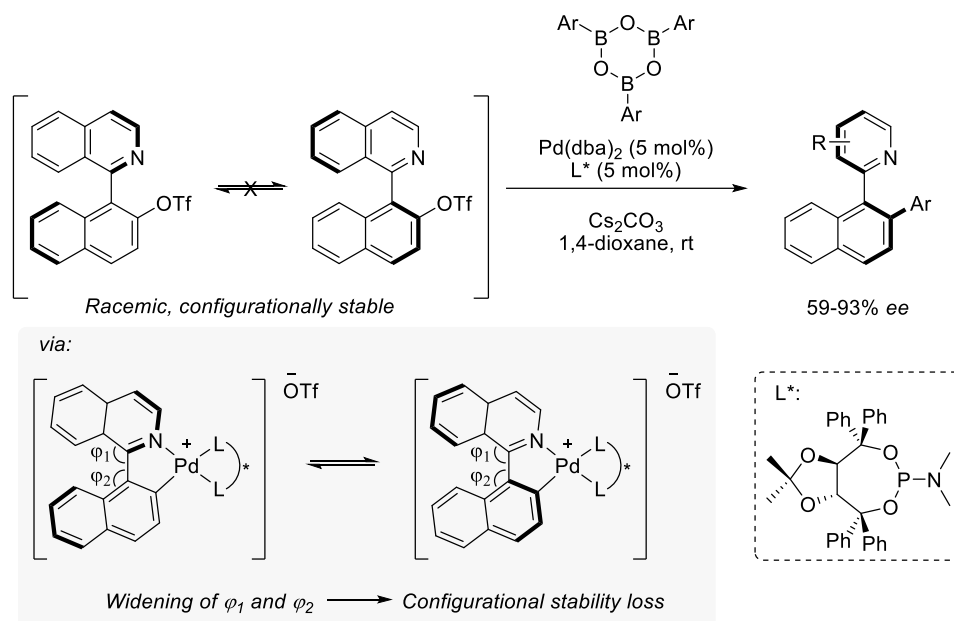
Scheme 56: [2+2+2] cycloadditions reactions for the atroposelective construction of stereogenic axis.

II.1.1.1. Dynamic Kinetic Asymmetric Transformations.

In 2013, our research group reported the first example of a DYKAT strategy applied to the synthesis of axially chiral heterobiaryls.¹⁰⁰ The reaction consists of the palladium-catalyzed Suzuki coupling between arylboroxine derivatives and naphthylisoquinoline triflates, using a TADDOL-derived phosphoramidite ligand. The formation of a five-membered palladacycle intermediate, facilitated by the poor

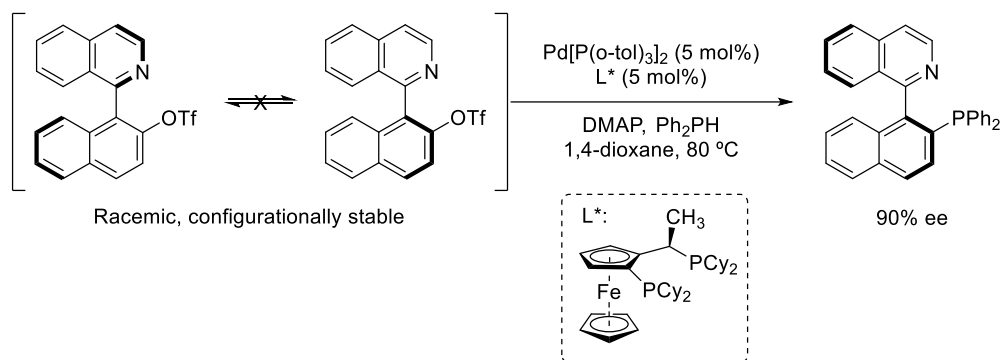
¹²³ N. Sakiyama, D. Hojo, K. Noguchi, K. Tanaka, *Chem. Eur. J.* **2011**, *17*, 1428 – 1432.

coordination ability of the triflate anion, was key for the success of the resolution. Indeed, the enantioselectivity was significantly lower when naphthylisoquinoline bromide was used as substrate. The resulting cationic palladacycle presented a significant widening of the angles φ_1 and φ_2 , which compromises its configurational stability, allowing for the interconversion between both diastereomeric intermediates (**scheme 57**).



Scheme 57: DYKAT strategy for the synthesis of axially chiral heterobiaryls developed by Fernández and Lassaletta.

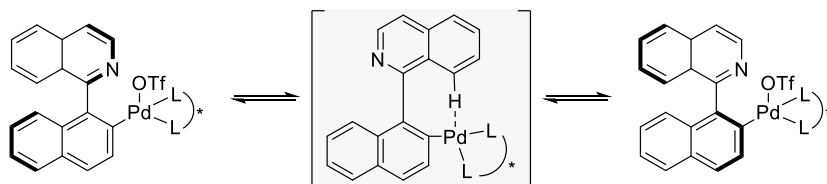
At the same time, Stoltz and Virgil reported a similar strategy for the asymmetric synthesis of QUINAP, using a palladium/JosiPhos catalyst (**scheme 58**).¹⁰¹ Although, (*S*)-QUINAP was obtained in good yields (86%) and excellent optical purity (90% *ee*; 95% *ee* after recrystallization), poor enantioselectivities were observed when other arylphosphines were tested.



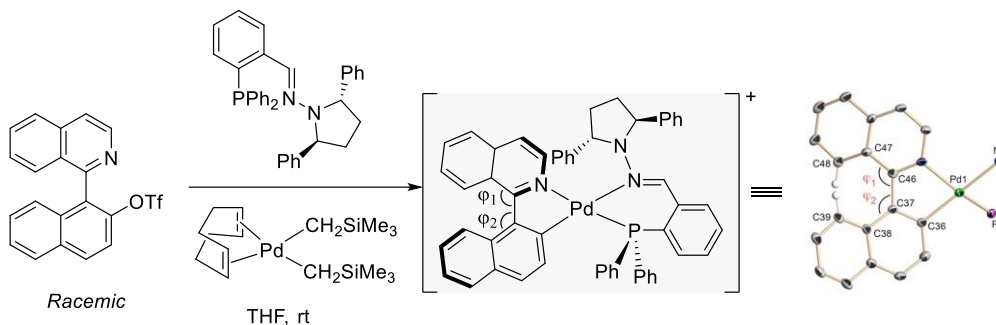
Scheme 58: DYKAT strategy developed by Stoltz and Virgil for the synthesis of QUINAP.

Stoltz and Virgil proposed that the isomerization of the palladacycle intermediate took place through an agostic interaction between the isoquinoline peri-hydrogen and the cationic palladium atom, that stabilized the intermediate (**scheme 59A**). This mechanistic proposal was merely speculative compared with the atropisomerization mechanism described by our research group (**scheme 59B**), which was supported by the isolation and further X-Ray analysis of the oxidative addition intermediate.

A. Stoltz and Virgil DYKAT proposed atropisomerization mechanism:



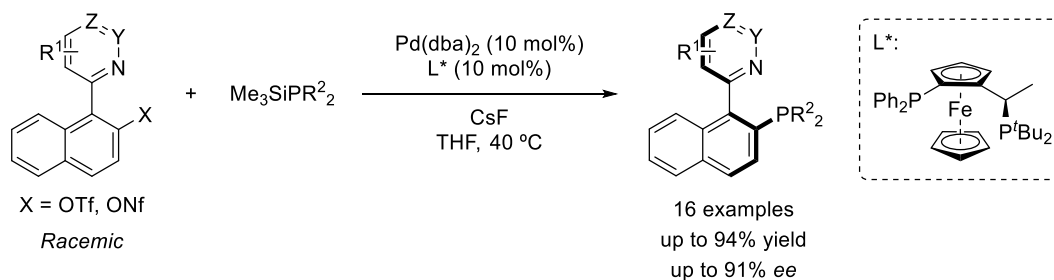
B: Fernández and Lassaletta atropisomerization mechanism:



Scheme 59: comparison of atropisomerization mechanisms.

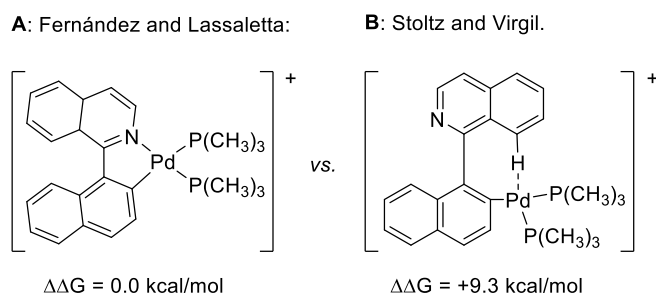
The DYKAT strategy was further extended in our research group to different C-C, C-P and C-N cross-coupling reactions.

Thus, in 2016, an improved DYKAT-based method was reported for the C-P bond formation.¹⁰² Likewise, the strategy was based on: (i) the poor coordination ability of the triflate anion, affording a cationic five-membered palladacycle intermediate; and (ii) the faster interconversion of the oxidative addition intermediates, compared with the translocation step, that allowed for the DYKAT. In this case, the use of silylphosphine reagents allowed for an excellent control of the translocation rate, due to their capacity to slowly release the active nucleophile specie. Under the optimized conditions, that were otherwise highly dependent on the reagents purity and dryness, excellent yield and enantioselectivity were obtained for a wide variety of axially chiral heterobiaryls, with (*R*)-QUINAP being obtained with 99% *ee* after recrystallization.



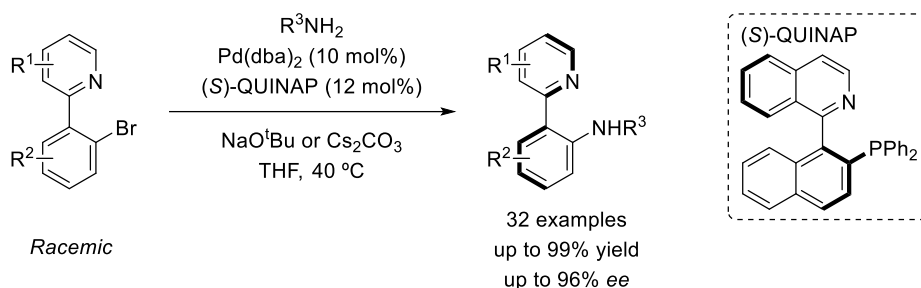
Scheme 60: dynamic kinetic asymmetric C-P cross-coupling for the synthesis of heterobiaryls.

Moreover, computational studies were carried out to elucidate the reaction mechanism. As previously stated, our research group proposed a five-membered cationic palladacycle oxidative addition intermediate (**scheme 61A**), while Stoltz and Virgil suggested an agostic Pd–H(8) interaction (**scheme 61B**), where the presence of the isoquinoline nitrogen did not play any role. DFT calculations revealed that the transition state proposed by Stoltz and Virgil was much more unstable ($\Delta\Delta G = +9.3$ kcal·mol⁻¹), being this energy difference substantially high to discard its participation in the mechanism.



Scheme 61: comparison of the stabilization interactions on the atropisomerization mechanisms.

Next, the DYKAT strategy was applied to the synthesis of axially chiral diamines through a Buchwald-Hartwig reaction.¹⁰³ In this work, the synthesis of IAN-type *N,N*-ligands was accomplished, affording excellent yields and optical purities (**scheme 62**).



Scheme 62: Dynamic Kinetic Asymmetric C-N cross-coupling via Buchwald-Hartwig amination.

Interestingly, when the oxidative addition intermediate was isolated from the heterobiaryl bromide, a complex mixture including cationic and neutral forms were observed. X-Ray analysis showed that the bromine atom remained coordinated to the Pd-atom while the isoquinoline and the 2-naphtyl rings were found to be placed almost perpendicular (**figure 8**). This was explained by the higher coordinating ability of the bromine compared with triflate. Addition of NaO^tBu led to an exchange of Br⁻ ligand for ^tBuO⁻, eased by the precipitation of NaBr, which enables the reaction to progress in a similar fashion as with the sulfonate analogues.

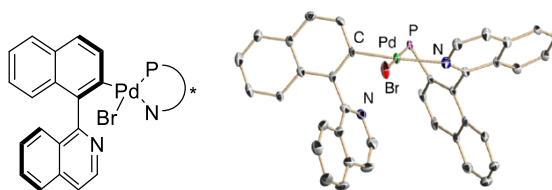
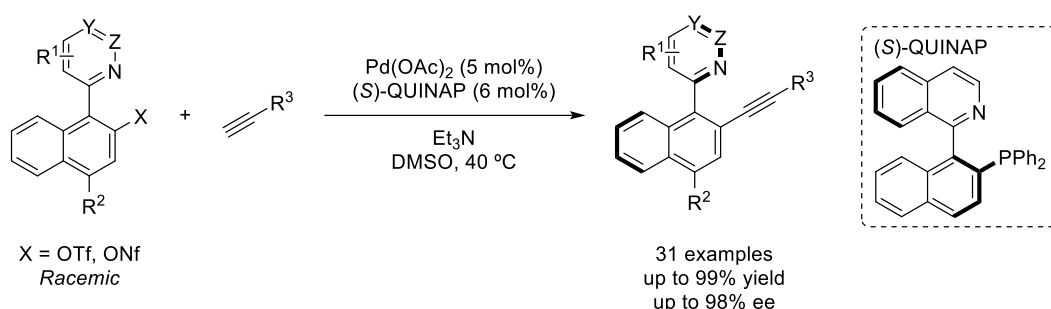


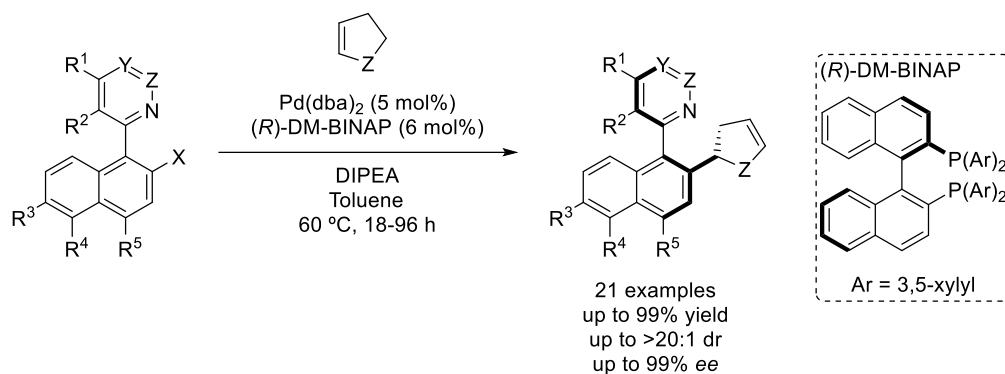
Figure 8: analysis of the oxidative addition intermediate.

The asymmetric alkylation of naphthyl isoquinoline sulfonates, by a Cu-free atroposelective Sonogashira cross-coupling,¹⁰⁴ was then performed using QUINAP as a chiral ligand (**scheme 63**). A large variety of terminal alkynes bearing aromatic and aliphatic substituents performed well in the reaction, affording excellent selectivities under mild conditions.



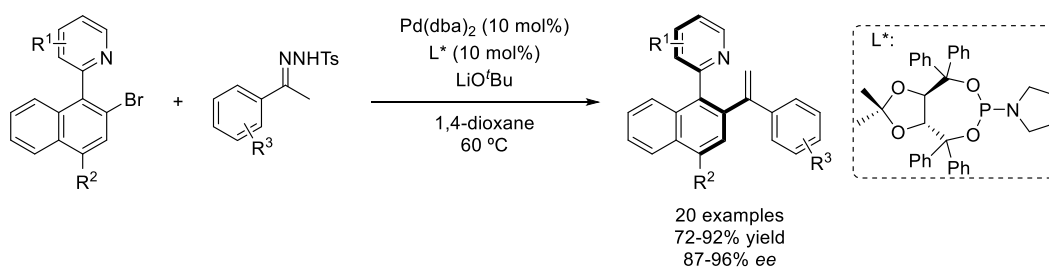
Scheme 63: Dynamic Kinetic Asymmetric alkylation of heterobiaryl sulfonates.

Examples of simultaneous generation of central and axial chirality are rare in literature. In 2018 our research group described a dynamic kinetic asymmetric Heck reaction for the synthesis of heterobiaryls bearing central and axial stereogenic elements.¹⁰⁵ This transformation was challenging since eight different stereoisomers could be obtained, considering the formation of the two stereogenic elements and the possible double bond migration in the cyclic alkene. Nevertheless, excellent yields and enantioselectivities were observed in the reaction of different heterobiaryl sulfonates with electron-rich cyclic and acyclic olefins, with diastereomeric ratios up to 20:1 and selective double bond migration (for cyclic systems) in nearly all cases (**Scheme 64**).



Scheme 64: DYKAT Heck reaction for the synthesis of heterobiaryls with central and axial chirality.

Very recently, our research group reported a dynamic kinetic asymmetric coupling between heterobiaryl bromides and *N*-tosyl hydrazones,¹⁰⁶ using a combination of $\text{Pd}(\text{dba})_2$ as precatalyst and TADDOL-derived phosphoramidite ligand, affording excellent enantioselectivities for a broad scope of axially chiral heterobiaryl styrenes (**scheme 65**).

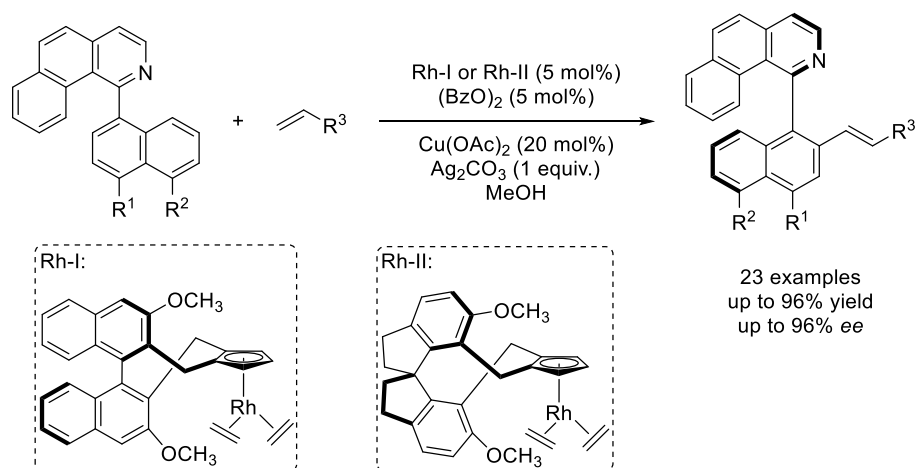


Scheme 65: Pd-catalyzed DYKAT for the synthesis of heterobiaryl styrenes.

II.1.1.2. Desymmetrizations.

An alternative approach to synthesize axially chiral naphthyl isoquinoline derivatives consist of desymmetrization reactions, in which achiral biaryl substrates are converted into an axially chiral compound, due to the increase in the rotational barrier.

You and co-workers reported in 2014^{124a} and further improved in 2016^{124b} a C-H functionalization using a Cp-rhodium catalysis. The alkenylation reaction afforded the axially chiral biaryls in good to excellent yields and enantioselectivities with either aryl or alkyl substituted olefins, under mild reaction conditions (room temperature).



Scheme 66: construction of axial chirality by rhodium-catalyzed asymmetric dehydrogenative Heck coupling.

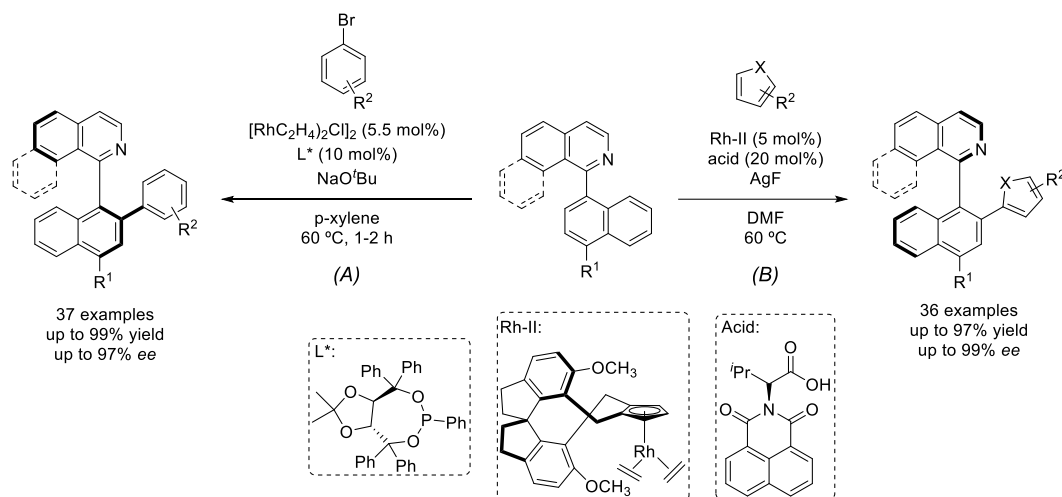
A few years later, the same research group described a C-H arylation reaction using a Rh/TADDOL-derived monodentate phosphite ligand.¹²⁵ In this case, configurationally labile naphthyl isoquinolines were coupled with different bromo-(hetero)aryl derivatives, bearing various substituents, leading to the corresponding axially chiral isoquinolines in up to 99% *ee* (**scheme 67A**). The potential of the obtained axially chiral quinolines was demonstrated, when the corresponding *N*-oxide was used as a ligand in the allylation of benzaldehyde with allyltrichlorosilane, affording high enantioselectivity (91% *ee*) for the resulting homoallylic alcohol.

Further on, You and co-workers used their previously developed Rh-II complex,^{124b} combined with a chiral carboxylic acid, for an enantioselective C-H/C-H

¹²⁴ a) J. Zheng, S.-L. You, *Angew. Chem. Int. Ed.* **2014**, *53*, 13244–13247. b) J. Zheng, W.-J. Cui, C. Zheng, S.-L. You, *J. Am. Chem. Soc.* **2016**, *138*, 5242–5245.

¹²⁵ a) Q. Wang, Z.-J. Cai, C.-X. Liu, Q. Gu, S.-L. You, *J. Am. Chem. Soc.* **2019**, *141*, 9504–9510.

cross-coupling reaction (**scheme 67B**).¹²⁶ Under the optimized conditions, the configurationally labile naphthyl isoquinoline substrate could be coupled with different heteroarenes bearing electronically different substituents, affording good to excellent yields and enantioselectivities. This methodology provided direct access to atropisomeric heterobiaryls, without the need to introduce reactive functionalities in the substrate.



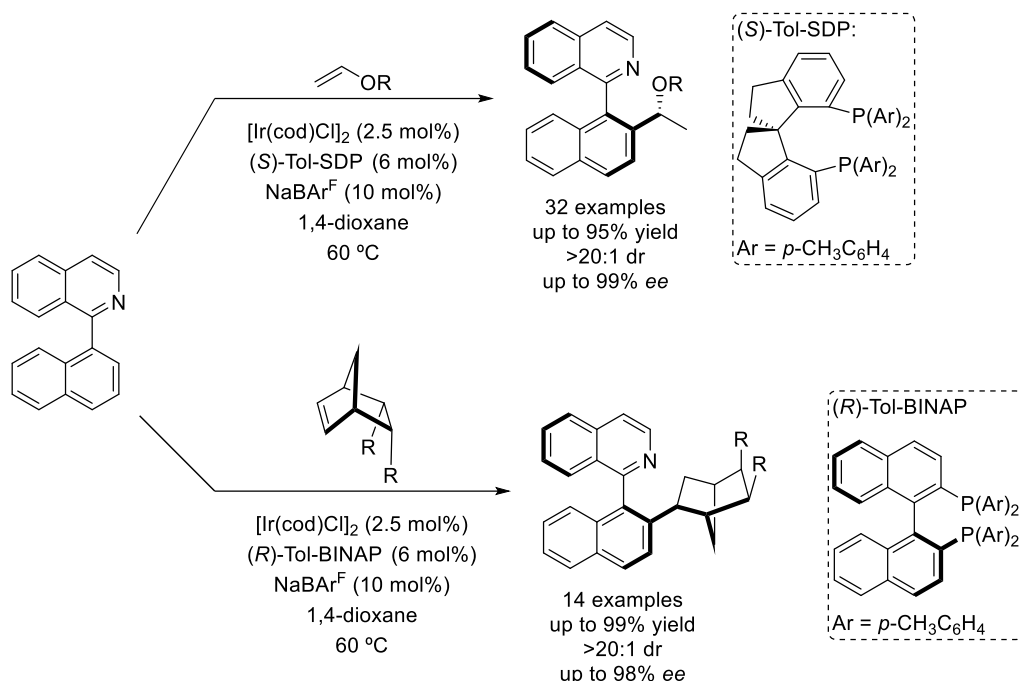
Scheme 67: Rh-catalyzed atroposelective C-H arylation and oxidative C-H/C-H cross-coupling reactions.

In 2019, our research group reported an Ir-catalyzed C-H activation methodology, taking advantage of the *ortho*-directing effect of the heterobiaryl *N*-atom.¹²⁷ This transformation had to overcome various difficulties such as the control in the formation of two chiral elements and the regioselective insertion of the olefin during the migratory insertion step. The combination of an Ir precatalyst with (*S*)-Tol-SDP as ligand and NaBAR^F, afforded a highly regio-, diastereo- (>20:1 dr) and enantioselective (up to 99% *ee*) desymmetrization of heterobiaryls, *via* hydroarylation of acyclic vinyl ethers, 2,3-dihydrofuran and norbornene derivatives.

¹²⁶ Q. Wang, W.-W. Zhang, H. Song, J. Wang, C. Zheng, Q. Gu, S.-L. You, *J. Am. Chem. Soc.* **2020**, *142*, 15678–15685.

¹²⁷ A. Romero-Arenas, V. Hornillos, J. Iglesias-Sigüenza, R. Fernández, J. López-Serrano, A. Ros, J. M. Lassaletta, *J. Am. Chem. Soc.* **2020**, *142*, 2628–2639.

Moreover, computational studies determined that the migratory insertion step into the Ir-C_{aryl} bond was the selectivity-determining step.



Scheme 68: Ir-catalyzed atroposelective desymmetrization of heterobiaryls *via* hydroarylation.

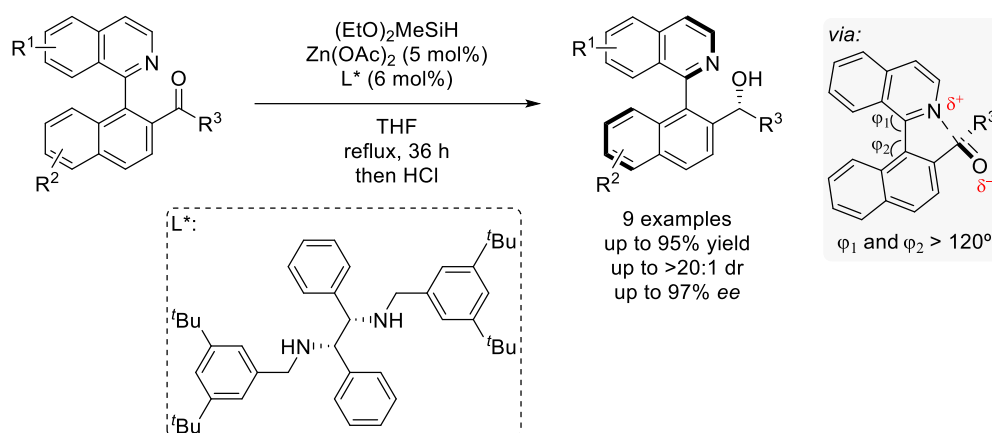
II.1.1.3. Dynamic Kinetic Resolution.

So far, only one dynamic kinetic resolution methodology has been described for the asymmetric synthesis of axially chiral heterobiaryls.

In 2018, our research group reported the first DKR for the asymmetric synthesis of axially chiral heterobiaryls *via* zinc-catalyzed asymmetric hydrosilylation.¹²⁸ The fast atropisomerization takes place through the formation of five-membered transition state, facilitated by a Lewis acid-base interaction between the nitrogen in the heterocycle and the ketone carbonyl, that produces the widening of the angles φ_1 and φ_2 . The use of Zn(OAc)₂ and a chiral diamine as ligand, combined with diethoxymethylsilane as reductant, afforded the corresponding heterobiaryl

¹²⁸ V. Hornillos, J. A. Carmona, A. Ros, J. Iglesias-Sigüenza, J. López-Serrano, R. Fernández, J. M. Lassaletta, *Angew. Chem. Int. Ed.* **2018**, *57*, 3777–3781.

alcohols, with central and axial chirality, in excellent yields and enantioselectivities and moderate to excellent diastereoselectivities. Nevertheless, in all cases, both diastereomers were easily isolated by flash chromatography.



Scheme 69: DKR of heterobiaryl ketones by zinc-catalyzed asymmetric hydrosilylation.

II.1.2. Quinolines.

The catalytic enantioselective synthesis of axially chiral quinoline derivatives remains more elusive than the isoquinoline analogues, despite the potential of this kind of structures as ligands for metal catalysis or for their promising biological activities.¹²⁹ These compounds present much lower configurational stability than the naphthalene analogues, due to the less steric hindrance of the nitrogen lone pair compared with a hydrogen (**figure 9**).

¹²⁹ a) F. Christ, A. Voet, A. Marchand, S. Nicolet, B. A. Desimmie, D. Marchand, D. Bardiot, N. J. Van der Veken, B. Van Remoortel, S. V. Strelkov, M. De Maeyer, P. Chaltin, Z. Debyser, *Nat. Chem. Biol.* **2010**, *6*, 442–448; b) L. D. Fader, E. Malenfant, M. Parisien, R. Carson, F. Bilodeau, S. Landry, M. Pesant, C. Brochu, S. Morin, C. Chabot, T. Halmos, Y. Bousquet, M. D. Bailey, S. H. Kawai, R. Coulombe, S. LaPlante, A. Jakalian, P. K. Bhardwaj, D. Wernic, P. Schroeder, M. Amad, P. Edwards, M. Garneau, J. Duan, M. Cordingley, R. Bethell, S. W. Mason, M. Bcs, P. Bonneau, M.-A. Poupart, A.-M. Faucher, B. Simoneau, C. Fenwick, C. Yoakim, Y. Tsantrizos, *ACS Med. Chem. Lett.* **2014**, *5*, 422–427.

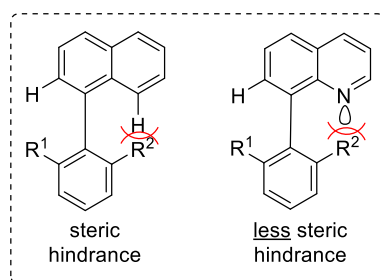
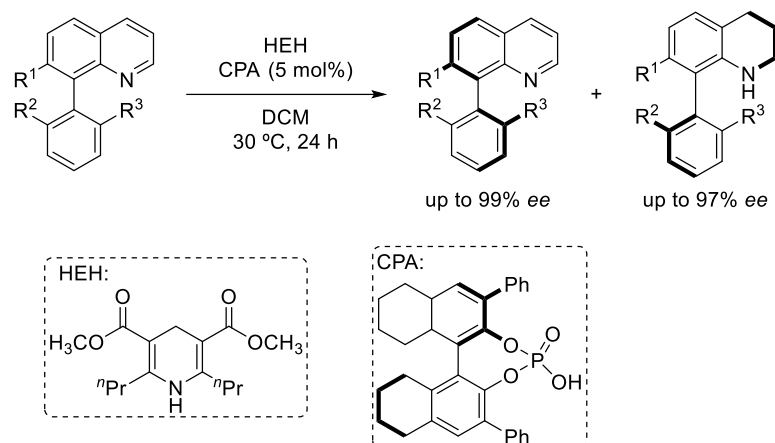


Figure 9: comparison of the configurational stability between axially chiral quinoline and naphthalene analogues.

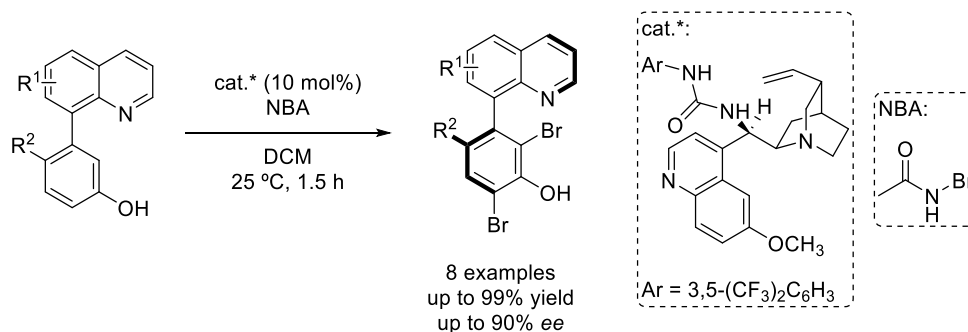
In 2016, the group of Zhou reported a kinetic resolution *via* asymmetric transfer hydrogenation of 5- or 8-substituted axially chiral quinoline derivatives, using a combination of a Hantzsch ester and a chiral phosphoric acid catalyst (**scheme 70**).¹³⁰ It should be emphasized the importance of introducing steric hindrance in the structure of Hantzsch ester to improve the selectivity of the kinetic resolution. The strategy was suitable for a variety of substrates bearing different substituents in the quinoline and the phenyl moiety at C5 or C8 position, affording high selectivity factors (*s*). Moreover, the recovered heterobiaryls present an exceptional configurational stability since heating to 80 °C for 4 h did not result in erosion of the optical purity.

¹³⁰ J. Wang, M.-W. Chen, Y. Ji, S.-B. Hu, Y.-G. Zhou, *J. Am. Chem. Soc.* **2016**, *138*, 10413–10416.



Scheme 70: KR via asymmetric transfer hydrogenation of axially chiral quinoline derivatives.

Later, Miyaji *et al.* described an enantioselective aromatic electrophilic halogenation for the synthesis of axially chiral 8-arylquinoline derivatives, using a bifunctional Cinchona-derived organocatalyst.¹³¹ Substrates bearing substituents at the 5- and 6-position of the quinoline provided moderate enantioselectivities, although they could be improved by a single recrystallization (**scheme 71**). In addition, bromination of mono-*ortho*-chlorinated substrates ($R^2 = \text{Cl}$), also worked well, yielding optically active heterobiaryls with two different halogen groups, that were interesting synthetic precursors for further derivatization.

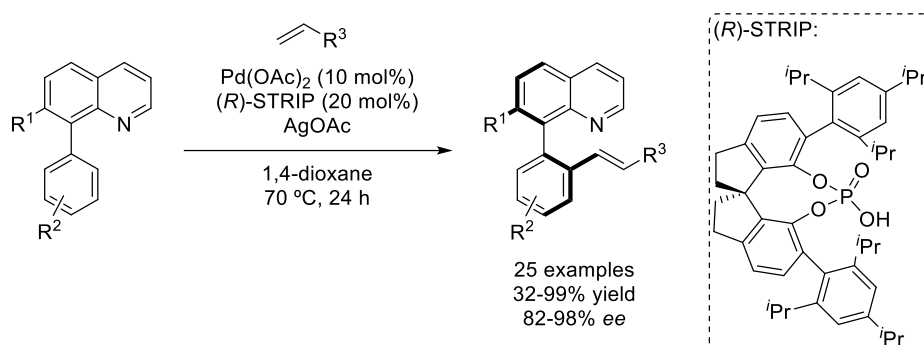


Scheme 71: aromatic electrophilic halogenation described by Miyaji and co-workers.

Two years later, Shi and co-workers identified a novel chiral spiro phosphoric acid organocatalyst (STRIP) that afforded excellent enantioselectivities in the Pd-

¹³¹ R. Miyaji, K. Asano, S. Matsubara, *Chem. Eur. J.* **2017**, *23*, 9996–10000.

catalyzed atroposelective C-H olefination of axially chiral quinoline-derived biaryls.¹³² Although reaction worked well for a variety of quinoline-derived biaryls, the enantioselectivity was very sensitive to the steric hindrance of the group at C2 position of the quinoline (R^1). In addition, substrates bearing electron-rich substituents presented higher reactivity than the electron-deficient ones, while optical purity was independent of the electronic effects (**scheme 72**). It was also found that decreasing the temperature resulted in an erosion of the optical purity. The nature of the olefin was also investigated, obtaining excellent yield and enantioselectivities for different acrylates and styrenes.

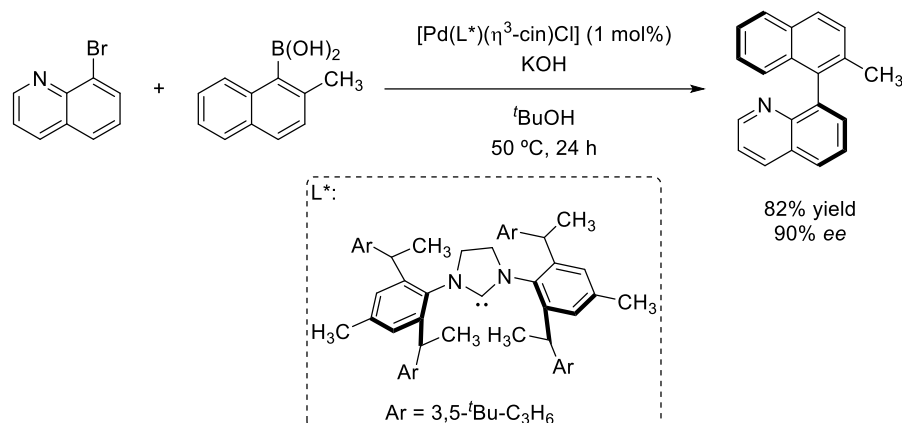


Scheme 72: enantioselective synthesis of biaryl atropisomers by Pd-catalyzed C-H olefination.

The same year, Shen *et al.* reported an enantioselective Suzuki-Miyaura cross-coupling for the synthesis of biaryl atropisomers.¹³³ The use of a bulky chiral *N*-heterocyclic carbene combined with a palladium complex resulted in excellent enantiocontrol for a wide variety of biaryls bearing different electronic substituents. However, only one example of a quinoline-based biaryl was reported, providing 90% *ee* (**scheme 73**).

¹³² J. Luo, T. Zhang, L. Wang, G. Liao, Q.-J. Yao, Y.-J. Wu, B.-B. Zhan, Y. Lan, X.-F. Lin, B.-F. Shi, *Angew. Chem. Int. Ed.* **2019**, *58*, 6708–6712.

¹³³ D. Shen, Y. Xu, S.-L. Shi, *J. Am. Chem. Soc.* **2019**, *141*, 14938–14945.



Scheme 73: axially chiral biaryls via Pd-catalyzed enantioselective Suzuki-Miyaura cross-coupling.

II.1.3. C-Carbonyl allylation via transfer hydrogenative coupling.

C-Allylation of carbonyl compounds is an outstanding process in which homoallylic alcohols are formed in a single step, enabling the construction of complex structures from simple starting materials. Most of the enantioselective versions of this methodology employed chiral allylboranes,^{134a,b} allylsilanes,^{134c,d} and allyltitanocenes;^{134e} or chiral Lewis acid and bases^{134f,g} to catalyzed the reaction (**figure 10**).

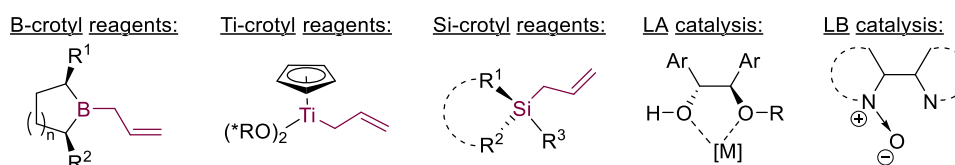


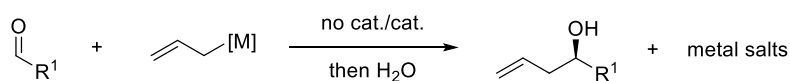
Figure 10: crotylmetal and Lewis acid and bases reagents.

However, these methods utilize stoichiometric quantities of the preformed allyl-metal reagent and therefore generates the same amounts of metal byproducts.

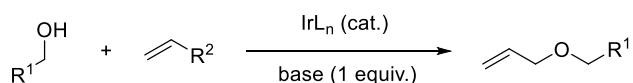
¹³⁴ a) T. Herold, R. W. Hoffmann, *Angew. Chem. Int. Ed. Engl.*, **1978**, 17 (10), 768–769. b) H. C. Brown, P. K. Jadhav, *J. Am. Chem. Soc.* **1983**, 105, 2092–2093. c) J. S. Panek, M. Yang, *J. Am. Chem. Soc.* **1991**, 113 (17), 6594–6600. d) J. W. A. Kinnaird, P. Y. Ng, K. Kubota, X. Wang, J. L. Leighton, *J. Am. Chem. Soc.* **2002**, 124, 7920–7921. e) M. Riediker, R. O. Duthaler, *Angew. Chem. Int. Ed.* **1989**, 28 (4), 494–495. f) V. Rauniyar, D. G. Hall, *Angew. Chem. Int. Ed.* **2006**, 45, 2426–2428. g) A. V. Malkov, L. Dufková, L. Farrugia, P. Kocovsky, *Angew. Chem. Int. Ed.* **2003**, 42, 3674–3677.

In 2008, the group of Krische developed an iridium catalyzed transfer hydrogenative allylation method, that avoids the employ of stoichiometric amounts of preformed organometallic reagents.¹³⁵ These findings were also noteworthy because iridium allylic substitution of alcohol nucleophiles was well known for presenting an *O*-allylation reactivity (**scheme 74**).¹³⁶

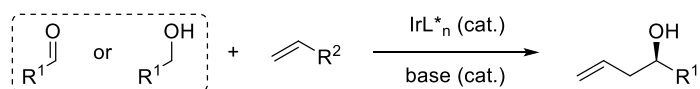
Classical C=O addition. Stoichiometric metals.



O-allylation via Conventional Allylic Substitution:



C-allylation via Transfer Hydrogenative Coupling:



Scheme 74: evolution of C=O addition chemistry beyond the use of stoichiometric metals.

Krische and co-workers investigated the use of allyl acetate as allyl source.^{135a,b} Under transfer hydrogenation conditions, the corresponding enantio-enriched alcohols could be obtained from either the alcohol or the aldehyde oxidation level, using an *ortho*-cyclometalated iridium complex as catalyst. The later presented enough stability to be isolated by flash chromatography and could be recycled multiple times without deterioration of performance. The reaction also required of catalytic amounts of Cs₂CO₃ and *m*-nitrobenzoic acid additives, while other carbonate bases were much less effective. Furthermore, reactions conducted using 2 or 5

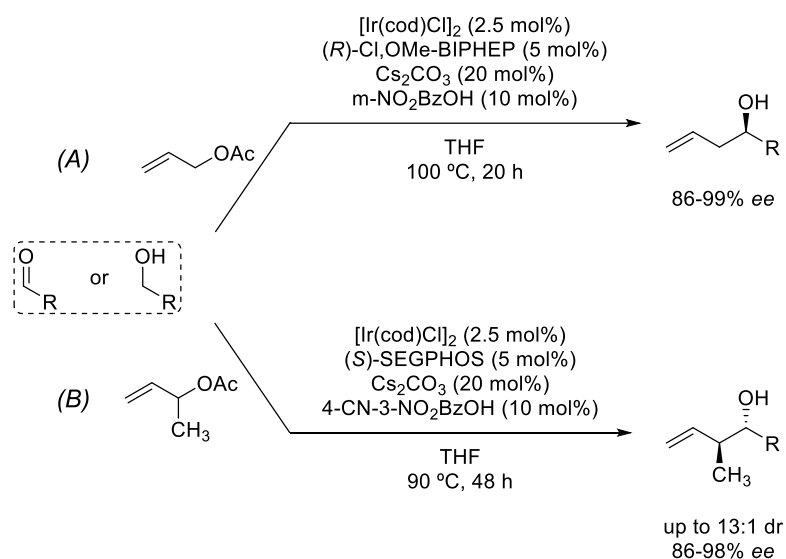
¹³⁵ a) I. S. Kim, M.-Y. Ngai, M. J. Krische, *J. Am. Chem. Soc.* **2008**, *130*, 20, 6340–6341. b) I. S. Kim, M.-Y. Ngai, M. J. Krische, *J. Am. Chem. Soc.* **2008**, *130*, 44, 14891–14899. c) I. S. Kim, S. B. Han, M. J. Krische, *J. Am. Chem. Soc.* **2009**, *131*, 7, 2514–2520.

¹³⁶ For selected bibliography a) F. López, T. Ohmura, J. F. Hartwig, *J. Am. Chem. Soc.*, **2003**, *125*, 3426–3427. b) C. Shu, J. F. Hartwig, *Angew. Chem. Int. Ed.* **2004**, *43*, 4794–4797. c) S. Ueno, J. F. Hartwig, *Angew. Chem. Int. Ed.* **2008**, *47*, 1928–1931.

equivalents of allyl acetate were not as effective than the reactions employing 10 equivalents.

Under the optimized conditions, the reaction between allyl acetate and allylic, aliphatic and benzylic alcohols or aldehydes (for the latter case, isopropanol is used as proton source), affords the corresponding enantioenriched homoallylic alcohols with excellent yields and optical purities. Interestingly, the use of aldehydes as coupling partners provided slightly higher enantioselectivities (**scheme 75A**).

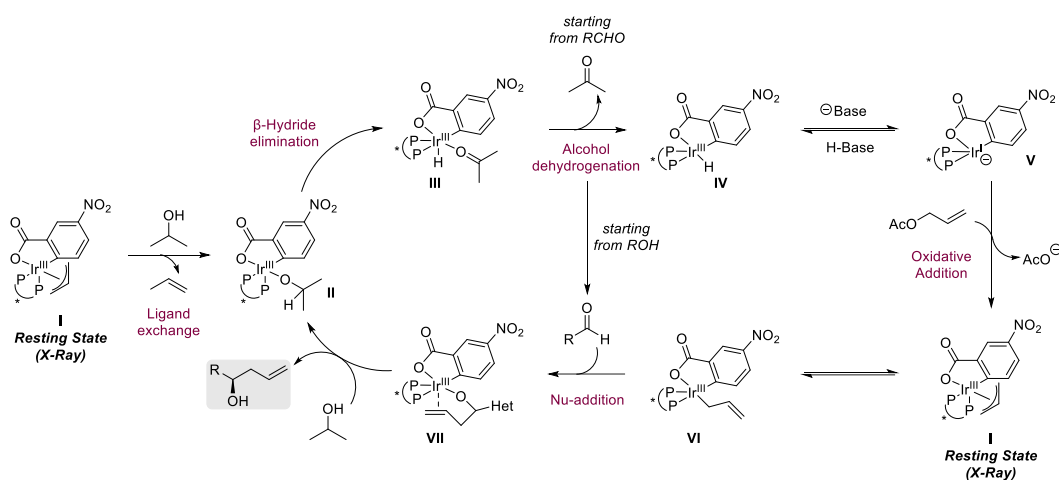
Moreover, the same research group extended the protocol for the highly enantio- and regioselective carbonyl crotylation reaction.^{135c} The process could also be carried out from the alcohol or aldehyde oxidation level, using the same first-generation catalyst, but employing (*S*)-SEGPHOS as a chiral ligand (**scheme 75B**). In this transformation, two chiral centers were formed, with an *anti*-diastereoselectivity that could be explained by the formation of a *cis*- π -crotyl complex. This transformation also afforded better results using aldehyde as reactants.



Scheme 75: enantioselective iridium-catalyzed carbonyl allylation and crotylation from the alcohol or aldehyde oxidation level developed by Krische.

Mechanistically, the catalytic cycle (**scheme 76**) starts with the π -allyl iridium (III) **I** resting state intermediate that undergoes protonolysis with the alcohol reagent,

delivering a pentacoordinate iridium (III) alkoxide **II** and propene. β -Hydride elimination provides an iridium (III) hydride **III** that is converted into an anionic iridium (I) intermediate **V** by deprotonation. Oxidative addition of allyl acetate provides again the π -allyl iridium (III) **I** resting state intermediate, that after nucleophilic addition to the aldehyde, generates an hexacoordinate 18-electron iridium alkoxide **VII**. The latter is reluctant to β -hydride elimination due to coordination of the double bond to the vacant site at iridium (III). This step was also found to be turnover limiting. Finally, ligand exchange with the alcohol reagent gives the pentacoordinate iridium (III) alkoxide **II** that re-enter again into the catalytic cycle, delivering the desired enantioenriched allylic alcohol.¹³⁷



Scheme 76: catalytic mechanism proposed for the iridium catalyzed transfer hydrogenative allylation.

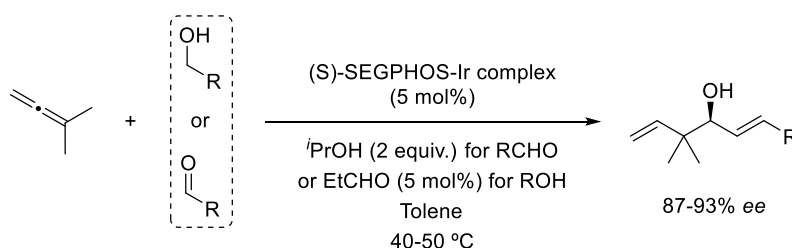
Reactions proceeding from the aldehyde oxidation level require of an alcohol additive (normally isopropanol) that would undergo ligand exchange with η^3 -allyl group followed by β -hydride elimination, to provide the required iridium (III) hydride. This additive is not required if an alcohol is used as a reactant, as it would itself perform the ligand exchange reaction, being delivered as an aldehyde to the reaction medium after β -hydride elimination. Furthermore, the possibility of performing the allylation from the alcohol oxidation level allowed for the use of

¹³⁷ A. Hassan, M. J. Krische, *Org. Process Res. Dev.* **2011**, *15*, 1236–1242.

reagents that are incompatible in conventional allylation processes, such as highly unstable 1,3-dialdehydes. In this case, 1,3-diols are stable and afford useful C₂-symmetric adducts in the absence of protecting groups.¹³⁸

Apart from the previously described carbonyl allylation and crotylation, the use of *ortho*-cyclometalated iridium catalyst was extended to different reactions, such as α -(trimethylsilyl) allylation,^{139a} α -(hydroxymethyl) allylation,^{139b} α -(trifluoromethyl) allylation,^{139c} and α -(hydroxy) allylation,^{139d} affording products bearing interesting functionalities that could be potentially used for further derivatization.

Additionally, allenes were also suitable substrates as allyl donors *via* iridium hydrometallation, promoting enantioselective carbonyl *tert*-prenylation also from the alcohol or aldehyde oxidation level.¹⁴⁰ In this case, the reactions were performed under surprisingly mild conditions (30-50 °C), affording excellent levels of enantioselectivity.



Scheme 77: enantioselective carbonyl *tert*-prenylation from the alcohol or aldehyde oxidation level.

¹³⁸ Y. Lu, I. S. Kim, A. Hassan, D. J. del Valle, M. J. Krische, *Angew. Chem. Int. Ed.* **2009**, *48*, 5018–5021.

¹³⁹ a) S. B. Han, X. Gao, M. J. Krische, *J. Am. Chem. Soc.* **2010**, *132*, 9153–9156. b) Y. J. Zhang, J. H. Zhang, M. J. Krische, *J. Am. Chem. Soc.* **2010**, *132*, 4562–4563. c) X. Gao, Y. J. Zhang, M. J. Krische, *Angew. Chem., Int. Ed.* **2011**, *50*, 4173–4175. d) S. B. Han, H. H. Han, M. J. Krische, *J. Am. Chem. Soc.* **2010**, *132*, 1760–1761.

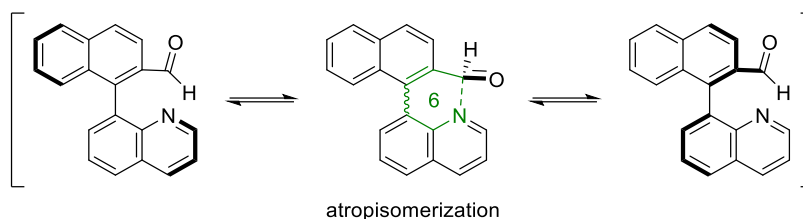
¹⁴⁰ S. B. Han, I. S. Kim, H. Han, M. J. Krische, *J. Am. Chem. Soc.* **2009**, *131*, 6916–6917.

II.2. Objectives.

Over the last few years, our research group has developed two different dynamization strategies for the synthesis of axially chiral (hetero)biaryls; The formation of palladacycle intermediates¹⁴¹ (DYKAT strategy) and, more recently, the use of Lewis acid-base interactions^{95,128} (DKR strategy). For the later, the group initially reported a diastereo- and highly enantioselective DKR of configurationally labile heterobiaryl ketones by zinc-catalyzed hydrosilylation of the carbonyl group, leading to secondary alcohols bearing axial and central chirality.¹²⁸ The atropisomerization was facilitated by the interaction between the carbonyl from the ketone and the nitrogen from the isoquinoline through a five-membered cyclic transition states (**scheme 69**). The interconversion between both atropisomers is consequence of the widening of the angles involved in the labilization of the stereogenic axis.

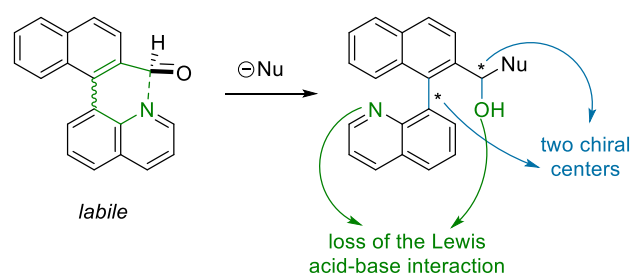
Considering the lack of asymmetric methodologies for the atroposelective synthesis of quinoline-derived atropisomers, we questioned whether it would be possible to apply this strategy for their enantioselective preparation. As a hypothesis, a Lewis acid-base interaction between the nitrogen from the quinoline and a carbonyl group strategically situated at 2' the other aryl ring would facilitate the interconversion between both atropisomers through the formation of six-membered cyclic transition states (**scheme 78**). Regarding the carbonyl functionality, two main functional groups could be introduced: aldehyde or ketone. In our case, we decided to explore the behaviour of an aldehyde moiety because is less hindered and more reactive than a ketone, facilitating the interaction.

¹⁴¹ For selected examples: a) A. Ros, B. Estepa, P. López-Ramírez, E. Álvarez, R. Fernández, J. M. Lassaletta, *J. Am. Chem. Soc.* **2013**, *135*, 42, 15730–15733. b) J. A. Carmona, V. Hornillos, P. López-Ramírez, A. Ros, J. Iglesias-Sigüenza, E. Gómez-Bengoia, R. Fernández, J. M. Lassaletta, *J. Am. Chem. Soc.*, **2018**, *140*, 11067 –11075. c) A. Romero-Arenas, V. Hornillos, J. Iglesias-Sigüenza, R. Fernández, J. López-Serrano, A. Ros, J. M. Lassaletta, *J. Am. Chem. Soc.* **2020**, *142*, 5, 2628–2639.



Scheme 78: labilization strategy via a six-membered cyclic transition state.

In this case, we decided to apply the asymmetric carbonyl allylation developed by Krische and co-workers^{135a,b} to disable the Lewis acid character of the carbonyl group and increase the rotational barrier, resulting in a DKR. It would allow for the synthesis of quinoline-derived atropisomers bearing central and axially chiral elements. In contrast to our previous DKR-based on Lewis pairs interactions, which proceed by a simple reduction of the carbonyl, a new carbon-carbon bond, which introduce the allyl group, an alcohol functionality and a new chiral center will be formed, allowing for further structural variability (**scheme 79**).

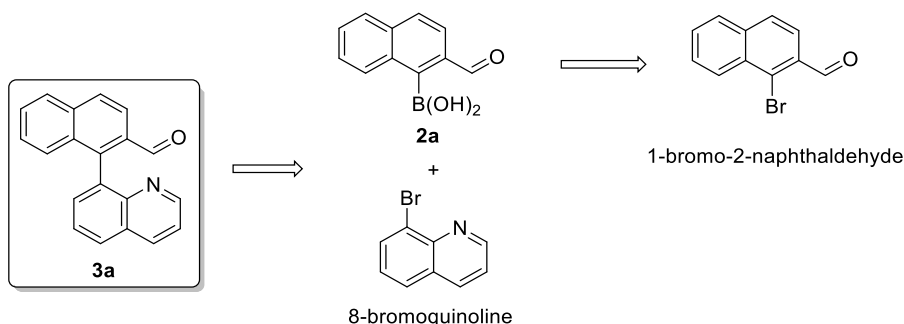


Scheme 79: strategy for the synthesis of enantioenriched quinoline-biaryl derivatives.

II.3. Results and discussion.

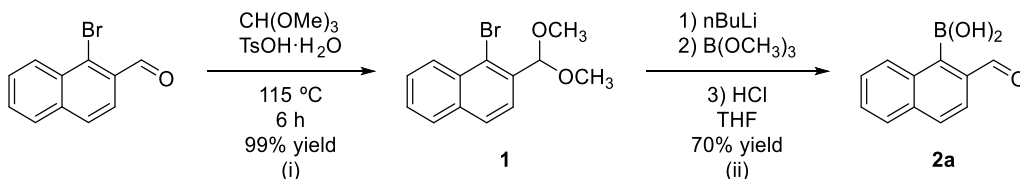
II.3.1. Substrate design and synthesis.

For the preparation of the model substrate **3a**, a retrosynthetic analysis suggested the route showed in **scheme 80** to be done.



Scheme 80: proposed retrosynthetic pathway for accessing naphthylquinoline derivative.

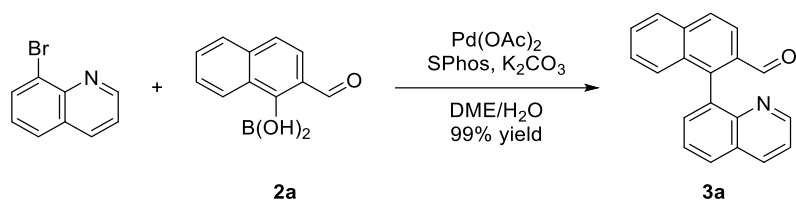
The aldehyde fragment **2a** was synthesized following literature procedures, from commercially available 1-bromo-2-naphthaldehyde, by first protecting the aldehyde with trimethyl orthoformate, followed by a lithiation-borylation reaction that allowed to obtain the boronic acid **2a** after aldehyde deprotection in acidic medium (**scheme 81**).¹⁴²



Scheme 81: synthetic route for the preparation of the boronic acid.

Considering that the 8-bromoquinoline coupling partner was commercially available, the next stage consisted of the Suzuki-Miyaura cross-coupling, to afford the corresponding biaryl **3a** in quantitative yields.

¹⁴² For each reaction step, the corresponding described procedures were followed. For step (i) and (ii): Y. E. Liu, Z. Lu, B. Li, J. Tian, F. Liu, J. Zhao, C. Hou, Y. Li, L. Niu, B. Zhao, *J. Am. Chem. Soc.*, **2016**, *138*, 10730 –10733.



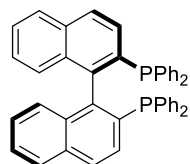
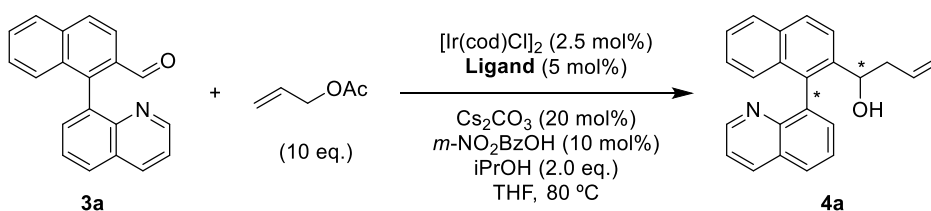
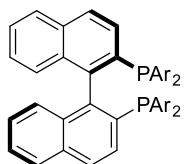
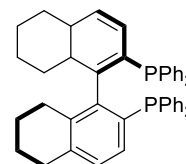
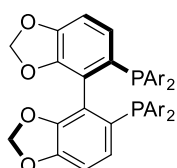
Scheme 82: Suzuki-Miyaura cross coupling for the synthesis of the naphthylquinoline derivative.

II.3.2. Reaction conditions optimization.

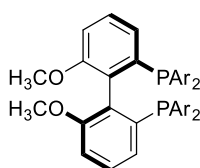
The optimization of the reaction parameters for the atroposelective *C*-allylation between **3a** and allyl acetate was carried out next.

The reaction is catalyzed by an *in situ* generated iridium complex from [Ir(cod)Cl]₂ and a C₂-symmetric bidentate phosphine ligands. We first explore the influence of the phosphine ligand, by using a variety of commercially available chiral C₂-symmetric bisphosphines, in combination with Cs₂CO₃ and *m*-nitrobenzoic acid as additives, with *i*PrOH as hydrogen donor, in THF at 80 °C.

The results were analysed after 48 h and are summarized in **Table 1**.

Table 1: ligand screening for the atroposelective C-allylation of **3a**.**L1:** (*R*)-BINAP**L2:** (*R*)-Tol-BINAP (Ar = *p*-Tolyl)
L3: (*R*)-DM-BINAP (Ar = 3,5-Xylyl)**L4:** (*R*)-H₈-BINAP**L5:** (*R*)-SEGPHOS (Ar = Ph)**L6:** (*R*)-DM-SEGPHOS

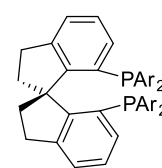
(Ar = 3,5-xylyl)

L7: (*S*)-DTBM-SEGPHOS(Ar = 3,5-*t*Bu-anisole)**L8:** (*R*)-MeO-BIPHEP

(Ar = Ph)

L9: (*R*)-DM-MeO-BIPEP

(Ar = 3,5-Xylyl)

**L10:** (*S*)-Tol-SDP(Ar = *p*-Tolyl)

Entry	Ligand	Conv. (%) ^b	d.r. ^b	ee _{major} (%) ^c	ee _{minor} (%) ^c
1	L1	85	3.6:1	95	95
2	L2	97	4.2:1	96	95
3	L3	89	4.6:1	96	94
4	L4	74	n.d.	n.d.	n.d.
5	L5	>99	2.9:1	98	97
6	L6	76	4.2:1	98	95
7	L7	n.r.	n.d.	n.d.	n.d.
8	L8	>99	3.0:1	96	98
9	L9	75	n.d.	n.d.	n.d.
10	L10	n.r.	n.d.	n.d.	n.d.

n.r. no reaction. N.d. not determined ^a Reaction performed at 0.1 mmol scale for **3a**. ^b Determined by ¹H-NMR spectroscopy. ^c Determined by HPLC on chiral stationary phases.

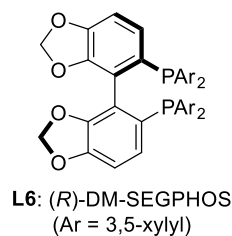
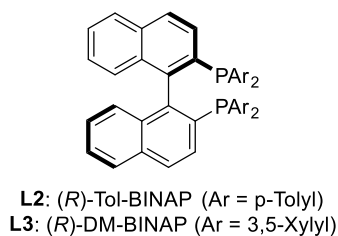
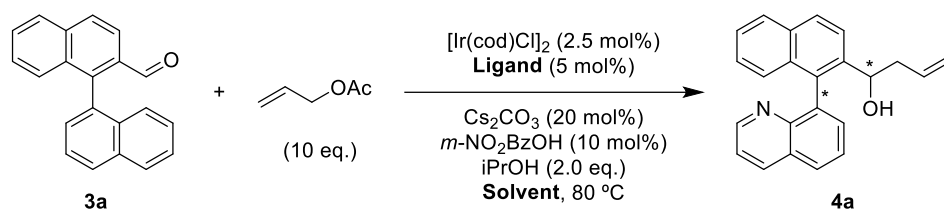
Initially, we applied the optimized reaction conditions described by Krische *et al.* for the allylation of simple aldehydes (**L1**, entry 1).^{135a} To our delight, the desired

product was obtained with high conversion (85%), 3.6:1 d.r. and excellent optical purity (95% *ee* for both diastereoisomers). An increase of diastereoselectivity (4.2:1 and 4.6:1 respectively) was observed for (*R*)-Tol-BINAP (**L2**, entry 2) and (*R*)-DM-BINAP (**L3**, entry 3), while the enantioselectivity remained excellent. In contrast, the use of (*R*)-SEGPHOS (**L5**, entry 5) or (*R*)-MeO-BIPHEP (**L8**, entry 8) led to a decrease on the diastereoselectivity, although full conversion was achieved in both cases.

Disappointingly, poor reactivities were obtained for (*R*)-H₈-BINAP (**L4**, entry 4) and (*R*)-DM-MeO-BIPHEP (**L9**, entry 9), while no reaction resulted, using (*S*)-DTBM-SEGPHOS (**L7**, entry 7) and (*S*)-Tol-SDP (**L10**, entry 10).

We then explore the influence of the solvent in the reaction (**table 2**), using the ligands that afforded the highest diastereo- and enantioselectivity (**L2**, **L3** and **L6**)

Table 2: solvent screening for the atroposelective *C*-allylation of **3a**.



Entry ^a	Ligand	Solvent	Conv. (%) ^b	d.r. ^b	<i>ee</i> _{major} (%) ^c	<i>ee</i> _{minor} (%) ^c
1	L2	1,4-Dioxane	97	4.1:1	96	94
2	L2	DME	95	4.4:1	96	94
3	L2	THF	97	4.2:1	96	95
4	L3	1,4-Dioxane	87	6.3:1	97	96

5	L3	MeCN	40	3.3:1	92	88
6	L3	DMF	63	3.5:1	92	84
7	L3	Toluene	79	2.9:1	91	55
8	L3	MTBE	<10	n.d.	n.d.	n.d.
9	L3	DME	>99	6.3:1	97	99
10	L3	DCE	<10	n.d.	n.d.	n.d.
11	L3	THF	89	4.6:1	96	94
12	L6	1,4-Dioxane	57	3.6:1	96	92
13	L6	DME	39	3.5:1	96	90
14	L6	THF	76	4.2:1	98	95

n.r. no reaction. n.d. not determined. ^a Reactions performed at 0.1 mmol scale of **3a**. ^b Determined by ¹H-NMR spectroscopy. ^c Determined by HPLC on chiral stationary phases.

Nearly no alteration in conversion and selectivity was observed using ligand **L2**, in 1,4-dioxane (entry 1) or DME (entry 2). On the other hand, when **L6** was used in the same solvents (entries 12 and 13), lower conversion and d.r. were observed respect to THF (entry 14), although the enantioselectivity remained excellent.

It must be noticed that the use of polar solvents such as MeCN and DMF (entries 5 and 6) led to an important decrease in the reactivity and diastereoselectivity, and slightly lower enantioselectivities. Similarly, the use of MTBE (entry 8) and dichloroethane (entry 10) resulted in less than 10% of conversion, and, therefore, diastereo- and enantioselectivities were not measured. To our delight, diastereoselectivity was improved when **L3** was used in combination with both 1,4-dioxane and DME (6.3:1), while conversion and optical purity remained excellent.

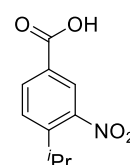
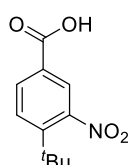
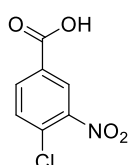
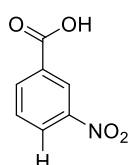
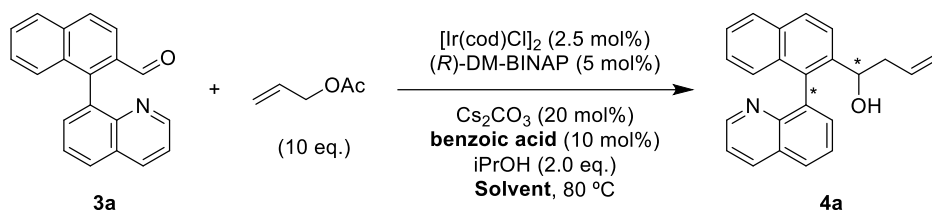
Combination of solvent and ligand was found to be key parameters, with **L3** being optimal in combination with 1,4-dioxane or DME.

To determine the effect of the *para*- substituent of *m*-nitrobenzoic acid,¹⁴³ on efficiency and selectivity,^{135a,b} different *m*-nitrobenzoic acid derivatives were tested,

¹⁴³ J. B. Johnson, T. Rovis, *Angew. Chem. Int. Ed.*, **2008**, *47*, 840–871.

using **L3** and 1,4-dioxane or DME as solvent. The results were analysed after 48 h and are summarized in **table 3**.

Table 3: screening of *m*-nitrobenzoic acid derivatives for the atroposelective *C*-allylation of **3a**.



Entry ^a	R	Solvent	Conv. (%) ^b	dr ^b	ee _{major} (%) ^c	ee _{minor} (%) ^c
1	H	1,4-Dioxane	87	6.3:1	97	96
2	Cl	1,4-Dioxane	90	5.5:1	95	95
3	<i>t</i> Bu	1,4-Dioxane	<10	n.d.	n.d.	n.d.
4	<i>i</i> Pr	1,4-Dioxane	<10	n.d.	n.d.	n.d.
5	H	DME	>99	6.3:1	97	99
6	Cl	DME	>99	5.3:1	96	92

n.r. no reaction. n.d. not determined. ^a Reactions performed at 0.1 mmol scale of **3a**. ^b Determined by ¹H-NMR spectroscopy. ^c Determined by HPLC on chiral stationary phases.

The use of *p*-chloro-*m*-nitrobenzoic acid (entry 2) did not affect selectivity and reactivity, obtaining similar values in 1,4-dioxane, and a slightly worse diastereomeric ratio in DME (entry 6). Remarkably, less than 10% conversion was observed when aliphatic bulky substituents were installed at the *para*-position of the benzoic acid (entries 3 and 4), and therefore, selectivities were not determined.

After all, we performed the reaction at 100 °C, to shorten the reaction time and determine if the products were configurationally stable at this temperature. To our delight, full conversion was achieved after 20 h, while maintaining the same

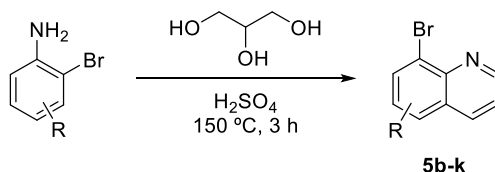
diastereomeric ratio 6.3:1 and enantioselectivities (97% *ee* for the major diastereomer and 99% *ee* for the minor diastereomer).

In view of these results, we decided to establish the use of 2.5 mol% of $[\text{Ir}(\text{cod})\text{Cl}]_2$, 5 mol% of (*R*)-DM-BINAP, 20 mol% of Cs_2CO_3 , 10 mol% of *m*-nitrobenzoic acid and 2 equiv. of *i*PrOH in DME at 100 °C, for 20 h, as the optimal reaction conditions.

II.3.3. Reaction scope.

With the optimized conditions in hand, we then moved to explore the DKR of different heterobiaryls aldehydes **3a-k** via Ir-catalyzed asymmetric allylation with allyl acetate.

We initially tested the effect of introducing different functional groups in the quinoline moiety, while the naphthaldehyde ring was kept unaltered. The required 8-bromoquinoline **5b-k** coupling partners were prepared in moderate to good yields, using the Skraup quinoline synthesis.¹⁴⁴



Scheme 83: Skraup reaction for the synthesis of quinoline derivatives.

A variety of substrates were then prepared by Suzuki-Miyaura cross-coupling (see also, **scheme 82**) in good to excellent yields (**figure 11**).

¹⁴⁴ H. Fang, J. Yan, B. Wang, *Molecules* **2004**, *9*, 178–184.

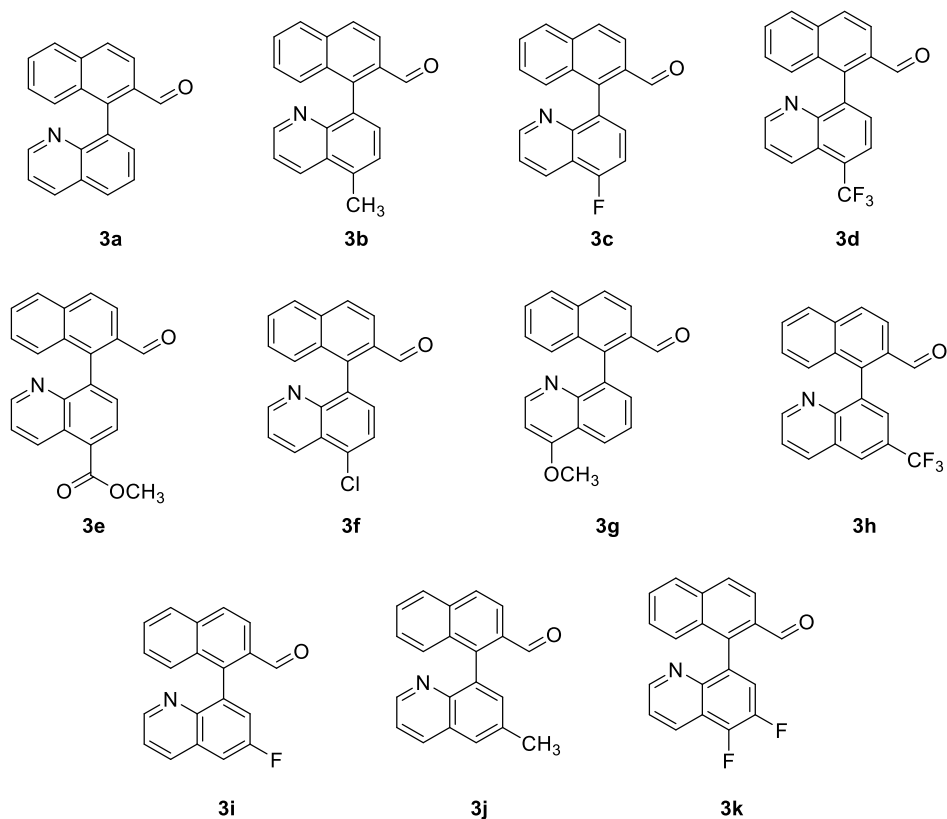
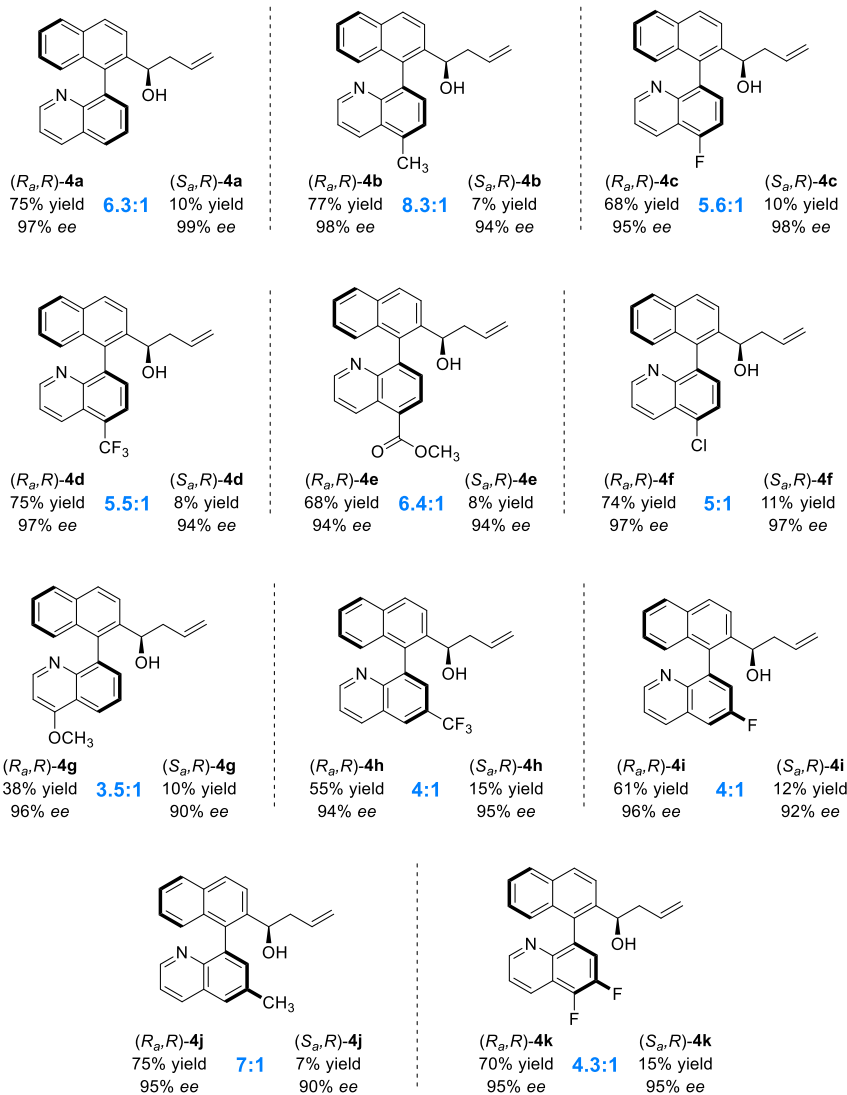
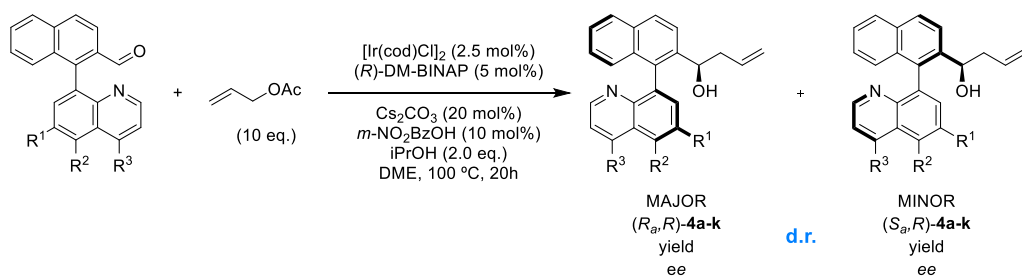


Figure 11: library of naphthylquinoline aldehydes synthesized.

This allylation reaction by DKR was successfully applied for the synthesis of alcohols **4a-k**, bearing central and axial chirality, in good diastereomeric ratios and excellent enantioselectivities, for the major and the minor diastereomers, in all cases. It must be highlighted that both diastereomers could be easily isolated by flash chromatography (**scheme 84**).



Scheme 84: scope of heterobiaryl scaffolds. Only major diastereomer structures are represented for simplicity.

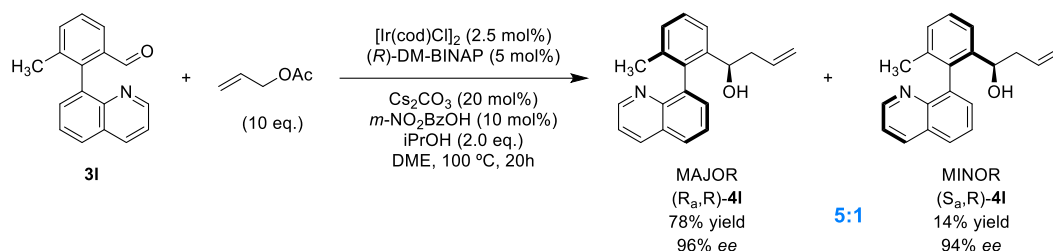
Aldehyde **3b**, with a methyl substituent at the C5 of the quinoline, provided the corresponding allylic alcohols **4b** in good diastereoselectivity (8.3:1 ratio), excellent optical purity (98 and 94% *ee* respectively) and 84% overall yield (77% and 7% of isolated major and minor isomers, respectively). In the same vein, electron-poor substituents at C5 of the quinoline (substrates **4c** and **4d**) were also well tolerated, affording good diastereomeric ratios and excellent enantioselectivities. For a substrate bearing a chloro group at the same position (**4f**), the diastereoselectivity slightly decrease (d.r. 5:1), but good overall yield (85%) and excellent 97% *ee* was observed for both diastereomers. Moreover, a product bearing an ester functionality at this position (**4e**) was also well tolerated in terms of yield (76% overall), diastereoselectivity (6.4:1 ratio) and enantioselectivity (94% *ee* for both isomers), offering a synthetically useful handle for further transformations. The selectivity decreases, however, when an electron-rich methoxy group is placed at C5 position of the quinoline ring (**4g**), affording the corresponding diastereomers in a moderate 48% yield and 3.5:1 ratio, while the enantioselectivity remained excellent (96% *ee* for the major isomer and 90% *ee* for the minor isomer).

Interestingly, a decrease in diastereoselectivity was observed in the reaction of substrates presenting electron-poor substituents at 6-position of the quinoline ring (4:1 d.r. for **4h** and **4i** and 4.3:1 d.r. for **4k**), whereas yield (70% for **4h**, 73% for **4i** and 85% for **4k**) and enantioselectivity (92-96% *ee*) remained excellent. On the other hand, when a methyl group is placed at this position (substrate **4j**), higher diastereomeric ratio is obtained (7:1) and good overall yield of 82% (75% and 7% for the major and minor isomers), although the enantioselectivity decrease for the minor diastereomer (90% *ee*) with respect of the major (95% *ee*).

Importantly, the carbonyl allylation by asymmetric transfer hydrogenation of the model heterobiaryl aldehyde **3a** could also be scaled-up to 1.63 mmol, affording the corresponding axially chiral allylic alcohol **4a** in good overall yield (75%: 68% major and 7% minor), the same excellent enantioselectivity (97% *ee* and 99% *ee* for

the major and the minor isomers, respectively) while diastereoselectivity was improved to 8:1 ratio.

We next explored other structural variations in the carbocyclic part of the substrate. A quinoline-derived compound, bearing a 3-methylbenzaldehyde residue (structure **31**) instead of the naphthalene ring, was studied in the reaction. To our delight, the desired biaryl carbinol **41** was successfully isolated in 92% overall yield (78% yield for the major isomer and 14% yield for the minor isomer) with 5:1 diastereomeric ratio, and 96% *ee* for the major diastereomer and 94% *ee* for the minor diastereomer (**scheme 85**).



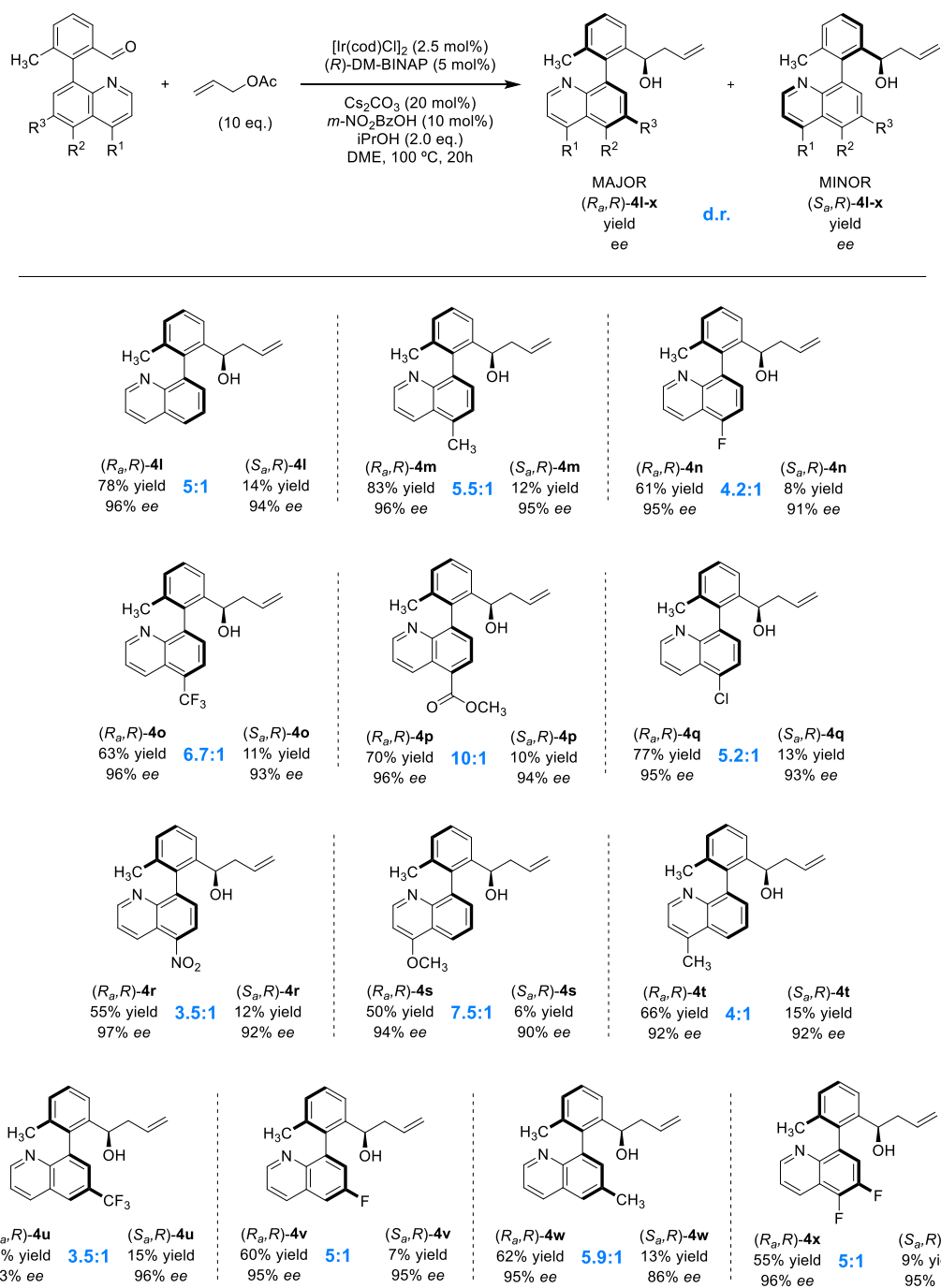
Scheme 85: asymmetric transfer hydrogenative carbonyl allylation performed on biaryl quinoline **31**.

Other 3-methyl-quinolin-benzaldehyde derivatives **3m-x** with different electron-rich and electron-deficient substituents were then studied as previously, affording good to excellent selectivities and yields (**scheme 86**). The highest diastereomeric ratio was obtained for product **4p** bearing an ester functionality at 5-position (10:1 ratio), with excellent optical purity (96% *ee* for the major and 94% *ee* for the minor isomers). Substrate **4r** with a nitro group at the same position also underwent the asymmetric allylation in moderate yields (55% and 12% yield for the major and minor isomers, respectively) and diastereoselectivity (3.5:1 ratio), but excellent optical purity (97% *ee* for the major and 92% *ee* for the minor isomers). Substrates presenting electron-poor substituents, such as fluoro- **4n**, trifluoromethyl- **4o** and chloro **4q** also engaged in the reaction, affording diastereomeric ratios between 4.2:1 and 6.7:1 d.r., and enantiomeric ratios among 91% and 96% *ee*. Moreover, placing an electron-rich methoxy at the C4 position (**4s**) resulted in an

increase of diastereoselectivity, (7.5:1 ratio) and 56% overall yield, although the minor diastereomer presented a slightly lower 90% *ee*, than the major (94% *ee*).

Better results were obtained for 5-methyl-substituted substrate **4m**, (95% overall yield, 5.5:1 d.r. and 96% *ee* and 95% *ee* for the major and minor isomer, respectively), than for a 4-methyl-substituted **4t** (81% overall yield, 4:1 diastereoselectivity, and 92% *ee* for both diastereomers).

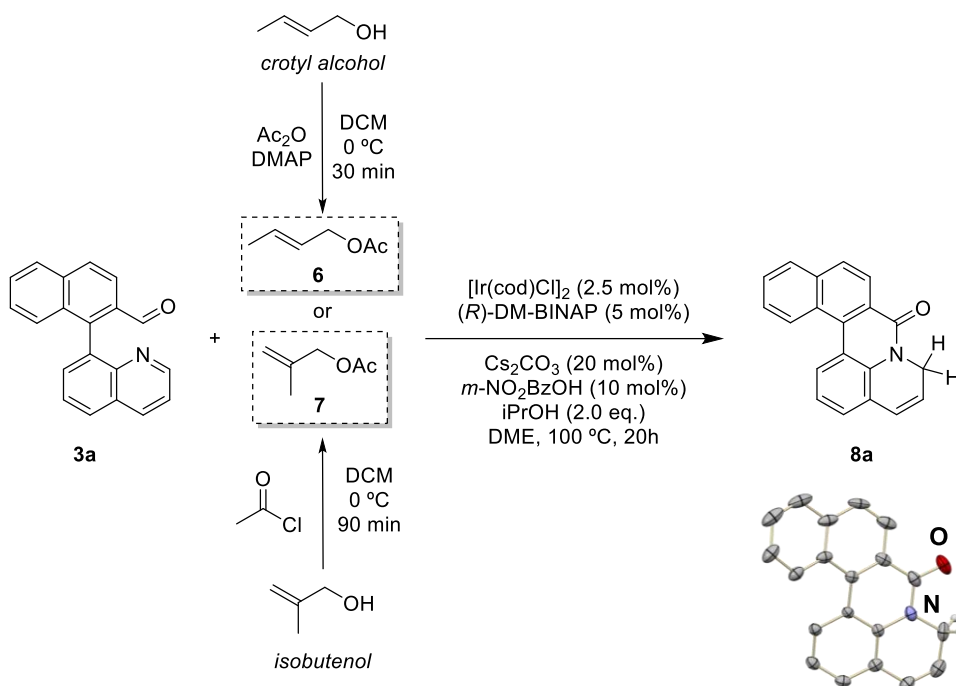
Finally, products bearing halides (**4u**, **4v** and **4x**) and methyl (**4w**) functionalities at C6 position were also well tolerated in terms of yield and selectivity.



Scheme 86: extension of the scope of heterobiaryl scaffolds. Only major diastereomer structures are represented for simplicity.

To summarize, up to 48 carbinols **4a-x** featuring axial and central chirality have been prepared in high yield (up to 95%), good diastereoselectivities (up to 10:1 d.r.) and excellent enantioselectivities (up to 99% *ee*), using this DKR method.

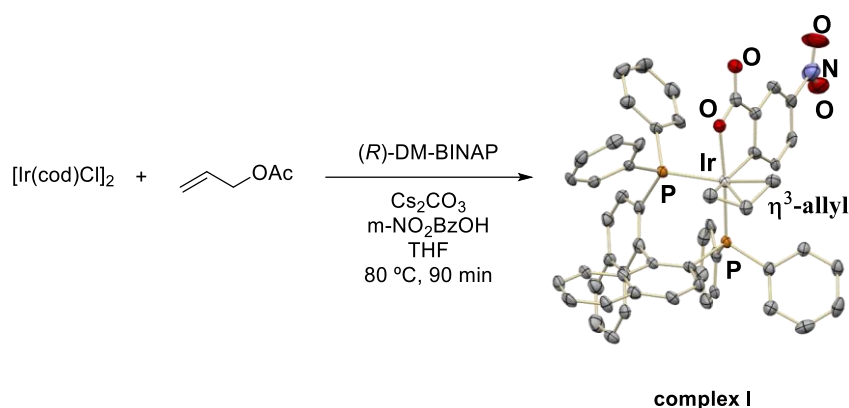
We next moved to study the suitability of allyl acetates in the reaction. To this end, crotyl alcohol and isobutenol were transformed into the corresponding acetates **6** and **7** respectively, and both were tested under the optimal reaction conditions using **3a** as substrate (**scheme 87**). Unexpectedly, the desired allyl alcohols were not observed with either **6** or **7**, and instead, a cyclic lactam **8a** was isolated, whose structure was confirmed by X-ray diffraction analysis.



Scheme 87: extension of the scope using crotyl or 2-methylallyl acetates.

Compound **8a** was formed through a prototropic rearrangement, probably catalyzed by a cyclometalated iridium complex intermediate, acting as a Lewis acid. The larger size of the crotyl and 2-methylallyl groups in combination with the steric hindrance of aldehyde **3a** may prevent allylation of the carbonyl, leaving the prototropic rearrangement as the unique reaction pathway.

We also could isolate the corresponding Ir-complex resting-state (**complex I**, **scheme 88**), which is the intermediate with the lowest energy (ΔG^\ddagger). This is the intermediate in which the catalyst spends most of the time during the reaction. Consequently, it is present at the highest concentration among all the catalytically active species and was found to be an active specie in the transfer hydrogenative carbonyl allylation.^{135a,b}

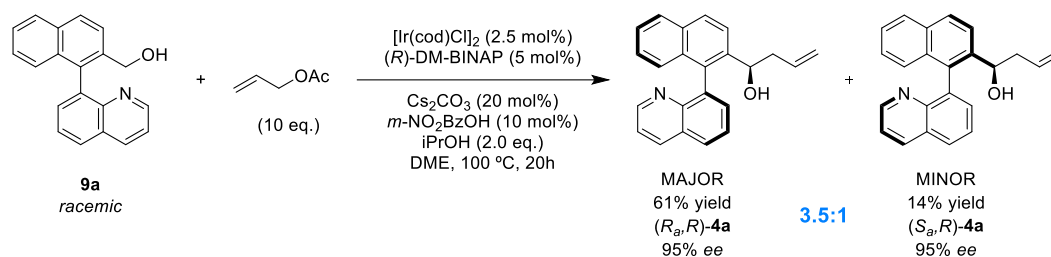


Scheme 88: isolation and characterization of the Ir-complex resting state.

II.3.4. Control experiments.

Some control experiments were then performed. One of the purposes was to confirm if racemization of **3a** proceed through a Lewis acid-base interaction between the aldehyde and the nitrogen from the quinoline, or it was otherwise facilitated by thermal racemization due to the elevated reaction temperature (100 °C). As it was previously mentioned, this carbonyl allylation could take place from either the aldehyde or the alcohol oxidation level. In this regard, C-allylation of alcohol **9a** was carried out, to determine the influence on selectivity and yield.

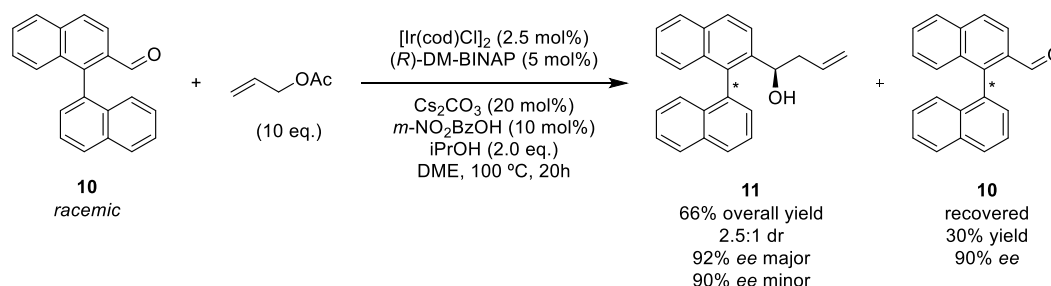
Racemic biaryl alcohol **9a** was subjected to the optimized reaction conditions, and after 20 h the desired isomers **4a** could be isolated in a 3.5:1 diastereomeric ratio, 75% overall yield and the same excellent 95% *ee* for both isomers (**scheme 89**).



Scheme 89: asymmetric carbonyl allylation using the alcohol-derivative **9a** as substrate.

However, the diastereomeric ratio was a bit lower (3.5:1 starting from the alcohol vs. 6.3:1 from the aldehyde) presumably because of the lack of time for an efficient racemization.

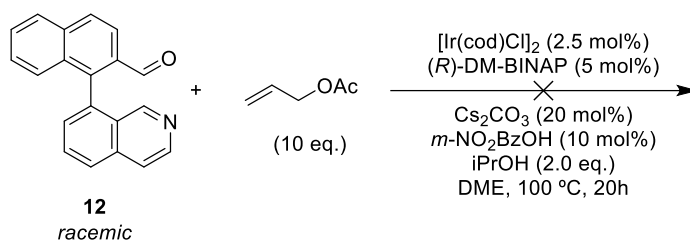
In another control experiment, *rac*-(1,1'-binaphthalene)-2-carbaldehyde **10** was subjected to the optimal conditions for the transfer hydrogenative carbonyl allylation (**scheme 90**). Biaryl **11** was isolated in 66% overall yield with 2.5:1 diastereoisomeric ratio and excellent enantioselectivity for both diastereomers. However, after 24 h, 30% of the starting material **10** was recovered, which presented 90% *ee*. This result indicates that compound **10** is configurationally stable and a simple kinetic resolution was taking place instead.



Scheme 90: asymmetric carbonyl allylation using the biaryl **10** as substrate.

Then, the influence of the position of the nitrogen atom in the heteroaromatic unit was studied, using the isoquinoline derivative **12**. A kinetic resolution was again expected to occur because of the impossibility for the formation of the Lewis acid-base pair (**scheme 91**). However, we observed a completely absence of reactivity. As

a reason, coordination of the less hindered N from the isoquinoline to a cyclometallated iridium complex intermediate, bearing a vacant coordination site, would render the catalyst ineffective.



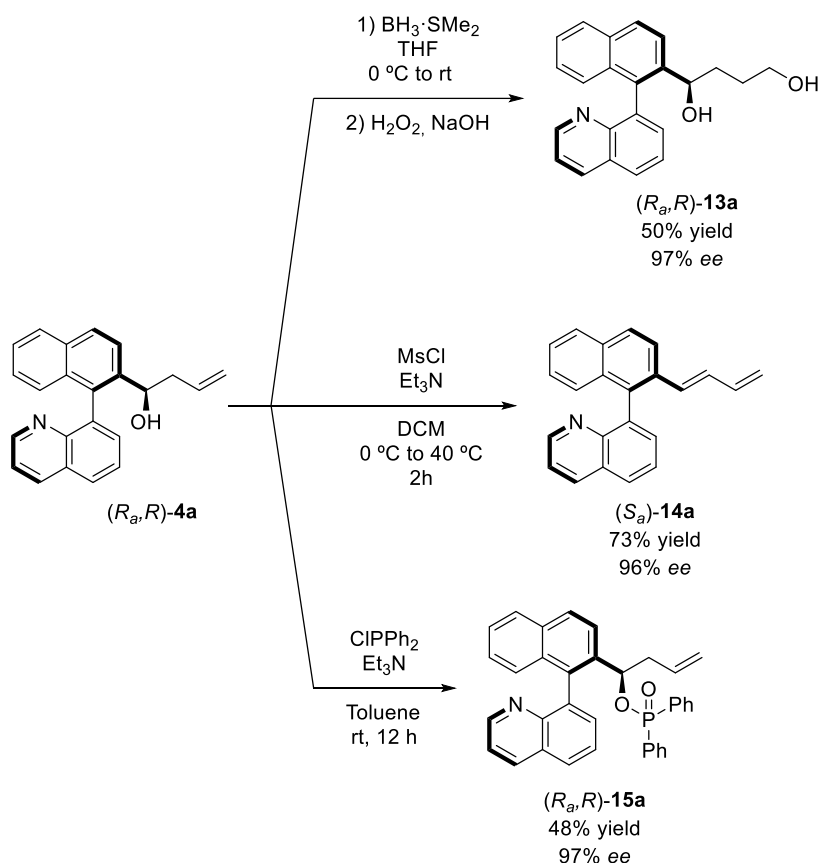
Scheme 91: asymmetric carbonyl allylation using the isoquinolinebiaryl **12** as substrate.

These results confirm that the racemization occurs through a Lewis acid-base interaction, after the aldehyde being delivered to the reaction medium.

II.3.5. Representative transformations.

To demonstrate the versatility of the resulting products, the major diastereomer of the model heterobiaryl alcohol **4a** was subjected to a variety of derivatization reactions.

First, biaryldiol **13a** was prepared by a hydroboration-oxidation reaction in moderate yield and with no erosion on the optical purity. Moreover, butadiene-derivative **14a** was obtained through the dehydration of **4a**, after reaction with mesyl chloride. Additionally, organophosphate (*R_aR*)-**15a** was prepared using chlorodiphenylphosphine and base, in moderate yields but maintaining the excellent enantioselectivity (**scheme 92**).



Scheme 92: representative transformations carried out over model substrate **4a**.

The absolute configuration of (R_a, R)-**15a** was determined by single-crystal X-Ray analysis and hence, the configuration of the major isomer (R_a, R)-**4a** was assigned to be the same (**figure 12**). On the other hand, the configuration of the minor diastereomer was assigned by chemical correlation after dehydration of (S_a, R)-**4a**, and comparison of the HPLC traces with the obtained for (S_a)-**14a**, which afforded the opposite enantiomer (R_a)-**4a**. The absolute configuration of all other products was assigned by analogy. It should be noted that the configuration of the axis is inverted in compounds **4a** and **14a**, due to the different priority order of the substituents at *ortho* positions of the naphthyl moiety.

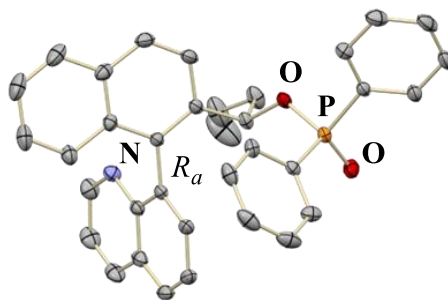


Figure 12: X-Ray diffraction analysis of compound 15a.

II.4. Conclusions.

An atroposelective Ir-catalyzed dynamic kinetic resolution (DKR) of aryl-quinoline derivatives by transfer hydrogenative coupling of allyl acetate has been described.

The allylation reaction takes place with simultaneous installation of central and axial chirality, reaching high diastereo- and excellent enantiomeric excesses, when using an *ortho*-cyclometalated iridium-DM-BINAP complex as catalyst.

The racemization of the substrates likely occurs through a Lewis acid-base interaction between the quinoline nitrogen atom and a carbonyl group.

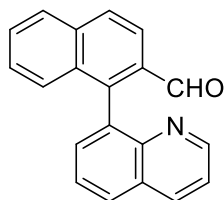
Moreover, the synthetic versatility of the resulting products has been demonstrated with their transformation into interesting derivatives with potential use as ligands in asymmetric catalysis, without erosion of the optical purity.

II.5. Experimental section.

II.5.1. General procedure for the synthesis of aldehydes 3a-x.

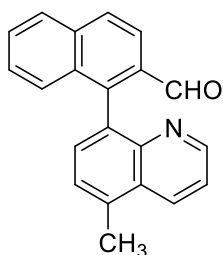
In a flame-dried Schlenk tube, under N₂ atmosphere, there are added the corresponding bromoquinoline **5b-k** (1 eq.), the corresponding (2-formylnaphthalen-1-yl)boronic acid **2a** or (2-formyl-6-methylphenyl)boronic acid **2b** (1.2 eq.), Pd(OAc)₂ (3.3 mol%), SPhos (4 mol%), K₂CO₃ (4.0 eq) followed by DME (0.2 M) and H₂O (0.5 M). The reaction mixture is stirred overnight at 80 °C. After completion, the reaction mixture is diluted with EtOAc and brine, and extracted with EtOAc. Collected organic phases are dried over MgSO₄, filtering and solvent is removed under vacuum. The residue is purified by column chromatography on silica gel (cyclohexane/EtOAc 4:1) to afford the desired quinolyl aldehyde **3a-x**.

1-(Quinolin-8-yl)-2-naphthaldehyde (3a). Following the general procedure from



8-bromo quinoline (7.2 mmol, 1.49g) and **2a**, afforded **3a** (2.04 g, 99% yield) as an amorphous yellow solid. ¹H NMR (400 MHz, CDCl₃) δ 9.69 (s, 1H), 8.83 – 8.74 (m, 1H), 8.28 (dd, *J* = 8.3, 1.8 Hz, 1H), 8.18 (d, *J* = 8.6 Hz, 1H), 8.07 – 7.98 (m, 3H), 7.95 (d, *J* = 8.2 Hz, 1H), 7.77 – 7.68 (m, 2H), 7.57 (t, *J* = 7.4 Hz, 1H), 7.45 – 7.36 (m, 5H), 7.33 (t, *J* = 7.6 Hz, 1H). ¹³C NMR (100 MHz, CDCl₃) δ 192.6, 151.1, 147.8, 144.5, 136.3, 135.0, 133.1, 132.7, 132.0, 129.1, 128.7, 128.6, 128.4, 128.3, 127.7, 126.7, 125.9, 122.2, 121.6. HRMS (ESI) calcd. for C₂₀H₁₄NO (M + H⁺) 284.1070. Found 248.1073.

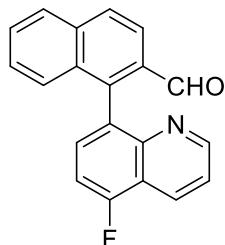
1-(5-Methylquinolin-8-yl)-2-naphthaldehyde (3b). Following the general



procedure from **5b** (1.0 mmol, 222 mg) and **2a**, afforded **3b** (265 mg, 89% yield) as an amorphous yellow solid. ¹H NMR (400 MHz, CDCl₃) δ 9.66 (s, 1H), 8.63 (d, *J* = 4.3 Hz, 1H), 8.26 – 8.19 (m, 1H), 8.16 (d, *J* = 8.6 Hz, 1H), 8.00 (d, *J* = 8.6 Hz, 1H), 7.94 (d, *J* = 8.2 Hz, 1H), 7.78 – 7.68 (m, 2H), 7.56 (ddd, *J* = 8.1, 6.5, 1.5 Hz, 1H), 7.40 – 7.34 (m, 2H), 7.32 (ddd, *J* = 8.4, 6.6, 1.3 Hz, 1H), 7.25 (d, *J* = 4.8 Hz,

1H), 2.82 (s, 3H). ¹³C NMR (100 MHz, CDCl₃) δ 192.69, 150.69, 147.60, 144.98, 144.45, 136.29, 135.46, 133.07, 132.40, 131.87, 128.53, 128.37, 128.33, 127.76, 126.63, 125.50, 125.00, 122.32, 122.16, 18.99. HRMS (ESI) calcd. for C₂₁H₁₆NO (M + H⁺) 298.1229. Found 298.1229.

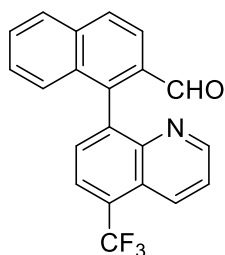
1-(5-Fluoroquinolin-8-yl)-2-naphthaldehyde (3c). Following the general



procedure from **5c** (1.0 mmol, 226 mg) and **2a**, afforded **3c** (283 mg, 91% yield) as an amorphous yellow solid. ¹H NMR (400 MHz, CDCl₃) δ 9.68 (d, J = 0.9 Hz, 1H), 8.82 (dd, J = 4.2, 1.8 Hz, 1H), 8.57 (dd, J = 8.5, 1.8 Hz, 1H), 8.16 (d, J = 8.6 Hz, 1H), 8.02 (d, J = 8.6 Hz, 1H), 7.95 (d, J = 8.2 Hz, 1H), 7.69 (dd, J = 8.0, 6.0 Hz, 1H), 7.58

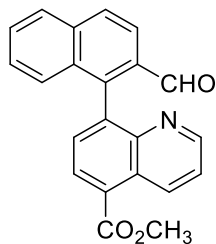
(ddd, J = 8.2, 5.8, 2.3 Hz, 1H), 7.49 (dd, J = 8.5, 4.2 Hz, 1H), 7.41 (dd, J = 9.3, 8.0 Hz, 1H), 7.35 (dd, J = 5.7, 1.4 Hz, 2H). ¹³C NMR (100 MHz, CDCl₃) δ 192.3, 158.2 (d, J = 257.6 Hz), 151.8, 148.3, 143.5, 136.3, 133.1, 132.1, 132.0, 130.9, 129.5 (d, J = 4.9 Hz), 128.9, 128.7, 128.4, 127.5, 126.8, 122.3, 121.7 (d, J = 3.0 Hz), 119.1 (d, J = 16.4 Hz), 109.7 (d, J = 19.4 Hz). ¹⁹F NMR (377 MHz, CDCl₃) δ -120.93. HRMS (ESI) calcd. for C₂₀H₁₃FNO (M + H⁺) 302.0976. Found 302.0981.

1-(5-(Trifluoromethyl)quinolin-8-yl)-2-naphthaldehyde (3d). Following the

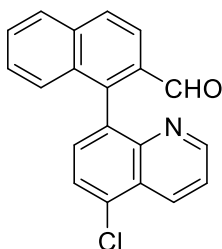


general procedure from **5d** (1.0 mmol, 276 mg) and **2a**, afforded **3d** (298 mg, 85% yield) as an amorphous yellow solid. ¹H NMR (400 MHz, CDCl₃) δ 9.68 – 9.59 (s, 1H), 8.84 (dd, J = 4.2, 1.7 Hz, 1H), 8.73 – 8.57 (d, J = 8.7 Hz, 1H), 8.17 (d, J = 8.7 Hz, 1H), 8.11 (d, J = 7.5 Hz, 1H), 8.05 (d, J = 8.7 Hz, 1H), 7.97 (d, J = 8.2 Hz, 1H), 7.82 (d, J = 7.4 Hz, 1H), 7.64 – 7.53 (m, 2H), 7.36 (ddd, J = 8.1, 6.7,

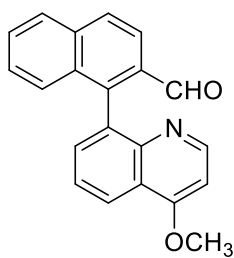
1.3 Hz, 1H), 7.32 – 7.28 (d, J = 8.7 Hz, 1H). ¹³C NMR (100 MHz, CDCl₃) δ 191.8, 151.5, 147.9, 142.9, 140.4, 136.2, 132.8, 132.6, 131.8, 130.9, 129.1, 128.8, 128.5, 127.3, 127.0, 127.2 (q, J = 31.6 Hz) 124.5, 124.4 (q, J = 5.6 Hz), 124.0 (q, J = 274.4 Hz), 122.7, 122.3. ¹⁹F NMR (377 MHz, CDCl₃) δ -59.1. HRMS (ESI) calcd. for C₂₁H₁₃F₃NO (M + H⁺) 352.0944. Found 352.0941.

Methyl 8-(2-formyl-6-methylphenyl)quinoline-5-carboxylate (3e).

the general procedure from **5e** (133 mg, 0.5 mmol) and **2a**, afforded **3e** (110 mg, 65% yield) as an amorphous yellow solid. ^1H NMR (400 MHz, CDCl_3) δ 9.64 (s, 1H), 9.46 (dd, $J = 8.8, 1.7$ Hz, 1H), 8.80 (dd, $J = 4.1, 1.8$ Hz, 1H), 8.43 (d, $J = 7.5$ Hz, 1H), 8.16 (d, $J = 8.6$ Hz, 1H), 8.03 (d, $J = 8.6$ Hz, 1H), 7.96 (d, $J = 8.2$ Hz, 1H), 7.79 (d, $J = 7.5$ Hz, 1H), 7.58 (ddd, $J = 8.1, 6.5, 1.5$ Hz, 1H), 7.53 (dd, $J = 8.8, 4.1$ Hz, 1H), 7.37 – 7.27 (m, 2H), 4.09 (s, 3H). ^{13}C NMR (100 MHz, CDCl_3) δ 191.9, 166.8, 151.1, 147.9, 143.6, 140.8, 136.2, 134.5, 132.6, 131.7, 131.3, 129.7, 128.9, 128.7, 128.4, 127.8, 127.4, 127.1, 126.9, 122.9, 122.3, 52.6. HRMS (ESI) calcd. for $\text{C}_{22}\text{H}_{16}\text{NO}_3$ ($\text{M} + \text{H}^+$) 342.1125. Found 342.1124.

1-(5-Chloroquinolin-8-yl)-2-naphthaldehyde (3f).

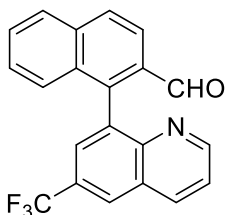
the general procedure from **5f** (1 mmol, 243 mg) and **2a**, afforded **3f** (227 mg, 72% yield) as an amorphous yellow solid. ^1H NMR (400 MHz, CDCl_3) δ 9.68 (s, 1H), 8.81 (dd, $J = 4.2, 1.7$ Hz, 1H), 8.72 (dd, $J = 8.6, 1.7$ Hz, 1H), 8.02 (d, $J = 8.6$ Hz, 1H), 7.95 (dd, $J = 8.2, 1.1$ Hz, 1H), 7.81 (d, $J = 7.7$ Hz, 1H), 7.68 (d, $J = 7.7$ Hz, 1H), 7.58 (ddd, $J = 8.1, 5.2, 2.8$ Hz, 1H), 7.53 (dd, $J = 8.6, 4.2$ Hz, 1H), 7.37 – 7.32 (m, 2H). ^{13}C NMR (100 MHz, CDCl_3) δ 192.2, 151.6, 148.3, 143.3, 136.3, 134.4, 133.2, 132.9, 132.4, 132.2, 131.9, 128.9, 128.7, 128.4, 127.4, 126.9, 126.4, 126.1, 122.4, 122.3. HRMS (ESI) calcd. for $\text{C}_{20}\text{H}_{13}\text{ClNO}$ ($\text{M} + \text{H}^+$) 318.0860. Found 318.0861.

1-(4-Methoxyquinolin-8-yl)-2-naphthaldehyde (3g).

the general procedure from **5g** (238 mg, 1.0 mmol) and **2a**, afforded **3g** (257 mg, 82% yield) as an amorphous yellow solid. ^1H NMR (400 MHz, CDCl_3) δ 9.67 (s, 1H), 8.62 (d, $J = 5.2$ Hz, 1H), 8.43 (dd, $J = 8.2, 1.7$ Hz, 1H), 8.15 (d, $J = 8.6$ Hz, 1H), 7.99 (d, $J = 8.6$ Hz, 1H), 7.93 (d, $J = 8.2$ Hz, 1H), 7.76 – 7.62 (m, 2H), 7.56 (s, 1H), 7.38 (d, $J = 1.3$ Hz, 1H), 7.34 (dd, $J = 6.7, 1.4$ Hz, 1H), 6.76 (d, $J = 5.2$ Hz, 1H), 4.10 (s, 3H). ^{13}C NMR (100 MHz, CDCl_3) δ 192.7, 162.3, 151.9, 148.6, 144.8, 136.3, 134.4, 133.0,

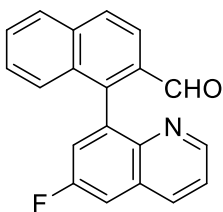
131.9, 128.5, 128.3, 127.7, 126.6, 124.8, 123.0, 122.2, 121.6, 100.4, 55.9. HRMS (ESI) calcd. for $C_{21}H_{16}NO_2$ ($M + H^+$) 314.1176. Found 314.1175.

1-(6-(Trifluoromethyl)quinolin-8-yl)-2-naphthaldehyde (3h). Following the



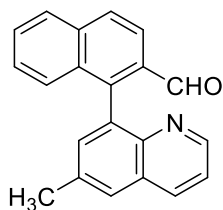
general procedure from **5h** (276 mg, 1.0 mmol) and **2a**, afforded **3h** (350 mg, 99%) as an amorphous yellow solid. 1H NMR (400 MHz, $CDCl_3$) δ 9.66 (s, 1H), 8.88 (dd, $J = 4.2, 1.8$ Hz, 1H), 8.45 – 8.36 (m, 2H), 8.18 (df, $J = 8.6$ Hz, 1H), 8.06 (d, $J = 8.6$ Hz, 1H), 8.02 – 7.94 (m, 2H), 7.61 (ddd, $J = 8.2, 6.7, 1.3$ Hz, 1H), 7.54 (dd, $J = 8.3, 4.2$ Hz, 1H), 7.38 (ddd, $J = 8.1, 6.7, 1.3$ Hz, 1H), 7.32 (dd, $J = 8.4, 1.3$ Hz, 1H). ^{13}C NMR (100 MHz, $CDCl_3$) δ 191.8, 153.1, 148.8, 142.5, 137.2, 136.9, 136.3, 132.7, 131.9, 129.2, 128.8, 128.5, 128.0 (q, $J = 33.0$), 127.9 (q, $J = 2.5$ Hz), 127.4, 127.2, 127.1, 126.9 (q, $J = 4.4$ Hz), 123.8 (q, $J = 273.3$ Hz), 122.8, 122.4. ^{19}F NMR (377 MHz, $CDCl_3$) δ -62.2. HRMS (ESI) calcd. for $C_{21}H_{13}F_3NO$ ($M + H^+$) 352.0944. Found 352.0944.

1-(6-Fluoroquinolin-8-yl)-2-naphthaldehyde (3i). Following the general



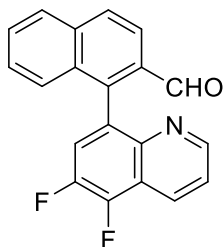
procedure from **5i** (226 mg, 1.0 mmol) and **2a**, afforded **3i** (210 mg, 70%) as an amorphous yellow solid. 1H NMR (400 MHz, $CDCl_3$) δ 9.67 (d, $J = 0.9$ Hz, 1H), 8.74 (ddd, $J = 4.1, 1.7, 0.6$ Hz, 1H), 8.24 (dd, $J = 8.4, 1.8$ Hz, 1H), 8.16 (d, $J = 8.6$ Hz, 1H), 8.04 (d, $J = 8.6$ Hz, 1H), 7.96 (dt, $J = 8.2, 1.1$ Hz, 1H), 7.66 (dd, $J = 8.5, 2.8$ Hz, 1H), 7.62 – 7.55 (m, 2H), 7.44 (ddd, $J = 8.3, 4.1, 0.8$ Hz, 1H), 7.39 – 7.36 (m, 2H). ^{13}C NMR (100 MHz, $CDCl_3$) δ 191.9, 159.4 (d, $J = 250.1$ Hz), 150.3, 145.1, 142.6, 138.1 (d, $J = 9.0$ Hz), 136.3, 135.8 (d, $J = 5.5$ Hz), 132.7, 131.8, 129.1, 128.9, 128.7, 128.5, 127.3, 126.9, 122.8, 122.6, 122.3 (d, $J = 8.7$ Hz), 111.8 (d, $J = 21.0$ Hz). ^{19}F NMR (377 MHz, $CDCl_3$) δ -113.30. HRMS (ESI) calcd. for $C_{20}H_{13}FNO$ ($M + H^+$) 302.0976. Found 302.0975.

1-(6-Methylquinolin-8-yl)-2-naphthaldehyde (3j). Following the general



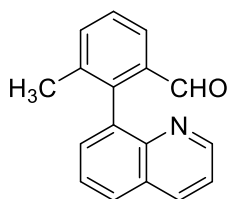
procedure from **5j** (222 mg, 1.0 mmol) and **2a**, afforded **3j** (258 mg, 87%) as an amorphous yellow solid. ^1H NMR (400 MHz, CDCl_3) δ 9.68 (s, 1H), 8.72 (dd, $J = 4.2, 1.8$ Hz, 1H), 8.19 (dd, $J = 8.3, 1.8$ Hz, 1H), 8.16 (d, $J = 8.6$ Hz, 1H), 8.00 (dd, $J = 8.7, 1.0$ Hz, 1H), 7.94 (dt, $J = 8.3, 0.9$ Hz, 1H), 7.79 (dd, $J = 2.1, 1.1$ Hz, 1H), 7.62 – 7.53 (m, 2H), 7.43 – 7.29 (m, 3H), 2.62 (s, 3H). ^{13}C NMR (100 MHz, CDCl_3) δ 192.7, 150.2, 146.5, 144.6, 136.3, 135.7, 135.6, 134.9, 134.7, 133.0, 131.9, 128.6, 128.6, 128.4, 127.9, 127.7, 126.7, 122.2, 121.6, 21.6. HRMS (ESI) calcd. for $\text{C}_{21}\text{H}_{16}\text{NO}$ ($\text{M} + \text{H}^+$) 298.1226. Found 298.1226.

1-(5,6-Difluoroquinolin-8-yl)-2-naphthaldehyde (3k). Following the general



procedure from **5k** (1.0 mmol, 244 mg) and **2a**, afforded **3k** (229 mg, 72% yield) as an amorphous yellow solid. ^1H NMR (400 MHz, CDCl_3) δ 9.67 (s, 1H), 8.78 (dd, $J = 4.3, 1.7$ Hz, 1H), 8.57 (dd, $J = 8.5, 1.8$ Hz, 1H), 8.15 (d, $J = 8.6$ Hz, 1H), 8.08 – 8.02 (m, 1H), 7.97 (d, $J = 8.3$ Hz, 1H), 7.67 (dd, $J = 10.4, 8.2$ Hz, 1H), 7.60 (ddd, $J = 8.2, 6.4, 1.6$ Hz, 1H), 7.55 – 7.49 (m, 1H), 7.42 – 7.32 (m, 2H). ^{13}C NMR (100 MHz, CDCl_3) δ 191.8, 150.9, 145.6 (dd, $J = 251.0, 11.5$ Hz), 144.3, 143.9 (dd, $J = 257.9, 12.9$ Hz), 141.6, 136.3, 132.8, 132.5 – 132.3 (m), 132.1, 129.3, 129.3 – 128.9 (m), 128.8, 128.5, 127.1, 122.9, 122.7, 122.4, 122.3 – 122.1 (m). ^{19}F NMR (377 MHz, CDCl_3) δ -139.2 (d, $J = 19.3$ Hz), -146.4 (d, $J = 19.4$ Hz). HRMS (ESI) calcd. for $\text{C}_{20}\text{H}_{12}\text{F}_2\text{NO}$ ($\text{M} + \text{H}^+$) 320.0881. Found 320.0883.

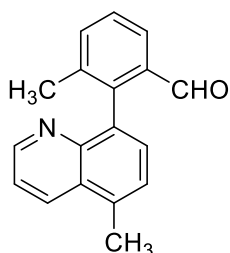
3-Methyl-2-(quinolin-8-yl)benzaldehyde (3l). Following the general procedure



from 8-bromo quinoline (98 mg, 0.6 mmol) and **2b**, afforded **3l** (105 mg, 85%) as an amorphous yellow solid. ^1H NMR (400 MHz, CDCl_3) δ 9.49 (s, 1H), 8.86 (dd, $J = 4.3, 1.7$ Hz, 1H), 8.41 (dd, $J = 8.5, 1.8$ Hz, 1H), 7.93 (d, $J = 8.0$ Hz, 1H), 7.57 (d, $J = 7.5$ Hz, 1H), 7.50 – 7.38 (m, 4H), 2.78 (s, 3H), 2.01 (s, 3H). ^{13}C NMR (100 MHz, CDCl_3) δ 192.8, 150.3, 147.2, 143.7, 138.2, 135.4, 135.4, 135.1, 134.4, 132.7,

131.2, 127.8, 127.8, 126.5, 124.7, 120.9, 20.2, 18.8. HRMS (ESI) calcd. for $C_{18}H_{16}NO$ ($M + H^+$) 262.1226. Found 262.1231.

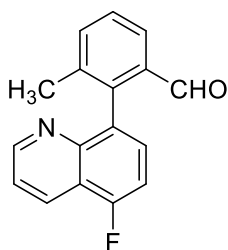
3-Methyl-2-(5-methylquinolin-8-yl)benzaldehyde (3m). Following the general



procedure from **5b** (98 mg, 0.6 mmol) and **2b**, afforded **3m** (110 mg, 85%) as an amorphous yellow solid. 1H NMR (400 MHz, $CDCl_3$) δ 9.49 (s, 1H), 8.86 (dd, $J = 4.3, 1.7$ Hz, 1H), 8.41 (dd, $J = 8.5, 1.8$ Hz, 1H), 7.93 (d, $J = 8.0$ Hz, 1H), 7.57 (d, $J = 7.5$ Hz, 1H), 7.50 – 7.38 (m, 4H), 2.78 (s, 3H), 2.01 (s, 3H). ^{13}C NMR (100 MHz, $CDCl_3$) δ 192.8, 150.3, 147.2, 143.7, 138.2, 135.4, 135.4, 135.1,

134.4, 132.7, 131.2, 127.8, 127.8, 126.5, 124.7, 120.9, 20.0, 18.8. HRMS (ESI) calcd. for $C_{18}H_{16}NO$ ($M + H^+$) 262.1226. Found 262.1231.

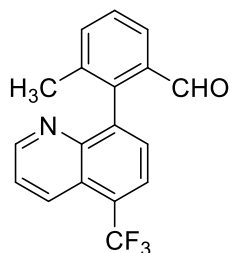
2-(5-Fluoroquinolin-8-yl)-3-methylbenzaldehyde (3n). Following the general



procedure from **5c** (98 mg, 0.6 mmol) and **2b**, afforded **3n** (90 mg, 70%) as an amorphous yellow solid. 1H NMR (400 MHz, $CDCl_3$) δ 9.49 (s, 1H), 8.90 (dd, $J = 4.2, 1.8$ Hz, 1H), 8.52 (dd, $J = 8.5, 1.8$ Hz, 1H), 7.93 (dd, $J = 7.8, 1.4$ Hz, 1H), 7.58 (d, $J = 7.5$ Hz, 1H), 7.55 – 7.43 (m, 3H), 7.33 (t, $J = 7.6$ Hz, 1H), 2.00 (s, 3H). ^{13}C NMR (100 MHz, $CDCl_3$) δ 192.4, 157.9 (d, $J = 257.0$ Hz), 151.6,

147.4, 142.3, 138.2, 135.5, 135.2, 132.5, 130.8 (d, $J = 8.7$ Hz), 129.5 (d, $J = 4.7$ Hz), 126.7 (d, $J = 306.7$ Hz), 121.5, 119.2 (d, $J = 16.2$ Hz), 109.8 (d, $J = 19.5$ Hz), 19.9. ^{19}F NMR (377 MHz, $CDCl_3$) δ -121.8. HRMS (ESI) calcd. for $C_{17}H_{13}FNO$ ($M + H^+$) 266.0976. Found 266.0974.

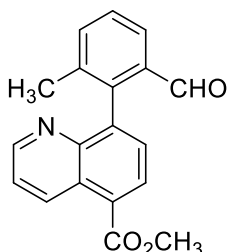
3-Methyl-2-(5-(trifluoromethyl)quinolin-8-yl)benzaldehyde (3o). Following the



general procedure from **5d** (230 mg, 1.4 mmol) and **2b**, afforded **3o** (291 mg, 92%) as an amorphous yellow solid. 1H NMR (400 MHz, $CDCl_3$) δ 9.49 (s, 1H), 8.93 (dd, $J = 4.2, 1.7$ Hz, 1H), 8.60 (dt, $J = 8.8, 1.8$ Hz, 1H), 8.03 (d, $J = 7.5$ Hz, 1H), 7.94 (dd, $J = 7.7, 1.5$ Hz, 1H), 7.65 (d, $J = 7.4$ Hz, 1H), 7.63 – 7.47 (m, 3H), 1.99 (s, 3H). ^{13}C NMR (100 MHz, $CDCl_3$) δ 191.8, 151.3, 147.1, 141.9, 141.8,

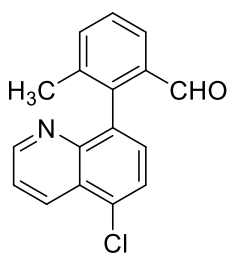
137.7, 135.5, 134.8, 132.8, 129.6, 128.4, 126.7 (q, $J = 31.2$ Hz), 125.6, 124.7, 124.6 (q, $J = 5.8$ Hz), 124.0 (q, $J = 273.2$ Hz), 122.5, 19.9. ^{19}F NMR (377 MHz, CDCl_3) δ -59.07. HRMS (ESI) calcd. for $\text{C}_{18}\text{H}_{13}\text{F}_3\text{NO}$ ($\text{M} + \text{H}^+$) 316.0944. Found 316.0941.

Methyl 8-(2-formyl-6-methylphenyl)quinoline-5-carboxylate (3p). Following



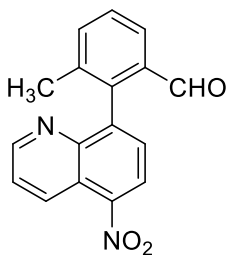
the general procedure from **5e** (133 mg, 0.5 mmol) and **2b**, afforded **3p** (108 mg, 71%) as an amorphous yellow solid. ^1H NMR (400 MHz, CDCl_3) δ 9.47 (s, 1H), 9.43 (dd, $J = 8.7, 1.7$ Hz, 1H), 8.88 (dd, $J = 4.2, 1.7$ Hz, 1H), 8.37 (d, $J = 7.5$ Hz, 1H), 7.93 (dd, $J = 7.8, 1.4$ Hz, 1H), 7.62 (d, $J = 7.4$ Hz, 1H), 7.58 (d, $J = 7.5$ Hz, 1H), 7.55 – 7.48 (m, 2H), 4.05 (s, 3H), 1.98 (s, 3H). ^{13}C NMR (100 MHz, CDCl_3) δ 191.9, 166.8, 150.9, 146.9, 142.5, 142.2, 137.6, 135.5, 134.7, 134.6, 130.0, 128.3, 127.3, 125.3, 122.7, 52.5, 19.9. HRMS (ESI) calcd. for $\text{C}_{19}\text{H}_{16}\text{NO}_3$ ($\text{M} + \text{H}^+$) 306.1125. Found 306.1122.

2-(5-Chloroquinolin-8-yl)-3-methylbenzaldehyde (3q). Following the general



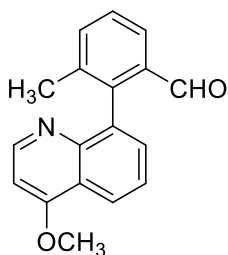
procedure from **5f** (244 mg, 1.0 mmol) and **2b**, afforded **3q** (287 mg, 99%) as an amorphous yellow solid. ^1H NMR (400 MHz, CDCl_3) δ 9.50 (s, 1H), 8.90 (dd, $J = 4.2, 1.7$ Hz, 1H), 8.68 (dd, $J = 8.6, 1.7$ Hz, 1H), 7.93 (ddd, $J = 7.7, 1.6, 0.7$ Hz, 1H), 7.74 (d, $J = 7.7$ Hz, 1H), 7.63 – 7.43 (m, 5H), 1.99 (s, 3H). ^{13}C NMR (100 MHz, CDCl_3) δ 192.2, 151.4, 147.4, 142.2, 138.0, 135.9, 135.5, 134.9, 133.2, 131.8, 131.0, 128.2, 126.6, 126.2, 125.2, 122.2, 19.9. HRMS (ESI) calcd. for $\text{C}_{17}\text{H}_{13}\text{ClNO}$ ($\text{M} + \text{H}^+$) 282.0860. Found 282.0862.

3-Methyl-2-(5-nitroquinolin-8-yl)benzaldehyde (3r). Following the general



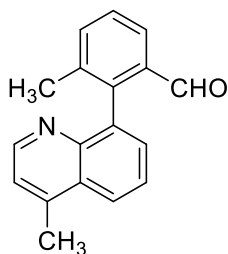
procedure from **5l** (253 mg, 1 mmol) and **2b**, afforded **3r** (209 mg, 73%) as an amorphous yellow solid. ^1H NMR (400 MHz, CDCl_3) δ 9.52 (s, 1H), 9.10 (dd, $J = 8.9, 1.7$ Hz, 1H), 8.93 (dd, $J = 4.2, 1.6$ Hz, 1H), 8.47 (d, $J = 7.9$ Hz, 1H), 7.96 – 7.89 (m, 1H), 7.74 – 7.50 (m, 4H), 1.98 (s, 3H). ^{13}C NMR (100 MHz, CDCl_3) δ 191.4, 151.7, 146.8, 145.5, 144.9, 140.8, 137.5, 135.7, 134.6, 132.2, 129.1, 128.8, 126.7, 124.1, 124.0, 121.4, 19.9. HRMS (ESI) calcd. for $\text{C}_{17}\text{H}_{13}\text{N}_2\text{O}_3$ ($\text{M} + \text{H}^+$) 293.0921. Found 293.0922.

2-(4-Methoxyquinolin-8-yl)-3-methylbenzaldehyde (3s). Following the general



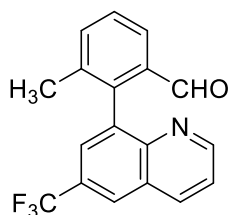
procedure from **5g** (238 mg, 1 mmol) and **2b**, afforded **3s** (261 mg, 94%) as an amorphous yellow solid. ^1H NMR (400 MHz, CDCl_3) δ 9.48 (s, 1H), 8.70 (d, $J = 5.2$ Hz, 1H), 8.33 (dd, $J = 8.1, 1.8$ Hz, 1H), 7.98 – 7.88 (m, 1H), 7.66 – 7.50 (m, 3H), 7.45 (t, $J = 7.7$ Hz, 1H), 6.76 (d, $J = 5.2$ Hz, 1H), 4.08 (s, 3H), 2.01 (s, 3H). ^{13}C NMR (100 MHz, CDCl_3) δ 192.8, 162.4, 151.8, 147.7, 143.7, 137.9, 135.8, 135.4, 134.9, 131.9, 127.9, 125.0, 124.7, 122.5, 121.7, 100.3, 55.9, 19.9. HRMS (ESI) calcd. for $\text{C}_{18}\text{H}_{16}\text{NO}_2$ ($\text{M} + \text{H}^+$) 278.1176. Found 278.1175.

3-Methyl-2-(4-methylquinolin-8-yl)benzaldehyde (3t). Following the general



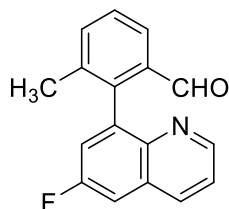
procedure from **5m** (98 mg, 0.6 mmol) and **2b**, afforded **3t** (110 mg, 85%) as an amorphous yellow solid. ^1H NMR (400 MHz, CDCl_3) δ 9.47 (s, 1H), 8.72 (d, $J = 4.4$ Hz, 1H), 8.13 (d, $J = 8.6$ Hz, 1H), 7.93 (d, $J = 7.7$ Hz, 1H), 7.65 (t, $J = 7.6$ Hz, 1H), 7.56 (d, $J = 6.0$ Hz, 2H), 7.46 (t, $J = 7.6$ Hz, 1H), 7.25 (d, $J = 4.5$ Hz, 1H), 2.78 (s, 3H), 2.00 (s, 3H). ^{13}C NMR (100 MHz, CDCl_3) δ 192.7, 150.5, 146.7, 144.5, 143.8, 137.9, 136.9, 135.4, 134.9, 131.2, 128.5, 127.9, 125.7, 124.7, 124.5, 122.2, 20.0, 18.9. HRMS (ESI) calcd. for $\text{C}_{18}\text{H}_{16}\text{NO}$ ($\text{M} + \text{H}^+$) 262.1226. Found 262.1230.

3-Methyl-2-(6-(trifluoromethyl)quinolin-8-yl)benzaldehyde (3u). Following the



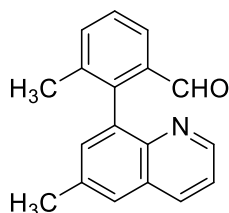
general procedure from **5h** (276 mg, 1 mmol) and **2b**, afforded **3u** (214 mg, 68%) as an amorphous yellow solid. ^1H NMR (400 MHz, CDCl_3) δ 9.52 (s, 1H), 8.96 (dd, $J = 4.2, 1.8$ Hz, 1H), 8.35 (dd, $J = 8.4, 1.8$ Hz, 2H), 8.30 – 8.25 (m, 1H), 7.96 (dd, $J = 7.8, 1.5$ Hz, 1H), 7.80 (d, $J = 2.1$ Hz, 1H), 7.64 – 7.58 (m, 1H), 7.56 – 7.49 (m, 2H), 2.02 (s, 3H). ^{13}C NMR (100 MHz, CDCl_3) δ 191.8, 152.9, 147.9, 141.4, 138.4, 137.3, 135.6, 134.9, 128.5, 127.6, 126.7, 126.7, 126.5 (q, $J = 271.6$ Hz), 126.36 (q, $J = 4.5$ Hz), 125.7, 122.6, 122.3, 19.9. ^{19}F NMR (377 MHz, CDCl_3) δ -62.2. HRMS (ESI) calcd. for $\text{C}_{18}\text{H}_{13}\text{F}_3\text{NO}$ ($\text{M} + \text{H}^+$) 316.0944. Found 316.0945.

2-(6-Fluoroquinolin-8-yl)-3-methylbenzaldehyde (3v). Following the general



procedure from **5i** (226 mg, 1 mmol) and **2b**, afforded **3v** (172 mg, 65%) as an amorphous yellow solid. ^1H NMR (400 MHz, CDCl_3) δ 9.53 (s, 1H), 8.80 (dd, $J = 4.3, 1.7$ Hz, 1H), 8.18 (dd, $J = 8.3, 1.8$ Hz, 1H), 7.94 (dd, $J = 7.8, 1.5$ Hz, 1H), 7.61 – 7.52 (m, 2H), 7.49 (t, $J = 7.6$ Hz, 1H), 7.43 – 7.36 (m, 2H), 2.02 (s, 3H). ^{13}C NMR (100 MHz, CDCl_3) δ 191.9, 159.5 (d, $J = 249.3$ Hz), 150.1 (d, $J = 2.7$ Hz), 144.2, 141.7, 139.6 (d, $J = 8.8$ Hz), 137.8, 135.8 (d, $J = 5.4$ Hz), 135.6, 134.9, 129.2 (d, $J = 10.3$ Hz), 128.4, 125.3, 122.2, 121.4 (d, $J = 25.8$ Hz), 111.3 (d, $J = 21.2$ Hz), 19.9. ^{19}F NMR (377 MHz, CDCl_3) δ -113.2. HRMS (ESI) calcd. for $\text{C}_{17}\text{H}_{13}\text{FNO}$ ($\text{M} + \text{H}^+$) 266.0976. Found 266.0983.

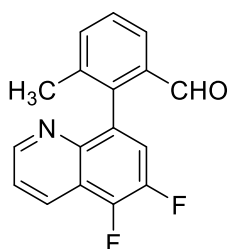
3-Methyl-2-(6-methylquinolin-8-yl)benzaldehyde (3w). Following the general



procedure from **5j** (222 mg, 1 mmol) and **2b**, afforded **3w** (232 mg, 89%) as an amorphous yellow solid. ^1H NMR (400 MHz, CDCl_3) δ 9.50 (s, 1H), 8.80 (dd, $J = 4.2, 1.8$ Hz, 1H), 8.14 (dd, $J = 8.3, 1.8$ Hz, 1H), 7.94 (dd, $J = 7.8, 1.5$ Hz, 1H), 7.73 – 7.67 (m, 1H), 7.57 (d, $J = 7.6$ Hz, 1H), 7.46 (t, $J = 7.7$ Hz, 1H), 7.42 (d, $J = 2.0$ Hz, 1H), 7.37 (dd, $J = 8.3, 4.2$ Hz, 1H), 2.58 (s, 3H), 2.02 (s, 3H). ^{13}C NMR (100 MHz, CDCl_3) δ 192.7, 150.0, 145.6, 143.4, 138.1, 136.1, 135.9, 135.7, 135.4, 134.9, 133.8, 128.5,

127.9, 127.4, 124.7, 121.4, 21.6, 20.0. HRMS (ESI) calcd. for C₁₈H₁₆NO (M + H⁺) 262.1226. Found 298.1228.

2-(5,6-Difluoroquinolin-8-yl)-3-methylbenzaldehyde (3x). Following the general



procedure from **5k** (244 mg, 1.0 mmol) and **2b**, afforded **3x** (283 mg, 99%) as an amorphous yellow solid. ¹H NMR (400 MHz, CDCl₃) δ 9.52 (s, 1H), 8.85 (dd, *J* = 4.3, 1.7 Hz, 1H), 8.52 (dd, *J* = 8.5, 1.8 Hz, 1H), 7.92 (dd, *J* = 7.7, 1.5 Hz, 1H), 7.59 (d, *J* = 7.5 Hz, 1H), 7.57 – 7.45 (m, 3H), 2.01 (s, 3H). ¹³C NMR (100 MHz, CDCl₃) δ 191.8, 150.8 (d, *J* = 2.7 Hz), 145.7 (dd, *J* = 250.0, 11.4 Hz), 143.5 (dd, *J* = 256.7, 13.0 Hz), 143.4, 140.6, 138.0, 135.6, 135.0, 134.1 – 133.8 (m), 129.2 – 129.0 (m), 128.5, 125.8, 121.9 (d, *J* = 3.3 Hz), 121.4 (d, *J* = 21.1 Hz), 120.2 (dd, *J* = 12.7, 2.6 Hz), 19.9. ¹⁹F NMR (377 MHz, CDCl₃) δ -139.2 (d, *J* = 19.4 Hz), -147.5 (d, *J* = 19.4 Hz). HRMS (ESI) calcd. for C₁₇H₁₂F₂NO (M + H⁺) 284.0881. Found 284.0885.

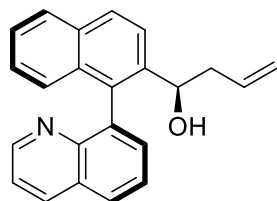
II.5.2. General procedure for the Ir-catalyzed asymmetric allylation of aldehydes **4a-x**.

In a flame-dried Schlenk tube, under N₂ atmosphere, there are added the corresponding aldehyde **3a-x** (0.2 mmol, 1.0 eq.), [Ir(cod)Cl]₂ (2.5 mol%), (*R*)-DM-BINAP (6 mol%), Cs₂CO₃ (0.2 eq.), *m*-nitrobenzoic acid (0.1 eq.) and anhydrous DME (0.2 M). Finally, allyl acetate (10 eq.) and anhydrous *i*PrOH (2 eq.) are subsequently added, and the reaction mixture is stirred at 100 °C for 20h. Upon reaction completion, the solvent is removed under reduced pressure and the residue is purified by flash column chromatography on silica gel (toluene/EtOAc 5:1) to isolate both diastereoisomers of allylic alcohols **4a-x**.

Note: racemic products for HPLC traces were prepared following the same general procedure using rac-BINAP instead of (R)-DM-BINAP.

1-(1-(Quinolin-8-yl)naphthalen-2-yl)but-3-en-1-ol (4a).

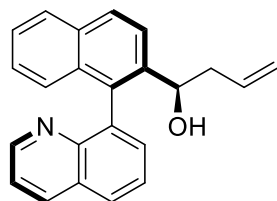
(*R_a,R*)-**4a** (49 mg, 75% yield): $[\alpha]_{\text{D}} +55.34$ (*c* 0.93, CHCl₃) for 97% *ee*. ¹H NMR (400



MHz, CDCl₃) δ 8.81 (dd, *J* = 4.2, 1.8 Hz, 1H), 8.29 (dd, *J* = 8.3, 1.8 Hz, 1H), 8.03 (d, *J* = 8.7 Hz, 1H), 8.00 (dd, *J* = 6.9, 2.8 Hz, 1H), 7.92 (d, *J* = 8.2 Hz, 1H), 7.85 (d, *J* = 8.7 Hz, 1H), 7.74 – 7.67 (m, 2H), 7.48 – 7.39 (m, 2H), 7.28 – 7.21 (m, 1H), 7.10

(d, *J* = 9.5 Hz, 1H), 5.59 – 5.45 (m, 1H), 4.98 – 4.84 (m, 2H), 4.51 (dd, *J* = 8.9, 3.9 Hz, 1H), 2.55 – 2.36 (m, 2H), 2.11 (br s, 1H). ¹³C NMR (100 MHz, CDCl₃) δ 150.5, 147.8, 139.3, 138.1, 136.4, 135.3, 134.9, 133.2, 132.9, 131.5, 128.6, 128.5, 128.2, 128.0, 126.9, 126.3, 125.9, 125.5, 123.6, 121.2, 117.6, 71.2, 42.6. HRMS (ESI) calcd. for C₂₃H₂₀NO (*M* + *H*⁺) 326.1539. Found 326.1537. HPLC (IA column, 90:10 *n*-Hex/*i*-PrOH, 30 °C, 1.0 mL/min): *t_R* 12.35 min (major) and 15.68 min (minor).

(*S_a,R*)-**4a** (6.5 mg, 10% yield): $[\alpha]_{\text{D}} +42.38$ (*c* 0.37, CHCl₃) for 99% *ee*. ¹H NMR (400

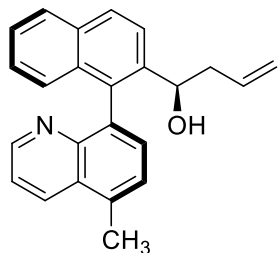


MHz, CDCl₃) δ 8.73 (dd, *J* = 4.2, 1.8 Hz, 1H), 8.31 (dd, *J* = 8.3, 1.8 Hz, 1H), 8.05 (d, *J* = 8.7 Hz, 1H), 8.00 (dd, *J* = 8.0, 1.7 Hz, 1H), 7.93 (d, *J* = 8.2 Hz, 1H), 7.89 (d, *J* = 8.7 Hz, 1H), 7.77 – 7.64 (m, 2H), 7.46 (ddd, *J* = 8.1, 6.7, 1.3 Hz, 1H), 7.41 (dd, *J* =

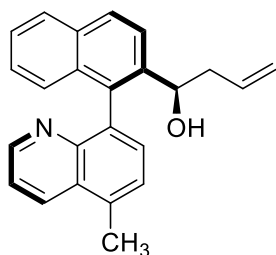
8.3, 4.2 Hz, 1H), 7.31 – 7.24 (m, 2H), 7.19 (d, *J* = 7.4 Hz, 0H), 5.71 – 5.56 (m, 1H), 5.09 – 4.86 (m, 2H), 4.52 (t, *J* = 7.1 Hz, 1H), 3.72 (s, 1H), 2.77 – 2.56 (m, 2H). ¹³C NMR (100 MHz, CDCl₃) δ 151.0, 147.4, 139.3, 137.6, 137.1, 135.0, 133.4, 133.2, 132.9, 129.2, 128.9, 128.8, 128.4, 128.3, 128.2, 126.6, 126.3, 126.1, 125.7, 123.6, 121.6, 117.1, 71.2, 40.3. HRMS (ESI) calcd. for C₂₃H₂₀NO (*M* + *H*⁺) 326.1539. Found 326.1538. HPLC (IA column, 90:10 *n*-Hex/*i*-PrOH, 30 °C, 1.0 mL/min): *t_R* 6.89 min (minor) and 9.03 min (major).

1-(1-(5-Methylquinolin-8-yl)naphthalen-2-yl)but-3-en-1-ol (4b).

(*R_a,R*)-4b (52.3 mg, 77% yield): [α]_D +42.95 (*c* 1.3, CHCl₃) for 98% *ee*. ¹H NMR (400 MHz, CDCl₃) δ 8.79 (dd, *J* = 4.1, 1.7 Hz, 1H), 8.46 (dd, *J* = 8.5, 1.8 Hz, 1H), 8.01 (d, *J* = 8.7 Hz, 1H), 7.90 (d, *J* = 8.2 Hz, 1H), 7.83 (d, *J* = 8.7 Hz, 1H), 7.61 – 7.50 (m, 2H), 7.48 – 7.38 (m, 2H), 7.26 – 7.19 (m, 1H), 7.12 (dd, *J* = 8.4, 1.2 Hz, 1H), 5.60 – 5.47 (m, 1H), 4.99 – 4.77 (m, 2H), 4.53 (dd, *J* = 8.9, 4.0 Hz, 1H), 2.84 (s, 3H), 2.58 – 2.30 (m, 2H), 2.09 (br s, 1H). ¹³C NMR (101 MHz, CDCl₃) δ 149.9, 148.0, 139.3, 136.1, 135.3, 135.2, 134.9, 133.3, 133.0, 132.7, 131.1, 128.4, 128.0, 127.7, 127.0, 126.9, 125.8, 125.5, 123.6, 120.8, 117.6, 71.2, 42.6, 18.8. HRMS (ESI) calcd. for C₂₄H₂₂NO (*M* + H⁺) 340.1696. Found 340.1693. HPLC (IC column, 90:10 *n*-Hex/*i*-PrOH, 30 °C, 1.0 mL/min): *t_R* 7.73 min (major) and 9.73 min (minor).

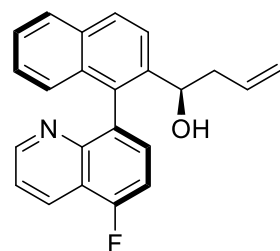


(*S_a,R*)-4b (4.8 mg, 7% yield): [α]_D +103.46 (*c* 0.9, CHCl₃) for 94% *ee*. ¹H NMR (400 MHz, CDCl₃) δ 8.75 (dd, *J* = 4.2, 1.7 Hz, 1H), 8.49 (dd, *J* = 8.5, 1.8 Hz, 1H), 8.03 (d, *J* = 8.7 Hz, 1H), 7.91 (d, *J* = 8.2 Hz, 1H), 7.86 (d, *J* = 8.6 Hz, 1H), 7.55 (d, *J* = 1.8 Hz, 2H), 7.51 – 7.40 (m, 2H), 7.28 – 7.21 (m, 1H), 7.18 (d, *J* = 8.5 Hz, 1H), 5.63 (ddt, *J* = 17.1, 10.2, 6.9 Hz, 1H), 5.00 (dd, *J* = 17.1, 1.8 Hz, 1H), 4.96 – 4.90 (m, 1H), 4.52 (t, *J* = 6.9 Hz, 1H), 3.67 (br s, 1H), 2.85 (s, 3H), 2.74 – 2.56 (m, 2H). HRMS (ESI) calcd. for C₂₄H₂₂NO (*M* + H⁺) 340.1696. Found 340.1691. HPLC (IA column, 90:10 *n*-Hex/*i*-PrOH, 30 °C, 1.0 mL/min): *t_R* 6.62 min (minor) and 9.91 min (major).

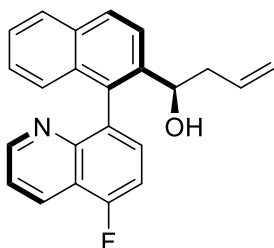


1-(1-(5-Fluoroquinolin-8-yl)naphthalen-2-yl)but-3-en-1-ol (4c).

(*R_a,R*)-**4c** (46.7 mg, 68% yield): [α]_D +42.81 (*c* 0.73, CHCl₃) for 95% *ee*. ¹H NMR (400 MHz, CDCl₃) δ 8.83 (dd, *J* = 4.2, 1.8 Hz, 1H), 8.58 (dd, *J* = 8.5, 1.8 Hz, 1H), 8.03 (d, *J* = 8.6 Hz, 1H), 7.92 (d, *J* = 8.2 Hz, 1H), 7.84 (d, *J* = 8.6 Hz, 1H), 7.63 (dd, *J* = 8.0, 6.1 Hz, 1H), 7.51 – 7.42 (m, 2H), 7.39 (dd, *J* = 9.5, 7.9 Hz, 1H), 7.28 – 7.20 (m, 1H), 7.12 – 7.03 (m, 1H), 5.60 – 5.45 (m, 1H), 4.98 – 4.84 (m, 2H), 4.50 (dd, *J* = 8.5, 4.3 Hz, 1H), 2.49 – 2.35 (m, 2H), 2.11 (s, 1H). ¹³C NMR (100 MHz, CDCl₃) δ 157.7 (d, *J* = 255.6 Hz), 151.3, 148.2, 139.6, 135.1, 134.1, 134.0 (d, *J* = 4.6 Hz), 133.2, 132.9, 130.9 (d, *J* = 8.4 Hz), 129.5, 128.8, 128.9, 126.7, 126.0, 125.6, 123.5, 121.3 (d, *J* = 2.4 Hz), 119.2 (d, *J* = 16.3 Hz), 117.8, 110.0 (d, *J* = 19.1 Hz), 71.0, 42.7. ¹⁹F NMR (377 MHz, CDCl₃) δ -122.5. HRMS (ESI) calcd. for C₂₃H₁₉FNO (*M* + *H*⁺) 344.1445. Found 344.1442. HPLC (IC column, 90:10 *n*-Hex/*i*-PrOH, 30 °C, 1.0 mL/min): *t_R* 5.78 min (major) and 6.99 min (minor).

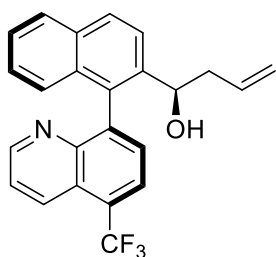


(*S_a,R*)-**4c** (6.9 mg, 10% yield): [α]_D +147.72 (*c* 0.8, CHCl₃) for 98% *ee*. ¹H NMR (400 MHz, CDCl₃) δ 8.79 (dd, *J* = 4.2, 1.8 Hz, 1H), 8.60 (dd, *J* = 8.5, 1.8 Hz, 1H), 8.05 (d, *J* = 8.7 Hz, 1H), 7.92 (d, *J* = 8.2 Hz, 1H), 7.87 (d, *J* = 8.6 Hz, 1H), 7.60 (dd, *J* = 8.0, 6.1 Hz, 1H), 7.51 (dd, *J* = 8.5, 4.2 Hz, 1H), 7.48 – 7.38 (m, 2H), 7.32 – 7.25 (m, 1H), 7.15 (d, *J* = 8.5 Hz, 1H), 5.61 (ddt, *J* = 17.1, 10.2, 6.9 Hz, 1H), 5.00 (dd, *J* = 17.2, 1.8 Hz, 1H), 4.96 – 4.91 (m, 1H), 4.46 (t, *J* = 7.1 Hz, 1H), 3.34 (s, 1H), 2.74 – 2.55 (m, 2H). ¹³C NMR (100 MHz, CDCl₃) δ 157.6 (d, *J* = 256.9 Hz), 151.6, 139.5, 134.7, 134.1, 133.4, 133.3, 133.2, 132.1 (d, *J* = 8.7 Hz), 130.1 (d, *J* = 4.8 Hz), 129.1, 129.0, 128.1, 126.3, 126.1, 125.7, 123.5, 121.6, 119.4 (d, *J* = 15.6 Hz), 117.2, 109.9 (d, *J* = 19.4 Hz), 71.1, 40.3. ¹⁹F NMR (377 MHz, CDCl₃) δ -122.3. HRMS (ESI) calcd. for C₂₃H₁₉FNO (*M* + *H*⁺) 344.1445. Found 344.1442. HPLC (IC column, 90:10 *n*-Hex/*i*-PrOH, 30 °C, 1.0 mL/min): *t_R* 7.13 min (major) and 8.14 min (minor).

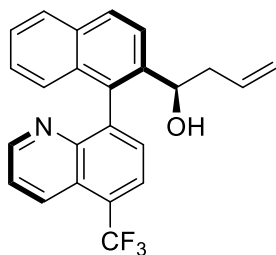


1-(1-(5-(Trifluoromethyl)quinolin-8-yl)naphthalen-2-yl)but-3-en-1-ol (4d).

(*R_a,R*)-**4d** (59 mg, 75% yield): $[\alpha]_D +34.32$ (*c* 0.44, CHCl₃) for 97% *ee*. ¹H NMR (400 MHz, CDCl₃) δ 8.86 (dd, *J* = 4.1, 1.7 Hz, 1H), 8.66 (dt, *J* = 8.7, 1.9 Hz, 1H), 8.08 (d, *J* = 7.5 Hz, 1H), 8.04 (d, *J* = 0.8 Hz, 1H), 7.97 – 7.91 (m, 1H), 7.86 (d, *J* = 8.6 Hz, 1H), 7.75 (d, *J* = 7.4 Hz, 1H), 7.56 (dd, *J* = 8.7, 4.1 Hz, 1H), 7.46 (ddd, *J* = 8.1, 6.8, 1.2 Hz, 1H), 7.31 – 7.25 (m, 1H), 7.01 (d, *J* = 8.5 Hz, 1H), 5.59 – 5.45 (m, 1H), 4.99 – 4.86 (m, 2H), 4.48 – 4.41 (m, 1H), 2.53 – 2.30 (m, 2H), 2.16 (br s 1H). ¹³C NMR (100 MHz, CDCl₃) δ 151.0, 147.9, 143.4, 139.0, 134.9, 133.9, 132.9, 132.8, 132.7, 129.9, 129.0, 128.1, 126.5, 126.4 (*q*, *J* = 30.7 Hz), 126.2, 125.8, 124.9 (*q*, *J* = 5.8 Hz), 124.6, 124.2 (*q*, *J* = 274.1 Hz), 123.5, 122.4, 118.0, 70.9, 42.7. ¹⁹F NMR (377 MHz, CDCl₃) δ -59.2. HRMS (ESI) calcd. for C₂₄H₁₉F₃NO (M + H⁺) 394.1413. Found 394.1410. HPLC (IA column, 90:10 *n*-Hex/*i*-PrOH, 30 °C, 1.0 mL/min): *t_R* 9.07 min (major) and 10.63 min (minor).

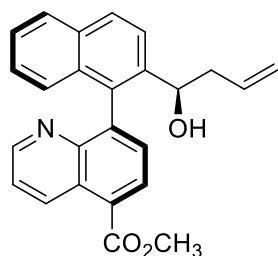


(*S_a,R*)-**4d** (6.3 mg, 8% yield): $[\alpha]_D +89.52$ (*c* 0.98, CHCl₃) for 94% *ee*. ¹H NMR (400 MHz, CDCl₃) δ 8.85 (dd, *J* = 4.2, 1.7 Hz, 1H), 8.68 (dt, *J* = 8.8, 1.8 Hz, 1H), 8.11 (d, *J* = 7.5 Hz, 1H), 8.08 (d, *J* = 8.7 Hz, 1H), 7.94 (d, *J* = 8.2 Hz, 1H), 7.88 (d, *J* = 8.7 Hz, 1H), 7.76 – 7.70 (m, 1H), 7.59 (dd, *J* = 8.7, 4.2 Hz, 1H), 7.47 (ddd, *J* = 8.2, 6.8, 1.2 Hz, 1H), 7.28 – 7.25 (m, 1H), 7.09 (dt, *J* = 8.4, 1.0 Hz, 1H), 5.60 (ddt, *J* = 17.1, 10.2, 7.0 Hz, 1H), 5.04 – 4.97 (m, 1H), 4.97 – 4.91 (m, 1H), 4.41 (t, *J* = 7.0 Hz, 1H), 3.12 (s, 1H), 2.74 – 2.56 (m, 2H). ¹³C NMR (100 MHz, CDCl₃) δ 151.2, 142.6, 139.2, 134.5, 133.8, 133.2, 132.6, 131.4, 129.5, 129.4, 128.2, 126.3, 126.0, 125.9, 124.9, 124.8, 124.7, 123.5, 122.7, 122.2, 117.4, 71.1, 40.4. ¹⁹F NMR (377 MHz, CDCl₃) δ -59.0. HRMS (ESI) calcd. for C₂₄H₁₉F₃NO (M + H⁺) 394.1413. Found 394.1410. HPLC (IC column, 90:10 *n*-Hex/*i*-PrOH, 30 °C, 1.0 mL/min): *t_R* 5.32 min (major) and 5.78 min (minor).



Methyl 8-(2-(1-hydroxybut-3-en-1-yl)naphthalen-1-yl)quinoline-5-carboxylate (4e).

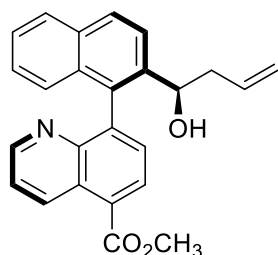
(*R_a,R*)-**4e** (52 mg, 68% yield): $[\alpha]_D +37.78$ (*c* 0.98, CHCl₃) for 94% *ee*. ¹H NMR (400



MHz, CDCl₃) δ 9.46 (dd, *J* = 8.8, 1.8 Hz, 1H), 8.80 (dd, *J* = 4.1, 1.8 Hz, 1H), 8.40 (d, *J* = 7.5 Hz, 1H), 8.01 (d, *J* = 8.7 Hz, 1H), 7.90 (d, *J* = 8.2 Hz, 1H), 7.82 (d, *J* = 8.7 Hz, 1H), 7.71 (d, *J* = 7.5 Hz, 1H), 7.50 (dd, *J* = 8.8, 4.1 Hz, 1H), 7.42 (t, *J* = 8.1 Hz, 1H), 7.27 – 7.18 (m, 1H), 7.00 (d, *J* = 8.4 Hz, 1H), 5.48 (dddd, *J* = 16.7, 10.2, 7.9, 6.4 Hz, 1H), 4.95 – 4.82 (m, 2H), 4.43 (dd,

J = 8.7, 4.1 Hz, 1H), 4.08 (s, 3H), 2.48 – 2.30 (m, 2H), 2.38 (s, 1H). ¹³C NMR (100 MHz, CDCl₃) δ 167.0, 150.6, 147.8, 143.9, 138.9, 135.0, 134.5, 134.4, 132.9, 132.7, 130.4, 130.2, 128.9, 128.1, 127.3, 127.0, 126.6, 126.1, 125.7, 123.5, 122.6, 117.9, 71.1, 52.5, 42.7. HRMS (ESI) calcd. for C₂₅H₂₂NO₃ (*M* + *H*⁺) 384.1594. Found 384.1591. HPLC (IA column, 90:10 *n*-Hex/*i*-PrOH, 30 °C, 1.0 mL/min): *t_R* 15.52 min (major) and 19.41 min (minor).

(*S_a,R*)-**4e** (8.1 mg, 8% yield): $[\alpha]_D +87.49$ (*c* 0.83, CHCl₃) for 94% *ee*. ¹H NMR (400 MHz,

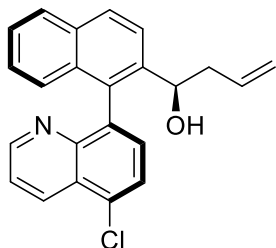


CDCl₃) δ 9.52 (dd, *J* = 8.8, 1.7 Hz, 1H), 8.79 (dd, *J* = 4.2, 1.7 Hz, 1H), 8.45 (d, *J* = 7.5 Hz, 1H), 8.06 (d, *J* = 8.7 Hz, 1H), 7.93 (d, *J* = 8.2 Hz, 1H), 7.87 (d, *J* = 8.7 Hz, 1H), 7.71 (d, *J* = 7.5 Hz, 1H), 7.56 (dd, *J* = 8.8, 4.1 Hz, 1H), 7.46 (t, *J* = 7.5 Hz, 1H), 7.26 (dd, *J* = 7.1, 1.5 Hz, 1H), 7.10 (d, *J* = 8.5 Hz, 1H), 5.59

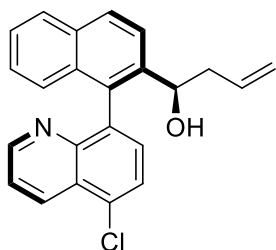
(ddt, *J* = 17.1, 10.2, 6.9 Hz, 1H), 5.05 – 4.90 (m, 2H), 4.43 (t, *J* = 7.1 Hz, 1H), 4.11 (s, 3H), 3.33 (s, 1H), 2.73 – 2.53 (m, 2H). ¹³C NMR (100 MHz, CDCl₃) δ 166.9, 150.9, 147.3, 143.3, 138.9, 135.2, 134.6, 134.4, 133.2, 132.6, 131.5, 130.1, 129.2, 128.2, 127.5, 126.9, 126.2, 125.8, 123.4, 122.8, 117.3, 71.2, 52.5, 40.2. HRMS (ESI) calcd. for C₂₅H₂₂NO₃ (*M* + *H*⁺) 384.1594. Found 384.1591. HPLC (IA column, 90:10 *n*-Hex/*i*-PrOH, 30 °C, 1.0 mL/min): *t_R* 7.15 min (minor) and 16.38 min (major).

1-(1-(5-Chloroquinolin-8-yl)naphthalen-2-yl)but-3-en-1-ol (4f).

(*R_a,R*)-**4f** (50 mg, 74% yield): $[\alpha]_D +36.08$ (*c* 1.13, CHCl₃) for 97% *ee*. ¹H NMR (400 MHz, CDCl₃) δ 8.81 (dd, *J* = 4.2, 1.7 Hz, 1H), 8.71 (dd, *J* = 8.6, 1.7 Hz, 1H), 8.01 (d, *J* = 8.6 Hz, 1H), 7.82 (d, *J* = 8.7 Hz, 1H), 7.77 (d, *J* = 7.7 Hz, 1H), 7.59 (d, *J* = 7.7 Hz, 1H), 7.51 (dd, *J* = 8.6, 4.2 Hz, 1H), 7.43 (t, *J* = 7.5 Hz, 1H), 7.26 – 7.17 (m, 1H), 7.05 (d, *J* = 8.5 Hz, 1H), 5.50 (ddt, *J* = 17.1, 10.1, 7.1 Hz, 1H), 4.95 – 4.83 (m, 2H), 4.47 (dd, *J* = 8.6, 4.3 Hz, 1H), 2.48 – 2.31 (m, 2H), 2.14 (s, 1H). ¹³C NMR (100 MHz, CDCl₃) δ 151.0, 148.3, 139.3, 137.5, 135.1, 134.1, 133.2, 133.0, 132.9, 131.3, 131.2, 129.1, 128.8, 128.1, 126.7, 126.5, 126.1, 125.6, 123.6, 122.0, 117.8, 71.0, 42.7. HRMS (ESI) calcd. for C₂₃H₁₉ClNO (*M* + H⁺) 360.1150. Found 360.1146. HPLC (IA column, 90:10 *n*-Hex/*i*-PrOH, 30 °C, 1.0 mL/min): *t_R* 11.63 min (major) and 14.05 min (minor).

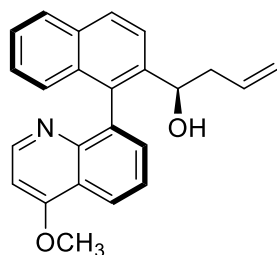


(*S_a,R*)-**4f** (7.5 mg, 11% yield): $[\alpha]_D +114.13$ (*c* 1.35, CHCl₃) for 97% *ee*. ¹H NMR (400 MHz, CDCl₃) δ 8.79 – 8.70 (m, 2H), 8.03 (d, *J* = 8.7 Hz, 1H), 7.90 (d, *J* = 8.2 Hz, 1H), 7.82 (dd, *J* = 17.7, 8.2 Hz, 2H), 7.57 (d, *J* = 7.7 Hz, 1H), 7.53 (dd, *J* = 8.6, 4.2 Hz, 1H), 7.48 – 7.39 (m, 1H), 7.30 – 7.21 (m, 1H), 7.12 (d, *J* = 8.6 Hz, 1H), 5.58 (ddt, *J* = 17.2, 10.2, 6.9 Hz, 1H), 5.03 – 4.88 (m, 2H), 4.43 (t, *J* = 7.1 Hz, 1H), 3.30 (s, 1H), 2.61 (qt, *J* = 14.0, 7.0 Hz, 2H). ¹³C NMR (100 MHz, CDCl₃) δ 151.4, 147.8, 139.3, 136.9, 134.6, 134.0, 133.8, 133.3, 132.9, 132.4, 131.4, 129.1, 128.1, 126.7, 126.4, 126.3, 126.2, 125.8, 123.5, 122.3, 117.2, 71.1, 40.3. HRMS (ESI) calcd. for C₂₃H₁₉ClNO (*M* + H⁺) 360.1150. Found 360.1146. HPLC (IA column, 90:10 *n*-Hex/*i*-PrOH, 30 °C, 1.0 mL/min): *t_R* 6.21 min (minor) and 9.14 min (major).



1-(1-(4-Methoxyquinolin-8-yl)naphthalen-2-yl)but-3-en-1-ol (4g).

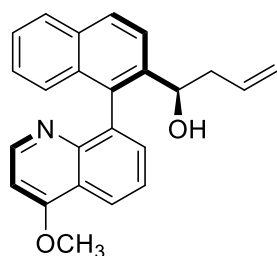
(*R_a,R*)-**4g** (38 mg, 38% yield): $[\alpha]_D^{25} +15.67$ (*c* 0.9, CHCl₃) for 96% *ee*. ¹H NMR (400 MHz,



CDCl₃) δ 8.61 (d, *J* = 5.2 Hz, 1H), 8.37 (t, *J* = 5.0 Hz, 1H), 7.98 (d, *J* = 8.6 Hz, 1H), 7.87 (d, *J* = 8.2 Hz, 1H), 7.80 (d, *J* = 8.6 Hz, 1H), 7.63 (d, *J* = 5.0 Hz, 2H), 7.40 (t, *J* = 7.5 Hz, 1H), 7.22 (t, *J* = 7.6 Hz, 1H), 7.07 (d, *J* = 8.5 Hz, 1H), 6.73 (d, *J* = 5.2 Hz, 1H), 5.52 (dddd, *J* = 16.7, 10.4, 7.9, 6.3 Hz, 1H), 4.95 – 4.84 (m,

2H), 4.51 (dd, *J* = 9.0, 3.8 Hz, 1H), 4.09 (s, 3H), 2.52 – 2.30 (m, 2H). ¹³C NMR (100 MHz, CDCl₃) δ 162.4, 151.4, 148.6, 139.1, 137.5, 135.4, 135.3, 133.2, 132.9, 131.9, 128.5, 127.9, 126.9, 125.9, 125.5, 125.3, 123.7, 122.1, 121.7, 117.6, 100.1, 71.3, 55.8, 42.6. HRMS (ESI) calcd. for C₂₄H₂₂NO₂ (*M* + *H*⁺) 356.1645. Found 356.1642. HPLC (IF column, 95:5 *n*-Hex/*i*-PrOH, 30 °C, 1.0 mL/min): *t_R* 24.87 min (minor) and 27.39 min (major).

(*S_a,R*)-**4g** (10 mg, 10% yield): $[\alpha]_D^{25} +124.19$ (*c* 0.73, CHCl₃) for 90% *ee*. ¹H NMR (400

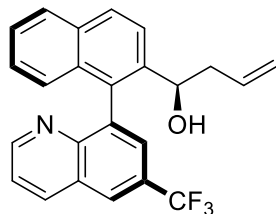


MHz, CDCl₃) δ 8.61 (d, *J* = 5.2 Hz, 1H), 8.40 (dd, *J* = 8.0, 1.9 Hz, 1H), 8.03 (d, *J* = 8.6 Hz, 1H), 7.91 (d, *J* = 8.2 Hz, 1H), 7.85 (d, *J* = 8.7 Hz, 1H), 7.72 – 7.61 (m, 2H), 7.44 (t, *J* = 7.4 Hz, 1H), 7.25 (d, *J* = 6.7 Hz, 1H), 7.18 (d, *J* = 8.5 Hz, 1H), 6.79 (d, *J* = 5.2 Hz, 1H), 5.62 (ddt, *J* = 17.1, 10.2, 6.9 Hz, 1H), 5.05 – 4.89 (m, 2H), 4.50 (t, *J* = 7.2 Hz, 1H), 4.13 (s, 3H), 3.86 (s, 1H), 2.76 –

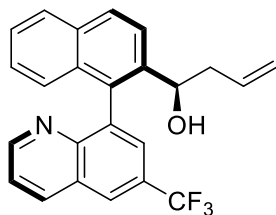
2.57 (m, 2H). ¹³C NMR (100 MHz, CDCl₃) δ 162.9, 151.8, 148.2, 139.0, 136.9, 135.3, 134.9, 133.3, 133.1, 128.8, 128.1, 126.6, 125.9, 125.6, 125.3, 123.4, 122.1, 121.9, 116.9, 100.5, 71.1, 55.9, 39.8. HRMS (ESI) calcd. for C₂₄H₂₂NO₂ (*M* + *H*⁺) 356.1645. Found 356.1643. HPLC (IA column, 90:10 *n*-Hex/*i*-PrOH, 30 °C, 1.0 mL/min): *t_R* 8.56 min (minor) and 10.39 min (major).

1-(1-(6-(Trifluoromethyl)quinolin-8-yl)naphthalen-2-yl)but-3-en-1-ol (4h).

(*R_a,R*)-**4h** (42.3 mg, 55% yield): [α]_D +33.05 (*c* 0.91, CHCl₃) for 94% *ee*. ¹H NMR (400 MHz, CDCl₃) δ 8.89 (dd, *J* = 4.2, 1.8 Hz, 1H), 8.37 (dd, *J* = 8.4, 1.9 Hz, 1H), 8.31 (d, *J* = 2.1 Hz, 1H), 8.03 (d, *J* = 8.7 Hz, 1H), 7.94 – 7.86 (m, 3H), 7.83 (d, *J* = 1.9 Hz, 1H), 7.51 (dd, *J* = 8.3, 4.2 Hz, 1H), 7.49 – 7.40 (m, 1H), 7.26 – 7.21 (m, 1H), 7.00 (dd, *J* = 8.6, 3.5 Hz, 1H), 5.57 – 5.42 (m, 1H), 4.96 – 4.77 (m, 2H), 4.44 (dd, *J* = 8.3, 4.4 Hz, 1H), 2.48 – 2.31 (m, 2H), 2.10 (s, 1H). ¹³C NMR (100 MHz, CDCl₃) δ 152.6, 148.8, 139.9, 139.5, 137.2, 134.9, 133.4, 132.9, 132.8, 129.1, 128.2, 127.5, 127.0, 127.0, 126.7 (q, *J* = 273.8 Hz), 126.4, 126.3, 126.0 (q, *J* = 4.13 Hz), 125.7, 123.6, 122.4, 117.8, 71.0, 42.7. ¹⁹F NMR (377 MHz, CDCl₃) δ -62.1. HRMS (ESI) calcd. for C₂₄H₁₉F₃NO (*M* + H⁺) 394.1413. Found 394.1409. HPLC (IF column, 90:10 *n*-Hex/*i*-PrOH, 30 °C, 1.0 mL/min): *t_R* 6.56 min (major) and 12.29 min (minor).

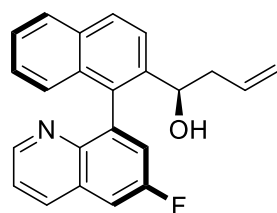


(*S_a,R*)-**4h** (12.1 mg, 15% yield): [α]_D +97.13 (*c* 2.27, CHCl₃) for 95% *ee*. ¹H NMR (300 MHz, CDCl₃) δ 8.79 (dd, *J* = 4.2, 1.8 Hz, 1H), 8.38 (dd, *J* = 8.3, 1.8 Hz, 1H), 8.30 (dt, *J* = 2.2, 1.2 Hz, 1H), 8.03 (t, *J* = 7.9 Hz, 1H), 7.96 – 7.90 (m, 1H), 7.88 – 7.83 (m, 2H), 7.52 – 7.43 (m, 2H), 7.35 – 7.28 (m, 1H), 7.17 – 7.03 (m, 1H), 5.57 (ddt, *J* = 17.2, 10.2, 7.0 Hz, 1H), 5.03 – 4.88 (m, 2H), 4.37 (t, *J* = 7.1 Hz, 1H), 2.72 – 2.49 (m, 2H). ¹³C NMR (75 MHz, CDCl₃) δ 152.9, 148.2, 139.4, 139.3, 137.7, 134.4, 133.3, 133.2, 132.7, 129.3, 129.2, 128.4, 128.2, 127.7, 127.1, 126.4 (q, *J* = 270.8 Hz), 126.1, 125.9 (q, *J* = 4.21 Hz), 125.8, 123.5, 122.7, 117.4, 71.2, 40.7. ¹⁹F NMR (377 MHz, CDCl₃) δ -62.4. HRMS (ESI) calcd. for C₂₄H₁₉FNO (*M* + H⁺) 394.1413. Found 394.1409. HPLC (IA column, 90:10 *n*-Hex/*i*-PrOH, 30 °C, 1.0 mL/min): *t_R* 6.18 min (minor) and 7.25 min (major).

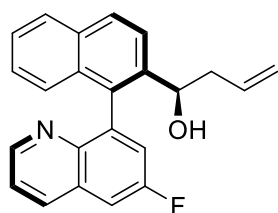


1-(1-(6-Fluoroquinolin-8-yl)naphthalen-2-yl)but-3-en-1-ol (4i).

(*R_aR*)-**4i** (41.9 mg, 61% yield): $[\alpha]_D +42.09$ (*c* 0.57, CHCl₃) for 96% *ee*. ¹H NMR (400 MHz, CDCl₃) δ 8.75 (dd, *J* = 4.2, 1.8 Hz, 1H), 8.24 (dd, *J* = 8.4, 1.8 Hz, 1H), 8.04 (d, *J* = 8.6 Hz, 1H), 7.92 (d, *J* = 8.1 Hz, 1H), 7.85 (d, *J* = 8.7 Hz, 1H), 7.61 (dd, *J* = 8.5, 2.9 Hz, 1H), 7.52 (dd, *J* = 8.8, 2.9 Hz, 1H), 7.48 – 7.40 (m, 2H), 7.30 – 7.23 (m, 1H), 7.08 (dd, *J* = 8.5, 1.1 Hz, 1H), 5.59 – 5.45 (m, 1H), 5.02 – 4.81 (m, 2H), 4.49 (dd, *J* = 8.7, 4.1 Hz, 1H), 2.50 – 2.33 (m, 2H), 2.12 (s, 1H). ¹³C NMR (100 MHz, CDCl₃) δ 159.8 (d, *J* = 249.2 Hz), 149.8, 145.1, 141.3 (d, *J* = 8.8 Hz), 139.3, 135.8 (d, *J* = 5.8 Hz), 135.1, 133.6, 132.9 (d, *J* = 11.5 Hz), 129.2, 129.1, 129.0, 128.1, 126.6, 126.2, 125.7, 123.5, 122.0, 121.63 (d, *J* = 25.3 Hz), 117.8, 111.1 (d, *J* = 20.8 Hz), 71.1, 42.7. ¹⁹F NMR (377 MHz, CDCl₃) δ -113.2. HRMS (ESI) calcd. for C₂₃H₁₉FNO (M + H⁺) 344.1445. Found 344.1442. HPLC (IA column, 90:19 *n*-Hex/*i*-PrOH, 30 °C, 1.0 mL/min): *t_R* 11.05 min (major) and 16.73 min (minor).

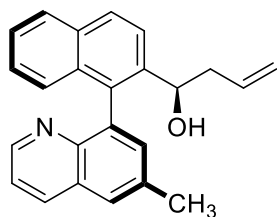


(*S_aR*)-**4i** (8.2 mg, 12% yield): $[\alpha]_D +59.76$ (*c* 1.16, CHCl₃) for 92% *ee*. ¹H NMR (400 MHz, CDCl₃) δ 8.72 (dd, *J* = 4.2, 1.8 Hz, 1H), 8.27 (dd, *J* = 8.4, 1.8 Hz, 1H), 8.06 (d, *J* = 8.7 Hz, 1H), 7.93 (d, *J* = 8.1 Hz, 1H), 7.87 (d, *J* = 8.7 Hz, 1H), 7.62 (dd, *J* = 8.5, 2.8 Hz, 1H), 7.53 – 7.44 (m, 3H), 7.33 – 7.29 (m, 1H), 7.18 – 7.15 (m, 1H), 5.62 (ddt, *J* = 17.2, 10.2, 7.0 Hz, 1H), 5.09 – 4.89 (m, 2H), 4.45 (t, *J* = 7.1 Hz, 1H), 3.43 (s, 1H), 2.77 – 2.56 (m, 2H). ¹³C NMR (100 MHz, CDCl₃) δ 159.7 (d, *J* = 249.8 Hz), 150.1, 144.5, 140.7 (d, *J* = 9.0 Hz), 139.2, 136.5 (d, *J* = 5.6 Hz), 134.6, 133.5, 133.3, 132.7, 129.5, 129.3, 128.2, 126.3, 126.1, 125.8, 123.4, 122.9 (d, *J* = 25.3 Hz), 122.3, 117.3, 111.0 (d, *J* = 21.4 Hz), 71.1, 40.2. ¹⁹F NMR (377 MHz, CDCl₃) δ -113.1. HRMS (ESI) calcd. for C₂₃H₁₉FNO (M + H⁺) 344.1445. Found 344.1443. HPLC (IA column, 90:10 *n*-Hex/*i*-PrOH, 30 °C, 1.0 mL/min): *t_R* 6.73 min (minor) and 9.24 min (major).

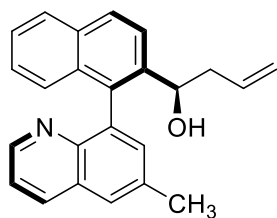


1-(1-(6-Methylquinolin-8-yl)naphthalen-2-yl)but-3-en-1-ol (4j).

(*R_a,R*)-**4j** (51 mg, 75% yield): [α]_D +21.15 (*c* 1.96, CHCl₃) for 95% *ee*. ¹H NMR (400 MHz, CDCl₃) δ 8.71 (dd, *J* = 4.2, 1.8 Hz, 1H), 8.17 (dd, *J* = 8.3, 1.8 Hz, 1H), 7.99 (d, *J* = 8.6 Hz, 1H), 7.89 (d, *J* = 8.2 Hz, 1H), 7.82 (d, *J* = 8.7 Hz, 1H), 7.73 (s, 1H), 7.51 (d, *J* = 2.0 Hz, 1H), 7.41 (t, *J* = 7.5 Hz, 1H), 7.35 (dd, *J* = 8.3, 4.2 Hz, 1H), 7.23 (t, *J* = 7.6 Hz, 1H), 7.10 (d, *J* = 8.5 Hz, 1H), 5.50 (dddd, *J* = 16.8, 10.2, 7.9, 6.4 Hz, 1H), 4.95 – 4.82 (m, 2H), 4.50 (dd, *J* = 9.0, 3.8 Hz, 1H), 2.59 (s, 3H), 2.51 – 2.31 (m, 2H). ¹³C NMR (100 MHz, CDCl₃) δ 149.7, 146.4, 139.2, 137.8, 136.1, 135.7, 135.3, 134.9, 133.6, 133.2, 132.9, 128.5, 128.0, 127.1, 126.9, 125.9, 125.5, 123.5, 121.2, 117.7, 71.1, 42.7, 21.6. HRMS (ESI) calcd. for C₂₄H₂₂NO (*M* + H⁺) 340.1696. Found 340.1694. HPLC (IA column, 90:10 *n*-Hex/*i*-PrOH, 30 °C, 1.0 mL/min): *t_R* 10.13 min (major) and 16.29 min (minor).

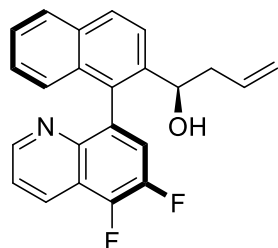


(*S_a,R*)-**4j** (4.6 mg, 7% yield): [α]_D +140.78 (*c* 0.58, CHCl₃) for 90% *ee*. ¹H NMR (400 MHz, CDCl₃) δ 8.66 (dd, *J* = 4.2, 1.8 Hz, 1H), 8.20 (dd, *J* = 8.3, 1.8 Hz, 1H), 8.01 (d, *J* = 8.7 Hz, 1H), 7.89 (d, *J* = 8.2 Hz, 1H), 7.84 (d, *J* = 8.7 Hz, 1H), 7.73 (s, 1H), 7.49 (d, *J* = 2.0 Hz, 1H), 7.46 – 7.34 (m, 2H), 7.24 (d, *J* = 9.8 Hz, 1H), 7.16 (d, *J* = 8.5 Hz, 1H), 5.61 (ddt, *J* = 17.1, 10.3, 6.9 Hz, 1H), 5.07 – 4.82 (m, 2H), 4.48 (t, *J* = 7.1 Hz, 1H), 3.65 (s, 1H), 2.68 (dt, *J* = 14.5, 7.3 Hz, 1H), 2.61 (s, 3H). ¹³C NMR (100 MHz, CDCl₃) δ 149.9, 145.9, 139.1, 137.1, 136.3, 136.0, 134.9, 133.3, 133.1, 128.8, 128.1, 126.9, 126.5, 125.9, 125.6, 123.4, 121.5, 116.9, 71.1, 40.0, 21.6. HRMS (ESI) calcd. for C₂₄H₂₂NO (*M* + H⁺) 340.1696. Found 340.1692. HPLC (IA column, 90:10 *n*-Hex/*i*-PrOH, 30 °C, 1.0 mL/min): *t_R* 5.78 min (minor) and 7.15 min (major).



1-(1-(5,6-Difluoroquinolin-8-yl)naphthalen-2-yl)but-3-en-1-ol (4k).

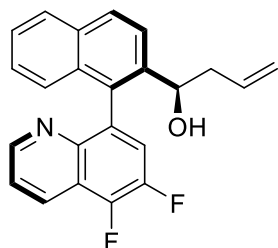
(*R_a,R*)-**4k** (50.6 mg, 70% yield): [α]_D +30.38 (*c* 0.76, CHCl₃) for 95% *ee*. ¹H NMR (400



MHz, CDCl₃) δ 8.80 (dd, *J* = 4.2, 1.1 Hz, 1H), 8.58 (dd, *J* = 8.5, 1.8 Hz, 1H), 8.04 (d, *J* = 8.7 Hz, 1H), 7.92 (d, *J* = 8.3 Hz, 1H), 7.84 (d, *J* = 8.6 Hz, 1H), 7.61 (dd, *J* = 10.6, 8.4 Hz, 1H), 7.51 (ddd, *J* = 8.5, 4.2, 0.9 Hz, 1H), 7.46 (ddd, *J* = 8.1, 6.8, 1.2 Hz, 1H), 7.32 – 7.23 (m, 1H), 7.05 (d, *J* = 8.1 Hz, 1H), 5.59 – 5.45

(m, 1H), 4.98 – 4.86 (m, 2H), 4.48 (ddd, *J* = 7.3, 4.7, 2.0 Hz, 1H), 2.50 – 2.34 (m, 2H), 2.16 (br s, 1H). ¹³C NMR (100 MHz, CDCl₃) δ 150.4, 145.9 (dd, *J* = 251.2, 11.9 Hz), 144.2, 143.4 (dd, *J* = 255.7, 13.1 Hz) 139.5, 135.5, 134.9, 132.9, 132.8, 129.2, 129.0, 128.2, 126.4, 126.3, 125.8, 123.5, 121.9, 121.8, 121.6, 120.1 (d, *J* = 12.4 Hz), 117.9, 70.9, 42.8. ¹⁹F NMR (377 MHz, CDCl₃) δ -140.3 (d, *J* = 19.4 Hz), -148.9 (d, *J* = 19.4 Hz). HRMS (ESI) calcd. for C₂₃H₁₈F₂NO (M + H⁺) 362.1351. Found 362.1348. HPLC (IC column, 90:10 *n*-Hex/*i*-PrOH, 30 °C, 1.0 mL/min): *t_R* 5.42 min (minor) and 6.01 min (major).

(*S_a,R*)-**4k** (10.8 mg, 15% yield): [α]_D +122.62 (*c* 1.3, CHCl₃) for 95% *ee*. ¹H NMR (400



MHz, CD₂Cl₂) δ 8.77 (ddd, *J* = 4.1, 1.7, 0.6 Hz, 1H), 8.62 (dd, *J* = 8.5, 1.7 Hz, 1H), 8.08 (d, *J* = 8.7 Hz, 1H), 7.96 (d, *J* = 8.2 Hz, 0H), 7.86 (d, *J* = 8.7 Hz, 1H), 7.65 – 7.54 (m, 2H), 7.50 (ddd, *J* = 8.1, 6.8, 1.2 Hz, 1H), 7.32 (ddd, *J* = 8.3, 6.8, 1.4 Hz, 1H), 7.15 (dd, *J* = 8.5, 1.0 Hz, 1H), 5.64 (ddt, *J* = 17.2, 10.2, 7.0 Hz, 1H),

5.06 – 4.94 (m, 2H), 4.46 – 4.36 (m, 1H), 2.88 (br s, 1H), 2.69 – 2.52 (m, 2H). ¹³C NMR (101 MHz, CD₂Cl₂) δ 150.8, 145.8 (dd, *J* = 251.3, 12.3 Hz), 143.8, 143.3 (dd, *J* = 254.5, 13.2 Hz), 139.9, 134.9, 134.7, 133.0, 132.8, 129.5, 129.4, 129.0, 128.0, 126.3, 126.0, 125.8, 123.6, 122.7, (d, *J* = 21.0 Hz), 122.2, 122.1, 117.0, 70.9, 40.9. ¹⁹F NMR (377 MHz, CD₂Cl₂) δ -140.3 (d, *J* = 19.4 Hz), -148.9 (d, *J* = 19.4 Hz). HRMS (ESI) calcd. for C₂₃H₁₈F₂NO (M + H⁺) 362.1351. Found 362.1348. HPLC (IC column, 90:10 *n*-Hex/*i*-PrOH, 30 °C, 1.0 mL/min): *t_R* 6.06 min (major) and 6.67 min (minor).

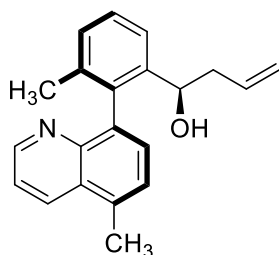
1-(3-Methyl-2-(quinolin-8-yl)phenyl)but-3-en-1-ol (4I).

(*R_a,R*)-**4I** (45 mg, 78% yield): $[\alpha]_D +4.3$ (*c* 0.71, CHCl₃) for 96% *ee*. ¹H NMR (400 MHz, CDCl₃): δ 8.87 (dd, *J* = 4.2, 1.8 Hz, 1H), 8.22 (dd, *J* = 8.3, 1.8 Hz, 1H), 7.88 (dd, *J* = 8.0, 1.6 Hz, 1H), 7.62 (dd, *J* = 8.0, 7.0 Hz, 1H), 7.59 – 7.49 (m, 2H), 7.44 – 7.36 (m, 2H), 7.30 – 7.25 (m, 1H), 5.53 – 5.30 (m, 1H), 4.90 – 4.68 (m, 2H), 4.36 (dd, *J* = 8.6, 4.0 Hz, 1H), 2.35 – 2.10 (m, 2H), 2.07 – 1.98 (s, 1H), 1.88 (s, 3H). ¹³C NMR (100 MHz, CDCl₃) δ 150.5, 146.9, 142.2, 139.2, 137.8, 136.9, 136.3, 135.3, 130.4, 128.9, 128.6, 128.1, 127.8, 126.4, 123.1, 121.1, 117.4, 70.9, 42.8, 20.7. HRMS (ESI) calcd. for C₁₉H₁₈NO (*M* + H⁺) 290.1539. Found 290.1538. HPLC (IC column, 90:10 *n*-Hex/*i*-PrOH, 30 °C, 1.0 mL/min): *t_R* 6.85 min (minor) and 7.21 min (major).

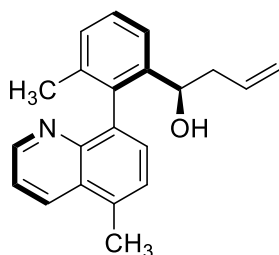
(*S_a,R*)-**4I** (8.1 mg, 14% yield): $[\alpha]_D +86.8$ (*c* 0.34, CHCl₃) for 94% *ee*. ¹H NMR (400 MHz, CDCl₃) δ 8.80 (dd, *J* = 4.3, 1.8 Hz, 1H), 8.25 (dd, *J* = 8.3, 1.8 Hz, 1H), 7.90 (d, *J* = 1.5 Hz, 1H), 7.63 (dd, *J* = 8.2, 7.1 Hz, 1H), 7.58 – 7.48 (m, 2H), 7.46 – 7.38 (m, 2H), 7.29 (d, *J* = 7.3 Hz, 1H), 5.59 (ddt, *J* = 17.1, 10.2, 6.9 Hz, 1H), 5.00 – 4.88 (m, 2H), 4.24 (dd, *J* = 7.7, 6.2 Hz, 1H), 3.28 (s, 1H), 2.51 (dt, *J* = 11.5, 6.9 Hz, 2H), 1.87 (s, 3H). ¹³C NMR (100 MHz, CDCl₃) δ 150.7, 146.7, 142.2, 138.8, 138.2, 136.9, 136.6, 135.2, 131.5, 129.5, 128.7, 128.3, 127.8, 126.4, 123.1, 121.4, 116.8, 70.8, 40.3, 20.9. HRMS (ESI) calcd. for C₂₀H₂₀NO (*M* + H⁺) 290.1539. Found 290.1538. HPLC (IA column, 90:10 *n*-Hex/*i*-PrOH, 30 °C, 1.0 mL/min): *t_R* 5.56 min (minor) and 6.25 min (major).

1-(3-Methyl-2-(5-methylquinolin-8-yl)phenyl)but-3-en-1-ol (4m).

(*R_a,R*)-**4m** (50 mg, 83% yield): $[\alpha]_D +7.8$ (*c* 1.33, CHCl₃) for 96% *ee*. ¹H NMR (400 MHz, CDCl₃) δ 8.86 (dd, *J* = 4.2, 1.8 Hz, 1H), 8.39 (dd, *J* = 8.5, 1.8 Hz, 1H), 7.54 – 7.49 (m, 1H), 7.45 (s, 2H), 7.44 – 7.32 (m, 2H), 7.30 – 7.25 (m, 1H), 5.56 – 5.36 (m, 1H), 4.94 – 4.72 (m, 2H), 4.38 (d, *J* = 5.0 Hz, 1H), 2.77 (s, 3H), 2.30 – 2.15 (m, 2H), 2.04 (d, *J* = 3.1 Hz, 1H), 1.88 (s, 3H). ¹³C NMR (100 MHz, CDCl₃) δ 149.88, 147.16, 142.34, 138.17, 137.24, 137.05, 135.39, 134.48, 132.70, 129.98, 128.84, 127.94, 127.85, 126.94, 123.10, 120.66, 117.30, 70.99, 42.74, 20.70, 18.73. HRMS (ESI) calcd. for C₂₁H₂₂NO (*M* + H⁺) 304.1696. Found 304.1693. HPLC (IA column, 90:10 *n*-Hex/*i*-PrOH, 30 °C, 1.0 mL/min): *t_R* 8.04 min (major) and 9.92 min (minor).

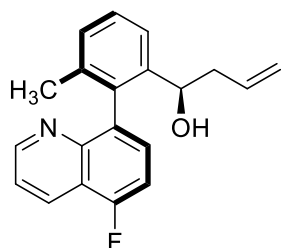


(*S_a,R*)-**4m** (6.9 mg, 12% yield): $[\alpha]_D +117.4$ (*c* 0.45, CHCl₃) for 95% *ee*. ¹H NMR (400 MHz, CDCl₃) δ 8.79 (dd, *J* = 4.2, 1.7 Hz, 1H), 8.42 (dd, *J* = 8.5, 1.8 Hz, 1H), 7.53 (d, *J* = 7.7 Hz, 1H), 7.50 – 7.35 (m, 4H), 7.29 (s, 1H), 5.60 (ddt, *J* = 17.1, 10.2, 6.9 Hz, 1H), 4.96 – 4.87 (m, 2H), 4.27 (t, *J* = 7.0 Hz, 1H), 3.30 (s, 1H), 2.77 (s, 3H), 2.61 – 2.43 (m, 2H), 1.87 (s, 3H). ¹³C NMR (100 MHz, CDCl₃) δ 150.1, 142.2, 138.6, 136.8, 136.7, 135.3, 134.5, 133.3, 131.1, 129.4, 128.1, 128.0, 126.9, 123.0, 120.9, 116.8, 70.7, 40.3, 21.0, 18.7. HRMS (ESI) calcd. for C₂₁H₂₂NO (*M* + H⁺) 304.1696. Found 304.1696. HPLC (IA column, 90:10 *n*-Hex/*i*-PrOH, 30 °C, 1.0 mL/min): *t_R* 7.50 min (minor) and 7.89 min (major).

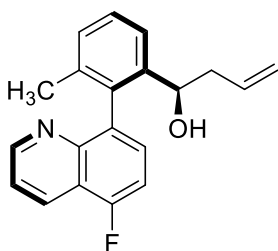


1-(2-(5-Fluoroquinolin-8-yl)-3-methylphenyl)but-3-en-1-ol (4n).

(*R_a,R*)-**4n** (36 mg, 61% yield): [α]_D +11.6 (*c* 1.7, CHCl₃) for 95% *ee*. ¹H NMR (400 MHz, CDCl₃) δ 8.90 (dd, *J* = 4.2, 1.8 Hz, 1H), 8.50 (dd, *J* = 8.5, 1.8 Hz, 1H), 7.51 (d, *J* = 1.7 Hz, 2H), 7.46 (dd, *J* = 8.5, 4.2 Hz, 1H), 7.41 (t, *J* = 7.7 Hz, 1H), 7.31 (dd, *J* = 9.5, 7.9 Hz, 1H), 5.55 – 5.29 (m, 1H), 4.90 – 4.73 (m, 2H), 4.33 (dt, *J* = 7.8, 3.6 Hz, 1H), 2.30 – 2.12 (m, 2H), 1.92 (d, *J* = 3.3 Hz, 1H), 1.86 (s, 3H). ¹³C NMR (100 MHz, CDCl₃) δ 157.4 (d, *J* = 255.9 Hz), 151.2, 147.3, 142.4, 140.4, 137.1, 137.1, 135.1, 129.7 (d, *J* = 8.4 Hz), 129.5 (d, *J* = 4.8 Hz), 128.9, 128.3, 123.1, 121.2, 119.2 (d, *J* = 16.4 Hz), 117.6, 110.0 (d, *J* = 19.0 Hz), 70.8, 42.9, 20.6. ¹⁹F NMR (377 MHz, CDCl₃) δ -123.0. HRMS (ESI) calcd. for C₂₀H₁₉FNO (*M* + *H*⁺) 308.1445. Found 308.1442. HPLC (IB column, 90:10 *n*-Hex/*i*-PrOH, 30 °C, 1.0 mL/min): *t_R* 5.19 min (minor) and 6.54 min (major).

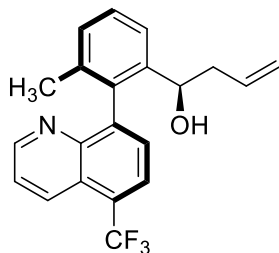


(*S_a,R*)-**4n** (3.6 mg, 8% yield): [α]_D +104.3 (*c* 0.63, CHCl₃) for 91% *ee*. ¹H NMR (400 MHz, CDCl₃) δ 8.85 (dd, *J* = 4.3, 1.8 Hz, 1H), 8.53 (dd, *J* = 8.5, 1.8 Hz, 1H), 7.54 (d, *J* = 7.8 Hz, 1H), 7.48 (dt, *J* = 8.7, 4.3 Hz, 1H), 7.47 – 7.39 (m, 2H), 7.36 – 7.28 (m, 2H), 5.58 (ddt, *J* = 17.1, 10.2, 6.9 Hz, 1H), 5.03 – 4.86 (m, 2H), 4.22 (dd, *J* = 7.7, 6.2 Hz, 1H), 3.04 (s, 1H), 2.50 (qt, *J* = 13.9, 7.0 Hz, 2H), 1.87 (s, 3H). ¹³C NMR (100 MHz, CDCl₃) δ 157.1 (d, *J* = 256.0 Hz), 151.5, 147.0, 142.4, 137.4, 136.8, 135.0, 134.7 (d, *J* = 6.9 Hz), 130.8 (d, *J* = 8.1 Hz), 130.1, 129.5, 128.5, 123.2, 121.5, 119.5, 117.0, 110.0 (d, *J* = 18.9 Hz), 70.7, 40.5, 20.9. ¹⁹F NMR (377 MHz, CDCl₃) δ -122.90. HRMS (ESI) calcd. for C₂₀H₁₉FNO (*M* + *H*⁺) 308.1445. Found 308.1447. HPLC (IA column, 90:10 *n*-Hex/*i*-PrOH, 30 °C, 1.0 mL/min): *t_R* 5.06 min (minor) and 5.92 min (major).

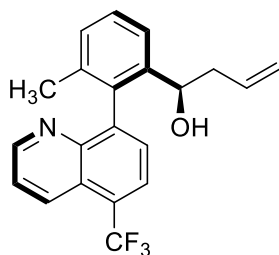


1-(3-Methyl-2-(5-(trifluoromethyl)quinolin-8-yl)phenyl)but-3-en-1-ol (4o).

(*R_a,R*)-**4o** (42 mg, 63% yield): $[\alpha]_D -5.35$ (*c* 0.52, CHCl₃) for 96% *ee*. ¹H NMR (400 MHz, CDCl₃) δ 8.94 (dd, *J* = 4.2, 1.7 Hz, 1H), 8.58 (dq, *J* = 8.7, 1.9 Hz, 1H), 8.01 (d, *J* = 7.5 Hz, 1H), 7.64 (d, *J* = 7.4 Hz, 1H), 7.61 – 7.50 (m, 2H), 7.43 (t, *J* = 7.7 Hz, 1H), 7.28 (d, *J* = 7.5 Hz, 1H), 5.44 (dddd, *J* = 16.9, 10.2, 7.7, 6.5 Hz, 1H), 4.92 – 4.74 (m, 2H), 4.27 (ddd, *J* = 7.3, 4.3, 2.2 Hz, 1H), 2.30 – 2.13 (m, 2H), 1.97 (d, *J* = 3.1 Hz, 1H), 1.86 (s, 3H). ¹³C NMR (100 MHz, CDCl₃) δ 150.9, 147.1, 144.4, 141.8, 136.9, 136.5, 134.9, 132.8, 129.0, 128.9, 128.5, 126.0 (q, *J* = 31.5 Hz), 125.0 (q, *J* = 6.0 Hz), 124.7, 124.1 (q, *J* = 273.3 Hz), 123.2, 122.3, 117.7, 70.7, 42.8, 20.6. ¹⁹F NMR (377 MHz, CDCl₃) δ -58.96. HRMS (ESI) calcd. for C₂₁H₁₉F₃NO (M + H⁺) 358.1413. Found 358.1409. HPLC (IA column, 90:10 *n*-Hex/*i*-PrOH, 30 °C, 1.0 mL/min): *t_R* 6.02 min (major) and 7.39 min (minor).

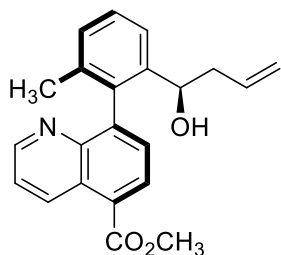


(*S_a,R*)-**4o** (8 mg, 11% yield): $[\alpha]_D +106.65$ (*c* 0.62, CHCl₃) for 93% *ee*. ¹H NMR (400 MHz, CDCl₃) δ 8.89 (dd, *J* = 4.2, 1.7 Hz, 1H), 8.65 – 8.56 (m, 1H), 8.01 (d, *J* = 7.5 Hz, 1H), 7.64 – 7.52 (m, 3H), 7.45 (t, *J* = 7.7 Hz, 1H), 7.30 (d, *J* = 7.6 Hz, 1H), 5.58 (ddt, *J* = 17.2, 10.2, 7.0 Hz, 1H), 5.01 – 4.89 (m, 2H), 4.17 (t, *J* = 6.9 Hz, 1H), 2.92 (s, 1H), 2.59 – 2.42 (m, 2H), 1.86 (s, 3H). ¹³C NMR (100 MHz, CDCl₃) δ 151.2, 144.0, 141.9, 137.2, 136.1, 134.8, 133.3, 129.9, 129.5, 128.7, 126.1 (q, *J* = 30.0 Hz), 124.9, 124.9, 124.8 (q, *J* = 5.8 Hz), 124.0 (q, *J* = 271.6 Hz), 123.3, 122.6, 117.2, 70.8, 40.6, 20.9. ¹⁹F NMR (377MHz, CDCl₃) δ -59.0. HRMS (ESI) calcd. for C₂₁H₁₉F₃NO (M + H⁺) 358.1413. Found 358.1411. HPLC (IA column, 90:10 *n*-Hex/*i*-PrOH, 30 °C, 1.0 mL/min): *t_R* 4.65 min (minor) and 5.63 min (major).

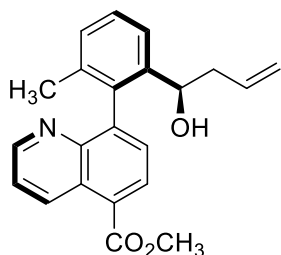


Methyl 8-(2-(1-hydroxybut-3-en-1-yl)-6-methylphenyl)quinoline-5-carboxylate (4p).

(*R_a,R*)-**4p** (48.3 mg, 70% yield): $[\alpha]_D +3.29$ (*c* 1.8, CHCl₃) for 96% *ee*. ¹H NMR (400 MHz, CDCl₃) δ 9.42 (dd, *J* = 8.7, 1.8 Hz, 1H), 8.89 (dd, *J* = 4.2, 1.7 Hz, 1H), 8.35 (d, *J* = 7.4 Hz, 1H), 7.61 (d, *J* = 7.4 Hz, 1H), 7.51 (dt, *J* = 8.2, 3.5 Hz, 2H), 7.42 (t, *J* = 7.7 Hz, 1H), 7.28 (s, 1H), 5.40 (ddd, *J* = 17.1, 9.9, 7.1 Hz, 1H), 4.96 – 4.74 (m, 2H), 4.29 (s, 1H), 4.05 (s, 3H), 2.20 (ddd, *J* = 14.4, 8.5, 5.1 Hz, 2H), 1.94 (d, *J* = 3.2 Hz, 1H), 1.85 (s, 3H). ¹³C NMR (100 MHz, CDCl₃) δ 166.9, 150.6, 147.0, 145.1, 141.8, 137.4, 136.4, 135.0, 134.5, 130.5, 129.1, 128.9, 128.4, 127.4, 126.6, 123.2, 122.5, 117.7, 70.8, 52.4, 42.9, 20.6. HRMS (ESI) calcd. for C₂₂H₂₂NO₃ (M + H⁺) 348.1594. Found 348.1592. HPLC (IB column, 90:10 *n*-Hex/*i*-PrOH, 30 °C, 1.0 mL/min): *t_R* 6.25 min (minor) and 6.97 min (major).

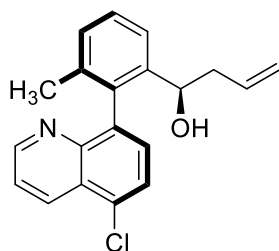


(*S_a,R*)-**4p** (6.2 mg, 10% yield): $[\alpha]_D +44.96$ (*c* 0.52, CHCl₃) for 94% *ee*. ¹H NMR (400 MHz, CDCl₃) δ 9.47 (dd, *J* = 8.8, 1.8 Hz, 1H), 8.87 (dd, *J* = 4.2, 1.7 Hz, 1H), 8.38 (d, *J* = 7.5 Hz, 1H), 7.57 (t, *J* = 8.0 Hz, 3H), 7.46 (t, *J* = 7.7 Hz, 1H), 7.32 (s, 1H), 5.68 – 5.50 (m, 1H), 5.03 – 4.87 (m, 2H), 4.21 (t, *J* = 7.0 Hz, 1H), 4.08 (s, 3H), 3.05 (s, 1H), 2.53 (qt, *J* = 14.0, 7.0 Hz, 2H), 1.88 (s, 3H). ¹³C NMR (100 MHz, CDCl₃) δ 166., 150.8, 146.8, 144.6, 141.8, 137.8, 136.0, 135.1, 134.9, 130.4, 130.2, 129.5, 128.6, 127.6, 126.6, 123.2, 122.7 117.1, 70.7, 52.4, 40.4, 20.9. HRMS (ESI) calcd. for C₂₂H₂₂NO₃ (M + H⁺) 348.1594. Found 348.1591. HPLC (IA column, 95:5 *n*-Hex/*i*-PrOH, 30 °C, 1.0 mL/min): *t_R* 7.94 min (minor) and 16.61 min (major).



1-(2-(5-Chloroquinolin-8-yl)-3-methylphenyl)but-3-en-1-ol (4q).

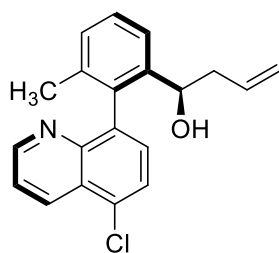
(*R_a,R*)-**4q** (50 mg, 77% yield): $[\alpha]_D +17.52$ (*c* 1.67, CHCl₃) for 95% *ee*. ¹H NMR (400



MHz, CDCl₃) δ 8.90 (dd, *J* = 4.1, 1.8 Hz, 1H), 8.66 (dd, *J* = 8.5, 1.8 Hz, 1H), 7.72 (d, *J* = 7.7 Hz, 1H), 7.56 – 7.47 (m, 3H), 7.41 (t, *J* = 7.7 Hz, 1H), 7.29 – 7.22 (m, 1H), 5.44 (dddd, *J* = 16.9, 10.2, 7.7, 6.5 Hz, 1H), 4.93 – 4.74 (m, 2H), 4.33 (dd, *J* = 8.5, 4.2 Hz, 1H), 2.31 – 2.13 (m, 2H), 2.02 (s, 1H), 1.87 (s, 3H). ¹³C

NMR (100 MHz, CDCl₃) δ 150.9, 147.5, 142.2, 138.6, 137.0, 136.9, 135.1, 133.2, 130.9, 130.1, 128.9, 128.3, 126.6, 123.2, 121.9, 117.6, 70.8, 42.9, 20.7. HRMS (ESI) calcd. for C₂₀H₁₉ClNO (*M* + H⁺) 324.1150. Found 324.1149. HPLC (IA column, 90:10 *n*-Hex/*i*-PrOH, 30 °C, 1.0 mL/min): *t_R* 7.46 min (major) and 9.11 min (minor).

(*S_a,R*)-**4q** (9.2 mg, 13% yield): $[\alpha]_D +85.86$ (*c* 1.28, CHCl₃) for 93% *ee*. ¹H NMR (400

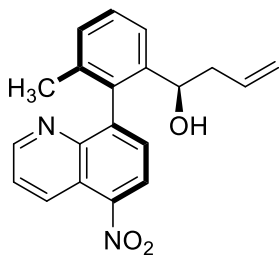


MHz, CDCl₃) δ 8.84 (dd, *J* = 4.2, 1.7 Hz, 1H), 8.69 (dd, *J* = 8.6, 1.7 Hz, 1H), 7.72 (d, *J* = 7.7 Hz, 1H), 7.54 (td, *J* = 6.6, 3.2 Hz, 2H), 7.47 – 7.39 (m, 2H), 7.28 (d, *J* = 7.5 Hz, 1H), 5.58 (ddt, *J* = 17.1, 10.2, 6.9 Hz, 1H), 5.01 – 4.89 (m, 2H), 4.21 (t, *J* = 6.9 Hz, 1H), 3.03 (s, 1H), 2.50 (tdd, *J* = 14.1, 7.5, 5.9 Hz, 2H), 1.87

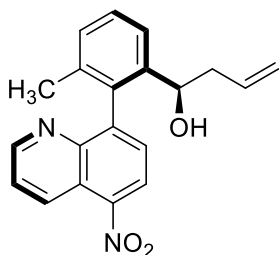
(s, 3H). ¹³C NMR (100 MHz, CDCl₃) δ 151.2, 147.2, 142.2, 138.2, 137.3, 136.52, 134.9, 133.7, 131.1, 131.0, 129.5, 128.5, 126.8, 126.5, 123.2, 122.2, 117.1, 70.7, 40.6, 20.9. HRMS (ESI) calcd. for C₂₀H₁₉ClNO (*M* + H⁺) 324.1150. Found 324.1147. HPLC (IA column, 90:10 *n*-Hex/*i*-PrOH, 30 °C, 1.0 mL/min): *t_R* 5.27 min (minor) and 6.63 min (major).

1-(3-Methyl-2-(5-nitroquinolin-8-yl)phenyl)but-3-en-1-ol (4r).

(*R_a,R*)-**4r** (31.8 mg, 55% yield): [α]_D -7.95 (*c* 0.31, CHCl₃) for 97% *ee*. ¹H NMR (400 MHz, CDCl₃) δ 9.11 (dd, *J* = 8.8, 1.7 Hz, 1H), 8.99 (dd, *J* = 4.1, 1.7 Hz, 1H), 8.48 (d, *J* = 7.9 Hz, 1H), 7.72 (d, *J* = 7.9 Hz, 1H), 7.67 (dd, *J* = 8.8, 4.1 Hz, 1H), 7.56 (ddt, *J* = 7.9, 1.3, 0.6 Hz, 1H), 7.47 (t, *J* = 7.7 Hz, 1H), 7.31 (ddd, *J* = 7.5, 1.4, 0.8 Hz, 1H), 5.53 – 5.38 (m, 1H), 4.91 (ddt, *J* = 10.2, 2.0, 1.0 Hz, 1H), 4.84 (ddt, *J* = 17.1, 2.0, 1.4 Hz, 1H), 4.26 (dd, *J* = 8.0, 4.7 Hz, 1H), 2.31 – 2.19 (m, 2H), 1.98 (s, 1H), 1.87 (s, 3H). ¹³C NMR (100 MHz, CDCl₃) δ 151.5, 147.2, 146.9, 145.1, 141.6, 136.5, 136.2, 134.7, 132.2, 129.1, 128.8, 128.7, 124.4, 123.9, 123.3, 121.4, 118.0, 70.7, 42.9, 20.6. HRMS (ESI) calcd. for C₂₀H₁₉N₂O₃ (M + H⁺) 335.1390. Found 335.1387. HPLC (IA column, 90:10 *n*-Hex/*i*-PrOH, 30 °C, 1.0 mL/min): *t_R* 10.79 min (major) and 15.58 min (minor).

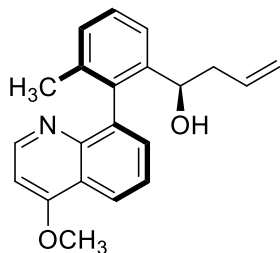


(*S_a,R*)-**4r** (6.9 mg, 12% yield): [α]_D +46.36 (*c* 0.43, CHCl₃) for 92% *ee*. ¹H NMR (400 MHz, CDCl₃) δ 9.14 (dd, *J* = 8.8, 1.7 Hz, 1H), 8.95 (dd, *J* = 4.1, 1.7 Hz, 1H), 8.48 (d, *J* = 7.9 Hz, 1H), 7.70 (dd, *J* = 8.8, 4.2 Hz, 1H), 7.65 (d, *J* = 7.9 Hz, 1H), 7.60 (d, *J* = 7.8 Hz, 1H), 7.49 (t, *J* = 7.7 Hz, 1H), 7.33 (d, *J* = 7.5 Hz, 1H), 5.58 (ddt, *J* = 17.2, 10.2, 7.0 Hz, 1H), 5.03 – 4.93 (m, 2H), 4.19 – 4.11 (m, 1H), 2.77 (s, 1H), 2.60 – 2.42 (m, 2H), 1.88 (s, 3H). ¹³C NMR (100 MHz, CDCl₃) δ 151.78, 146.8, 146.6, 145.1, 141.7, 139.3, 135.8, 134.6, 132.7, 129.6, 129.0, 124.2, 124.1, 123.4, 121.7, 1119.7, 117.5, 70.8, 40.8, 20.8. HRMS (ESI) calcd. for C₂₀H₁₉N₂O₃ (M + H⁺) 335.1390. Found 335.1391. HPLC (IA column, 90:10 *n*-Hex/*i*-PrOH, 30 °C, 1.0 mL/min): *t_R* 7.73 min (minor) and 10.02 min (major).

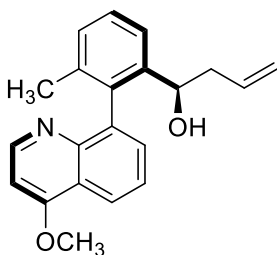


1-(2-(4-Methoxyquinolin-8-yl)-3-methylphenyl)but-3-en-1-ol (4s).

(*R_aR*)-**4s** (32 mg, 50% yield): [α]_D +12.95 (*c* 0.68, CHCl₃) for 94% *ee*. ¹H NMR (400 MHz, CDCl₃) δ 8.70 (d, *J* = 5.2 Hz, 1H), 8.28 (dd, *J* = 8.0, 1.8 Hz, 1H), 7.61 – 7.46 (m, 3H), 7.38 (t, *J* = 7.6 Hz, 1H), 7.24 (s, 1H), 6.74 (d, *J* = 5.2 Hz, 1H), 5.53 – 5.38 (m, 1H), 4.91 – 4.76 (m, 2H), 4.37 (dd, *J* = 8.8, 3.9 Hz, 1H), 4.08 (s, 3H), 2.33 – 2.11 (m, 2H), 1.87 (s, 3H). ¹³C NMR (100 MHz, CDCl₃) δ 162.4, 151.3, 147.8, 142.1, 138.1, 136.9, 135.4, 130.7, 128.9, 127.9, 125.4, 123.2, 121.7, 121.7, 117.4, 100.1, 71.1, 55.8, 42.7, 20.7. HRMS (ESI) calcd. for C₂₁H₂₂NO₂ (M + H⁺) 320.1645. Found 320.1642. HPLC (IA column, 90:10 *n*-Hex/*i*-PrOH, 30 °C, 1.0 mL/min): *t_R* 9.28 min (major) and 11.98 min (minor).

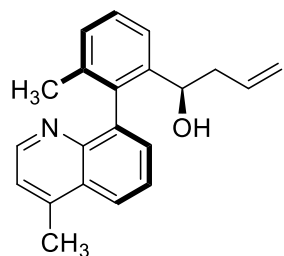


(*S_aR*)-**4s** (4 mg, 6% yield): [α]_D +111.29 (*c* 0.83, CHCl₃) for 90% *ee*. ¹H NMR (400 MHz, CDCl₃) δ 8.64 (d, *J* = 5.2 Hz, 1H), 8.28 (dd, *J* = 8.3, 1.6 Hz, 1H), 7.62 – 7.45 (m, 3H), 7.41 (t, *J* = 7.7 Hz, 1H), 7.18 (d, *J* = 7.5 Hz, 1H), 6.76 (d, *J* = 5.3 Hz, 1H), 5.60 (ddt, *J* = 17.1, 10.2, 6.9 Hz, 1H), 5.01 – 4.87 (m, 2H), 4.26 (dd, *J* = 7.7, 6.3 Hz, 1H), 4.08 (s, 3H), 2.63 – 2.44 (m, 2H), 1.88 (s, 3H). ¹³C NMR (101 MHz, CDCl₃) δ 162.9, 151.7, 147.6, 142.0, 138.7, 138.2, 136.5, 135.3, 131.8, 129.5, 129.0, 128.2, 125.4, 122.9, 121.9, 121.7, 116.7, 70.7, 55.9, 39.9, 21.0. HRMS (ESI) calcd. for C₂₁H₂₂NO₂ (M + H⁺) 320.1645. Found 320.1643. HPLC (IA column, 90:10 *n*-Hex/*i*-PrOH, 30 °C, 1.0 mL/min): *t_R* 6.28 min (minor) and 7.56 min (major).

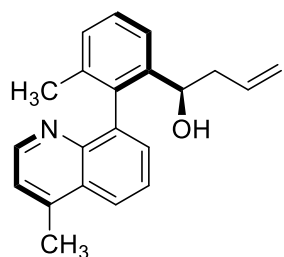


1-(3-Methyl-2-(4-methylquinolin-8-yl)phenyl)but-3-en-1-ol (4t).

(*R_a,R*)-**4t** (40 mg, 66% yield): $[\alpha]_D^{25} +18.41$ (*c* 0.93, CHCl₃) for 92% *ee*. ¹H NMR (400 MHz, CDCl₃) δ 8.71 (d, *J* = 4.3 Hz, 1H), 8.07 (dd, *J* = 8.3, 1.5 Hz, 1H), 7.64 (dd, *J* = 8.4, 7.0 Hz, 1H), 7.58 – 7.45 (m, 2H), 7.39 (t, *J* = 7.6 Hz, 1H), 7.28 – 7.19 (m, 2H), 5.52 – 5.37 (m, 1H), 4.97 – 4.67 (m, 2H), 4.36 (dt, *J* = 8.6, 3.5 Hz, 1H), 2.77 (s, 3H), 2.36 – 2.18 (m, 2H), 2.02 (d, *J* = 3.3 Hz, 1H), 1.87 (s, 3H). ¹³C NMR (100 MHz, CDCl₃) δ 150.1, 146.7, 144.4, 142.1, 139.7, 138.3, 136.8, 135.4, 130.1, 128.9, 128.6, 127.9, 126.0, 123.8, 123.1, 121.9, 117.4, 71.0, 42.7, 20.7, 19.0. HRMS (ESI) calcd. for C₂₁H₂₂NO (*M* + *H*⁺) 304.1696. Found 304.1695. HPLC (IA column, 90:10 *n*-Hex/*i*-PrOH, 30 °C, 1.0 mL/min): *t_R* 7.84 min (major) and 8.71 min (minor).

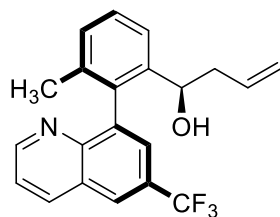


(*S_a,R*)-**4t** (9 mg, 15% yield): $[\alpha]_D^{25} +111.22$ (*c* 1.02, CHCl₃) for 92% *ee*. ¹H NMR (400 MHz, CDCl₃) δ 8.65 (d, *J* = 4.4 Hz, 1H), 8.07 (dd, *J* = 8.4, 1.5 Hz, 1H), 7.64 (dd, *J* = 8.4, 7.0 Hz, 1H), 7.57 – 7.45 (m, 2H), 7.42 (d, *J* = 7.6 Hz, 1H), 7.31 – 7.22 (m, 2H), 5.60 (ddt, *J* = 17.1, 10.2, 6.9 Hz, 1H), 5.01 – 4.87 (m, 2H), 4.24 (t, *J* = 7.0 Hz, 1H), 3.42 (s, 1H), 2.78 (s, 3H), 2.64 – 2.44 (m, 2H), 1.87 (s, 3H). ¹³C NMR (100 MHz, CDCl₃) δ 150.3, 146.4, 145.2, 142.0, 139.3, 138.7, 136.5, 135.3, 131.2, 129.5, 128.8, 128.2, 126.0, 123.7, 123.0, 122.2, 116.8, 70.7, 40.1, 29.7, 20.9. HRMS (ESI) calcd. for C₂₁H₂₂NO (*M* + *H*⁺) 304.1696. Found 304.1697. HPLC (IA column, 90:10 *n*-Hex/*i*-PrOH, 30 °C, 1.0 mL/min): *t_R* 5.25 min (minor) and 6.05 min (major).



1-(3-Methyl-2-(6-(trifluoromethyl)quinolin-8-yl)phenyl)but-3-en-1-ol (4u).

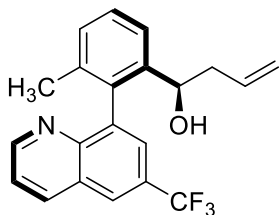
(*R_a,R*)-**4u** (43.6 mg, 61% yield): $[\alpha]_D -7.20$ (*c* 0.38, CHCl₃) for 93% *ee*. ¹H NMR (400



MHz, CDCl₃) δ 8.98 (dd, *J* = 4.2, 1.8 Hz, 1H), 8.32 (dd, *J* = 8.3, 1.8 Hz, 1H), 8.21 (s, 1H), 7.78 (d, *J* = 2.1 Hz, 1H), 7.57 – 7.48 (m, 2H), 7.43 (t, *J* = 7.7 Hz, 1H), 7.29 (s, 1H), 5.51 – 5.36 (m, 1H), 4.89 – 4.72 (m, 2H), 4.29 (dt, *J* = 7.9, 3.7 Hz, 1H), 2.20 (dt, *J* = 14.2, 6.7 Hz, 2H), 1.92 (d, *J* = 3.2 Hz, 1H), 1.86 (s, 3H).

¹³C NMR (100 MHz, CDCl₃) δ 152.5, 148.0, 142.1, 140.9, 137.2, 136.7, 136.4, 134.9, 129.1, 128.6, 128.2, 127.6, 126.0 (*q*, *J* = 2.6 Hz), 125.6 (*q*, *J* = 4.5 Hz), 123.3, 122.3, 117.6, 70.9, 42.9, 20.6. ¹⁹F NMR (377 MHz, CDCl₃) δ -62.2. HRMS (ESI) calcd. for C₂₁H₁₉F₃NO (*M* + *H*⁺) 358.1413. Found 358.1411. HPLC (IA column, 90:10 *n*-Hex/*i*-PrOH, 30 °C, 1.0 mL/min): *t_R* 6.16 min (major) and 10.72 min (minor).

(*S_a,R*)-**4u** (10.7 mg, 15% yield): $[\alpha]_D +76.9$ (*c* 1.05, CHCl₃) for 96% *ee*. ¹H NMR (400

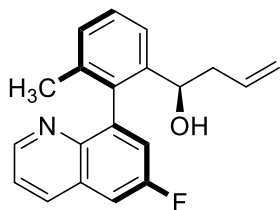


MHz, CDCl₃) δ 8.93 (dd, *J* = 4.2, 1.8 Hz, 1H), 8.35 (dd, *J* = 8.3, 1.8 Hz, 1H), 8.24 – 8.18 (m, 1H), 7.70 (d, *J* = 2.2 Hz, 1H), 7.61 – 7.51 (m, 2H), 7.45 (t, *J* = 7.7 Hz, 1H), 7.30 (d, *J* = 7.5 Hz, 1H), 5.57 (ddt, *J* = 17.2, 10.2, 7.0 Hz, 1H), 5.01 – 4.89 (m, 2H), 4.16 (ddd, *J* = 7.7, 6.2, 1.6 Hz, 1H), 2.89 (s, 1H), 2.61 – 2.39 (m, 2H),

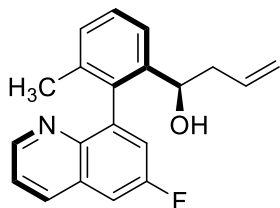
1.87 (s, 3H). ¹³C NMR (100 MHz, CDCl₃) δ 152.8, 147.7, 142.2, 140.6, 137.7, 136.7, 136.3, 134.7, 129.6, 128.8, 128.4, 127.9, 127.7, 127.1 (*q*, *J* = 3.2 Hz), 126.7 (*q*, *J* = 288.0 Hz), 125.6 (*q*, *J* = 4.5 Hz), 123.3, 122.5, 70.9, 40.8, 20.9. ¹⁹F NMR (377 MHz, CDCl₃) δ -62.4. HRMS (ESI) calcd. for C₂₁H₁₉F₃NO (*M* + *H*⁺) 358.1413. Found 358.1410. HPLC (IA column, 90:10 *n*-Hex/*i*-PrOH, 30 °C, 1.0 mL/min): *t_R* 5.32 min (minor) and 5.80 min (major).

1-(2-(6-Fluoroquinolin-8-yl)-3-methylphenyl)but-3-en-1-ol (4v).

(*R_a,R*)-**4v** (36.4 mg, 60% yield): $[\alpha]_D +12.65$ (*c* 2.18, CHCl₃) for 95% *ee*. ¹H NMR (400 MHz, CDCl₃) δ 8.82 (dd, *J* = 4.2, 1.7 Hz, 1H), 8.17 (dd, *J* = 8.3, 1.8 Hz, 1H), 7.56 – 7.46 (m, 2H), 7.46 – 7.35 (m, 3H), 7.28 (s, 1H), 5.51 – 5.36 (m, 1H), 4.91 – 4.70 (m, 2H), 4.33 (dt, *J* = 6.8, 3.1 Hz, 1H), 2.30 – 2.12 (m, 2H), 1.98 (s, 1H), 1.89 (s, 3H). ¹³C NMR (100 MHz, CDCl₃) δ 159.8 (d, *J* = 249.3 Hz), 149.7 (d, *J* = 2.7 Hz), 144.2, 142.3 (d, *J* = 8.9 Hz), 142.1, 136.6, 136.5, 135.8 (d, *J* = 5.6 Hz), 135.1, 129.2 (d, *J* = 10.2 Hz), 129.0, 128.5, 123.2, 121.9, 120.5 (d, *J* = 25.3 Hz), 117.6, 110.6 (d, *J* = 21.3 Hz), 70.8, 42.9, 20.6. ¹⁹F NMR (377 MHz, CDCl₃) δ -113.1. HRMS (ESI) calcd. for C₂₀H₁₉FNO (M + H⁺) 308.1445. Found 308.1443. HPLC (IA column, 90:10 *n*-Hex/*i*-PrOH, 30 °C, 1.0 mL/min): *t_R* 7.21 min (major) and 10.15 min (minor).

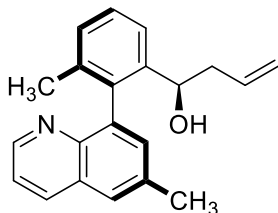


(*S_a,R*)-**4v** (4.3 mg, 7% yield): $[\alpha]_D +93.72$ (*c* 0.57, CHCl₃) for 95% *ee*. ¹H NMR (400 MHz, CDCl₃) δ 8.77 (dd, *J* = 4.2, 1.7 Hz, 1H), 8.20 (dd, *J* = 8.4, 1.7 Hz, 1H), 7.55 (d, *J* = 7.8 Hz, 1H), 7.50 (dd, *J* = 8.5, 2.9 Hz, 1H), 7.47 – 7.41 (m, 2H), 7.39 – 7.28 (m, 2H), 5.60 (ddt, *J* = 17.1, 10.2, 7.0 Hz, 1H), 5.03 – 4.91 (m, 2H), 4.21 (t, *J* = 7.1 Hz, 1H), 3.14 (s, 1H), 2.52 (qt, *J* = 13.7, 6.9 Hz, 2H), 1.90 (s, 1H). ¹³C NMR (100 MHz, CDCl₃) δ 159.8 (d, *J* = 249.3 Hz), 150.0 (d, *J* = 2.9 Hz), 143.9, 142.0, 141.9, 136.9, 136.3, 136.2, 134.9, 129.6, 129.5 (d, *J* = 10.5 Hz), 128.7, 123.2, 122.1, 121.6 (d, *J* = 25.3 Hz), 117.1, 110.6 (d, *J* = 21.2 Hz), 70.8, 40.4, 20.9. ¹⁹F NMR (377 MHz, CDCl₃) δ -113.0. HRMS (ESI) calcd. for C₂₀H₁₉FNO (M + H⁺) 308.1445. Found 308.1445. HPLC (IA column, 90:10 *n*-Hex/*i*-PrOH, 30 °C, 1.0 mL/min): *t_R* 5.51 min (minor) and 6.60 min (major).

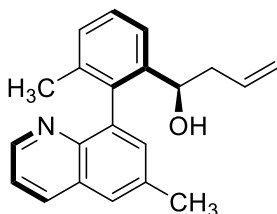


1-(3-Methyl-2-(6-methylquinolin-8-yl)phenyl)but-3-en-1-ol (4w).

(*R_aR*)-**4w** (42.3 mg, 55% yield): $[\alpha]_D +33.05$ (*c* 0.91, CHCl₃) for 95% *ee*. ¹H NMR (400 MHz, CDCl₃) δ 8.79 (dd, *J* = 4.2, 1.8 Hz, 1H), 8.12 (dd, *J* = 8.3, 1.8 Hz, 1H), 7.64 (s, 1H), 7.51 (d, *J* = 7.8 Hz, 1H), 7.43 – 7.31 (m, 3H), 7.27 (s, 1H), 5.52 – 5.37 (m, 1H), 4.90 – 4.71 (m, 2H), 4.37 (dt, *J* = 8.8, 3.2 Hz, 1H), 2.57 (s, 3H), 2.32 – 2.12 (m, 2H), 1.99 (s, 1H), 1.89 (s, 3H). ¹³C NMR (100 MHz, CDCl₃) δ 149.6, 145.6, 142.2, 138.9, 137.8, 136.8, 136.2, 135.6, 135.3, 132.5, 128.9, 128.6, 128.0, 126.7, 123.0, 121.1, 117.4, 70.9, 42.9, 21.6, 20.7. HRMS (ESI) calcd. for C₂₁H₂₂NO (*M* + *H*⁺) 304.1696. Found 304.1694. HPLC (IA column, 90:10 *n*-Hex/*i*-PrOH, 30 °C, 1.0 mL/min): *t_R* 6.44 min (major) and 8.78 min (minor).

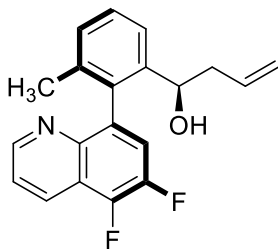


(*S_aR*)-**4w** (7.6 mg, 13% yield): $[\alpha]_D +40.56$ (*c* 0.42, CHCl₃) for 86% *ee*. ¹H NMR (400 MHz, CDCl₃) δ 8.73 (dd, *J* = 4.3, 1.8 Hz, 1H), 8.15 (dd, *J* = 8.3, 1.8 Hz, 1H), 7.64 (s, 1H), 7.53 (d, *J* = 7.8 Hz, 1H), 7.46 – 7.33 (m, 3H), 7.29 (s, 1H), 5.61 (ddt, *J* = 17.1, 10.2, 6.9 Hz, 1H), 5.02 – 4.88 (m, 2H), 4.26 (t, *J* = 7.0 Hz, 1H), 3.37 (s, 1H), 2.57 (s, 3H), 2.58 – 2.44 (m, 2H), 1.88 (s, 3H). ¹³C NMR (100 MHz, CDCl₃) δ 149.8, 145.4, 142.2, 138.4, 138.2, 136.6, 136.2, 136.1, 135.3, 133.7, 129.5, 128.8, 128.2, 126.6, 123.0, 121.4, 116.7, 70.7, 40.2, 21.6, 21.0. HRMS (ESI) calcd. for C₂₁H₂₂NO (*M* + *H*⁺) 304.1696. Found 304.1695. HPLC (IA column, 90:10 *n*-Hex/*i*-PrOH, 30 °C, 1.0 mL/min): *t_R* 4.95 min (minor) and 5.47 min (major).

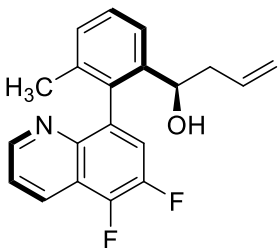


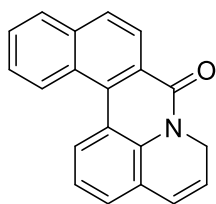
1-(2-(5,6-Difluoroquinolin-8-yl)-3-methylphenyl)but-3-en-1-ol (4x).

(*R_a,R*)-**4x** (35.2 mg, 55% yield): $[\alpha]_D +8.03$ (*c* 1.85, CHCl₃) for 96% *ee*. ¹H NMR (400 MHz, CDCl₃) δ 8.87 (dd, *J* = 4.3, 1.8 Hz, 1H), 8.50 (dd, *J* = 8.5, 1.8 Hz, 1H), 7.54 – 7.37 (m, 4H), 7.27 (d, *J* = 8.2 Hz, 1H), 5.52 – 5.37 (m, 1H), 4.91 – 4.74 (m, 2H), 4.34 – 4.26 (m, 1H), 2.22 (q, *J* = 6.6 Hz, 2H), 1.96 (d, *J* = 3.0 Hz, 1H), 1.87 (s, 3H). ¹³C NMR (100 MHz, CDCl₃) δ 150.4 (d, *J* = 2.8 Hz), 146.0 (dd, *J* = 250.2, 12.3 Hz), 143.1 (dd, *J* = 255.2, 12.8 Hz), 143.4, 142.2, 136.9, 136.7 – 136.4 (m), 135.8, 134.9, 129.1, 129.0 – 128.9 (m), 128.6, 123.2, 121.7 (d, *J* = 3.3 Hz), 120.6 (d, *J* = 20.6 Hz), 120.2 (d, *J* = 14.1 Hz), 117.7, 70.7, 42.9, 20.6. ¹⁹F NMR (377 MHz, CDCl₃) δ -139.1 (d, *J* = 19.8 Hz), -148.6 (d, *J* = 19.6 Hz). HRMS (ESI) calcd. for C₂₀H₁₈F₂NO (M + H⁺) 326.1351. Found 326.1353. HPLC (IA column, 90:10 *n*-Hex/*i*-PrOH, 30 °C, 1.0 mL/min): *t_R* 6.02 min (major) and 8.73 min (minor).

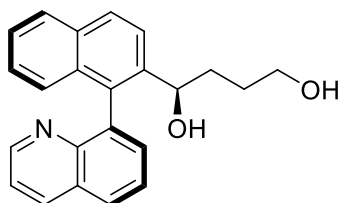


(*S_a,R*)-**4x** (5.9 mg, 9% yield): $[\alpha]_D +118.17$ (*c* 0.8, CHCl₃) for 95% *ee*. ¹H NMR (400 MHz, CDCl₃) δ 8.82 (dd, *J* = 4.2, 1.7 Hz, 1H), 8.53 (dd, *J* = 8.5, 1.8 Hz, 1H), 7.53 (td, *J* = 8.8, 5.8 Hz, 2H), 7.51 – 7.36 (m, 2H), 7.29 (d, *J* = 7.6 Hz, 1H), 5.59 (ddt, *J* = 17.1, 10.2, 7.0 Hz, 1H), 5.03 – 4.92 (m, 2H), 4.18 (t, *J* = 7.0 Hz, 1H), 2.92 (s, 1H), 2.60 – 2.41 (m, 2H), 1.89 (s, 3H). ¹³C NMR (100 MHz, CDCl₃) δ 150.7, 143.2, 142.3, 136.5, 136.3 – 136.2, 136.1, 134.8, 129.7 – 129.5, 129.5, 128.9, 123.3, 122.0 (d, *J* = 2.4 Hz), 121.6 (d, *J* = 20.7 Hz), 120.5 (dd, *J* = 12.5 Hz), 117.3, 70.7, 40.6, 20.9. ¹⁹F NMR (377 MHz, CDCl₃) δ -139.0 (d, *J* = 19.2 Hz), -148.4 (d, *J* = 19.1 Hz). HRMS (ESI) calcd. for C₂₀H₁₈F₂NO (M + H⁺) 326.1351. Found 326.1354. HPLC (IA column, 90:10 *n*-Hex/*i*-PrOH, 30 °C, 1.0 mL/min): *t_R* 5.08 min (minor) and 6.14 min (major).



6H,8H-benzo[k]pyrido[3,2,1-de]phenanthridin-8-one (8a).

^1H NMR (400 MHz, CDCl_3) δ 8.88 (d, $J = 9.0$ Hz, 1H), 8.49 (d, $J = 8.6$ Hz, 1H), 8.44 (d, $J = 10.1$ Hz, 1H), 8.01 (dd, $J = 7.5, 1.9$ Hz, 1H), 7.95 (d, $J = 8.6$ Hz, 1H), 7.75 – 7.61 (m, 2H), 7.26 – 7.14 (m, 2H), 6.56 (dt, $J = 10.1, 2.2$ Hz, 1H), 6.08 (dt, $J = 10.1, 3.6$ Hz, 1H), 5.08 (dd, $J = 3.6, 2.2$ Hz, 2H). ^{13}C NMR (100 MHz, CDCl_3) δ 161.1, 136.2, 134.0, 132.4, 128.9, 128.7, 128.6, 127.9, 127.9, 127.4, 126.6, 126.5, 124.6, 124.0, 123.5, 122.7, 122.4, 121.9, 118.6, 45.7.

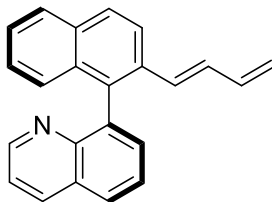
II.5.3. Derivatization reactions.**(R)-1-((S)-1-(Quinolin-8-yl)naphthalen-2-yl)butane-1,4-diol ((R_a,R)-13)**

Following a described procedure.¹⁴⁵ Borane tetrahydrofuran complex solution (24 μL , 0.25 mmol) was added to a solution of (R_a,R)-**4a** (32 mg, 0.1 mmol) in anhydrous THF (1 mL) at 0 $^\circ\text{C}$, then allowed to reach rt. Then NaOH (270 μL) and H_2O_2 (270 μL) were added, the organic layer was separated, and the aqueous phase was extracted with CH_2Cl_2 (2 mL \times 3). The organic layers were combined and concentrated to give an orange oil. This was purified by flash column chromatography (20:1 DCM/MeOH) to afford the title compound as a white foam (17 mg, 50% yield). ^1H NMR (400 MHz, CDCl_3) δ 8.75 (dd, $J = 4.2, 1.8$ Hz, 1H), 8.29 (dd, $J = 8.3, 1.8$ Hz, 1H), 7.99 (t, $J = 7.5$ Hz, 2H), 7.88 (d, $J = 8.2$ Hz, 1H), 7.81 (d, $J = 8.6$ Hz, 1H), 7.76 – 7.62 (m, 2H), 7.46 – 7.37 (m, 2H), 7.23 (t, $J = 7.7$ Hz, 1H), 7.05 (d, $J = 8.5$ Hz, 1H), 4.49 (dd, $J = 8.3, 4.2$ Hz, 1H), 3.26 (dd, $J = 6.9, 5.2$ Hz, 2H), 1.87 – 1.74 (m, 1H), 1.70 (dd, $J = 14.6, 7.2$ Hz, 1H), 1.40 – 1.11 (m, 3H). ^{13}C NMR (100 MHz, CDCl_3) δ 150.4, 147.6, 139.9, 138.1,

¹⁴⁵ G. Pandey, R. Laha, P. K. Mondal, *Chem. Commun.*, **2019**, 55, 9689–9692.

136.5, 134.7, 133.1, 132.8, 131.5, 128.6, 128.5, 128.2, 127.9, 126.8, 126.4, 125.9, 125.5, 123.6, 121.3, 71.9, 62.5, 34.7, 29.3.

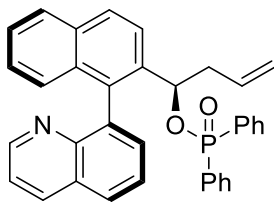
(*R,E*)-8-(2-(Buta-1,3-dien-1-yl)naphthalen-1-yl)quinoline ((*R_a*)-14).



Mesyl chloride (25 μ L, 0.32 mmol) was added over a solution of (*R_aR*)-**4a** (85 mg, 0.26 mmol) in anhydrous DCM (2 mL) and Et₃N (44 μ L, 0.32 mmol) at 0 °C, then heated to 40 °C. Then saturated NaHCO₃ was added, the organic layer was separated, and the aqueous phase was extracted with CH₂Cl₂ (2 mL \times 3). The organic layers were combined and concentrated to give an orange oil. This was purified by flash column chromatography (7:1 toluene/ethyl acetate) to afford the title compound as a white foam (58 mg, 73% yield) in 96% *ee*. ¹H NMR (400 MHz, CDCl₃) δ 8.79 (dd, *J* = 4.2, 1.8 Hz, 1H), 8.27 (dd, *J* = 8.3, 1.8 Hz, 1H), 7.98 (dd, *J* = 8.1, 1.6 Hz, 1H), 7.97 – 7.85 (m, 2H), 7.69 (dd, *J* = 8.1, 7.0 Hz, 1H), 7.62 (dd, *J* = 7.0, 1.6 Hz, 1H), 7.44 – 7.34 (m, 1H), 7.06 (dd, *J* = 8.5, 1.2 Hz, 2H), 6.89 – 6.78 (m, 1H), 6.25 – 6.03 (m, 2H), 5.31 – 5.20 (m, 1H), 5.02 (ddt, *J* = 10.0, 1.6, 0.8 Hz, 1H). ¹³C NMR (100 MHz, CDCl₃) δ 150.7, 147.5, 138.2, 137.6, 136.4, 136.2, 133.6, 133.0, 132.4, 131.9, 130.3, 129.1, 128.5, 128.3, 128.1, 127.9, 126.9, 126.3, 126.0, 125.6, 122.7, 121.2, 117.3. HPLC (IA column, 95:5 *n*-Hex/*i*-PrOH, 30 °C, 0.8 mL/min): *t_R* 7.61 min (major) and 8.28 min (minor).

From (*S_aR*)-**4a**, HPLC (IA column, 95:5 *n*-Hex/*i*-PrOH, 30 °C, 0.8 mL/min): *t_R* 7.65min (minor) and 8.32 min (major).

(R)-1-((S)-1-(Quinolin-8-yl)naphthalen-2-yl)but-3-en-1-yl diphenylphosphinate ((R_a)-15).



Following a described procedure,¹⁴⁶ to a solution of **4a** (32 mg, 0.1 mmol) in anhydrous toluene (1 mL) at rt, and Et₃N (28 μL, 0.2 mmol) and chlorodiphenylphosphine (37 μL, 0.2 mmol) were added dropwise. Reaction was stirred at rt for 12 h. Solvent was removed under reduced pressure and crude was purified by flash column chromatography (20:1 DCM/ethyl acetate) to afford the title compound as a white foam (25 mg, 48% yield). ¹H NMR (400 MHz, CDCl₃) δ 8.71 (dd, *J* = 4.1, 1.9 Hz, 1H), 8.20 (d, *J* = 8.3 Hz, 1H), 8.05 – 7.90 (m, 2H), 7.87 (dd, *J* = 12.0, 8.2 Hz, 2H), 7.77 (d, *J* = 7.5 Hz, 2H), 7.61 (d, *J* = 7.5 Hz, 2H), 7.50 – 7.32 (m, 7H), 7.29 (d, *J* = 7.6 Hz, 2H), 7.18 (t, *J* = 7.6 Hz, 1H), 6.94 (d, *J* = 8.5 Hz, 1H), 6.69 (d, *J* = 7.0 Hz, 1H), 5.70 – 5.55 (m, 1H), 5.15 (t, *J* = 5.8 Hz, 1H), 4.83 – 4.66 (m, 2H), 2.54 (t, *J* = 6.6 Hz, 2H). ¹³C NMR (100 MHz, CDCl₃) δ 150.3, 147.6, 136.8, 136.5, 136.3, 134.7, 133.9, 133.2, 132.9, 132.5, 132.4, 131.9, 131.9, 131.5, 131.4, 131.3, 131.0, 129.1, 128.4, 128.3, 128.3, 128.2, 128.1, 127.9, 126.9, 126.3, 125.9, 125.7, 125.3, 123.9, 121.1, 117.5, 75.6, 75.6, 42.5, 29.7. ³¹P NMR (162 MHz, CDCl₃) δ 29.9.

¹⁴⁶ R. Ewals, E. B. Eggeling, A. C. Hewat, P. C. J. Kamer, P. W. N. M. van Leeuwen, D. Vogt, *Chem. Eur. J.* **2000**, 6 (8), 1271-1504.

CHAPTER III

Biocatalytic Atroposelective Synthesis of Axially Chiral N-Arylindoles via Dynamic Kinetic Resolution.

Part of this chapter is published in:

P. Rodríguez-Salamanca, G. de Gonzalo, J. A. Carmona, J. López-Serrano, J. Iglesias-Sigüenza, R. Fernández, J. M. Lassaletta, V. Hornillos.

ACS Catal. **2023**, *13*, 1, 659–664.

III. Biocatalytic atroposelective synthesis of axially chiral N-arylindoles via Dynamic Kinetic Resolution.

III.1. Introduction.

III.1.1. C-N axial chirality.

As previously shown in **Chapter I**, most synthesized axially chiral molecules are restricted to those having a stereogenic carbon-carbon (C-C) axis.^{8a,b,c,147} In stark contrast, the catalytic atroposelective synthesis of C-N axially chiral molecules are relatively less explored.^{8d,148,149} Among these, axially chiral indoles are particularly important motives, which exist in a variety of alkaloids, bioactive molecules and chiral phosphine ligands (**Figure 13**).^{150,151}

¹⁴⁷ For selected examples, see: a) D. Zhang, Q. Wang, *Coord. Chem. Rev.* **2015**, *286*, 1–16; b) J. Wencel-Delord, A. Panossian, F. R. Leroux, F. Colobert, *Chem. Soc. Rev.* **2015**, *44*, 3418–3430; c) P. Loxq, E. Manoury, R. Poli, E. Deydier, A. Labande, *Coord. Chem. Rev.* **2016**, *308*, 131–190; d) M. Mancinelli, G. Bencivenni, D. Pecorari, A. Mazzanti, *Eur. J. Org. Chem.* **2020**, 4070–4086; e) V. Corti, G. Bertuzzi, *Synthesis* **2020**, *52*, 2450–2468; f) D.-J. Cheng, Y.-D. Shao, *Adv. Synth. Catal.* **2020**, *362*, 3081–3099; g) J. K. Cheng, S. H. Xiang, S. Li, L. Ye, B. Tan, *Chem. Rev.* **2021**, *121*, 4805–4902; h) Q. Zhao, C. Peng, Y.-T. Wang, G. Zhan, B. Han, *Org. Chem. Front.* **2021**, *8*, 2772–2785; i) C.-X. Liu, W.-W. Zhang, S.-Y. Yin, Q. Gu, S.-L. You, *J. Am. Chem. Soc.* **2021**, *143*, 14025–14040.

¹⁴⁸ For selected examples, see: a) I. Takahashi, Y. Suzuki, O. Kitagawa, *Org. Prep. Proced. Int.* **2014**, *46*, 1–23; b) E. Kumarasamy, R. Raghunathan, M. P. Sibi, J. Sivaguru, *Chem. Rev.* **2015**, *115*, 11239–11300; c) D. Bonne, J. Rodriguez, *Chem. Commun.* **2017**, *53*, 12385–12393; d) O. Kitagawa, *Acc. Chem. Res.* **2021**, *54*, 719–730.

¹⁴⁹ For a recent review on methods based on stereoselective C-N bond formation see: J. Frey, S. Choppin, F. Colobert, J. Wencel-Delord, *Chimia* **2020**, *74*, 883–889.

¹⁵⁰ For selected examples, see: a) M. R. Finlay, M. Anderton, S. Ashton, P. Ballard, P. A. Bethel, M. R. Box, R. H. Bradbury, S. J. Brown, S. Butterworth, A. Campbell, C. Chorley, N. Colclough, D. A. Cross, G. S. Currie, M. Grist, L. Hassall, G. B. Hill, D. James, M. James, P. Kemmitt, T. Klinowska, G. Lamont, S. G. Lamont, N. Martin, H. L. McFarland, M. J. Mellor, J. P. Orme, D. Perkins, P. Perkins, G. Richmond, P. Smith, R. A. Ward, M. J. Waring, D. Whittaker, S. Wells, G. L. Wrigley, *J. Med. Chem.* **2014**, *57*, 8249–8267. b) J. W. M. Huggins, W. T. Barker, J. T. Baker, N. A. Hahn, R. J. Melander, C. Melander, *ACS Med. Chem. Lett.* **2018**, *9*, 702–707. c) K. M. Foote, K. Blades, A. Cronin, S. Fillery, S. S. Guichard, L. Hassall, I. Hickson, X. Jacq, P. J. Jewsbury, T. M. McGuire, J. W. Nissink, R. Odedra, K. Page, P. Perkins, A. Suleman, K. Tam, P. Thommes, R. Broadhurst, C. Wood, *J. Med. Chem.* **2013**, *56*, 2125–2138.

¹⁵¹ For selected examples, see: a) G. Bringmann, T. Gulder, T. A. M. Gulder, M. Breuning, *Chem. Rev.* **2011**, *111*, 563–639; b) M. C. Kozlowski, B. J. Morgan, E. C. Linton, *Chem. Soc. Rev.* **2009**,

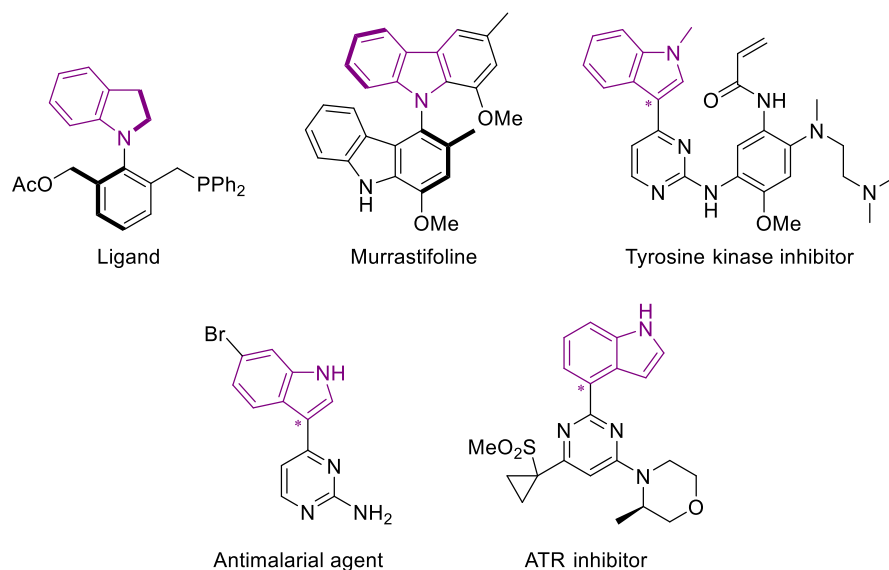


Figure 13: representative examples of important structures with C-N axial chirality.

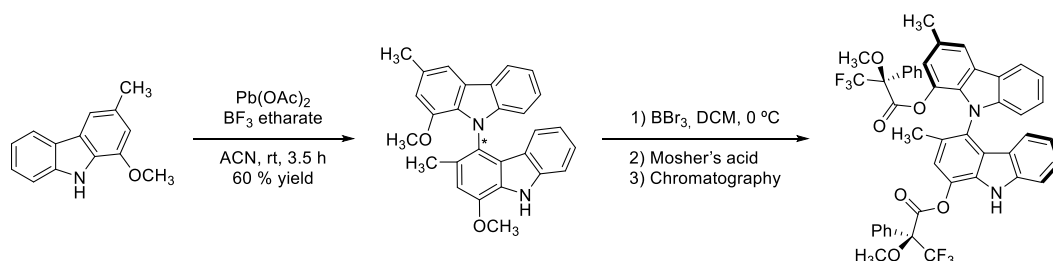
In these systems, the rotation about the C–N axis is generally easier than in C–C biaryl compounds due to the relatively larger C–N–C angles, associated with a five-membered heterocyclic ring.¹⁴⁸ Moreover, their stability generally relies on the steric factors of the substituents around the C–N axis and, thus, most of these axially chiral C–N atropisomers contain substituents in the *ortho* position of the aromatic unit attached to nitrogen. The structural properties of the C–N axis often led to a decrease in the configurational stability, which increases the difficulty of their enantioselective synthesis. Therefore, the catalytic enantioselective synthesis of indole derivatives bearing axial chirality is of significant importance and has become a growing area of research.

In 2001, Bringmann *et al.*¹⁵² described the first total synthesis of the natural product Murrastifoline-F, *via* an oxidative C–N homocoupling of a carbazole precursor, using $\text{Pb}(\text{OAc})_2$. Due to the restricted rotation around the C–N axis, the

38, 3193–3207; c) J. E. Smyth, N. M. Butler, P. A. Keller, *Nat. Prod. Rep.* **2015**, *32*, 1562–1583; d) A. Zask, J. Murphy, G. A. Ellestad, *Chirality* **2013**, *25*, 265–274.

¹⁵² G. Bringmann, S. Tasler, H. Endress, J. Kraus, K. Messer, M. Wohlfarth, W. Lobin, *J. Am. Chem. Soc.* **2001**, *123*, 2703–2711.

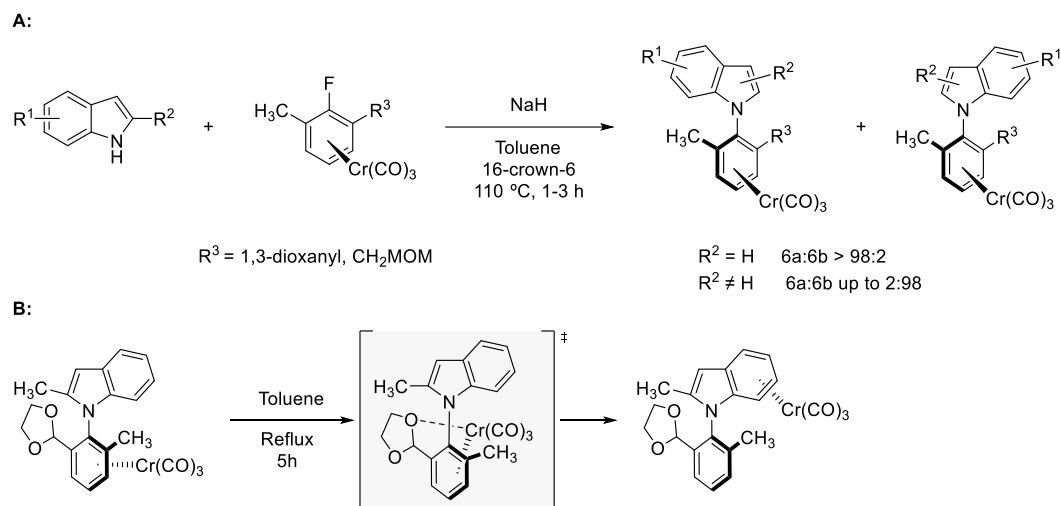
enantiomers of the coupling product could be detected through liquid chromatography-circular dichroism (LC-CD). The cleavage of the methoxy groups and additional derivatization with Mosher's acid allowed the isolation of the resulting diastereomers by preparative chromatography. Analysis of the absolute configuration determined the *M*-isomer to be the major product (**scheme 93**).



Scheme 93: first atroposelective synthesis of Murrastifoline-F.

Later, Uemura and co-workers developed an atroposelective synthesis of axially chiral *N*-aryl indoles through a nucleophilic substitution reaction of haloarene chromium complexes, presenting planar chirality, with indoles (**scheme 91A**).¹⁵³ The location of the substituent R¹ determined the stereochemistry of the C-N axis. When the indole ring had no substitution or 3-methyl substitution, the resulting chromium moiety was oriented *anti* with respect to the indole aryl ring. In contrast, when it was C2- substituted, the benzene ring of the indole was oriented *syn* toward the chromium tricarbonyl group. Interestingly, it was found that after heating in toluene, the chromium tricarbonyl group migrated from the *N*-aryl to the indole arene ring, in products containing a 1,3-dioxolanyl group (**scheme 94B**). X-Ray analysis revealed that the 1,3-dioxolane group was oriented *syn* to the chromium tricarbonyl moiety in the migrated product, indicating that the former could help for the transfer of the tricarbonyl chromium group by coordination.

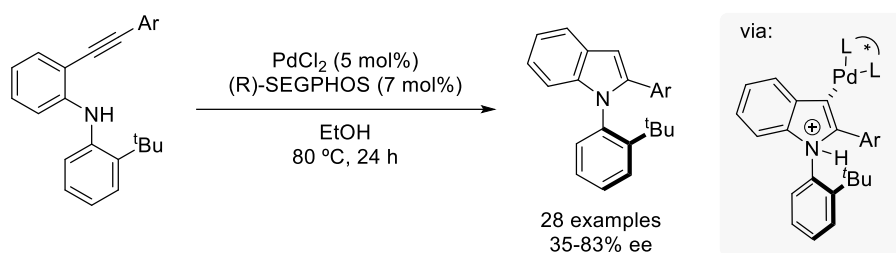
¹⁵³ a) K. Kamikawa, S. Kinoshita, H. Matsuoka, M. Uemura, *Org. Lett.* **2006**, *8*, 1097–1100. b) K. Kamikawa, S. Kinoshita, M. Furuyso, S. Takemoto, H. Matsuoka, M. Uemura, *J. Org. Chem.* **2007**, *72*, 3394–3402.



Scheme 94: stereoselective nucleophilic aromatic substitution reactions of planar chiral arene chromium complexes for the synthesis of *N*-arylindoles.

Kitagawa *et al.* reported in 2010^{154a} and further extended in 2016^{154b} the synthesis of axially chiral indoles through a Pd-catalyzed 5-endo-hydroaminocyclization of orthoalkynylanilines. The entitled products were obtained in moderate to good optical purity using (*R*)-SEGP_{HOS} as the chiral ligand (**scheme 95**). This transformation was the first asymmetric synthesis of such a structural motif, catalyzed by transition metals. The reaction performed well for aromatic alkynes but struggled for highly deactivated and aliphatic ones. The enantioselectivity could be improved with the presence of a substituent in the *ortho* position in the aromatic alkyne (60% *ee* for R = Ph, 80-83% *ee* for *ortho*-substituted substrates). This observation was rationalized by the dynamic axial chirality generated around the C(alkynyl)–C(phenyl) bond. Therefore, substrates with a bulky substituent at the *ortho*-position transferred more efficiently the chiral information from the ligand through the C(alkynyl)–C(phenyl) bond.

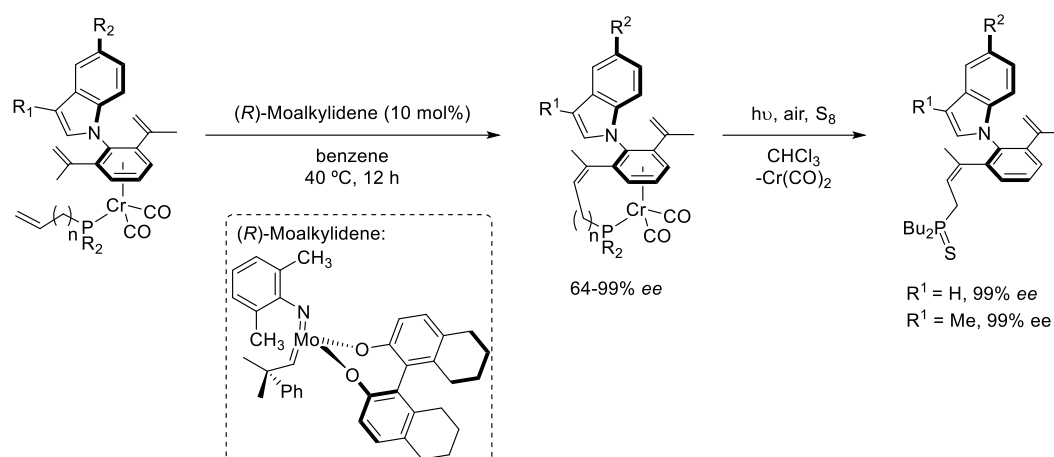
¹⁵⁴ a) N. Ototake, Y. Morimoto, A. Mokuya, H. Fukaya, Y. Shida, O. Kitagawa, *Chem. Eur. J.* **2010**, *16*, 6752–6755. b) Y. Morimoto, S. Shimizu, A. Mokuya, N. Ototake, A. Saito, O. Kitagawa, *Tetrahedron* **2016**, *72*, 5221–5229.



Scheme 95: synthesis of axially chiral indoles via a Pd-catalyzed 5-endo-hydroaminocyclization.

Kamikawa *et al.* described a desymmetrization of planar-prochiral (*p*-arene)chromium complexes for the synthesis of *N*-arylindoles bearing planar and axial chirality, through an enantioselective ring-closing metathesis, using (*R*)-Moalkylidene as catalyst.¹⁵⁵ In these substrates the aryl ring of the indole is oriented *anti* with respect to the $\text{Cr}(\text{CO})_2$ group (**scheme 96**). The presence of electron-donating groups on the phosphine moiety was essential to obtain good reactivity and high enantioselectivity. The reaction did not take place for substrates with poorer electron-donating groups on the R_2 groups of the allylphosphine. The proximal isopropenyl groups obstruct the rotation around the (*p*-arene)-indolyl single bond, fixing their orientation in the *anti*-configuration. The *p*-arene moiety can be removed under mild conditions through the exposure of chloroform solution to sunlight under air, affording axially chiral *N*-arylindoles without loss of the optical purity. The released phosphine was trapped by elemental sulfur. It was also established that the geometry of the internal olefin formed was exclusively *cis*.

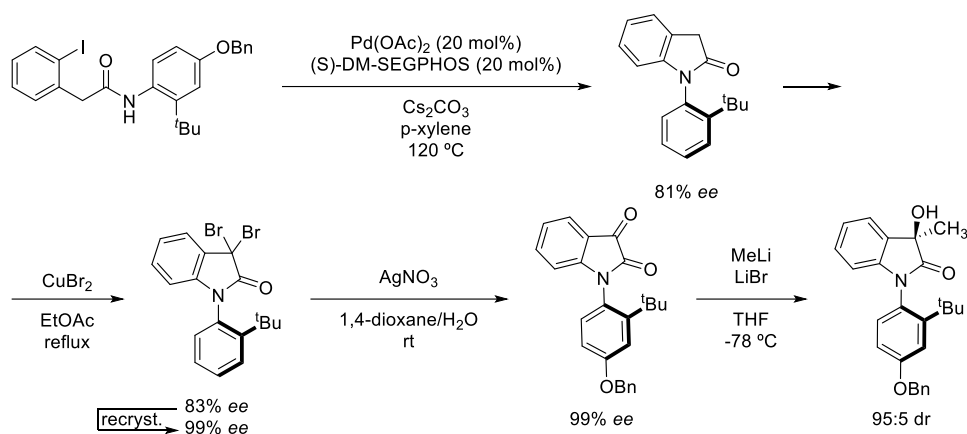
¹⁵⁵ a) S. Kinoshita, K. Kamikawa, *Tetrahedron* **2016**, 72, 5202–5207. b) K. Kamikawa, S. Arae, W.-Y. Wu, C. Nakamura, T. Takahashi, M. Ogasawara, *Chem. Eur. J.* **2015**, 21, 4954–4957.



Scheme 96: desymmetrization of planar-prochiral (*p*-arene)chromium complexes developed by Kamikawa.

In 2015, Nakazaki and co-workers reported a method for the synthesis of *N*-arylisatins, presenting C–N axial chirality, through an enantioselective intramolecular *N*-arylation reaction.¹⁵⁶ Cyclization of the amide using $Pd(OAc)_2$ and (*S*)-DM-SEGPHOS as the ligand afforded *N*-aryloxindole in moderate enantioselectivity. This product was further transformed into the dibrominated derivative, whose optical purity could be increased to >99 % *ee* after recrystallization (**scheme 97**). This product was successfully converted into the *N*-arylisatin-dione under mild conditions without loss of the enantiomeric purity. Finally, a diastereoselective 1,2-addition of MeLi, took place from the opposite side of the *tert*-butyl group, the less hindered face of the isatin, affording 3,3- disubstituted oxindole scaffold in good yield and high diastereoselectivity.

¹⁵⁶ A. Nakazaki, K. Miyagawa, N. Miyata, T. Nishikawa, *Eur. J. Org. Chem.* **2015**, 21, 4603–4606.



Scheme 97: atropisomeric synthesis of C–N arylsatin derivatives through asymmetric intramolecular *N*-arylation.

Direct N–C cross coupling in hindered systems usually involves harsh reaction conditions that compromise the configurational stability of the C–N axis. The group of Colobert, Wencel-Delord and co-workers reported in 2018 a synthetic solution to this problem, describing the distereoselective synthesis of axially chiral *N*-arylated indolines by Cu-catalyzed Ullmann coupling of highly electrophilic hypervalent iodine reagents (**scheme 98A**).¹⁵⁷ Taking advantage of the high reactivity of sterically hindered chiral iodanes, the reaction could be performed at low temperature, affording the axially chiral C–N motifs in a highly atroposelective manner. To control the stereochemical course of the reaction, a traceless sulfoxide auxiliary placed in the *ortho*-position of the iodine atom was used. It was found that nature of the iodane counteranion had a minimal impact on selectivity. Mechanistically, it was proposed that a π,π -stabilizing interaction between the *p*-tolyl group of the chiral auxiliary and the aromatic part of the indoline controlled the chemoselectivity.

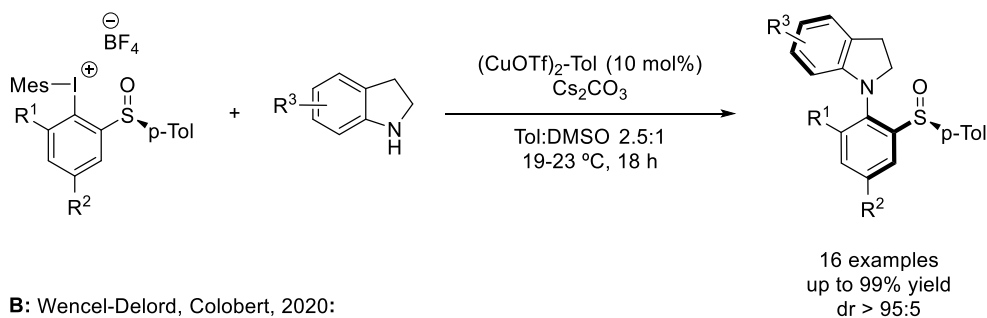
More recently, the same group described the Cu(I) catalyzed enantioselective version of the same reaction (**scheme 98B**),¹⁵⁸ using a chiral bisoxazoline ligand. It

¹⁵⁷ J. Rae, J. Frey, S. Jerhaoui, S. Choppin, J. Wencel-Delord, F. Colobert, *ACS Catal.* **2018**, *8*, 2805–2809.

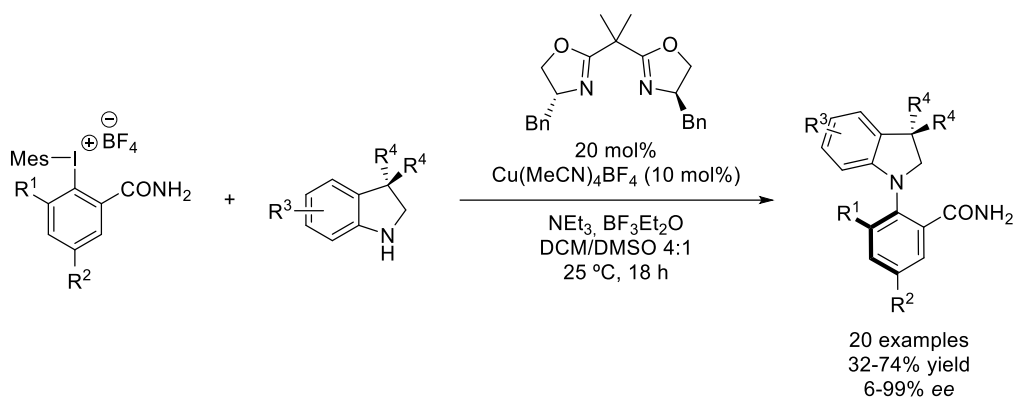
¹⁵⁸ J. Frey, A. Malekafzali, I. Delso, S. Choppin, F. Colobert, J. Wencel-Delord, *Angew. Chem. Int. Ed.* **2020**, *59*, 8844–8848; *Angew. Chem.* **2020**, *132*, 8929–8933.

was found that substrates with reduced steric hindrance at R¹ provided nearly racemic products while halogen-substituted iodanes afforded the corresponding indolines in good yields and enantioselectivities. An intermolecular hydrogen bond was found, between the N atom of the indoline and the amide motif, in the crystal structure of one of the products, with important implications for the success of the reaction.

A: Wencel-Delord, Colobert, 2018:



B: Wencel-Delord, Colobert, 2020:

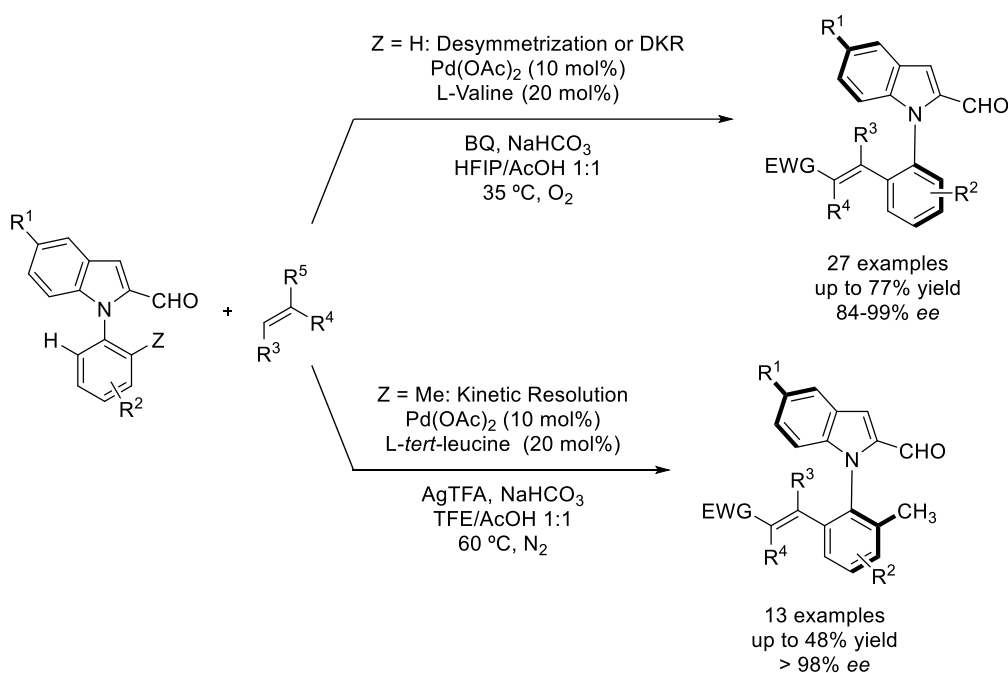


Scheme 98: asymmetric synthesis of axially chiral *N*-aryl indolines *via* Cu catalysis.

Xie, Zhang and co-workers reported an atroposelective C–H olefination of *N*-aryl indoles with electron-poor alkenes catalyzed by Pd(II) (**Scheme 99**).¹⁵⁹ The authors described three different situations depending on the substitution pattern of the starting material: first, for atroposelective C–H olefination/desymmetrization reactions [Z = H, R²(meta) = R²(meta')], the use of Pd(OAc)₂ as the precatalyst, L-valine

¹⁵⁹ J. Zhang, Q. Xu, J. Wu, J. Fan, M. Xie, *Org. Lett.* **2019**, *21*, 6361–6365.

as the ligand and benzoquinone (BQ) as an external oxidant, allowed the preparation of a wide variety of alkenylated products in good yields and high enantioselectivities. Yields and selectivities were also high for the catalytic C–H olefination by dynamic kinetic resolution of configurationally labile *N*-aryl indoles under the same catalytic system. Finally, a catalytic C–H alkenylation by kinetic resolution was developed for configurationally stable substrates, bearing an extra *ortho* substituent. In this case, the alkenylated *N*-aryl indoles needed *tert*-leucine as the ligand and AgTFA as the oxidant, leading to the desired product with excellent selectivity factors of up to 459.

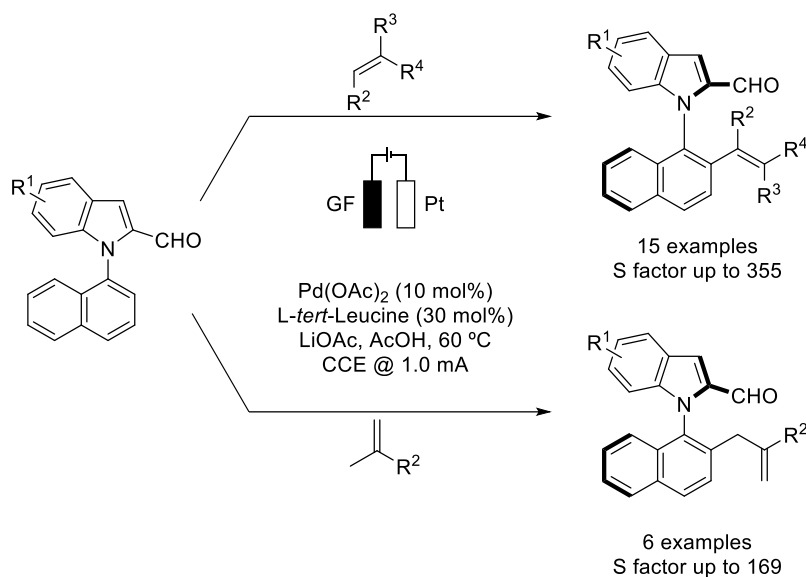


Scheme 99: construction of *N*-C axial chirality through atroposelective C–H olefination.

Very recently, Ackermann and co-workers reported the alkenylation of *N*-naphthyl indole carbaldehydes using a similar kinetic resolution strategy. An electrocatalytic approach was used in this case, to avoid the need of an external oxidant (**scheme 100**).¹⁶⁰ Excellent selectivity factors of up to $s = 355$ were obtained

¹⁶⁰ U. Dhawa, T. Wdowik, X. Hou, B. Yuan, J. C. A. Oliveira, L. Ackermann, *Chem. Sci.* **2021**, *12*, 14182–14188.

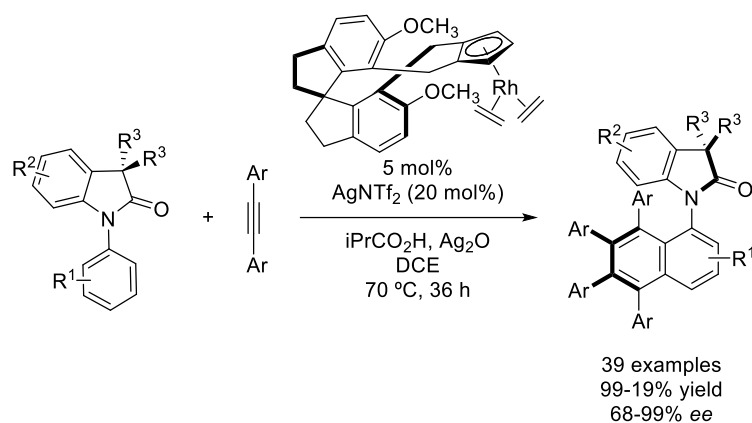
for a variety of electron-poor olefins. Interestingly, 1-1'-disubstituted alkenes showed an unprecedented selectivity towards the allyl product with *s* factor up to 169.



Scheme 100: electrocatalytic construction of N-C axial chirality through atroposelective C-H olefination.

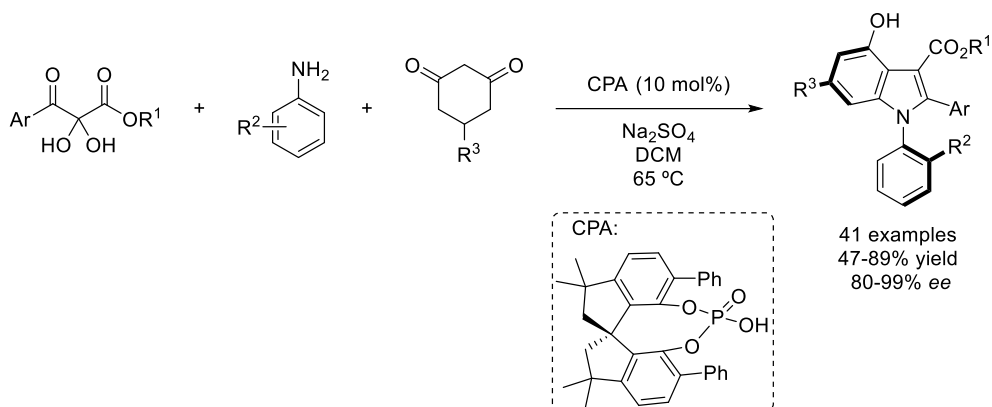
Subsequently, Wang *et al.* developed a Rh(III)-catalyzed Satoh-Miura-type reaction between *N*-aryloxindoles and alkynes as an alternative methodology to construct C-N axial chirality. Chiral *N*-aryloxindoles were obtained with high yields and enantioselectivities with the combination of a Rh(III)-precatalyst and a spirocyclic cyclopentadienyl ligand,¹⁶¹ affording moderate to excellent enantioselectivities for a variety of compounds (**scheme 101**). According to mechanistic studies, the C-H activation step proceeds through a carboxylate-assisted concerted metalation-deprotonation mechanism resulting in a six-membered rhodacyclic intermediate in which the two enantiotopic C-H bonds were better differentiated by the bulky isobutyrate additive.

¹⁶¹ H. Li, X. Yan, J. Zhang, W. Guo, J. Jiang, J. Wang, *Angew. Chem. Int. Ed.* **2019**, *58*, 6732–6736.



Scheme 101: asymmetric construction of C-N axial chirality by asymmetric dual C-H activation.

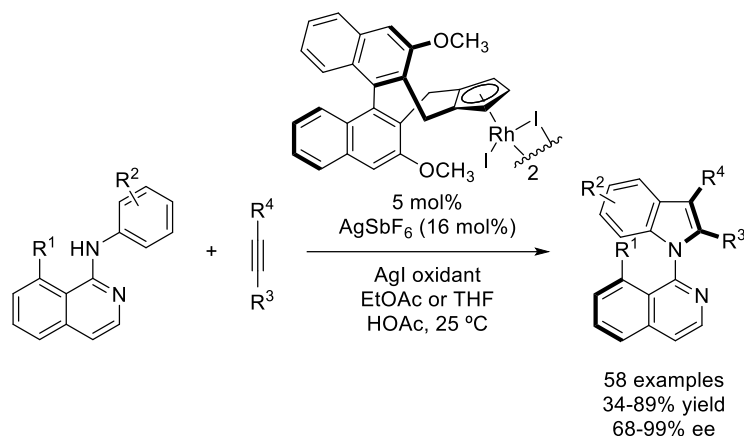
The group of Lin described the first three-component cascade heteroannulation reaction of 2,3-diketoesters, *ortho*-substituted aryl anilines and 1,3-cyclohexanediones, using a chiral spirocyclic phosphoric acid organocatalyst (**scheme 102**).¹⁶² Under the optimized conditions, substituents with different electronic properties in the aromatic ring of the 2,3-diketoester as well as structural modifications in anilines (R^2) and 1,3-cyclohexanediones (R^3), were well tolerated in the reaction, affording excellent yields and enantioselectivities.



Scheme 102: atroposelective phosphoric acid catalyzed three-component cascade reaction.

¹⁶² L. Wang, J. Zhong, X. Lin, *Angew. Chem. Int. Ed.* **2019**, *58*, 15824–15828; *Angew. Chem.* **2019**, *131*, 15971–15975.

Very recently, Wang, Lan, Li and co-workers performed an oxidative [3+2] annulation of anilines with alkynes via Rh(III)-catalyzed C–H activation, using the isoquinoline N atom as a directing group (**scheme 103**).¹⁶³ The reaction proceeds under mild conditions, with high enantioselectivity and high functional group tolerance, when Cramer’s CpOMeRh(III)/AgSbF₆ catalyst and Ag(I) salts as the oxidant were used.



Scheme 103: rhodium-catalyzed atroposelective construction of indoles via C–H bond activation.

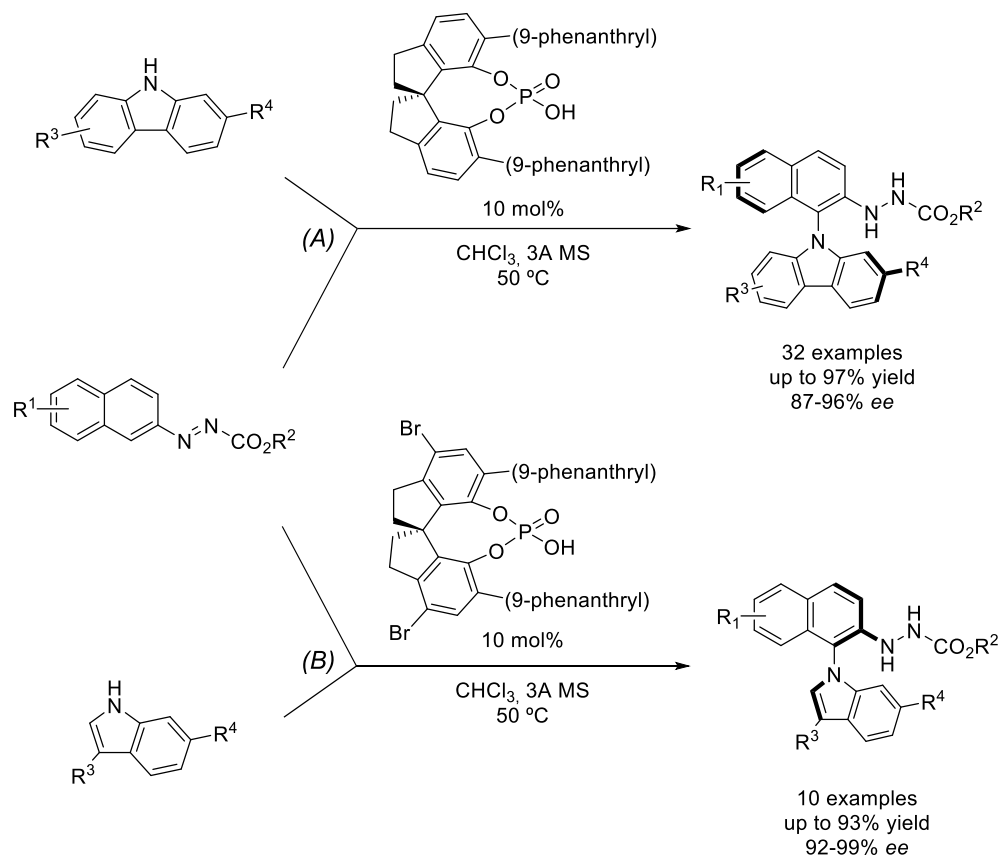
Conversely, Tan *et al.* reported the synthesis of axially chiral *N*-arylcarbazoles in good to excellent enantioselectivities, *via* acid-catalyzed atroposelective C–H amination of azonaphthalenes with carbazoles using spinol-derived chiral phosphoric acid as the catalyst (**scheme 104A**).¹⁶⁴ This methodology represents the first organocatalytic method for the synthesis of such chiral motifs. No external oxidant was needed because this reaction is redox neutral. The configurational stability of the resulting products was ensured by a sterically hindered group at the C2 position of the carbazole substrate. Replacement of the R¹ or R² group in the ester functionality also gave the desired products in excellent yields and with a similar optical purity.

¹⁶³ L. Sun, H. Chen, B. Liu, J. Chang, L. Kong, F. Wang, Y. Lan, X. Li, *Angew. Chem. Int. Ed.* **2021**, *60*, 8391–8395; *Angew. Chem.* **2021**, *133*, 8472–8476.

¹⁶⁴ W. Xia, Q.-J. An, S.-H. Xiang, Y.-B. Wang, B. Tan, *Angew. Chem. Int. Ed.* **2020**, *59*, 6775–6779; *Angew. Chem.* **2020**, *132*, 6841–6845.

Mechanistically, a H-bond activation and a central to axial chirality transfer rearomatization process was proposed, assisted by the CPA.

Indoles were also effective in this transformation, although a bulky R^3 substituent at C3 was required together with a different catalyst, to generate the desired products with high enantioselectivity (**scheme 104B**). Furthermore, it was found that the introduction of a methyl group at C3 of the azonaphthalene significantly increased the yield and had a positive impact on the enantioselectivity.

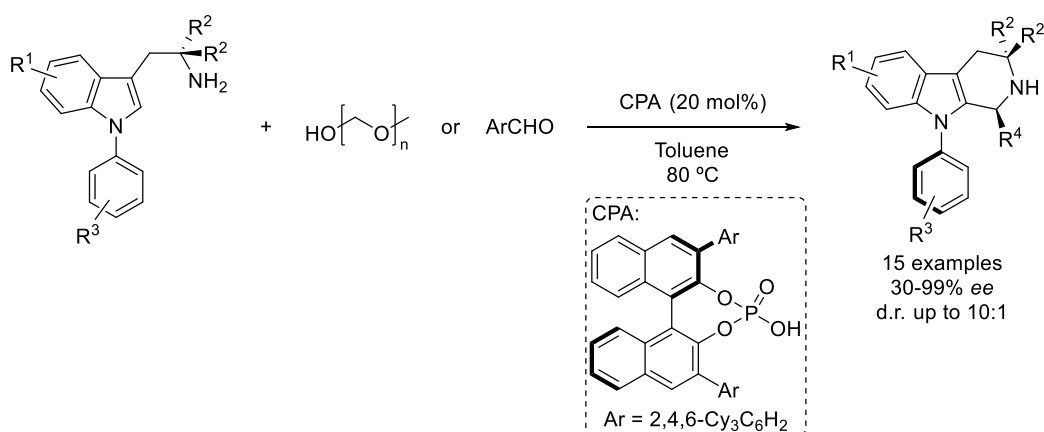


Scheme 104: chiral phosphoric acid catalyzed atroposelective C-H amination of arenes.

Recently, Kwon and co-workers described a Pictet-Spengler reaction between *N*-aryl indoles and paraformaldehyde,¹⁶⁵ for the atroposelective synthesis of *N*-aryl-

¹⁶⁵ A. Kim, A. Kim, S. Park, S. Kim, H. Jo, K. M., Ok, S. K. Lee, J. Song, Y. Kwon, *Angew. Chem. Int. Ed.* **2021**, *60*, 12279–12283; *Angew. Chem.* **2021**, *133*, 12387–12391.

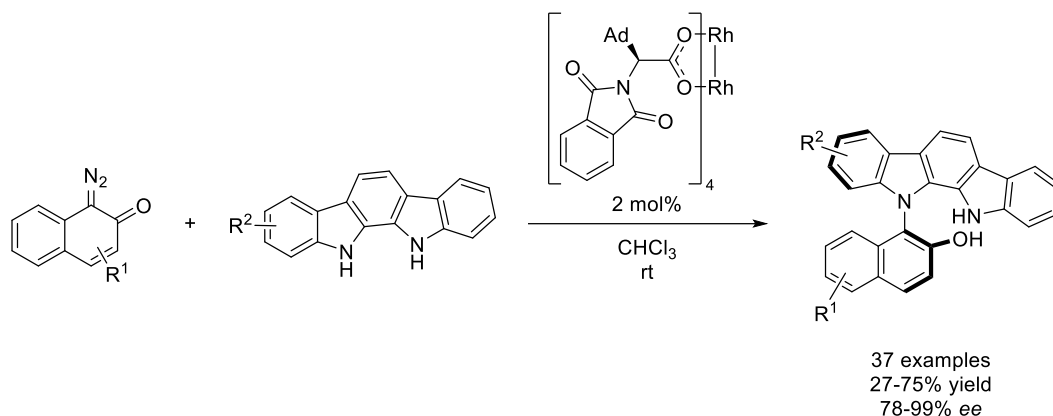
tetrahydro- β -carbolines (**scheme 105**). A bifunctional activation that includes acidic activation of the electrophile and interaction between the phosphate counterion and the indole N–H was needed. The lack of a N–H group in these substrates was solved by introducing an *ortho*-amino hydrogen bond donor into the bottom aromatic ring. Hence, by means of a chiral phosphoric acid, excellent yields and enantioselectivities were obtained for a variety of substrates. In addition, the reaction also works with different activated benzaldehydes, which additionally allows to control both central and axial chirality (4:1 to 10:1 d.r., >99% ee).



Scheme 105: chiral phosphoric acid-catalyzed atroposelective Pictet-Spengler reaction of *N*-arylindoles.

More recently, Wang and co-workers reported on a highly atroposelective synthesis of axially chiral *N*-arylindolocarbazoles, by Rh(II)-catalyzed intermolecular N–H insertion of diazonaphthoquinone-derived carbenes into indolocarbazole precursors.¹⁶⁶ The reaction afforded moderate to good yields and excellent enantioselectivities under mild conditions by using phthalimido-derived dirhodium catalyst Rh₂(S-PTAD)₄ (**scheme 106**). This methodology allows for the late-stage functionalization of natural products and bioactive molecules and for the synthesis of novel *N*-naphthylindolocarbazole-derived chiral phosphoric acids.

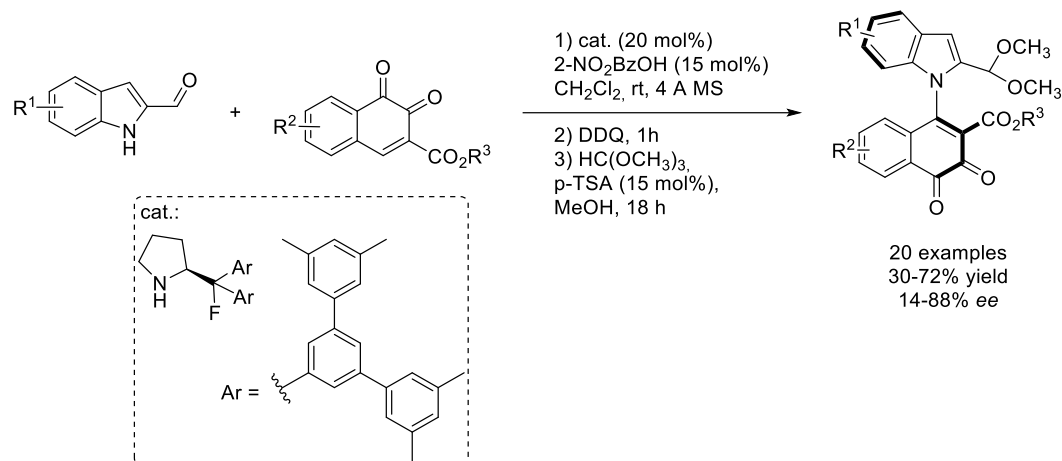
¹⁶⁶ Q. Ren, T. Cao, C. He, M. Yang, H. Liu, L. Wang, *ACS Catal.* **2021**, *11*, 6135–6140.



Scheme 106: synthesis of *N*-arylindolocarbazoles via Rh(II)-catalyzed intermolecular carbene N-H insertion.

The group of Jørgensen has recently described an atroposelective addition of indole-2-carboxaldehydes to *ortho*-quinone derivatives affording C-N axially chiral products by means of a fluorine-substituted proline-based organocatalyst (**scheme 106**).¹⁶⁷ It was found that the reaction needed DDQ to avoid the formation of the corresponding naphthalene-1,2-diol product. Interestingly, the reaction was highly dependent on the solvent used and the acidity of the co-catalyst. Bulkier substituents on the ester moiety of the *ortho*-quinone afforded better enantioselectivities, and overall, a large library of C-N atropisomers was obtained in good levels of regio- and enantioselectivity.

¹⁶⁷ V. Corti, M. K. Thøgersen, V. J. Enemærke, N. M. Rezaee, C. L. Barlose, K. A. Jørgensen, *Chem. Eur. J.* **2022**, e202202395.



Scheme 107: amino catalytic enantioselective addition of indole-2-carboxaldehydes to quinone derivatives.

III.1.2. ADHs as catalyst.

ADH biocatalysts have demonstrated to be an effective tool for oxidation and reduction chemistry, accomplishing the electron transfer from a donor molecule to an acceptor carbonyl compound.¹⁶⁸ Alcohol dehydrogenases (ADHs or also known as ketoreductases KREDs) are oxidoreductases enzymes that depends on external nicotinamide adenine dinucleotide (phosphate) cofactors (NAD(P)H) as the reductant.¹⁸ Although this enzymes may be seen unattractive due to their dependence on this highly expensive cofactor, the problem could be easily overcome through the use of cofactor regeneration strategies. These relies on a sacrificial and inexpensive reductant such as isopropanol (IPA), that is oxidized to acetone, or glucose, generally known as recycling system. Commonly, isopropanol is also used as the hydride source.

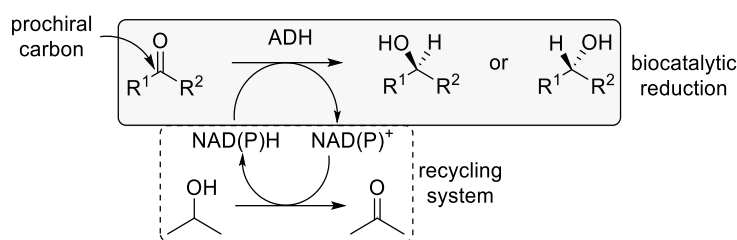
It is important to establish efficient cofactor regeneration strategies when using purified enzymes, due to the high costs of these compounds. In this regard, to regenerate the nicotinamide cofactor, the desired bioreduction is combined with a

¹⁶⁸ Nealon, C.M., Musa, M.M., Patel, J.M., Philips, R.S. *ACS Catal.* **2015**, 5, 2100–2114.

chemical, photochemical, electrochemical or enzymatic reaction, and can be developed by two approaches:¹⁶⁹

1. Coupled enzyme approach, in which the NAD(P)H is regenerated by a second enzymatic system.

2. Coupled substrate approach, in which the bioreduction and the oxidation of the cosubstrate (typically IPA), are catalyzed by ADH. The presence of IPA and acetone as coproducts increase the substrate solubility, but because the ketone reduction is under thermodynamic control, it is needed a large excess of IPA.



Scheme 108: ADHs catalytic system.

ADHs are mainly found to belong to one of the next four protein superfamilies:

(i) Short-chain dehydrogenases/reductases (SDR) are nonmetal-dependant enzymes of about 250 to 300 amino acids residues and present very good functional group tolerance. Within this family, they can be classified based on coenzyme specificities.¹⁷⁰

(ii) Medium-chain dehydrogenases/reductases (MDR) that present around 350-residue subunits and are zinc-dependant, employing the metal for the activation of the carbonyl group through a Lewis acid-base interaction. This superfamily can be divided into separated families, based on sequence similarities.¹⁷¹

¹⁶⁹ G. de Gonzalo, I. Lavandera, (2020). Recent Advances in Selective Biocatalytic (Hydrogen Transfer) Reductions, in Johannes F. Teichert (Ed.) *Homogeneous Hydrogenation with Non-Precious Catalysts* (1st ed., pp. 227–259). Wiley-VCH Verlag GmbH & Co. KGaA

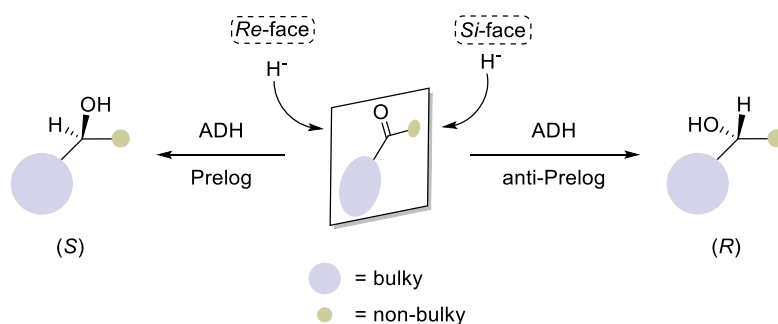
¹⁷⁰ Y. Kallberg, U. Oppenmann, H. Jörnvall, B. Persson, *Eur. J. Biochem.* **2002**, 269 (18), 4409 - 4417.

¹⁷¹ B. Persson, J. Hedlund, H. Jörnvall, *Cell Mol Life Sci.* **2008**, 65 (24), 3879-3894.

(iii) Long-chain dehydrogenases/reductases (LDR) that constitutes a diverse protein family and accept a wide variety of substrates, such as polyols.

(iv) Aldo-keto reductases (AKR) are involved in metabolic reactions of endogenous compounds and xenobiotics and accept a wide range of substrates.

The absolute configuration of the product will be determined by the binding of the substrate in the enzyme active site, due to the relative position of the carbonyl group. The hydride from the NAD(P)H coenzyme can attack the carbonyl substrate from the *Re* or *Si* face, forming the corresponding enantioenriched alcohol (**scheme 109**). Although most ADHs are known to attack on the *Re*-face of the carbonyl and deliver the “Prelog”-type (*S*)-alcohols, many ADHs with the “anti-Prelog”-stereopreference has emerged over the past years.



Scheme 109: ADHs stereopreference regarding the Prelog rule.

ADHs displays excellent stereopreference on prochiral carbonyl compounds, when the substituents R^1 and R^2 are sufficiently different in size.¹⁷² On the other hand, there are not many examples describing successful stereoselective reductions using ADHs, in compounds where the substituents present lower size difference.¹⁷³ In the past few years, protein engineering has emerged as a promising approach to overcome this limitation.¹⁶⁹

¹⁷² H. Gröger, W. Hummel, S. Borchert, M. Krauber, **2012**, *Reduction of ketones and aldehydes to alcohols*, In: *Enzyme Catalysis in Organic Synthesis*, 3 ed. (eds. K. Drauz, H. Gröger, O. May), 1037-1110. Weinheim: Wiley-VCH.

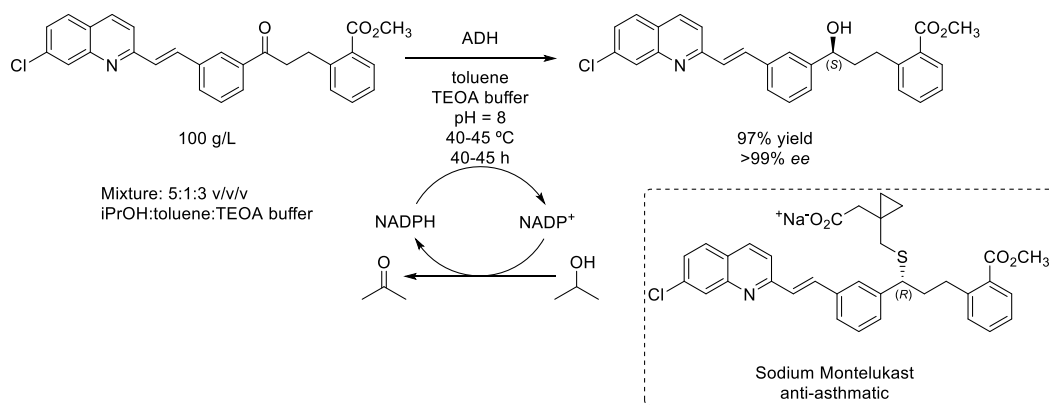
¹⁷³ M. D. Truppo, D. Pollard, P. Devine, *Org. Lett.* **2007**, 9, 335-338.

ADHs has been widely used for the synthesis of bioactive molecules such as antidepressants, anti-asthmatics and anticholesterol drugs, among others, as well as for the preparation of fine chemicals.¹⁷⁴ This successful implementation lays on the excellent robustness of this type of enzymes in organic solvents, allowing the use of isopropanol not only for cofactor regeneration and the ultimate hydride source, but also as organic cosolvent.

For example, Montelukast sodium is an anti-asthmatic agent that is obtained from the (*S*)-alcohol precursor. The asymmetric reduction developed by Merck¹⁷⁵ need of stoichiometric amounts of (–)-B-chlorodiisopinocampheylborane. Although the substrate presents a sterically hindered ketone and functionalities that are sensitive to reductive conditions, the use of various enzymes from Codexis resulted in high selectivity and activity (**scheme 110**). Furthermore, they were found to be stable under the high temperatures and concentrations in the organic solvents used. The process was successfully scaled up to 230 kg, due to the easy purification of the product through precipitation during the reaction.

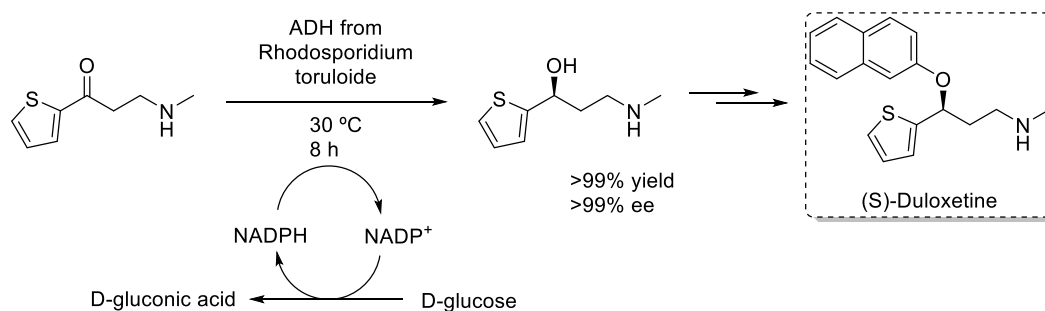
¹⁷⁴ Y.-G. Zheng, H.-H. Yin, D.-F. Yu, X. Chen, X.-L. Tang, X.-J. Zhang, Y.-P. Xue, Y.-J. Wang, Z.-Q. Liu, *Appl. Microbiol. Biotechnol.* **2017**, *101*, 987-1001

¹⁷⁵ A. O. King, E. G. Corley, R. K. Anderson, R. D. Larsen, T. R. Verhoeven, P. J. Reider, *J. Org. Chem.*, **1993**, *58*, 14, 3731–3735.



Scheme 110: synthesis of key intermediate of montelukast using ADHs as catalyst.

The antidepressant (*S*)-duloxetine was first prepared by Eli Lilly *via* an stereoselective reduction of the prochiral ketone precursor. However, several additional steps were needed, and trace metal contamination was found. In 2016, Chen and co-workers developed a highly efficient method to obtain (*S*)-duloxetine in only four steps, employing an ADH from *Rhodospiridium toruloide* for the enantiodetermining step.¹⁷⁶ The procedure allows for high substrate concentration (1000 mM), and proceed with excellent yield and enantioselectivity (**scheme 111**).



Scheme 111: synthesis of key intermediate of (*S*)-duloxetine using ADHs as catalyst.

The first example of kinetic resolution of biaryl compounds using ADHs was described by Miyano and co-workers in 1988,¹⁷⁷ using baker's yeast as whole cell biocatalytic system (**scheme 112**). In this context, 2'-methoxy-2-formylbinaphthyl was

¹⁷⁶ X. Chen, Z.-Q. Liu, C.-P. Lin, Y.-C. Zheng, *Bioorganic Chemistry* **2016**, *65*, 82–89.

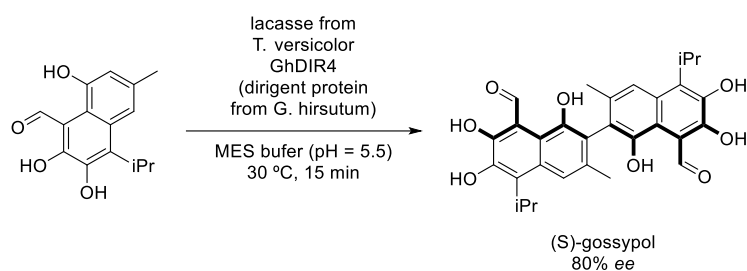
¹⁷⁷ K. Kawahara, M. Matsumoto, H. Hashimoto, S. Miyano, *Chem. Lett.* **1988**, 1163-1164.

axially chiral biaryls, but it remains a challenging transformation in the field of synthetic biocatalysis.

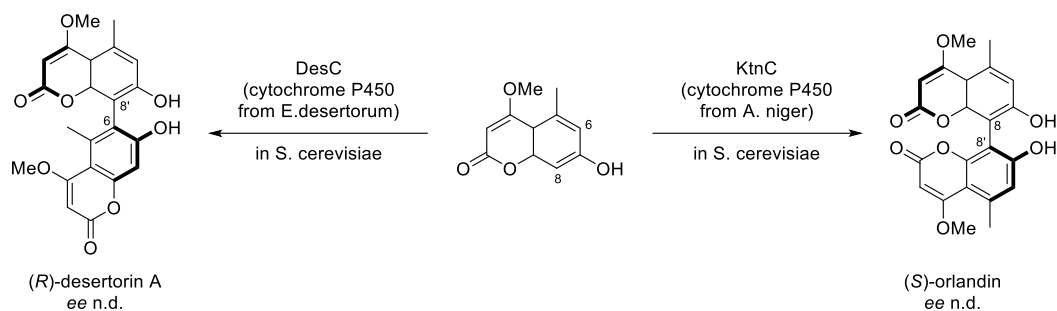
In 2015, Wang and Schaller's research group reported the atroposelective synthesis of (*S*)-gossypol,^{179a} a natural product present in flowers, that acts as a defence compound against insect pests and pathogens. Using of the enzyme lacase from *Trametes versicolor* alone, afforded the racemic product, but in combination with protein GhDIR4 from *Gossypium hirsutum* allowed for the synthesis of the desired (*S*)-gossypol in moderate 80% enantioselectivity (**scheme 114A**). In the same year Müller *et al.* described the use of two different monooxygenases that provided excellent enantioselectivity in the atroposelective dimerization of 7-demethylsiderin (**scheme 114B**).^{179b} Fermentation with enzyme KtnC from *Aspergillus niger*, in baker's yeast, successfully provided (*S*)-orlandin (8,8'-dimer), while fermentation with enzyme DesC from *Emericella desertorum*, afforded (*R*)-desertorin A (6,8'-regioisomer).

¹⁷⁹ a) I. Effenberger, B. Zhang, L. Li, Q. Wang, Y. Liu, I. Klaiber, J. Pfannstiel, Q. Wang, A. Schaller, *Angew. Chem. Int. Ed.* **2015**, *54*, 14660–14663. b) L. S. Mazzaferro, W. Hüttel, A. Fries, M. Müller, *J. Am. Chem. Soc.* **2015**, *137*, 12289–12295.

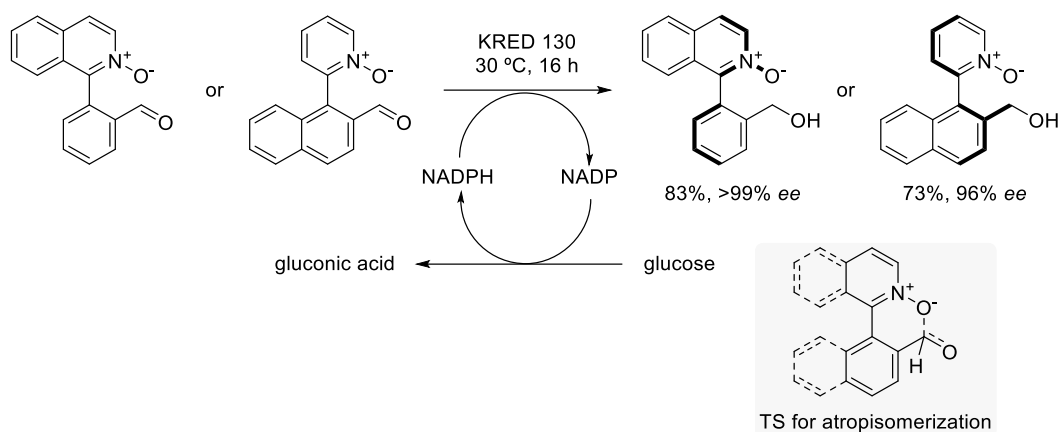
A: Wang and Schaller, 2015:



B: Müller, 2015:

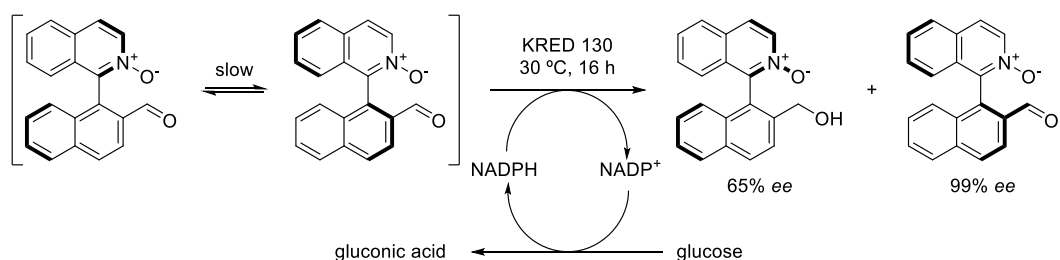
**Scheme 114:** oxidative couplings developed by Wang and Schaller, and Müller.

In 2016 Turner and Clayden described the first biocatalytic dynamic kinetic resolution for the asymmetric synthesis of biaryl atropisomers.⁹⁷ Labile aldehyde-*N*-oxide substrates were incubated with different commercially available KREDs, and high enantioselectivities and conversions could be obtained using KRED 130 (**scheme 115**). In this case, glucose is oxidized to gluconic acid (recycling system). An intramolecular interaction between the aldehyde and the *N*-oxide oxygen atom is responsible for the racemization of the process through a six-membered transition state, supported by molecular modelling. Although the process resembles to the Bringman's lactones, in this case there is no covalent bond, but a transition state with a bonding interaction.



Scheme 115: biocatalytic dynamic kinetic resolution for the synthesis of atropisomeric biaryls *via* Lewis acid-base interaction.

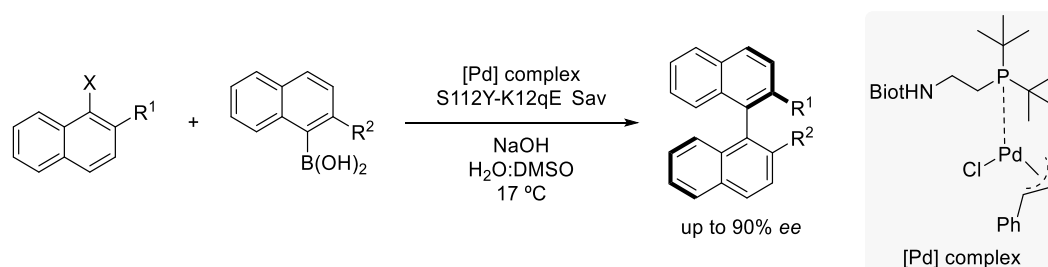
The corresponding naphthylisoquinoline *N*-oxide presented an inefficiently low racemization rate due to its hindered tetra-*ortho*-substituted system. For this reason, a kinetic resolution takes place, affording the (*R*)-alcohol product in moderate enantioselectivity (65% *ee*), while the unreacted starting material was recovered in 46% yield and optically pure (**scheme 116**). When the system was heated over 100 °C, product decomposition occurs before racemization, making impossible to determine the racemization rate.



Scheme 116: biocatalytic kinetic resolution for the synthesis of tetra-substituted *N*-oxide biaryls.

III.1.3. Alternative systems.

Recently, Ward and co-workers reported a palladium-catalyzed Suzuki-Miyaura coupling, assisted by an asymmetric artificial enzyme “Suzukiase”,¹⁸⁰ that was attached to the catalyst thorough a biotin-streptavidin interaction (**scheme 117**). The succeed of the transformation was based on the well-defined second coordination sphere of the artificial metalloenzymes, combined with an electron-rich phosphine ligand, affording enantioselectivities up to 90% *ee*.

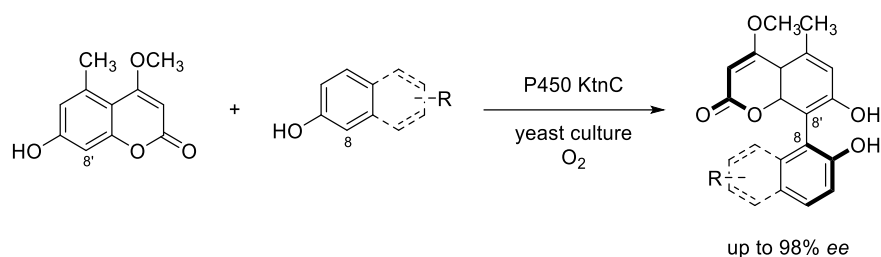


Scheme 117: Suzuki-Miyaura coupling for the synthesis of axially chiral biaryls using an artificial enzyme “Suzukiase”.

Very recently, Narayan and co-workers reported the use of both wild-type and engineered P450 enzymes for the successful regio- and atroposelective unnatural oxidative cross-coupling reaction between coumarin derivative and different non-native phenols (**scheme 118**).¹⁸¹ The reaction tolerates a range of coumarin derivatives bearing electron-donating and electron-withdrawing groups, overcomes the steric and electronic restrictions usually observed in small-molecule oxidative cross-coupling reactions, and thus providing biocatalytic access to a wide range of biaryl scaffolds. For most of the cross-coupling products, the site selectivity for the dimer was the same as in the natural reaction; however, when the steric hindrance was increased at the C4-position of the coumarin coupling partner, a rare 6,6'-connectivity for the minor cross-coupling product was observed.

¹⁸⁰ A. Chatterjee, H. Mallin, J. Klehr, J. Vallapurackal, A. D. Finke, L. Vera, M. Marsh, T. R. Ward, *Chem. Sci.* **2016**, 7, 673-677.

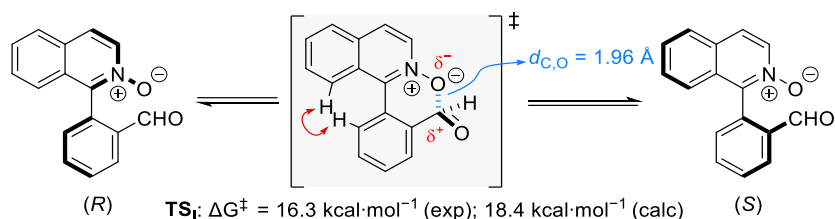
¹⁸¹ L. E. Zetsche, J. A. Yazarians, S. Chakrabarty, M. E. Hinze, L. A. M. Murray, A. L. Lukowski, A. Joyce, A. R. H. Narayan, *Nature* **2022**, 603, 79-85.



Scheme 118: biocatalytic oxidative cross-coupling reactions for the synthesis of axially chiral diols.

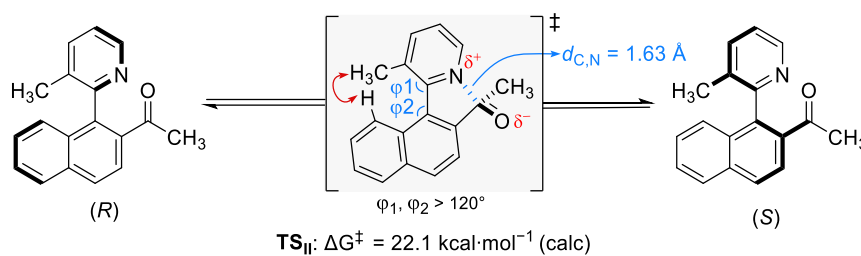
III.2. Objectives and substrate design.

We questioned for the possibility to employ a DKR for the enantioselective biocatalytic synthesis of axially chiral biaryls, based on the use of Lewis acid-base interactions (LABI) as a racemization strategy. For the *N*-oxide biaryls described by Turner, Clayden (**scheme 119**), the bonding interaction between the *N*-oxide and the carbonyl group facilitates the labilization at room temperature through a six-membered cyclic transition state, with an experimental rotational barrier of 16.3 kcal·mol⁻¹ (**TS_I**).



Scheme 119: labilization of the *N*-oxide biaryl through a Lewis acid-base interaction developed by Turner and Clayden.

We recently described the atroposelective synthesis of heterobiaryl carbinols with central and axial chirality, *via* Zn-catalyzed hydrosilylation of heterobiaryl ketones.¹²⁸ In this case, the Lewis acid-base interaction between the nitrogen from the 3-methyl pyridine and the carbonyl from the ketone, forces a five-membered cyclic transition state (**TS_{II}**) which causes the widening of the φ_1 and φ_2 angles, facilitating the racemization of *ortho,ortho'*-trisubstituted substrates (**scheme 120**).



Scheme 120: labilization strategy developed by Fernández and Lassaletta via a five-membered cyclic transition state.

In this regard, we decided to study the DKR of simple biaryl compounds *via* a Lewis acid-base interaction between a formyl and a dimethyl amino groups, strategically situated at the *ortho* positions. This interaction would act as a “*lubricant*”, decreasing the rotational barrier of the substrates, and therefore facilitating rotation around the stereogenic axis.

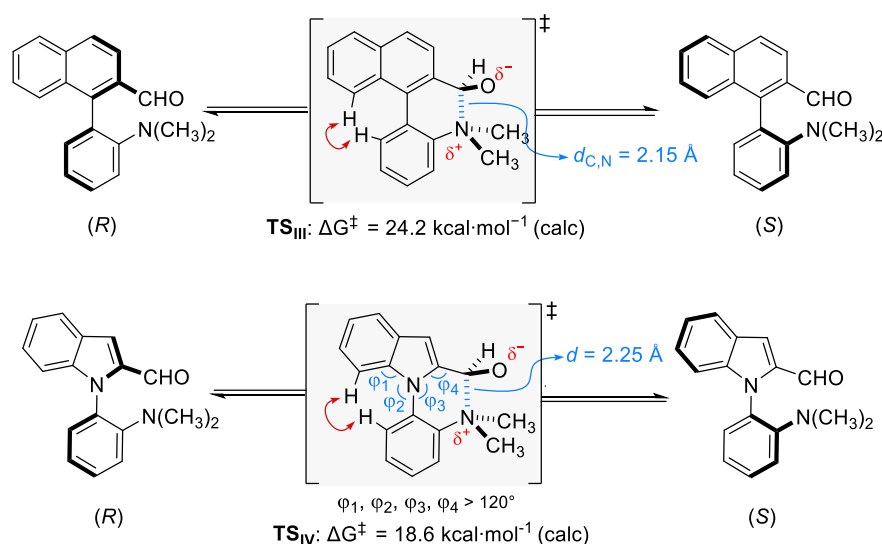
Initially, we decided to study the resolution of biphenyl derivatives (**scheme 121** upper), in which racemization should occur through a six-membered cyclic transition state **TS_{III}**, similar to **TS_I**. As a challenge, the bigger size of the dimethylamino group may debilitate the interaction with the carbonyl, and even steric repulsive interactions between the carbonyl oxygen atom and the nearest *N*-Me group could occur. Furthermore, a rotational barrier of $24.2 \text{ kcal}\cdot\text{mol}^{-1}$ was computationally determined, making uncertain its suitability as substrate in conditions compatible with biocatalytic DKR transformations.

To address this limitation, we decided to study *N*-aryl indoles analogues (**scheme 121** lower), where a lower rotational barrier for the labilization at room temperature would be expected due to two main reasons:

1. The predicted structure of the transition state **TS_{IV}** would present a longer distance between the interacting dimethylamino and the carbonyl group (2.25 \AA), as well as longer distances between the hydrogen atoms on the other side of the axis, decreasing the steric hindrance. This is due to the presence of a five-membered pyrrole unit in the indole fragment, instead of a phenyl ring, making the angles φ_1 , φ_2 , φ_3 , and φ_4 significantly wider than the prototypical 120° angles.

2. The indole ring, as a result of the partial pyramidalization of the N atom, presents a lower aromaticity¹⁸² than expected, that would minimize the steric hindrance in **TS_{IV}**.

A computational study [DFT/B3PW91-D/6-311++g(2d,p)/CPM *-n*-hexane] carried out by Professor Joaquín López-Serrano from the University of Seville (US-CSIC), validated these hypothesis through DFT calculations. It was determined that the longer distance between the *N,N*-dimethylamino group and the CHO group in **TS_{IV}** ($d_{\text{CN}} = 2.25 \text{ \AA}$) compared with **TS_{III}** ($d_{\text{CN}} = 2.15 \text{ \AA}$), and the lower aromaticity of the indole ring due to the partial pyramidalization of the N atom, relieve the steric hindrance between the H-H atoms in **TS_{IV}**, facilitating the labilization. Thus, the calculated racemization barrier of the biaryl analogue was found to be higher (24.8 kcal·mol⁻¹) than the calculated barrier for the formyl indole (18.6 kcal·mol⁻¹).

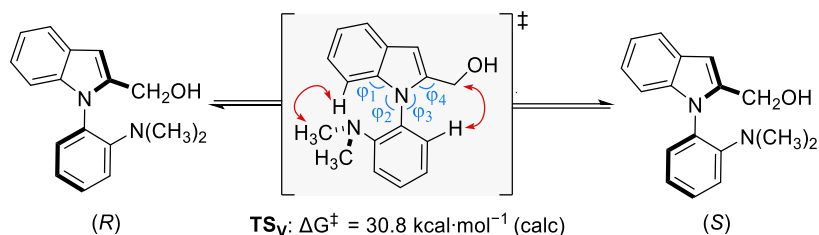


Scheme 121: comparison of aryl- and indole- biaryls racemization barrier.

For comparative purposes, the rotational barrier around the axis for the reduced indole-alcohol in **TS_V** was also computationally determined and as expected,

¹⁸² A. R. Katritzky, C. A. Ramsden, J. A. Joule, V. V. Zhdankin (2010) *Handbook of heterocyclic Chemistry*, 3rd ed., Elsevier, Amsterdam.

it was found to be significantly higher (30.8 kcal·mol⁻¹) than the precursor formyl indole.



Scheme 122: barrier of rotation around the axis for the reduced indole-alcohol.

We envisioned that the stabilization of the axis could be achieved by elimination of the Lewis acid character of the carbonyl group through a biocatalytic reduction via Dynamic Kinetic Resolution, affording configurationally stable enantioenriched axially chiral *N*-arylindole amino-alcohols. In this context, an asymmetric biocatalytic reduction combined with a DKR appeared as an attractive strategy. However, this transformation is particularly challenging because the racemization of the starting material must take place faster than the enantioselective bio-reduction, and should proceed at the temperature range at which these enzymes operates (20-50 °C).

III.3. Results and discussion.

III.3.1. Synthesis of starting materials.

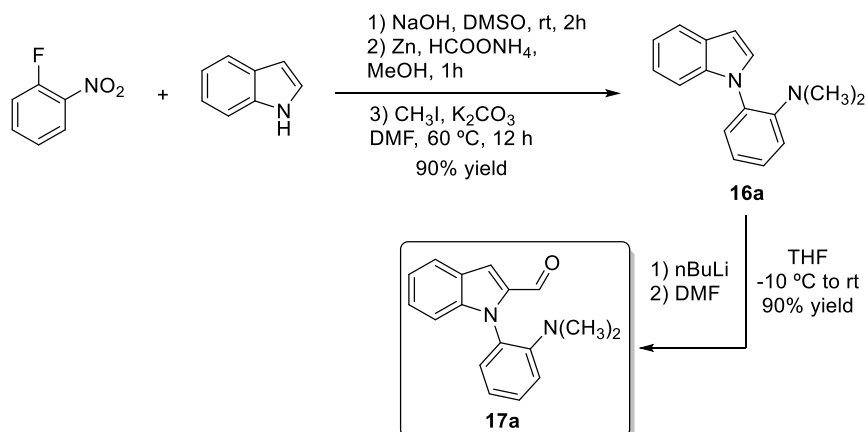
For the synthesis of the target racemic starting material, we followed a four-step synthetic procedure well described in literature. Thus, 1-fluoro-2-nitrobenzene, undergoes nucleophilic aromatic substitution with 1*H*-indole,¹⁸³ followed by the reduction of the nitro group to amine.¹⁸⁴ Finally, dimethylation of the primary amine using methyl iodide¹⁸⁵ and treatment of the resulting *N*-aryl indole with *n*-butyl

¹⁸³ Y.-S. Fan, Y.-J. Jiang, D. An, D. Sha, J. C. Antilla, S. Zhang, *Org. Lett.* **2014**, *16*, 6112–6115

¹⁸⁴ T. U. Thikekar, C.-M. Sun, *Adv. Synth. Catal.* **2017**, *359*, 3388 – 3396.

¹⁸⁵ Q.-C. Mu, Y.-X. Nie, X.-F. Bai, J. Chen, L. Yang, Z. Xu, L. Li, C.-G. Xia, L.-W. Xu, *Chem. Sci.*, **2019**, *10*, 9292–9301.

lithium and dimethyl formamide¹⁸⁶ allowed to obtain the desired indole C2-carbaldehyde **17a**, as shown in **scheme 123**.



Scheme 123: proposed synthetic pathway for the synthesis of the target starting material **17a**.

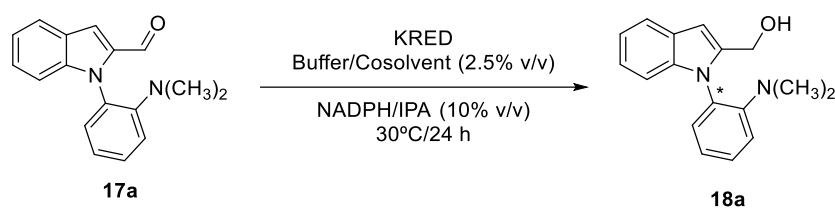
III.3.2. DKR of heterobiaryl aldehydes catalyzed by ketoreductases.

III.3.2.1. Screening of ketoreductases.

A set of commercially available ketoreductases from Codexis were tested for the desired Dynamic Kinetic Resolution using substrate **17a**. The reaction was performed at 30 °C, at analytical scale (10 mM substrate, 1.0 mL), in a buffer containing 2.5% v/v DMSO or THF, with isopropanol for the NADPH cofactor recycling, and the results were analysed after 24 h.

Results are summarized in **table 4**.

¹⁸⁶ K. Grudzień, B. Trzaskowski, M. Smoleń, R. Gajda, K. Woźniak, K. Grela, *Dalton Trans.*, **2017**, 46, 11790–11799.

Table 4: screening of enzymes for the biocatalytic reduction of **17a**.

Entry ^a	KRED	Cosolvent	Conv. (%) ^b	ee (%) ^c	Config. 18a ^d
1	P1-B02	DMSO	96	5	<i>R</i>
2	P1-C01	DMSO	90	40	<i>R</i>
3	P2-B02	DMSO	95	42	<i>S</i>
4	P2-D03	DMSO	97	≤3	n.d.
5	P2-D11	DMSO	56	45	<i>S</i>
6	P2-D12	DMSO	90	23	<i>S</i>
7	P2-G03	DMSO	41	71	<i>S</i>
8	P2-C02	DMSO	72	40	<i>S</i>
9	P1-B12	DMSO	95	81	<i>S</i>
10	P3-G09	DMSO	76	91	<i>S</i>
11	P3-G09	THF	94	94	<i>S</i>
12	P1-A12	DMSO	55	59	<i>S</i>
13	P1-H08	THF	48	94	<i>S</i>
14	P1-H08	DMSO	31	81	<i>S</i>
15	P1-B05	DMSO	90	45	<i>R</i>
16	P2-H07	DMSO	92	96	<i>S</i>
17	P2-B10	DMSO	83	50	<i>S</i>
18	P2-C11	DMSO	24	98	<i>S</i>
19	P3-B03	DMSO	57	95	<i>S</i>
20	P1-A04	DMSO	56	97	<i>S</i>
21	P1-A04	THF	50	93	<i>S</i>
22	P3-H12	DMSO	65	97	<i>S</i>
23	P3-H12	THF	88	94	<i>S</i>

n.d. not determined. ^a Reaction performed at 0.1 mmol scale. ^b Estimated by GS. ^c Determined by HPLC on chiral stationary phases. ^d Absolute configuration was determined by X-Ray analysis.

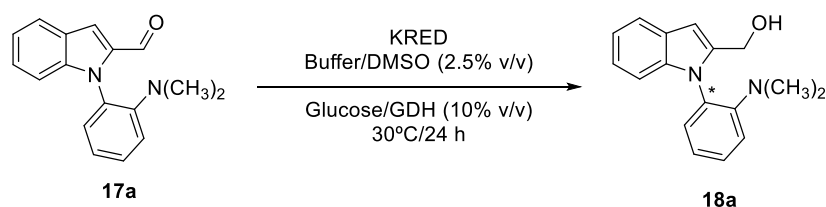
To our delight, various commercially available KRED afforded the desired axially chiral alcohol (*S*)-**18a**, which was found to be configurationally stable. Interestingly, KREDs P2-G03, P3-G09, P3-B03 and P3-H12 (entries **7**, **10** and **11**, **19**,

and **22** and **23**, respectively) showed high enantioselectivities but moderate conversions. On the other hand, P1-B02, P1-C01, P2-B02, P2-B02, P2-D12, P1-B12 and P1-B05 (entries **1**, **2**, **3**, **4**, **6**, **9** and **15**) afforded good to excellent conversions but poor enantiomeric excess. Only P2-H07 (entry **16**) afforded desired alcohol derivative (*S*)-**2a** with excellent conversion (91%) and optical purity (96% *ee*).

When the co-solvent was slightly modified from 2.5% v/v DMSO to 2.5% v/v THF, for enzyme P3-G09 (entry **11**), both conversion and optical purity were improved. On the other hand, the use of 2.5% v/v THF for enzyme P3-H12 (entry **23**), resulted in a significant increase in conversion (from 65% to 88%) and a slightly decrease in enantioselectivity (from 97% to 94% *ee*).

We next explored glucose/glucose dehydrogenase (GDH) dependent KREDs, under the same reaction conditions. The results are summarized in **table 5**.

Table 5: screening of enzymes for the biocatalytic reduction of **17a**.



Entry ^a	KRED	Conv. (%) ^b	ee (%) ^c	Config. 18a ^d
1	101	84	92	<i>R</i>
2	119	97	92	<i>R</i>
3	130	67	90	<i>R</i>
4	NADH 101	83	91	<i>R</i>
5	NADH 110	96	63	<i>R</i>

^a Reaction performed at 0.1 mmol scale. ^b Estimated by GS. ^c Determined by HPLC on chiral stationary phases. ^d Absolute configuration was determined by X-Ray analysis.

Remarkably, when glucose/GDH dependent KREDs were used, the resulting axially chiral alcohol **18a** presented the opposite axial configuration (*R*), with excellent conversion (from 67% to 97%) and high enantiomeric excess in all cases. In

particular, the use of KRED 119 (entry **2**) provided the best results in terms of conversion and enantioselectivity (97% and 92% respectively).

It should be pointed out that the formation of both atropoisomers (*R*) and (*S*) of the heterobiaryl alcohol **18a**, with excellent conversion and optical purities in both cases (96% *ee* for (*S*)-**18a** in table 4, entry **16**, and 92% *ee* for (*R*)-**18a** in table 4, entry **2**), constitute an important feature of this methodology, given the impossibility of using the same enzyme with opposite configuration.

Hence, in view of this results, and because active sites of the enzymes are highly dependent on the structure of the reacting molecule, KREDs P2-H07, P2-G03, P3-G09, P3-B03 and 119 were selected as the optimal enzymes to study the scope of the reaction.

III.3.3. Reaction scope.

The biocatalytic atroposelective reduction strategy was extended to a range of aldehydes substrates (**17b-m**) to explore their reactivity and enzyme-substrate compatibility. The different indole C2-carbaldehyde derivatives were synthesized in moderate to good yields following the same synthetic route as previously described, starting from commercially available substituted 1*H*-indoles and 1-fluoro-2-nitrobenzene derivatives (**figure 14**).

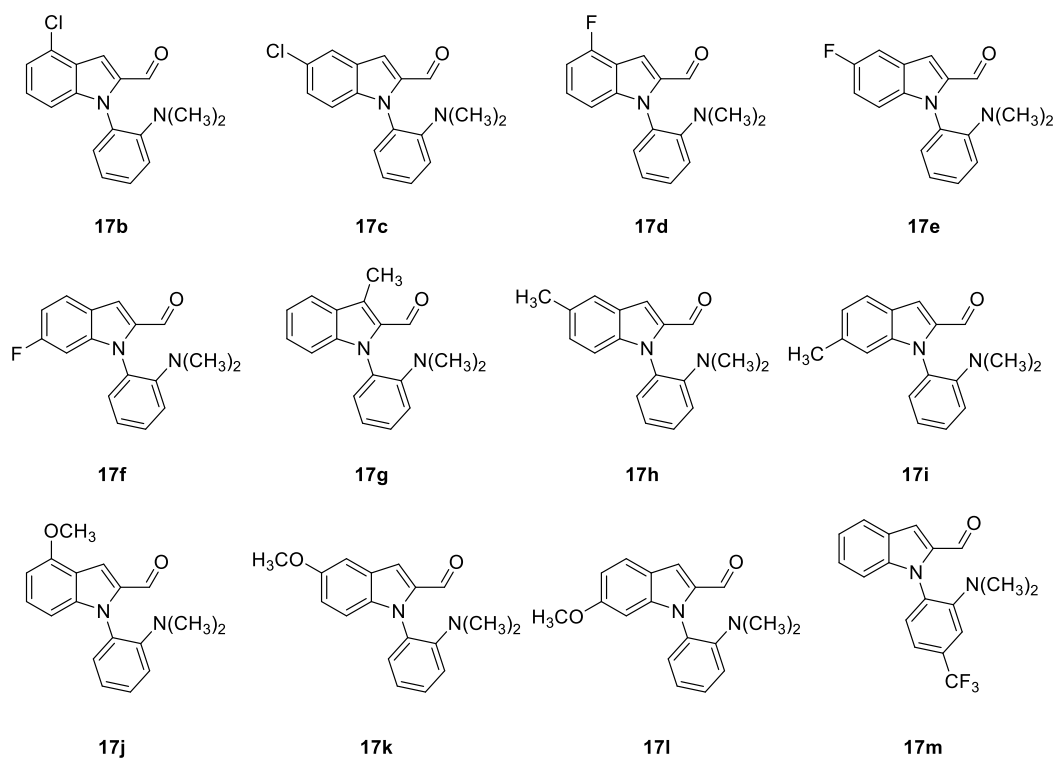
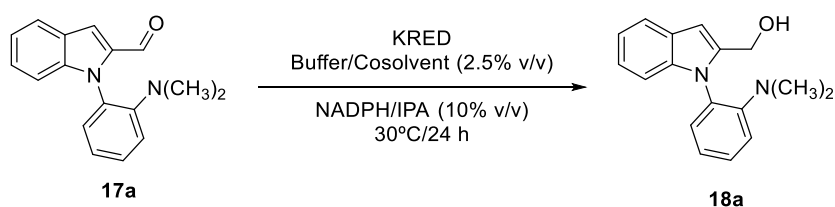


Figure 14: library of indole aldehydes synthesized.

Each substrate was subjected to the reaction conditions using the five most efficient KREDs found above, in presence of DMSO or THF as cosolvent.

The results are summarized in **table 6**.

Table 6: scope of the biocatalytic reduction of the indole-aldehydes.



Entry ^a	Aldehyde	KRED	Cosolvent	X	Conv. (%) ^b	ee (%) ^c
1	17b	P2-H07	DMSO	4-Cl	67	47
2	17b	P3-B03	DMSO	4-Cl	44	51

3	17b	P3-G09	DMSO	4-Cl	52	67
4	17b	P1-A04	DMSO	4-Cl	26	37
5	17b	P2-G03	DMSO	4-Cl	45	75
6	17b	P2-G03	THF	4-Cl	75	88
7	17b	P2-G03	Cyrene	4-Cl	43	81
8	17b	101	DMSO	4-Cl	26	19
9	17b	119	DMSO	4-Cl	43	69
10	17b	119	THF	4-Cl	29	75
11	17c	P2-H07	DMSO	5-Cl	87	97
12	17c	P3-B03	DMSO	5-Cl	61	97
13	17c	P3-G09	DMSO	5-Cl	66	94
14	17c	P2-G03	DMSO	5-Cl	57	93
15	17c	101	DMSO	5-Cl	49	76
16	17c	119	DMSO	5-Cl	67	59
17	17d	P2-H07	DMSO	4-F	42	41
18	17d	P3-B03	DMSO	4-F	52	47
19	17d	P3-G09	DMSO	4-F	95	91
20	17d	P3-G09	THF	4-F	80	90
21	17d	P2-G03	DMSO	4-F	89	47
22	17d	101	DMSO	4-F	37	53
23	17d	119	DMSO	4-F	19	70
24	17d	119	THF	4-F	33	68
25	17e	P2-H07	DMSO	5-F	94	99
26	17e	P3-B03	DMSO	5-F	91	98
27	17e	P3-G09	DMSO	5-F	88	97
28	17e	P2-G03	DMSO	5-F	90	96
29	17e	119	DMSO	5-F	81	75
30	17f	P2-H07	DMSO	6-F	90	97
31	17f	P3-B03	DMSO	6-F	95	97
32	17f	P3-G09	DMSO	6-F	95	97
33	17f	P2-G03	DMSO	6-F	90	92
34	17f	119	DMSO	6-F	45	68
35	17g	P2-H07	DMSO	3-CH ₃	45	31
36	17g	P3-B03	DMSO	3-CH ₃	38	19
37	17g	P3-G09	DMSO	3-CH ₃	33	63
38	17g	P3-G09	THF	3-CH ₃	45	50
39	17g	P2-G03	DMSO	3-CH ₃	27	23
40	17g	101	DMSO	3-CH ₃	35	62

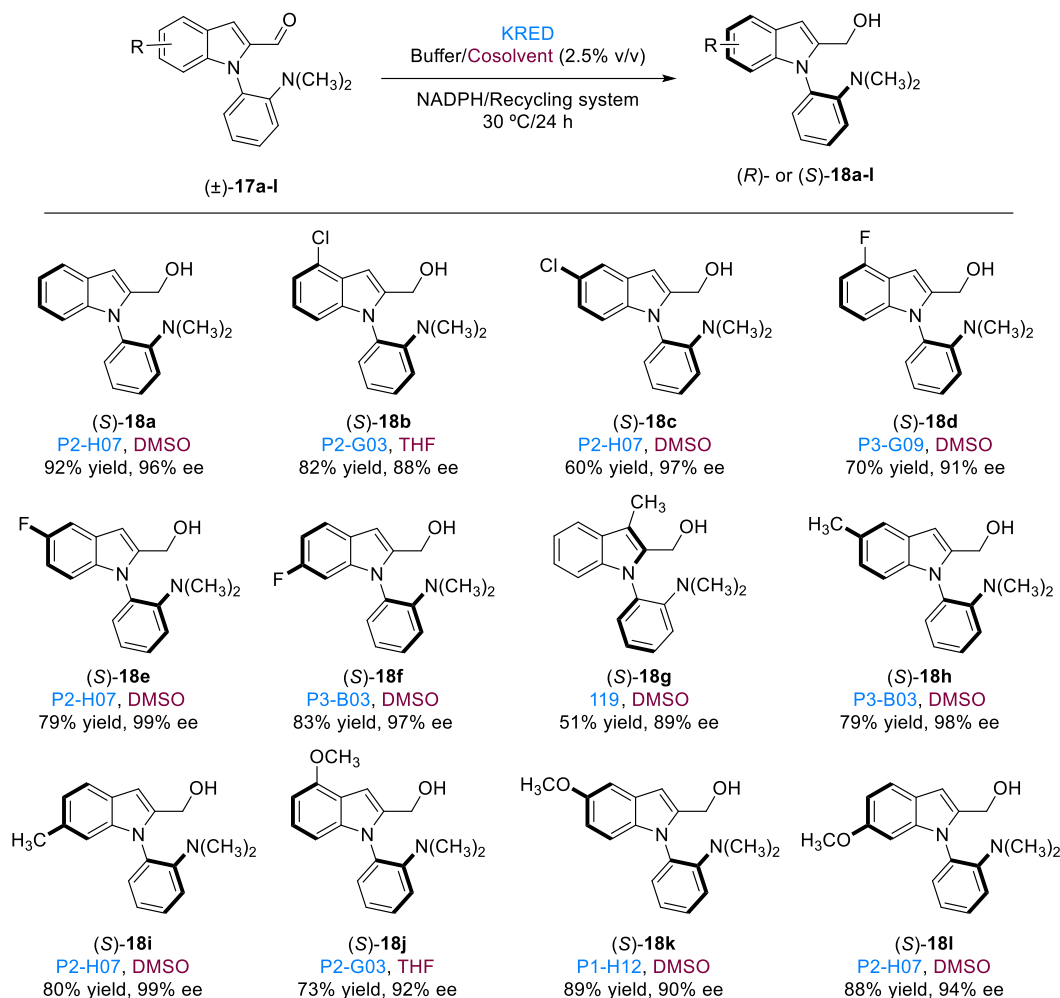
41	17g	119	DMSO	3-CH ₃	55	89
42	17g	119	THF	3-CH ₃	50	77
43	17h	P2-H07	DMSO	5-CH ₃	91	95
44	17h	P3-B03	DMSO	5-CH ₃	90	98
45	17h	P3-G09	DMSO	5-CH ₃	89	93
46	17h	P1-H12	DMSO	5-CH ₃	82	89
47	17h	119	DMSO	5-CH ₃	78	79
48	17i	P2-H07	DMSO	6-CH ₃	85	99
49	17i	P3-B03	DMSO	6-CH ₃	66	98
50	17i	P3-G09	DMSO	6-CH ₃	60	93
51	17i	P1-H12	DMSO	6-CH ₃	65	99
52	17i	119	DMSO	6-CH ₃	49	77
53	17j	P2-H07	DMSO	4-OCH ₃	42	65
54	17j	P3-B03	DMSO	4-OCH ₃	57	60
55	17j	P3-G09	DMSO	4-OCH ₃	59	83
56	17j	P3-G09	THF	4-OCH ₃	27	88
57	17j	P3-H12	DMSO	4-OCH ₃	30	68
58	17j	P2-G03	DMSO	4-OCH ₃	87	81
59	17j	P2-G03	THF	4-OCH ₃	77	92
60	17j	P2-G03	Cyrene	4-OCH ₃	35	82
61	17j	101	DMSO	4-OCH ₃	22	76
62	17j	119	DMSO	4-OCH ₃	58	29
63	17k	P2-H07	DMSO	5-OCH ₃	67	90
64	17k	P3-B03	DMSO	5-OCH ₃	74	90
65	17k	P3-G09	DMSO	5-OCH ₃	90	89
66	17k	P1-H12	DMSO	5-OCH ₃	92	90
67	17k	P1-H12	THF	5-OCH ₃	90	83
68	17k	119	DMSO	5-OCH ₃	43	72
69	17l	P2-H07	DMSO	6-OCH ₃	94	94
70	17l	P3-B03	DMSO	6-OCH ₃	72	95
71	17l	P3-G09	DMSO	6-OCH ₃	80	90
72	17l	P1-H12	DMSO	6-OCH ₃	65	95
73	17l	119	DMSO	6-OCH ₃	52	70

^a Reaction performed at 0.1 mmol scale. ^b Estimated by GS. ^c Determined by HPLC on chiral stationary phases.

Pleasingly, the use of the selected KREDs under the optimized conditions allowed to obtain the corresponding alcohols with high conversion and excellent

optical purity in nearly all cases. As an exception, the 4-(trifluoromethyl)phenyl-indole derivative **17m**, remained unreacted with all the enzymes used.

Bioreductions of aldehydes **17a-l** were scaled up to 15 mg of substrate to obtain synthetically useful amounts of the resulting chiral alcohols for further transformations and characterization. The results are summarized in **scheme 124**.



Scheme 124: summarized scope of the biocatalytic reduction.

As it is shown, halogenated heterobiaryls aldehydes **17b-f** were converted into the (S) - or (R) -alcohols with excellent conversions and optical purities (up to 99% *ee*). It must be remarked that the enantioselectivities were higher for aldehydes

bearing a chloride or fluorine atom at 5- and 6- position of the indole ring (**18c**, **18e** and **18f**), compared with the 4-substituted analogues (**18b** and **18d**).

Furthermore, the reaction also tolerated both 5- and 6-methyl-1*H*-indole derivatives **18h** and **18i**, affording the corresponding alcohols in good conversions (85-90%) and excellent enantioselectivities (98% and 99% *ee* respectively). However, for methyl C3-substituted indole (**18g**), poor conversion and selectivities were observed using isopropanol dependant enzymes (**table 6**, entries 35-39), and the best result was obtained with glucose/glucose dehydrogenase (GDH) dependent KRED 119 (55% conversion and 89% *ee*).

Finally, methoxy derivatives (**18j**, **18k** and **18l**) followed the same trend as the fluorine and chloride derivatives: 5- and 6-methoxy-indoles performed better (up to 90% conversion and 94% *ee*) than the 4- analogue, that presented lower conversion (77%) but equivalent enantiomeric excess.

In general, the presence of a substituent at 4-position caused a negative effect on the conversion and selectivity of the bioreduction, while the same substituents in positions 5- and 6- resulted in excellent results. This effect seems to be related to the steric interactions within the enzyme cage, more than with the electronic nature of the substituents.

It was also possible to determine the absolute configuration of the products **18a** by X-Ray diffraction analysis, showing a (*S_a*)-configuration for the major enantiomer (**figure 15**).

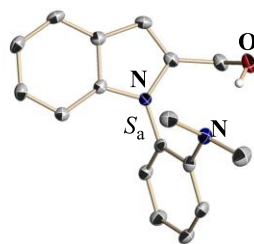
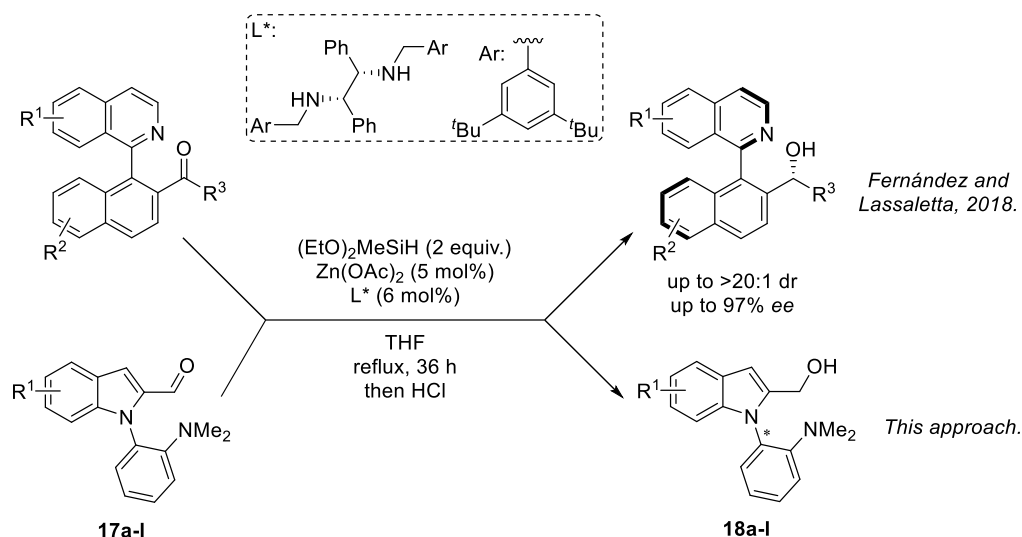


Figure 15: X-Ray diffraction analysis of compound **18a**.

Because different enzymes have been used to carry out the scope of this reaction, in order to determine the absolute configuration of the final products, we performed the reduction of the same substrates using a Zn-catalyzed enantioselective hydrosilylation reaction (**scheme 125**).¹²⁸ Knowing the absolute configuration of (*S*)-**18a** by X-ray diffraction analysis, we could compare the HPLC traces of all products **18** with those obtained by the enantioselective hydrosilylation, assuming a uniform stereochemical outcome for the latter.



Scheme 125: asymmetric hydrosilylation reaction conditions to confirm the absolute configuration.

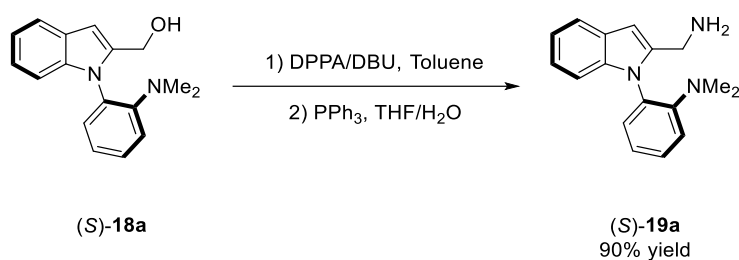
This analysis revealed that the major enantiomer in the biocatalytic reduction was the opposite than in the hydrosilylation reaction. Therefore, we could conclude that for the biocatalytic reduction (results showed in **scheme 124**), the absolute

configuration for the alcohol-indole derivatives **18a-l** was (*S_a*), except for 3-methyl indole derivative **18g**, that present (*R*) axial configuration.

III.3.4. Representative transformations.

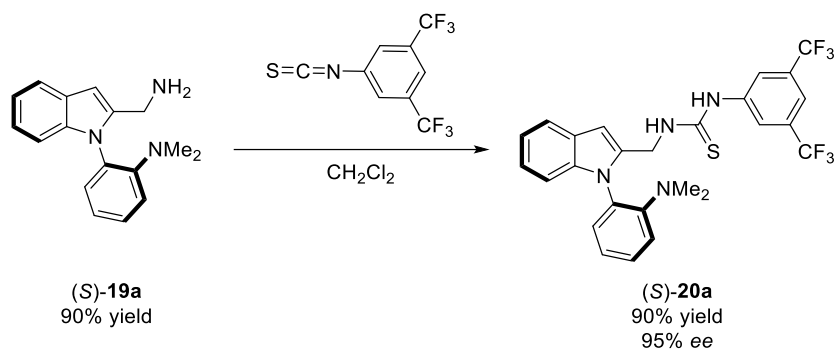
To illustrate the synthetic potential of the reduced products, some derivatization of the model substrate **18a** were performed.

As shown in **scheme 126**, axially chiral diamine (*S*)-**19a** was obtained with excellent yields (90%) through the displacement of the primary alcohol (*S*)-**18a** using diphenylphosphoryl azide (DPPA) and DBU, followed by Staudinger reaction with PPh₃ in a THF/H₂O mixture.



Scheme 126: synthesis of axially chiral diamine **19a**.

Next, condensation of (*S*)-**18a** with 1-isothiocyanato-3,5-bis(trifluoromethyl)benzene afforded a bifunctional thiourea derivative (*S*)-**20a**, with potential use as organocatalyst (**scheme 127**), in excellent yields (90%).



Scheme 127: synthesis of axially chiral thiourea derivative.

Importantly, no racemization was observed during any of these transformations.

III.4. Racemization studies.

We next studied the configurational stability of enantioenriched compound (*S*)-**18a** and compare the experimental results with the obtained by DFT calculations. In this regard we determined the rotational barrier around the C-N bond. The rate of decay in *ee* values at 60 °C and at rt, in a mixture of solvents 8:2 hexane/IPA was measured by taking aliquots at regular time intervals. The change of *ee* was monitored by HPLC on a chiral stationary phase.

In the **figure 16**, $\ln(ee)$ vs *t* (time, hours) is plotted. It can be observed the decrease in optical purity over time, according to first order kinetics, when the sample is heated at 60 °C (orange line). Nonetheless, the compound presents high configurational stability at r.t. (blue line), and it took nearly 19 days to reach half of its initial value.

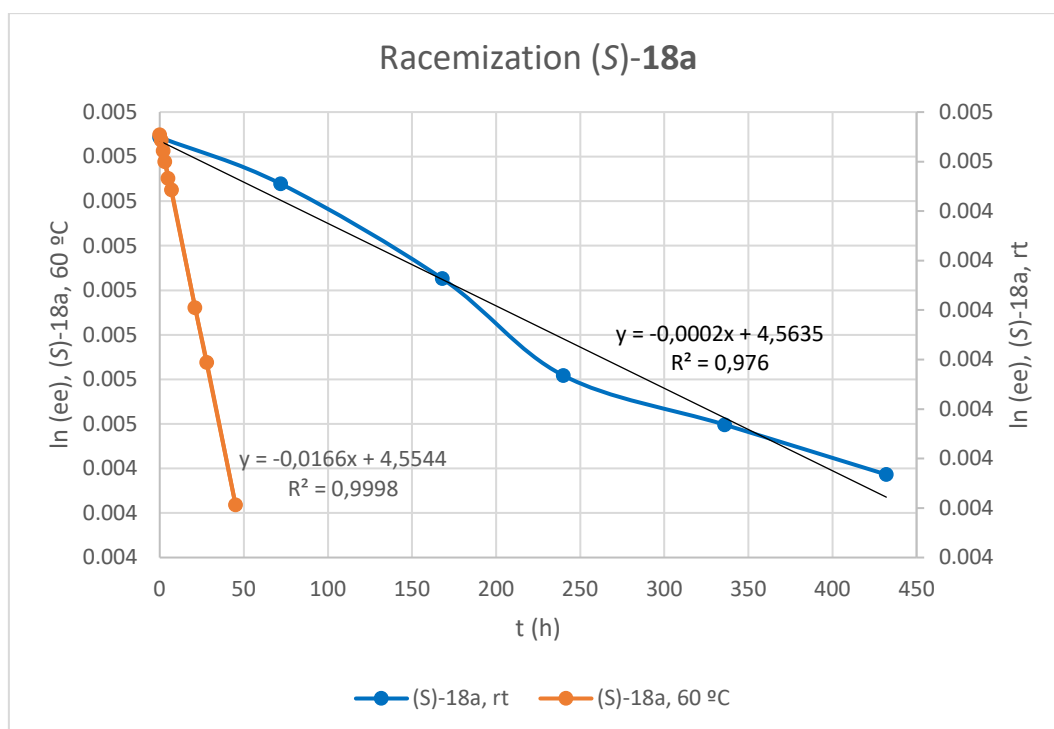


Figure 16: comparison of $\ln(ee)$ vs t (time, hours) of (S)-18a at rt and 60 °C.

With these results in hand, we could experimentally determine the half-life time to racemization, which is defined as the time taken for the enantiomeric excess of the sample to reach half of its initial value ($t_{1/2}$), the rate of racemization (k_{rac}) and the corresponding activation energies of racemization ($\Delta G^\ddagger(T)$).¹⁸⁷

$$t_{1/2} = \frac{\ln 2}{k_{rac}} \quad \text{being} \quad \ln(ee) = -k_{rac}t$$

$$\Delta G^\ddagger(T) = -RT \ln \frac{k_{rac}h}{k_B T}$$

In this regard, being k_B the Boltzmann constant ($1.380662 \times 10^{-23} \text{ J K}^{-1}$), h the Plank constant ($6.626176 \times 10^{-34} \text{ J s}$), R the universal gas constant ($8.31441 \text{ J K}^{-1} \text{ mol}^{-1}$) and T the temperature (K), we were able to calculate:

$$k_{rac}(60 \text{ }^\circ\text{C}) = 1,66 \cdot 10^{-2} \text{ h}^{-1}$$

$$t_{1/2} = 42 \text{ h}$$

¹⁸⁷ F. Pellati, G. Cannazza, S. Benventi, *Journal of Chromatography A*, **2010**, 1217, 3503–3510.

$$\Delta G(T) = 1.16 \cdot 10^2 \text{ kJ/mol} = 28 \text{ kcal/mol}$$

The experimental barrier for the racemization of the reduced alcohol (*S*)-**18a** was found to be 28 kcal mol⁻¹, which is consistent with the DFT calculated barrier of 30.8 kcal mol⁻¹ (**section III.2**), granting the configurational stability of the products.

III.5. Conclusions.

To summarize, in this chapter a highly efficient enantioselective biocatalytic DKR of configurationally labile *N*-arylindole aldehydes has been developed, which afforded a series of axially chiral *N*-arylindole aminoalcohols with excellent conversions and optical purities, under very mild reaction conditions.

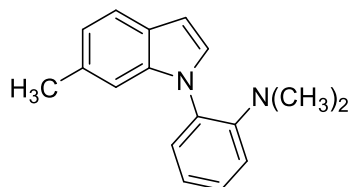
In this case, the labilization of the axis occurs by a weak Lewis acid-base interaction between the aldehyde carbonyl and the dimethyl amino groups through a six-membered cyclic transition state.

To demonstrate the versatility of the resulting products, derivatizations toward highly functionalized compounds, with potential used as ligands u organocatalyst, have been performed, with no erosion in the enantioselectivity.

In must be highlighted that this strategy represents the first successful approach for the atroposelective synthesis of axially chiral compounds featuring a C-N axis, using biocatalytic methodologies.

III.6. Experimental Section.

III.6.1. General procedure for the synthesis of *N,N*-Dimethyl-2-(6-methyl-1*H*-indol-1-yl)aniline. (**16i**)



To a stirred solution of 6-methyl-1*H*-indole (181 mg, 0.82 mmol, 1.0 equiv.) in dry DMSO (0.85 M), 1-fluoro-2-nitrobenzene (1.1 equiv.) and NaOH (1.5 equiv.) were added under nitrogen atmosphere, and the reaction mixture was stirred for 2 h. Upon completion of reaction, the mixture was poured in H₂O and ethyl acetate. The aqueous layer was extracted with ethyl acetate (3 x 20 mL) and the combined organic layers were dried over Mg₂SO₄ and concentrated in vacuo to furnish the corresponding coupling product, that was directly used in the next step without additional purification.

A mixture of 6-methyl-1-(2-nitrophenyl)-1*H*-indole (1 equiv.), HCOONH₄ (5.0 equiv.) and Zn (10 equiv.) in dry methanol (0.16 M) was stirred at room temperature for 1 h. Upon completion of reaction, the mixture was filtered through a Celite pad, and the solvent was evaporated. The crude was dissolved in DCM, the precipitated ammonium formate was filtered off and the solvent was evaporated under reduced pressure. The product was used in the next step without further purification.

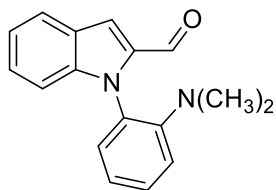
To a stirred solution of 2-(6-methyl-1*H*-indol-1-yl)aniline (1.0 equiv.) and K₂CO₃ (3.0 equiv.) in CH₃CN (0.5 M) was added iodomethane (3.0 equiv.) and the mixture was stirred to reflux for 12h. After cooling to room temperature, the reaction was hydrolysed with H₂O (100 mL) and extracted with ethyl acetate (3 x 50 mL). The combined organic layers were dried over Mg₂SO₄, filtered and concentrated under reduced pressure. The crude residue was purified by flash chromatography using cyclohexane/ethyl acetate 9:1, affording **16i** (200 mg, 98% yield).

^1H NMR (400 MHz, CDCl_3) δ 7.57 (d, $J = 8.0$ Hz, 1H), 7.33 (dt, $J = 7.2, 1.4$ Hz, 2H), 7.30 (d, $J = 3.3$ Hz, 1H), 7.13 – 7.09 (m, 2H), 7.07 – 6.98 (m, 2H), 6.64 (d, $J = 3.0$ Hz, 1H), 2.45 (s, 3H), 2.42 (s, 6H). ^{13}C NMR (100 MHz, CDCl_3) δ 149.0, 136.4, 131.7, 130.4, 128.8, 128.2, 128.0, 126.4, 121.8, 120.8, 120.2, 118.4, 110.7, 102.7, 41.9, 21.9. HRMS (ESI) calcd. for $\text{C}_{17}\text{H}_{19}\text{N}_2$ ($\text{M} + \text{H}^+$) 251.1543. Found 251.1541.

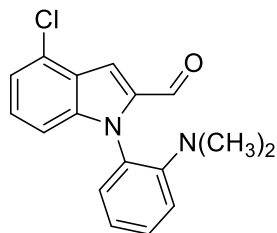
III.6.2. General procedure for the synthesis of 1-(2-(dimethylamino)phenyl)-1*H*-indole-2-carbaldehydes. (17a-l)

To a stirred solution of the corresponding 2-(1*H*-indol-1-yl)-*N,N*-dimethylaniline derivatives (1.0 equiv.) in THF (0.31 M), 1.6 M *n*BuLi in hexane (1.5 equiv.) was added dropwise at 0 °C. The reaction mixture was stirred at 0 °C for 10 min, followed by 1h at rt. Then, *N,N*-dimethylformamide (2.0 equiv.) was added at 0 °C and the reaction mixture was allowed to reach room temperature. After completion, the reaction mixture was quenched with sat. NH_4Cl aq. solution and extracted with ethyl acetate (2 x 50 mL). Organic layer was washed with brine, dried over anhydrous Na_2SO_4 , filtered and evaporated. The crude was purified by flash chromatography using ethyl acetate in hexane as eluent. The desired fractions were concentrated under reduced pressure to afford the corresponding 1-(2-(dimethylamino)phenyl)-1*H*-indole-2-carbaldehydes **17a-l**.

1-(2-(Dimethylamino)phenyl)-1*H*-indole-2-carbaldehyde (17a). Prepared

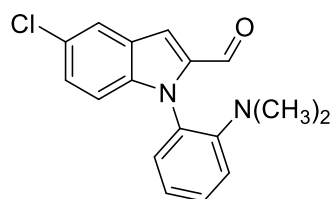


following general procedure using the corresponding 1*H*-indol **16a** (160 mg, 0.6 mmol) to obtain **17a** (160 mg, 90% yield) as yellow solid. ^1H NMR (400 MHz, CDCl_3) δ 9.62 (s, 1H), 7.78 (d, $J = 8.0$ Hz, 1H), 7.50 (s, 1H), 7.39 (td, $J = 8.0, 1.6$ Hz, 1H), 7.36 – 7.31 (m, 3H), 7.23 – 7.19 (m, 1H), 7.15 – 7.09 (m, 2H), 2.30 (s, 6H). ^{13}C NMR (100 MHz, CDCl_3) δ 182.4, 149.3, 138.7, 135.6, 129.2, 129.1, 128.3, 126.9, 126.6, 123.1, 121.9, 121.7, 119.1, 111.3, 110.9, 41.9. HRMS (ESI) calcd. for $\text{C}_{17}\text{H}_{17}\text{N}_2\text{O}$ ($\text{M} + \text{H}^+$) 265.1341. Found 265.1339.

4-Chloro-1-(2-(dimethylamino)phenyl)-1*H*-indole-2-carbaldehyde (17b).

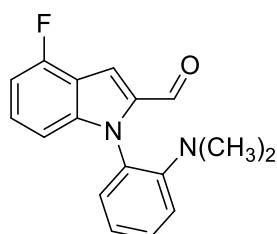
Prepared following general procedure using the corresponding 4-chloro-1*H*-indol **16b** (816 mg, 3.36 mmol) to obtain **17b** (990 mg, 99% yield) as yellow solid. ¹H NMR (400 MHz, CDCl₃) δ 9.58 (s, 1H), 7.55 (s, 1H), 7.41 (t, *J* = 7.5 Hz, 1H), 7.34 (d, *J* = 6.6 Hz, 1H), 7.22 (m, 3H), 7.13 (t, *J* = 7.8

Hz, 2H), 2.30 (s, 6H). ¹³C NMR (100 MHz, CDCl₃) δ 182.0, 149.2, 139.2, 135.9, 129.6, 128.9, 128.4, 128.1, 126.8, 126.1, 122.1, 121.3, 119.3, 109.9, 109.2, 42.0. HRMS (ESI) calcd. for C₁₇H₁₆ClN₂O (M + H⁺) 299.0951. Found 299.0947.

5-Chloro-1-(2-(dimethylamino)phenyl)-1*H*-indole-2-carbaldehyde (17c).

Prepared following general procedure using the corresponding 5-chloro-1*H*-indol **16c** (254 mg, 1.0 mmol) to obtain **17c** (149 mg, 50% yield) as yellow solid. ¹H NMR (400 MHz, CDCl₃) δ 9.54 (s, 1H), 7.84 -

7.67 (m, 1H), 7.42 (t, *J* = 7.7 Hz, 1H), 7.38 (s, 1H), 7.36 - 7.32 (m, 1H), 7.31 - 7.27 (m, 1H), 7.24 (d, *J* = 8.9 Hz, 1H), 7.15 - 7.12 (m, 2H), 2.29 (s, 6H). ¹³C NMR (100 MHz, CDCl₃) δ 182.2, 149.2, 136.9, 136.5, 129.5, 128.9, 127.9, 127.8, 127.3, 126.9, 122.2, 122.1, 119.3, 112.5, 109.8, 41.9. HRMS (ESI) calcd. for C₁₇H₁₆ClN₂O (M + H⁺) 299.0951. Found 299.0945.

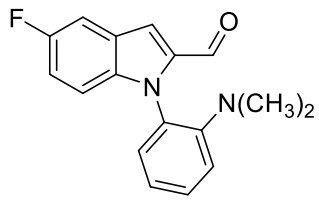
1-(2-(Dimethylamino)phenyl)-4-fluoro-1*H*-indole-2-carbaldehyde (17d).

Prepared following general procedure using the corresponding 4-fluoro-1*H*-indol **16d** (1.46 g, 5.72 mmol) to obtain **17d** (1.3 g, 80% yield) as green solid. ¹H NMR (400 MHz, CDCl₃) δ 9.52 (s, 1H), 7.52 (s, 1H), 7.42 (td, *J* = 7.8, 1.6 Hz, 1H), 7.39 - 7.35 (m, 1H), 7.30 - 7.22 (m, 1H), 7.15 (t, *J* =

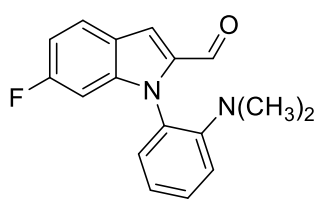
7.3 Hz, 2H), 7.08 (d, *J* = 8.4 Hz, 1H), 6.87 (dd, *J* = 9.9, 7.8 Hz, 1H), 2.32 (s, 6H). ¹³C NMR (100 MHz, CDCl₃) δ 181.9, 157.5 (d, *J* = 251.8 Hz), 149.2, 140.8 (d, *J* = 9.6 Hz), 135.6, 129.5, 128.9, 128.2, 126.9 (d, *J* = 7.9 Hz), 122.1, 119.3, 116.9 (d, *J* = 22.9 Hz), 107.3 (d,

$J = 4.0$ Hz), 106.8, 106.0 (d, $J = 18.6$ Hz), 41.9. ^{19}F NMR (377 MHz, CDCl_3) δ -119.57. HRMS (ESI) calcd. for $\text{C}_{17}\text{H}_{16}\text{FN}_2\text{O}$ ($\text{M} + \text{H}^+$) 283.1247. Found 283.1241.

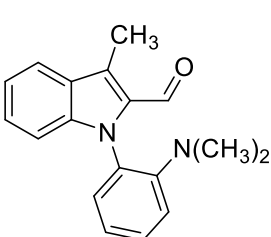
1-(2-(Dimethylamino)phenyl)-5-fluoro-1*H*-indole-2-carbaldehyde (17e).

 Prepared following general procedure using the corresponding 5-fluoro-1*H*-indol **16e** (207 mg, 0.76 mmol) to obtain **17e** (172 mg, 80% yield) as dark yellow solid. ^1H NMR (400 MHz, CDCl_3) δ 9.57 (s, 1H), 7.48 – 7.35 (m, 4H), 7.30 – 7.24 (m, 1H), 7.19 – 7.09 (m, 3H), 2.33 (s, 6H). ^{13}C NMR (100 MHz, CDCl_3) δ 182.2, 158.7 (d, $J = 238.1$ Hz), 149.2, 136.7, 135.3, 129.4, 128.9, 128.1, 127.1 (d, $J = 10.3$ Hz), 122.1, 119.3, 115.5 (d, $J = 26.9$ Hz), 112.4 (d, $J = 9.4$ Hz), 110.2 (d, $J = 5.4$ Hz), 107.2 (d, $J = 23.4$ Hz), 41.9. ^{19}F NMR (377 MHz, CDCl_3) δ -121.7. HRMS (ESI) calcd. for $\text{C}_{17}\text{H}_{16}\text{FN}_2\text{O}$ ($\text{M} + \text{H}^+$) 283.1247. Found 283.1243.

1-(2-(Dimethylamino)phenyl)-6-fluoro-1*H*-indole-2-carbaldehyde (17f).

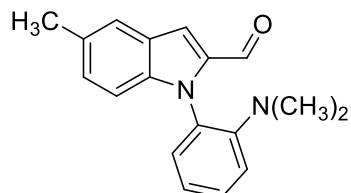
 Prepared following general procedure using the corresponding 6-fluoro-1*H*-indol **16f** (1.6 g, 5.5 mmol) to obtain **17f** (1.1 g, 75% yield) as green solid. ^1H NMR (400 MHz, CDCl_3) δ 9.52 (s, 1H), 7.71 (dd, $J = 8.8, 5.3$ Hz, 1H), 7.43 (s, 1H), 7.42 – 7.38 (m, 1H), 7.33 (dd, $J = 7.7, 1.7$ Hz, 1H), 7.20 – 7.08 (m, 2H), 7.02 – 6.88 (m, 2H), 2.33 (s, 6H). ^{13}C NMR (100 MHz, CDCl_3) δ 181.8, 162.5 (d, $J = 244.4$ Hz), 149.2, 139.2 (d, $J = 12.4$ Hz), 136.5 (d, $J = 3.9$ Hz), 129.5, 128.8, 128.0, 124.4 (d, $J = 10.3$ Hz), 123.5, 122.0, 119.2, 111.4 (d, $J = 4.8$ Hz), 111.2, 97.4 (d, $J = 26.9$ Hz), 41.9. ^{19}F NMR (377 MHz, CDCl_3) δ -113.15. HRMS (ESI) calcd. for $\text{C}_{17}\text{H}_{16}\text{FN}_2\text{O}$ ($\text{M} + \text{H}^+$) 283.1247. Found 283.1239.

1-(2-(Dimethylamino)phenyl)-3-methyl-1*H*-indole-2-carbaldehyde (17g).

 Prepared following general procedure using the corresponding 3-methyl-1*H*-indol **16g** (225 mg, 0.90 mmol) to obtain **17g** (278 mg, 90% yield) as yellow solid. ^1H NMR (400 MHz, CDCl_3) δ 9.64 (s, 1H), 7.75 (d, $J = 8.0$ Hz, 1H), 7.46 – 7.31 (m, 3H), 7.29 – 7.24 (m, 2H), 7.20 (t, $J = 7.5$ Hz, 1H),

7.10 (t, $J = 7.2$ Hz, 2H), 2.74 (s, 3H), 2.31 (s, 6H). ^{13}C NMR (100 MHz, CDCl_3) δ 183.8, 149.4, 137.6, 130.7, 129.3, 129.0, 128.3, 128.0, 126.7, 122.6, 121.8, 121.1, 120.9, 118.9, 111.1, 41.9, 9.7. RMS (ESI) calcd. for $\text{C}_{18}\text{H}_{19}\text{N}_2\text{O}$ ($\text{M} + \text{H}^+$) 279.1497. Found 279.1494.

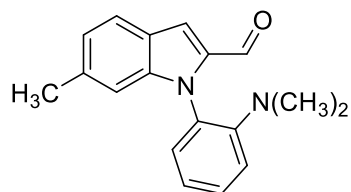
1-(2-(Dimethylamino)phenyl)-5-methyl-1*H*-indole-2-carbaldehyde (17h).



Prepared following general procedure using the corresponding 5-methyl-1*H*-indol **16h** (187 mg, 0.75 mmol) to obtain **17h** (125 mg, 60% yield) as yellow solid. ^1H NMR (400 MHz, CDCl_3) δ 9.55 (s, 1H), 7.54 (s,

1H), 7.43 – 7.31 (m, 3H), 7.23 – 7.16 (m, 2H), 7.13 (d, $J = 7.7$ Hz, 2H), 2.46 (s, 3H), 2.30 (s, 6H). ^{13}C NMR (100 MHz, CDCl_3) δ 182.4, 149.3, 137.3, 135.7, 131.1, 129.1, 129.1, 128.5, 128.4, 127.2, 122.3, 121.9, 119.1, 111.0, 110.4, 41.9, 21.4. HRMS (ESI) calcd. for $\text{C}_{18}\text{H}_{19}\text{N}_2\text{O}$ ($\text{M} + \text{H}^+$) 279.1497. Found 279.1498.

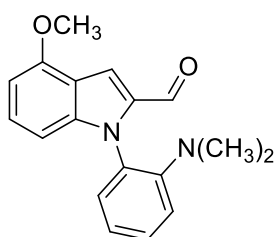
1-(2-(Dimethylamino)phenyl)-6-methyl-1*H*-indole-2-carbaldehyde (17i).



Prepared following general procedure using the corresponding 6-methyl-1*H*-indol **16i** (200 mg, 0.80 mmol) to obtain **17i** (122 mg, 55% yield) as yellow solid. ^1H NMR (400 MHz, CDCl_3) δ 9.54 (s, 1H), 7.65 (d,

$J = 8.2$ Hz, 1H), 7.45 – 7.41 (m, 1H), 7.39 – 7.35 (m, 1H), 7.14 (ddd, $J = 7.1, 3.8, 2.3$ Hz, 3H), 7.10 – 7.03 (m, 2H), 2.44 (s, 3H), 2.33 (s, 6H). ^{13}C NMR (100 MHz, CDCl_3) δ 182.2, 149.3, 139.3, 137.0, 135.3, 129.2, 129.1, 128.4, 124.9, 123.7, 122.7, 121.8, 119.1, 111.2, 110.8, 41.9, 22.2. HRMS (ESI) calcd. for $\text{C}_{18}\text{H}_{19}\text{N}_2\text{O}$ ($\text{M} + \text{H}^+$) 279.1497. Found 279.1496.

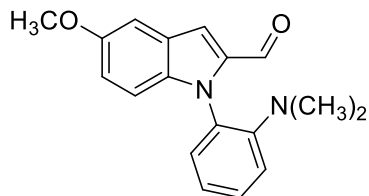
1-(2-(Dimethylamino)phenyl)-4-methoxy-1*H*-indole-2-carbaldehyde (17j).



Prepared following general procedure using the corresponding 4-methoxy-1*H*-indol **16j** (726 mg, 3.04 mmol) to obtain **17j** (880 mg, 76% yield) as yellow solid. ^1H NMR (400 MHz, CDCl_3) δ 9.55 (s, 1H), 7.59 (s, 1H), 7.38 (t, $J = 7.0$ Hz, 2H), 7.34 (t, $J = 6.6$ Hz, 1H), 7.26 (t, $J = 8.1$ Hz, 1H),

7.16 – 7.06 (m, 1H), 6.87 (d, $J = 8.5$ Hz, 1H), 6.56 (d, $J = 7.7$ Hz, 1H), 3.99 (s, 3H), 2.33 (s, 6H). ^{13}C NMR (100 MHz, CDCl_3) δ 181.9, 154.9, 149.4, 140.3, 134.7, 129.2, 129.2, 128.5, 127.7, 121.7, 119.0, 118.6, 109.3, 104.2, 100.6, 55.5, 41.9. HRMS (ESI) calcd. for $\text{C}_{18}\text{H}_{19}\text{N}_2\text{O}_2$ ($\text{M} + \text{H}^+$) 295.1447. Found 295.1439.

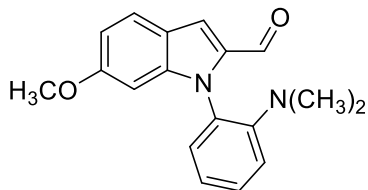
1-(2-(Dimethylamino)phenyl)-5-methoxy-1*H*-indole-2-carbaldehyde (17k).



Prepared following general procedure using the corresponding 5-methoxy-1*H*-indol **16k** (236 mg, 0.89 mmol) to obtain **17k** (144 mg, 55% yield) as yellow solid. ^1H NMR (400 MHz, CDCl_3) δ 9.54 (s, 1H),

7.45 – 7.29 (m, 3H), 7.20 (d, $J = 9.1$ Hz, 1H), 7.16 – 7.07 (m, 3H), 7.02 (dd, $J = 9.1, 2.5$ Hz, 1H), 3.87 (s, 3H), 2.31 (s, 6H). ^{13}C NMR (100 MHz, CDCl_3) δ 182.3, 155.4, 149.3, 135.7, 134.2, 129.2, 129.1, 128.3, 127.3, 121.8, 119.1, 118.3, 112.3, 110.1, 102.6, 55.7, 41.9. HRMS (ESI) calcd. for $\text{C}_{18}\text{H}_{19}\text{N}_2\text{O}_2$ ($\text{M} + \text{H}^+$) 295.1447. Found 295.1444.

1-(2-(Dimethylamino)phenyl)-6-methoxy-1*H*-indole-2-carbaldehyde (17l).



Prepared following general procedure using the corresponding 6-methoxy-1*H*-indol **16l** (1.80 g, 6.8 mmol) to obtain **17l** (400 mg, 20% yield) as yellow solid. ^1H NMR (400 MHz, CDCl_3) δ 10.17 (s, 1H), 7.77

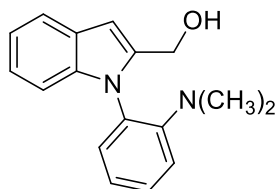
(d, $J = 8.7$ Hz, 1H), 7.34 – 7.27 (m, 2H), 7.19 (d, $J = 3.2$ Hz, 1H), 7.01 (td, $J = 7.7, 4.6$ Hz, 2H), 6.89 (d, $J = 8.7$ Hz, 1H), 6.66 (d, $J = 3.3$ Hz, 1H), 3.95 (s, 3H), 2.29 (s, 6H). ^{13}C NMR (100 MHz, CDCl_3) δ 187.6, 158.2, 147.3, 133.5, 132.7, 130.9, 127.8, 126.9, 126.7, 125.4, 120.9, 118.1, 113.2, 105.5, 103.8, 56.9, 41.5. HRMS (ESI) calcd. for $\text{C}_{18}\text{H}_{19}\text{N}_2\text{O}_2$ ($\text{M} + \text{H}^+$) 295.1447. Found 295.1445.

III.6.3. General procedure for the racemic reduction of 1-(2-(dimethylamino)phenyl)-1*H*-indole-2-carbaldehydes. ((\pm)-18a-l**)**

To a solution of the corresponding aldehyde **17a-l** (1.0 equiv.) in a 1:1 mixture MeOH/DCM (0.1 M) was added sodium borohydride (2.0 equiv.) at 0 °C, and the resulting mixture stirred at rt for 1 h. The mixture was then poured into brine,

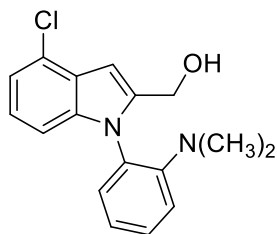
extracted with ethyl acetate and the combined organic extracts washed with brine, dried over sodium sulphate, filtered, and evaporated to afford the corresponding racemic alcohols (\pm)-**18a-l**.

(\pm)-(1-(2-(Dimethylamino)phenyl)-1*H*-indol-2-yl)methanol (18a). ^1H NMR (400



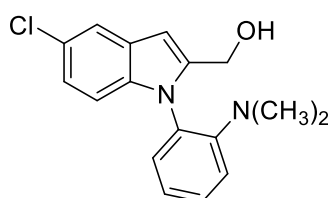
MHz, CDCl_3) δ 7.71 (d, $J = 8.5$ Hz, 1H), 7.48 (t, $J = 7.6$ Hz, 1H), 7.30 – 7.24 (m, 2H), 7.23 – 7.17 (m, 2H), 7.16 – 7.09 (m, 1H), 6.78 (s, 1H), 5.06 (br s, 1H), 4.59 (d, $J = 12.8$ Hz, 1H), 4.36 (d, $J = 12.8$ Hz, 1H), 2.46 (s, 6H). ^{13}C NMR (100 MHz, CDCl_3) δ 149.7, 140.8, 138.4, 131.4, 130.0, 129.6, 128.4, 123., 122.6, 120.9, 120.5, 119.3, 110.5, 103.6, 56.7, 42.8. HRMS (ESI) calcd. for $\text{C}_{17}\text{H}_{19}\text{N}_2\text{O}$ ($\text{M} + \text{H}^+$) 267.1497. Found 267.1490.

(\pm)-(4-Chloro-1-(2-(dimethylamino)phenyl)-1*H*-indol-2-yl)methanol (18b) ^1H

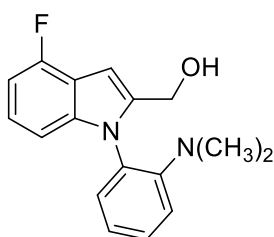


NMR (400 MHz, CDCl_3) δ 7.47 (m, 1H), 7.24 (s, 1H), 7.21 – 7.17 (m, 2H), 7.15 (d, $J = 7.6$ Hz, 1H), 7.07 (t, $J = 7.8$ Hz, 1H), 6.95 (d, $J = 8.1$ Hz, 1H), 6.84 (s, 1H), 5.22 (br s, 1h) 4.55 (d, $J = 12.7$ Hz, 1H), 4.27 (d, $J = 12.8$ Hz, 1H), 2.43 (s, 6H). ^{13}C NMR (100 MHz, CDCl_3) δ 149.6, 141.5, 139.0, 131.2, 129.9, 129.6, 127.1, 126.2, 123.6, 123.1, 120.2, 119.4, 109.1, 102.1, 56.7, 42.9. HRMS (ESI) calcd. for $\text{C}_{17}\text{H}_{18}\text{ClN}_2\text{O}$ ($\text{M} + \text{H}^+$) 301.1108. Found 301.1100.

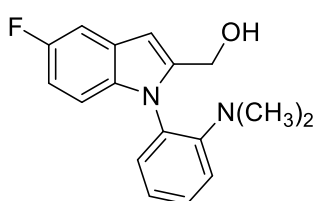
(\pm)-(5-Chloro-1-(2-(dimethylamino)phenyl)-1*H*-indol-2-yl)methanol (18c). ^1H



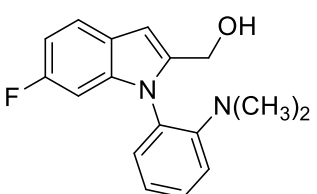
NMR (400 MHz, CDCl_3) δ 7.61 (d, $J = 2.0$ Hz, 1H), 7.46 (dt, $J = 8.7, 4.5$ Hz, 1H), 7.24 (d, $J = 8.3$ Hz, 1H), 7.19 (d, $J = 4.4$ Hz, 2H), 7.11 (dd, $J = 8.7, 2.1$ Hz, 1H), 6.97 (d, $J = 8.7$ Hz, 1H), 6.67 (s, 1H), 4.52 (d, $J = 12.8$ Hz, 1H), 4.25 (d, $J = 12.7$ Hz, 1H), 2.42 (s, 6H). ^{13}C NMR (100 MHz, CDCl_3) δ 149.6, 142.1, 136.7, 131.1, 129.8, 129.6, 129.2, 126.0, 123.6, 122.8, 120.2, 119.4, 111.4, 103.1, 56.7, 42.8. HRMS (ESI) calcd. for $\text{C}_{17}\text{H}_{18}\text{ClN}_2\text{O}$ ($\text{M} + \text{H}^+$) 301.1102. Found 301.1100.

(±)-(1-(2-(Dimethylamino)phenyl)-4-fluoro-1*H*-indol-2-yl)methanol (18d). ¹H

NMR (400 MHz, CDCl₃) δ 7.47 (ddd, *J* = 8.7, 6.5, 2.5 Hz, 1H), 7.25 – 7.14 (m, 3H), 7.07 (td, *J* = 8.0, 5.1 Hz, 1H), 6.89 – 6.78 (m, 3H), 5.26 (s, 1H), 4.53 (d, *J* = 12.7 Hz, 1H), 4.26 (d, *J* = 12.8 Hz, 1H), 2.43 (s, 6H). ¹³C NMR (100 MHz, CDCl₃) δ 156.4 (d, *J* = 247.7 Hz), 149.6, 140.9 (d, *J* = 10.9 Hz), 140.8, 131.2, 129.9, 129.8, 123.6, 122.9 (d, *J* = 7.9 Hz), 119.4, 117.4 (d, *J* = 22.7 Hz), 106.6 (d, *J* = 3.6 Hz), 105.3 (d, *J* = 19.2 Hz), 99.5, 56.7, 42.8. ¹⁹F NMR (377 MHz, CDCl₃) δ -122.2. HRMS (ESI) calcd. for C₁₇H₁₈FN₂O (M + H⁺) 285.1403. Found 285.1396.

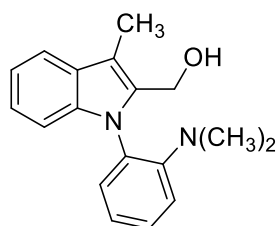
(±)-(1-(2-(Dimethylamino)phenyl)-5-fluoro-1*H*-indol-2-yl)methanol (18e). ¹H

NMR (400 MHz, CDCl₃) δ 7.46 (ddd, *J* = 8.7, 6.2, 2.7 Hz, 1H), 7.29 (dd, *J* = 9.4, 2.5 Hz, 1H), 7.26 – 7.14 (m, 3H), 6.97 (dd, *J* = 8.9, 4.5 Hz, 1H), 6.90 (td, *J* = 9.0, 2.5 Hz, 1H), 6.68 (s, 1H), 4.52 (d, *J* = 12.7 Hz, 1H), 4.25 (d, *J* = 12.7 Hz, 1H), 2.42 (s, 6H). ¹³C NMR (100 MHz, CDCl₃) δ 158.3 (d, *J* = 235.1 Hz), 149.6, 142.3, 134.9, 131.2, 129.8, 129.7, 128.5 (d, *J* = 10.2 Hz), 123.6, 119.4, 111.1 (d, *J* = 9.7 Hz), 110.8 (d, *J* = 26.2 Hz), 105.6 (d, *J* = 23.6 Hz), 103.5 (d, *J* = 4.7 Hz), 56.8, 42.8. ¹⁹F NMR (377 MHz, CDCl₃) δ -124.1. HRMS (ESI) calcd. for C₁₇H₁₈FN₂O (M + H⁺) 285.1403. Found 285.1396.

(±)-(1-(2-(Dimethylamino)phenyl)-6-fluoro-1*H*-indol-2-yl)methanol (18f). ¹H

NMR (400 MHz, CDCl₃) δ 7.55 (dd, *J* = 8.6, 5.3 Hz, 1H), 7.49 – 7.43 (m, 1H), 7.25 – 7.16 (m, 3H), 6.91 (t, *J* = 9.1 Hz, 1H), 6.73 (d, *J* = 9.8 Hz, 1H), 6.70 (s, 1H), 5.29 (s, 1H), 4.50 (d, *J* = 12.7 Hz, 1H), 4.25 (d, *J* = 12.8 Hz, 1H), 2.44 (s, 6H). ¹³C NMR (100 MHz, CDCl₃) δ 160.3 (d, *J* = 238.4 Hz), 149.6, 141.3 (d, *J* = 3.7 Hz), 138.4 (d, *J* = 11.8 Hz), 131.0, 129.8, 129.7, 124.7, 123.7, 121.6 (d, *J* = 9.9 Hz), 119.4, 109.1 (d, *J* = 24.3 Hz), 103.6, 96.9 (d, *J* = 26.5 Hz), 56.7, 42.8. ¹⁹F NMR (377 MHz, CDCl₃) δ -119.73. HRMS (ESI) calcd. for C₁₇H₁₈FN₂O (M + H⁺) 285.1403. Found 285.1397.

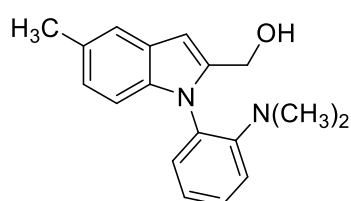
(±)-(1-(2-(Dimethylamino)phenyl)-3-methyl-1*H*-indol-2-yl)methanol (18g). ¹H



NMR (400 MHz, CDCl₃) δ 7.69 – 7.54 (m, 1H), 7.51 – 7.39 (m, 1H), 7.24 (dd, *J* = 8.4, 1.4 Hz, 2H), 7.20 (dd, *J* = 4.9, 1.6 Hz, 1H), 7.19 – 7.15 (m, 2H), 7.08 – 7.01 (m, 1H), 5.36 (s, 1H), 4.62 (d, *J* = 12.9 Hz, 1H), 4.17 (d, *J* = 12.9 Hz, 1H), 2.47 (s, 3H), 2.42 (s, 6H). ¹³C NMR (100 MHz, CDCl₃) δ 149.8, 137.4,

136.7, 131.4, 130.5, 129.3, 129.0, 123.6, 122.6, 119.7, 119.2, 119.1, 111.1, 110.1, 54.4, 42.9, 8.8. HRMS (ESI) calcd. for C₁₈H₂₁N₂O (*M* + *H*⁺) 281.1654. Found 281.1648.

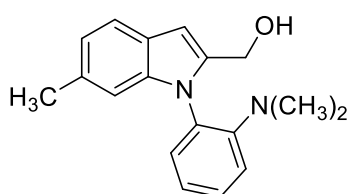
(±)-(1-(2-(Dimethylamino)phenyl)-5-methyl-1*H*-indol-2-yl)methanol (18h). ¹H



NMR (400 MHz, CDCl₃) δ 7.43 (t, *J* = 8.7 Hz, 2H), 7.30 – 7.11 (m, 3H), 7.05 – 6.92 (m, 2H), 6.65 (s, 1H), 4.52 (d, *J* = 12.7 Hz, 1H), 4.25 (d, *J* = 12.7 Hz, 1H), 2.46 (s, 3H), 2.43 (s, 6H). ¹³C NMR (100 MHz, CDCl₃) δ 149.6, 140.8, 136.8, 131.3, 130.2, 129.6, 129.4, 128.6, 124.1, 123.5,

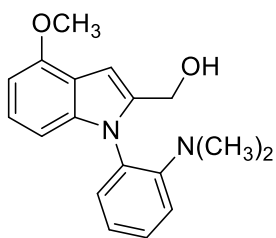
120.5, 119.2, 110.1, 103.2, 56.9, 42.8, 21.4. HRMS (ESI) calcd. for C₁₈H₂₁N₂O (*M* + *H*⁺) 281.1648. Found 281.1648.

(±)-(1-(2-(Dimethylamino)phenyl)-6-methyl-1*H*-indol-2-yl)methanol (18i). ¹H

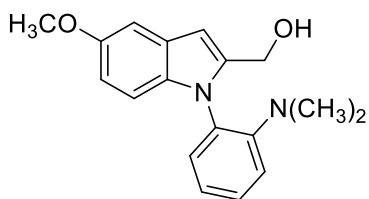


NMR (400 MHz, CDCl₃) δ 7.53 (d, *J* = 8.0 Hz, 1H), 7.46 (t, *J* = 8.7, 1H), 7.26 – 7.17 (m, 3H), 6.99 (dd, *J* = 8.0, 1.5 Hz, 1H), 6.84 (s, 1H), 6.68 (s, 1H), 5.45 (br s, 1H), 4.51 (d, *J* = 12.7 Hz, 1H), 4.24 (d, *J* = 12.7 Hz, 1H), 2.44 (s, 3H), 2.40 (s, 6H). ¹³C NMR (100 MHz, CDCl₃) δ 149.7, 140.1,

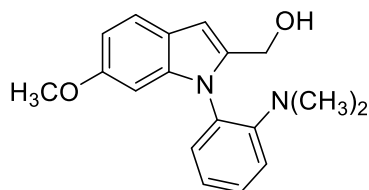
138.8, 132.4, 131.4, 130.2, 129.4, 126.1, 123.5, 122.2, 120.5, 119.2, 110.3, 103.5, 56.8, 42.8, 21.8. HRMS (ESI) calcd. for C₁₈H₂₁N₂O (*M* + *H*⁺) 281.1648. Found 281.1646.

(±)-(1-(2-(Dimethylamino)phenyl)-4-methoxy-1*H*-indol-2-yl)methanol (18j)

^1H NMR (400 MHz, CDCl_3) δ 7.45 (t, J = 7.7 Hz, 1H), 7.25 – 7.14 (m, 3H), 7.08 (t, J = 8.0 Hz, 1H), 6.83 (s, 1H), 6.67 (d, J = 8.2 Hz, 1H), 6.57 (d, J = 7.8 Hz, 1H), 5.40 (s, 1H), 4.52 (d, J = 12.7 Hz, 1H), 4.25 (d, J = 12.7 Hz, 1H), 3.99 (s, 3H), 2.43 (s, 6H). ^{13}C NMR (100 MHz, CDCl_3) δ 153.4, 149.6, 139.7, 139.3, 131.4, 130.2, 129.6, 123.4, 123.3, 119.2, 118.8, 103.9, 100.9, 100.3, 56.8, 55.4, 42.8. HRMS (ESI) calcd. for $\text{C}_{18}\text{H}_{21}\text{N}_2\text{O}_2$ ($\text{M} + \text{H}^+$) 297.1603. Found 297.1592.

(±)-(1-(2-(Dimethylamino)phenyl)-5-methoxy-1*H*-indol-2-yl)methanol (18k).

^1H NMR (400 MHz, CDCl_3) δ 7.46 – 7.42 (m, 1H), 7.25 – 7.14 (m, 3H), 7.11 (d, J = 2.4 Hz, 1H), 6.95 (d, J = 8.8 Hz, 1H), 6.82 (dd, J = 8.9, 2.5 Hz, 1H), 6.65 (s, 1H), 5.40 (s, 1H), 4.51 (d, J = 12.7 Hz, 1H), 4.24 (d, J = 12.7 Hz, 1H), 3.86 (s, 3H), 2.43 (s, 6H). ^{13}C NMR (100 MHz, CDCl_3) δ 154.7, 149.6, 141.2, 133.6, 131.3, 130.2, 129.5, 128.6, 123.5, 119.2, 112.7, 111.2, 103.3, 102.4, 56.9, 55.8, 42.8. HRMS (ESI) calcd. for $\text{C}_{18}\text{H}_{21}\text{N}_2\text{O}_2$ ($\text{M} + \text{H}^+$) 297.1603. Found 297.1595.

(±)-(1-(2-(Dimethylamino)phenyl)-6-methoxy-1*H*-indol-2-yl)methanol (18l).

^1H NMR (400 MHz, CDCl_3) δ 7.57 (d, J = 8.7 Hz, 1H), 7.39 (t, J = 8.6 Hz, 1H), 7.29 – 7.24 (m, 1H), 7.12 – 7.02 (m, 2H), 7.01 (d, J = 3.3 Hz, 1H), 6.91 (d, J = 8.7 Hz, 1H), 6.61 (d, J = 3.3 Hz, 1H), 4.57 (d, J = 12.1 Hz, 1H), 4.28 (d, J = 12.1 Hz, 1H), 3.92 (s, 3H), 2.44 (s, 6H). ^{13}C NMR (100 MHz, CDCl_3) δ 154.8, 148.7, 135.1, 132.6, 130.6, 130.3, 129.3, 124.6, 121.7, 120.9, 118.2, 113.3, 106.2, 103.1, 56.9, 54.7, 42.4. HRMS (ESI) calcd. for $\text{C}_{18}\text{H}_{21}\text{N}_2\text{O}_2$ ($\text{M} + \text{H}^+$) 297.1603. Found 297.1596.

III.6.4. General procedure for the enantioselective bioreduction of heterobiaryl aldehydes 17a-l catalyzed by commercially available KREDs.

Procedure A: Codexis KRED (P1-A04, P2-H07, P1-H12 P3-B03, P3-G09 or P2-G03, 10 mg) was added to a 2.0 mL Eppendorf tube with 875 μL of NaPi buffer 100

mM pH 7.0 containing NADP⁺ (1.0 g/L), and the tube was shaken until KRED was dissolved. To this mixture, a solution of heterobiaryl aldehyde **17a-I** (0.01 mmol) in IPA (100 μ L) and the corresponding organic cosolvent (25 μ L) was added. Then, the Eppendorf tube was closed and kept under orbital shaking at 220 rpm at 30 °C for 24 hours. After this time, the product was extracted with ethyl acetate (3 \times 0.5 mL), the combined organic layers were dried over anhydrous Na₂SO₄ and filtered. The solution was concentrated, measuring then the reaction conversion and the enantiomeric excess of alcohol (*S*)-**18a-I** by GC/MS and HPLC, respectively.

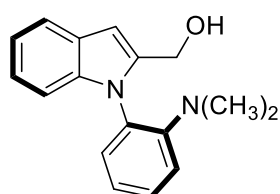
Procedure B: Unless otherwise stated, a solution of the starting aldehyde **17a-I** (0.01 mmol) in 25 μ L DMSO and 975 μ L NaPi buffer 100 mM pH 7.0 with NADP⁺ (1.0 g/L), GHD Codexis® CDX-901 (1.0 g/L) and glucose (3.8 g/L) was added to a 2.0 mL Eppendorf tube containing KRED 101 or KRED 119 (10 mg). The reaction was shaken at 220 rpm at 30 °C for 24 h. After this time, the product was extracted with ethyl acetate (3 \times 0.5 mL), the combined organic layers were dried over anhydrous Na₂SO₄ and filtered. The solution was concentrated, measuring the conversion and the enantiomeric excess of alcohol (*R*)-**18a-I** by GC/MS and HPLC, respectively.

III.6.5. General procedure for the multimilligram bioreduction of heterobiaryl aldehydes **17a-I** catalyzed by KREDs.

Procedure A: Codexis KRED P2-H07, P3-B03, P3-G09 or P2-G03 (20 mg) was added to a glass vial with 1.75 μ L of NaPi buffer 100 mM pH 7.0 containing NADP⁺ (1.0 g/L), and the tube was shaken until KRED was dissolved. To this mixture, a solution of heterobiaryl aldehyde **17a-I** (10.6-13.4 mg, 0.04 mmol) in IPA (200 μ L) and the corresponding organic cosolvent DMSO or THF (50 μ L) was added. Then, the vial was closed and kept under orbital shaking at 220 rpm at 30 °C for 48-60 hours. After this time, the product was extracted with ethyl acetate (3 \times 1.0 mL), the combined organic layers were dried over anhydrous Na₂SO₄ and filtered. The solution was concentrated, measuring then the reaction conversion and the enantiomeric excess of alcohol (*S*)-**18a-f** and (*S*)-**18h-I** by GC/MS and HPLC, respectively.

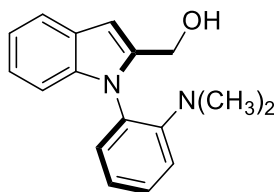
Procedure B: Unless otherwise stated, a solution of the starting aldehyde **17a** (10.6 mg, 0.04 mmol) or **17g** (11.2, 0.04 mmol) in 50 μ L DMSO and 1.95 mL NaPi buffer 100 mM pH 7.0 with NADP⁺ (1.0 g/L), GDH Codexis® CDX-901 (1.0 g/L) and glucose (3.8 g/L) was added to a glass vial tube containing KRED 119 (20 mg). The reaction was shaken at 220 rpm at 30 °C for 48 h for **17a** and 72 h for **17g**. After this time, the product was extracted with ethyl acetate (3 \times 1.0 mL), the combined organic layers were dried over anhydrous Na₂SO₄ and filtered. The solution was concentrated, measuring the conversion and the enantiomeric excess of alcohol (*R*)-**18a** or (*R*)-**18g** by GC/MS and HPLC, respectively.

(S)-**(1-(2-(Dimethylamino)phenyl)-1*H*-indol-2-yl)methanol (18a)**. Following the



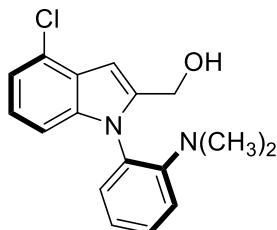
general **procedure A**, (*S*)-**18a** was obtained as a white solid (9.8 mg, 92% yield). $[\alpha]_{\text{D}}^{20} +6.6$ (*c* 1.12, CHCl₃) for 96% *ee*. HPLC (ID column, 95:5 n-Hex/*i*-PrOH, 30 °C, 0.8 mL/min): t_{R} 17.30 min (*S*) and 20.01 min (*R*).

(R)-**(1-(2-(Dimethylamino)phenyl)-1*H*-indol-2-yl)methanol (18a)**. Following



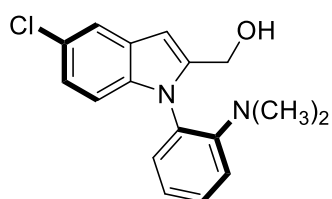
the general **procedure B**, (*R*)-**18a** was obtained as a white solid (9.4 mg, 88% yield). $[\alpha]_{\text{D}}^{20} -2.9$ (*c* 1.12, CHCl₃) for 92% *ee*. HPLC (ID column, 95:5 n-Hex/*i*-PrOH, 30 °C, 0.8 mL/min): t_{R} 17.23 min (*S*) and 19.80 min (*R*).

(S)-**(4-Chloro-1-(2-(dimethylamino)phenyl)-1*H*-indol-2-yl)methanol (18b)**.



Following the general **procedure A**, (*S*)-**18b** was obtained as a yellow oil (9.8 mg, 82% yield). $[\alpha]_{\text{D}}^{20} +11.6$ (*c* 1.23, CHCl₃) for 88% *ee*. HPLC (ID column, 95:5 n-Hex/*i*-PrOH, 30 °C, 0.8 mL/min): t_{R} 15.33 min (*S*) and 19.66 min (*R*).

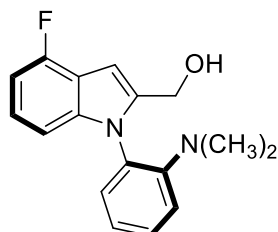
(*S*)-(5-Chloro-1-(2-(dimethylamino)phenyl)-1*H*-indol-2-yl)methanol (18c).



16.91 min (*S*).

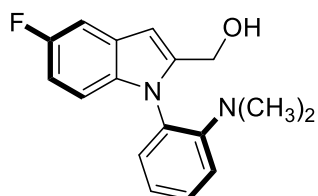
Following the general **procedure A**, (*S*)- **18c** was obtained as a yellow oil (7.2 mg, 60% yield). $[\alpha]_D^{20} -6.2$ (c 0.50, CHCl_3) for 97% *ee*. HPLC (IA column, 95:5 n-Hex/*i*-PrOH, 30 °C, 1.0 mL/min): t_R 15.62 min (*R*) and

(*S*)-(1-(2-(Dimethylamino)phenyl)-4-fluoro-1*H*-indol-2-yl)methanol (18d).



Following the general **procedure A**, (*S*)- **18d** was obtained as a yellow oil (7.9 mg, 70% yield). $[\alpha]_D^{20} +4.1$ (c 0.63, CHCl_3) for 91% *ee*. HPLC (ID column, 95:5 n-Hex/*i*-PrOH, 30 °C, 0.8 mL/min): t_R 15.61 min (*S*) and 17.93 min (*R*).

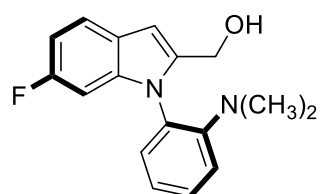
(*S*)-(1-(2-(Dimethylamino)phenyl)-5-fluoro-1*H*-indol-2-yl)methanol (18e).



(*R*).

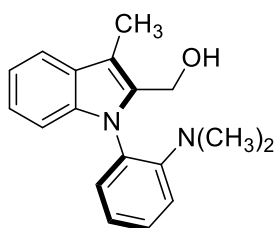
Following the general **procedure A**, (*S*)- **18e** was obtained as a yellow oil (9.0 mg, 79% yield). $[\alpha]_D^{20} +3.6$ (c 1.38, CHCl_3) for 99% *ee*. HPLC (OD column, 98:2 n-Hex/*i*-PrOH, 30 °C, 1.0 mL/min): t_R 17.03 min (*S*) and 18.22 min

(*S*)-(1-(2-(Dimethylamino)phenyl)-6-fluoro-1*H*-indol-2-yl)methanol (18f).

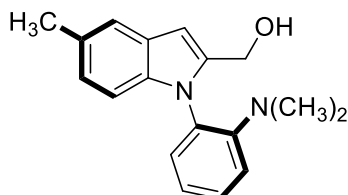


16.89 min (*R*).

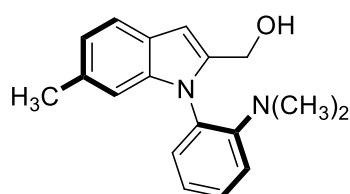
Following the general **procedure A**, (*S*)- **18f** was obtained as a yellow oil (9.4 mg, 83% yield). $[\alpha]_D^{20} +16.0$ (c 0.88, CHCl_3) for 97% *ee*. HPLC (ID column, 95:5 n-Hex/*i*-PrOH, 30 °C, 0.8 mL/min): t_R 13.69 min (*S*) and

(*R*)-1-(2-(Dimethylamino)phenyl)-3-methyl-1*H*-indol-2-yl)methanol (18g).

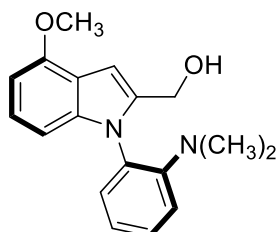
Following the general **procedure B**, (*R*)- **18g** was obtained as a yellow oil (5.7 mg, 51% yield). $[\alpha]_{\text{D}}^{20}$ -47.18 (c 1.12, CHCl_3) for 89% *ee*. HPLC (OD column, 98:2 n-Hex/*i*-PrOH, 30 °C, 1.0 mL/min): t_{R} 10.45 min (*S*) and 11.78 min (*R*).

(*S*)-1-(2-(Dimethylamino)phenyl)-5-methyl-1*H*-indol-2-yl)methanol (18h).

Following the general **procedure A**, (*S*)- **18h** was obtained as a yellow oil (8.9 mg, 79% yield). $[\alpha]_{\text{D}}^{20}$ -6.87 (c 0.50, CHCl_3) for 98% *ee*. HPLC (OD column, 98:2 n-Hex/*i*-PrOH, 30 °C, 1.0 mL/min): t_{R} 13.98 min (*S*) and 16.14 min (*R*).

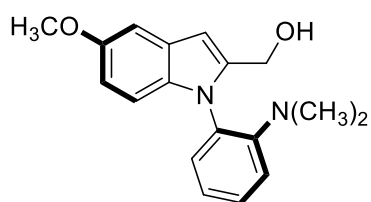
(*S*)-1-(2-(Dimethylamino)phenyl)-6-methyl-1*H*-indol-2-yl)methanol (18i).

Following the general **procedure A**, (*S*)- **18i** was obtained as a yellow oil (9.0 mg, 80% yield). $[\alpha]_{\text{D}}^{20}$ -14.91 (c 1.12, CHCl_3) for 99% *ee*. HPLC (ID column, 95:5 n-Hex/*i*-PrOH, 30 °C, 0.8 mL/min): t_{R} 13.38 min (*S*) and 16.31 min (*R*).

(*S*)-1-(2-(Dimethylamino)phenyl)-4-methoxy-1*H*-indol-2-yl)methanol (18j).

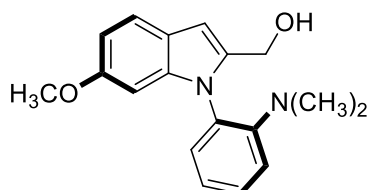
Following the general **procedure A**, (*S*)- **18j** was obtained as a yellow oil (8.7 mg, 73% yield). $[\alpha]_{\text{D}}^{20}$ $+11.8$ (c 0.50, CHCl_3) for 92% *ee*. HPLC (ID column, 95:5 n-Hex/*i*-PrOH, 30 °C, 0.8 mL/min): t_{R} 35.23 min (*R*) and 38.01 min (*S*).

(*S*)-(1-(2-(Dimethylamino)phenyl)-5-methoxy-1*H*-indol-2-yl)methanol (18k).



Following the general **procedure A**, (*S*)- **18k** was obtained as a yellow oil (10.6 mg, 89% yield). $[\alpha]_{\text{D}}^{20} +5.7$ (c 1.71, CHCl_3) for 90% *ee*. HPLC (OD column, 98:2 n-Hex/*i*-PrOH, 30 °C, 1.0 mL/min): t_{R} 21.52 min (*S*) and 24.08 min (*R*).

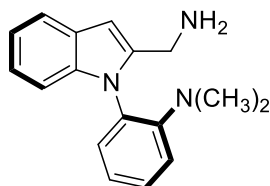
(*S*)-(1-(2-(Dimethylamino)phenyl)-6-methoxy-1*H*-indol-2-yl)methanol (18l).



Following the general **procedure A**, (*S*)- **18l** was obtained as a yellow oil (10.4 mg, 88% yield). $[\alpha]_{\text{D}}^{20} -13.6$ (c 0.15, CHCl_3) for 94% *ee*. HPLC (IA column, 95:5 n-Hex/*i*-PrOH, 30 °C, 1.0 mL/min): t_{R} 10.42 min (*S*) and 11.41 min (*R*).

III.6.6. Derivatization reactions of **18a**.

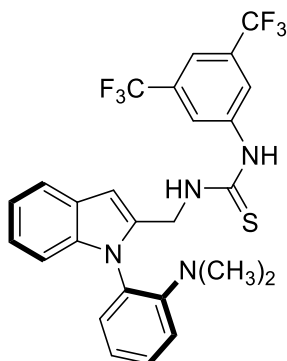
Synthesis of diamine (*S*)-**19a**.



Following a described procedure,¹²⁸ to a solution of (*S*)-**18a** (11 mg, 0.04 mmol) and DPPA (14 μL , 0.06 mmol) in toluene (0.21 mL) at 0° C, was added DBU (11 μL , 0.07 mmol) via syringe. The mixture was stirred at rt for 2 h. Ethyl acetate (0.2 mL) was added, and the mixture was washed with water, brine, dried over anhydrous Na_2SO_4 , filtrated and concentrated in vacuo. The reaction crude was directly used for the next step without further purification. The reaction crude was dissolved in THF (100 μL), and PPh_3 (18 mg, 0.07 mmol) was added portionwise. After 5 min, H_2O (8 μL , 0.44 mmol) was added and the mixture was stirred at rt for 12 h. Then, the reaction mixture was concentrated in vacuo. Purification by flash chromatography (9:1 EtOAc/MeOH) afforded (*S*)-**19a** (5.2 mg, 90%) as a light-yellow oil. ^1H NMR (400

MHz, CDCl₃) δ 7.64 – 7.59 (m, 1H), 7.39 (dd, *J* = 7.3, 1.7 Hz, 1H), 7.21 (dd, *J* = 7.7, 1.7 Hz, 1H), 7.16 – 7.08 (m, 4H), 7.04 (td, *J* = 7.5, 1.4 Hz, 1H), 6.58 (s, 1H), 3.79 (s, 2H), 2.40 (s, 6H). ¹³C NMR (100 MHz, CDCl₃) δ 150.2, 143.3, 138.1, 130.8, 129.3, 128.4, 128.3, 121.7, 121.3, 120.1, 120.1, 118.6, 110.4, 100.3, 42.2, 38.7. HRMS (ESI) calcd. for C₁₇H₂₀N₃ (M + H⁺) 266.1657. Found 266.1650. [α]_D²⁰ –7.94 (c 0.36, CHCl₃).

Synthesis of thiourea (S)-20a.



Following a described procedure,¹²⁸ amine (S)-**19a** (5.2 mg, 0.02 mmol) was added to a solution of 3,5-bis(trifluoromethyl)phenyl isothiocyanate (4 μL, 0.02 mmol) in CH₂Cl₂ (100 μL). The resulting mixture was stirred for 3 h at rt. The solvent was removed under reduced pressure and the product was purified by flash column chromatography (4:1 n-hexane/EtOAc) to afford (S)-**20a** (9.6 mg, 90%) as a light-yellow oil. ¹H NMR (400 MHz, CDCl₃) δ 8.00 (s, 1H), 7.70 – 7.58 (m, 3H), 7.54 – 7.34 (m, 1H), 7.31 (s, 1H), 7.17 (qt, *J* = 6.9, 3.4 Hz, 2H), 7.13 – 7.02 (m, 3H), 6.76 (s, 1H), 4.98 (s, 1H), 4.44 (dd, *J* = 15.3, 3.6 Hz, 1H), 2.31 – 2.05 (m, 6H). ¹³C NMR (100 MHz, CDCl₃) δ 180.4, 149.9, 139.4, 138.3, 135.3, 132.9 (q, *J* = 33.5 Hz), 130.8, 129.8, 128.6, 127.9, 123.6, 122.7 (q, *J* = 273.0 Hz), 120.7, 120.7, 119.1, 110.3, 103.5, 42.6, 42.2. ¹⁹F NMR (377 MHz, CDCl₃) δ -63.03. HRMS (ESI) calcd. for C₂₆H₂₃F₆N₄S (M + H⁺) 537.1548. Found 537.1539. [α]_D²⁰ -3.04 (c 0.37, CHCl₃) for 95% *ee*. HPLC (IA column, 95:5 n-Hex/i-PrOH, 30 °C, 1.0 mL/min): t_R 35.23 min (*R*) and 38.01 min (*S*).

CHAPTER IV

*Asymmetric synthesis of
dibenzo[b,d]azepines by Cu-catalyzed
reductive or borylative cyclization.*

Part of this chapter is published in:

P. Rodríguez-Salamanca, R. Martín-de la Calle, V. Rodríguez, P.
Merino, R. Fernández, J. M. Lassaletta, V. Hornillos.

Chem. Sci. **2021**,*12*, 15291-15297.

IV. Asymmetric synthesis of dibenzo[*b,d*]azepines by Cu-catalyzed reductive or borylative cyclization.

IV.1. Introduction.

IV.1.1. Synthesis of dibenzoazepine derivatives. State-of-the-art.

Bridged biaryls are a particular class of atropoisomers in which the biaryl unit is incorporated into a cyclic system, with the *ortho*, *ortho'* substituents being replaced by a bridge. Over the last few years, this class of compounds has attracted increasing attention due to their particular structures and promising pharmacological profiles, and for their use as chiral ligands, organocatalyst and in material science.¹⁸⁸ Some relevant examples are shown in **figure 17**.

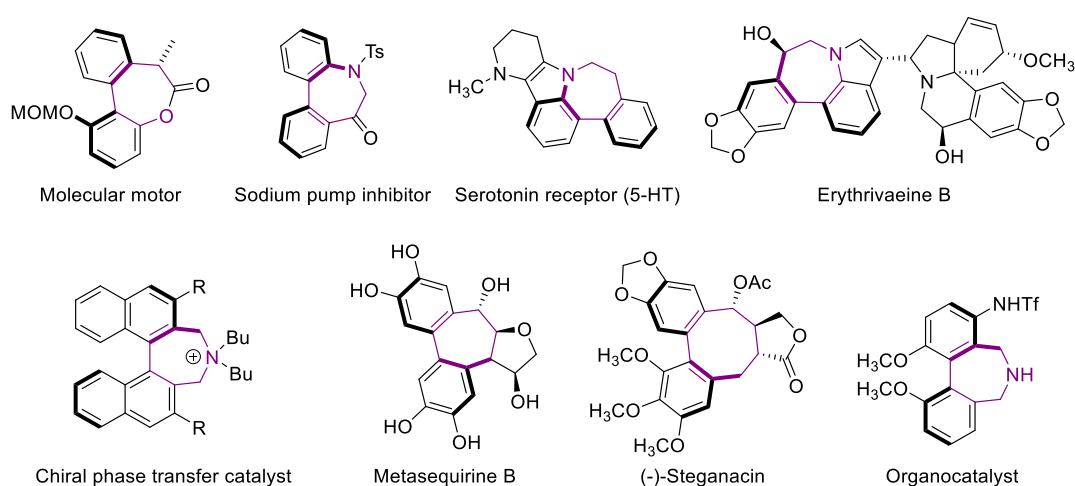


Figure 17: examples of bridged biaryls compounds.

In these systems, the configurational stability is directly connected with the ring size. Thus, in systems presenting a five-membered ring, rotation around the

¹⁸⁸ a) G. Bringmann, T. Gulder, T. A. M. Gulder and M. Breuning, *Chem. Rev.* **2011**, *111*, 563–639; b) J. E. Smyth, N. M. Butler and P. A. Keller, *Nat. Prod. Rep.* **2015**, *32*, 1562–1583; c) J. Wencel-Delord, A. Panossian, F. R. Leroux and F. Colobert, *Chem. Soc. Rev.* **2015**, *44*, 3418–3430; d) Y.-B. Wang and B. Tan, *Acc. Chem. Res.* **2018**, *51*, 534–547; e) J. K. Cheng, S.-H. Xiang, S. Li, L. Ye and B. Tan, *Chem. Rev.* **2021**, *121*, 4805–4902; f) J. M. Lassaletta, *Atropisomerism and Axial Chirality*, *World Scientific*, New Jersey, **2019**.

stereogenic axis is usually not hindered at room temperature. On the other hand, six-membered ring biaryls are still labile, but can be turned configurationally stable by introducing a bulky R groups at the *ortho* position.¹⁸⁹ Seven-membered bridged biaryls present higher configurational stability and can be resolved as atropisomers at room temperature. The configurational stability in these compounds can also be determined by introducing a stereogenic element in the bridge, originating a thermodynamic atropodiastereomeric equilibrium, which is shifted towards the most stable isomer (**figure 18**).²²

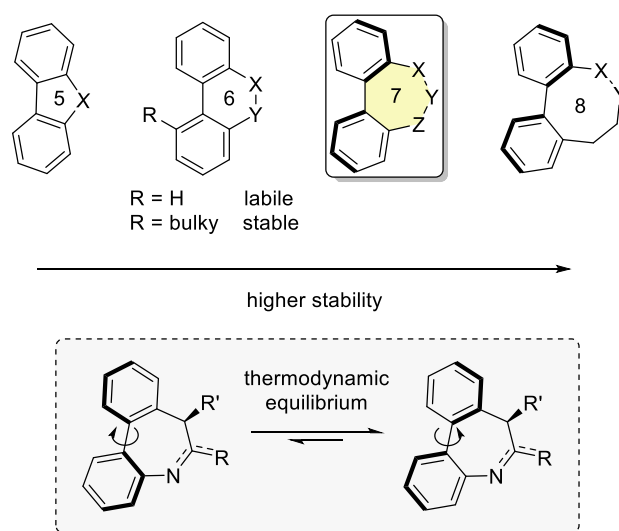


Figure 18: comparison of the configurational stability of bridged biaryls.

The most distinctive class of 7-membered bridged biaryls are dibenzoazepines. However, the asymmetric synthesis of these compounds has mainly relied on the use of chiral auxiliaries or starting materials from the chiral pool, generally requiring synthetic procedures that involves several steps.¹⁹⁰

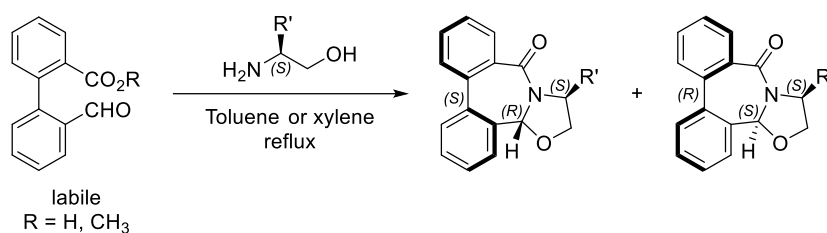
In 2007, Wallace *et al.*¹⁹¹ reported a method for the synthesis of biaryl-fused lactams, with central and axial chirality, using configurationally labile biaryl

¹⁸⁹ G. Bringmann, H. Busse, U. Dauer, S. Güssregen, M. Stahl, *Tetrahedron* **1995**, *51*, 3149–3158.

¹⁹⁰ L. A. Saudan, G. Bernardinelli, E. P. Kündig, *Synlett* **2000**, *4*, 483–486.

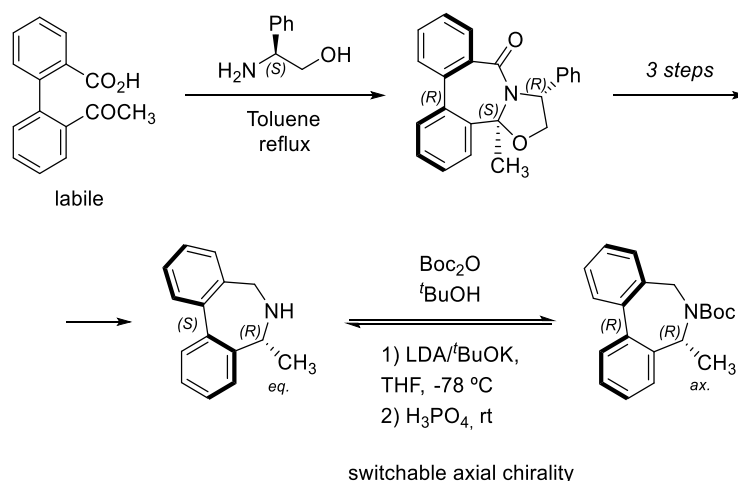
¹⁹¹ D. J. Edwards, D. House, H.M. Sheldrake, S.J. Stone, T.W. Wallace, *Org. Biomol. Chem.* **2007**, *5*, 2658–2669.

substrates. Interestingly, a chirality relay effect was observed by which the configuration of the axis is controlled by the near C4 stereogenic center (**scheme 128**).



Scheme 128: synthesis of biaryl-fused lactams reported by Wallace.

A few years later the same research group expanded the strategy to the synthesis of dibenz[*c,e*]azepine derivatives.¹⁹² Interestingly, it was found that the configuration of the stereogenic axis could be inverted when the secondary amine was *N*-Boc protected. In this case, the 5-methyl substituent adopt a pseudo-axial orientation, which inverts the configuration of the axis (**scheme 129**).

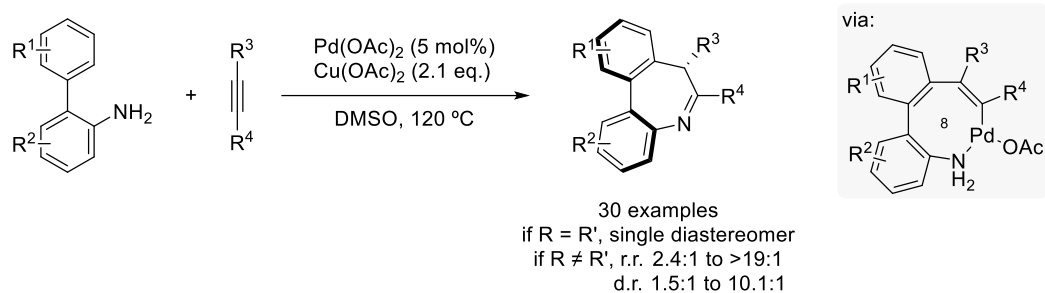


Scheme 129: synthesis of dibenz[*c,e*]azepine derivatives reported by Wallace.

On the other hand, imine containing dibenzo[*b,d*]azepines were synthesized by Luan and co-workers through a palladium(II)-catalyzed [5+2] annulation of *o*-

¹⁹² S. L. Pira, T. W. Wallace, J. P. Graham, *Org. Lett.* **2009**, *11*, 1663–1666.

arylanilines and alkynes.¹⁹³ Notably, for symmetrical alkynes ($R = R'$), a single diastereomer was observed while the use of unsymmetrical ones ($R \neq R'$) resulted into a mixture of two separable regioisomers. Some control experiments indicated that the C-H activation was the rate-determining step and that the formation of the eight-membered palladacycle determined the regioselectivity of the reaction (**scheme 130**).

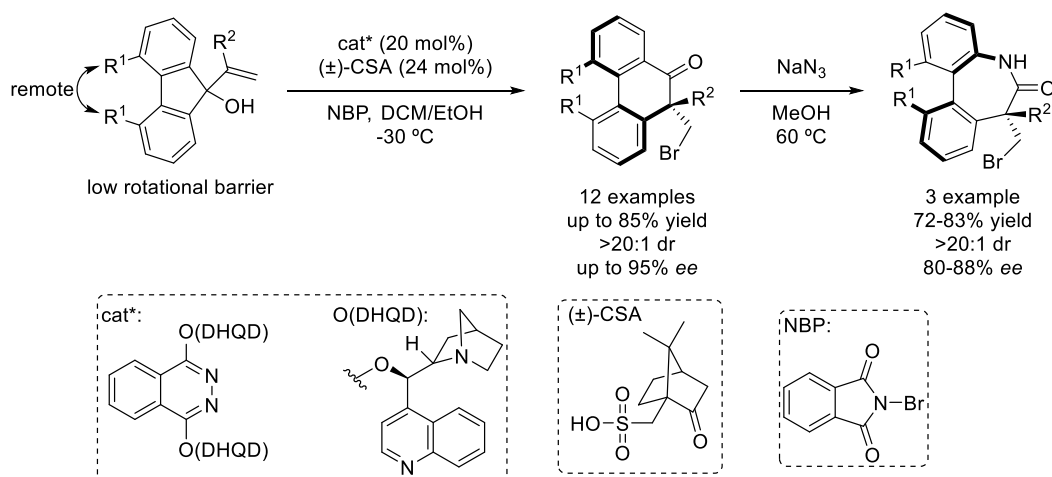


Scheme 130: synthesis of imine-containing dibenzo[*b,d*]azepines through a [5+2] annulation.

In 2007, Yeung and co-workers reported the synthesis of axially chiral biaryl structures through an organocatalytic enantioselective semipinacol rearrangement *via* dynamic kinetic resolution.¹⁹⁴ Their strategy was based on the use of a 4,5-dimethylfluorene system, where the two methyl units are farther than the *ortho*-substituents in a typical biaryl system, resulting in a low racemization barrier (**scheme 131**). Under the optimal conditions, a wide variety of compounds could be prepared in good yield and enantioselectivity, and excellent diastereomeric ratio, except for *ortho*-phenyl substituted products. Moreover, a second ring-expansion could be performed through an intramolecular Schmidt reaction, giving seven-membered dibenzolactams. Interestingly, it was found that the axial chirality was inverted after this second ring-expansion.

¹⁹³ Z. Zuo, J. Liu, J. Nan, L. Fan, W. Sun, Y. Wang, X. Luan, *Angew. Chem. Int. Ed.* **2015**, *54*, 15385–15389.

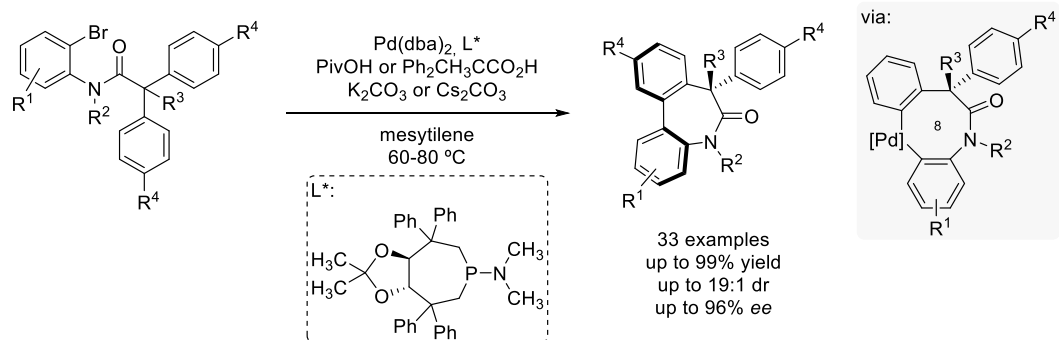
¹⁹⁴ Y. Liu, Y.-L. S. Tse, F. Y. Kwong, Y.-Y. Yeung, *ACS Catal.* **2017**, *7*, 7, 4435–4440.



Scheme 131: synthesis of bridged biaryls through organocatalytic enantioselective DKR-semipinacol rearrangement.

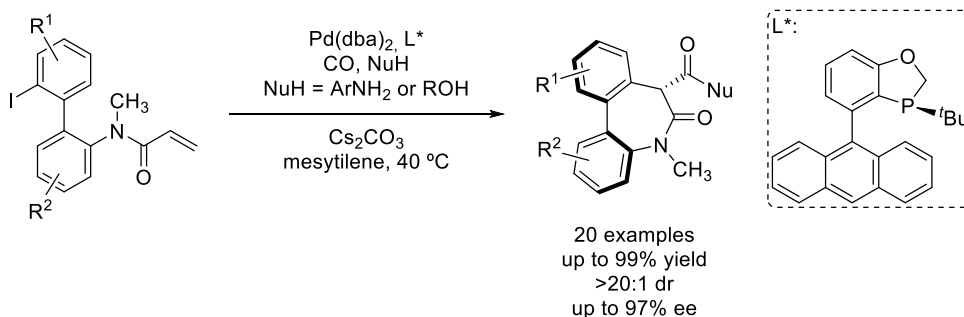
The group of Cramer has also reported the synthesis of dibenzoazepine derivatives through intramolecular C-H arylation using Pd(0) as catalyst.¹⁹⁵ The main challenge of this method consists of the difficult formation of the eight-membered palladacycle intermediate. Authors based their strategy on the cooperative effect between a chiral TADDOL phosphoramidite ligand and a bulky carboxylate, with the enantiotopic concerted metalation deprotonation being the enantiodiscriminating step (**scheme 132**). Under the optimal conditions, a wide variety of functional groups were tolerated in the aryl rings, although for R² = H, the reaction failed to give the desired product. Moreover, the bulkiness of the *N*-alkyl group was crucial to obtain high levels of enantioselectivity.

¹⁹⁵ a) T. Saget, N. Cramer, *Angew. Chem. Int. Ed.* **2013**, *52*, 7865-7868. b) C.G. Newton, E. Braconi, J. Kuziola, M. D. Wodrich, N. Cramer, *Angew. Chem. Int. Ed.* **2018**, *57*, 11040-11044.



Scheme 132: axially chiral dibenzazepinones by a Pd-catalyzed atropenantioselective C-H arylation.

Very recently, Luo and Zhu described the synthesis of dibenzo[*b,d*]azepin-6-ones containing a thermodynamically controlled stereogenic axis *via* cyclocarbopalladation-initiated carbonylation cascade reactions, using alcohols and anilines as nucleophiles (**scheme 133**).¹⁹⁶ A iodo-substituted acrylamide containing a rigid biaryl backbone and a flexible and less hindered terminal alkene was designed to overcome the challenges associated with this transformation, such as a competing carbonylation before insertion of the alkene and a β -H elimination of σ -alkylpalladium species. The reaction worked with excellent enantio- and diastereocontrol for a wide variety of substrates bearing electron donating and withdrawing groups.

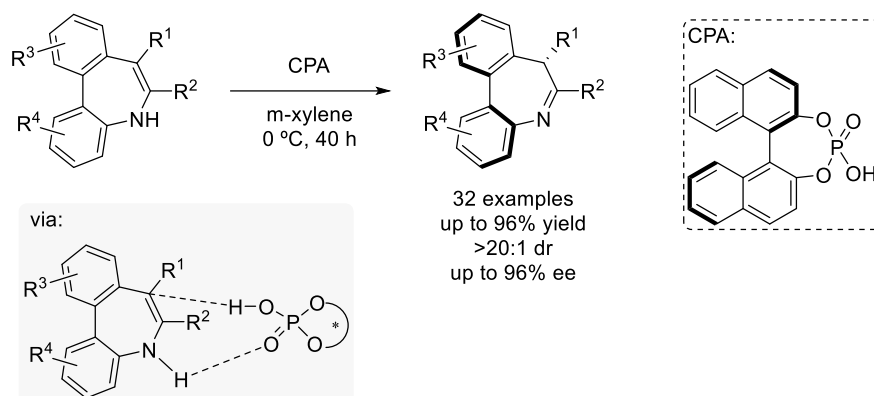


Scheme 133: Pd-catalyzed enantioselective synthesis of dibenzo[*b,d*]azepin-6-one derivatives.

To the best of our knowledge, the tautomerization of metastable enamines assisted by a chiral phosphoric acid (CPA) catalyst is the only catalytic method for the

¹⁹⁶ H. Hu, Y. Peng, T. Yu, S. Cheng, S. Luo, Q. Zhu, *Org. Lett.* **2021**, *23*, 3636–3640.

synthesis of chiral dibenzo[*b,d*]azepines with high yields and enantioselectivities.¹⁹⁷ Mechanistically, the authors proposed that the chiral phosphoric acid activated first the proton from the amino group by the basic oxygen, and then the OH deliver its proton to the enamine group in an enantioselective manner, *via* an eight-membered cyclic transition state (**scheme 135**).



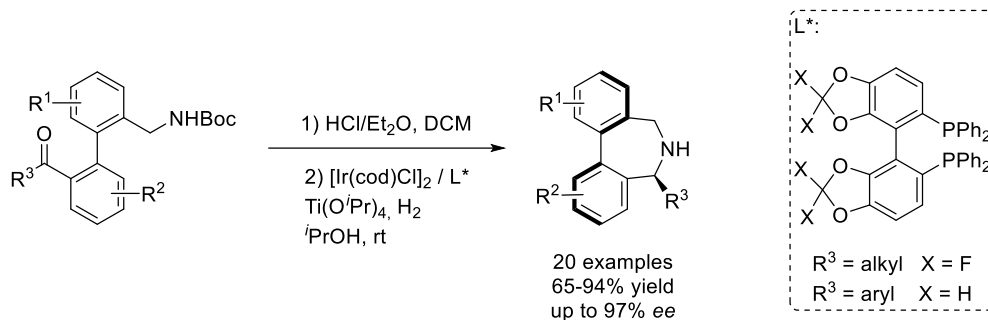
Scheme 134: organocatalytic enantioselective tautomerization of metastable enamines.

More recently, the group of Yin and Zhang reported two methods to obtain chiral dibenz[*c,e*]azepines through an intramolecular asymmetric reductive amination (ARA). They first prepared aryl-bridged aminoketones^{198a} via one pot *N*-Boc deprotection followed by Ir-catalyzed ARA sequence (**scheme 136A**). However, the enantioselectivity was found to be very sensitive to the steric bulkiness of the substituent R^3 . In 2020 the same research group reported a Ru-catalyzed ARA, followed by a spontaneous ring-closing cascade reaction to construct biaryl-bridged NH lactams,^{198b} in excellent yield and enantioselectivity. In this case the reaction was not sensitive to the bulkiness of substituent R^3 (**scheme 136B**).

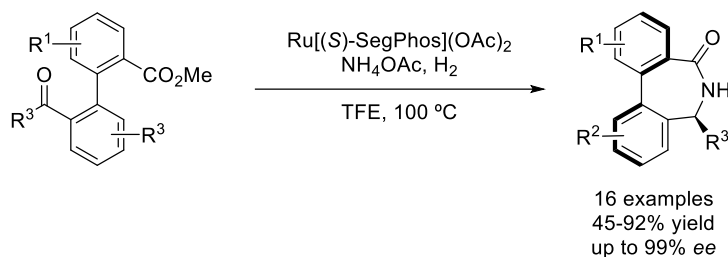
¹⁹⁷ J. Liu, X. Yang, Z. Zuo, J. Nan, Y. Wang, X. Luan, *Org. Lett.* **2018**, *20*, 244–247.

¹⁹⁸ a) T. Yang, X. Guo, Q. Yin, X. Zhang, *Chem. Sci.* **2019**, *10*, 2473–2477. b) Y. Zhang, Y-Q. Liu, L. Hu, X. Zhang, Q. Yin, *Org. Lett.* **2020**, *22*, 6479–6483.

A: Yin and Zhang, 2019.



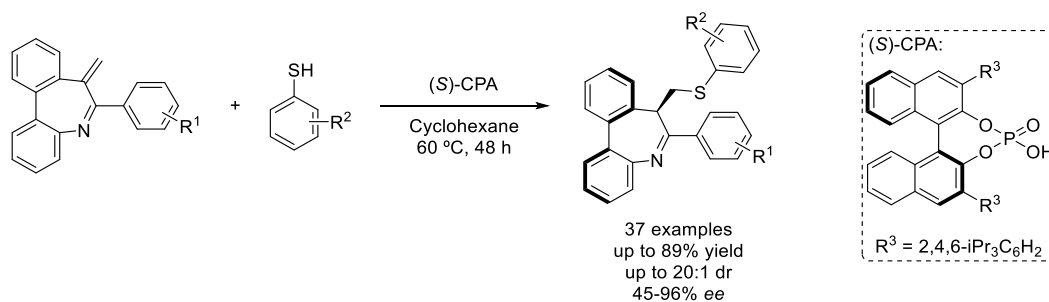
B: Yin and Zhang, 2020.

**Scheme 135:** intramolecular ARA/ring-closing cascade reaction.

In 2020, Zhao, Zhu and co-workers reported the first synthesis of arylthio-dibenzo[*b,d*]azepines through an asymmetric conjugate addition of thiophenol derivatives (**scheme 136**).¹⁹⁹ Their interest were based on the importance of organosulfur compounds as bioactive molecules and natural products. The corresponding α,β -unsaturated cyclic imine substrates were prepared by Pd-catalyzed intermolecular imidoylation and an intramolecular Heck annulation. Interestingly, aryl iodides bearing electron-withdrawing groups gave higher yields than those with electron-neutral and -donating substituents. The use of different CPAs was studied, and it was found that the steric hindrance at R³ have an important influence on the reactivity and enantioselectivity. Under the optimal conditions, excellent enantioselectivities (up to 96% *ee*) and yields were obtained for a wide range of aryl thiols and cyclic imines. A plausible catalytic cycle was proposed, in which after protonation of the imine substrate by the CPA and addition of the thiol,

¹⁹⁹ W. Hu, X. Wang, Y. Peng, S. Luo, J. Zhao, Q. Zhu, *Org. Lett.* **2022**, *24*, 3642–3646.

an enamine intermediate was formed. Finally, the stereogenic center is established through enantioselective proton transfer.



Scheme 136: imidoylative Heck cyclization and CPA-catalyzed thio-Michael addition/enantioselective protonation for the synthesis of 7-aryltiomethyl dibenzo[*b,d*]azepines.

In view of this results, catalytic asymmetric synthesis of axially chiral dibenzo[*b,d*]azepines remains limited and challenging. Hence, the development of a simple catalytic enantioselective method, providing access to these structural motifs, is a desirable goal.

IV.1.2. Reductive hydroamination.

Hydroamination reactions involve the addition of a hydrogen and an amino group into a C-C multiple bonds of an alkene, alkyne, diene or allene, representing an important tool for the synthesis of complex amines.²⁰⁰ This protocol results optimal from the atom economy point of view. Over the years, this transformation has been performed using a wide variety of synthetic strategies, among which the use of rare-

²⁰⁰ R. Y. Liu, S. L. Buchwald, *Acc. Chem. Res.* **2020**, *53*, 1229–1243.

earth and noble metal-based catalysis,²⁰¹ Brønsted acid catalysis,²⁰² free radicals,²⁰³ pericyclic reactions²⁰⁴ and photocatalysis²⁰⁵ stand out.

Traditionally, the amine nitrogen reacts as a nucleophile in a Markovnikov manner, while the proton acts as electrophile. Although traditional hydroamination methodologies represent reliable approaches that are selective and efficient, until recently, there was a lack of stereoselective methods that could be applied for both functionalized and unfunctionalized substrates. In this regard, a polarity-reverse (*umpolung*) mechanism has been developed in the past decade, where the hydride derived from a reducing reagent act as a nucleophile, while the amino group is turned as the electrophile.

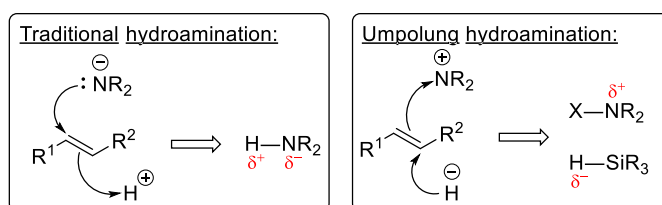


Figure 19: comparison between traditional and umpolung hydroamination.

The use of copper(I) hydride species as key catalytic intermediates for enantio- and regioselective hydroamination reactions was reported by two different research groups in 2013. Hirano and Miura (**scheme 137A**),²⁰⁶ and Buchwald

²⁰¹ L. Huang, M. Arndt, K. Gooßen, H. Heydt, L. J. Gooßen, *Chem. Rev.* **2015**, *115*, 2596–2697.

²⁰² a) B. Schlummer, J. F. Hartwig, *Org. Lett.* **2002**, *4*, 9, 1471–1474. b) L. L. Anderson, J. Arnold, R. G. Bergman, *J. Am. Chem. Soc.* **2005**, *127*, 42, 14542–14543. c) N. D. Saphiro, V. Rauniyar, G. L. Hamilton, J. Wu, F. D. Toste, *Nature* **2011**, *470*, 245–249. d) J.-S. Lin, P. Yu, L. Huang, P. Zhang, B. Tan, X.-Y. Liu, *Angew. Chem.* **2015**, *127*, 7958–7962.

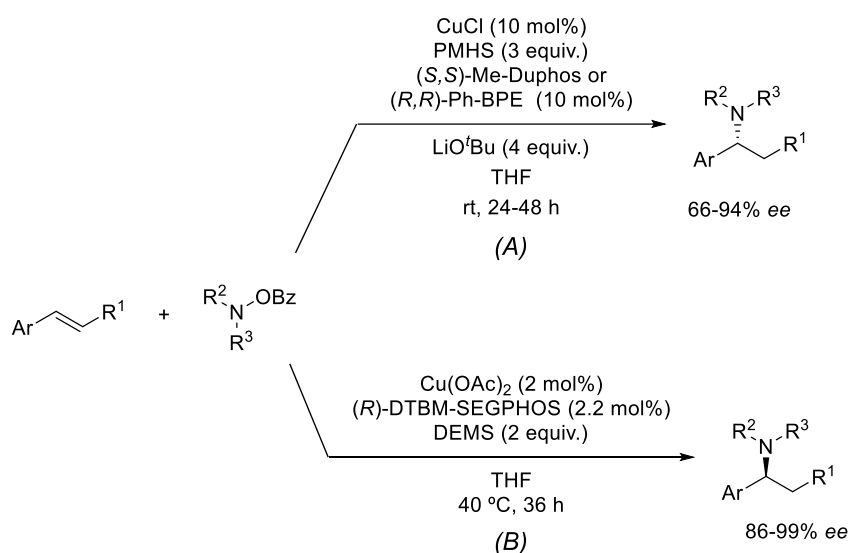
^{203a)} J. Kemper, A. Studer, *Angew. Chem. Int. Ed.* **2005**, *44*, 4914–4917. b) J. Guin, C. Mück-Lichtenfeld, S. Grimme, A. Studer, *J. Am. Chem. Soc.* **2007**, *129*, 4498–4503. c) T. M. Nguyen, D. A. Nicewicz, *J. Am. Chem. Soc.* **2013**, *135*, 9588–9591. d) A. J. Musacchio, L. Q. Nguyen, G. H. Beard, R. R. Knowles, *J. Am. Chem. Soc.* **2014**, *136*, 12217–12220.

²⁰⁴ a) A. M. Beauchemin, J. Moran, M.-E. Lebrun, C. Soguain, E. Dimitrijevic, L. Zhang, S. I. Gorelsky, *Angew. Chem. Int. Ed.* **2008**, *47*, 1410–1413. b) A. R. Brown, C. Uyeda, C. A. Brotherton, E. N. Jacobsen, *J. Am. Chem. Soc.* **2013**, *135*, 6747–6749.

²⁰⁵ A. Trowbridge, S. M. Walton, M. J. Gaunt, *Chem. Rev.* **2020**, *120*, 5, 2613–2692.

²⁰⁶ Y. Miki, K. Hirano, T. Satoh, M. Miura, *Angew. Chem.* **2013**, *125*, 11030–11034.

(**scheme 137B**)²⁰⁷ simultaneously described the enantioselective hydroamination of styrenes via CuH catalysis. They demonstrated that the transformation could take place using copper(I) reduced *in situ* from copper(II) acetate or copper(I)-*tert*-butoxide generated from copper(I) chloride, in combination with chiral phosphine ligands. The hydride source consisted of inexpensive and environmentally benign poly(methylhydrosiloxane) (PMHS) or its monomeric analogue diethoxymethylsilane (DEMS). In both cases, tertiary amines were obtained from a variety of styrenes, in excellent yield and enantioselectivities, and exclusively in a Markovnikov fashion, that could be explained by the formation of a stabilized benzylcopper intermediates. Under the same reaction conditions, the use of terminal alkenes provided the corresponding anti-Markovnikov linear aliphatic amines.



Scheme 137: asymmetric hydroamination of styrenes reported by Hirano and Miura, and Buchwald.

The hydroamination methodology was later extended to oxa- and azabicyclic alkenes,²⁰⁸ using a wide range of amine electrophiles, affording the hydroamination products from moderate to excellent enantioselectivity (**scheme 138A**).

²⁰⁷ S. Zhu, N. Niljianskul, S. L. Buchwald, *J. Am. Chem. Soc.* **2013**, *135*, 15746–15749.

²⁰⁸ Y. Miki, K. Hirano, T. Satoh, M. Miura, *Org. Lett.* **2014**, *16*, 1498–1501.

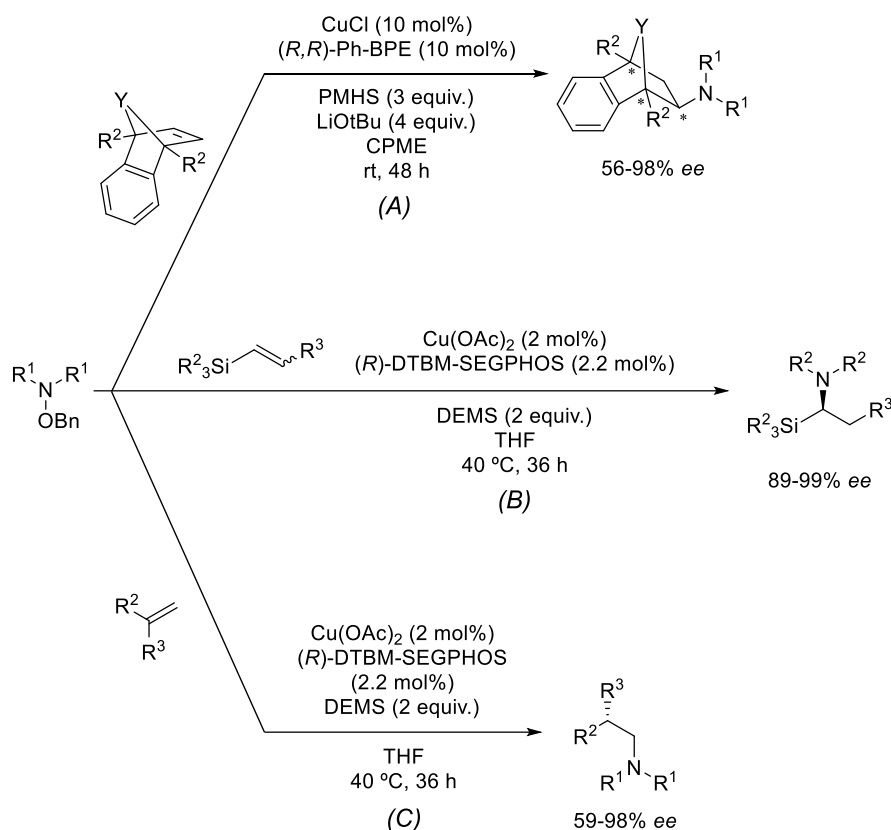
Moreover, the group of Buchwald described the synthesis of α -amino-silanes,²⁰⁹ in excellent yields and enantioselectivities, using its previously reported CuH-catalytic system. Interestingly, it was observed that the same enantiomer was always obtained when using either (*E*)- and (*Z*)- alkene isomer, with exclusive Markovnikov regioselectivity. This behavior was explained by the hyperconjugative stabilization of the alkylcopper intermediate by the silyl group (**scheme 138B**).

Buchwald research group also studied this transformation for 1,1-disubstituted alkenes,²¹⁰ which are poorly reactive and present a difficult enantioinduction owing to the similar enantiotopic faces. However, the desired anti-Markovnikov β -chiral amines could be obtained in good enantioselectivity when the size difference between the substituents of the alkene was significantly high. Furthermore, the method tolerates a wide range of functional groups and was suitable for the hydroamination of unactivated internal alkenes,²¹¹ using an electrophilic aminating reagent bearing a more electron-rich benzoyl group that is less prone to reduction. For unsymmetrical alkenes, the resulting products were obtained in a moderate regioselectivity, but each regioisomer was obtained optically pure (**scheme 138C**).

²⁰⁹ N. Niljianskul, S. Zhu, S. L. Buchwald, *Angew. Chem. Int. Ed.* **2015**, *54*, 1638–1641.

²¹⁰ S. Zhu, S. L. Buchwald, *J. Am. Chem. Soc.* **2014** *136*, 15913–15916.

²¹¹ Y. Yang, S.-L. Shi, D. Niu, P. Liu, S. L. Buchwald, *Science* **2015**, *349*, 62–66.

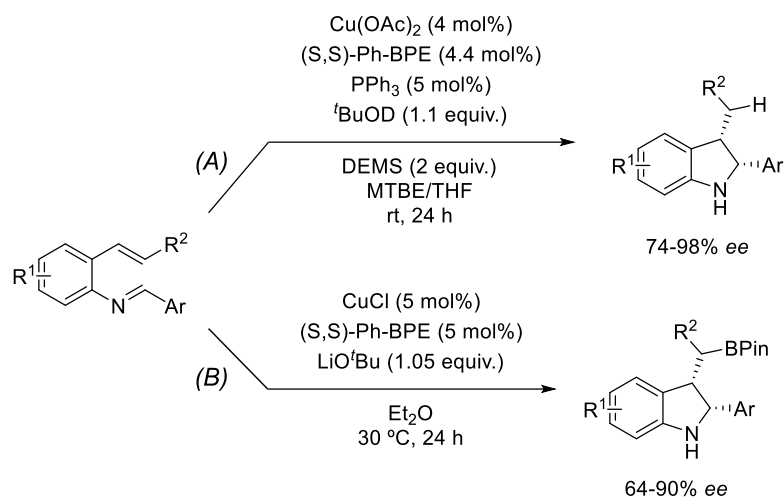


Scheme 138: copper-catalyzed enantioselective hydroamination with different substituted alkenes.

Considering the previous experience in the activation of alkenes using CuH-catalysis, the group of Buchwald further extent this methodology to the intramolecular hydrocupration followed by 1,2-addition to the attached imine electrophiles.²¹² Thus, the synthesis of enantioenriched indolines bearing two chiral centers was carried out in good yields and stereoselectivities (**scheme 139A**). Interestingly, the use of *tert*-BuOD instead of *tert*-BuOH increased the yield of the reaction, a phenomenon explained by the deuterium isotopic effect, in which the protonolysis of the alkylcopper intermediate that would lead to de undesired reduced product was slower than with *tert*-BuOH.

²¹² E. Ascic, S.L. Buchwald, *J. Am. Chem. Soc.* **2015**, *137*, 4666–4669.

Three years later, the group of Yun employ this strategy for the synthesis of enantioenriched borylated indolines (**scheme 139B**).²¹³ In this case, a chiral β -boryl benzylcopper intermediate is formed before the 1,2 addition to the imine.

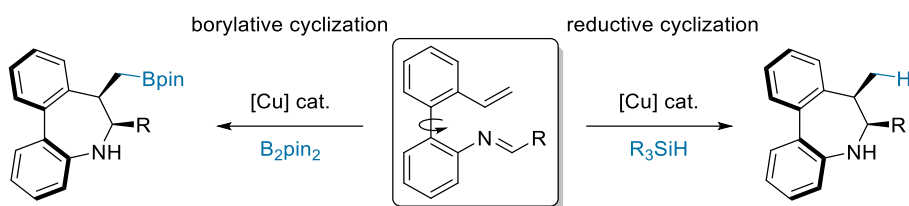


Scheme 139: diastereo- and enantioselective CuH-catalyzed synthesis of 2,3-disubstituted (borylated) indolines by Buchwald (A) and Yun (B).

IV.2. Objectives.

Considering these precedents, the limitations of the previously described methodologies for the synthesis of dibenzo[*b,d*]azepines and the inherent interest of our research group for the atroposelective synthesis of biaryl compounds, we envisioned that secondary ketimines from *ortho*-vinyl, *ortho'*-amino biaryls could be appropriate substrates to perform reductive or borylative cyclizations for the construction of axially chiral dibenzo[*b,d*]azepine derivatives (**scheme 140**).

²¹³ D.-X. Li, J. Kim, J. W. Yang, J. Yun, *Chem.-Asian J.* **2018**, *13*, 2365-2368.



Scheme 140: reductive or borylative cyclization for the synthesis of bridged biaryl derivatives.

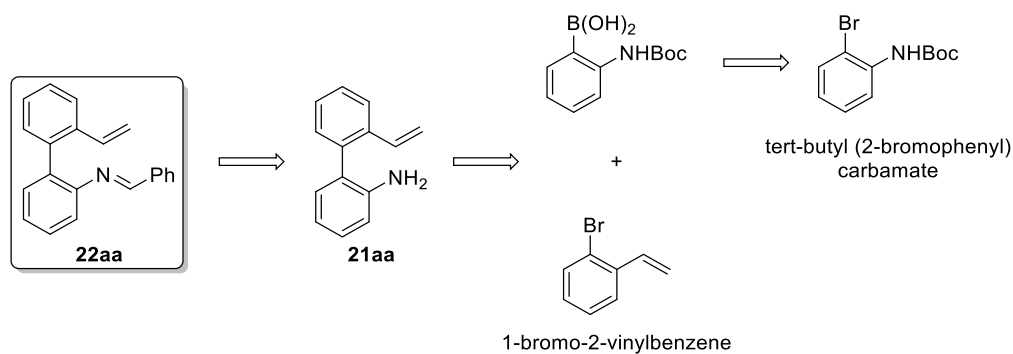
This strategy would allow for the simultaneous generation of axial and central chirality and would require an exquisite control of the regio-, diastereo- and enantioselectivity. Moreover, point-to-axial chirality transfer is an uncommon and promising strategy that allows the introduction of axial chirality in structurally complex compounds, involving the internal transfer of stereochemical information from a sp^3 carbon to the chiral axis.

IV.3. Results and discussion.

IV.3.1. Synthesis of starting materials.

This chapter describes the study of a copper-catalyzed asymmetric reductive intramolecular cyclization using Schiff bases from *ortho*-vinyl, *ortho'*-amino biaryls. Thus, the synthesis of the substrates and their precursors will be first described. A retrosynthetic analysis of these structures suggests following the proposed route on **scheme 141**. Lithium/halogen exchange of commercially available *tert*-butyl (2-bromophenyl)carbamate with *tert*-butyl lithium was followed by addition of trimethyl borate, to obtain the corresponding boronic acid. A Suzuki cross-coupling reaction was then performed between the latter and commercial 1-bromo-2-vinylbenzene. The desired biphenyl-amine was obtained after deprotection of the Boc protecting group using trifluoroacetic acid.

Further condensation between the isolated biphenyl-amine with different aldehydes afforded the desired biaryl-imines. For the study of the reaction conditions, benzaldehyde was selected to prepare the imine model substrate.



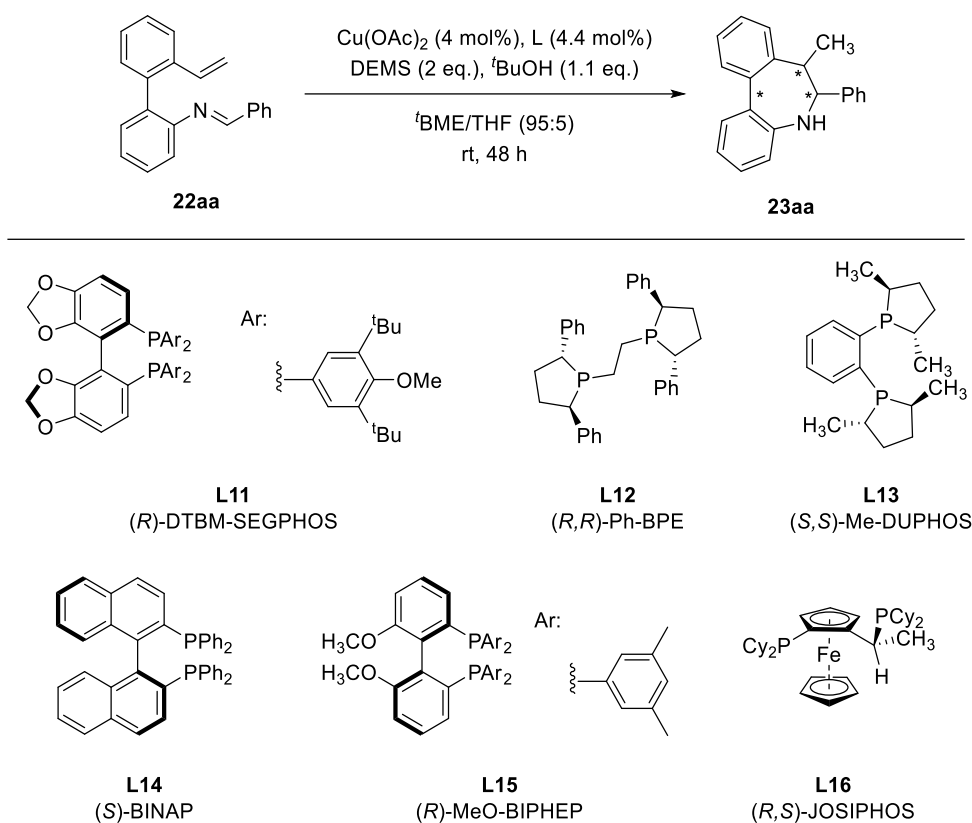
Scheme 141: retrosynthetic analysis for the synthesis of the target biphenyl-amine.

IV.3.2. Asymmetric intramolecular reductive cyclization.

IV.3.2.1. Screening of ligands.

Chiral C_2 -symmetric biphosphines are commonly used ligands in copper(I)-catalyzed reactions, due to their capacity to act as π acids and stabilize low valent organometallic complexes, such as Cu(I).²¹⁴ Thus, a variety of commercially available chiral biphosphine ligands were tested under the reaction conditions previously described by Buchwald,²¹² and the results were analyzed after 48 h, as summarized in **table 7**.

²¹⁴ J. M. Thomas, P. K. Madarasi, C. Sivasankar, A. G. Samuelson, (2019) Chapter 7 in *Copper(I) chemistry of Phosphines, Functionalized Phosphines and Phosphorus Heterocycles* (165-236).

Table 7: commercial ligand screening for the reductive cyclization.

Entry ^a	Ligand	Conv. (%) ^b	ee (%) ^c
1	(<i>R</i>)-DTBM-SEGPHOS (L11)	<10	n.d.
2 ^d	(<i>R,R</i>)-Ph-BPE (L12)	99 (99 yield)	98
3	(<i>S,S</i>)-Me-DUPHOS (L13)	<20	n.d.
4	(<i>S</i>)-BINAP (L14)	<5	n.d.
5	(<i>R</i>)-MeO-BIPHEP (L15)	42	77
6	(<i>R</i>)-(<i>S</i>)-JOSIPHOS (L16)	<20	n.d.

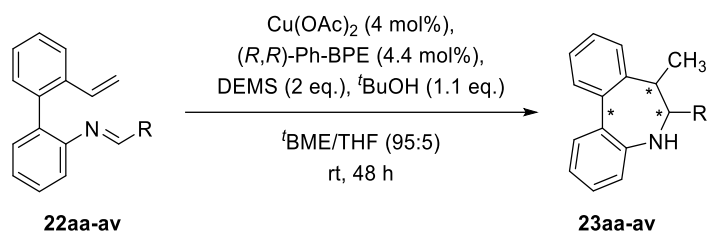
n.d. not determined. ^a Reaction performed on 0.2 mmol scale of **22aa**. ^b Estimated by ¹H-NMR spectroscopy. ^c Determined by HPLC on chiral stationary phases. ^d A single diastereomer was observed by ¹H NMR in the crude reaction mixture.

(*R*)-DTBM-SEGPHOS (**L11**), (*S,S*)-Me-DUPHOS (**L13**), (*S*)-BINAP (**L14**) and (*R,S*)-JOSIPHOS (**L16**) (entries 1, 3, 4 and 6 respectively) gave low reactivities as

determined by $^1\text{H-NMR}$ analysis and, therefore, the enantiomeric excess was not determined. Moderate conversion and enantioselectivities were observed using (*R*)-MeO-BIPHEP (**L15**) (entry 5). To our delight, (*R,R*)-Ph-BPE (**L12**) (entry 2) afforded the desired dibenzo[*b,d*]azepine with 99% isolated yield, excellent diastereoselectivity, with only one observed diastereomer by $^1\text{H-NMR}$ of the crude reaction (>20:1), and 98% of enantiomeric excess.

IV.3.2.1. Reaction scope.

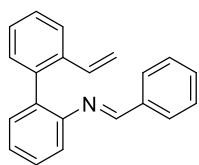
With the optimized conditions established ($\text{Cu}(\text{OAc})_2$ 4 mol%, (*R,R*)-Ph-BPE 4.4 mol%, diethoxymethylsilane 2 equivalents, *tert*-butanol 1.1 equivalents in a mixture of solvents 95:5 *t*BME/THF at room temperature for 48 h, **scheme 142**), the next step consisted of the study of electronic and steric effects of substituents on the intramolecular reductive cyclization.



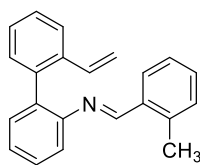
Scheme 142: model reaction for the atroposelective synthesis of dibenzo[*b,d*]azepine derivatives.

Hence, the structural modifications were divided on two main groups. On the one hand a variety of commercially available aldehydes presenting different electronic and steric properties were evaluated (**figure 20A and B**); on the other hand, different substitutions in the biaryls were also introduced, while maintaining the phenyl ring in the aldimine (**figure 20C**).

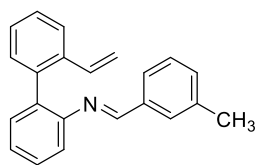
A: Aryl derivatives.



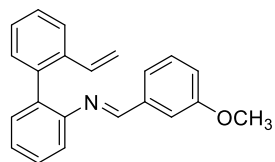
22aa



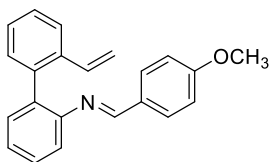
22ab



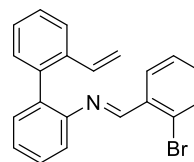
22ac



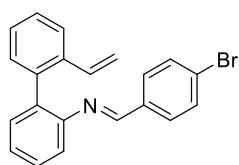
22ad



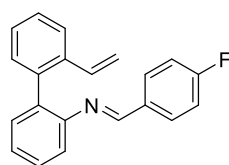
22ae



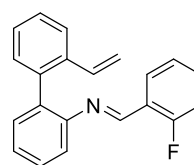
22af



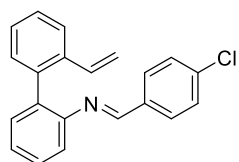
22ag



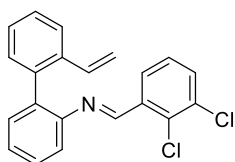
22ah



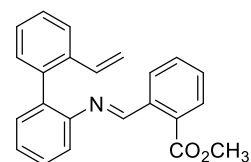
22ai



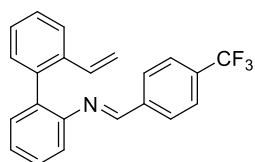
22aj



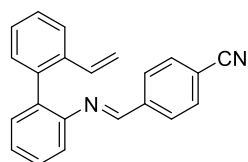
22ak



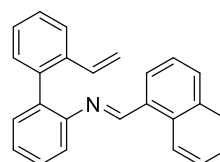
22al



22am

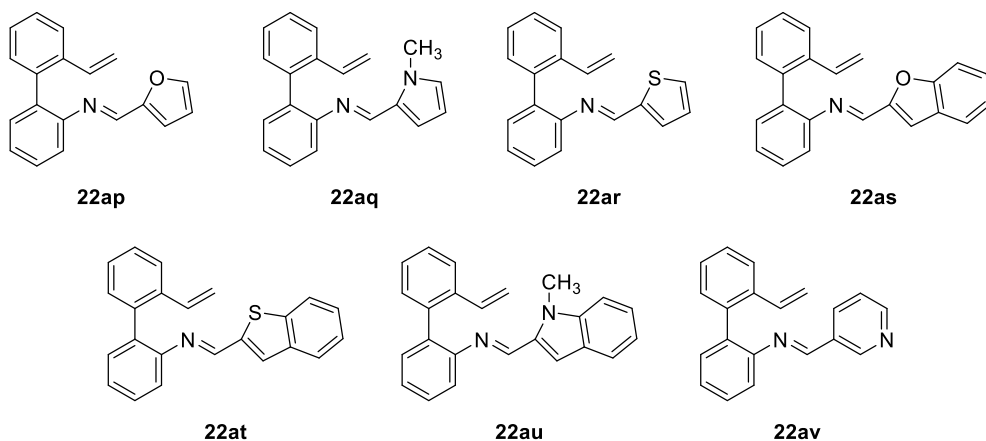


22an



22ao

B: Heterocyclic derivatives.



C: Biaryl derivatives.

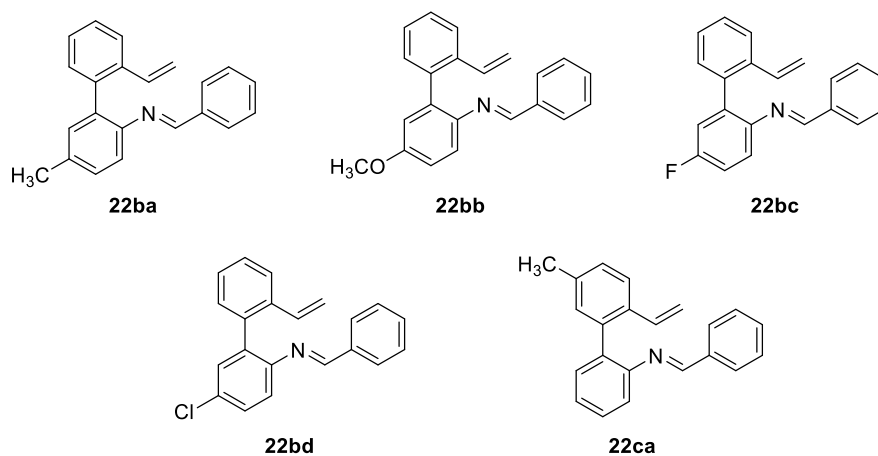


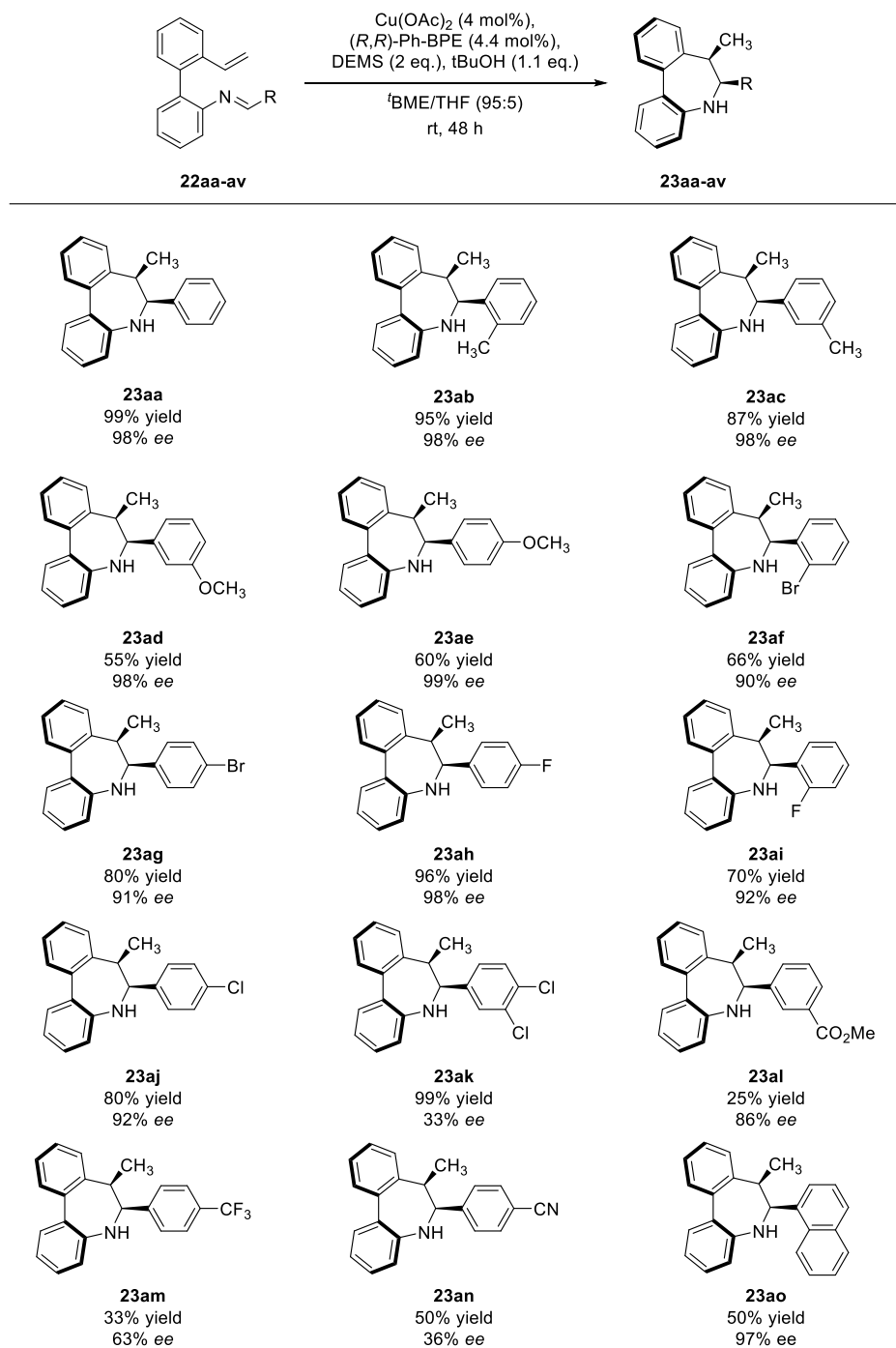
Figure 20: library of synthesized biaryl-imines.

The selected biaryl-imines were obtained in good to excellent yields and their reactivity was explored under the previously optimized reaction conditions.

As shown in **scheme 143**, the reaction presents very good functional group tolerance and can be applied to a variety of biaryl-imines, obtaining very high stereoselectivities. To our delight, only one diastereomer was observed in all cases by NMR spectroscopy (>20:1 diastereomeric ratio). Substrates featuring electron-rich substituents on the aldimine aryl ring such as methyl group **23ab** and **23ac** afforded the corresponding dibenzoazepines derivatives with similar results as for the model

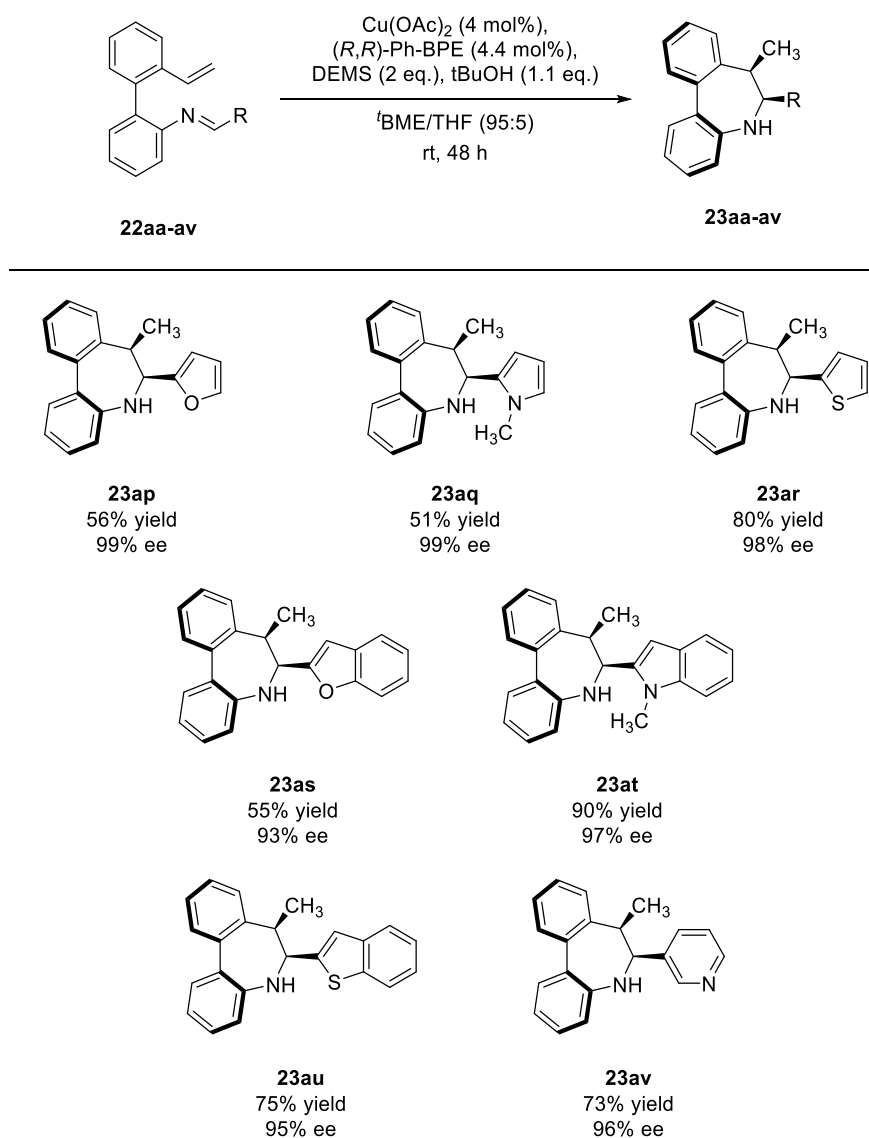
substrate. Additionally, dibenzoazepines bearing methoxy substituents **23ad** and **23ae** were obtained with slightly poorer yield (55% yield for the *ortho*-position and 60% for the *para*-position) but excellent enantioselectivities (98% *ee* in both cases). In the same vein, the presence of substituents at the *ortho*-position has very little effect on reactivity and enantioselectivity, as demonstrated for the synthesis of **23ab**, **23af** and **23ai**. Besides that, fluorinated substrates placed on the phenyl ring of the imine were also well tolerated, as highlighted for compounds **23ah** and **23ai**. However, the enantioselectivity drops to 33% *ee* for a substrate presenting two chloro-groups on the phenyl ring (**23ak**), to 63% *ee* for the presence of a -CF₃ group (**23am**) and to 36% *ee* for a nitrile group placed at the *para*-position (**23an**).

Moreover, products bearing a halide (**23af**, **23ag**, **23aj** and **23ak**) or ester (**23al**) functionalities were also well tolerated, affording 66-99% yields and moderate to high enantioselectivities (up to 92%), and offering synthetic handles for further transformations.



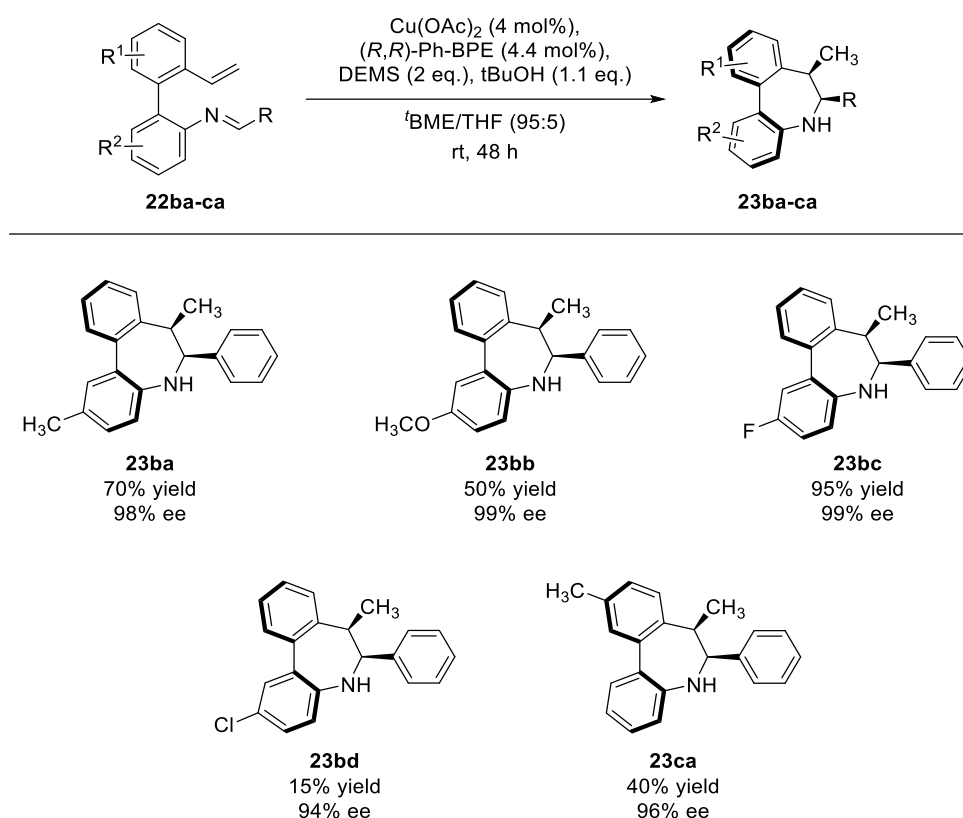
Scheme 143: substrate scope for the asymmetric synthesis of dibenzo[*b,d*]azepines.

Furthermore, the reaction also tolerates a variety of heterocyclic substrates, such as furan (**23ap**), *N*-methyl pyrrole (**23aq**), thiophene (**23ar**), pyridine (**23av**) and fused heterocyclic derivatives (benzofuran **23as**, *N*-methylindole **23at** and thianaphthene **23au**), affording good yields (51-90%) and excellent enantioselectivities (93-99% ee).



Scheme 144: substrate scope of heterobiaryls for the asymmetric synthesis of dibenzo[*b,d*]azepines.

We next explored the scope of the reaction with respect of substitution on the biaryl frame (**scheme 146**). When different electron-donating and withdrawing groups were placed on the lower fragment of the biaryl moiety (**23ba**, **23bb**, **23bc** and **23bd**), very good yields (up to 95%) and enantioselectivities (94-99% ee) were observed, except for the chloride derivative **23bd** that was isolated in only 15% yield. On the other hand, when a methyl group was placed on the upper fragment of the biaryl (**23ca**), the corresponding dibenzoazepine derivative was obtained in moderate 40% yield and excellent enantioselectivity (96% ee).



Scheme 145: substrate scope of the biaryl frame for the asymmetric synthesis of dibenzo[b,d]azepines by Cu-catalyzed reductive cyclization.

Additionally, **23aa** was also prepared in 2 mmol reaction scale, affording the desired product with similar yield (93%) and the same enantiomeric excess (98% ee) and diastereomeric ratio (>20:1).

It was also possible to determine the absolute configuration of the products **23ag** and **23aj** by X-Ray diffraction analysis, revealing a $S_a,6S,7R$ configuration for the major diastereomer, while the other products were assigned by analogy. Moreover, the central to axial chirality relay phenomenon was confirmed by a dihedral angle of 39° between the two aryl groups in both compounds. It should be noted that the *cis*-diastereomers were exclusively formed in all cases.

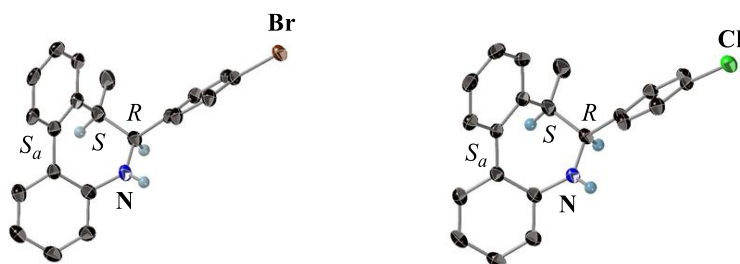
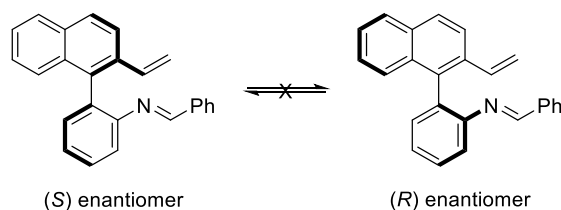


Figure 21: X-Ray diffraction analysis of compounds **23ag** and **23aj**.

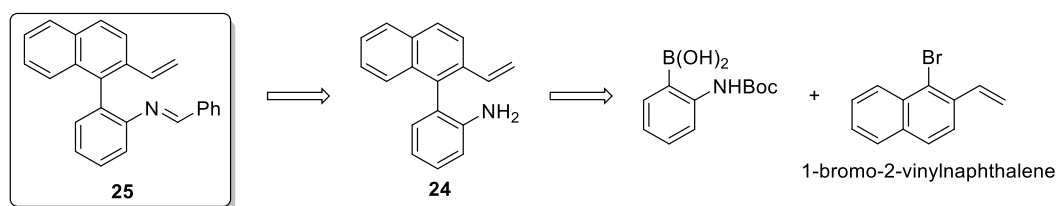
IV.3.2.3. Kinetic resolution.

Following the study of the intramolecular reductive cyclization through enantioselective copper catalysis, we decided to evaluate the reactivity of a configurationally stable biarylimine substrate presenting three substituents around the axis. In this case, interconversion between the two atropoisomers is not possible and therefore, a kinetic resolution (KR) could take place (**scheme 146**).



Scheme 146: configurationally stable biaryl-imines.

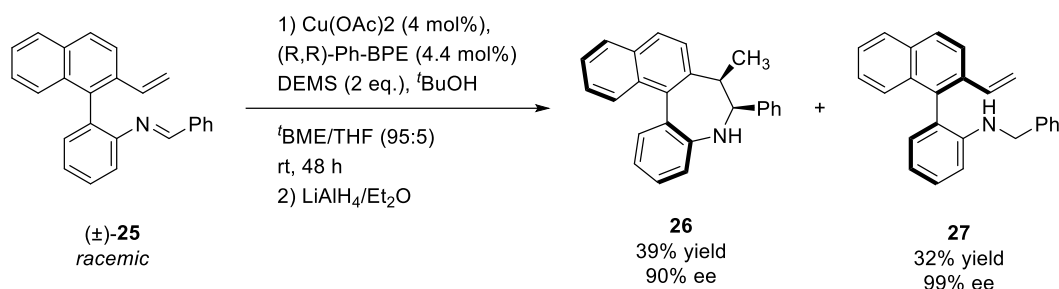
The substrate **25** was prepared starting from 1-bromo-2-vinylnaphtalene as the organohalide partner for the Suzuki-Miyaura cross coupling, following the same synthetic strategy previously reported (**scheme 147**).



Scheme 147: retrosynthetic analysis for the synthesis of biaryl-imine **25**.

It was ideally expected for one of the atropisomers to be fully transformed into the desired dibenzoazepine derivative, while the other was recovered unreacted.

To our delight, under the previously optimized conditions, the reaction stopped at 50% conversion, despite the use of an excess of silane (2 equiv.). A dibenzoazepine derivative **26** was isolated in 39% yield and 90% *ee*, while the enantioenriched starting material, was reduced *in situ* with lithium aluminium hydride to afford the corresponding amine **27** in 32% yield and nearly enantiopure form (>99% *ee*) (**scheme 148**). This biaryl-2-amine **27**, featuring only axial chirality, shows an interesting structure with potential applications in asymmetric catalysis.



Scheme 148: kinetic resolution reductive cyclization of the configurationally stable biaryl-imine substrate **25**.

The effectiveness of a kinetic resolution is judged by the selectivity factor (*s*), which is defined as the difference in energies between the diastereomeric transition states in the selectivity-determining step of the reaction.²¹⁵ It is expressed as the rate constant for the reaction of the fast-reacting enantiomer divided by the rate constant

²¹⁵ Keith, J.M., Larrow, J.F. Jacobsen, E.N. *Adv. Synth. Catal.* **2001**, 343, 5–26

of the slow-reacting enantiomer, assuming first kinetic order. It can also be expressed in terms of conversion (C), enantiomeric excess of the enantioenriched starting material (ee_s) and enantiomeric excess of the enantioenriched product (ee_p),²¹⁶ as depicted in the following equation.

$$s_{\text{factor}} = \frac{k_{\text{fast}}}{k_{\text{slow}}} = \frac{\ln [(1-C)(1-ee_s)]}{\ln [(1-C)(1+ee_s)]} \text{ being } C = \frac{ee_s}{(ee_s+ee_p)}$$

In our case, the value of the selectivity factor was found to be $s = 99$, meaning that the kinetic resolution reaction proceeds with high efficiency.

Finally, attempts to synthesize configurationally stable biaryl-2-imine derivatives with different electron-rich and -deficient groups on the aldimine aryl ring were unsuccessful, due to the instability of the substrates under the reaction conditions.

IV.3.3. Intramolecular borilative cyclization.

IV.3.3.1. Screening of ligands.

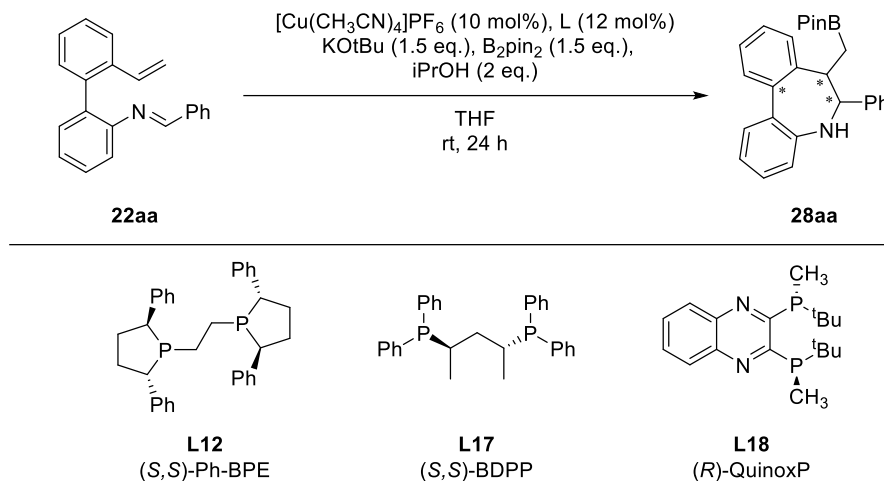
Considering that 2'-vinyl-biphenyl-2-imines substrates would form very similar organocopper intermediates after the insertion of the vinyl group into the *in situ* formed L*Cu-Bpin catalyst, we decided to study the intramolecular copper catalyzed borylative cyclization, as an alternative approach. In this case, the resulting axially chiral dibenzo[*b,d*]azepines would present a pinacol methyl boronate group at the 7-position instead of a methyl unit. The BPin group is an important handle for further derivatization, being possible to transform the C(sp³)-B bond into C-O, C-N or C-C bonds.²¹⁷

²¹⁶ Gao, D-W., Gu, Q., You, S-L. *ACS Catal.* **2014**, *4*, 8, 2741–2745.

²¹⁷ For selected examples, see: a) T. Awano, T. Ohmura, M. Suginome, *J. Am. Chem. Soc.* **2011**, *133*, 51, 20738–20741. b) S. L. Poe, J. P. Morken, *Angew. Chem. Int. Ed.* **2011**, *50*, 4189–4192. c) M. Tortosa, *Angew. Chem. Int. Ed.* **2011**, *50*, 3950–3953. d) D. Leonori, V. K. Aggarwal, *Acc. Chem. Res.* **2014**, *47*, 10, 3174–3183. e) D. Imao, B. W. Glasspoole, V. S. Laberge, C. M. Crudden, *J. Am. Chem. Soc.* **2009**, *131*, 14, 5024–5025. f) E. Fernández, A. Whiting (2015). *Synthesis and Application of Organoboron Compounds*. (1st ed.). Springer.

For the optimization reaction, based on the described conditions by Yun²¹³ and more recently, Procter *et al.*,²¹⁸ a screening of ligands was carried out using $[\text{Cu}(\text{CH}_3\text{CN})_4]\text{PF}_6$ as pre-catalyst and imine **22aa** as model substrate (**table 8**).

Table 8: commercial ligand screening for the borylative cyclization.



Entry ^a	Ligand	Conv. (%) ^b	<i>ee</i> (%) ^c
1	(<i>S,S</i>)-Ph-BPE (L12)	99	93
2	(<i>S,S</i>)-BDPP (L17)	99	20
3	(<i>R</i>)-QuinoxP (L18)	99	0
4 ^{d,e}	(<i>S,S</i>)-Ph-BPE (L12)	99 (85 yield)	98

^a Reaction performed on 0.2 mmol scale of **22aa**. ^b Estimated by ¹H-NMR spectroscopy. ^c Determined by HPLC on chiral stationary phases. ^d A single diastereomer was observed by ¹H NMR in the crude reaction mixture. ^e $[\text{Cu}]$ (5 mol%)/ L^* (6 mol%).

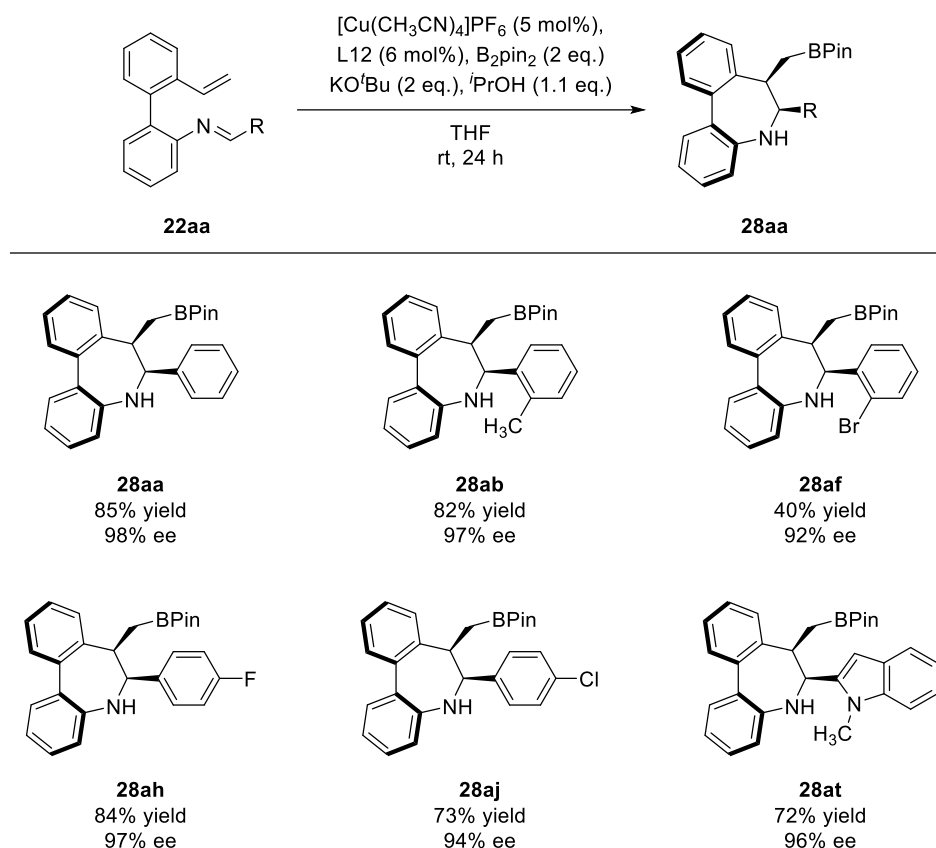
We studied different phosphine ligands, and surprisingly, all afforded the desired axially chiral borylated dibenzoazepine in full conversion in 24 h at room temperature. However, with (*S,S*)-BDPP **L17** (entry 2) and (*R*)-QuinoxP **L18** (entry 3) poor enantiomeric excess were obtained (20% *ee* and racemic, respectively). Again, (*S,S*)-Ph-BPE (**L12**) (entry 1) was found to give the best results in the reaction, affording excellent reactivity and enantiomeric excess (99% conversion determined

²¹⁸ Dherbassy, Q., Manna, S., Shi, C., Prasitwatcharakorn, W., Crisenza, G. E. M., Perry, G. J. P., Procter, D. J. *Angew. Chem. Int. Ed.* **2021**, *60*, 14355–14359.

by $^1\text{H-NMR}$ and 93% *ee*), and only one diastereomer observed in $^1\text{H-NMR}$ of the crude reaction mixture. Decreasing the catalytic loading to 5 mol% (entry 4) improved the optical purity to 98%, while the diastereomeric ratio remained excellent. The resulting borylated dibenzoazepine **28aa** was isolated in 85% yield.

IV.3.3.2. Reaction scope.

Under the optimized reaction conditions, the most representative imines previously synthesized were studied.



Scheme 149: substrate scope for the asymmetric synthesis of borylated dibenzo[*b,d*]azepines by Cu-catalyzed borylative cyclization.

As shown in **scheme 149**, borylative cyclization of selected 2'-vinyl-biphenyl-2-imines proceeded efficiently, leading in all cases to the desired dibenzoazepine derivatives in good to excellent yields, excellent enantioselectivities and only one

diastereomer observed by $^1\text{H-NMR}$ in the crude reaction mixture. For instance, methyl substitution at the *ortho*-position of the aryl (**28ab**) afforded the product with similar results as for the model compound. However, when a bromo substituent was placed at the *ortho*-position a decrease of yield was observed, while the selectivity was slightly lower. Alternatively, imines bearing electron-poor substituents at the *para*-position of the aldimine aryl ring **28ah** and **28aj** provided excellent enantioselectivities (97% *ee* and 94% *ee*, respectively). Additionally, the use of *N*-methylindole **28at** also led to the desired product in good yields (72%) and excellent enantioselectivity (96% *ee*), demonstrating the effectiveness of the method for heterocyclic substrates.

Single crystal X-ray analysis of compound **28aa** revealed the absolute configuration $S_a,6S,7R$ (**figure 22**), which is the same as for **23ag** and **23aj**.

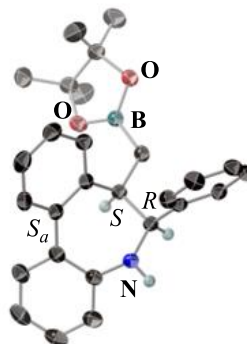
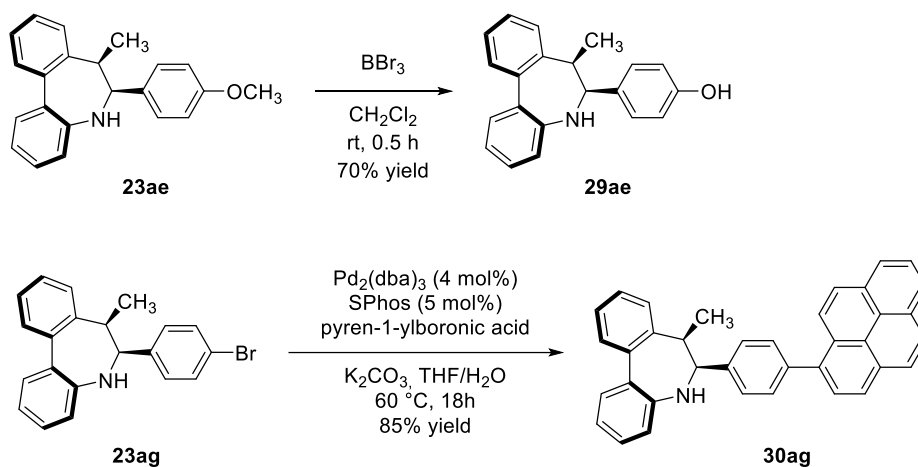


Figure 22: Ray diffraction analysis of compound **28aa**.

IV.3.4. Representative transformations.

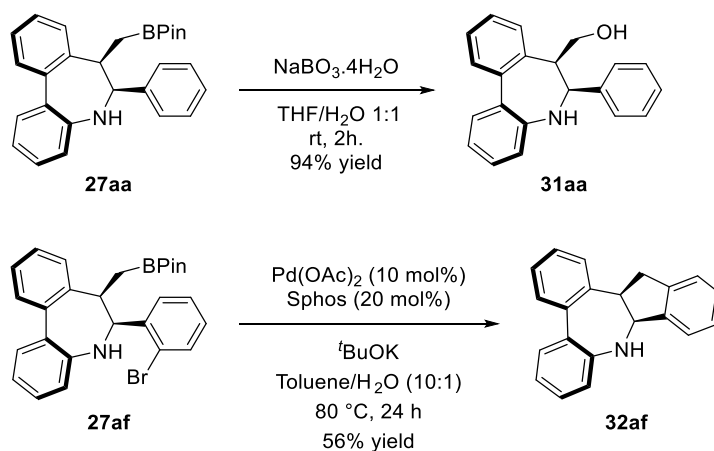
To illustrate the synthetic potential of the obtained products, derivatizations of selected dibenzoazepines were performed. As shown in **scheme 150**, *O*-demethylation reaction of **23ae** afforded the corresponding phenol product **29ae** in good yields. This transformation represents an alternative for the synthesis of this phenol-derivative since the corresponding aldimine substrate was not stable under the reaction conditions.

Additionally, a pyrene substituted compound **30ag** was obtained through a Suzuki-Miyaura coupling, affording an interesting fluorescent analogue that can be used in biological studies because of its emitting properties.



Scheme 150: demethylation reaction and Suzuki-Miyaura cross-coupling.

On the other hand, borylated axially chiral dibenzoazepine was oxidized with sodium perborate to obtain the corresponding alcohol **31aa** in excellent yield. Furthermore, intramolecular Suzuki coupling of **27af** afforded the tricyclic tetrahydrodibenzoindenoazepine **32af** in moderate yields (**scheme 151**).



Scheme 151: oxidation of -BPin and intramolecular Suzuki-Miyaura coupling.

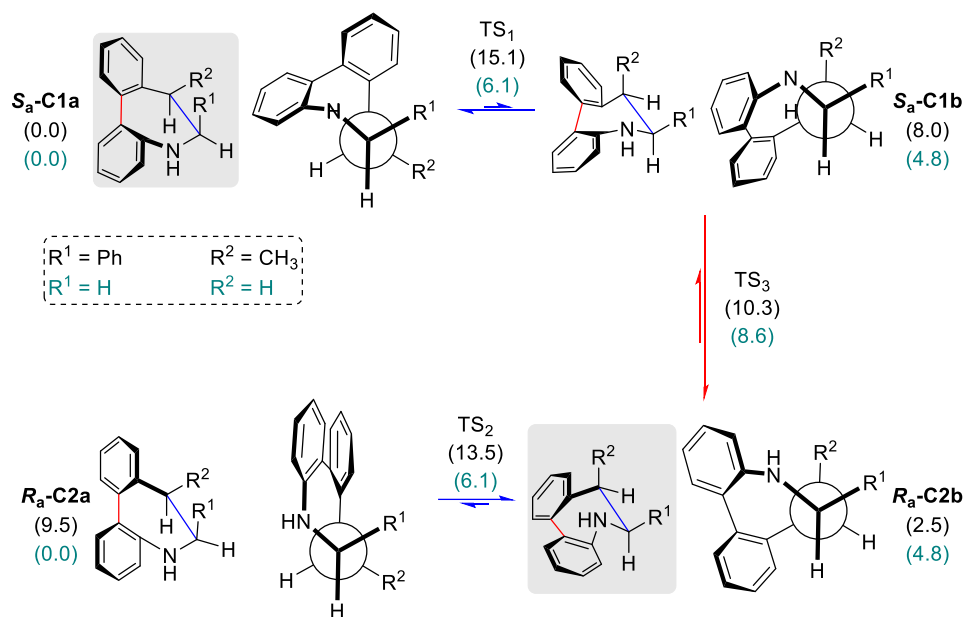
IV.3.5. Mechanistic studies.

Professor Pedro Merino, from University of Zaragoza, studied the configurational stability of these dibenzo[*b,d*]azepines in order to gain deeper insight on the origin of the high diastereoselectivity observed for the reaction. The obtained dibenzoazepine compounds can adopt a boat **a** and a half-chair **b** conformations (a third conformation can be located but at a considerable higher energy, so it would not be considered) depending on the pseudo-axial and pseudo-equatorial orientation of the substituents at the stereogenic centers.^{219,220} As illustrated in **scheme 152**, the calculations for the epimerization showed that *S_a,6*S*,7*R*-C1a* was found to be the most stable conformation for **23aa**, a result that matched with the experimental results observed in the X-Ray structures of **23ag**, **23aj** and **27aa**. Noteworthy, interconversion between *S_a,6*S*,7*R*-C1a* and *R_a,6*S*,7*R*-C2a* was found to be no possible due to steric reasons, and thus, axial epimerization by biphenyl bond rotation requires a conversion between **a** to **b** conformations, through TS₁ and TS₃.

As shown in the following scheme, the free energy barrier for the *S_a,6*S*,7*R*-C1a*/*S_a,6*S*,7*R*-C1b* interconversion (TS₁) was located at 15.1 kcal/mol, while the interconversion between *R_a,6*S*,7*R*-C2a*/*R_a,6*S*,7*R*-C2b* conformers (TS₂) was found to be 13.5 kcal/mol. This difference in the free energy explained the favoured *S_a,6*S*,7*R*-C1a* and *R_a,6*S*,7*R*-C2b* conformations, respectively.

²¹⁹ S. Saebo, J. E. Boggs, *J. Mol. Struct.: THEOCHEM*, **1982**, *87*, 365–373.

²²⁰ J. Messinger, V. Buss, *J. Org. Chem.*, **1992**, *57*, 3320–3328.



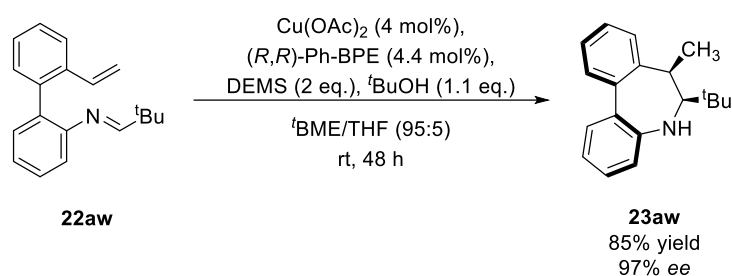
Scheme 152: conformational study.

The first transformation between $S_a,6S,7R\text{-C1a}$ and $S_a,6S,7R\text{-C1b}$ was found to be the limiting state, with an energy barrier of 15.1 kcal/mol. Those values showed that a fast equilibrium is established at 25 °C, having a kinetic constant of 52.11 s⁻¹ with $t_{1/2}$ of 0.0133 and therefore the observed population of conformers depends on their relative stability, meaning that the studied transformation is under thermodynamic control.

It must be noted that when no substituents are present (R¹ = R² = H, **scheme 152**, green data) the calculated free energies are lower than those for compound **23aa**, as expected by virtue of the lower steric hindrance presented.

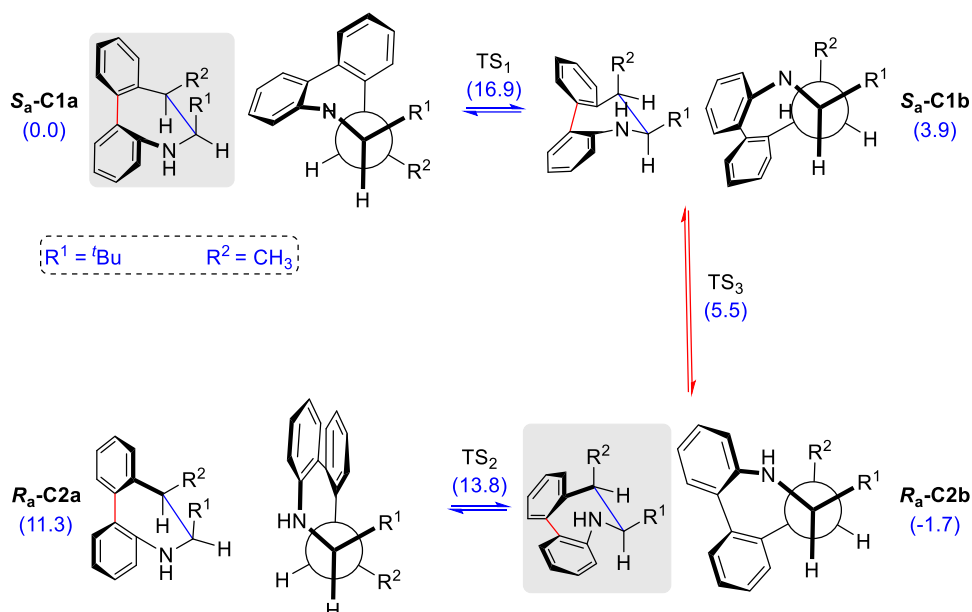
For the most stable atropisomers ($S_a,6S,7R\text{-C1a}$ and $R_a,6S,7R\text{-C2b}$, in grey shadow in **scheme 152**), the calculated relative energies presented a 2.5 kcal/mol difference, corresponding to a predicted 99:1 *er* ratio. In view of the assumed DFT experimental error and the high diastereomeric excess values obtained, it could be concluded that, essentially, only $S_a,6S,7R\text{-C1a}$ will be observed, which is in agreement with the experimental results.

With these results in hand, we wondered if the equilibrium would be shifted by replacing the phenyl group in the aldimine moiety by a bulkier *tert*-butyl group. The corresponding Schiff base **22aw** using pivalaldehyde as precursor was synthesized following the same procedure described in **scheme 142**, affording the biphenyl imine **22aw** with 40% yield. Subsequently, it was subjected to the optimized conditions for the intramolecular reductive cyclization, providing the dibenzoazepine derivative **23aw** in 85% yield, 97% optical purity and >20:1 d.r., as shown in **scheme 153**.



Scheme 153: enantioselective reductive cyclization affording dibenzo[*b,d*]azepine **23aw**.

Interestingly, as shown in the data in **scheme 154** in blue, DFT calculations predicted that, in this case, $R_a6S,7R$ -**C2b** conformation presented the lowest energy (0.0 kcal/mol for $S_a6S,7R$ -**C1a** and -1.7 kcal/mol for $R_a6S,7R$ -**C2b**), value that corresponds with a 95:5 ratio at 25 °C. In this case, the rate limited state is also the interconversion of $S_a6S,7R$ -**C1a**/ $S_a6S,7R$ -**C1b** (TS_1 with a barrier of 16.9 kcal/mol).



Scheme 154: conformational study of compound **23aw**.

As stated above, DFT calculation predicted that the diastereomer with the opposite configuration in the axis ($R_a6S,7R\text{-C2b}$) was the most stable.

Quantitative NCI calculations were carried out for the conformers derived from **23aa** ($R^1 = \text{CH}_3$, $R^2 = \text{Ph}$) and **23aw** ($R^1 = \text{CH}_3$, $R^2 = \text{tert-Bu}$), in order to obtain a picture of non-covalent interactions. From the analysis of the surfaces, showed in **figure 23** (where thin, delocalized green surface indicates Van der Waals interactions; small, lenticular, bluish surfaces indicate strong interactions such as hydrogen bondings; and steric clashes are shown as red isosurfaces), it can be concluded that conformer $S_a6S,7R\text{-C1a}$ of compound **23aa** is the one with less repulsive interactions.

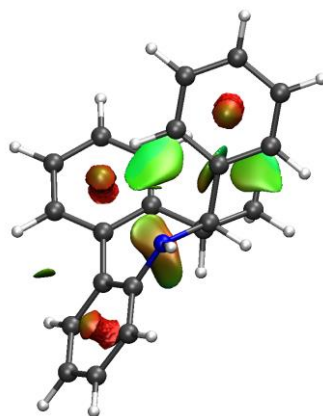


Figure 23: NCI analysis of conformers for compound **23aa**.

On the other hand, for compound **23aw**, the less repulsive interactions were observed in conformer *R_a6S,7R-C2b*, as DFT calculation predicted, shown in **figure 24**.

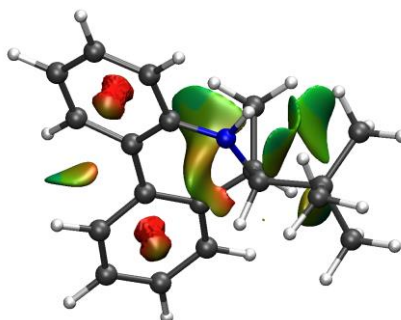


Figure 24: NCI analysis of conformers for compound **23aw**.

Low temperature ¹H-NMR analysis was also carried out for compound **23aa** (**figure 25** upper) and compound **23aw** (**figure 25** lower) and even at temperatures as low as -60 °C, no new signals were observed, meaning that the atropodiastereoisomeric equilibrium is completely shifted towards the thermodynamic product, either in **23aa** or **23aw**.

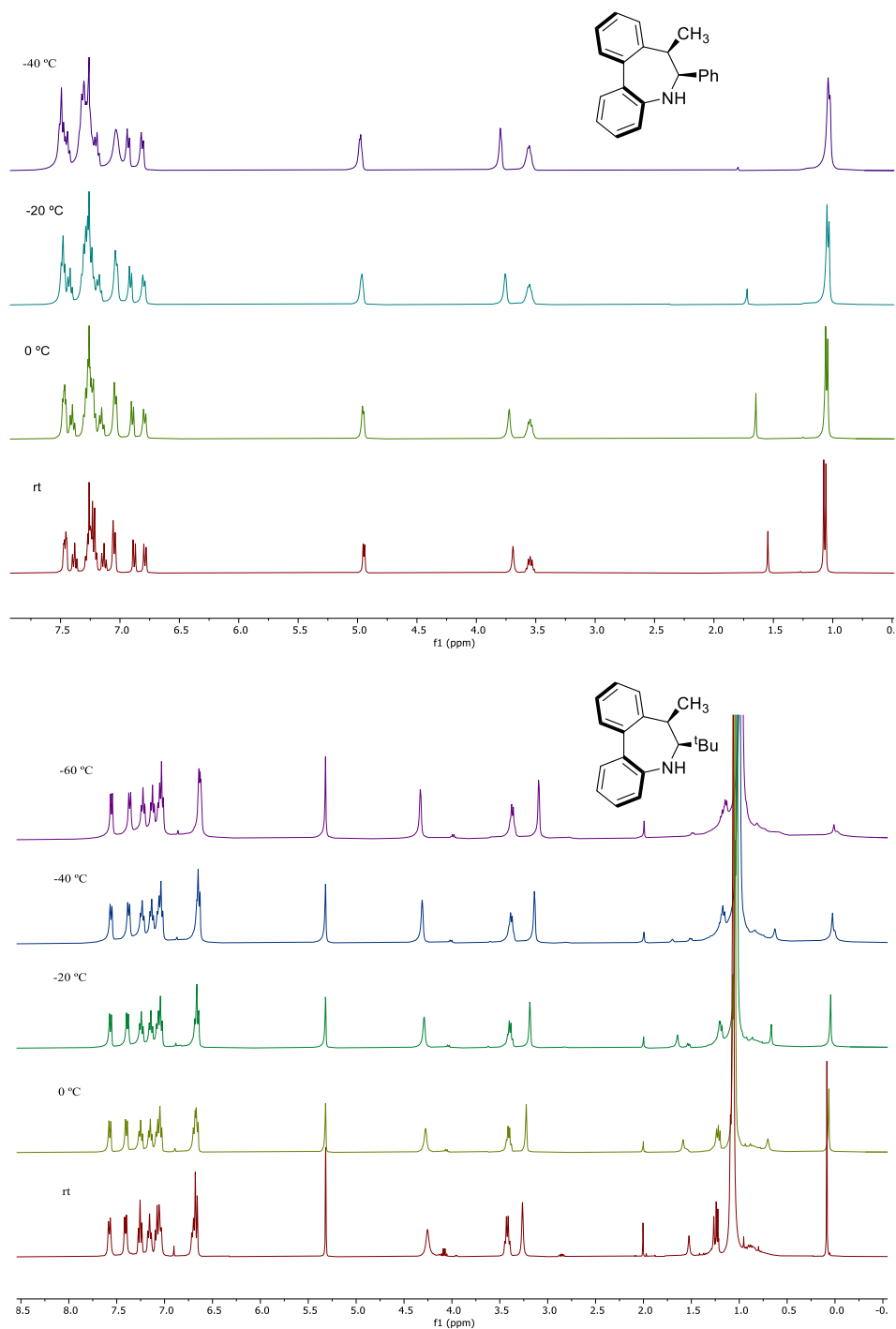


Figure 25: comparison of low temperature ¹H-NMR analysis of compound 23aa and compound 23aw.

The $R_a,6S,7R$ absolute configuration for **23aw** was assigned based on the previously discussed DFT calculations and by the comparison of a NOESY experiment between **23aa** and **23aw**.

As it is shown in following **figure 26** for **23aa**, due to the relative gauche disposition between H7 and the -CH₃ group, it could be observed the correlation between the two signals as a blue dot in the corresponding NOESY experiment.

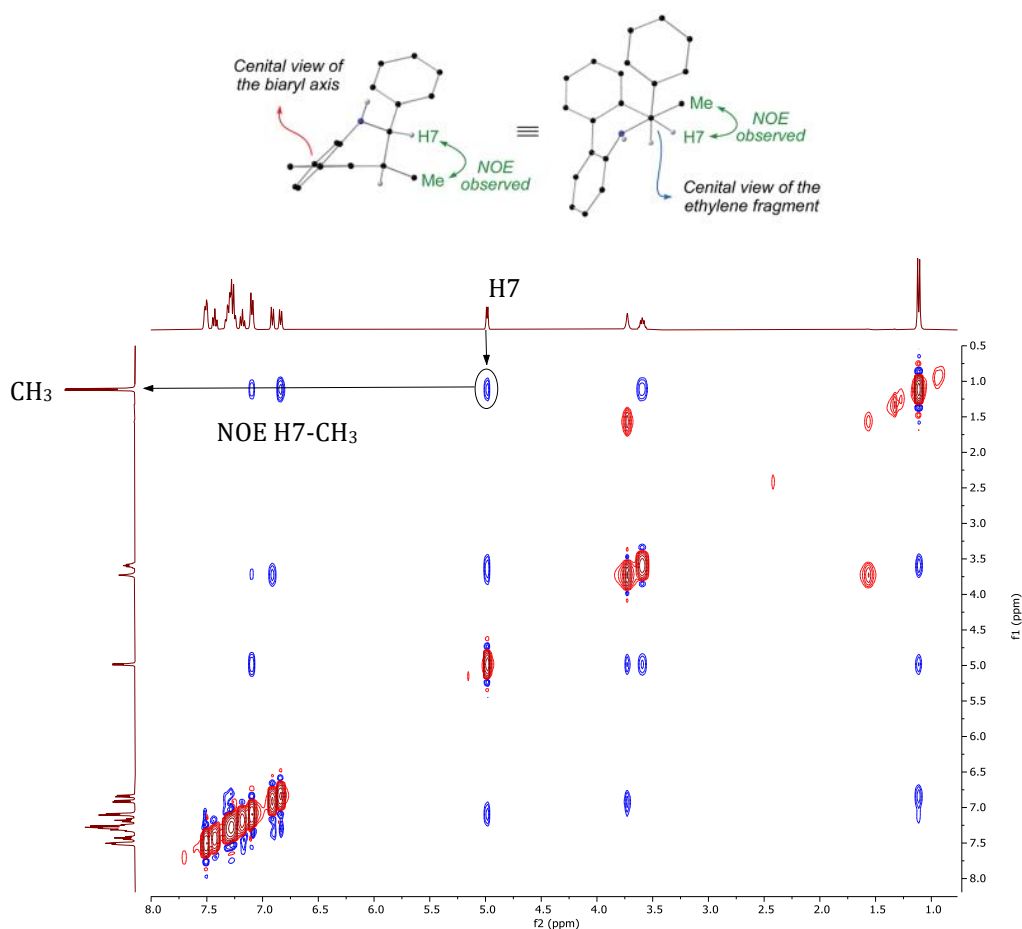


Figure 26: NOESY experiment for compound **23aa**.

However, as it can be observed in **figure 27**, for **23aw** the absence of a NOE between H7 and the CH₃ by the lack of the blue dot signal, proved the different

disposition of the corresponding groups, explained by the $R_a,6S,7R$ configuration. These results are in agreement with the DFT calculations.

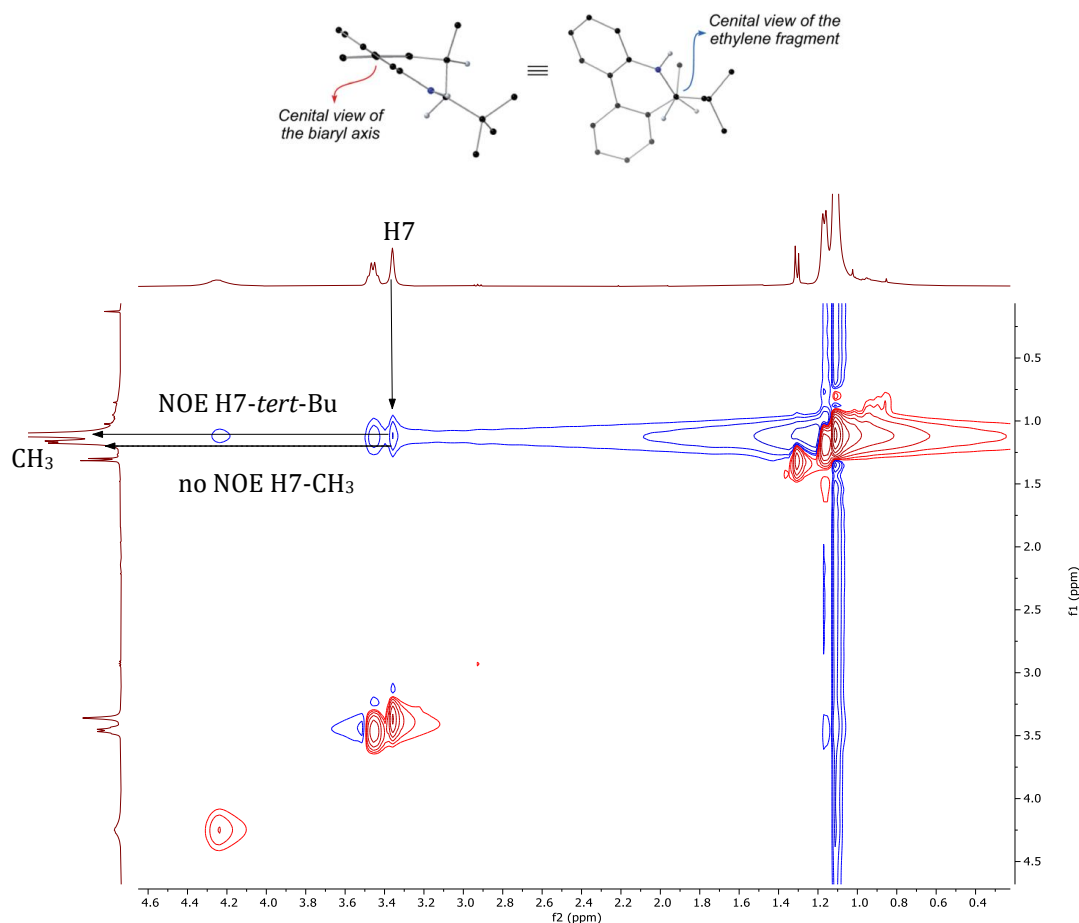


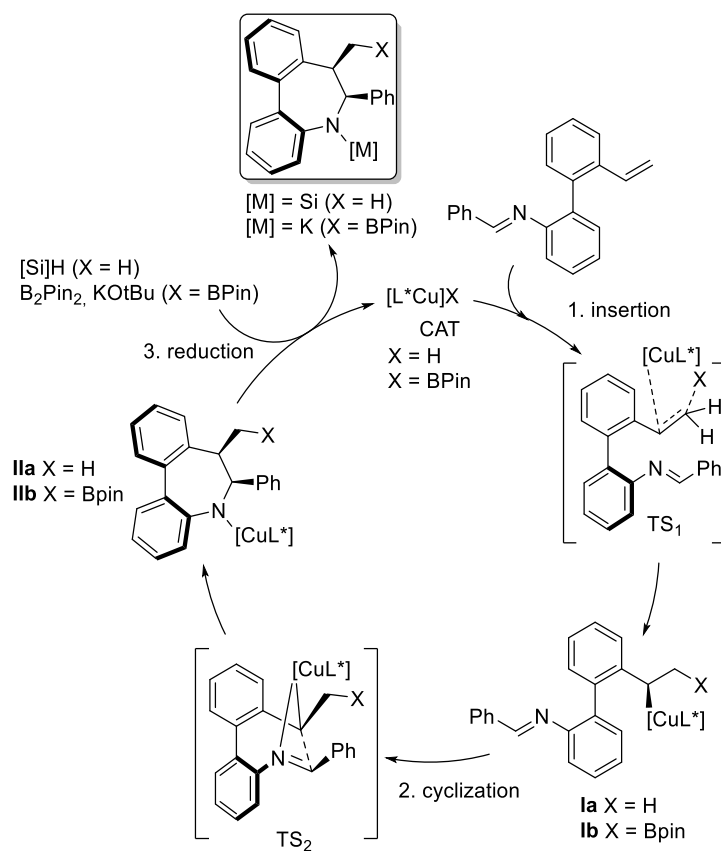
Figure 27: expansion of NOESY experiment (4.6-0.4 ppm) of compound **23aw**.

Based on the mechanistic studies carried out by Buchwald²²¹ and Hartwig²²² on asymmetric hydroamination and asymmetric hydroboration of alkenes, respectively, we proposed a catalytic cycle for the intramolecular reductive or borylative cyclization of dibenzoazepines, showed in **scheme 155**. The catalytic cycle begin with the insertion (**1**) of the *in situ* formed [L*Cu]X catalyst **CAT** (X = H) into the

²²¹ Y. Yang, S.-L. Shi, D. Niu, P. Liu, S. L. Buchwald, *Science*, **2015**, 349, 62–66.

²²² Y. Xi, J. F. Hartwig, *J. Am. Chem. Soc.*, **2017**, 139, 12758–12772.

double bond, through a four membered transition state (**TS₁**), in which the formation of the Cu-C bond and the delivery of the hydride to the olefin carbon occurs simultaneously, forming complex **Ia**. Buchwald and Hartwig described that the alkene insertion determined the enantio- and regioselectivity of the reaction. Successively, *cis*-selective cyclization via a well-organized transition state **TS₂** assisted by coordination of the imine nitrogen, afforded complex **IIa** that further reacted with [Si]H (for the reductive cyclization), in order to regenerate the [L*Cu]H active species, delivering the desired enantioenriched dibenzo[*b,d*]azepine. A similar model and catalytic cycle can be proposed for the borylative cyclization (X = Bpin).



Scheme 155: proposed catalytic mechanism for the asymmetric synthesis of dibenzo[*b,d*]azepines by Cu-catalyzed reductive or borylative cyclization.

IV.4. Conclusions.

To summarize this chapter, we have developed a novel methodology for the enantioselective synthesis of dibenzo[*b,d*]diazepines bearing both central and axial chirality through copper-catalyzed asymmetric intramolecular reductive or borylative cyclizations.

The resulting products were obtained with good yields and excellent diastereo- and enantioselectivities, under mild conditions.

Furthermore, axially chiral biaryl-2-amines were also obtained featuring nearly perfect enantioselectivity *via* a kinetic resolution process.

Computational studies confirmed that the axial chirality is controlled by a thermodynamic equilibrium completely shifted to the diastereomer with lower energy, and the configuration of the axis is controlled by the nature of the imine R group.

IV.5. Experimental Section.

IV.5.1. Synthesis of starting materials.

IV.5.1.1. General procedure for the synthesis of amine precursors.

Procedure A: Following a described procedure.²²³ An oven-dried round-bottom flask equipped with a magnetic stir bar was charged with Pd(dba)₂ (5 mol%), SPhos (6 mol%) and the reaction vessel was capped then evacuated and backfilled with N₂ using the Schlenk line (this process was repeated a total of three times). Thoroughly degassed THF (0.20 M) was then added via syringe and the resulting mixture was stirred for 5 min at room temperature. Then, the corresponding 1-bromo-2-vinylbenzene (1.0 equiv.), the corresponding phenylboronic acid (1.25 equiv.), K₂CO₃ (3.0 equiv.) and H₂O (0.6 M for a THF/H₂O = 3:1) were added, and the resulting mixture was placed in a preheated oil bath and stirred at 60 °C for 18 h. The reaction crude was allowed to reach room temperature, water (30 mL) was added, and the resulting mixture was extracted with AcOEt (3 × 15 mL). The combined organic layer was dried over anhydrous Na₂SO₄, filtered and concentrated in vacuo. The crude mixture was purified by flash column chromatography.

Procedure B: Following a described procedure.²²⁴ The corresponding carbamate (1.0 equiv.) was treated with TFA (8.0 equiv.) in DCM (0.40 mL) at rt. After 30 min, the solvent was blown off with N₂, the residue was diluted with DCM, basified with sat. NaHCO₃, extracted with DCM, dried over MgSO₄, and concentrated in vacuo. The residue was purified by column chromatography.

Procedure C: An oven-dried round-bottom flask equipped with a magnetic stir bar was charged with Pd₂(dba)₃ (3 mol%), SPhos (6 mol%) and the reaction vessel was capped then evacuated and backfilled with N₂. Thoroughly degassed THF (0.20 M) was then added via syringe and the resulting mixture was stirred for 5 min at room temperature. Then, the corresponding 1-bromo-2-vinylbenzene derivative (1.0

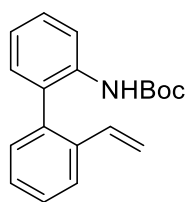
²²³ X.-J. Dai; O. D. Engl; T. Leon, S.L. Buchwald, *Angew. Chem., Int. Ed.*, 2019, **58**, 3407–3411.

²²⁴ S. W. Youn, S.J. Pastine, D. Sames, *Org. Lett.*, **2004**, *6*, 581–584.

equiv.), the corresponding phenylboronic acid (1.25 equiv.), K_2CO_3 (3.0 equiv.) and H_2O (0.6 M for a THF/ H_2O = 3:1) were added, and the resulting mixture was placed in a preheated oil bath and stirred at 60 °C for 18 h. The reaction crude was allowed to reach room temperature, water (30 mL) was added, and the resulting mixture was extracted with AcOEt (3 × 15 mL). The residue was directly treated TFA (8.0 equiv.) in DCM (0.40 M) at rt. After 30 min, the solvent was blown off with N_2 , the residue was diluted with DCM, basified with sat. $NaHCO_3$, extracted with DCM, dried over $MgSO_4$, and concentrated in vacuo. The residue was purified by column chromatography.

Procedure D: An oven-dried round-bottom flask equipped with a magnetic stir bar was charged with $Pd_2(dba)_3$ (3 mol%), SPhos (6 mol%) and the reaction vessel was capped then evacuated and backfilled with N_2 . Thoroughly degassed THF (0.2 M) was then added via syringe and the resulting mixture was stirred for 5 min at room temperature. Then, the corresponding bromo-vinylbenzene derivative (1.0 equiv.), phenylboronic acid (1.25 equiv.), K_2CO_3 (3.0 equiv.) and H_2O (0.6 M for a THF/ H_2O = 3:1) were added, and the resulting mixture was placed in a preheated oil bath and stirred at 60 °C for 18 h. The reaction crude was allowed to reach room temperature, water (30 mL) was added, and the resulting mixture was extracted with AcOEt (3 × 15 mL). The combined organic layer was dried over anhydrous Na_2SO_4 , filtered and concentrated in vacuo. The residue was then solved in DCM (0.45 M) and HCl (4M in dioxane, 10 equiv.) was added at 0 °C. The reaction was then allowed to reach rt and after 2 h, the solvent was removed under vacuum. The resulting mixture was dissolved with DCM, basified with sat. $NaHCO_3$, extracted with DCM, dried over $MgSO_4$, and concentrated in vacuo. The residue was purified by column chromatography.

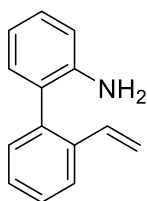
Tert-butyl (2'-vinyl-[1,1'-biphenyl]-2-yl)carbamate (33). Prepared following



general **procedure A** using the corresponding 1-bromo-2-vinylbenzene (701 mg, 3.83 mmol). The crude mixture was purified by flash column chromatography (20:1 hexane/EtOAc) to afford **33**

as a yellow oil (941 mg, 83% yield). $^1\text{H NMR}$ (400 MHz, CDCl_3) δ 8.13 (d, $J = 8.3$ Hz, 1H), 7.75 (dd, $J = 7.7, 1.6$ Hz, 1H), 7.48-7.37 (m, 3H), 7.27-7.24 (m, 1H), 7.17-7.10 (m, 2H), 6.49 (dd, $J = 17.5, 11.0$ Hz, 1H), 6.14 (s, 1H), 5.75 (dd, $J = 17.5, 1.2$ Hz, 1H), 5.21 (dd, $J = 11.0, 1.2$ Hz, 1H), 1.47 (s, 9H). $^{13}\text{C NMR}$ (100 MHz, CDCl_3) δ 152.9, 136.6, 136.4, 136.0, 134.6, 134.5, 130.7, 130.4, 129.8, 128.5, 128.5, 128.3, 125.5, 122.8, 119.6, 115.6, 115.5, 80.4, 28.3.

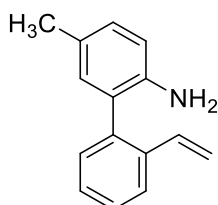
2'-Vinyl-[1,1'-biphenyl]-2-amine (21aa). Prepared following general **procedure B**



using the corresponding carbamate **33** (1403 mg, 4.75 mmol). The residue was purified by column chromatography on silica gel by eluting 15:1 hexane/EtOAc to give **21aa** (862 mg, 93%) as a white solid. $^1\text{H NMR}$ (400 MHz, CDCl_3) δ 7.75 (d, $J = 7.0$ Hz, 1H), 7.40 (m,

2H), 7.30 (m, 1H), 7.24 (td, $J = 7.7, 1.7$ Hz, 1H), 7.09 (dd, $J = 7.7, 1.7$ Hz, 1H), 6.88 (t, $J = 7.5$ Hz, 1H), 6.83 (d, $J = 8.1$ Hz, 1H), 6.63 (dd, $J = 17.6, 11.0$ Hz, 1H), 5.77 (d, $J = 17.6$ Hz, 1H), 5.22 (d, $J = 11.0$ Hz, 1H), 3.62 (s, 2H). $^{13}\text{C NMR}$ (100 MHz, CDCl_3) δ 143.5, 137.8, 136.3, 135.0, 130.8, 130.7, 128.7, 128.2, 128.0, 126.6, 125.2, 118.6, 115.5, 114.9.

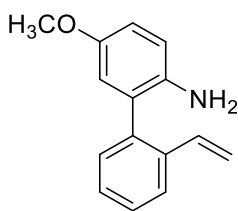
5-Methyl-2'-vinyl-[1,1'-biphenyl]-2-amine (21ba). Prepared following general



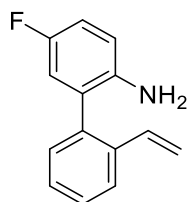
procedure C using the corresponding 1-bromo-2-vinylbenzene (94 μL , 0.73 mmol). The residue was purified by column chromatography on silica gel by eluting 15:1 hexane/EtOAc to give **21ba** as a colorless oil (151 mg, 99% yield). $^1\text{H NMR}$ (400 MHz, CDCl_3) δ 7.74-7.72 (m, 1H), 7.42-7.33 (m, 2H), 7.29-7.26

(m, 1H), 7.03 (d, $J = 8.1$ Hz, 1H), 6.89 (s, 1H), 6.71 (d, $J = 8.1$ Hz, 1H), 6.68-6.58 (m, 1H) 5.77 (dt, $J = 17.6, 1.6$ Hz, 1H), 5.20 (dt, $J = 11.0, 1.5$ Hz, 1H), 3.41 (br s, 2H), 2.31 (s, 3H). $^{13}\text{C NMR}$ (100 MHz, CDCl_3) δ 141.4, 138.2, 136.2, 135.1, 131.2, 130.7, 129.2, 128.2, 127.9, 127.5, 126.6, 125.1, 115.5, 114.7, 20.5.

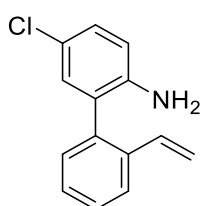
5-Methoxy-2'-vinyl-[1,1'-biphenyl]-2-amine (21bb). Following the general **procedure C**, using 1-bromo-2-vinylbenzene (90 μ L, 0.69 mmol). The residue was purified by column chromatography on silica gel by eluting 15:1 hexane/EtOAc to give **21bb** as a colorless oil (110 mg, 71% yield). $^1\text{H NMR}$ (400 MHz, CDCl_3) δ 7.71 (d, $J = 7.2$ Hz, 1H), 7.54-7.32 (m, 2H), 7.30-7.16 (m, 1H), 6.81 (dd, $J = 8.7, 2.9$ Hz, 1H), 6.72 (d, $J = 8.6$ Hz, 1H), 6.66 (d, $J = 2.9$ Hz, 1H), 6.61 (dd, $J = 17.6, 11.0$ Hz, 1H), 5.75 (dd, $J = 17.6, 1.2$ Hz, 1H), 5.20 (dd, $J = 11.0, 1.2$ Hz, 1H), 3.76 (s, 3H), 3.16 (br s, 2H). $^{13}\text{C NMR}$ (100 MHz, CDCl_3) δ 152.4, 137.9, 137.6, 136.2, 134.9, 130.5, 128.2, 128.0, 127.6, 125.2, 116.6, 115.8, 115.0, 114.7, 55.8.



5-Fluoro-2'-vinyl-[1,1'-biphenyl]-2-amine (21bc). Following the general **procedure C**, using 1-bromo-2-vinylbenzene (106 μ L, 0.82 mmol). The residue was purified by column chromatography on silica gel by eluting 15:1 hexane/EtOAc to give **21bc** as a colorless oil (131 mg, 75% yield). $^1\text{H NMR}$ (400 MHz, CDCl_3) δ 7.72 (d, $J = 7.5$ Hz, 1H), 7.44-7.35 (m, 2H), 7.25 (dd, $J = 7.5, 1.6$ Hz, 1H), 6.93 (td, $J = 8.5, 3.0$ Hz, 1H), 6.81 (dd, $J = 9.0, 3.0$ Hz, 1H), 6.71 (dd, $J = 8.8, 4.8$ Hz, 1H), 6.59 (dd, $J = 17.5, 11.0$ Hz, 1H), 5.76 (dd, $J = 17.6, 1.1$ Hz, 1H), 5.22 (dd, $J = 11.0, 1.1$ Hz, 1H), 3.41 (s, 2H). $^{13}\text{C NMR}$ (100 MHz, CDCl_3) δ 156.0 (d, $J = 236.5$ Hz), 140.1 (d, $J = 2.2$ Hz), 136.8 (d, $J = 1.5$ Hz), 136.2, 134.6, 130.4, 128.3, 125.3, 117.1, 116.9, 116.1, 116.0, 115.3, 115.2, 115.0. $^{19}\text{F NMR}$ (377 MHz, CDCl_3) δ -126.9.

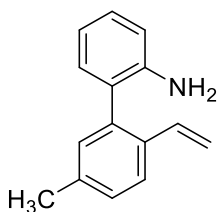


5-chloro-2'-vinyl-[1,1'-biphenyl]-2-amine (21bd). Following the general **procedure C**, using 1-bromo-2-vinylbenzene (47 μ L, 0.36 mmol). The residue was purified by column chromatography on silica gel by eluting 15:1 hexane/EtOAc to give **21bd** as a colorless oil (91 mg, 99% yield). $^1\text{H NMR}$ (400 MHz, CDCl_3) δ 7.70 (dd, $J = 7.4, 1.6$ Hz, 1H), 7.39 - 7.30 (m, 2H), 7.27 - 7.18 (m, 1H), 7.14 (dd, $J = 8.5, 2.5$ Hz, 1H), 7.03 (d, $J = 2.5$ Hz, 1H), 6.68 (d, $J = 8.5$ Hz, 1H), 6.56 (dd, $J = 17.5, 11.0$ Hz, 1H), 5.75 (dd, $J = 17.5, 1.2$ Hz, 1H), 5.21 (dd, $J = 11.0, 1.1$ Hz, 1H), 3.52 (s, 2H). $^{13}\text{C NMR}$ (100MHz, CDCl_3) δ 143.4,



142.6, 136.5, 136.2, 134.5, 130.5, 130.2, 129.0, 128.5, 128.4, 128.4, 127.7, 125.5, 125.3, 122.8, 116.3, 115.4.

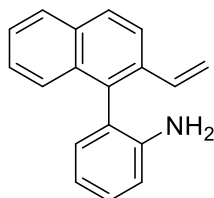
5'-Methyl-2'-vinyl-[1,1'-biphenyl]-2-amine (21ca). Following the general



procedure D, using 2-bromo-4-methyl-1-vinylbenzene (307 mg, 1.56 mmol). The residue was purified by column chromatography on silica gel by eluting 15:1 hexane/EtOAc to give **21ca** as a yellow oil (135 mg, 42% yield). ¹H NMR (400 MHz, CDCl₃) δ 7.68 (d, *J* = 8.0 Hz, 1H), 7.26-7.22 (m, 2H), 7.15 (s, 1H)

7.10 (dd, *J* = 7.5, 1.6 Hz, 1H), 6.88 (t, *J* = 7.4 Hz, 1H), 6.80 (d, *J* = 8.0 Hz, 1H), 6.63 (dd, *J* = 17.6, 11.0 Hz, 1H), 5.75 (d, *J* = 17.6 Hz, 1H), 5.18 (dd, *J* = 11.0, 1.3 Hz, 1H), 3.56 (s, 2H), 2.44 (s, 3H). ¹³C NMR (100 MHz, CDCl₃) δ 144.0, 138.1, 137.9, 134.9, 133.5, 131.3, 130.7, 128.8, 128.6, 126.6, 125.1, 118.3, 115.2, 113.9, 21.2.

2-(2-Vinylnaphthalen-1-yl)aniline (24). Following the general **procedure D**, 1-



bromo-2-vinylnaphthalene (197 mg, 0.85 mmol). The residue was purified by column chromatography on silica gel by eluting 1:4 hexane/toluene to give **23** as a colorless oil (144 mg, 97% yield). ¹H NMR (400 MHz, CDCl₃) δ 7.92-7.87 (m, 3H), 7.53 (d, *J* =

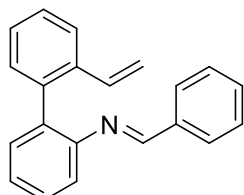
8.4 Hz, 1H), 7.49 (ddd, *J* = 8.1, 6.7, 1.3 Hz, 1H), 7.44-7.37 (m, 1H), 7.32 (td, *J* = 7.7, 1.6 Hz, 1H), 7.09 (dd, *J* = 7.4, 1.6 Hz, 1H), 6.94 (td, *J* = 7.4, 1.1 Hz, 1H), 6.87 (dd, *J* = 8.0, 1.1 Hz, 1H), 6.72 (dd, *J* = 17.6, 11.0 Hz, 1H), 5.87 (dd, *J* = 17.6, 1.1 Hz, 1H), 5.28 (dd, *J* = 11.1, 1.0 Hz, 1H), 3.36 (s, 2H). ¹³C NMR (100 MHz, CDCl₃) δ 144.6, 135.2, 134.5, 133.6, 133.5, 132.6, 131.6, 128.9, 128.2, 128.0, 126.6, 126.6, 126.1, 123.5, 122.7, 118.5, 115.4, 115.2.

IV.5.1.2. General procedure for the synthesis of aldimines substrates.

Aldimines **22** were made from corresponding aniline using a literature protocol. A mixture of aniline derivative (1.0 equiv) and MgSO₄ (360 mg/mmol aniline) was evacuated/refilled with N₂ three times. To this mixture, anhydrous toluene was added, followed by the addition of aldehyde derivative (1.1 equiv) and glacial acetic

acid (286 $\mu\text{L}/\text{mmol}$ aniline). Then, the reaction mixture was stirred overnight at 80 $^{\circ}\text{C}$ and cooled to room temperature. The mixture was filtered through celite, and the filtrate was concentrated in vacuo. The residue was purified via flash column chromatography with silica gel (eluting with 20:1 Hexane/ Et_3N) to yield the corresponding imine.

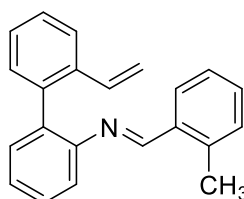
(*E*)-1-Phenyl-*N*-(2'-vinyl-[1,1'-biphenyl]-2-yl)methanimine (22aa). Prepared



following general procedure, using **21aa** (59 mg, 0.3 mmol), to obtain **22aa** (81 mg, 95% yield) as yellow oil. ^1H NMR (400 MHz, CDCl_3) δ 8.32 (s, 1H), 7.68-7.65 (m, 2H), 7.62 (m, 1H), 7.46-7.36 (m, 4H), 7.35-7.26 (m, 5H), 7.12 (ddd, $J = 7.8, 1.2, 0.6$

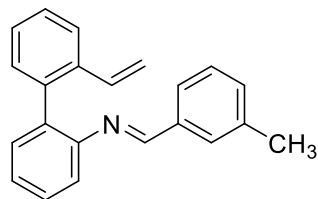
Hz, 1H), 6.60 (dd, $J = 17.5, 11.0$ Hz, 1H), 5.60 (dd, $J = 17.5, 1.3$ Hz, 1H), 5.10 (dd, $J = 11.0, 1.3$ Hz, 1H). ^{13}C NMR (100 MHz, CDCl_3) δ 160.5, 150.6, 138.7, 136.4, 136.3, 136.07, 136.05, 134.4, 131.2, 131.1, 130.9, 128.7, 128.5, 127.3, 127.1, 125.3, 124.8, 118.8, 114.0. HRMS (ESI) calcd. for $\text{C}_{21}\text{H}_{18}\text{N}$ ($\text{M} + \text{H}^+$) 284.1439. Found 284.1431.

(*E*)-1-*o*-Tolyl-*N*-(2'-vinyl-[1,1'-biphenyl]-2-yl)methanimine (22ab). Prepared

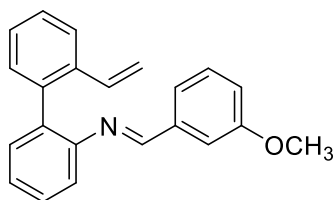


following general procedure, using **21aa** (59 mg, 0.3 mmol), to obtain **22ab** (80 mg, 90% yield) as yellow oil. ^1H NMR (400 MHz, CDCl_3) δ 8.54 (s, 1H), 7.72 (d, $J = 7.7$ Hz, 1H), 7.63 (d, $J = 7.3$ Hz, 1H), 7.45 (m, 1H), 7.36-7.25 (m, 6H), 7.21 (m, 1H), 7.13

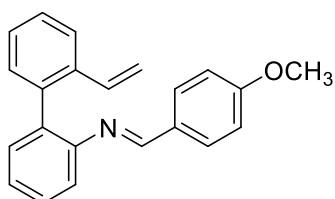
(m, 2H), 6.61 (dd, $J = 17.6, 11.0$ Hz, 1H), 5.61 (d, $J = 17.5$ Hz, 1H), 5.11 (d, $J = 11.0$ Hz, 1H), 2.35 (s, 3H). ^{13}C NMR (100 MHz, CDCl_3) δ 160.1, 151.3, 138.9, 138.5, 136.3, 135.9, 134.2, 134.1, 131.1, 130.84, 130.83, 130.6, 128.6, 128.5, 127.3, 127.2, 126.1, 125.2, 124.8, 119.1, 114.1, 19.5. HRMS (ESI) calcd. for $\text{C}_{22}\text{H}_{20}\text{N}$ ($\text{M} + \text{H}^+$) 298.1596. Found 298.1587.

(*E*)-1-*m*-Tolyl-*N*-(2'-vinyl-[1,1'-biphenyl]-2-yl)methanimine (22ac).

Prepared following general procedure, using **21aa** (59 mg, 0.3 mmol) to obtain **22ac** (80 mg, 90% yield) as a yellow oil. $^1\text{H NMR}$ (400 MHz, CDCl_3) δ 8.27 (s, 1H), 7.63 (m, 1H), 7.50-7.41 (m, 3H), 7.34-7.23 (m, 7H), 7.11 (dd, $J = 7.8, 1.2$ Hz, 1H), 6.60 (dd, $J = 17.5, 11.0$ Hz, 1H), 5.61 (dd, $J = 17.5, 1.4$ Hz, 1H), 5.11 (dd, $J = 11.0, 1.4$ Hz, 1H), 2.37 (s, 3H). $^{13}\text{C NMR}$ (100 MHz, CDCl_3) δ 160.9, 150.8, 138.7, 138.2, 136.4, 136.3, 136.1, 134.2, 131.9, 131.2, 130.9, 129.1, 128.5, 128.4, 127.3, 127.1, 126.0, 125.2, 124.8, 118.9, 114.0, 21.3. HRMS (ESI) calcd. for $\text{C}_{22}\text{H}_{20}\text{N}$ ($\text{M} + \text{H}^+$) 298.1596. Found 298.1593.

(*E*)-1-(3-Methoxyphenyl)-*N*-(2'-vinyl-[1,1'-biphenyl]-2-yl)methanimine (22ad).

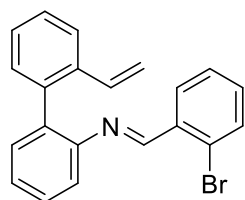
Prepared following general procedure, using **21aa** (98 mg, 0.5 mmol) to obtain **22ad** (126 mg, 80% yield) as a yellow oil. $^1\text{H NMR}$ (400 MHz, CDCl_3) δ 8.30 (s, 1H), 7.74-7.59 (m, 1H), 7.45 (ddd, $J = 7.9, 6.8, 2.1$ Hz, 1H), 7.35-7.28 (m, 6H), 7.26 (m, 1H), 7.21 (dt, $J = 7.5, 1.3$ Hz, 1H), 7.14 (ddd, $J = 7.9, 1.3, 0.6$ Hz, 1H), 6.99 (ddd, $J = 8.2, 2.7, 1.1$ Hz, 1H), 6.62 (dd, $J = 17.5, 11.0$ Hz, 1H), 5.62 (dd, $J = 17.5, 1.3$ Hz, 1H), 5.12 (dd, $J = 11.0, 1.3$ Hz, 1H), 3.80 (s, 3H). $^{13}\text{C NMR}$ (100 MHz, CDCl_3) δ 160.2, 159.8, 150.3, 138.8, 137.9, 136.3, 136.1, 134.5, 131.1, 130.9, 129.5, 128.6, 127.3, 127.1, 125.5, 124.7, 122.1, 118.6, 118.0, 113.9, 111.8, 55.3. HRMS (ESI) calcd. for $\text{C}_{22}\text{H}_{20}\text{NO}$ ($\text{M} + \text{H}^+$) 314.1545. Found 314.1537.

(*E*)-1-(4-Methoxyphenyl)-*N*-(2'-vinyl-[1,1'-biphenyl]-2-yl)methanimine (22ae).

Prepared following general procedure, using **21aa** (98 mg, 0.5 mmol) to obtain **22ae** (145 mg, 93% yield) as a yellow oil. $^1\text{H NMR}$ (400 MHz, CDCl_3) δ 8.28 (s, 1H), 7.69-7.62 (m, 3H), 7.45 (m, 1H), 7.38-7.30 (m, 5H), 7.14 (d, $J = 7.9$ Hz, 1H), 6.92 (m, 2H), 6.65 (dd, $J = 17.5, 11.0$ Hz, 1H), 5.64 (d, $J = 17.5$ Hz, 1H), 5.13 (d, $J = 11.0$ Hz, 1H), 3.85 (s, 3H). $^{13}\text{C NMR}$ (100 MHz, CDCl_3) δ 162.1, 159.8, 150.9, 139.0, 136.4, 136.2, 134.4, 131.2, 131.0, 130.4, 129.6, 128.6, 127.3, 127.1,

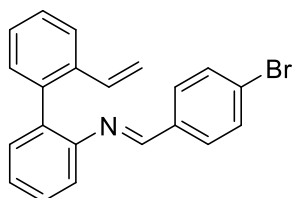
125.0, 124.8, 118.9, 114.0, 113.9, 55.4. HRMS (ESI) calcd. for C₂₂H₂₀NO (M + H⁺) 314.1545. Found 314.1541.

(E)-1-(2-Bromophenyl)-N-(2'-vinyl-[1,1'-biphenyl]-2-yl)methanimine (22af).



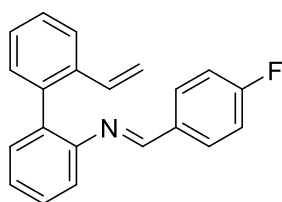
Prepared following general procedure, using **21aa** (59 mg, 0.3 mmol) to obtain **22af** (104 mg, 95% yield) as yellow oil. ¹H NMR (400 MHz, CDCl₃) δ 8.69 (s, 1H), 7.82-7.79 (m, 1H), 7.64-7.62 (m, 1H), 7.57-7.55 (m, 1H), 7.48-7.44 (m, 1H), 7.37-7.25 (m, 7H), 7.17-7.15 (m, 1H), 6.57 (dd, *J* = 17.5, 11.0 Hz, 1H), 5.60 (dd, *J* = 17.5, 1.3 Hz, 1H), 5.11 (dd, *J* = 11.0, 1.3 Hz, 1H). ¹³C NMR (100 MHz, CDCl₃) δ 159.7, 150.3, 138.6, 136.3, 135.9, 134.8, 134.5, 132.9, 132.1, 131.2, 130.8, 129.2, 128.6, 127.6, 127.4, 127.1, 125.8, 125.6, 124.8, 118.9, 114.1. HRMS (ESI) calcd. for C₂₁H₁₇BrN (M + H⁺) 362.0544. Found 362.0540.

(E)-1-(4-Bromophenyl)-N-(2'-vinyl-[1,1'-biphenyl]-2-yl)methanimine (22ag).



Prepared following general procedure, using **21aa** (98 mg, 0.5 mmol) to obtain **22ag** (155 mg, 85% yield) as a yellow oil. ¹H NMR (400 MHz, CDCl₃) δ 8.22 (s, 1H), 7.58 (d, *J* = 7.5 Hz, 1H), 7.49 (s, 4H), 7.41 (ddd, *J* = 7.9, 6.1, 2.9 Hz, 1H), 7.32-7.26 (m, 4H), 7.25-7.21 (m, 1H), 7.08 (d, *J* = 7.7 Hz, 1H), 6.52 (dd, *J* = 17.5, 11.0 Hz, 1H), 5.55 (dd, *J* = 17.5, 1.3 Hz, 1H), 5.05 (dd, *J* = 11.0, 1.3 Hz, 1H). ¹³C NMR (100 MHz, CDCl₃) 159.1, 150.2, 138.7, 136.3, 136.0, 135.3, 134.5, 131.9, 131.2, 130.9, 130.1, 128.6, 127.5, 127.2, 125.7, 124.8, 118.6, 114.1. HRMS (ESI) calcd. for C₂₁H₁₆BrN (M + H⁺) 362.0544. Found 362.0538.

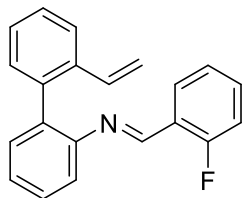
(E)-1-(4-Fluorophenyl)-N-(2'-vinyl-[1,1'-biphenyl]-2-yl)methanimine (22ah).



Prepared following general procedure, using **21aa** (98 mg, 0.5 mmol) to obtain **22ah** (137 mg, 91% yield) as a yellow oil. ¹H NMR (400 MHz, CDCl₃) δ 8.24 (s, 1H), 7.61 (m, 3H), 7.41 (m, 1H), 7.29 (m, 5H), 7.04 (m, 3H), 6.55 (dd, *J* = 17.5, 11.0 Hz, 1H), 5.57 (d, *J* = 17.5 Hz, 1H), 5.06 (d, *J* = 11.0 Hz, 1H). ¹³C NMR (100 MHz, CDCl₃) δ 164.6 (d, *J* = 251.6 Hz), 159.0, 150.3, 138.7, 136.3,

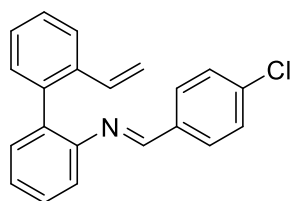
136.0, 134.5, 132.8, 131.2, 130.8, 130.7, 130.6, 128.6, 127.4, 127.1, 125.4, 124.7, 118.7, 115.8, 115.6, 114.0. ^{19}F NMR (377 MHz, CDCl_3) δ -108.6. HRMS (ESI) calcd. for $\text{C}_{21}\text{H}_{17}\text{FN}$ ($\text{M} + \text{H}^+$) 302.1435. Found 302.1337.

(E)-1-(2-Fluorophenyl)-N-(2'-vinyl-[1,1'-biphenyl]-2-yl)methanimine (22ai).



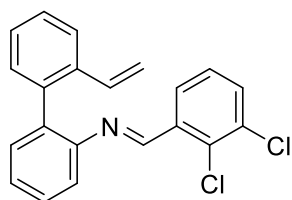
Prepared following general procedure, using **21aa** (59 mg, 0.3 mmol) to obtain **22ai** (76 mg, 85% yield) as yellow oil. ^1H NMR (400 MHz, CDCl_3) δ 8.65 (s, 1H), 7.78 (t, $J = 6.9$ Hz, 1H), 7.62 (d, $J = 7.6$ Hz, 1H), 7.46-7.26 (m, 7H), 7.14-7.05 (m, 3H), 6.57 (dd, $J = 17.5, 10.9$ Hz, 1H), 5.60 (dd, $J = 17.5, 1.4$ Hz, 1H), 5.10 (dd, $J = 10.9, 1.4$ Hz, 1H). ^{13}C NMR (100 MHz, CDCl_3) δ 162.7 (d, $J = 253.1$ Hz), 153.7 (d, $J = 5.1$ Hz), 150.6, 138.7, 136.4, 136.0, 134.7, 132.7 (d, $J = 8.8$ Hz), 131.1, 130.8, 128.6, 128.1, 127.4, 127.1, 125.7, 124.7, 124.4 (d, $J = 3.6$ Hz), 124.1 (d, $J = 9.2$ Hz), 118.6, 115.6 (d, $J = 21.0$ Hz), 114.0. ^{19}F NMR (377 MHz, CDCl_3) δ -121.7. HRMS (ESI) calcd. for $\text{C}_{21}\text{H}_{17}\text{FN}$ ($\text{M} + \text{H}^+$) 302.1435. Found 302.1337.

(E)-1-(4-Chlorophenyl)-N-(2'-vinyl-[1,1'-biphenyl]-2-yl)methanimine (22aj).



Prepared following general procedure, using **21aa** (98 mg, 0.5 mmol) to obtain **22aj** (111 mg, 70% yield) as a colorless oil. ^1H NMR (400 MHz, CDCl_3) δ 8.25 (s, 1H), 7.56 (m, 3H), 7.42 (m, 1H), 7.31 (m, 7H), 7.09 (d, $J = 7.8$ Hz, 1H), 6.54 (dd, $J = 17.6, 11.0$ Hz, 1H), 5.57 (d, $J = 17.5$ Hz, 1H), 5.07 (d, $J = 11.0$ Hz, 1H). ^{13}C NMR (100 MHz, CDCl_3) δ 159.0, 150.2, 138.6, 137.1, 136.3, 136.0, 134.9, 134.5, 131.2, 130.8, 129.8, 128.9, 128.6, 127.4, 127.1, 125.6, 124.8, 118.6, 114.0. HRMS (ESI) calcd. for $\text{C}_{21}\text{H}_{17}\text{ClN}$ ($\text{M} + \text{H}^+$) 318.1050. Found 318.1042

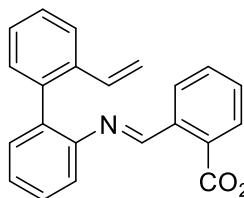
(E)-1-(3,4-Dichlorophenyl)-N-(2'-vinyl-[1,1'-biphenyl]-2-yl)methanimine (22ak).



Prepared following general procedure, using **21aa** (59 mg, 0.3 mmol) to obtain **22ak** (75 mg, 71% yield) as yellow oil. ^1H NMR (400 MHz, CDCl_3) δ 8.22 (s, 1H), 7.74 (s, 1H), 7.63 (d, $J = 7.5$ Hz, 1H), 7.45 (m, 3H), 7.39-7.23 (m, 5H), 7.10 (d, $J = 7.8$ Hz, 1H), 6.55 (dd, $J = 17.5, 11.0$ Hz, 1H), 5.60 (d, $J = 17.5$ Hz, 1H), 5.10

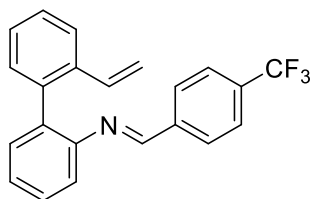
(*d*, *J* = 11.0 Hz, 1H). ¹³C NMR (100 MHz, CDCl₃) δ 157.7, 149.8, 138.5, 136.32, 136.27, 135.9, 135.1, 134.5, 133.0, 131.2, 130.8, 130.7, 130.2, 128.6, 127.5 (2C), 127.2, 125.9, 124.8, 118.5, 114.1. HRMS (ESI) calcd. for C₂₁H₁₆Cl₂N (M + H⁺) 352.0660. Found 352.0654.

Methyl (*E*)-3-(((2'-vinyl-[1,1'-biphenyl]-2-yl)imino)methyl)benzoate (22al).

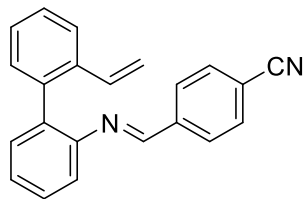


Prepared following general procedure, using **21aa** (98 mg, 0.5 mmol) to obtain **22al** (145 mg, 85% yield) as colorless oil. ¹H NMR (400 MHz, CDCl₃) δ 8.33 (s, 1H), 8.26 (s, 1H), 8.07 (d, *J* = 7.7 Hz, 1H), 7.86 (d, *J* = 7.8 Hz, 1H), 7.60 (d, *J* = 6.7 Hz, 1H), 7.42 (m, 2H), 7.33-7.25 (m, 5H), 7.10 (d, *J* = 7.4 Hz, 1H), 6.56 (dd, *J* = 17.5, 11.0 Hz, 1H), 5.57 (dd, *J* = 17.5, 1.3 Hz, 1H), 5.08 (dd, *J* = 11.0, 1.3 Hz, 1H), 3.92 (s, 3H). ¹³C NMR (100 MHz, CDCl₃) δ 166.6, 159.4, 150.2, 138.6, 136.8, 136.3, 136.0, 134.5, 132.2, 132.0, 131.2, 130.8, 130.6, 131.4, 128.8, 128.6, 127.4, 127.2, 125.7, 124.8, 118.7, 114.0, 52.3. HRMS (ESI) calcd. for C₂₃H₂₀NO₂ (M + H⁺) 342.1494. Found 342.1486.

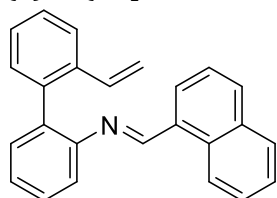
(*E*)-1-(4-(Trifluoromethyl)phenyl)-*N*-(2'-vinyl-[1,1'-biphenyl]-2-



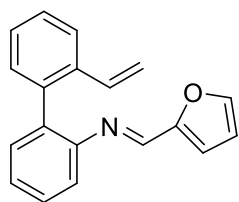
yl)methanimine (22am). Prepared following general procedure, using **21aa** (98 mg, 0.5 mmol) to obtain **22am** (126 mg, 72% yield) as colorless oil. ¹H NMR (400 MHz, CDCl₃) δ 8.35 (s, 1H), 7.82-7.69 (m, 2H), 7.68-7.57 (m, 3H), 7.44 (ddd, *J* = 7.8, 6.2, 2.7 Hz, 1H), 7.36-7.26 (m, 5H), 7.13 (d, *J* = 8.4 Hz, 1H), 6.57 (dd, *J* = 17.5, 11.0 Hz, 1H), 5.59 (dd, *J* = 17.5, 1.3 Hz, 1H), 5.09 (dd, *J* = 11.0, 1.3 Hz, 1H). ¹³C NMR (100 MHz, CDCl₃) δ, 158.8, 149.9, 139.4 (q, *J* = 1.4 Hz), 138.5, 136.3, 136.0, 134.7, 132.5 (q, *J* = 32.5 Hz), 131.2, 130.8, 128.8, 128.6, 127.5, 127.2, 126.0, 125.5 (q, *J* = 3.9 Hz), 124.8, 123.9 (d, *J* = 272.5 Hz), 118.5, 114.1. ¹⁹F NMR (377 MHz, CDCl₃) δ -62.8. HRMS (ESI) calcd. for C₂₂H₁₇F₃N (M + H⁺) 352.1313. Found 352.1307.

(*E*)-4-(((2'-Vinyl-[1,1'-biphenyl]-2-yl)imino)methyl)benzonitrile (22an).

Prepared following general procedure, using **21aa** (98 mg, 0.5 mmol) to obtain **22an** (145 mg, 94% yield) as orange oil. ¹H NMR (400 MHz, CDCl₃) δ 8.32 (s, 1H), 7.73-7.69 (m, 2H), 7.66-7.58 (m, 3H), 7.52-7.37 (m, 1H), 7.35-7.22 (m, 5H), 7.11 (d, *J* = 7.8 Hz, 1H), 6.52 (dd, *J* = 17.5, 11.0 Hz, 1H), 5.56 (dd, *J* = 17.6, 1.3 Hz, 1H), 5.06 (dd, *J* = 11.0, 1.3 Hz, 1H). ¹³C NMR (100 MHz, CDCl₃) δ 158.1, 149.6, 140.1, 138.4, 136.3, 135.9, 134.9, 132.4, 131.3, 130.8, 128.9, 128.7, 127.6, 127.2, 126.3, 124.8, 118.5, 118.3, 114.2, 114.1. HRMS (ESI) calcd. for C₂₂H₁₇N₂ (M + H⁺) 309.1392. Found 309.1386.

(*E*)-1-(Naphthalen-1-yl)-*N*-(2'-vinyl-[1,1'-biphenyl]-2-yl)methanimine (22ao).

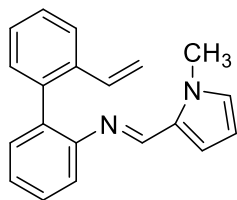
Prepared following general procedure, using **21aa** (98 mg, 0.5 mmol) to obtain **22ao** (141 mg, 85% yield) as a yellow oil. ¹H NMR (400 MHz, CDCl₃) δ 8.88 (s, 1H), 8.67 (d, *J* = 8.6 Hz, 1H), 7.89 (d, *J* = 8.2 Hz, 1H), 7.84 (dd, *J* = 8.2, 1.3 Hz, 1H), 7.78 (dd, *J* = 7.2, 1.2 Hz, 1H), 7.68 (d, *J* = 6.8 Hz, 1H), 7.53-7.46 (m, 3H), 7.43-7.29 (m, 6H), 7.23 (dd, *J* = 7.8, 1.2 Hz, 1H), 6.67 (dd, *J* = 17.5, 11.0 Hz, 1H), 5.63 (dd, *J* = 17.5, 1.3 Hz, 1H), 5.11 (dd, *J* = 11.0, 1.3 Hz, 1H). ¹³C NMR (100 MHz, CDCl₃) δ 160.8, 151.1, 139.2, 136.4, 135.9, 135.0, 133.8, 131.8, 131.7, 131.2, 130.9, 130.8 (x2), 128.8, 128.4, 127.4, 127.3, 127.3, 126.1, 125.6, 125.2, 125.0, 124.8, 118.3, 114.3. HRMS (ESI) calcd. for C₂₅H₂₀N (M + H⁺) 334.1596. Found 334.1587.

(*E*)-1-(Furan-2-yl)-*N*-(2'-vinyl-[1,1'-biphenyl]-2-yl)methanimine (22ap).

Prepared following general procedure, using **21aa** (98 mg, 0.5 mmol) to obtain **22ap** (55 mg, 40% yield) as orange oil. ¹H NMR (400 MHz, CDCl₃) δ 8.06 (s, 1H), 7.61 (dd, *J* = 7.0, 1.7 Hz, 1H), 7.51 (d, *J* = 1.7 Hz, 1H), 7.44-7.39 (m, 1H), 7.34-7.26 (m, 5H), 7.09 (d, *J* = 7.8 Hz, 1H), 6.77 (d, *J* = 3.4 Hz, 1H), 6.55 (dd, *J* = 17.5, 11.0 Hz, 1H), 6.48-6.45 (d, *J* = 1.7 Hz, 1H), 5.59 (dd, *J* = 17.6, 1.3 Hz, 1H), 5.11 (dd, *J* = 11.0, 1.3 Hz, 1H). ¹³C NMR (100 MHz, CDCl₃) δ 152.3, 150.6, 149.2, 145.4,

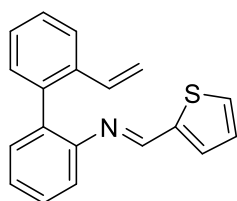
138.5, 136.4, 136.0, 133.9, 131.4, 131.0, 128.5, 127.4, 127.2, 125.3, 124.9, 119.5, 115.2, 114.2, 111.9. HRMS (ESI) calcd. for C₁₉H₁₆NO (M + H⁺) 274.1232. Found 274.1229.

(*E*)-1-(1-Methyl-1*H*-pyrrol-2-yl)-*N*-(2'-vinyl-[1,1'-biphenyl]-2-yl)methanimine



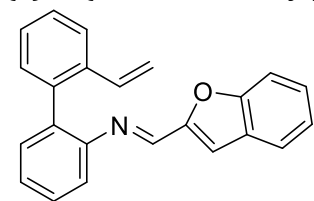
(22aq). Prepared following general procedure, using **21aa** (98 mg, 0.5 mmol) to obtain **22aq** (108 mg, 75% yield) as yellow oil. ¹H NMR (400 MHz, CDCl₃) δ 8.25 (s, 1H), 7.66 (d, *J* = 7.5 Hz, 1H), 7.44 (s, 1H), 7.36-7.25 (m, 5H), 7.14 (d, *J* = 7.9 Hz, 1H), 6.85-6.47 (m, 3H), 6.16 (s, 1H), 5.64 (d, *J* = 17.5 Hz, 1H), 5.11 (d, *J* = 11.0 Hz, 1H), 3.57 (s, 3H). ¹³C NMR (100 MHz, CDCl₃) δ 151.0, 150.2, 139.8, 136.2, 136.1, 135.6, 130.7, 130.7, 130.5, 129.1, 128.7, 127.1, 127.1, 124.9, 124.3, 118.7, 117.5, 113.8, 108.3, 36.9. HRMS (ESI) calcd. for C₂₀H₁₉N₂ (M + H⁺) 287.1548. Found 287.1540.

(*E*)-1-(Thiophen-2-yl)-*N*-(2'-vinyl-[1,1'-biphenyl]-2-yl)methanimine (22ar).



Prepared following general procedure, using **21aa** (98 mg, 0.5 mmol) to obtain **22ar** (75 mg, 52% yield) as yellow oil. ¹H NMR (400 MHz, CDCl₃) δ 8.38 (s, 1H), 7.63 (d, *J* = 7.2 Hz, 1H), 7.42 (d, *J* = 5.9 Hz, 2H), 7.37-7.25 (m, 6H), 7.14 (d, *J* = 7.8 Hz, 1H), 7.07 (t, *J* = 4.4 Hz, 1H), 6.58 (dd, *J* = 17.5, 11.0 Hz, 1H), 5.61 (d, *J* = 17.5 Hz, 1H), 5.11 (d, *J* = 11.0 Hz, 1H). ¹³C NMR (100 MHz, CDCl₃) δ 153.4, 150.0, 143.2, 138.6, 136.4, 136.1, 134.4, 131.4, 131.2, 130.9, 130.3, 128.5, 127.5, 127.3, 127.1, 125.4, 124.8, 119.0, 114.1. HRMS (ESI) calcd. for C₁₉H₁₆NS (M + H⁺) 290.1003. Found 290.1000.

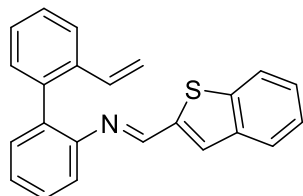
(*E*)-1-(Benzofuran-2-yl)-*N*-(2'-vinyl-[1,1'-biphenyl]-2-yl)methanimine (22as).



Prepared following general procedure, using **21aa** (98 mg, 0.5 mmol) to obtain **22as** (124 mg, 77% yield) as yellow oil. ¹H NMR (400 MHz, CDCl₃) δ 8.17 (s, 1H), 7.67-7.57 (m, 2H), 7.53 (dd, *J* = 8.3, 0.9 Hz, 1H), 7.43 (ddd, *J* = 7.9, 6.4, 2.5 Hz, 1H), 7.36 (ddd, *J* = 8.4, 7.2, 1.3 Hz, 1H), 7.33-7.23 (m, 6H), 7.18-7.12 (m, 1H), 7.06 (d, *J* = 0.9 Hz, 1H), 6.56 (dd, *J* = 17.6, 11.0 Hz, 1H), 5.59 (dd, *J* = 17.5, 1.3

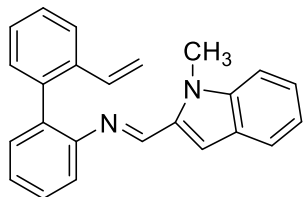
Hz, 1H), 5.12 (dd, $J = 11.0, 1.3$ Hz, 1H). ^{13}C NMR (100 MHz, CDCl_3) δ 155.8, 153.2, 150.4, 150.2, 138.3, 136.4, 135.9, 133.7, 131.5, 131.0, 128.5, 127.8, 127.5, 127.3, 126.8, 125.7, 125.1, 123.4, 122.2, 119.8, 114.4, 112.1, 112.0. HRMS (ESI) calcd. for $\text{C}_{23}\text{H}_{18}\text{NO}$ ($\text{M} + \text{H}^+$) 324.1388. Found 324.1380.

(E)-1-(Benzo[b]thiophen-2-yl)-N-(2'-vinyl-[1,1'-biphenyl]-2-yl)methanimine

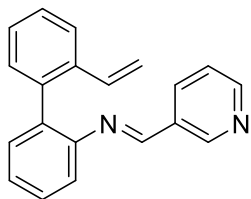


(22at). Prepared following general procedure, using **21aa** (98 mg, 0.5 mmol) to obtain **22at** (157 mg, 93% yield) as yellow oil. ^1H NMR (400 MHz, CDCl_3) δ 8.46 (s, 1H), 7.77 (d, $J = 7.3$ Hz, 2H), 7.59 (s, 1H), 7.54 (s, 1H), 7.47-7.38 (m, 1H), 7.36-7.27 (m, 7H), 7.15 (d, $J = 7.7$ Hz, 1H), 6.55 (dd, $J = 17.5, 11.0$ Hz, 1H), 5.59 (dd, $J = 17.5, 1.4$ Hz, 1H), 5.09 (dd, $J = 11.0, 1.4$ Hz, 1H). ^{13}C NMR (100 MHz, CDCl_3) δ 154.1, 149.7, 143.5, 141.3, 139.3, 138.5, 136.5, 136.0, 134.6, 131.3, 130.9, 128.8, 128.5, 127.4, 127.1, 126.3, 125.8, 124.9, 124.7, 124.5, 122.8, 118.9, 114.2. HRMS (ESI) calcd. for $\text{C}_{23}\text{H}_{18}\text{NS}$ ($\text{M} + \text{H}^+$) 340.1160. Found 340.1152.

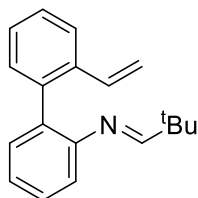
(E)-1-(1-Methyl-1H-indol-2-yl)-N-(2'-vinyl-[1,1'-biphenyl]-2-yl)methanimine



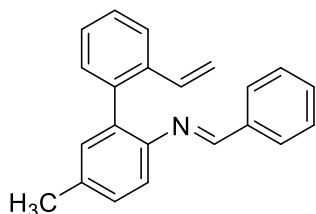
(22au). Prepared following general procedure, using **21aa** (98 mg, 0.5 mmol) to obtain **22au** (132 mg, 79% yield) as yellow oil. ^1H NMR (400 MHz, CDCl_3) δ 8.47 (s, 1H), 7.74-7.60 (m, 2H), 7.48 (ddd, $J = 7.9, 6.8, 2.2$ Hz, 1H), 7.41-7.28 (m, 7H), 7.23-7.19 (m, 1H), 7.14 (ddd, $J = 7.9, 6.1, 1.9$ Hz, 1H), 6.90 (d, $J = 0.7$ Hz, 1H), 6.62 (dd, $J = 17.6, 11.0$ Hz, 1H), 5.64 (dd, $J = 17.6, 1.3$ Hz, 1H), 5.11 (dd, $J = 11.0, 1.3$ Hz, 1H), 3.73 (s, 3H). ^{13}C NMR (100 MHz, CDCl_3) δ 151.7, 150.4, 140.4, 139.5, 136.3, 135.9, 135.7, 130.8, 130.7, 128.8, 127.3, 127.2, 126.9, 125.6, 124.5, 124.5, 121.8, 120.1, 117.4, 114.1, 111.7, 31.7. HRMS (ESI) calcd. for $\text{C}_{24}\text{H}_{21}\text{N}_2$ ($\text{M} + \text{H}^+$) 337.1705. Found 337.1699.

(E)-1-(Pyridin-3-yl)-N-(2'-vinyl-[1,1'-biphenyl]-2-yl)methanimine (22av).

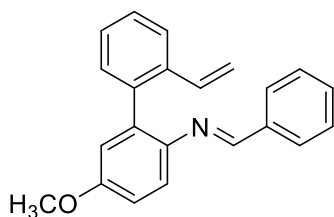
Prepared following general procedure, using **21aa** (59 mg, 0.3 mmol) to obtain **22av** (77 mg, 90% yield) as yellow oil. ^1H NMR (400 MHz, CDCl_3) δ 8.81 (s, 1H), 8.64 (d, $J = 4.8$ Hz, 1H), 8.36 (s, 1H), 7.98 (d, $J = 7.8$ Hz, 1H), 7.62 (d, $J = 7.4$ Hz, 1H), 7.45 (m, 1H), 7.38-7.24 (m, 6H), 7.14 (d, $J = 7.8$ Hz, 1H), 6.56 (dd, $J = 17.5, 11.0$ Hz, 1H), 5.59 (d, $J = 17.5$ Hz, 1H), 5.09 (d, $J = 11.0$ Hz, 1H). ^{13}C NMR (100 MHz, CDCl_3) δ 157.4, 151.8, 150.7, 145.0, 138.5, 136.3, 136.0, 134.9, 134.7, 132.0, 131.2, 130.8, 128.6, 127.5, 127.2, 126.0, 124.8, 123.7, 118.4, 114.1. HRMS (ESI) calcd. for $\text{C}_{20}\text{H}_{17}\text{N}_2$ ($\text{M} + \text{H}^+$) 285.1392. Found 285.1389.

(E)-2,2-dimethyl-N-(2'-vinyl-[1,1'-biphenyl]-2-yl)propan-1-imine (22aw).

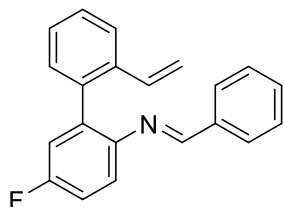
Prepared following general procedure, using **21aa** (130 mg, 0.67 mmol) to obtain **22aw** (71 mg, 40% yield) as a yellow oil. ^1H NMR (400 MHz, CD_2Cl_2) δ 7.60 (dd, $J = 7.6, 1.6$ Hz, 1H), 7.42 (s, 1H), 7.36-7.24 (m, 3H), 7.21-7.13 (m, 3H), 6.87 (dt, $J = 7.8, 0.9$ Hz, 1H), 6.44 (dd, $J = 17.6, 11.0$ Hz, 1H), 5.62 (dd, $J = 17.6, 1.3$ Hz, 1H), 5.10 (dd, $J = 11.0, 1.3$ Hz, 1H), 0.89 (s, 9H). ^{13}C NMR (100 MHz, CD_2Cl_2) δ 173.8, 151.3, 138.7, 136.1, 135.7, 132.7, 130.9, 130.6, 128.3, 127.2, 127.0, 124.4, 124.2, 119.4, 113.8, 36.5, 26.0. HRMS (ESI) calcd. for $\text{C}_{19}\text{H}_{22}\text{N}$ ($\text{M} + \text{H}^+$) 264.1752. Found 264.1747.

(E)-N-(5-Methyl-2'-vinyl-[1,1'-biphenyl]-2-yl)-1-phenylmethanimine (22ba).

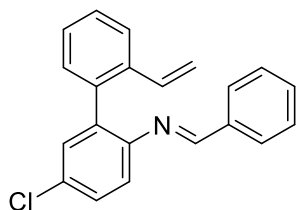
Prepared following general procedure, using **21ba** (155 mg, 0.73 mmol) to obtain **22ba** (195 mg, 90% yield) as a yellow oil. ^1H NMR (400 MHz, CDCl_3) δ 8.31 (s, 1H), 7.71-7.56 (m, 3H), 7.43-7.22 (m, 7H), 7.14 (s, 1H), 7.04 (d, $J = 8.0$ Hz, 1H), 6.61 (dd, $J = 17.5, 11.0$ Hz, 1H), 5.60 (dd, $J = 17.5, 1.4$ Hz, 1H), 5.09 (dd, $J = 11.0, 1.3$ Hz, 1H), 2.43 (s, 3H). ^{13}C NMR (100 MHz, CDCl_3) δ 159.9, 148.1, 139.0, 136.6, 136.3, 136.2, 135.1, 134.5, 131.8, 130.9, 130.9, 129.1, 128.6, 128.5, 127.3, 127.1, 124.7, 118.5, 113.9, 21.0. HRMS (ESI) calcd. for $\text{C}_{22}\text{H}_{20}\text{N}$ ($\text{M} + \text{H}^+$) 298.1596. Found 298.1587.

(E)-N-(5-Methoxy-2'-vinyl-[1,1'-biphenyl]-2-yl)-1-phenylmethanimine (22bb).

Prepared following general procedure, using **21bb** (110 mg, 0.49 mmol) to obtain **22bb** (123 mg, 80% yield) as a yellow oil. ¹H NMR (400 MHz, CDCl₃) δ 8.33 (s, 1H), 7.65-7.63 (m, 3H), 7.39-7.29 (m, 6H), 7.13 (d, *J* = 8.7 Hz, 1H), 6.98 (dd, *J* = 8.7, 2.9 Hz, 1H), 6.89 (d, *J* = 2.9 Hz, 1H), 6.62 (dd, *J* = 17.5, 11.0 Hz, 1H), 5.61 (dd, *J* = 17.5, 1.3 Hz, 1H), 5.09 (dd, *J* = 11.0, 1.3 Hz, 1H), 3.85 (s, 3H). ¹³C NMR (100 MHz, CDCl₃) δ 158.9, 157.5, 143.6, 138.8, 136.7, 136.4, 136.3, 136.1, 130.8, 128.6, 128.5, 127.4, 127.1, 124.8, 119.4, 116.3, 114.1, 114.0, 55.6. HRMS (ESI) calcd. for C₂₂H₂₀NO (M + H⁺) 314.1545. Found 314.1536.

(E)-N-(5-Fluoro-2'-vinyl-[1,1'-biphenyl]-2-yl)-1-phenylmethanimine (22bc).

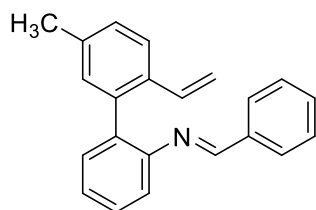
Prepared following general procedure, using **21bc** (133 mg, 0.62 mmol) to obtain **22bc** (70 mg, 37% yield) as a yellow oil. ¹H NMR (400 MHz, CDCl₃) δ 8.29 (s, 1H), 7.65-7.60 (m, 3H), 7.44-7.24 (m, 6H), 7.15-7.08 (m, 2H), 7.05 (dd, *J* = 8.8, 2.5 Hz, 1H), 6.58 (dd, *J* = 17.5, 11.0 Hz, 1H), 5.60 (dd, *J* = 17.5, 1.2 Hz, 1H), 5.12 (dd, *J* = 11.0, 1.2 Hz, 1H). ¹³C NMR (100 MHz, CDCl₃) δ 161.7, 160.48 (d, *J* = 1.5 Hz), 159.3, 146.7 (d, *J* = 2.9 Hz), 137.7 (d, *J* = 1.5 Hz), 136.4 (d, *J* = 7.8 Hz), 136.33, 136.31, 135.7, 131.2, 130.6, 128.7, 128.6, 127.7, 127.2, 125.0, 119.8 (d, *J* = 8.4 Hz), 117.8 (d, *J* = 22.5 Hz), 115.1 (d, *J* = 22.2 Hz), 114.5. ¹⁹F NMR (377 MHz, CDCl₃) δ -118.3. HRMS (ESI) calcd. for C₂₁H₁₇FN (M + H⁺) 302.1345. Found 302.1337.

(E)-N-(5-chloro-2'-vinyl-[1,1'-biphenyl]-2-yl)-1-phenylmethanimine (22bd).

Prepared following general procedure, using **21ca** (135 mg, 0.65 mmol) to obtain **22bd** (140 mg, 72% yield) as a yellow oil. ¹H NMR (400 MHz, CDCl₃) δ 8.26 (s, 1H), 7.66 - 7.61 (m, 2H), 7.59 (dd, *J* = 7.6, 1.6 Hz, 1H), 7.44 - 7.35 (m, 4H), 7.33 (dd, *J* = 7.2, 1.7 Hz, 1H), 7.30 (d, *J* = 2.4 Hz, 2H), 7.29 - 7.19 (m, 2H), 7.03 (d, *J* = 8.4 Hz, 1H), 6.54 (dd, *J* = 17.5, 11.0 Hz, 1H), 5.58 (dd, *J* = 17.5, 1.3 Hz, 1H), 5.11 (dd, *J* = 11.0, 1.3 Hz, 1H). ¹³C NMR (100 MHz, CDCl₃) δ 160.9,

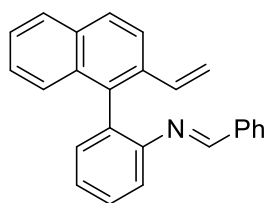
149.2, 137.4, 136.3, 136.2, 136.1, 135.7, 131.3, 130.9, 130.6, 128.8, 128.6, 128.5, 127.8, 127.2, 124.9, 119.9, 114.6. HRMS (ESI) calcd. for C₂₁H₁₆ClN (M + H⁺) 318.1050. Found 318.1045.

(E)-N-(5'-Methyl-2'-vinyl-[1,1'-biphenyl]-2-yl)-1-phenylmethanimine (22ca).



Prepared following general procedure, using **21ca** (135 mg, 0.65 mmol) to obtain **22ca** (140 mg, 72% yield) as a yellow oil. ¹H NMR (400 MHz, CDCl₃) δ 8.30 (s, 1H), 7.66-7.4 (m, 2H), 7.50 (d, *J* = 7.9 Hz, 1H), 7.43-7.35 (m, 4H), 7.33-7.28 (m, 2H), 7.13-7.08 (m, 3H), 6.53 (dd, *J* = 17.5, 11.0 Hz, 1H), 5.52 (dd, *J* = 17.5, 1.4 Hz, 1H), 5.02 (dd, *J* = 11.0, 1.4 Hz, 1H), 2.36 (s, 3H). ¹³C NMR (100 MHz, CDCl₃) δ 160.5, 150.6, 138.7, 136.8, 136.5, 135.9, 134.6, 133.7, 131.4, 131.1, 131.0, 128.7, 128.5, 128.5, 128.2, 125.4, 124.6, 118.7, 113.0, 21.2. HRMS (ESI) calcd. for C₂₂H₂₀N (M + H⁺) 298.1596. Found 298.1594.

(E)-1-Phenyl-N-(2-(2-vinylnaphthalen-1-yl)phenyl)methanimine (25).



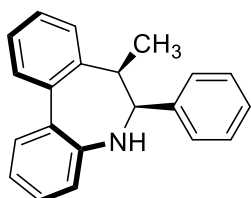
Prepared following general procedure, using **24** (144 mg, 0.59 mmol) to obtain **25** (147 mg, 80% yield) as yellow oil. ¹H NMR (400 MHz, CDCl₃) δ 8.21 (s, 1H), 7.92-7.67 (m, 3H), 7.64-7.46 (m, 2H), 7.41 (ddd, *J* = 8.1, 4.0, 2.4 Hz, 3H), 7.35 (ddt, *J* = 8.2, 3.9, 2.2 Hz, 2H), 7.32-7.27 (m, 2H), 7.27-7.16 (m, 3H), 6.64 (dd, *J* = 17.6, 11.0 Hz, 1H), 5.73 (dd, *J* = 17.5, 1.2 Hz, 1H), 5.19 (dd, *J* = 11.0, 1.1 Hz, 1H). ¹³C NMR (100 MHz, CDCl₃) δ 160.2, 151.7, 136.2, 136.0, 135.7, 133.1, 132.9, 131.8, 131.6, 131.0, 128.8, 128.5, 128.4, 127.8, 127.6, 126.9, 126.0, 125.5, 125.3, 122.4, 119.1, 114.5. HRMS (ESI) calcd. for C₂₅H₂₀N (M + H⁺) 334.1596. Found 334.1592.

IV.5.2. General procedure for the synthesis of dibenzazepines by CuH-catalyzed intramolecular cyclization.

A flamed-dried Schlenk tube equipped with a magnetic stir bar was charged with Cu(OAc)₂ (4 mol%) and (*R,R*)-Ph-BPE (4.4 mol%). Anhydrous THF (300 μL) was added via syringe and the reaction mixture was stirred for 15 min, until a blue

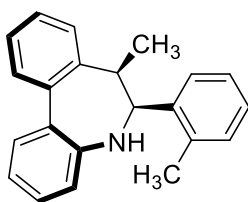
homogeneous solution was obtained. Diethoxymethylsilane (DEMS, 2.0 equiv) was added via syringe and stirring was continued for 10 min at room temperature. Into a separate flamed-dried Schlenk tube aldimine **22** (0.2 mmol, 1 equiv) was dissolved in anhydrous MTBE (1 mL) and transferred via syringe to the reaction tube containing the catalyst. Anhydrous *t*BuOH (1.1 equiv) was added via microsyringe and the reaction mixture was stirred at room temperature under N₂ for 48 h. The reaction mixture was then quenched with saturated aqueous Na₂CO₃ solution, extracted with EtOAc and the combined organic layers were concentrated *in vacuo*. The resulting crude product was purified by flash column chromatography (30:1 hexane/EtOAc) on silica gel to obtain dibenzo[*b,d*]azepine derivatives **23**.

(*S_a,6*S*,7*R)-7-Methyl-6-phenyl-6,7-dihydro-5*H*-dibenzo[*b,d*]azepine (23aa).**



Prepared following general procedure, using **22aa** and further purification by flash chromatography afforded **23aa** (56 mg, 99% yield) as colorless oil. $[\alpha]_{\text{D}}^{20} +52.3$ (*c* 0.51, CHCl₃) for 98% *ee*. ¹H NMR (400 MHz, CDCl₃) δ 7.50 (m, 2H), 7.42 (t, *J* = 7.3 Hz, 1H), 7.29 (m, 5H), 7.18 (t, *J* = 7.4 Hz, 1H), 7.09 (d, *J* = 7.2 Hz, 2H), 6.92 (d, *J* = 7.7 Hz, 1H), 6.83 (d, *J* = 7.6 Hz, 1H), 4.98 (d, *J* = 5.1 Hz, 1H), 3.59 (s, 1H), 1.11 (d, *J* = 7.0 Hz, 3H). ¹³C NMR (100 MHz, CDCl₃) δ 144.8, 141.00, 140.4, 139.7, 133.7, 129.4, 128.9 (2C), 128.8, 128.3, 127.6, 127.4 (2C), 126.7, 126.6, 126.1, 122.5, 120.7, 58.2, 37.9, 15.0. HRMS (ESI) calcd. for C₂₁H₂₀N (M + H⁺) 286.1517. Found 286.1588. HPLC (IA column, 95:5 *n*-Hex/*i*-PrOH, 30 °C, 1.0 mL/min): *t_R* 4.90 min (major) and 6.84 min (minor).

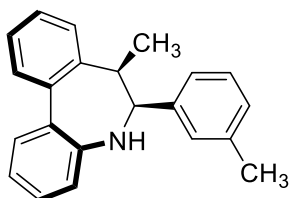
(*S_a,6*S*,7*R)-7-Methyl-6-(*o*-tolyl)-6,7-dihydro-5*H*-dibenzo[*b,d*]azepine (23ab).**



Prepared following general procedure, using **22ab** and further purification by flash chromatography afforded **23ab** (48 mg, 95% yield) as colorless oil. $[\alpha]_{\text{D}}^{20} +4.0$ (*c* 0.48, CHCl₃) for 98% *ee*. ¹H NMR (400 MHz, CDCl₃) δ 7.52-7.49 (m, 2H), 7.43 (t, *J* = 7.5 Hz, 1H), 7.29 (m, 2H), 7.18 (m, 3H), 7.02 (m, 2H), 6.94 (m, 2H), 5.39 (d, *J* = 5.1 Hz, 1H), 3.59 (m, 1H), 2.45 (s, 3H), 1.11 (d, *J* = 7.1 Hz, 3H). ¹³C NMR (100 MHz,

CDCl₃) δ 144.9, 140.7, 140.2, 139.5, 135.9, 133.2, 130.0, 129.5, 129.0, 128.7, 128.5, 127.1, 126.8, 126.7 (2C), 125.3, 122.4, 120.7, 68.6, 39.3, 20.1, 14.0. HRMS (ESI) calcd. for C₂₂H₂₂N (M + H⁺) 300.1752. Found 300.1743. HPLC (IA column, 95:5 *n*-Hex/*i*-PrOH, 30 °C, 1.0 mL/min): t_R 5.02 min (major) and 7.36 min (minor).

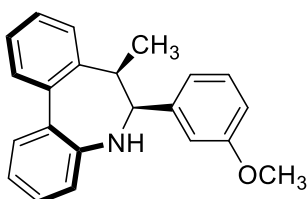
(*S*_a,6*S*,7*R*)-7-Methyl-6-(*m*-tolyl)-6,7-dihydro-5*H*-dibenzo[*b,d*]azepine (23ac).



Prepared following general procedure, using **22ac** and further purification by flash chromatography afforded **23ac** (44 mg, 87% yield) as colorless oil. [α]_D²⁰ +24.7 (*c* 0.25, CHCl₃) for 98% *ee*. ¹H NMR (400 MHz, CDCl₃) δ 7.52-7.49 (m,

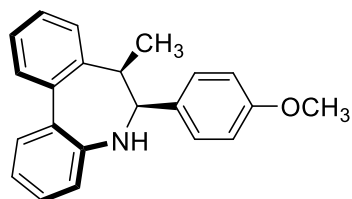
2H), 7.42 (td, *J* = 7.5, 1.3 Hz, 1H), 7.33-7.26 (m, 2H), 7.19-7.10 (m, 3H), 6.92-6.84 (m, 4H), 4.94 (d, *J* = 5.1 Hz, 1H), 3.57 (dd, *J* = 7.2, 5.1 Hz, 1H), 2.29 (s, 3H), 1.10 (d, *J* = 7.2 Hz, 3H). ¹³C NMR (100 MHz, CDCl₃) δ 144.8, 140.9, 140.3, 139.9, 136.9, 133.6, 129.7, 129.4, 128.7, 128.3, 128.3, 127.3, 126.6 (2C), 126.2, 126.0, 122.5, 120.7, 75.4, 37.9, 21.4, 15.0. HRMS (ESI) calcd. for C₂₂H₂₂N (M + H⁺) 300.1752. Found 300.1745. HPLC (IA column, 95:5 *n*-Hex/*i*-PrOH, 30 °C, 1.0 mL/min): t_R 6.12 min (major) and 10.70 min (minor).

(*S*_a,6*S*,7*R*)-6-(3-Methoxyphenyl)-7-methyl-6,7-dihydro-5*H*-



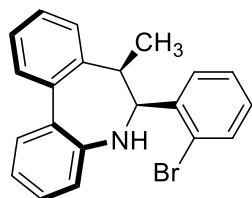
dibenzo[*b,d*]azepine (23ad). Prepared following general procedure, using **22ad** and further purification by flash chromatography afforded **23ad** (34 mg, 55% yield) as yellow oil. [α]_D²⁰ +92.5 (*c* 0.54, CHCl₃) for 98% *ee*. ¹H NMR

(400 MHz, CDCl₃) δ 7.45 (ddd, *J* = 7.6, 3.7, 1.5 Hz, 2H), 7.37 (td, *J* = 7.5, 1.3 Hz, 1H), 7.31-7.20 (m, 2H), 7.18-7.10 (m, 2H), 6.88 (dd, *J* = 7.7, 1.2 Hz, 1H), 6.85-6.78 (m, 2H), 6.68 (dt, *J* = 7.6, 1.3 Hz, 1H), 6.55 (dd, *J* = 2.7, 1.5 Hz, 1H), 4.93 (d, *J* = 5.0 Hz, 1H), 3.57 (s, 3H), 3.57-3.51 (m, 1H), 1.08 (d, *J* = 7.2 Hz, 3H). ¹³C NMR (100 MHz, CDCl₃) δ 158.8, 144.8, 142.7, 140.4, 139.8, 133.6, 129.4, 128.8, 128.3, 128.2, 126.6, 126.2, 122.4, 121.4, 120.7, 114.1, 113.4, 75.4, 55.0, 37.8, 15.0. HRMS (ESI) calcd. for C₂₂H₂₂NO (M + H⁺) 316.1701. Found 316.1691. HPLC (IA column, 95:5 *n*-Hex/*i*-PrOH, 30 °C, 1.0 mL/min): t_R 5.93 min (major) and 13.15 min (minor).

(*S_a,6*S*,7*R)-6-(4-Methoxyphenyl)-7-methyl-6,7-dihydro-5*H*-**

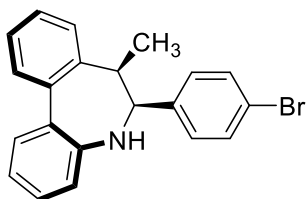
dibenzo[*b,d*]azepine (23ae). Prepared following general procedure, using **22ae** and further purification by flash chromatography afforded **23ae** (38 mg, 60% yield) as yellow oil. $[\alpha]_{\text{D}}^{20} +7.1$ (*c* 0.57, CHCl₃) for 99%

ee. ¹H NMR (400 MHz, CDCl₃) δ 7.46 (dt, *J* = 7.7, 2.0 Hz, 2H), 7.38 (td, *J* = 7.5, 1.2 Hz, 1H), 7.32-7.20 (m, 3H), 7.13 (td, *J* = 7.5, 1.2 Hz, 1H), 6.96 (d, *J* = 8.6 Hz, 2H), 6.87 (dd, *J* = 7.8, 1.2 Hz, 1H), 6.81 (d, *J* = 7.7 Hz, 1H), 6.76 (d, *J* = 8.6 Hz, 2H), 4.90 (d, *J* = 5.1 Hz, 1H), 3.79 (s, 3H), 3.65 (brad s, 1H), 3.51 (dt, *J* = 12.0, 6.1 Hz, 1H), 1.05 (d, *J* = 7.1 Hz, 2H). ¹³C NMR (100 MHz, CDCl₃) δ 159.1, 144.9, 140.5, 133.7, 133.1, 129.9, 129.3, 128.7, 128.2, 126.7, 126.6, 127.1, 122.5, 120.7, 112.7, 74.9, 55.2, 37.9, 15.0. HRMS (ESI) calcd. for C₂₂H₂₂NO (*M* + *H*⁺) 316.1701. Found 316.1689. HPLC (IA column, 95:5 *n*-Hex/*i*-PrOH, 30 °C, 1.0 mL/min): *t_R* 8.58 min (major) and 10.91 min (minor).

(*S_a,6*S*,7*R)-6-(2-Bromophenyl)-7-methyl-6,7-dihydro-5*H*-dibenzo[*b,d*]azepine**

(23af). Prepared following general procedure, using **22af** and further purification by flash chromatography afforded **23af** (47 mg, 66% yield) as colorless oil. $[\alpha]_{\text{D}}^{20} +35.0$ (*c* 0.26, CHCl₃) for 90% *ee*. ¹H NMR (400 MHz, CDCl₃) δ 7.57 (dd, *J* = 7.8, 1.6 Hz,

1H), 7.49 (m, 2H), 7.43 (td, *J* = 7.5, 1.3 Hz, 1H), 7.30 (m, 2H), 7.18 (td, *J* = 7.5, 1.3 Hz, 1H), 7.15-7.05 (m, 2H), 6.97 (m, 2H), 6.90 (d, *J* = 7.7 Hz, 1H), 5.64 (d, *J* = 5.3 Hz, 1H), 3.87-3.34 (m, 2H), 1.19 (d, *J* = 7.2 Hz, 3H). ¹³C NMR (100 MHz, CDCl₃) δ 144.7, 140.4, 140.2, 139.8, 133.6, 132.3, 131.3, 129.4, 128.9, 128.8, 128.4, 126.84, 126.82, 126.6, 126.5, 124.7, 122.7, 120.9, 72.0, 38.6, 14.1. HRMS (ESI) calcd. for C₂₁H₁₉BrN (*M* + *H*⁺) 364.0701. Found 364.0509. HPLC (IA column, 95:5 *n*-Hex/*i*-PrOH, 30 °C, 1.0 mL/min): *t_R* 4.78 min (major) and 6.55 min (minor).

(*S_a*,6*S*,7*R*)-6-(4-Bromophenyl)-7-methyl-6,7-dihydro-5*H*-dibenzo[*b,d*]azepine

(23ag). Prepared following general procedure, using **22ag**

and further purification by flash chromatography afforded

23ag (58 mg, 80% yield) as colorless oil. $[\alpha]_{\text{D}}^{20}$ -8.1 (*c*

0.26, CHCl₃) for 91% *ee*. ¹H NMR (400 MHz, CDCl₃) δ 7.46

(d, *J* = 3.5 Hz, 2H), 7.39 (t, *J* = 7.5 Hz, 1H), 7.33 (d, *J* = 8.0 Hz, 2H), 7.25 (q, *J* = 7.2 Hz,

2H), 7.17 (q, *J* = 8.6, 7.5 Hz, 1H), 6.90 (t, *J* = 8.1 Hz, 3H), 6.77 (d, *J* = 7.7 Hz, 1H), 4.91 (d,

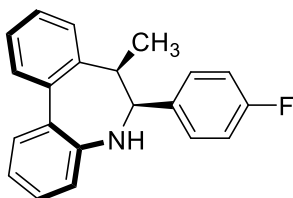
J = 5.0 Hz, 1H), 3.69 (s, 1H), 3.58-3.47 (m, 1H), 1.05 (d, *J* = 7.2 Hz, 3H). ¹³C NMR (100

MHz, CDCl₃) 144.3, 140.3, 139.7, 139.0, 133.7, 130.6, 130.5, 129.4, 129.1, 128.8, 128.3,

126.9, 126.0, 122.9, 121.5, 120.8, 74.9, 37.4, 15.0. HRMS (ESI) calcd. for C₂₁H₁₉BrN (*M*

+ *H*⁺) 364.0701. Found 364.0692. HPLC (IB column, 95:5 *n*-Hex/*i*-PrOH, 30 °C, 1.0

mL/min): t_{R} 7.38 min (minor) and 10.27 min (major).

(*S_a*,6*S*,7*R*)-6-(4-Fluorophenyl)-7-methyl-6,7-dihydro-5*H*-dibenzo[*b,d*]azepine

(23ah). Prepared following general procedure, using **22ah**

and further purification by flash chromatography afforded

23ah (58 mg, 96% yield) as colorless oil. $[\alpha]_{\text{D}}^{20}$ +26.2 (*c*

0.50, CHCl₃) for 98% *ee*. ¹H NMR (400 MHz, CDCl₃) δ 7.50-

7.46 (m, 2H), 7.41 (td, *J* = 7.5, 1.3 Hz, 1H), 7.31-7.24 (m, 2H), 7.17 (td, *J* = 7.5, 1.2 Hz,

1H), 7.04-7.00 (m, 2H), 6.96-6.85 (m, 3H), 6.79 (d, *J* = 7.7 Hz, 1H), 4.94 (d, *J* = 5.0 Hz,

1H), 3.54 (dt, *J* = 12.3, 6.1 Hz, 1H), 1.07 (d, *J* = 7.2 Hz, 3H). ¹³C NMR (100 MHz, CDCl₃)

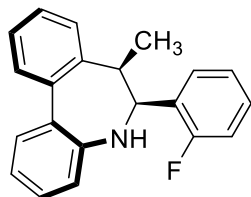
δ 162.4 (d, *J* = 245.2 Hz), 144.5, 140.4, 139.2, 136.5, 133.7, 130.3 (d, *J* = 7.9 Hz), 129.4,

128.8, 128.3, 126.7, 126.8, 126.0, 122.8, 120.8, 114.2 (d, *J* = 21.1 Hz), 74.8, 37.6, 15.0.

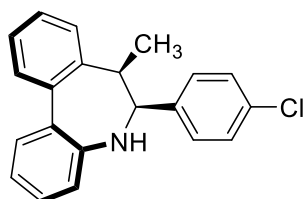
¹⁹F NMR (377 MHz, CDCl₃) δ -115.2. HRMS (ESI) calcd. for C₂₁H₁₉FN (*M* + *H*⁺) 304.1502.

Found 304.1492. HPLC (IB column, 95:5 *n*-Hex/*i*-PrOH, 30 °C, 1.0 mL/min): t_{R} 10.81

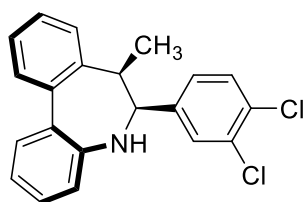
min (minor) and 12.27 min (major).

(*S_a,6*S*,7*R)-6-(2-Fluorophenyl)-7-methyl-6,7-dihydro-5*H*-dibenzo[*b,d*]azepine**

(23ai). Prepared following general procedure, using **22ai** and further purification by flash chromatography afforded **23ai** (42 mg, 70% yield) as colorless oil. $[\alpha]_D^{20} +44.0$ (*c* 0.48, CHCl₃) for 92% *ee*. ¹H NMR (400 MHz, CDCl₃) δ 7.49 (m, 2H), 7.42 (td, *J* = 7.5, 1.3 Hz, 1H), 7.32-7.17 (m, 4H), 7.05 (m, 1H), 6.97-6.88 (m, 3H), 6.84 (dd, *J* = 8.0, 1.0 Hz, 1H), 5.50 (d, *J* = 5.2 Hz, 1H), 3.62 (m, 1H), 1.16 (dd, *J* = 7.2, 2.3 Hz, 3H). ¹³C NMR (100 MHz, CDCl₃) δ 160.7 (d, *J* = 245.2 Hz), 144.5, 140.3, 139.3, 133.7, 130.6 (d, *J* = 4.1 Hz), 129.4, 128.8, 128.7, 128.6, 128.3, 126.81, 126.77, 126.0, 123.3 (d, *J* = 3.6 Hz), 122.8, 120.9, 114.4 (d, *J* = 22.8 Hz), 66.0, 37.8, 14.1 (d, *J* = 1.5 Hz). ¹⁹F NMR (377 MHz, CDCl₃) δ -118.5. HRMS (ESI) calcd. for C₂₁H₁₉FN (M + H⁺) 304.1502. Found 304.1494. HPLC (IA column, 95:5 *n*-Hex/*i*-PrOH, 30 °C, 1.0 mL/min): *t_R* 6.36 min (major) and 8.39 min (minor).

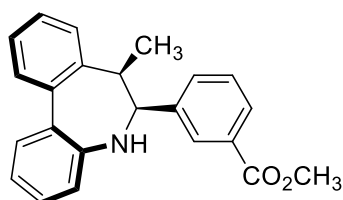
(*S_a,6*S*,7*R)-6-(4-Chlorophenyl)-7-methyl-6,7-dihydro-5*H*-dibenzo[*b,d*]azepine**

(23aj). Prepared following general procedure, using **22aj** and further purification by flash chromatography afforded **23aj** (51 mg, 80% yield) as colorless oil. $[\alpha]_D^{20} +3.7$ (*c* 0.49, CHCl₃) for 92% *ee*. ¹H NMR (400 MHz, CDCl₃) δ 7.46 (ddd, *J* = 7.6, 3.7, 1.5 Hz, 2H), 7.39 (td, *J* = 7.5, 1.2 Hz, 1H), 7.33-7.22 (m, 3H), 7.21-7.11 (m, 3H), 6.98 (d, *J* = 8.4 Hz, 2H), 6.94-6.86 (m, 1H), 6.77 (d, *J* = 7.7 Hz, 1H), 4.92 (d, *J* = 5.0 Hz, 1H), 3.66 (br s, 1H), 3.58-3.51 (m, 1H), 1.06 (d, *J* = 7.2 Hz, 3H). ¹³C NMR (100 MHz, CDCl₃) 144.5, 140.4, 139.4, 139.1, 133.7, 133.3, 130.2, 129.4, 128.8, 128.3, 127.6, 126.8, 126.8, 126.0, 122.8, 120.8, 74.9, 37.5, 15.0. HRMS (ESI) calcd. for C₂₁H₁₉ClN (M + H⁺) 320.1206. Found 320.1195. HPLC (IB column, 95:5 *n*-Hex/*i*-PrOH, 30 °C, 1.0 mL/min): *t_R* 7.08 min (minor) and 9.24 min (major).

(*S_a*,6*S*,7*R*)-6-(3,4-Dichlorophenyl)-7-methyl-6,7-dihydro-5*H*-

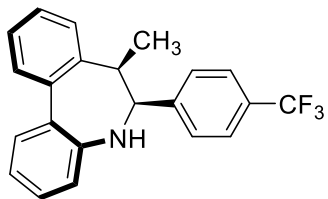
dibenzo[*b,d*]azepine (23ak). Prepared following general procedure, using **22ak** and further purification by flash chromatography afforded **23ak** (68 mg, 99% yield) as colorless oil. $[\alpha]_D^{20} -5.3$ (*c* 0.45, CHCl₃) for 33% *ee*. ¹H NMR (400 MHz, CDCl₃) δ 7.49 (m, 2H), 7.43 (td, *J* = 7.5, 1.3 Hz,

1H), 7.29 (m, 3H), 7.19 (td, *J* = 7.5, 1.2 Hz, 1H), 7.13 (d, *J* = 2.0 Hz, 1H), 6.92-6.87 (m, 2H), 6.79 (d, *J* = 7.7 Hz, 1H), 4.92 (d, *J* = 4.9 Hz, 1H), 3.58 (dd, *J* = 7.2, 5.0 Hz, 1H), 1.11 (d, *J* = 7.2 Hz, 3H). ¹³C NMR (100 MHz, CDCl₃) δ 144.2, 141.3, 140.2, 138.6, 133.6, 131.4, 131.3, 130.8, 129.5, 129.3, 128.8, 128.4, 128.2, 127.0, 126.9, 125.9, 122.9, 120.7, 74.4, 37.4, 15.0. HRMS (ESI) calcd. for C₂₁H₁₈Cl₂N (M + H⁺) 354.0816. Found 354.0792. HPLC (IA column, 95:5 *n*-Hex/*i*-PrOH, 30 °C, 1.0 mL/min): *t_R* 6.05 min (major) and 6.65 min (minor).

Methyl**3-((*S_a*,6*S*,7*R*)-7-Methyl-6,7-dihydro-5*H*-dibenzo[*b,d*]azepin-6-**

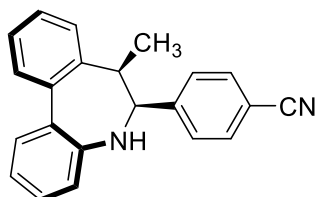
yl)benzoate (23al). Prepared following general procedure, using **22al** and further purification by flash chromatography afforded **23al** (18 mg, 25% yield) as a white solid. $[\alpha]_D^{20} +31.4$ (*c* 0.64, CHCl₃) for 86% *ee*. ¹H

NMR (400 MHz, CDCl₃) δ 7.93 (dt, *J* = 7.6, 1.6 Hz, 1H), 7.74 (s, 1H), 7.46 (td, *J* = 7.4, 1.5 Hz, 2H), 7.39 (td, *J* = 7.5, 1.3 Hz, 1H), 7.29-7.17 (m, 4H), 7.14 (td, *J* = 7.5, 1.2 Hz, 1H), 6.88 (dd, *J* = 7.8, 1.2 Hz, 1H), 6.72 (d, *J* = 7.7 Hz, 1H), 5.01 (d, *J* = 5.0 Hz, 1H), 3.88 (s, 3H), 3.70 (br s, 1H), 3.63-3.54 (m, 1H), 1.07 (d, *J* = 7.2 Hz, 3H). ¹³C NMR (100 MHz, CDCl₃) δ 167.2, 144.6, 141.5, 140.4, 139.1, 133.5, 133.4, 130.1, 129.4, 129.3, 128.9, 128.8, 128.4, 127.5, 126.8, 125.9, 122.6, 120.7, 75.1, 52.0, 37.6, 15.0. HRMS (ESI) calcd. for C₂₃H₂₂NO₂ (M + H⁺) 344.1651. Found 344.1643. HPLC (IB column, 95:5 *n*-Hex/*i*-PrOH, 30 °C, 1.0 mL/min): *t_R* 15.32 min (minor) and 18.26 min (major).

(*S_a*,6*S*,7*R*)-7-Methyl-6-(4-(trifluoromethyl)phenyl)-6,7-dihydro-5*H*-

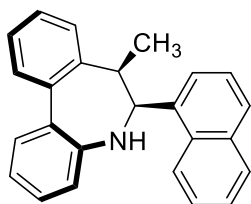
dibenzo[*b,d*]azepine (23am). Prepared following general procedure, using **22am** and further purification by flash chromatography afforded **23am** (24 mg, 33% yield) as white solid. $[\alpha]_D^{20} +21.9$ (*c* 0.50, CHCl₃) for 63%

ee. ¹H NMR (400 MHz, CDCl₃) δ 7.50-7.46 (m, 4H), 7.42 (td, *J* = 7.5, 1.2 Hz, 1H), 7.33-7.28 (m, 1H), 7.25 (td, *J* = 7.6, 1.5 Hz, 1H), 7.20-7.16 (m, 3H), 6.91 (dd, *J* = 7.8, 1.2 Hz, 1H), 6.76 (d, *J* = 7.7 Hz, 1H), 5.03 (d, *J* = 5.1 Hz, 1H), 3.70 (br s, 1H), 3.61 (qd, *J* = 7.1, 4.9 Hz, 1H), 1.10 (d, *J* = 7.2 Hz, 3H). ¹³C NMR (100 MHz, CDCl₃) δ 145.0, 144.4, 140.4, 138.9, 133.6, 129.7 (q, *J* = 32.3 Hz), 129.5, 129.2, 128.8, 128.3, 126.9, 125.9, 124.3, 124.2, 124.27 (d, *J* = 272.1 Hz), 122.8, 120.8, 75.1, 37.5, 14.9. HRMS (ESI) calcd. for C₂₂H₁₉F₃N (M + H⁺) 354.1470. Found 354.1458. HPLC (IB column, 95:5 *n*-Hex/*i*-PrOH, 30 °C, 1.0 mL/min): *t_R* 6.11 min (minor) and 7.60 min (major). ¹⁹F NMR (377 MHz, CDCl₃) δ -62.3.

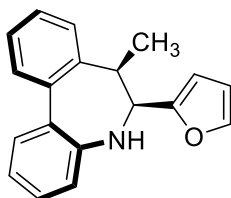
4-((*S_a*,6*S*,7*R*)-7-Methyl-6,7-dihydro-5*H*-dibenzo[*b,d*]azepin-6-yl)benzonitrile

(23an). Prepared following general procedure, using **22an** and further purification by flash chromatography afforded **23an** (31 mg, 50% yield) as yellow oil. $[\alpha]_D^{20} -$

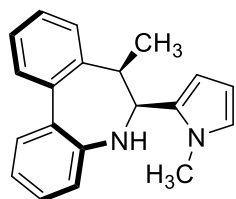
10.5 (*c* 0.28, CHCl₃) for 36% *ee*. ¹H NMR (400 MHz, CDCl₃) δ 7.51-7.43 (m, 4H), 7.39 (td, *J* = 7.5, 1.2 Hz, 1H), 7.33-7.25 (m, 1H), 7.21 (td, *J* = 7.5, 1.4 Hz, 1H), 7.18-7.10 (m, 3H), 6.88 (dd, *J* = 7.8, 1.2 Hz, 1H), 6.68 (d, *J* = 7.7 Hz, 1H), 5.00 (d, *J* = 4.9 Hz, 1H), 3.63-3.56 (m, 1H), 1.07 (d, *J* = 7.2 Hz, 3H). ¹³C NMR (100 MHz, CDCl₃) δ 146.4, 144.1, 140.2, 138.4, 133.5, 131.2, 129.6, 129.6, 128.9, 128.4, 127.1, 126.9, 125.8, 123.0, 120.8, 119.0, 111.4, 75.1, 37.3, 14.9. HRMS (ESI) calcd. for C₂₂H₁₉N₂ (M + H⁺) 311.1548. Found 311.1540. HPLC (IB column, 98:2 *n*-Hex/*i*-PrOH, 30 °C, 1.0 mL/min): *t_R* 33.61 min (minor) and 36.80 min (major).

(*S_a*,6*S*,7*R*)-7-Methyl-6-(naphthalen-1-yl)-6,7-dihydro-5*H*-dibenzo[*b,d*]azepine

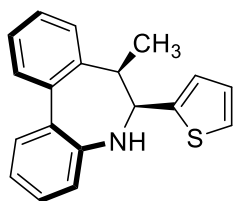
(23ao). Prepared following general procedure, using **22ao** and further purification by flash chromatography afforded **23ao** (33 mg, 50% yield) as colorless oil. $[\alpha]_{\text{D}}^{20} +6.8$ (*c* 0.53, CHCl₃) for 97% *ee*. ¹H NMR (400 MHz, CDCl₃) δ 8.20 (d, *J* = 8.5 Hz, 1H), 7.89 (d, *J* = 9.4 Hz, 1H), 7.77 (dd, *J* = 5.8, 3.7 Hz, 1H), 7.53-7.49 (m, 4H), 7.41 (td, *J* = 7.5, 1.3 Hz, 1H), 7.35-7.23 (m, 4H), 7.18-7.10 (m, 1H), 6.92 (dd, *J* = 7.8, 1.2 Hz, 1H), 6.83 (d, *J* = 7.7 Hz, 1H), 6.03 (br s, 1H), 4.22-3.43 (m, 2H), 1.02 (d, *J* = 7.2 Hz, 3H). ¹³C NMR (100 MHz, CDCl₃) δ 145.1, 140.6, 140.3, 137.3, 133.5, 133.1, 132.2, 129.6, 129.0, 128.8, 128.6, 127.8, 126.8, 126.8, 126.7, 125.8, 125.2, 125.0, 122.8, 122.3, 120.6, 67.0, 39.9, 14.9. HRMS (ESI) calcd. for C₂₅H₂₂N (*M* + *H*⁺) 336.1752. Found 336.1741. HPLC (IA column, 95:5 *n*-Hex/*i*-PrOH, 30 °C, 1.0 mL/min): *t_R* 6.55 min (major) and 11.42 min (minor).

(*S_a*,6*S*,7*R*)-6-(Furan-2-yl)-7-methyl-6,7-dihydro-5*H*-dibenzo[*b,d*]azepine

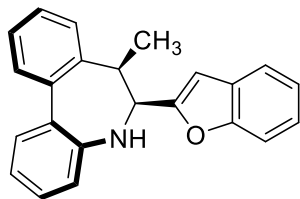
(23ap). Prepared following general procedure, using **22ap** and further purification by flash chromatography afforded **23ap** (31 mg, 56% yield) as colorless oil. $[\alpha]_{\text{D}}^{20} +31.8$ (*c* 0.50, CHCl₃) for 99% *ee*. ¹H NMR (400 MHz, CDCl₃) δ 7.47-7.44 (m, 2H), 7.38 (t, *J* = 7.7 Hz, 1H), 7.35-7.26 (m, 3H), 7.15 (t, *J* = 7.5 Hz, 1H), 7.05 (d, *J* = 7.5 Hz, 1H), 6.92 (d, *J* = 7.8 Hz, 1H), 6.30 (dd, *J* = 3.2, 1.8 Hz, 1H), 5.97 (d, *J* = 3.2 Hz, 1H), 5.06 (d, *J* = 5.0 Hz, 1H), 3.73 (s, 1H), 3.51-3.40 (m, 1H), 1.18 (d, *J* = 7.2 Hz, 3H). ¹³C NMR (100 MHz, CDCl₃) δ 155.5, 144.1, 141.4, 140.0, 139.9, 133.6, 129.4, 128.6, 128.3, 126.8, 126.7, 125.7, 122.8, 120.9, 110.1, 107.5, 68.8, 38.0, 14.4. HRMS (ESI) calcd. for C₁₉H₁₈NO (*M* + *H*⁺) 276.1388. Found 276.1380. HPLC (IA column, 95:5 *n*-Hex/*i*-PrOH, 30 °C, 1.0 mL/min): *t_R* 6.76 min (major) and 8.19 min (minor).

(*S_a,6*S*,7*R)-7-Methyl-6-(1-methyl-1*H*-pyrrol-2-yl)-6,7-dihydro-5*H*-**

dibenzo[*b,d*]azepine (23aq). Prepared following general procedure, using **22aq** and further purification by flash chromatography afforded **23aq** (29 mg, 51% yield) as colorless oil. $[\alpha]_{\text{D}}^{20}$ -14.4 (c 0.16, CHCl_3) for 99% *ee*. $^1\text{H NMR}$ (400 MHz, CDCl_3) δ 7.48 (m, 2H), 7.39 (td, $J = 7.5, 1.4$ Hz, 1H), 7.35-7.22 (m, 2H), 7.12 (dd, $J = 7.5, 1.3$ Hz, 1H), 7.12-7.03 (m, 1H), 6.86 (dd, $J = 7.8, 1.2$ Hz, 1H), 6.54 (t, $J = 2.3$ Hz, 1H), 6.08 (dd, $J = 3.5, 2.7$ Hz, 1H), 5.89 (s, 1H), 5.12 (d, $J = 4.8$ Hz, 1H), 3.72 (br s, 1H), 3.46 (qd, $J = 7.1, 4.7$ Hz, 1H), 3.35 (s, 3H), 1.15 (d, $J = 7.1$ Hz, 3H). $^{13}\text{C NMR}$ (100 MHz, CDCl_3) δ 144.8, 141.2, 140.3, 131.8, 129.8, 129.08, 128.7, 128.3, 127.0, 126.8, 126.3, 123.0, 122.1, 120.6, 109.0, 106.5, 67.3, 39.6, 34.6, 14.5. HRMS (ESI) calcd. for $\text{C}_{20}\text{H}_{21}\text{N}_2$ ($\text{M} + \text{H}^+$) 289.1705. Found 289.1703. HPLC (IA column, 95:5 *n*-Hex/*i*-PrOH, 30 °C, 1.0 mL/min): t_{R} 6.78 min (major) and 9.60 min (minor).

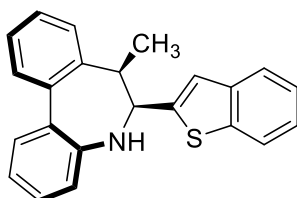
(*S_a,6*S*,7*R)-7-Methyl-6-(thiophen-2-yl)-6,7-dihydro-5*H*-dibenzo[*b,d*]azepine**

(23ar). Prepared following general procedure, using **22ar** and further purification by flash chromatography afforded **23ar** (47 mg, 80% yield) as colorless oil. $[\alpha]_{\text{D}}^{20}$ $+44.5$ (c 0.51, CHCl_3) for 98% *ee*. $^1\text{H NMR}$ (400 MHz, CDCl_3) δ 7.48-7.45 (m, 2H), 7.40 (t, $J = 7.5$ Hz, 1H), 7.30-7.25 (m, 2H), 7.19-7.15 (m, 2H), 6.99-6.94 (m, 2H), 6.91-6.88 (m, 2H), 5.26 (d, $J = 5.0$ Hz, 1H), 3.93 (br s, 1H), 3.48 (dt, $J = 12.2, 6.1$ Hz, 1H), 1.18 (d, $J = 7.1$ Hz, 3H). $^{13}\text{C NMR}$ (100 MHz, CDCl_3) δ 145.2, 144.0, 140.4, 139.1, 134.2, 129.4, 128.7, 128.3, 126.8, 126.7, 126.4, 125.6, 125.3, 124.8, 123.1, 120.9, 71.4, 37.7, 14.9. HRMS (ESI) calcd. for $\text{C}_{19}\text{H}_{18}\text{NS}$ ($\text{M} + \text{H}^+$) 292.1160. Found 292.1154. HPLC (IA column, 95:5 *n*-Hex/*i*-PrOH, 30 °C, 1.0 mL/min): t_{R} 6.64 min (major) and 11.95 min (minor).

(*S_a*,6*S*,7*R*)-6-(Benzofuran-2-yl)-7-methyl-6,7-dihydro-5*H*-dibenzo[*b,d*]azepine

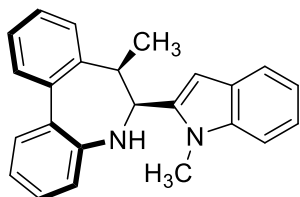
(23as). Prepared following general procedure, using **22as** and further purification by flash chromatography afforded **23as** (36 mg, 55% yield) as colorless oil. $[\alpha]_{\text{D}}^{20}$ -36.3 (c 0.51, CHCl_3) for 93% *ee*. $^1\text{H NMR}$ (400 MHz, CDCl_3) δ 7.50-

7.46 (m, 4H), 7.40 (td, $J = 7.5, 1.3$ Hz, 1H), 7.32-7.25 (m, 3H), 7.25-7.15 (m, 2H), 7.04 (d, $J = 7.7$ Hz, 1H), 6.94 (dd, $J = 7.7, 1.2$ Hz, 1H), 6.36 (s, 1H), 5.17 (d, $J = 5.0$ Hz, 1H), 3.78 (br s, 1H), 3.55 (td, $J = 7.2, 5.2$ Hz, 1H), 1.27 (d, $J = 7.3$ Hz, 3H). $^{13}\text{C NMR}$ (100 MHz, CDCl_3) δ 158.7, 154.6, 144.0, 140.0, 139.7, 133.7, 129.5, 128.7, 128.4, 128.3, 126.9, 126.9, 125.9, 123.8, 123.0, 122.6, 121.0, 120.9, 111.2, 104.6, 69.1, 38.0, 14.6. HRMS (ESI) calcd. for $\text{C}_{23}\text{H}_{20}\text{NO}$ ($\text{M} + \text{H}^+$) 326.1445. Found 326.1539. HPLC (IA column, 95:5 *n*-Hex/*i*-PrOH, 30 °C, 1.0 mL/min): t_{R} 8.92 min (major) and 10.34 min (minor).

(*S_a*,6*S*,7*R*)-6-(Benzo[*b*]thiophen-2-yl)-7-methyl-6,7-dihydro-5*H*-

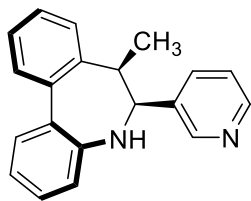
dibenzo[*b,d*]azepine (23at). Prepared following general procedure, using **22at** and further purification by flash chromatography afforded **22at** (51 mg, 75% yield) as colorless oil. $[\alpha]_{\text{D}}^{20}$ -41.1 (c 0.50, CHCl_3) for 95% *ee*. $^1\text{H NMR}$ (400 MHz, CDCl_3) δ 7.76-7.73 (m, 2H), 7.53-7.50 (m,

2H), 7.46 (ddt, $J = 7.5, 6.5, 1.4$ Hz, 1H), 7.40-7.28 (m, 4H), 7.25-7.18 (m, 1H), 7.17 (s, 1H), 7.09-7.03 (m, 1H), 6.92 (dd, $J = 7.7, 1.2$ Hz, 1H), 5.32 (d, $J = 5.1$ Hz, 1H), 3.95 (br s, 1H), 3.60-3.53 (m, 1H), 1.28 (d, $J = 7.2$ Hz, 3H). $^{13}\text{C NMR}$ (100 MHz, CDCl_3) δ 146.6, 144.0, 140.4, 139.9, 139.1, 139.0, 134.2, 129.5, 128.8, 128.3, 126.9, 126.9, 126.6, 123.9, 123.8, 123.2, 122.4, 121.9, 121.0, 72.1, 37.6, 15.0. HRMS (ESI) calcd. for $\text{C}_{23}\text{H}_{20}\text{NS}$ ($\text{M} + \text{H}^+$) 342.1316. Found 342.1305. HPLC (IA column, 95:5 *n*-Hex/*i*-PrOH, 30 °C, 1.0 mL/min): t_{R} 12.07 min (major) and 16.44 min (minor).

(*S_a,6*S*,7*R)-7-Methyl-6-(1-methyl-1*H*-indol-2-yl)-6,7-dihydro-5*H*-**

dibenzo[b,d]azepine (23au). Prepared following general procedure, using **22au** and further purification by flash chromatography afforded **23au** (60 mg, 90% yield) as yellow oil. $[\alpha]_{\text{D}}^{20}$ -18.6 (*c* 0.51, CHCl₃) for 97% *ee*. ¹H NMR

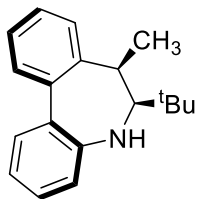
(400 MHz, CDCl₃) δ 7.59 (d, *J* = 7.8 Hz, 1H), 7.57-7.48 (m, 2H), 7.44 (t, *J* = 7.5 Hz, 1H), 7.33-7.28 (m, 3H), 7.23 (t, *J* = 7.5 Hz, 1H), 7.19-7.12 (m, 2H), 7.04 (d, *J* = 7.6 Hz, 1H), 6.92 (d, *J* = 7.8 Hz, 1H), 6.28 (s, 1H), 5.34 (d, *J* = 5.0 Hz, 1H), 3.79 (br s, 1H), 3.64-3.54 (m, 1H), 3.49 (s, 3H), 1.19 (d, *J* = 7.1 Hz, 3H). ¹³C NMR (100 MHz, CDCl₃) δ 144.5, 140.8, 140.3, 139.3, 138.2, 132.9, 129.8, 128.8, 127.2, 127.2, 127.0, 126.4, 122.5, 121.3, 120.8, 120.4, 119.5, 109.2, 102.5, 68.1, 39.2, 30.7, 14.6. HRMS (ESI) calcd. for C₂₄H₂₃N₂ (*M* + *H*⁺) 339.1861. Found 339.1849. HPLC (IA column, 95:5 *n*-Hex/*i*-PrOH, 30 °C, 1.0 mL/min): *t_R* 8.36 min (major) and 10.84 min (minor).

(*S_a,6*S*,7*R)-7-Methyl-6-(pyridin-3-yl)-6,7-dihydro-5*H*-dibenzo[b,d]azepine**

(23av). Prepared following general procedure, using **22av** and further purification by flash chromatography afforded **23av** (42 mg, 73% yield) as white solid. $[\alpha]_{\text{D}}^{20}$ +31.3 (*c* 0.53, CHCl₃) for 96% *ee*. ¹H NMR (400 MHz, CDCl₃) δ 8.49 (d, *J* = 3.9

Hz, 1H), 8.33 (s, 1H), 7.47-7.43 (m, 2H), 7.38 (td, *J* = 7.5, 1.2 Hz, 1H), 7.31-7.19 (m, 3H), 7.15 (td, *J* = 7.5, 1.2 Hz, 1H), 7.09 (dd, *J* = 7.9, 4.7 Hz, 1H), 6.89 (dd, *J* = 7.8, 1.2 Hz, 1H), 6.72 (d, *J* = 7.7 Hz, 1H), 4.97 (d, *J* = 4.9 Hz, 1H), 3.65 (s, 1H), 3.64-3.56 (m, 1H), 1.08 (d, *J* = 7.2 Hz, 3H). ¹³C NMR (100 MHz, CDCl₃) δ 150.1, 149.1, 144.4, 140.4, 138.7, 136.4, 133.6, 129.5, 128.9, 128.4, 127.0, 125.7, 122.8, 122.6, 120.8, 72.9, 37.4, 14.9. HRMS (ESI) calcd. for C₂₀H₁₉N₂ (*M* + *H*⁺) 287.1548. Found 287.1543. HPLC (IA column, 95:5 *n*-Hex/*i*-PrOH, 30 °C, 1.0 mL/min): *t_R* 14.97 min (major) and 23.91 min (minor).

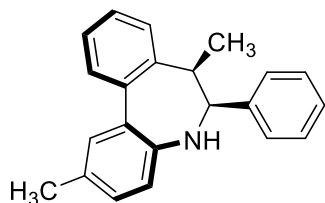
(*R_a*,6*S*,7*R*)-6-(*tert*-butyl)-7-methyl-6,7-dihydro-5*H*-dibenzo[*b,d*]azepine



(23aw). Prepared following general procedure, using **22aw** and further purification by flash chromatography afforded **23aw** (45 mg, 85% yield) as colorless oil. $[\alpha]_D^{20} -165.1$ (*c* 0.41, CHCl₃) for 97% ee. ¹H NMR (400 MHz, CDCl₃) δ 7.62 (d, *J* = 7.5 Hz, 1H), 7.46

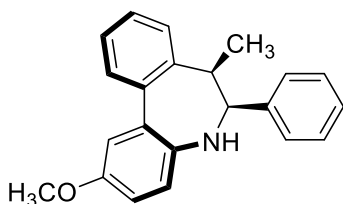
(d, *J* = 7.7 Hz, 1H), 7.29 (t, *J* = 7.5 Hz, 1H), 7.19 (t, *J* = 7.1 Hz, 1H), 7.11 (t, *J* = 7.4 Hz, 1H), 7.05 (d, *J* = 6.6 Hz, 1H), 6.74 (t, *J* = 7.0 Hz, 1H), 6.67 (d, *J* = 8.0 Hz, 1H), 4.22 (s, 1H), 3.43 (d, *J* = 7.1 Hz, 1H), 3.33 (s, 1H), 1.14 (d, *J* = 7.0 Hz, 3H), 1.08 (s, 9H). ¹³C NMR (100 MHz, CDCl₃) δ 147.9, 145.7, 138.4, 132.2, 130.7, 128.2, 127.6, 126.4, 126.1, 123.5, 117.2, 117.0, 69.2, 43.1, 35.3, 27.5, 14.1. HRMS (ESI) calcd. for C₁₉H₂₄N (M + H⁺) 266,1909. Found 266.1904. HPLC (IA column, 95:5 *n*-Hex/*i*-PrOH, 30 °C, 1.0 mL/min): *t_R* 5.54 min (minor) and 6.23 min (major).

(*S_a*,6*S*,7*R*)-2,7-Dimethyl-6-phenyl-6,7-dihydro-5*H*-dibenzo[*b,d*]azepine (23ba).

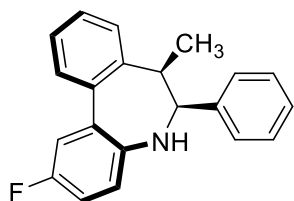


Prepared following general procedure, using **22ba** and further purification by flash chromatography afforded **23ba** (42 mg, 70% yield) as yellow oil. $[\alpha]_D^{20} +25.1$ (*c* 0.38, CHCl₃) for 98% ee. ¹H NMR (400 MHz, CDCl₃) δ 7.49 (dd, *J* = 7.6, 1.4 Hz, 1H), 7.40 (td, *J* = 7.5, 1.3 Hz, 1H), 7.29-

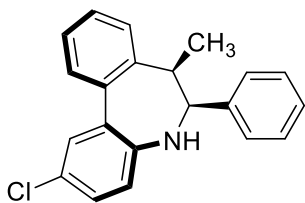
7.21 (m, 5H), 7.11-7.06 (m, 3H), 6.82-6.80 (m, 2H), 4.91 (d, *J* = 5.3 Hz, 1H), 3.56-3.49 (m, 1H), 2.42 (s, 3H), 1.06 (d, *J* = 7.2 Hz, 3H). ¹³C NMR (100 MHz, CDCl₃) δ 142.3, 141.0, 140.5, 139.8, 133.9, 132.0, 129.9, 129.3, 129.0, 128.1, 127.6, 127.4, 126.7, 126.6, 126.1, 120.8, 75.6, 37.8, 20.9, 15.0. HRMS (ESI) calcd. for C₂₂H₂₂N (M + H⁺) 300.1752. Found 300.1744. HPLC (IA column, 95:5 *n*-Hex/*i*-PrOH, 30 °C, 1.0 mL/min): *t_R* 5.50 min (major) and 7.04 min (minor).

(*S_a,6S,7R*)-2-Methoxy-7-methyl-6-phenyl-6,7-dihydro-5H-dibenzo[*b,d*]azepine

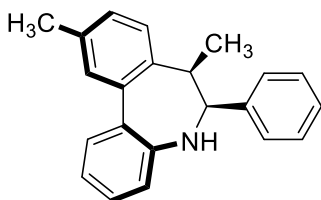
(23bb). Prepared following general procedure, using **22bb** and further purification by flash chromatography afforded **23bb** (33 mg, 50% yield) as yellow oil. $[\alpha]_{\text{D}}^{20}$ -31.2 (*c* 0.25, CHCl_3) for 99% *ee*. ^1H NMR (400 MHz, CDCl_3) δ 7.49 (d, *J* = 7.4 Hz, 1H), 7.40 (t, *J* = 7.4 Hz, 1H), 7.28-7.20 (m, 5H), 7.08-7.03 (m, 3H), 6.88-6.82 (m, 3H), 4.86 (d, *J* = 5.5 Hz, 1H), 3.86 (s, 3H), 3.48 (m, 1H), 1.03 (d, *J* = 7.2 Hz, 3H). ^{13}C NMR (100 MHz, CDCl_3) δ 155.8, 140.8, 140.4, 139.9, 138.1, 135.8, 128.9, 127.9, 127.6, 127.5, 126.9, 126.6, 126.2, 122.0, 114.7, 113.9, 75.7, 55.7, 37.7, 15.0. HRMS (ESI) calcd. for $\text{C}_{22}\text{H}_{22}\text{NO}$ ($\text{M} + \text{H}^+$) 316.1701. Found 316.1690. HPLC (IA column, 95:5 *n*-Hex/*i*-PrOH, 30 °C, 1.0 mL/min): t_{R} 6.18 min (major) and 9.58 min (minor).

(*S_a,6S,7R*)-2-Fluoro-7-methyl-6-phenyl-6,7-dihydro-5H-dibenzo[*b,d*]azepine

(23bc). Prepared following general procedure, using **22bc** (and further purification by flash chromatography afforded **23bc** (57 mg, 95% yield) as yellow oil. $[\alpha]_{\text{D}}^{20}$ -2.5 (*c* 0.58, CHCl_3) for 99% *ee*. ^1H NMR (400 MHz, CDCl_3) δ 7.47-7.39 (m, 2H), 7.31-7.18 (m, 5H), 7.08-7.04 (m, 2H), 6.99 (td, *J* = 8.4, 3.0 Hz, 1H), 6.85-6.82 (m, 2H), 4.90 (d, *J* = 5.4 Hz, 1H), 3.58 (s, 1H), 3.51 (dd, *J* = 7.4, 5.6 Hz, 1H), 1.07 (d, *J* = 7.2 Hz, 3H). ^{13}C NMR (100 MHz, CDCl_3) δ 159.1 (d, *J* = 239.9 Hz), 140.9, 140.7, 139.7 (d, *J* = 27.9 Hz), 135.9 (d, *J* = 7.8 Hz), 128.9, 128.0, 127.7, 127.5, 127.3, 126.7, 126.3, 121.89 (d, *J* = 8.0 Hz), 115.63 (d, *J* = 22.7 Hz), 114.95 (d, *J* = 22.1 Hz), 75.6, 37.7, 29.8, 15.0. ^{19}F NMR (377 MHz, CDCl_3) δ -121.8. HRMS (ESI) calcd. for $\text{C}_{21}\text{H}_{19}\text{FN}$ ($\text{M} + \text{H}^+$) 304.1502. Found 304.1492. HPLC (IA column, 95:5 *n*-Hex/*i*-PrOH, 30 °C, 1.0 mL/min): t_{R} 5.43 min (major) and 7.85 min (minor).

(*S_a*,6*S*,7*R*)-2-chloro-7-methyl-6-phenyl-6,7-dihydro-5*H*-dibenzo[*b,d*]azepine

(23bd). Prepared following general procedure, using **22bd** and further purification by flash chromatography afforded **23bd** (10 mg, 15% yield) as colorless oil. $[\alpha]_D^{20} +58.7$ (*c* 0.26, CHCl₃) for 94% *ee*. ¹H NMR (400 MHz, CDCl₃) δ 7.47 – 7.34 (m, 3H), 7.29 – 7.16 (m, 5H), 7.01 (dt, *J* = 6.9, 1.5 Hz, 2H), 6.79 (dd, *J* = 8.1, 6.1 Hz, 2H), 4.91 (d, *J* = 5.0 Hz, 1H), 3.68 (s, 1H), 3.55 – 3.44 (m, 1H), 1.06 (d, *J* = 7.2 Hz, 3H). ¹³C NMR (101 MHz, CDCl₃) δ 143.4, 140.6, 139.7, 139.2, 129.0, 128.8, 128.4, 128.2, 127.7, 127.5, 127.2, 126.8, 126.2, 121.8, 77.2, 77.2, 14.9. HRMS (ESI) calcd. for C₂₁H₁₉ClN (*M* + *H*⁺) 320.1206. Found 320.1197. HPLC (IA column, 95:5 *n*-Hex/*i*-PrOH, 30 °C, 1.0 mL/min): *t_R* 6.17 min (major) and 8.99 min (minor).

(*S_a*,6*S*,7*R*)-7,10-Dimethyl-6-phenyl-6,7-dihydro-5*H*-dibenzo[*b,d*]azepine

(23ca). Prepared following general procedure, using **22ca** and further purification by flash chromatography afforded **23ca** (24 mg, 40% yield) as colorless oil. $[\alpha]_D^{20} +6.3$ (*c* 0.43, CHCl₃) for 96% *ee*. ¹H NMR (400 MHz, CDCl₃)

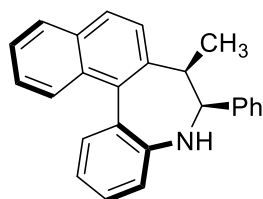
δ 7.46 (dd, *J* = 7.5, 1.6 Hz, 1H), 7.29-7.19 (m, 5H), 7.13 (td, *J* = 7.5, 1.2 Hz, 1H), 7.07-7.03 (m, 3H), 6.87 (dd, *J* = 7.7, 1.2 Hz, 1H), 6.69 (d, *J* = 7.8 Hz, 1H), 4.91 (d, *J* = 5.1 Hz, 1H), 3.67 (s, 1H), 3.49 (dt, *J* = 12.4, 6.1 Hz, 1H), 2.43 (s, 3H), 1.03 (d, *J* = 7.2 Hz, 3H). ¹³C NMR (100 MHz, CDCl₃) δ 144.9, 141.1, 140.2, 136.7, 136.0, 133.9, 129.3, 129.0, 128.9, 128.6, 127.5, 127.4, 126.0, 122.5, 120.8, 75.4, 37.5, 21.2, 15.0. HRMS (ESI) calcd. for C₂₂H₂₂N (*M* + *H*⁺) 300.1752. Found 300.1748. HPLC (IA column, 95:5 *n*-Hex/*i*-PrOH, 30 °C, 1.0 mL/min): *t_R* 4.99 min (major) and 6.77 min (minor).

IV.5.3. General procedure for the kinetic resolution of **25** followed by reduction of the remaining enantioenriched imine.

A flamed-dried Schlenk tube equipped with a magnetic stir bar was charged with Cu(OAc)₂ (4 mol%) and (*R,R*)-Ph-BPE (4.4 mol%). Anhydrous THF (300 μ L) was added via syringe and the reaction mixture was stirred for 15 min, until a blue

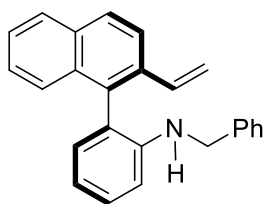
homogeneous solution was obtained. Diethoxymethylsilane (DEMS, 2.0 equiv) was added via syringe and stirring was continued for 10 min at room temperature. Into a separate flamed-dried Schlenk tube aldimine **25** (0.2 mmol, 1 equiv) was dissolved in anhydrous MTBE (1 mL) and transferred via syringe to the reaction tube containing the catalyst. Anhydrous *t*BuOH (1.1 equiv) was added via microsyringe and the reaction mixture was stirred at room temperature under N₂ for 48 h. The reaction mixture was then quenched with saturated aqueous Na₂CO₃ solution, extracted with EtOAc and the combined organic layers were concentrated *in vacuo*. The residue was dissolved in Et₂O (1.25 mL) and slowly added over a suspension of LiAlH₄ (15 mg) in Et₂O (0.4 mL) at 0°C. The mixture was then allowed to reach room temperature and stirred for 2h. Saturated aqueous NH₄Cl solution was then added, and the mixture was extracted with AcOEt (3 × 3 mL). The combined organic layer was dried over anhydrous Na₂SO₄, filtered and concentrated *in vacuo*. The crude mixture was purified by flash column chromatography (4:1 hexane/toluene) on silica gel to obtain **26** (21 mg, 39% yield) and **27** (17 mg, 32% yield) as light-yellow oils.

(*S_a,6*S*,7*R)-7-Methyl-6-phenyl-6,7-dihydro-5*H*-benzo[*b*]naphtho[1,2-*d*]azepine**



(26). $[\alpha]_{\text{D}}^{20} +18.3$ (*c* 0.43, CHCl₃) for 90% *ee*. ¹H NMR (400 MHz, CDCl₃) δ 8.08 (d, *J* = 9.0 Hz, 1H), 7.95-7.88 (m, 2H), 7.64-7.59 (m, 2H), 7.47 – 7.42 (m, 2H), 7.39-7.32 (m, 4H), 7.27-7.22 (m, 3H), 6.80 (d, *J* = 7.7 Hz, 1H), 4.34 (d, *J* = 11.2 Hz, 1H), 3.49-3.41 (m, 1H), 1.15 (d, *J* = 6.9 Hz, 3H). ¹³C NMR (100 MHz, CDCl₃) δ 145.0, 144.9, 139.1, 135.6, 133.2, 132.0, 131.1, 130.4, 128.9, 128.5, 128.2, 128.0, 127.7, 126.7, 126.3, 126.0, 125.1, 123.0, 122.0, 121.5, 77.0, 38.5, 16.2. HRMS (ESI) calcd. for C₂₅H₂₂N (M + H⁺) 336.1752. Found 336.1745. HPLC (IA column, 95:5 *n*-Hex/*i*-PrOH, 30 °C, 1.0 mL/min): *t_R* 6.29 min (major) and 9.85 min (minor).

(*R*)-*N*-(2-(2-Vinylnaphthalen-1-yl)benzyl)aniline (27**).** $[\alpha]_{\text{D}}^{20} -6.0$ (*c* 0.43, CHCl₃)

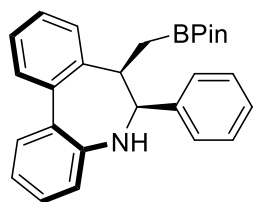


for >99% *ee*. ¹H NMR (400 MHz, CDCl₃) δ 7.86 (m, 3H), 7.51-7.46 (m, 2H), 7.41-7.37 (m, 1H), 7.30 (ddd, *J* = 8.7, 7.5, 1.7 Hz, 1H), 7.23-7.18 (m, 3H), 7.15-7.13 (m, 2H), 7.05 (dd, *J* = 7.4, 1.7 Hz, 1H), 6.87 (td, *J* = 7.4, 1.1 Hz, 1H), 6.78 (d, *J* = 8.2 Hz, 1H), 6.69 (dd, *J* = 17.6, 11.0 Hz, 1H), 5.85 (dd, *J* = 17.6, 1.0 Hz, 1H),

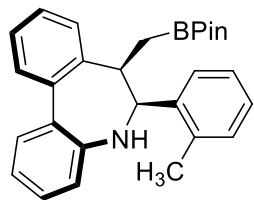
5.28 (dd, *J* = 11.0, 1.0 Hz, 1H), 4.25 (d, *J* = 4.2 Hz, 2H). ¹³C NMR (100 MHz, CDCl₃) δ 145.3, 139.2, 135.2, 134.1, 133.9, 133.5, 132.9, 131.3, 129.0, 128.4, 128.4, 128.0, 127.0, 127.0, 126.6, 126.6, 126.1, 123.6, 122.7, 117.6, 115.3, 111.3, 48.0. HRMS (ESI) calcd. for C₂₅H₂₂N (*M* + H⁺) 336.1752. Found 336.1745. HPLC (OJ-H column, 98:2 *n*-Hex/*i*-PrOH, 30 °C, 1.0 mL/min): *t*_R 12.70 min (major) and 25.47 min (minor).

IV.5.4. General procedure for the synthesis of borylated dibenzazepines **28** by Cu-catalyzed intramolecular borylative cyclization.

To a 10 mL reaction vial was added Cu(MeCN)₄PF₆ (5 mol %), (–)-1,2-Bis((2*R*,5*R*)-2,5-diphenylphospholano)ethane (0.012 mmol), KO^tBu (0.3 mmol) and THF (1.0 mL). The mixture was stirred at room temperature for 10-15 min before the addition of B₂pin₂ (0.3 mmol). After brief stirring (10 min), a solution of **22** (0.2 mmol) in anhydrous THF (0.7 mL) was then added at room temperature under nitrogen atmosphere. Degassed and dry isopropanol (0.4 mmol) was added under nitrogen atmosphere and the reaction mixture was then stirred at r.t. for 12 h. After reaction completion, the resulting solution was filtered through a silica plug, and the crude material was concentrated in vacuo. The resulting crude product was purified by flash column chromatography on silica gel to obtain borylated dibenzo[*b,d*]azepine derivatives **28**.

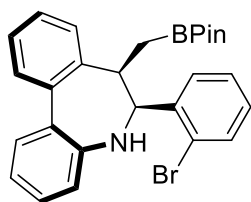
(*S*_a,6*S*,7*R*)-6-Phenyl-7-((4,4,5,5-tetramethyl-1,3,2-dioxaborolan-2-yl)methyl)-**6,7-dihydro-5*H*-dibenzo[*b,d*]azepine (28aa).**

Prepared following general procedure, using **22aa** (56 mg, 0.2 mmol) to obtain **28aa** (72 mg, 85% yield) as colorless oil. $[\alpha]_{\text{D}}^{20} +46$ (*c* 0.55, CHCl₃) for 98% *ee*. ¹H NMR (400 MHz, CDCl₃) δ 7.50–7.43 (m, 2H), 7.35 (t, *J* = 7.3 Hz, 1H), 7.29–7.18 (m, 5H), 7.14 (t, *J* = 7.2 Hz, 1H), 7.06 (m, 2H), 6.87 (d, *J* = 7.7 Hz, 1H), 6.80 (br s, 1H), 5.02 (d, *J* = 4.9 Hz, 1H), 3.76–3.62 (m, 2H), 1.14 (s, 6H), 1.06 (s, 6H), 0.94 (d, *J* = 8.2 Hz, 2H). ¹³C NMR (100 MHz, CDCl₃). δ 145.0, 141.0, 140.5, 139.9, 134.0, 129.3, 129.0, 128.6, 128.1, 127.4, 127.4, 126.4, 122.4, 120.8, 83.1, 75.9, 39.3, 24.7, 24.5, 12.7. ¹¹B NMR (160 MHz, CDCl₃): δ 33.9 ppm. HRMS (ESI) calcd. for C₂₇H₃₁BNO₂ (*M* + *H*⁺) 412,2448. Found 412.2438. HPLC (IA column, 95:5 *n*-Hex/*i*-PrOH, 30 °C, 1.0 mL/min): *t*_R 5.04 min (major) and 6.46 min (minor).

(*S*_a,6*S*,7*R*)-7-((4,4,5,5-Tetramethyl-1,3,2-dioxaborolan-2-yl)methyl)-6-(*o*-**tolyl)-6,7-dihydro-5*H*-dibenzo[*b,d*]azepine (28ab).**

Prepared following general procedure, using **22ab** (60 mg, 0.2 mmol) to obtain **28ab** (70 mg, 82% yield) as colorless oil. $[\alpha]_{\text{D}}^{20} +19$ (*c* 0.52, CHCl₃) for 97% *ee*. ¹H NMR (400 MHz, CDCl₃) δ 7.50–7.45 (m, 2H), 7.36 (t, *J* = 7.5 Hz, 1H), 7.25–7.21 (m, 3H), 7.15–7.10 (m, 3H), 7.01–6.87 (m, 4H), 5.37 (d, *J* = 5.1 Hz, 1H), 3.72 (br s, 1H), 2.43 (s, 3H), 1.05 (s, 6H), 0.95 (m, 8H). ¹³C NMR (100 MHz, CDCl₃) δ 144.4, 140.0, 136.0, 130.0, 129.4, 128.6, 127.3, 127.1, 126.7, 126.5, 125.3, 123.1, 121.1, 83.0, 70.3, 40.0, 24.7, 24.4, 20.2, 11.2. ¹¹B NMR (160 MHz, CDCl₃): δ 33.4 ppm. HRMS (ESI) calcd. for C₂₈H₃₃BNO₂ (*M* + *H*⁺) 426,2604. Found 426.2598. HPLC (IA column, 95:5 *n*-Hex/*i*-PrOH, 30 °C, 1.0 mL/min): *t*_R 4.68 min (major) and 6.49 min (minor).

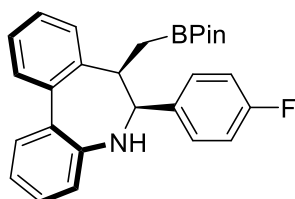
(*S_a,6*S*,7*R)-6-(2-Bromophenyl)-7-((4,4,5,5-tetramethyl-1,3,2-dioxaborolan-2-yl)methyl)-6,7-dihydro-5*H*-dibenzo[*b,d*]azepine (28af).**



Prepared following general procedure, using **22af** (72 mg, 0.2 mmol) to obtain **28af** (29 mg, 40% yield) as colorless oil.

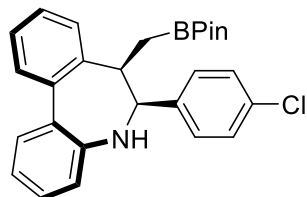
$[\alpha]_D^{20} +57$ (*c* 1.33, CHCl₃) for 92% *ee*. ¹H NMR (400 MHz, CDCl₃) δ 7.54 (d, *J* = 8.2 Hz, 1H), 7.50–7.44 (m, 2H), 7.38 (t, *J* = 7.5 Hz, 1H), 7.30–7.21 (m, 2H), 7.19–7.13 (m, 1H), 7.10–7.03 (m, 3H), 6.99–6.80 (m, 2H), 5.63 (d, *J* = 5.2 Hz, 1H), 3.81 (br s, 1H), 3.63 (br s, 1H), 1.07 (s, 6H), 0.96 (s, 8H). ¹³C NMR (100 MHz, CDCl₃) δ 144.7, 140.5, 140.2, 139.6, 134.1, 132.3, 131.3, 129.3, 128.8, 128.7, 128.3, 127.0, 126.6, 126.5, 126.4, 124.8, 122.7, 121.0, 83.0, 73.1, 40.1, 24.7, 24.4, 11.4. ¹¹B NMR (160 MHz, CDCl₃): δ 32.7 ppm. HRMS (ESI) calcd. for C₂₇H₃₀BBrNO₂ (*M* + *H*⁺) 490,1553. Found 490.1545. HPLC (IA column, 95:5 *n*-Hex/*i*-PrOH, 30 °C, 1.0 mL/min): *t_R* 4.44 min (major) and 5.76 min (minor).

(*S_a,6*S*,7*R)-6-(4-Fluorophenyl)-7-((4,4,5,5-tetramethyl-1,3,2-dioxaborolan-2-yl)methyl)-6,7-dihydro-5*H*-dibenzo[*b,d*]azepine (28ah).**



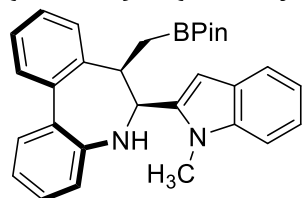
Prepared following general procedure, using **22ah** (60 mg, 0.2 mmol) to obtain **28ah** (72 mg, 84% yield) as colorless oil. $[\alpha]_D^{20} -59$ (*c* 0.70, CHCl₃) for 97%

ee. ¹H NMR (400 MHz, CDCl₃) δ 7.48–7.43 (m, 2H), 7.35 (t, *J* = 7.2 Hz, 1H), 7.29–7.12 (m, 4H), 7.05–6.96 (m, 2H), 6.93–6.83 (m, 3H), 6.77 (d, *J* = 7.0 Hz, 1H), 4.99 (d, *J* = 5.1 Hz, 1H), 3.68 (br s, 1H), 1.13 (s, 6H), 1.05 (s, 6H), 0.89 (m, 2H). ¹³C NMR (100 MHz, CDCl₃) δ 162.3 (d, *J* = 245.2 Hz), 144.1, 140.2, 139.3, 136.2, 134.1, 130.5, 130.5, 129.3, 128.7, 128.3, 126.6, 126.6, 126.4, 123.0, 121.0, 114.1 (d, *J* = 21.1 Hz), 83.2, 75.1, 39.0, 24.7, 24.5, 12.4. ¹⁹F NMR (377 MHz, CDCl₃) δ -115.4. ¹¹B NMR (160 MHz, CDCl₃): δ 33.9 ppm. HRMS (ESI) calcd. for C₂₇H₃₀BFNO₂ (*M* + *H*⁺) 430,2354. Found 430.2345. HPLC (IB column, 95:5 *n*-Hex/*i*-PrOH, 30 °C, 1.0 mL/min): *t_R* 5.95 min (minor) and 6.30 min (major).

(*S*_a,6*S*,7*R*)-6-(4-Chlorophenyl)-7-((4,4,5,5-tetramethyl-1,3,2-dioxaborolan-2-**yl)methyl)-6,7-dihydro-5*H*-dibenzo[*b,d*]azepine**

(28aj). Prepared following general procedure, using **22aj** (64 mg, 0.2 mmol) to obtain **28aj** (65 mg, 73% yield) as colorless oil. $[\alpha]_D^{20} +19$ (*c* 0.51, CHCl₃) for 94% *ee*. ¹H NMR

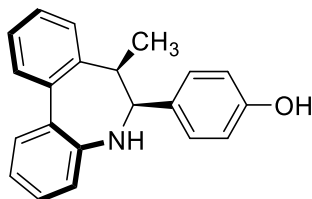
(400 MHz, CDCl₃) δ 7.47-7.42 (m, 2H), 7.34 (t, *J* = 7.2 Hz, 1H), 7.27-7.12 (m, 6H), 6.98-6.96 (m, 2H), 6.91 (d, *J* = 7.1 Hz, 1H), 6.76 (d, *J* = 7.2 Hz, 1H), 4.98 (d, *J* = 5.2 Hz, 1H), 3.66 (br s, 1H), 1.13 (s, 6H), 1.04 (s, 6H), 0.90-0.86 (m, 2H). ¹³C NMR (100 MHz, CDCl₃) δ 140.0, 139.0, 134.2, 133.3, 130.4, 129.3, 128.7, 128.3, 127.5, 126.8, 126.4, 123.3, 121.1, 83.2, 75.1, 38.8, 24.7, 24.5, 12.4. ¹¹B NMR (160 MHz, CDCl₃): δ 33.7 ppm. HRMS (ESI) calcd. for C₂₇H₃₀BClNO₂ (M + H⁺) 446,2058. Found 446.2049. HPLC (IB column, 95:5 *n*-Hex/*i*-PrOH, 30 °C, 1.0 mL/min): *t*_R 5.87 min (minor) and 7.01 min (major).

(*S*_a,6*S*,7*R*)-6-(1-Methyl-1*H*-indol-2-yl)-7-((4,4,5,5-tetramethyl-1,3,2-**dioxaborolan-2-yl)methyl)-6,7-dihydro-5*H*-**

dibenzo[*b,d*]azepine (28au). Prepared following general procedure, using **22au** (67 mg, 0.2 mmol) to obtain **28au** (67 mg, 72% yield) as colorless oil. $[\alpha]_D^{20} +1.0$ (*c* 0.53, CHCl₃) for 96% *ee*. ¹H NMR (400 MHz, CDCl₃) δ 7.57 (d, *J* = 7.8 Hz, 1H), 7.52-7.50 (m, 2H), 7.39 (td, *J* = 7.5, 1.3 Hz, 1H), 7.29-7.24 (m, 4H), 7.23-7.19 (m, 1H), 7.17-7.04 (m, 3H), 6.91 (d, *J* = 7.8 Hz, 1H), 6.31 (br s, 1H), 5.39 (d, *J* = 4.8 Hz, 1H), 3.73 (br s, 1H), 3.50 (br s, 3H), 1.09 (s, 6H), 1.03 (m, 8H). ¹³C NMR (100 MHz, CDCl₃) δ 144.3, 140.2, 138.2, 129.9, 129.0, 128.7, 127.2, 126.9, 126.8, 121.2, 120.4, 119.4, 109.2, 102.6, 83.1, 30.6, 27.0, 24.8, 24.5, 11.8. ¹¹B NMR (160 MHz, CDCl₃): δ 34.3 ppm. HRMS (ESI) calcd. for C₃₀H₃₄BN₂O₂ (M + H⁺) 465,2713. Found 465.2706. HPLC (IA column, 95:5 *n*-Hex/*i*-PrOH, 30 °C, 1.0 mL/min): *t*_R 9.32 min (major) and 10.60 min (minor).

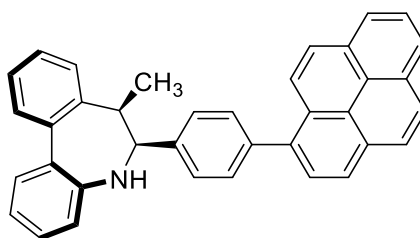
IV.5.5. Representative transformations.

Synthesis of **29ae** by demethylation of **23ae**.



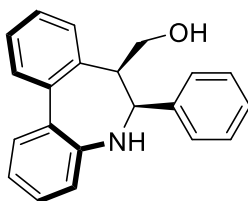
Following a described procedure,²²⁵ Boron tribromide (18 μ L, 0.19 mmol) was added to a solution of **23ae** (21 mg, 0.07 mol) in CH₂Cl₂ (1 mL) at -40 °C, then stirred for 30 min at rt. Saturated NaHCO₃ solution (2 mL) was added, the organic layer was separated and the aqueous phase was extracted with CH₂Cl₂ (2 mL \times 3). The organic layers were combined and concentrated to give an orange oil. This was purified by flash column chromatography (9:1 toluene/Et₃N) to afford the title compound as a white foam (14 mg, 70% yield). [α]_D²⁰ -17.1 (*c* 0.6, CHCl₃). ¹H NMR (400 MHz, CDCl₃) δ 7.45 (t, *J* = 1.7 Hz, 1H), 7.43 (t, *J* = 1.7 Hz, 1H), 7.36 (td, *J* = 7.3, 1.3 Hz, 1H), 7.28 – 7.20 (m, 3H), 7.12 (td, *J* = 7.5, 1.3 Hz, 1H), 6.90–6.85 (m, 3H), 6.80 (d, *J* = 8.1 Hz, 1H), 6.67 (m, 2H), 4.87 (d, *J* = 5.1 Hz, 1H), 3.52–3.45 (m, 1H), 1.04 (d, *J* = 7.2 Hz, 3H). ¹³C NMR (100 MHz, CDCl₃) δ 155.3, 144.9, 140.4, 139.8, 133.7, 132.9, 130.0, 129.3, 128.7, 128.2, 126.7, 126.5, 126.1, 122.5, 120.7, 114.3, 74.9, 37.8, 15.0. HRMS (ESI) calcd. for C₂₁H₂₀NO (M + H⁺) 302.1545. Found 302.1539.

²²⁵ C. W. Lim, O. Tissot, A. Mattison, M. W. Hooper, J. M. Brown, A. R. Cowley, D. I. Hulmes, A. J. Blacker, *Org. Process Res. Dev.*, **2003**, 7, 379–384.

Synthesis of **30ag** by Suzuki-Miyaura reaction.

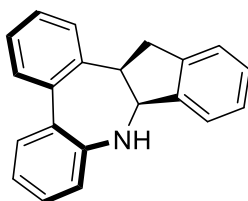
Following a described procedure.²²³ An oven-dried schlenk tube equipped with a magnetic stir bar was charged with Pd₂(dba)₃ (3.2 mg, 3 mol%), SPhos (2.8 mg, 6 mol%) and the reaction vessel was capped then evacuated and backfilled with N₂ using the Schlenk line. Thoroughly degassed THF (0.6 mL) was then added via syringe and the resulting mixture was stirred for 5 min at room temperature. Then, **23ag** (42 mg, 0.12 mmol), pyren-1-ylboronic acid (35 mg, 0.14 mmol), K₂CO₃ (48 mg, 0.35 mmol) and H₂O (0.2 mL for a THF/H₂O = 3:1) were added, and the resulting mixture was placed in a preheated oil bath and stirred at 60 °C for 18 h. The reaction crude was allowed to reach room temperature, water (3 mL) was added and the resulting mixture was extracted with AcOEt (3 × 5 mL). The combined organic layer was dried over anhydrous Na₂SO₄, filtered and concentrated *in vacuo*. The crude mixture was purified by flash column chromatography (4:1 cyclohexane/toluene) to afford **30ag** as a yellow oil (48 mg, 85% yield). [α]_D²⁰ -123.4 (*c* 0.51, CHCl₃). ¹H NMR (400 MHz, CDCl₃) δ 8.27–8.19 (m, 4H), 8.13 (m, 2H), 8.08–8.02 (m, 3H), 7.58–7.52 (m, 4H), 7.47 (td, *J* = 7.5, 1.4 Hz, 1H), 7.38–7.32 (m, 2H), 7.30–7.27 (m, 2H), 7.22 (t, *J* = 7.4 Hz, 1H), 7.03–6.99 (m, 2H), 5.12 (d, *J* = 5.1 Hz, 1H), 3.71–3.65 (m, 1H), 1.25 (d, *J* = 7.2 Hz, 3H). ¹³C NMR (100 MHz, CDCl₃) δ 140.5, 140.2, 139.4, 137.5, 134.0, 131.5, 131.0, 130.5, 129.8, 129.5, 129.0, 128.8, 128.5, 128.4, 127.7, 127.4, 127.4, 127.1, 127.0, 126.3, 126.0, 125.31, 125.1, 125.0, 124.9, 124.8, 124.7, 121.1, 75.4, 37.7, 15.1. HRMS (ESI) calcd. for C₃₇H₂₈N (M + H⁺) 486.2222. Found 486.2210.

Oxidation of organoboronate **28aa** for the synthesis of **31aa**.



Sodium perborate tetrahydrate (38 mg, 0.24 mmol) was added in one portion to a solution of boryl dibenzoazepine **28aa** (20 mg, 0.048 mmol) in aqueous THF (560 μ L, THF/H₂O = 1/1), and the mixture was stirred for 2 h. After diluting the reaction mixture with water (3 mL), the aqueous solution was extracted with EtOAc (3 \times 5 mL). The combined organic layer was dried over Na₂SO₄ and the solvent evaporated. The residue was purified by flash column chromatography (SiO₂, *n*-pentane/AcOEt 1:1), affording product **31aa** (14 mg, 96% yield) as a yellow solid. $[\alpha]_{\text{D}}^{20}$ +42 (*c* 0.78, CHCl₃). ¹H NMR (400 MHz, CDCl₃) δ 7.50-7.45 (m, 2H), 7.40 (t, *J* = 7.5 Hz, 1H), 7.29-7.20 (m, 6H), 7.14 (d, *J* = 7.4 Hz, 1H), 7.12-7.07 (m, 2H), 6.88 (d, *J* = 7.7 Hz, 1H), 6.65 (d, *J* = 7.2 Hz, 1H), 5.23 (d, *J* = 5.0 Hz, 1H), 3.79-3.70 (m, 2H), 3.58 (q, *J* = 7.2 Hz, 1H). ¹³C NMR (100 MHz, CDCl₃) δ 144.8, 140.9, 140.6, 136.2, 133.1, 129.4, 128.9, 128.7, 128.5, 127.8, 127.7, 127.0, 126.8, 125.6, 122.6, 120.9, 71.2, 61.7, 46.1, 26.9. HRMS (ESI) calcd. for C₂₁H₂₀NO (*M* + H⁺) 302,1545. Found 302.1537.

Intramolecular Suzuki Coupling for the synthesis of **32af**.



Following a described procedure,²²³ Pd(OAc)₂ (3.6 mg, 0.016 mmol), KO^tBu (54 mg, 0.48 mmol), and Sphos (13 mg, 0.032 mmol) were added to a dry Schlenk tube equipped with a stir bar. The tube was evacuated and refilled with N₂. A solution of boryl dibenzoazepine **28af** (78 mg, 0.16 mmol) in toluene (1.6 mL) and H₂O (0.2 mL)

was introduced to the Schlenk tube by syringe, respectively. The resulting reaction mixture was stirred vigorously at 80 °C for 24 h. The reaction mixture was concentrated in vacuum and the residue was purified by flash column chromatography (SiO₂, *n*-pentane/AcOEt 20:1) to afford **32af** (25 mg, 56% yield) as a solid. $[\alpha]_{\text{D}}^{20} +167$ (*c* 0.48, CHCl₃). ¹H NMR (400 MHz, CDCl₃) δ 7.46–7.31 (m, 6H), 7.29–7.25 (m, 2H), 7.18 (t, *J* = 7.3 Hz, 1H), 7.08 (t, *J* = 7.4 Hz, 1H), 7.02 (d, *J* = 7.4 Hz, 1H), 6.96 (t, *J* = 8.1 Hz, 1H), 6.46 (d, *J* = 7.6 Hz, 1H), 5.27 (d, *J* = 8.5 Hz, 1H), 3.84 (q, *J* = 9.0 Hz, 1H), 2.93 (dd, *J* = 16.3, 9.0 Hz, 1H), 2.77 (dd, *J* = 16.2, 9.3 Hz, 1H). ¹³C NMR (100 MHz, CDCl₃) δ 144.5, 143.7, 143.1, 140.3, 139.3, 136.4, 130.0, 129.8, 129.1, 128.9, 128.3, 127.9, 127.8, 127.6, 127.4, 126.0, 124.4, 124.2, 124.1, 75.1, 48.5, 39.1. HRMS (ESI) calcd. for C₂₁H₁₈N (M + H⁺) 284,1439. Found 284.1436.

APPENDIX I: Abbreviations

Å	Ångstrom
AcO	Acetate
AcOEt	Ethyl Acetate
ADH	Alcohol dehydrogenase
Aq	Aqueous
Ar	Aryl
Bn	Benzyl
Boc	<i>tert</i> -Butoxycarbonyl
BOX	Bisoxazoline
B ₂ pin ₂	Bis(pinacolato)diboron
tBu	<i>tert</i> -Butyl
nBuLi	<i>n</i> -Butyl lithium
CAL	Candida Antarctica
Cat	Catalyst
Cat*	Chiral catalyst
cod	1,5-Cyclooctadiene
CPA	Chiral Phosphoric Acid
m-CPBA	<i>meta</i> -Chloroperbenzoic acid
CPME	Cyclopentyl methyl ether
dba	Dibenzylidenacetone
DBU	1,8-Diazabicyclo[5.4.0]undec-7-ene

DCE	1,2-Dichloroethane
DCM	Dichloromethane
DEMS	Diethoxymethylsilane
DFT	Density Functional Theory
DIPEA	<i>N,N</i> -Diisopropylethylamine
DKR	Dynamic Kinetic Resolution
DMA	<i>N,N</i> -Dimethylacetamide
DMAP	4-Dimethylaminopyridine
DME	1,2-Dimethoxyethane
DMF	<i>N,N</i> -Dimethylformamide
DMSO	Dimethylsulphoxide
DPPA	Diphenyl phosphoryl azide
DQ	1,4-Benzoquinone
DYKAT	Dynamic Kinetic Asymmetric Transformation
eq.	Equivalents
ESI	Electrospray Ionization
Et	Ethyl
EtOH	Ethanol
<i>n</i> -Hex	<i>n</i> -Hexane
HFIP	1,1,1,3,3,3-Hexafluoro-2-propanol
HPLC	High Performance Liquid Chromatography
HRMS	High Resolution Mass Spectrometry
<i>i</i> Pr	<i>iso</i> -Propyl

iPrOH	<i>iso</i> -Propanol
KRED	Ketoreductases
L	Ligand
L*	Chiral ligand
LA	Lewis Acid
LB	Lewis Base
mmol	Milimolar
M	Metal
Me	Methyl
MeCN	Acetonitrile
MeOH	Methanol
MS	Molecular sieve
Ms	Mesyl
MTBE	<i>tert</i> -Butyl methyl ether
NADH	Nicotinamide adenine dinucleotide
NADPH	Nicotinamide adenine dinucleotide phosphate
NBP	<i>N</i> -bromophthalimide
n.d.	Not determined
n.r.	No reaction
NHC	<i>N</i> -Heterocyclic carbene
NMR	Nuclear Magnetic Resonance
NOESY	Nuclear Overhauser Effect Spectroscopy
Nu	Nucleophile

O ^t Bu	<i>tert</i> -Butoxide
ONf	Nonaflate
OTf	Triflate
PCL	Poly(ϵ -caprolactone)
Ph	Phenyl
PMHS	Polymethylhydrosiloxane
ppm	Parts per million
R	General substituent
rt	Room temperature
^t Bu	<i>tert</i> -Butyl
^t BuOH	<i>tert</i> -Butanol
TEOA	Triethanolamine
TFA	Trifluoroacetic acid
TFE	Trifluoroethanol
TLC	Thin Layer Chromatography
THF	Tetrahydrofuran
Tol	Toluene
tR	Retention time
Ts	Tosyl
TS	Transition State
X	Halogen
Xyl	Xylyl
δ	Chemical shift

APPENDIX II: General Methods

NMR Spectroscopy

¹H-NMR were recorded using a Bruker Advance DRX-500, and Bruker Advance DRX-400 spectrometers at 500 and 400 MHz respectively. ¹³C-NMR spectra were recorded using Bruker Advance DRX-400 spectrometer at 100 MHz. Solutions in commercial deuterated solvents were used to prepare samples, CDCl₃, CD₂Cl₂ or CD₃OD. Residual solvent peaks were used as an internal reference for ¹H-NMR spectra (CDCl₃ δ 7.26 ppm, CD₂Cl₂ δ 5.32 ppm, or CD₃OD δ 3.31 ppm) and ¹³C-NMR spectra (CDCl₃ δ 77.2 ppm, CD₂Cl₂ δ 53.8 ppm, or CD₃OD, 9.0 ppm). Coupling constants (J) are quoted to the nearest 0.1 Hz. The following abbreviations (or combinations thereof) were used to describe ¹H-NMR multiplicities: s = singlet, d = doublet, t = triplet, q = quartet, hept = heptet, m = multiplet, br = broad.

Mass Spectrometry

High Resolution Mass Spectrometry (HRMS) measurements were performed either by Kratos MS-80 RFA or Micromass AutoSpecQ (ESI) by General Services from University of Seville (CITIUS). In HRMS characterization, m/z found value for molecular peak was compared with that calculated from more abundant isotopes.

Chromatography

Analytical thin layer chromatography (TLC) was employed to monitor reactions progress. This technique was performed with commercial aluminium plates coated with 0.25 mm silica gel (Merck, silica gel 60 F254). Compounds were detected under UV-light at 254 nm and by dipping the plates in different home-made stains like mostain (20 g of ammonium molybdate tetrahydrate, 0.4 g of Ce(SO₄)₂ and 400 mL of 10% aqueous H₂SO₄), phosphomolybdic (5% solution of phosphomolybdic in EtOH), permanganate (10 g KMnO₄, 66 g K₂CO₃, 17 mL AcOH, 1 L H₂O), or ninhydrin (0.1% solution of ninhydrin in EtOH). Flash chromatography purifications were performed with Merck silica gel 60 (0.040-0.063 μm grade) and eluting by gravity or

using compressed air pressure. As eluents, solvent mixtures are indicated for each case.

Optical Rotations

Optical rotations were measured on a Perkin-Elmer 341 MC using a 1.0 cm cell with a Na ($\lambda = 589$ nm) yellow light.

X-ray Analysis

X-ray diffraction analyses were performed at the X-ray services from Centro de Investigación, Tecnología e Innovación de la Universidad de Sevilla (CITIUS), equipped with a BRUKER APEX II diffractometer. This equipment has the possibility of employ three different irradiation lamps: copper, tungsten, or silver. Furthermore, it includes a four circles goniometer with Kappa geometry, and a high sensitivity CCD detector. It is also possible to cool the samples thanks to a liquid nitrogen cooling system Cryostream 700 Plus from Oxford, which allows the execution of experiments from 80 to 500 K, with a 0.1 K stability.

Experimental procedures, reagents and glassware

Commercially available chemicals were used as purchased, or where specified, purified by standard techniques. Solvent compositions are given in (v/v). All reactions were carried out under an atmosphere of nitrogen in flame-dried glassware with magnetic stirring, unless otherwise indicated. MeCN, THF, DCM, and DMF were purified by an Innovative Technology Solvent Delivery System. All other solvents were used as purchased. Diethoxymethylsilane (DEMS) was purchased from Sigma-Aldrich (stored at 4°C) and used as received. Anhydrous ^tBuOH were purchased from Sigma-Aldrich in a Sure-Seal® bottle and used as received.

Anhydrous solvents

Anhydrous toluene and DCM were directly used after collection from PureSolv MD3 Solvent Purification System. THF was dried over Na with benzophenone as

indicator, and distilled just before every single use. 1,4-Dioxane was dried over CaH and distilled.

